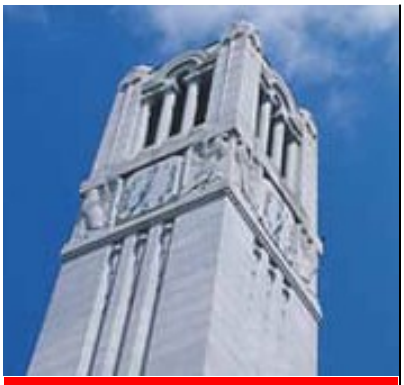

NC STATE UNIVERSITY

Constructed Facilities Laboratory
Department of Civil, Construction, and Environmental Engineering

Research Report
No. RD-06-05
FHWA/NC/2006-13

DEVELOPMENT OF A SIMPLIFIED PROCEDURE TO PREDICT DEAD LOAD DEFLECTIONS OF SKEWED AND NON-SKEWED STEEL PLATE GIRDER BRIDGES

Prepared by:

Seth T. Fisher, ***Research Assistant***

Todd W. Whisenhunt, ***Research Assistant***

Nuttapone Paoinchantara, ***Research Assistant***

Emmett A. Sumner, Ph.D., P.E., ***Co-Principle Investigator***

Sami Rizkalla, Ph.D., P.Eng., ***Co-Principle Investigator***

Prepared for:

North Carolina Department of Transportation
Research and Analysis Group
1 South Wilmington Street
Raleigh, North Carolina 27601

Constructed Facilities Laboratory
NC STATE UNIVERSITY

February 2006

Constructed Facilities Laboratory
2414 Campus Shore Drive
North Carolina State University
Raleigh, NC 27695-7533
Tel: (919) 513-1733
Fax: (919) 513-1765
Email: cfl@ncsu.edu
Web Site: www.cfl.ncsu.edu

Research Report

DEVELOPMENT OF A SIMPLIFIED PROCEDURE TO PREDICT DEAD LOAD DEFLECTIONS OF SKEWED AND NON-SKEWED STEEL PLATE GIRDER BRIDGES

Prepared by

Seth T. Fisher
Todd W. Whisenhunt
Nuttapone Paoinchantara
Research Assistants

Emmett A. Sumner, Ph.D., P.E.
Co-Principle Investigator

Sami Rizkalla, Ph.D., P.Eng.
Co-Principle Investigator

Submitted to

North Carolina Department of Transportation
Research and Analysis Group
1 South Wilmington Street
Raleigh, North Carolina 27601

NCSU-CFL Report No. RD-06-05
NCDOT Report No. FHWA/NC/2006-13

February 2006

Constructed Facilities Laboratory (CFL)
Department of Civil, Construction, and Environmental Engineering
North Carolina State University
Raleigh, NC 27695

Technical Report Documentation Page

1. Report No. FHWA/NC/2006-13	2. Government Accession No.	3. Recipient's Catalog No.
4. Title and Subtitle Development Of A Simplified Procedure To Predict Dead Load Deflections Of Skewed And Non-Skewed Steel Plate Girder Bridges		5. Report Date February 15, 2006 6. Performing Organization Code
7. Author(s) Seth T. Fisher, Todd W. Whisenhunt, Nuttapone Paoinchantara, Emmett A. Sumner, Sami H. Rizkalla		8. Performing Organization Report No.
9. Performing Organization Name and Address Department of Civil, Construction, and Environmental Engineering North Carolina State University Raleigh, North Carolina 27695		10. Work Unit No. (TRAIS) 11. Contract or Grant No.
12. Sponsoring Agency Name and Address North Carolina Department of Transportation Research and Analysis Group 1 South Wilmington Street Raleigh, North Carolina 27601		13. Type of Report and Period Covered Final Report July 1, 2003 - December 31, 2005 14. Sponsoring Agency Code 2004-14
Supplementary Notes:		

16. Abstract

Many of today's steel bridges are being constructed with longer spans and higher skew. The bridges are often erected in stages to limit traffic interruptions or to minimize environmental impacts. The North Carolina Department of Transportation (NCDOT) has experienced numerous problems matching the final deck elevations between adjacent construction stages due to inaccuracies in predicting the dead load deflections of steel plate girder bridges. In response to these problems, the NCDOT has funded this research project (Project No. 2004-14 - *Developing a Simplified Method for Predicting Deflection in Steel Plate Girders Under Non-composite Dead Load for Stage-constructed Bridges*). The primary objective of this research was to develop a simplified procedure to predict the dead load deflection of skewed and non-skewed steel plate girder bridges. In developing the simplified procedure, ten steel plate girder bridges were monitored during placement of the concrete deck to observe the deflection of the girders. Detailed three-dimensional finite element models of the bridge structures were generated in the commercially available finite element analysis program ANSYS. The finite element modeling results were validated through correlation with the field measured deflection results. With confidence in the ability of the developed finite element models to capture bridge deflection behavior, a preprocessor program was written to automate the finite element model generation. Subsequently, a parametric study was conducted to investigate the effect of skew angle, girder spacing, span length, cross frame stiffness, number of girders within the span, and exterior to interior girder load ratio on the girder deflection behavior. The results from the parametric were used to develop an empirical simplified procedure, which modifies traditional SGL predictions to account for skew angle, girder spacing, span length, and exterior to interior girder load ratio. Predictions of the deflections from the simplified procedure and from SGL analyses were compared to the deflections predicted from finite element models (ANSYS) and the field measured deflections to validate the procedure. It was concluded that the simplified procedure may be utilized to more accurately predict dead load deflection of simple span, steel plate girder bridges. Additionally, an alternative prediction method has been proposed to predict deflections in continuous span, steel plate girder bridges with equal exterior girder loads, and supplementary comparisons were made to validate this method

17. Key Words Skew bridges, plate girder bridges, camber, deflection, finite element method, structural steel, dead loads	18. Distribution Statement		
19. Security Classif. (of this report) Unclassified	20. Security Classif. (of this page) Unclassified	21. No. of Pages 389	22. Price

Form DOT F 1700.7 (8-72) **Reproduction of completed page authorized**

Disclaimer

The contents of this report reflect the views of the author(s) and not necessarily the views of the University. The author(s) are responsible for the facts and the accuracy of the data presented herein. The contents do not necessarily reflect the official views or policies of the North Carolina Department of Transportation or the Federal Highway Administration at the time of publication. This report does not constitute a standard, specification, or regulation.

Acknowledgments

Funding for this research was provided by the North Carolina Department of Transportation (project no. 2004-14 - *Developing a Simplified Method for Predicting Deflection in Steel Plate Girders Under Non-Composite Dead Load for Stage-Constructed Bridges*). Appreciation is extended to all of the NCDOT personnel that assisted in conducting the field measurements and coordination of this research project.

Executive Summary

Many of today's steel bridges are being constructed with longer spans and higher skew. The bridges are often erected in stages to limit traffic interruptions or to minimize environmental impacts. The North Carolina Department of Transportation (NCDOT) has experienced numerous problems matching the final deck elevations between adjacent construction stages due to inaccuracies in predicting the dead load deflections of steel plate girder bridges. In response to these problems, the NCDOT has funded this research project (Project No. 2004-14 - *Developing a Simplified Method for Predicting Deflection in Steel Plate Girders Under Non-composite Dead Load for Stage-constructed Bridges*).

The primary objective of this research was to develop a simplified procedure to predict the dead load deflection of skewed and non-skewed steel plate girder bridges. In developing the simplified procedure, ten steel plate girder bridges were monitored during placement of the concrete deck to observe the deflection of the girders. Detailed three-dimensional finite element models of the bridge structures were generated in the commercially available finite element analysis program ANSYS. The finite element modeling results were validated through correlation with the field measured deflection results. With confidence in the ability of the developed finite element models to capture bridge deflection behavior, a preprocessor program was written to automate the finite element model generation. Subsequently, a parametric study was conducted to investigate the effect of skew angle, girder spacing, span length, cross frame stiffness, number of girders within the span, and exterior to interior girder load ratio on the girder deflection behavior.

The results from the parametric were used to develop an empirical simplified procedure, which modifies traditional SGL predictions to account for skew angle, girder spacing, span length, and exterior to interior girder load ratio. Predictions of the deflections from the simplified procedure and from SGL analyses were compared to the deflections predicted from finite element models (ANSYS) and the field measured deflections to validate the procedure. It was concluded that the simplified procedure may be utilized to more accurately predict dead load deflection of simple span, steel plate girder bridges. Additionally, an alternative prediction method has been proposed to predict deflections in continuous span, steel plate girder bridges with equal exterior girder loads, and supplementary comparisons were made to validate this method.

Table of Contents

List of Figures

List of Tables

DEVELOPMENT OF A SIMPLIFIED PROCEDURE TO PREDICT DEAD LOAD DEFLECTIONS OF SKEWED AND NON-SKEWED STEEL PLATE GIRDER BRIDGES

1.0 Introduction

1.1 Background

1.1.1 General

Many current and upcoming bridge construction projects in North Carolina incorporate steel plate girder bridges. Due to currently increasing site constraints, many of these bridges are being designed for longer spans at higher skews than in the past. In addition, they are being constructed in stages to maintain traffic flow on existing roadways. The development of higher strength steel allows for the design of longer spans with more slender cross-sections. As a result, the deflection of the girder is a more significant factor in the design. Therefore, it is important to accurately predict girder deflections during construction so that desired vertical elevation of the bridge deck can be achieved.

Specifically, designers must accurately predict non-composite girder dead load deflections to produce the girder camber tables. The non-composite girder deflection is the deflection resulting from loads occurring during construction, prior to the curing of the concrete deck (i.e. prior to composite action between the steel girders and concrete deck). They include: girder self weight, other structural steel (cross frames, end bent diaphragms, connector plates, bearing stiffeners and web stiffeners), stay-in-place (SIP) metal deck forms, deck reinforcing steel (rebar), and concrete deck slab. Additional dead loads during construction consist of the overhang falsework, deck concrete screeding machine, and

construction live load (personnel). Some of these loads are temporary and the resulting elastic deflections are assumed to recover after unloading.

The North Carolina Department of Transportation (NCDOT) has experienced numerous problems in accurately predicting the non-composite girder deflections, resulting in many costly construction delays and maintenance and safety issues. As a result, the NCDOT has funded this research project (Project Number 2004-14 - *Developing a Simplified Method for Predicting Deflection in Steel Plate Girders Under Non-Composite Dead Load for Stage-Constructed Bridges*). The primary goal of the research project is to develop a method to more accurately predict the non-composite girder deflections of skewed and non-skewed steel plate girder bridges. This report presents the results of a two and an half year project which has supported three Master's of Science student's research. The contents of this report is the culmination of the three student's theses; Whisenhunt (2004), Paoinchantara (2005) and Fisher (2006).

1.1.2 Current Analysis and Design

Typically, non-composite dead load deflections are predicted using single girder line (SGL) analysis. This method does not account for any transverse load distribution transmitted through intermediate cross frames and/or the SIP forms. The predicted deflection is directly dependent on the calculated dead load, which is determined according to the tributary width of the deck slab. If the girders are equally spaced, the interior girders are predicted to deflect the same and the exterior girders are predicted to deflect accordingly with the respective slab overhang dimension. A typical cross-section with girders, connector plates, cross frames, SIP forms, and the concrete deck is illustrated in Figure 1.1. Note that the tributary width used for prediction of an interior and exterior girder is dimensioned.

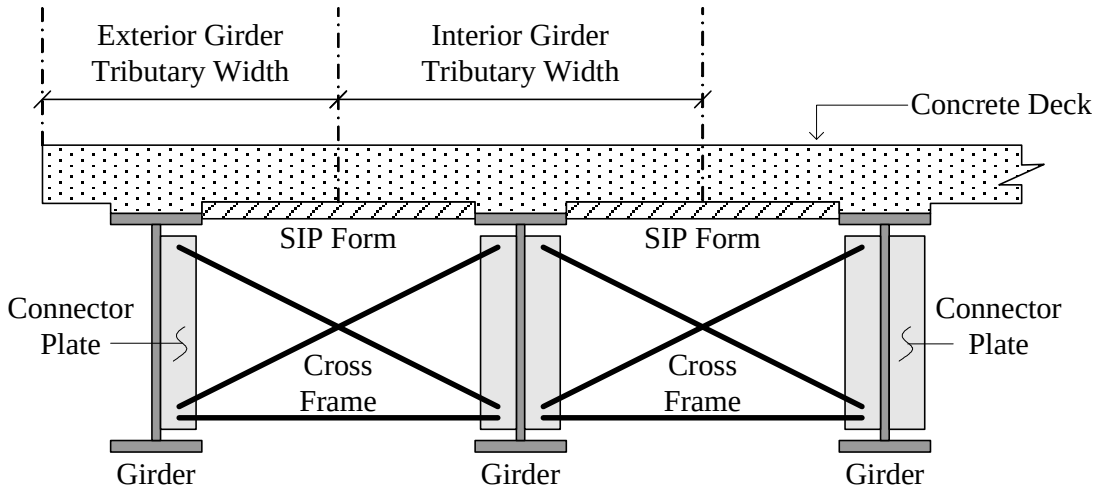

Figure 1.1: Traditional Single Girder Line Prediction Technique

Various construction issues may result from the use of traditional SGL analysis. When girders deflect less than expected, the deck slab and/or concrete covering the top layer of rebar may be too thin, resulting in rapid deck deterioration. When the girders deflect more than expected, dead loads are greater than accounted for in design.

Additionally, unexpected girder deflections may cause misaligned bridge decks during stage construction. During the first stage of construction, one half of the bridge superstructure is constructed while traffic is maintained on the existing structure. During the second stage, traffic is directed onto the first stage structure while the second half is being constructed. In the final stage, a closure strip is poured between the two stages. Figure 1.2 illustrates the differential deflection between construction phases as a result of inaccurate deflection predictions.

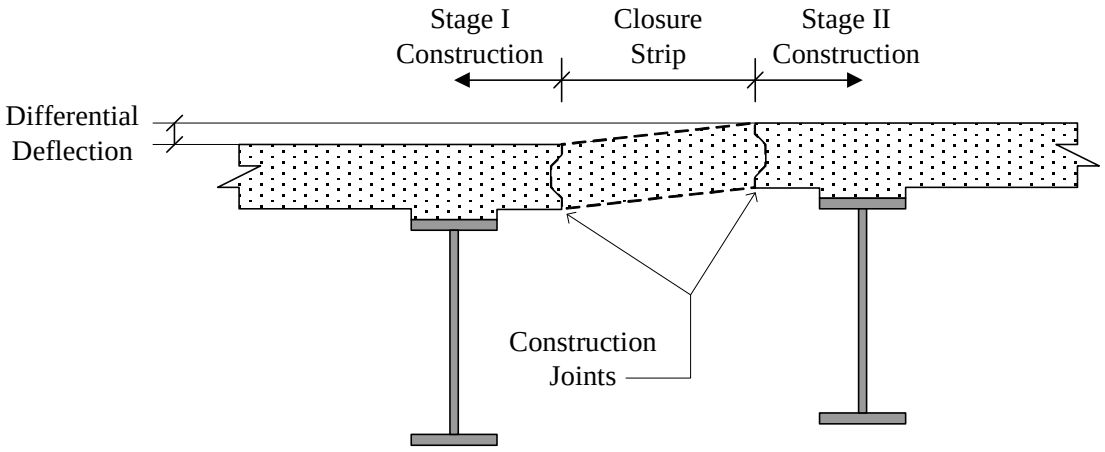

Figure 1.2: Misaligned Concrete Deck Elevations in Staged Construction

Misaligned bridge decks can cause numerous construction delays. For instance, the deck surface may require grinding to smooth the deck surface, which reduces the slab thickness and the cover concrete. The grinding maintenance could prove costly if the thinner deck causes a premature deterioration of the bridge deck.

1.1.3 Bridge Components

There are bridge components common to each of the bridges incorporated into this study. The bridges are comprised of steel plate girders, steel intermediate cross frames, steel end and interior bent diaphragms, reinforced concrete decks, and SIP metal deck forms. A discussion of each bridge component is included herein.

Steel plate girders consist of steel plates for each of the following: top flange, bottom flange, web, bearing stiffeners, intermediate web stiffeners, connector plates. Additionally, shear studs are welded to the top flange. Intermediate cross frames are steel members (typically structural tees or angles) utilized to laterally brace the plate girders along the span. The steel plate girders, intermediate cross frames and intermediate web stiffeners are displayed in Figure 1.3.

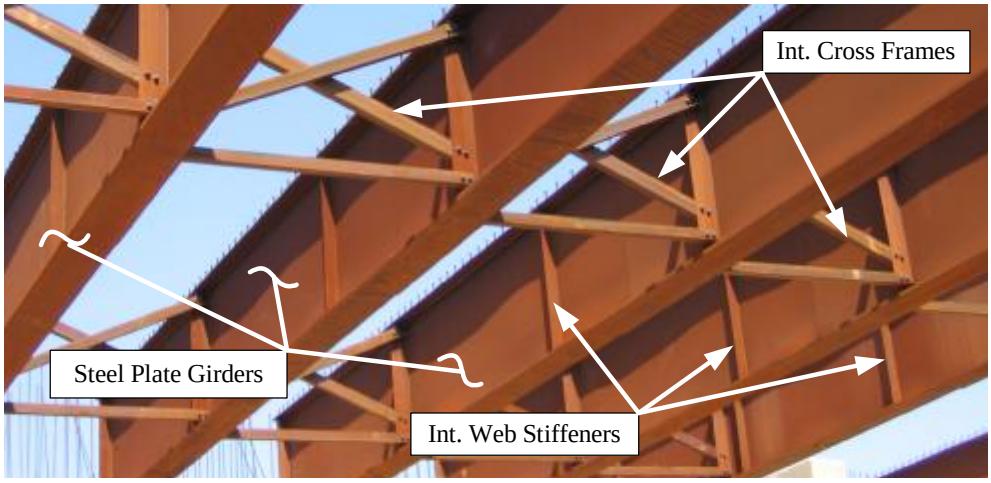

Figure 1.3: Steel Plate Girders, Intermediate Cross Frames and Intermediate Web Stiffeners

End and interior bent diaphragms consist of structural steel members utilized to laterally brace steel plate girders at supports. The diaphragm members are typically steel channels, structural tees and angles. An end bent diaphragm is presented in Figure 1.4. Note: interior bent diaphragms are commonly detailed identical to intermediate cross frames.

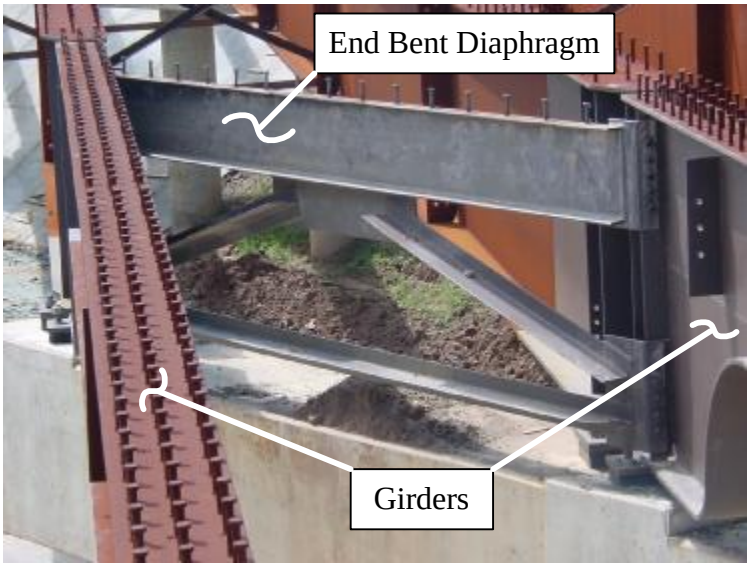

Figure 1.4: End Bent Diaphragm

SIP metal deck forms support wet concrete loads between adjacent girders during deck construction. The forms remain a bridge component throughout its lifespan, but are assumed to not provide vertical load support subsequent to the concrete curing. SIP forms are pictured in Figure 1.5 and Figure 1.6 illustrates a typical connection detail of the SIP forms to the top girder flange.

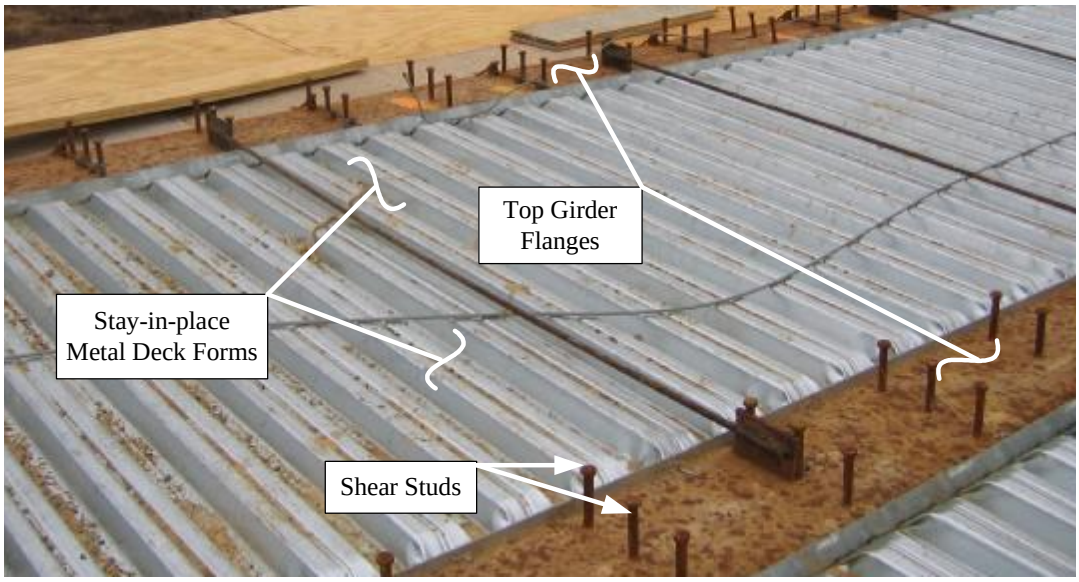

Figure 1.5: SIP Metal Deck Forms

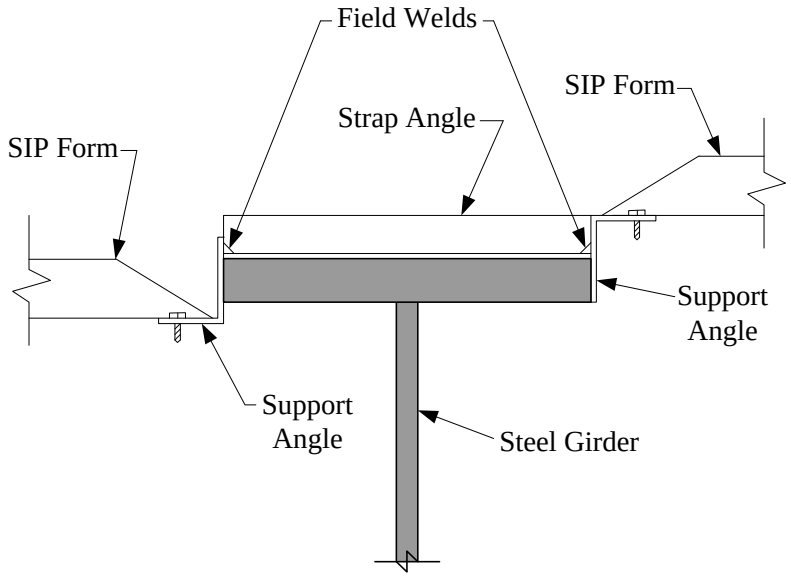

Figure 1.6: SIP Metal Deck Form Connection Detail

Girder bearing supports are located between the bottom girder flange and the supporting abutment at the ends of the girders. Pot bearings and elastomeric bearing pads were utilized by the bridges in this study. Pot bearings (see Figure 1.7) can allow girder end rotations, restrain all lateral movements, or allow lateral translation in one direction (along the length of the girder). Elastomeric bearing pads (see Figure 1.8) are capable of similar restrictions.

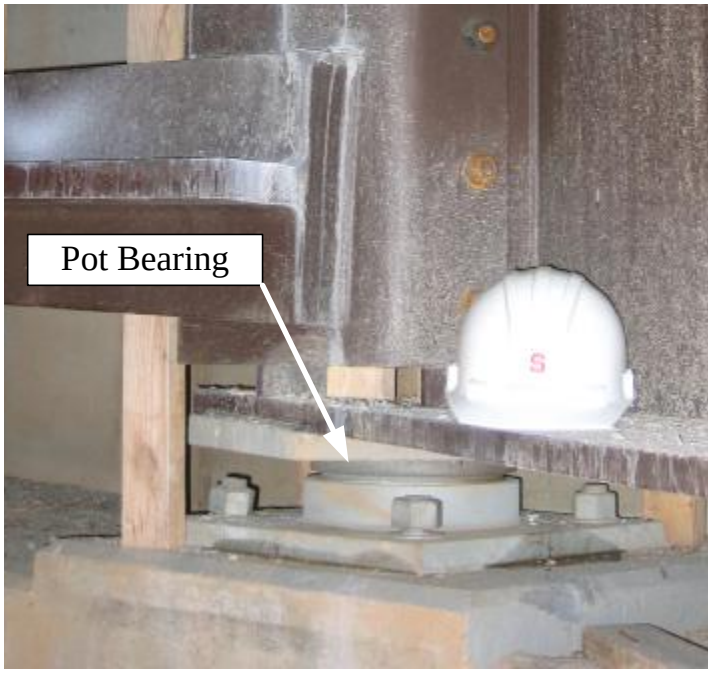

Figure 1.7: Pot Bearing Support

Figure 1.8: Elastomeric Bearing Pad Support

1.1.4 Equivalent Skew Offset

Skewed bridges are defined as bridges with support abutments constructed at angles other than 90 degrees (in plan view) from the longitudinal centerline of the girders.

Depending on the direction of stationing, a bridge may be defined with an angle less than, equal to, or greater than 90 degrees (see Figure 1.9).

An equivalent skew offset has been defined for this research so that bridges defined with skews less than 90 degrees may be compared directly to bridges defined with skews greater than 90 degrees. The equivalent skew offset, θ, is calculated by Equation 1.1 and the result defines the skew severity (i.e. the larger the number, the more severe the skew). Note that if the skew angle (via the bridge construction plans) was equal to 90, the equivalent skew offset would be equal to zero.

$$q = |\boldsymbol{skew} - \mathbf{90}| \qquad \text{(eq 1.1)}$$

where: ***skew*** = skew angle defined in bridge plans

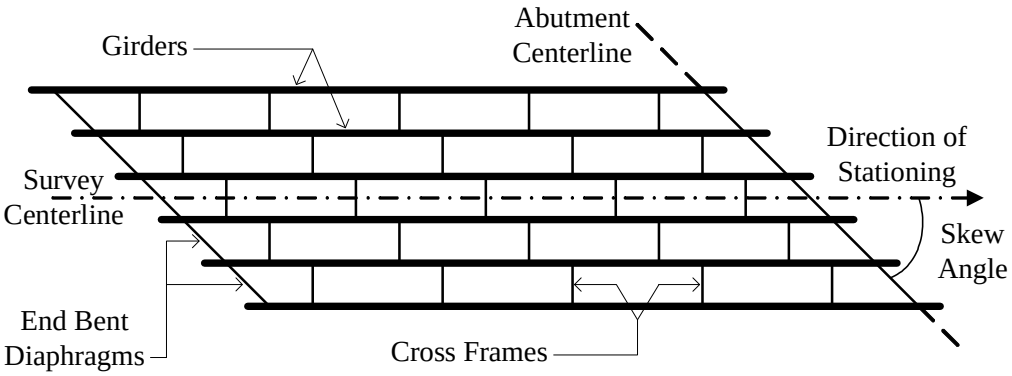

a) Skew Angle < 90 degrees

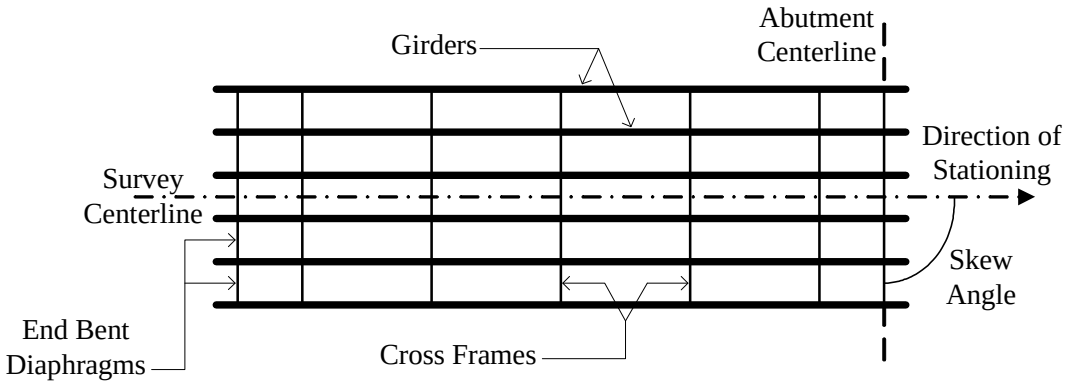

b) Skew Angle = 90 degrees

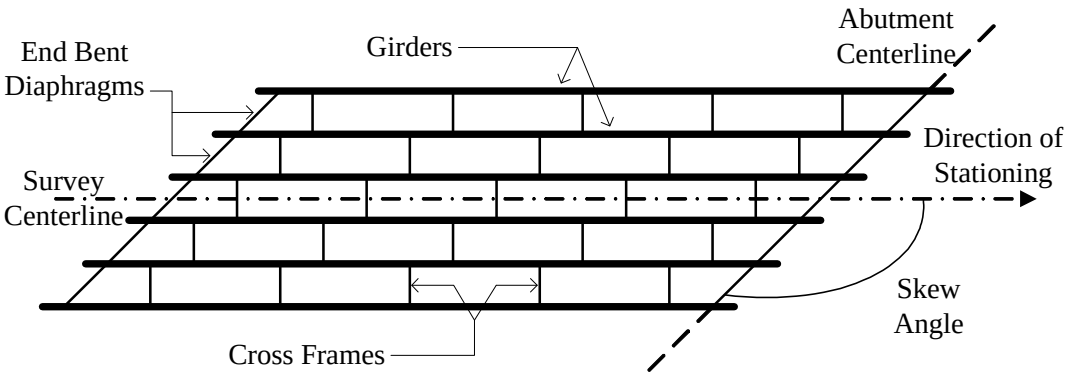

c) Skew Angle > 90 degrees

Figure 1.9: Skew Angle and Bridge Orientation (Plan View)

1.2 Objective and Scope

The primary objective of this research is to develop a simplified method to predict dead load deflections of skewed and non-skewed steel plate girder bridges by completing the following tasks:

- Measure girder deflections in the field during the concrete deck placement.
- Develop three-dimensional finite element models to simulate deflections measured in the field. The field measurements are used here to validate our modeling technique.
- Investigate alternate less sophisticated modeling techniques and a general analysis program such as SAP 2000
- Utilize the three-dimensional finite element models to conduct a parametric study for evaluating key parameters and their effect on non-composite deflection behavior.
- Develop the simplified procedure from the results of the parametric study.
- Verify the method by comparing all predicted deflection to those measured in the field.

1.3 Outline of Report

The following is a brief outline of the major topics covered in this report:

- Section 2 presents a literature review that summarizes previous research regarding the first research phase, bridge construction issues as related to bridge parameters, parametric studies and preprocessor programs for automated finite element generation.

- Section 3 presents descriptions of the bridges included in the study, the field measurement procedures implemented to monitor the bridges during construction, and a summary of the field measured deflections.
- Section 4 presents the detailed finite element modeling procedure, the development of the preprocessor program, and a summary of the simulated deflection results.
- Section 5 presents the details of an investigation into simplified modeling techniques using the general analysis program SAP2000.
- Section 6 presents the parametric study, its results, and the development of the simplified procedure for simple span bridges with equal exterior-to-interior girder load ratios, simple span bridges with unequal exterior-to-interior girder load ratios, and continuous span bridges with equal exterior-to-interior girder load ratios.
- Section 7 presents the comparisons of field measured deflections to SGL predictions, ANSYS modeling predictions, and predictions from the developed simplified procedure.
- Section 8 presents observations and conclusions drawn from the research and recommendations made for predicting dead load deflections of skewed and non-skewed steel plate girder bridges.
- Appendix A presents a flow chart outlining the simplified procedure.
- Appendix B presents sample calculations utilizing the simplified procedure to predict girder deflections.
- Appendices C-L present the following for the ten bridges monitored as a part of this research: a detailed description of the bridge components, elevation and plan

view illustrations, a summary of non-composite field measured deflections, a description of the finite element model, and a summary of the deflections predicted by the finite element models.

- Appendix M and N present sample calculations of the SIP metal deck properties that were used in the ANSYS and SAP2000 modeling respectively.

2.0 Literature Review

2.1 Overview

The following literature review outlines previous research related to construction issues of steel plate girder bridges such as differential girder deflections and problems during concrete deck construction. It will be shown that there is little research available on the behavior of steel plate girder bridges during deck construction and that there is an overall need for detailed research on this topic. Research on the influence of parameters such as bridge skew, cross-frame behavior, stay-in-place (SIP) metal deck forms, and rate of deck placement is also presented.

A large part of this research involves the finite element modeling of steel plate girder bridges with reinforced concrete decks. There have been several techniques developed for finite element bridge modeling. A review of previous and current techniques used in the finite element modeling of these bridges is included herein.

2.2 Construction Issues

Errors in predicting accurate dead load deflections of steel plate girder bridges during deck construction have been documented as far back as the early 1970's. Hilton (1972) measured deflections of single span steel plate girder bridges during deck construction. The study only included bridges with spans less than or equal to 100 feet and concrete decks that were screeded longitudinally (parallel to the span) during construction. Hilton indicated that conventional methods of calculating the construction dead load deflections of these bridges assume that each bridge girder deflects independently of the adjacent girders connected via cross-frames. He noted that the dead load deflections of girders fully loaded with wet concrete would be partially restrained by the cross-frames connected to girders not yet fully

loaded. He also noted that following the wet concrete too closely with the screeding machine can result in insufficient deck slab thicknesses and can contribute to the partial restraint of the girder deflections by the cross-frames. Hilton concluded the following: predicted dead load deflections calculated using the conventional methods tend to be larger than what is observed in the field, the entire bridge superstructure deflects as a unit because of the connections between the steel girders and the cross-frames, and that using the conventional methods to predict dead load deflections in conjunction with longitudinal screeding would be "risky" in bridges with high skew angles.

A limited amount of other research has been found that documents steel bridge behavior during deck construction. Some literature has been found that discuss problems encountered during staged bridge construction and the effects of bridge skew on differential girder deflections and out-of-plane girder rotations. Most of the related literature discusses erection techniques designed to limit the amount of unpredicted steel bridge girder behavior during construction and offers little input on how to account for these construction issues in the analysis and design of the bridges. The following sections provide an overview of this literature.

2.2.1 Differential Deflections/Girder Rotations

Swett (1998) and Swett et al. (2000) observed that if a bridge is not skewed and the deck is symmetric about the centerline of the bridge, then the dead load deflections are vertical. However, many bridges are skewed and/or the decks are not symmetric about the centerline which leads to a twisting displacement of the girders as well as vertical deflection. This combination of displacements can cause enough distortion to prevent adequate matching of the final deck elevations in staged construction.

AASHTO/NSBA (2002) stated that the point of maximum deflection for girders in a bridge with skewed abutments or piers will be at mid-span if the effects of bracing are ignored. This can result in significant differential deflection between girders since these points do not align across the width of the bridge. AASHTO/NSBA also noted that when the girders are connected with cross-frames, the girder webs will also rotate transversely from the weight of the concrete pour. These displacements have not significantly affected bridge performance in the past but are now becoming more of a problem because of the increased use of lighter, high strength steel girder sections.

AASHTO/NSBA (2002) also recommends that the bridge designer should evaluate the effects of differential deflections and girder rotations that may result for skewed, curved, or stage constructed bridges. It noted that consideration should be given to how the members are to be detailed, fabricated, and installed. Also, the installation details should include the orientation of the end and intermediate cross-frames relative to the girder line and the condition under which they should fit: no-load fit, steel dead-load, or full dead-load. AASHTO/NSBA states that installing girders vertically out of plumb can compensate for the rotation that may occur during the deck casting. It also recommends that only the horizontal members of the cross-frames be used between stages prior to the second stage deck pour. This would allow vertical deflection of the second structure while preventing lateral or twisting displacements.

Norton (2001) and Norton et al. (2003) monitored the behavior of a 74.45 meter single span, steel-composite plate girder bridge with a 55 degree skew during deck placement. They indicated that during construction, the girders were erected out of plumb in an effort to control the girder rotation due to construction dead loads and two screeding

machines (each spanning half of the bridge width) were staggered transverse to the bridge centerline so that the concrete could be poured as close to parallel with the skewed abutments as possible. They also indicated that when the concrete deck on a skewed bridge is poured perpendicular to the centerline of the bridge, the girders near the acute corner will deflect more than the girders near the obtuse corner and rotation of the bridge cross section will occur. After the deck placement it was observed that the girder webs were not vertical.

2.2.2 Staged Construction Problems

ACI (1992) stated that construction sequencing of the deck and closure pours is important in the prevention of large differential deflections between two stages of bridge construction. Differences in the stiffness of the two structures can influence the distribution of loads, which could negate assumed distribution factors used in the design. Resulting deflections may overload the stage 1 structure if they are connected prior to the pour. In cases where large dead load deflections are anticipated, the stages should remain separate until the stage 2 deck has sufficiently cured and connected before the closure strip is cast.

Swett (1998) and Swett et al. (2000) studied a straight steel girder bridge that deflected 90 mm less at mid-span than expected. They created a finite element model of the bridge to compare calculated deflections to actual measured deflections. The field measured deflections were based on survey data taken during different stages of construction. Concrete dead load estimates were calculated based on nominal dimensions from the construction drawings and a unit weight of concrete equal to 150 pcf. It was assumed that the unit weight of concrete would account for the weight of the rebar in the deck slab and that the concrete remained wet during the entire concrete deck placement (no composite action developed). These loads were applied to the finite element model and deflections from the model were

compared to the surveyed deflection data. Swett and Swett et al. determined that the model produced deflections within "acceptable accuracy" of the field measured deflections. Once the model was correlated to the field data, it was used to examine the stresses and deflections associated with six proposed construction methods involving staged construction. Three of these methods involve the connection of the two stages with the cross-frames prior to the stage 2 deck pour. They observed that these methods can be used to control the twisting action and lateral movement of the stage two girders. The other methods studied require that the two stages remain independent of each other while the second stage deck is cast. They stated that the structure could be torsionally stiffened by using either of the following: a balanced deck pour, a two phase stage 2 deck pour, or the addition of lateral members to the stage 2 girders. Swett and Swett et al. concluded that all of their proposed methods are suitable for reducing differential deflection in steel bridges provided that the appropriate one is chosen for each project. They performed their research in response to construction problems that had been experienced by the Washington State Department of Transportation (WSDOT) during the staged construction of steel bridges. They conducted a nationwide survey and found that numerous state highway agencies had also experienced similar difficulties.

Swett (1998) and Swett et al. (2000) also noted that in most cases of staged construction, the girders of each stage are connected with cross frames to allow them to act as a single unit during deck placement. They indicated that the cross-frames between two stages are usually not connected until the stage 2 deck has been cast. If stage 1 and 2 are connected during the stage 2 deck pour then unwanted stresses are introduced to the cross-frames and stage 1 girders, if they are separate then unacceptable displacements are incurred.

2.3 Parameters

Several bridge parameters such as skew angle, cross-frames and end bent diaphragms, and SIP metal deck forms are being investigated in this study to determine if they have a significant affect on the deflection of steel bridges during deck placement. An overview of existing literature pertaining to these parameters is presented in the following sections.

2.3.1 Skew Angle

Gupta and Kumar (1983) studied the effect of skew angle on the behavior of slab on girder bridges. They defined skew angle as the angle between the centerline of a bridge and the perpendicular to the face of abutments. They concluded that careful analysis is required of bridges with greater than 30 degrees of skew.

Bakht (1988) stated that it is considered safe to analyze skewed bridges as right bridges (zero skew) when the skew angle is less than 20 degrees (similar to skew definition defined above by Gupta and Kumar) and the spans are equal. He also stated that other factors besides skew angle must be considered when analyzing bridges with larger skew angles as right bridges. Bakht demonstrated that an increase in skew angle can affect the composite load distribution to the girders through the change in relative load position and the change of flexural rigidity of adjacent girders.

A study by Bishara (1993) involving cross-frame analysis and design supported conclusions reached by Bishara and Elmir (1990). They stated that differential deflections between adjacent girders are the major cause for internal cross-frame forces. The greatest amount of differential deflection occurred between exterior and adjacent girders near the obtuse corner of skewed bridges. Another conclusion was that skew is not a contributing factor when the skew angle is less than 20 degrees (similar to skew definition defined above

by Gupta and Kumar). However, when the skew angle is greater than 20 degrees, the internal cross-frame forces increase with an increase in skew angle. They also determined that the analysis for dead load deflections of girders should comply with actual construction procedure. For example, analyze each girder as a non-composite section subjected to self weight loading and the loading provided by the connected cross-frames and then analyze all of the interconnected girders as a space structure with the weight of the deck slab applied as line loads to the individual girders.

2.3.2 Cross-frames/Diaphragms

Bishara (1993) stated that cross-frames provide lateral load resistance, live load distribution, and reduce the buckling length of the compression flanges of steel girders. He also referenced Chen et al. (1986) when he stated that cross-frames have a significant effect on the load distribution not accounted for in design. Bishara (1993) developed a procedure that can be used to evaluate internal forces in the cross-frames of single span, steel girder bridges. To develop the procedure, he validated and employed a three-dimensional finite element modeling scheme in a study of 36 bridges of different geometric configuration. Parameters included in the study were skew angle, span length, deck width, and cross-frame spacing. Bishara concluded that his procedure was successful in computing internal cross-frames forces.

Helwig and Wang (2003) related cross-frames to truss systems that resist axial forces and diaphragms to beam systems that develop bending moments that brace the girders against buckling. They discuss the importance of cross-frames and diaphragms before and after deck construction. They determined that prior to and during deck construction is the critical stage in preventing buckling of the girders. The cross-frames and diaphragms prevent

the twist of the girder cross-section while they support their own weight and all construction loads. After construction these braces support the bottom of the girders against wind load and provide stability in negative moment regions. Helwig and Wang indicated that many cross-frames and diaphragms are standardized in size and not designed specifically for each application. This leads to oversized bracing that attracts large live load forces which typically results in fatigue problems in the areas where the braces and girders connect. This behavior is more critical in skewed bridges where girder and cross-frame interaction is increased because of skew. They referred to research by Keating and Alan (1992) that confirmed this problem.

2.3.3 Stay-in-place Metal Deck Forms

Currah (1993) and Soderberg (1994) investigated the bracing ability of SIP metal deck forms acting as shear diaphragms. Currah (1993) indicated that the shear stiffness of SIP deck forms is dependent upon material strength, modulus of elasticity, deck thickness, deck profile, pitch of deck corrugations, deck panel span, presence of end closures, number of end fasteners, number of seam fasteners, and flexibility of the SIP supporting members. The primary objective of his study was to determine the shear stiffness of SIP deck panels without any affects from the supports used to attach the forms to the girders. Currah also investigated the potentially mitigating affect of the SIP supporting members on the shear strength of the diaphragm system. The SIP forms used in his study were supported by thin angles that are either welded to the top flanges of the girders or the use of connecting strap angles that saddle the top flanges. Currah noted that both connection details can introduce an eccentricity in the transfer of the lateral loads from the SIP forms to the top girder flanges. He concluded that the flexibility of the supporting angles should be carefully considered if

the SIP decking is to be considered as a lateral bracing element. Some of the diaphragm system stiffnesses were reduced by more than 80 percent when using the typical eccentric support angle instead of a rigid connection. Currah (1993) also used the Diaphragm Design Manual (SDI, 1991) to evaluate the shear strength and shear stiffness of bridge SIP deck forms and compare them to experimental values. The Steel Deck Institute (SDI) method was modified to account for the differences found in bridge applications of SIP forms. Soderberg (1994) continued the work of Currah by further investigating the connection stiffness of SIP metal deck forms and also determined ways to improve the connection.

Helwig (1994) studied the lateral bracing ability of SIP metal deck forms commonly used in steel bridge construction. He stated that prior to deck placement the steel must support all construction loads until composite behavior is developed. Therefore, lateral-torsional buckling of the steel plate girders is critical during the non-composite stage of construction. Helwig stated that SIP metal deck forms provide continuous bracing against lateral movement along the girder thus behaving as a shear diaphragm. He used finite element analysis on twin girder systems with a shear diaphragm at the top flange. These analyses were used to determine the effect of the deck shear rigidity on buckling capacity of a twin girder system. The finite element results were compared to existing solutions for beams braced by shear diaphragms. These solutions were used to develop a design approach for single span and continuous girders braced by the SIP forms. It was found that this design approach reduces the number of cross-frames required to laterally brace the girders.

Jetann et al. (2002) continued to study the lateral bracing ability of stay-in-place metal forms in steel plate girder bridges and focused on improving the connection detail between the top girder flanges and the SIP forms. The goal of the research was to develop a

connection that would allow more of the shear strength of the forms to be developed thus enabling the form system to behave as a reliable bracing element for the girders. They conducted laboratory tests that were designed to evaluate the strength the metal deck forms system that includes the strength of the connection of the forms to the girders. Their tests included a system that utilized the typical connection used bridge construction. Jetann et al. presented their results and concluded that simple modifications to the connection can greatly improve the shear strength and stiffness of the SIP metal deck form system.

2.4 Bridge Modeling

Numerous studies have been conducted using finite element models of highway bridges. Three-dimensional modeling programs have allowed researchers to accurately analyze and predict the behavior of bridges with different geometric configurations. A summary of widely used finite element modeling techniques and other related research is presented below.

2.4.1 Finite Element Modeling Techniques

Schilling (1982) developed lateral distribution factors for fatigue using finite element analysis with the program ANSYS. He stated that the deck slab is the main element that distributes loads in both composite and non-composite steel bridges. He also stated that the diaphragms and cross-frames contribute little to load distribution due to their small relative stiffness and infrequent spacing and that full depth cross-frames have a greater effect. He neglected the cross-frame contribution in his models which used triangular isoparametric plate elements for the slab and beam elements for the girders. Schilling achieved good agreement between the factors he developed and ones calculated from the field measurements of actual bridges.

Bishara and Elmir (1990) used the finite element program ADINA to create models of single span steel plate girder bridges to investigate the interaction between cross-frames and girders. The concrete deck was modeled using triangular plate elements and the girders were divided into two top and bottom halves with each half discretized as beam elements. The top girder half was rigidly connected to the deck slab using constraint equations and was also connected to the bottom girder half using steel link elements. The cross-frames were represented with beam elements and the web stiffeners were neglected in the models. Finite element models were created for bridges with varying skew angles and one for a bridge with no skew and the sizes of the cross-frame members were varied. The models were first used to investigate the affects of dead load by analyzing each girder individually as a non-composite section subjected to self weight loading and the loading provided by the connected cross-frames. The entire system of the interconnected girders was then analyzed as a space frame with the weight of the deck slab applied as line loads to the individual girders. The effects of applying live loads to the models were also investigated. Some of the key conclusions obtained from the study are as follows: in the non-skewed bridge models under total dead, tensile forces were developed in all of the chord members of the intermediate cross-frames and only compressive forces were developed in the diagonals; in the skewed bridge models, the cross-frame members developed tensile or compressive forces with the maximum compressive forces occurring near the ends of the exterior girders closest to the obtuse angle of the bridge and the maximum tensile forces occurred in the chord members near mid-span; vertical deflections were insensitive to the size of the cross-frame members used; differential deflections reached up to 1 inch from the application of dead load only. It was noted that using beam elements to represent the cross-frames produced shear, bending,

and axial forces at the connection points to the girders. However, it was shown that the axial force was the dominant force and the other internal forces were insignificant when compare to the axial force.

Bishara et al. (1993) derived wheel-load distribution factors from the finite element analyses of 36 medium-length, single span, skewed, steel composite bridges. They used the finite element program ADINA to create the bridge models. The girder webs were modeled with shell elements, the transverse web stiffeners with truss elements, and the flanges with isobeam elements. The concrete slab, modeled with thin triangular plate elements, was connected to the top girder flanges with rigid elements. Cross-frames were represented by beam elements. This discretization scheme was validated by comparing theoretical results with field measured stress data gathered from a 137 ft single span, skewed plate girder bridge loaded with six dump trucks of known weight. The finite element model provided stresses approximately 8 percent higher than what was measured.

Helwig (1994) studied the effect of SIP deck forms on buckling capacity of straight girders using the finite element program ANSYS. He determined that the forms would provide minimal rotational restraint to the girders because of the relatively thin sheet metal used in the forms and the flexible connection used to attach the forms to the girders. Typical connections of the forms to the girders are with self tapping screws to angles attached to the top flange of the girder. Therefore the model developed would only provide shear stiffness. Helwig used four-node shell elements to represent the forms. Coupling the translational degrees of freedom of the corner nodes of the form elements to the centerline nodes of the top flanges would allow only shearing deformation. To avoid local buckling problems that occurred in preliminary models, the forms were given a unit thickness and the modulus of

elasticity was varied to achieve the desired shear rigidity. The linear relationship between plate buckling and elastic modulus would allow easier adjustment to the rigidity because plate buckling is a function of the cube of the plate thickness. In addition to varying the elastic modulus, local buckling was controlled by modeling the corrugations in the metal forms with beam elements which would stiffen the forms out-of-plane. Helwig (1994) used existing closed form solutions by Winter (1958) and Plaut (1993) for "fully braced" beams to check the accuracy of his models. Helwig's results matched those of Plaut and found that Winter's method underestimates displacements.

Ebeido and Kennedy (1995, 1996) studied the influence of bridge skew, among other factors, on moment and shear distribution factors for single span, skewed steel composite bridges. A finite element model was created using ABAQUS. The concrete deck slab was modeled using shell elements and the girders and diaphragms were modeled using 3-D beam elements. The multipoint constraint option was employed to produce a shear connection between the slab and girders. Ebeido and Kennedy made comparisons between the theoretical finite element models and six experimental bridge models. The results of simulated truck load tests showed good agreement between the experimental and theoretical models. They then used the finite element modeling scheme in an extensive parametric study of prototype composite bridges. The results of which were used to derive expressions for shear and moment distribution factors.

Tabsh and Sahajwani (1997) used ANSYS to create three dimensional finite element models of slab-on-girder bridges with irregular geometry. They used the models to verify their approximate method of analyzing these types of bridges. The modeling approach was based on the research of Bishara et al. (1993). The girder flanges and diaphragms were

modeled with 3-D beam elements and the girder webs and deck slabs were modeled with rectangular shell elements. To simulate composite behavior, the centroids of the deck slabs and top girder flanges were connected with rigid 3-D links. This model had been verified in the work of Sahajwani (1995). Tabsh and Sahajwani concluded that their models were in agreement with their approximate analysis method.

Tarhini et al. (1995) and Mabsout et al. (1997a) evaluated wheel load distribution factors of steel girder bridges with four finite element modeling techniques. The first three techniques were modeled using SAP90 and the final with ICES-STRUDL II. The first method, based on the research of Hays et al. (1986), involves representing the concrete slab as quadrilateral shell elements and the modeling steel girders with space frame elements. The centroids of the slab and girders were coincided to represent their connection. The second method, which was based on the research of Imbsen and Nutt (1978), is similar to the first but instead used rigid links to connect the slab and girders eccentrically. The research of Brockenbrough (1986) was the basis for the third method, which idealized the slab and girder webs as shell elements and the girder flanges as space frame elements. The slab and girder flanges were connected with rigid links. The final method, based on research from Tarhini and Frederick (1992), uses an isotropic eight node brick element to represent the concrete slab and quadrilateral shell elements to represent the girder flanges and webs. Mabsout et al. (1997a, 1997b) compared the load factors obtained from the models to factors calculated from both AASHTO (1996) and an equation developed by Nutt et al. (1987). They achieved good correlation between the Nutt et al. values and the first and fourth of the above methods. All of the modeling methods produced distribution factors below the AASHTO (1996) factors.

Mabsout et al. (1998) continued the research by performing a parametric study of the effect of continuity on the wheel load distribution factors for continuous steel girder bridges using the first and fourth finite element modeling techniques mentioned above. All elements used in the two methods were considered to be linearly elastic. Their research supports the use of the NCHRP 12-26 formulas, along with a correction factor, for continuous bridges and concluded that AASHTO (1996) load factors are overly conservative.

Swett (1998) modeled the Gulch Bridge in Washington using SAP2000. Two-dimensional and 3-dimensional models were both created to compare theoretical deflections and rotations with actual measured data. He concluded that the 3-D model should be used to further analyze six proposed construction techniques since it represented the realistic behavior of the bridge better than the 2-D model. The 3-D model consisted of frame elements for the girder flanges, diaphragms, and lateral members and shell elements for the girder webs. The diaphragms and the lateral members were connected to the girders by nodes placed at the intersection of the web and flanges. After a sensitivity study was conducted for mesh refinement, the model was calibrated against field deflection data collected by the WSDOT. Swett then concluded that the model produced acceptable results and was considered to be dependable for analyzing the different construction techniques.

Berglund and Schultz (2001) studied the effects of differential deflections between adjacent girders on local web distortion of composite bridges. Finite element modeling was used to predict the differential deflections of adjacent girders that cause this distortion. SAP2000 Nonlinear was used to create the models. To ensure a more accurate full scale modeling technique, they first conducted mesh convergence studies on finite element models of simple, two-girder, skewed bridges. Their modeling technique involved using shell

elements for the girder webs and deck and frame elements for the girder flanges, and diaphragms. Rigid elements were used to create the composite action between the deck slab and the top of the girders. The diaphragms were connected to the girders at one point located in the center of the web to simulate pinned behavior. The model was further refined by providing field measured dimensions that were not provided in bridge plans. They concluded that the model produced reasonable vertical deflection predictions.

Norton et al. (2003) developed a two-dimensional and three-dimensional computer model of a skewed, steel-composite plate girder bridge. It was concluded that the 2-D model yielded less accurate results than the 3-D finite element model. They used SAP2000 to create the 3-D bridge model. Frame elements were chosen to model the girder flanges, stiffeners, and cross-frames and shell elements were used for the girder webs and wet concrete deck. The connection between the deck and the girders was represented by rigid links and a modulus of elasticity of 10 ksi was assumed for the wet concrete deck. Nodes were placed at the top of the web, neutral axis, and the bottom of the web for the girder cross section and the cross-frames connections were assumed to be rigid. The initial rotation of the girders used in the field was also incorporated into the model. Four different load stages were used to recreate the loading sequence used in the deck pour. The SAP2000 model predicted vertical deflections that were 0.3-10.0 percent higher than deflections measured in the field.

Fu and Lu (2003) discussed the importance of using nonlinear finite element analysis when analyzing and modeling steel-girder composite bridges. They made comparisons between the field measured deflections of a two span continuous bridge reported by Yam and Chapman (1972) and theoretical deflections obtained from both a nonlinear finite element

analysis and an analysis using the traditionally used transformed section method. Fu and Lu noted that the concrete deck, under working loads, is a nonlinear material and the transformed section method assumes the concrete deck is linearly elastic. They used plate elements to model the steel girder flanges and plane stress elements for the webs. The shear studs were modeled with bar elements that provide a dimensionless link between the deck and girders. Fu and Lu concluded that their nonlinear finite element method yielded results close to the experimental results while the transformed section method did not.

Egilmez et al. (2003) continued the work of Helwig (1994) and improved the finite element modeling technique used to represent the SIP metal deck forms. The improved modeling technique was based on the method developed by Helwig and Yura (2003). This method involved creating a shear diaphragm truss panel consisting of two-node truss elements spanning between two girders. The truss panel was connected to the top girder flange by coupling the translational degrees of freedom between the nodes along the centerline of the top flange and the ends of the truss panel. The models were calibrated by adjusting the areas of the truss members in the panels to match laboratory test results of a real two girder system subjected to lateral displacement and buckling tests. The twin girder system used only 8 foot panels at each end of the girders near the support. This was done in an effort to capture the true shear stiffness of the system because these are the regions where the largest top flange lateral shear deformation occurs during buckling. Full SIP form decking between the two girders was also tested in the lab. However, the finite element model representing the fully decked case was considerably less stiff than the actual system. A three dimensional beam element was then added to the finite element model by rigidly linking the beam element to the top flange of one girder in the lateral direction. This was

done to more accurately represent the in-plane flexural behavior (plane of the SIP forms) of the SIP forms. This model was then calibrated to match the laboratory results by adjusting the moment of inertia of the beam element.

Helwig and Wang (2003) studied the behavior of cross-frames and diaphragms in skewed steel girder bridges. ANSYS was used to model steel plate girders, transverse stiffeners, cross-frames, and diaphragms. Eight node shell elements were used to represent the girder flanges, web, transverse stiffeners, and in some cases the I-shaped diaphragms. The aspect ratio of the web elements were held close to one and each flange was divided into two elements across their width. The cross-frames were modeled using 3-D truss elements that connected to the top and bottom of the girder web. The transverse stiffeners were connected to the top and bottom of the girder web but not to the flanges. This was done to prevent additional warping restraint from the stiffeners.

Helwig and Wang (2003) referred to previous research by Shi (1997) that provided a basis for their research. Shi used finite element models to determine the bracing requirements of skewed steel girder bridges. The compression flanges in these models were actually made discontinuous at the bracing points to prevent end warping restraint to the girders. This was done to correlate the model with results from previously developed expressions for the buckling capacity for singly and doubly symmetric beams. These expressions assume that the beam is free to warp at the ends of the unbraced length.

In some cases Helwig and Wang (2003) used small I-shaped members to connect the top flanges of adjacent girders. To avoid warping restraint from these flange braces, nodes at the flange tips and the corresponding brace nodes were coupled in the vertical direction while the middle flange node was coupled laterally with the corresponding bracing node. The

models by Helwig and Wang (2003) and Shi (1997) were compared to previously developed equations that predict the buckling capacity of beams. They achieved good agreement between the models and the expressions. The models were then used to modify other expressions that predict bracing requirements in bridges with supports normal to the girder center line. These expressions were modified to account for skewed supports and brace orientation.

2.4.2 Related Research

Consideration of time dependent material properties may prove to be necessary in modeling bridges in different stages of construction, i.e. during the concrete deck pour.

Melhem et al. (1996) used actual beam specimens and concrete cylinders to develop a computer program that determines how the modulus of elasticity of fresh concrete changes with time. They developed the following expression from the test data and concluded it to be valid only up to the age of 10 hours.

$$E_c(t) = 1.325 \times 10^6 (1 - e^{-0.37t})^{10} \qquad (2.1)$$

Where: E_c = Elastic Modulus of Concrete, psi

t = Time, hours

A polynomial was then used to extrapolate values of the modulus between 10 hours and the 28 day value given by the ACI code, which is a function of the compressive strength of concrete. Melhem et al. stated that the development of the modulus of elasticity of concrete is affected by its degree of confinement and should be multiplied by a factor K. A confinement factor of K=0.8-0.9 was determined to be realistic based on the test beams;

however the actual value of *K* for a bridge is unknown. The findings from this research were deemed meaningful, however comparisons with actual field data were recommended.

Paracha (1997) continued the research of the computer program created by Melhem et al. (1996). She concluded that the program would be useful in calculating dead load deflections during deck placement and help determine a proper deck pouring sequence.

2.5 Parametric Studies

A large portion of this project has been dedicated to a parametric study, completed to determine which bridge parameters affect non-composite deflection behavior in steel plate girder bridges. A few related sources have been reviewed.

Bishara (1993) conducted a parametric study to evaluate internal cross frame forces in simple span, steel girder bridges. He investigated 36 finite element models of various configurations by varying skew angle, span length, deck width and cross frame spacing. As a result, Bishara (1993) developed a procedure to analyze internal cross frame forces with acceptable accuracy.

Bishara and Elmir (1990) investigated the interaction between cross frames and girders by generating multiple finite element models and varying skew angles and cross frame member sizes. He concluded: in skewed bridge models, the maximum compression force developed in a cross frame occurs at the exterior girder near the obtuse angle, and vertical deflections were insensitive to the size of the cross frame members.

Ebeido and Kennedy (1996) studied the influence of bridge skew on moment and shear distribution factors for simple span, skewed steel composite bridges. A finite element scheme was then implemented to derive expressions for the distribution factors.

Martin et al. (2000) conducted a parametric study to investigate the relative effects of various design parameters on the dynamic response of bridges. In the study, bridge characteristics (stiffness and mass) and loading parameters (magnitude, frequency, and vehicle speed) were varied. Martin et al. (2000) concluded that the most important factors affecting dynamic response are the basic flexibility (mass and stiffness) of the structure.

Buckler et al. (2000) investigated the effect of girder spacing on bridge deck response by varying the girder spacing and span length in finite element bridge models. It was concluded that increasing girder spacing can significantly increase both tensile and compressive stresses in the deck.

2.6 Preprocessor Programs

Manually generating or revising finite element bridge models can be a very time consuming task. It is beneficial to incorporate a preprocessor program to automate the model generation, especially when several models must be analyzed (as in a parametric study). The subsequent review includes sources related to this issue.

Austin et al. (1993) presents preprocessor software for generating three-dimensional finite element meshes, applying truck loadings, and specifying boundary conditions for straight, non-skewed highway bridges. The software, "XBUILD," is written in the C programming language and creates input files in a format acceptable to the finite element analysis program ANSYS.

Barefoot et al. (1997) discusses a preprocessor program developed to model bridges with steel I-section girders and concrete deck slabs. The program is an ASCII batch file written in the ANSYS Parametric Design Language (ADPL) and allows efficient generation, and modification, of detailed finite element models in ANSYS.

Padur et al. (2002) describes a preprocessor program, "UCII Bridge Modeler," that has been developed to automate the generation of steel stringer bridges in SAP90 or SAP2000. The program is written in Microsoft Visual Basic and is designed to accept user-defined input through a graphical user interface and to output a file formatted as input to SAP90.

2.7 Need for Research

There is a limited amount of literature available that documents in detail construction issues of steel plate girder bridges such as differential deflections between adjacent girders, out-of-plane girder rotations, and problems that occur during staged bridge construction. Some sources were found that focus on preventing these problems during construction using several different erection techniques but few actually deal with accurately predicting such problematic behavior. There is an obvious need for research that will help further the understanding of the true behavior of steel bridges during construction.

Research has shown that several parameters of steel plate girder bridges affect the way the bridges behave during and after construction. Influence of skew angle, function of cross-frames and diaphragms, and influence of SIP metal deck forms, has been identified as parameters that are of interest to this research because of their potential affects on bridge behavior. As part of this research, skew angle, cross frame stiffness, girder spacing, span length, number of girders and girder overhang will be investigated to establish relationships between them and non-composite dead load deflection behavior in steel plate girder bridges.

There is a substantial amount of research available that involves the finite element modeling of steel bridges. Several methods have been reviewed and considered to develop a technique that would be suitable for this research. The methods that were developed and

implemented by Helwig (1994), Egilmez et al. (2003), and Helwig and Wang (2003) have been identified as the basis for the finite element modeling used in this research.

3.0 Field Measurement Procedure and Results

3.1 Introduction

As part of this research to study girder deflection behavior, ten steel plate girder bridges were monitored during the concrete deck construction phase. The bridges include: seven simple span bridges, two two-span continuous bridges, and one three-span continuous bridge. This section discusses the measured bridges, the field measurement procedure, and the measurement results.

3.2 Bridge Selection

The bridges selected for this project met certain criteria. The first obvious requirement was that the bridges were under construction during the field data collection phase of the project. Also, a range of geometric properties was desirable in order to observe different deflection behaviors during construction. Table 3.1 summarizes the targeted range of the geometric bridge properties considered in the bridge selection process.

Table 3.1: Targeted Range of Geometric Properties

Bridge Property	Range
Span Type	Simple, 2-Span Cont., 3-Span Cont.
Equivalent Skew Offset	0 - 75 degrees
Number of Girders	4 - 12
Span Length	50 - 250 feet
Girder Spacing	6 - 12 feet

3.3 Bridges Studied

3.3.1 General Characteristics

There are characteristics common to all ten bridges measured for this research project. They are as follows:

- The steel plate girders are straight and connected by intermediate cross frames.
- Stay-in-place (SIP) metal deck forms were used to support fresh concrete during the deck placement.
- The concrete was cast parallel to the support abutment centerline (see Figure 3.1).

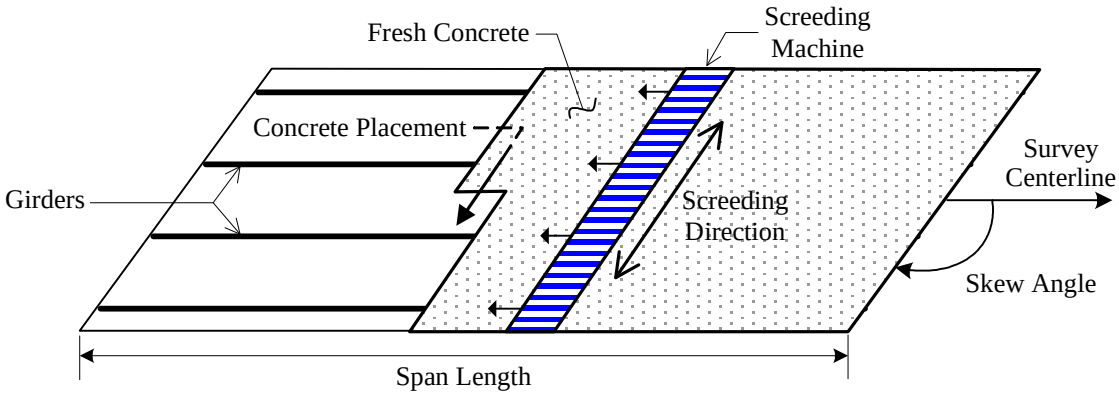

Figure 3.1: Typical Concrete Placement on Skewed Bridge

Some of the bridges utilized elastomeric bearing pads at the girder support locations. The settlements at these bearings were monitored and subtracted from the measured deflections within the span for direct correlation to the finite element analysis, which restrains vertical translation due to the modeled boundary conditions. In some cases, pot bearing supports were not monitored as deflections at this type of support are minimal.

Atypical to simple span bridges, sequence concrete pours are utilized for deck construction on most continuous span bridges (including all three in this study), in which the deck placement is completed in two or more separate pours. Specific characteristics of the five bridges, including pour sequence details, are included in Appendices.

3.3.2 Specific Bridges

A complete list of the ten bridges included in the combined study is presented in Table 3.2, which includes the key parameters of each. The first seven bridges are simple span, listed by increasing equivalent skew offset, whereas the last three are continuous span, listed accordingly. Descriptions of the ten bridges measured in part of this report are included herein.

Table 3.2: Summary of Bridges Measured

	Span Type	Number of Girders	Span Length (ft)	Girder Spacing (ft)	Nominal Skew Angle (deg)	Equivalent Skew Offset (deg)
Eno	Simple	5	236	9.6	90	0
Bridge 8	Simple	6	153	11.3	60	30
Avondale	Simple	7	144	11.2	53	37
US-29	Simple	7	124	7.8	46	44
Camden NB	Simple	6	144	8.7	150	60
Camden SB	Simple	7	144	8.7	150	60
Wilmington St	Simple	5	150	8.3	152	62
Bridge 14	2-Span Cont.	5	102, 106	10.0	66	24
Bridge 10	2-Span Cont.	4	156, 145	9.5	147	57
Bridge 1	3-Span Cont.	7	164, 234, 188	9.7	58	32

3.3.2.1 Eno River Bridge (NC 157 over Eno River, Project # U-2102)

The Eno River bridge is a single span, stage-constructed bridge located in Durham, North Carolina. The girders consist of HPS70W steel which is a high performance weathering steel with a yield stress of 70 ksi. The deflection measurements were recorded at the quarter points along the span during placement of the concrete bridge deck for all five girders of the second stage of construction. The duration of the placement of the concrete deck lasted approximately 10 hours. Figure 3.2 contains a picture of the Eno River bridge.

Figure 3.2- Eno River Bridge in Durham, North Carolina

3.3.2.1 Bridge 8 (US 64 Bypass Eastbound over Smithfield Rd, Project # R-2547C)

Bridge 8 (see Figure 3.3) is located in Knightdale, North Carolina and is one of the two simple span structures included in this report. The site included two completely separate (but close to symmetric) bridges, one eastbound over Smithfield Rd and the other westbound. Only the eastbound structure was monitored and included in this study. Deflections were measured on this six girder bridge at three positions along the girder span, including the one-quarter point and three-quarter point locations. The third location was about 16.5 feet offset from the accurate mid-point location, due to traffic limitations on Smithfield Rd. The single deck placement lasted approximately 5 hours. Bridge 8 is illustrated in Figure 3.4.

Figure 3.3: Bridge 8 in Knightdale, North Carolina

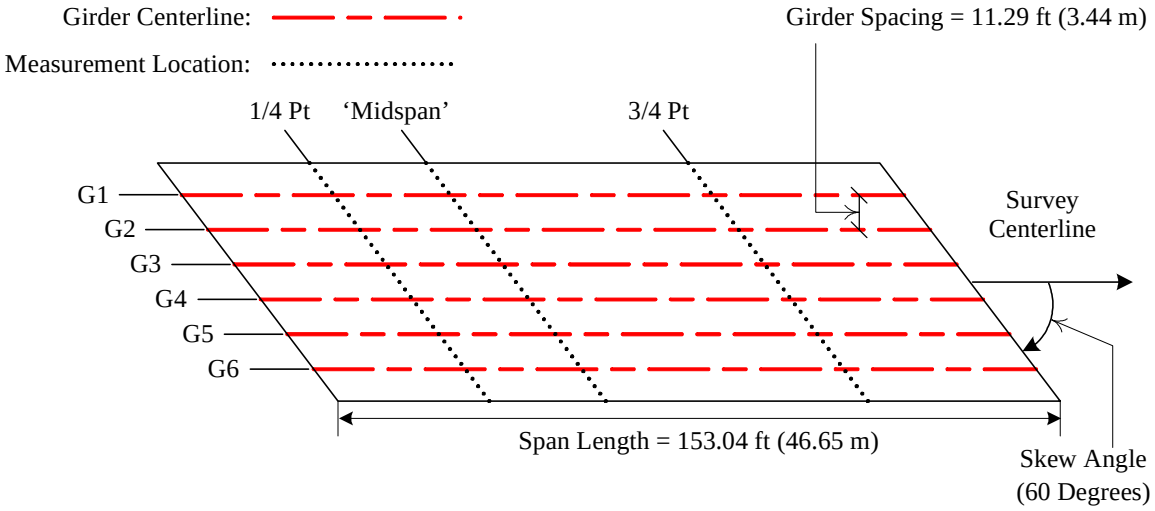

Figure 3.4: Plan View Illustration of Bridge 8 (Not to Scale)

3.3.2.2 Avondale Bridge (I-85 Southbound over Avondale Drive, Project # I-306DB)

The Avondale bridge is a single span bridge with seven steel plate girders located on the southbound lanes (SBL) of I-85 in Durham, North Carolina. The girders were fabricated from American Association of State Highway and Transportation Officials (AASHTO) M270 steel which is a weathering steel with a yield stress of 50 ksi. The bridge was erected in a single stage with a concrete deck that is curved in plan view resulting in unsymmetrical overhangs. The deflections were measured and recorded during the concrete deck placement

at the quarter points along the span. The duration of the deck placement was approximately 6 hours. Figure 3.5 contains a picture of the Avondale bridge.

Figure 3.5- Avondale Bridge in Durham, North Carolina

3.3.2.3 US 29 Bridge (US 29 over NC 150, Project # R-0984B)

The US 29 bridge is a seven girder, single span/single stage constructed structure located on the southbound lanes of US 29 crossing over NC 150 near Reidsville, North Carolina. The girders were fabricated from AASHTO M270 weathering steel which has a yield stress of 50 ksi. The deflections measured were taken at the one-quarter and three-quarter point locations along the span. Deflection readings were also taken approximately 5 feet from mid-span. Deflections could not be measured at the exact mid-point along the span due to traffic limitations on NC 150. A chemical retarder was used in the deck concrete to delay the development of concrete stiffness for the duration of the deck placement, which lasted approximately 6 hours. Figure 3.6 is a picture of the US 29 bridge site.

Figure 3.6- US 29 Bridge Site near Reidsville, North Carolina

3.3.2.4 Camden Bridge (I-85 over Camden Avenue, Project # I-306DC)

The Camden bridge is a stage-constructed bridge located on I-85 in Durham, North Carolina. The girders consist of AASHTO M270 weathering steel with a yield stress of 50 ksi. The deflections from the northbound (NBL) and southbound (SBL) bridges were subject of this study and were constructed in the third and fourth stages of a five stage construction sequence. This sequence consisted of erecting four bridges in the first four stages and then connecting the deck slabs of all of the bridges with a closure strip in the fifth construction stage. Deflections were measured at the quarter points along the spans of the NBL and SBL bridges. The Camden NBL bridge consists of seven girders and the Camden SBL bridge consists of six girders. The duration of deck placement for each bridge was approximately 4-5 hours. A picture of the Camden bridge is contained in Figure 3.7.

Figure 3.7- Camden Bridge in Durham, North Carolina

3.3.2.5 Wilmington St Bridge (Wilmington St over Norfolk Southern Railroad, Project # B-3257)

The Wilmington St Bridge is a five girder, simple span bridge near downtown Raleigh, North Carolina (see Figure 3.8). The entire structure consists of three simple spans built in staged construction across the Norfolk Southern Railroad. The middle, southbound simple span was monitored for this investigation. Deflections were measured at the one-quarter point, the three-quarter point and at a location about 15 feet offset from the mid-span, due to railway clearance restrictions. The deck placement for this bridge lasted approximately 5 hours. The Wilmington St Bridge is illustrated in Figure 3.9.

Figure 3.8: Wilmington St Bridge in Raleigh, North Carolina

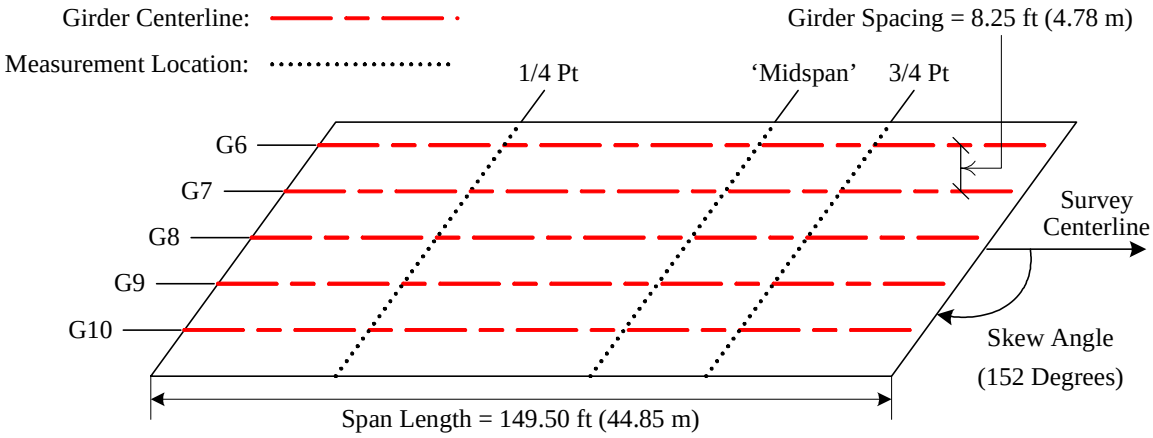

Figure 3.9: Plan View Illustration of the Wilmington St Bridge (Not to Scale)

3.3.2.6 Bridge 14 (Bridge on Ramp RPBDY1 over US 64 Business, Project # R-2547CC)

Bridge 14 is a five girder, two-span continuous structure, also located in Knightdale, North Carolina (see Figure 3.10). For this structure, deflections were measured for all five girders at the following locations: the four-tenths point of Span A (predicted maximum deflection point), the three-tenths point of Span B and the six-tenths point of Span B (predicted maximum deflection point). A two sequence concrete deck pour was utilized.

The first pour lasted about 4 hours, whereas the second lasted close to 5 hours. Bridge 14 is illustrated in Figure 3.11.

Figure 3.10: Bridge 14 in Knightdale, North Carolina

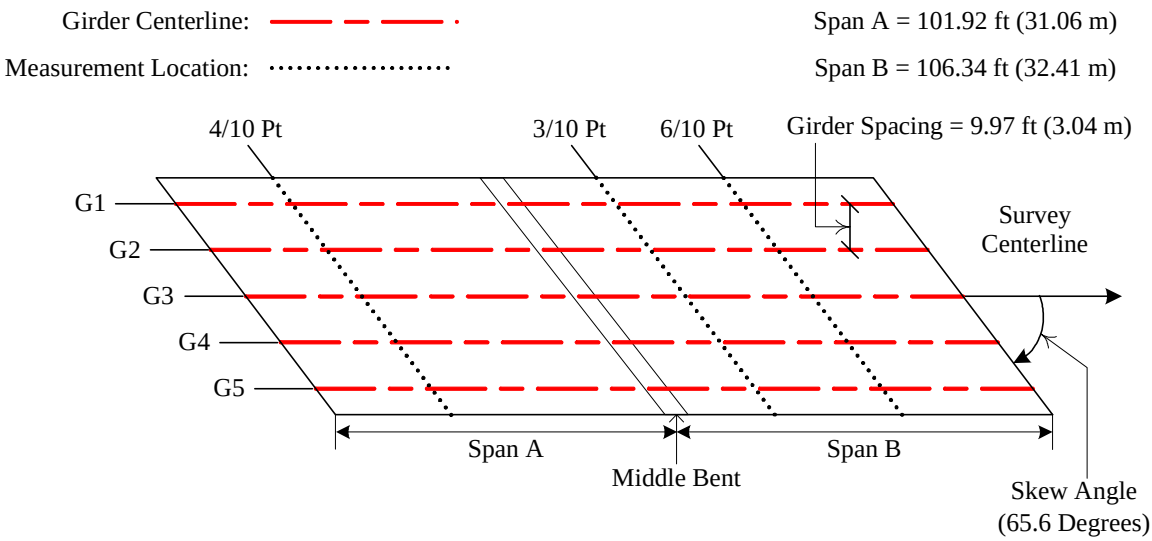

Figure 3.11: Plan View Illustration of Bridge 14 (Not to Scale)

3.3.2.7 Bridge 10 (Knightdale Eagle Rock Rd over US 64 Bypass, Project # R-2547CC)

Bridge 10 is a four girder, two-span continuous structure located in Knightdale, North Carolina (see Figure 3.12). During construction, deflections were measured on all four girders at four separate locations along the span. These locations included the four-tenths

(predicted maximum deflection point) and seven-tenths points of span B along with the two-tenths and six-tenths (predicted maximum deflection point) points of span C. The construction process involved a sequenced deck placement, the first and second pours taking about 2 and 7 hours to complete, respectively. Figure 3.13 is an illustration of Bridge 10.

Figure 3.12: Bridge 10 in Knightdale, North Carolina

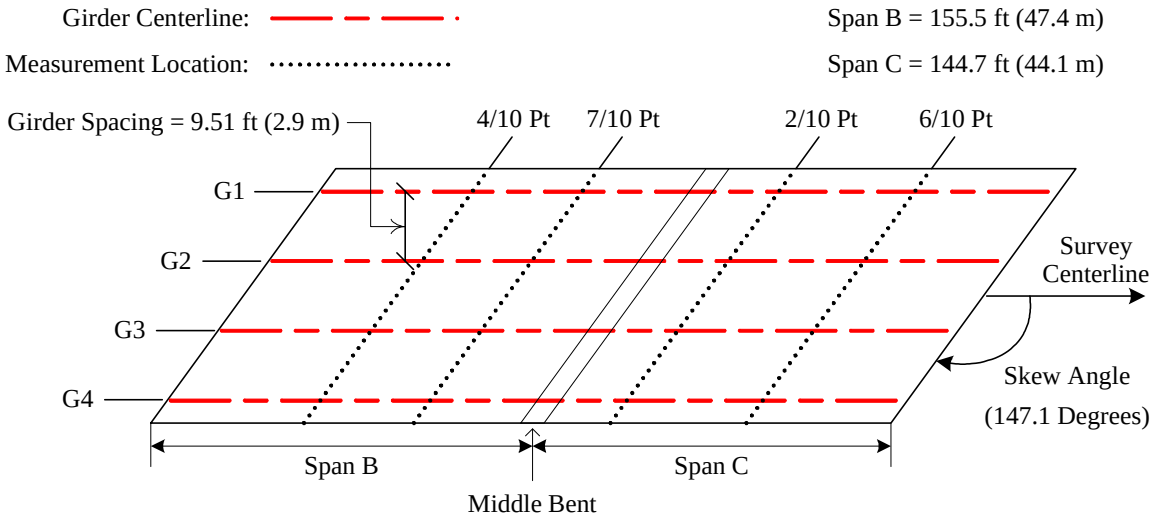

Figure 3.13: Plan View Illustration of Bridge 10 (Not to Scale)

3.3.2.8 Bridge 1 (Rogers Lane Extension over US 64 Bypass, Project # R-2547BB)

Bridge 1, in Raleigh NC (pictured in Figure 3.14), is unique to the study in that it is the only three-span continuous bridge monitored. The desired measurement locations were at the predicted maximum deflection points of all three spans; these were the four-tenths point of Span A, the mid-point of Span B and the six-tenths point of Span C. Due to Crabtree Creek below Span B and the Norfolk Southern Railroad below Span C, measurement points were offset from those locations. Span B was monitored at its four-tenths point, 23 feet from the mid-point and Span C was monitored at its thirty five-hundredths point, some 66 feet from the six-tenths point. The deck construction involved three separate concrete pours. Pours 1, 2 and 3 lasted about 4, 7 and 9 hours respectively. Figure 3.15 is an illustration of Bridge 1.

Figure 3.14: Bridge 1 in Raleigh, North Carolina

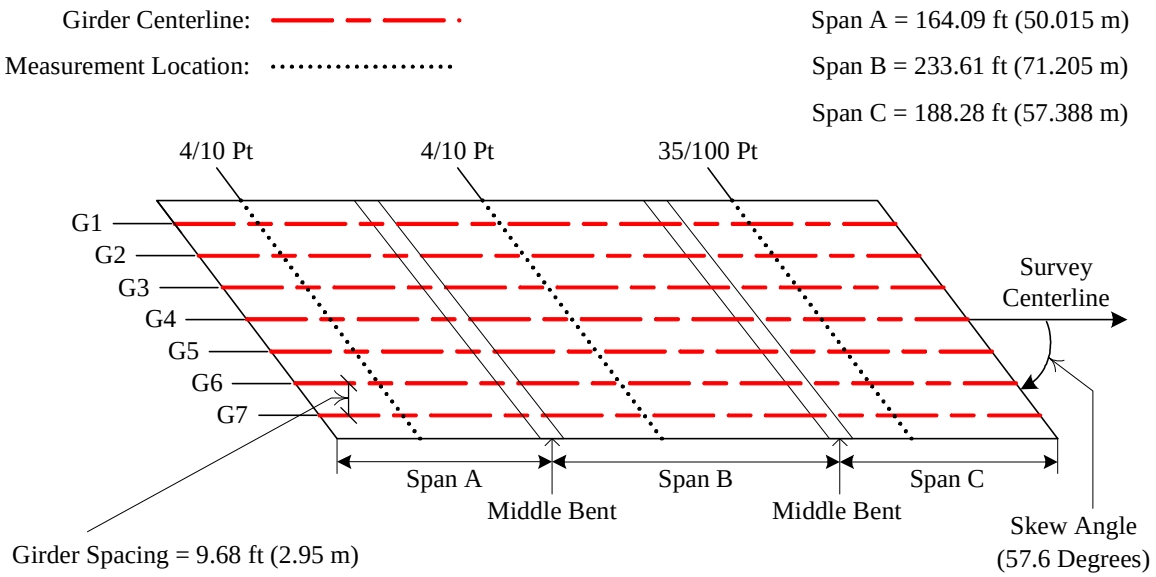

Figure 3.15: Plan View Illustration of Bridge 1 (Not to Scale)

3.4 Field Measurement

3.4.1 Overview

Two different techniques, conventional and alternate, were employed to measure the deflection of the girders during construction. Nine of the bridges were monitored using the conventional technique while the Wilmington St Bridge was monitored using an alternate technique. Both measurement procedures are described herein.

3.4.2 Conventional Method

3.4.2.1 Instrumentation

String potentiometers were used to measure girder deflections during the concrete deck placement. The potentiometers were calibrated in the laboratory to establish the linear relationship between the output voltage and the distance traveled by the string. Utilizing this relationship, voltage readings recorded in the field were readily converted to deflections.

The string potentiometers were placed on a firm surface directly beneath measurement locations and connected to the bottom flange of the girder by way of steel extension wire. The wire was adjoined to the girder by securing it to a perforated steel angle clamped to the bottom flange with c-clamps. Also, small weights were tied to the wire between the girder and potentiometer to keep constant tension in the system. The string potentiometer, extension wire, and small weight are pictured in Figure 3.16. The perforated steel angle, c-clamps, and extension wire are pictured in Figure 3.17.

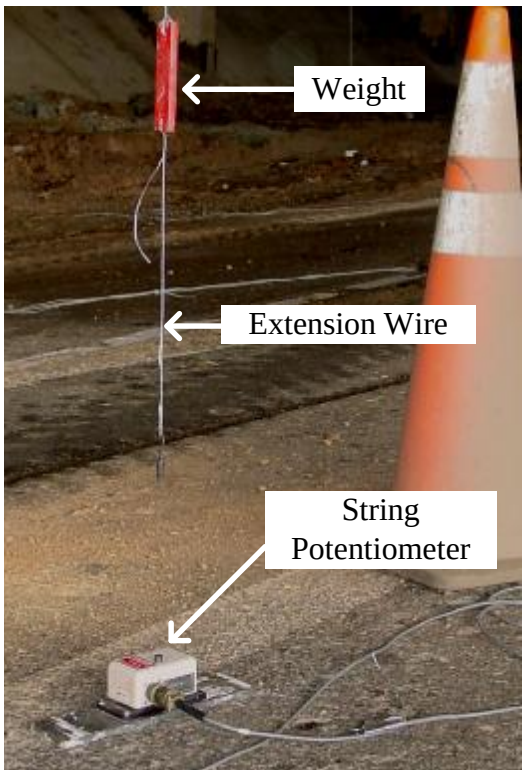

Figure 3.16: Instrumentation: String Potentiometer, Extension Wire, and Weight

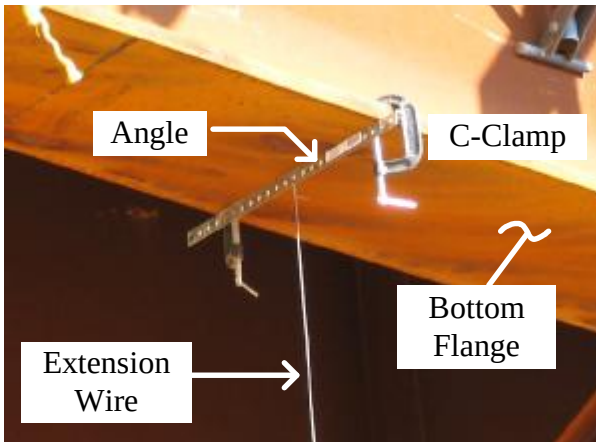

Figure 3.17: Instrumentation: Perforated Steel Angle, C-clamps, and Extension Wire

The potentiometers were connected to a switch and balance unit and a constant voltage power supply. A multimeter was used to read the voltage for each potentiometer connected to the switch and balance unit. The switch and balance units, power supply, and multimeter are pictured in Figure 3.18.

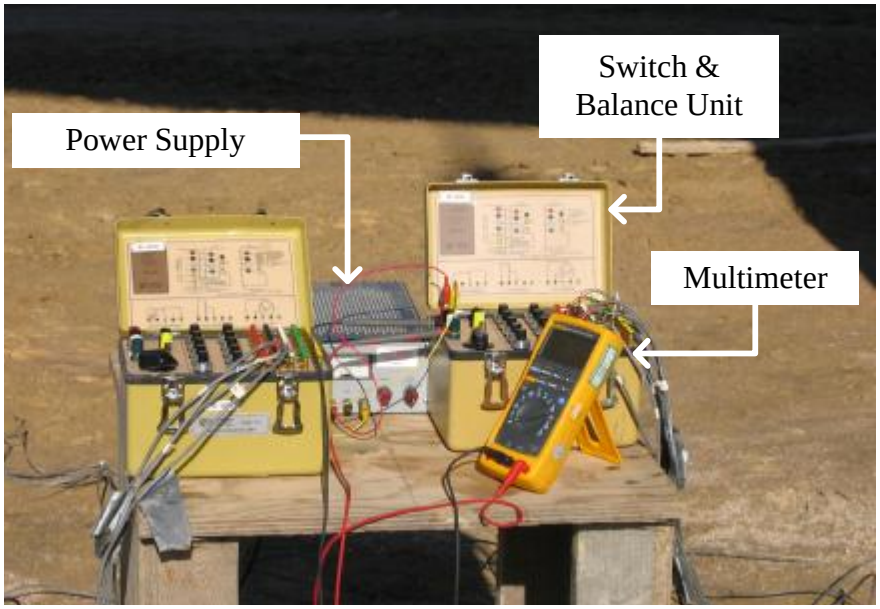

Figure 3.18: Instrumentation: Switch & Balance, Power Supply, and Multimeter

Dial gages were positioned next to the girder bearings of each girder to monitor bearing settlements (see Figure 3.19). The dial gages are accurate to 0.0001 inches, well within the desired accuracy of this project.

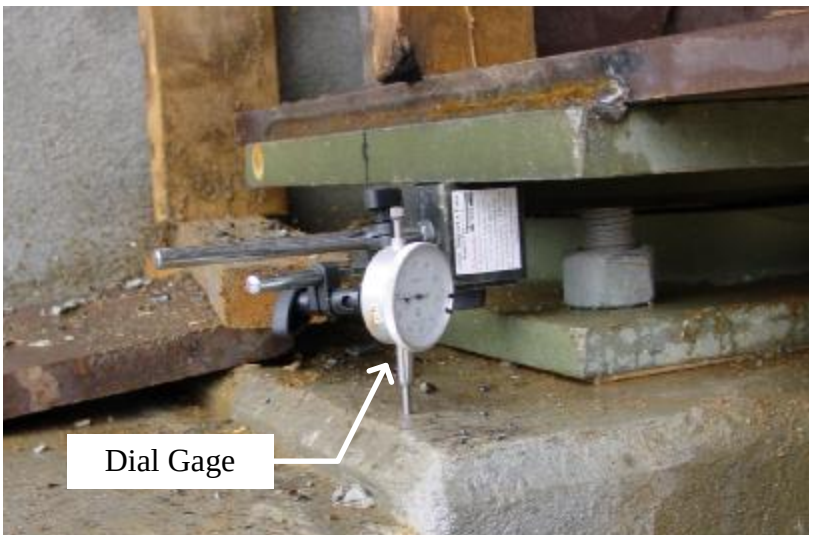

Figure 3.19: Instrumentation: Dial Gage

3.4.2.2 Procedure

Voltage readings for each string potentiometer were recorded before, during and after the concrete deck placement, and the dial gage readings were typically recorded only before and after the deck placement. To ensure dependable readings, the calibration of each string potentiometer was checked against approximate manual tape measurements both before and after the concrete pour.

3.4.2.3 Potential Sources of Error

The string potentiometers used in this research are very sensitive and can relay very small variances in voltage. Small wind gusts or vibrations from nearby traffic may have caused such variances, though they were considered insignificant to the measured

deflections. During the hydration process, concrete in contact with the top flanges can reach temperatures much greater than that of the surrounding environment. It is possible for the temperature gradient between the top and bottom flanges to decrease the dead load deflection as the top flange attempts to expand. Such variations are not fully accounted for in this research.

3.4.3 Alternate Method: Wilmington St Bridge

3.4.3.1 Instrumentation

Due to construction schedule overlap with Bridge 1, the Wilmington St Bridge was monitored using an alternate method. Similar to the conventional method, the tell-tail method utilized a steel extension wire attached to a perforated steel angle, which was clamped to the bottom flanges with c-clamps (as pictured in Figure 3.17). Again, small weights were tied to the bottom of the extension wire to keep constant tension in the system. The weights themselves additionally served as elevation markers to measure the girder deflection. Wooden stakes were driven next to each suspended weight as a stationary measurement reference. The tell-tail setup including the suspended weight and the wooden stake is pictured in Figure 3.20.

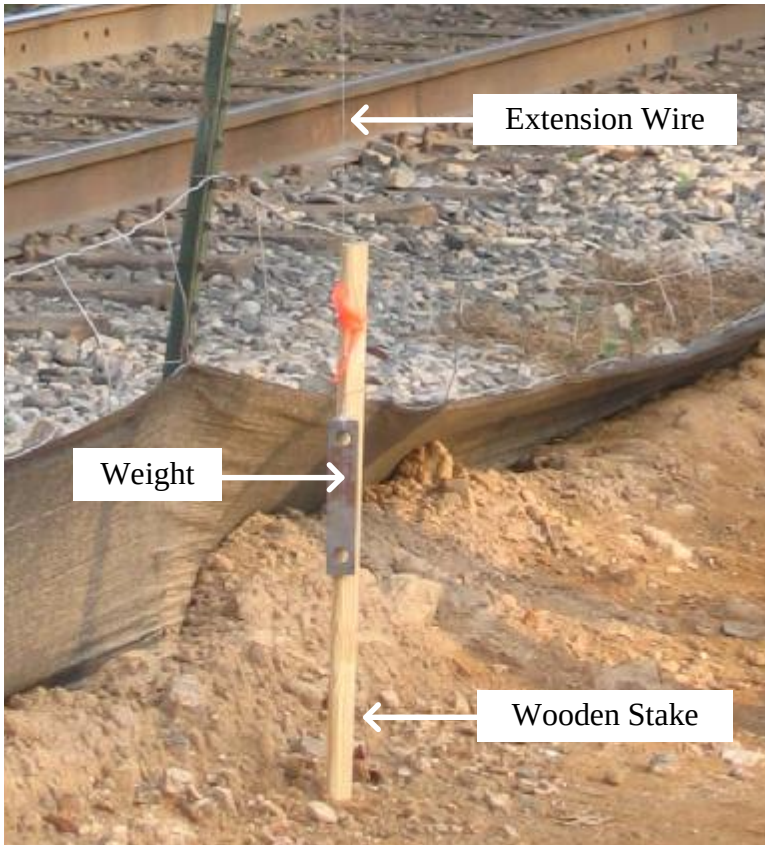

Figure 3.20: Instrumentation: Tell-Tail (Weight, Extension Wire, and Wooden Stake)

3.4.3.2 Procedure

Deflections were measured by marking the wooden stakes at the bottom of the suspended weights as the bridge girders deflected. Measurements were recorded immediately prior to the concrete deck placement, at three instances during the pour, and after the entire deck had been cast. After gathering the wooden stakes, manual measurements were made in the laboratory to determine the magnitude of deflection each girder experienced. Note: the steel plate girders rested on pot bearings, thus, bearing settlements were not monitored during construction of the Wilmington St Bridge.

3.5 Summary of Measured Deflections

Table 3.3 summarizes the field measured deflections recorded for the ten bridges included in this research. Deflections from the sequenced concrete pours were super-imposed for the continuous span structures and all tabulated deflections are in inches. Note that the girders are generically labeled A-G. Each bridge incorporates the appropriate labels depending on its number of girders. For instance, Bridge 10 only has four girders and they are labeled A-D, with girders A and D representing the exterior girders. Similarly, Bridge 1 has seven girders labeled A-G, with girders A and G now representing the exterior girders. For a given bridge, the dashed entries correspond to girders not monitored in the field and the boxes labeled "na" refer to nonexistent girders. As previously discussed, continuous span bridges have more than one location of predicted maximum deflection. Therefore, Table 3.3 includes the deflections at each of the predicted maximum deflection locations for all three continuous span bridges. A detailed deflection summary is available in the Appendices; included are deflection measurements of each pour sequence for the continuous span structures.

Table 3.3: Total Measured Vertical Deflection (inches)

	Span Location	Girder A	Girder B	Girder C	Girder D	Girder E	Girder F	Girder G
Eno	Mid-Span	6.94	6.41	5.88	5.14	4.89	na	na
Bridge 8	Mid-Span	2.89	3.14	3.17	3.26	3.30	3.24	na
Avondale	Mid-Span	4.79	4.94	-	5.08	-	5.36	5.47
US-29	Mid-Span	4.44	4.13	-	3.98	-	4.31	4.65
Camden NB	Mid-Span	3.18	3.29	3.47	na	3.28	3.08	na
Camden SB	Mid-Span	2.97	3.11	-	3.27	-	3.11	2.9
Wilmington St	Mid-Span	5.04	4.19	3.78	3.70	3.80	na	na
Bridge 14	4/10 Span A	0.87	0.79	0.97	0.85	0.51	na	na
	6/10 Span B	1.55	1.45	1.66	1.50	1.64	na	na
Bridge 10	4/10 Span B	1.97	1.91	1.74	2.02	na	na	na
	6/10 Span C	2.07	1.64	1.66	1.64	na	na	na
Bridge 1	4/10 Span A	1.99	1.73	-	1.53	-	1.77	2.03
	4/10 Span B	4.59	4.38	-	4.18	-	3.99	3.96
	35/100 Span C	1.27	1.13	-	1.21	-	1.41	1.72

The deflections from Table 3.3 were plotted and displayed in Figure 3.21. For clarity, only the "span B" deflections have been plotted for each continuous span bridge. It is apparent that there are five different bridge deflection behaviors for each of the five structures. The Wilmington St Bridge is the only bridge with unequal overhangs, thus unequal exterior girder loads. The inequality justifies the general slope from left to right, but not the "hat" shape observed. The other four deflected shapes appear essentially flat, with minor slopes for Bridge 8 and Bridge 1.

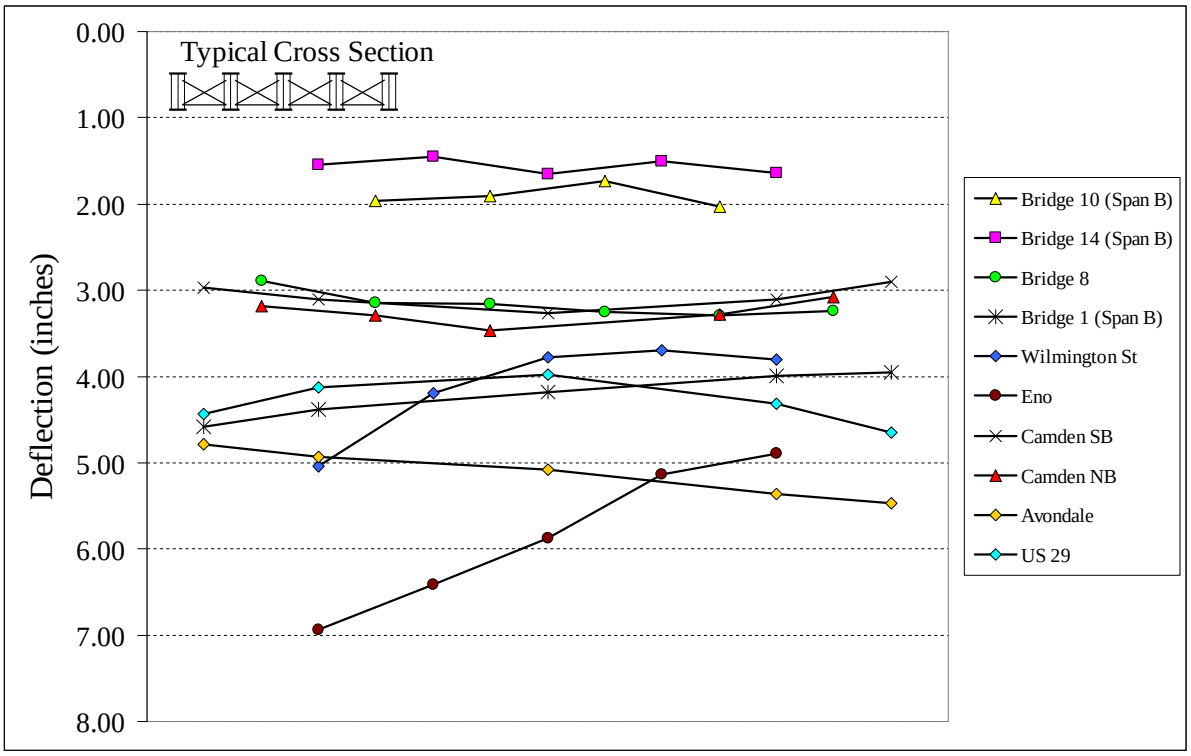

Figure 3.21: Plot of Non-composite Deflections

3.6 Summary

Ten steel plate girder bridges have been monitored during the concrete deck placement. Of the ten, seven are simple span, two are two-span continuous and one is three-span continuous. The bridges were selected based upon their geometric parameters which were believed to directly contribute to each bridge's deflection behavior during construction. The measured deflection results were used to validate the finite element modeling technique as described in the subsequent sections of this report.

4.0 Finite Element Modeling and Results

4.1 Introduction

Detailed finite element models of steel plate girder bridges have been created using the commercially available finite element analysis program ANSYS (ANSYS 2003). Initially, the models were developed to predict the bridge girder deflections which were compared to field measured values. These comparisons were used to validate the finite element modeling technique. With the confidence in the ability of ANSYS models to accurately predict non-composite girder deflections, a preprocessor program was developed in MATLAB to automate the procedure of processing detailed bridge information and generating commands to create the finite element models. The preprocessor program greatly reduced the time and effort spent generating the models and allowed for the administration of an extensive parametric study to determine which bridge components affect deflection behavior.

This section will discuss: the finite element models, the modeling procedure, the MATLAB preprocessor program, and modeling assumptions. Also included are the deflection results, predicted by the ANSYS models, for all ten bridges measured in this research project.

4.2 General

Static analysis is used to determine structural displacements, stresses, strains, and forces caused by loads that do not generate significant inertia and damping effects (ANSYS 2003). Therefore, without the presence of non-linear effects, the finite element bridge models of this research implement a static and linear analysis.

There are two linear elastic material property sets defined in each model, one for the structural steel and the other for the concrete deck. All structural steel elements are defined with an elastic modulus of 29,000 ksi (200,000 MPa) and a Poisson's ratio of 0.3. The concrete elements are defined with an elastic modulus, E_c, calculated by,

$$E_c = 57,000\sqrt{f'_c} \qquad \text{(eq 4.1)}$$

where f'_c is the compressive strength of the concrete (in psi). The Poisson's ratio for the concrete elements is defined as 0.2 a sensitivity study conducted as a part of this research indicated that the models were nearly insensitive to adjustments of this ratio for concrete.

MATLAB is a matrix-based, high-level computing language commonly used to solve technical computing problems. MATLAB was chosen for this facet of the research project for the author's familiarity of both MATLAB and the C programming language, which is closely related to the computing language incorporated into MATLAB. Statistically, output files are commonly between 2,000 and 6,000 lines of commands, while the MATLAB files programmed to generate the output consist of about 5,000 lines of code.

4.3 Bridge Components

The finite element models developed in this research include specifically detailed bridge components. Generally, these components include facets of the plate girders, the cross frames, the stay-in-place (SIP) metal deck forms and the concrete deck, each of which will be addressed in the following subsections. Note that in the subsequent discussion, a centerline distance refers to the distance from the centerline of the top flange of the girder section to the centerline of the girder bottom flange.

4.3.1 Plate Girders

4.3.1.1 Girder

The plate girders are modeled by creating six keypoints to outline the geometric cross-section (web and flanges), according to actual centerline dimensions. To establish the entire girder framework, the keypoints are then copied to desired locations along to span and areas are generated between the keypoints. Figure 4.1 displays perspective and cross-section views of a single girder modeled in ANSYS.

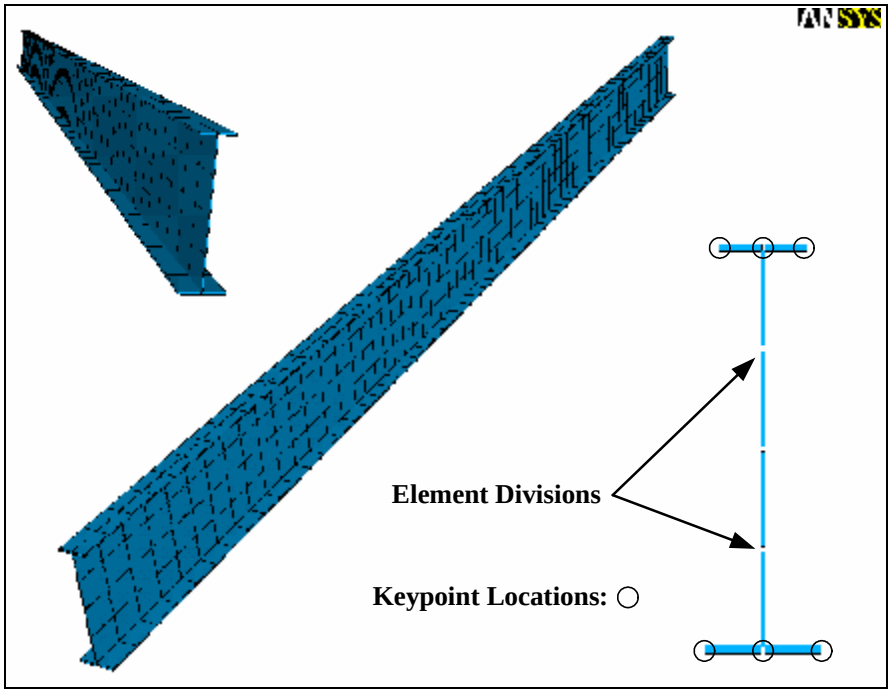

Figure 4.1: Single Plate Girder Model

Along a typical span, girder cross-sections vary in size. In developing a model, the centerline dimension is kept constant and defined by the section with the highest moment of inertia. The section properties are then adjusted by applying real constant sets appropriately within ANSYS, i.e. changing the plate thicknesses. The constant centerline assumption

differs from reality in that web depths are typically constant along the span. Therefore, the centerline dimension fluctuates as the flange thickness is changed. A sensitivity study conducted as a part of this research resolved that the centerline assumption has minimal effect on the bridge deflection behavior.

4.3.1.2 Bearing Stiffeners, Intermediate Web Stiffeners, and Connector Plates

Bearing stiffeners, intermediate web stiffeners, and connector plates are typical of the ten studied bridges. Bearing stiffeners are present to stiffen the web at support bearing locations, intermediate web stiffeners are utilized for web stiffening along the span, and connector plates are used doubly as links between the intermediate cross frames and girder, and as additional web stiffeners.

The bearing stiffeners, intermediate web stiffeners, and connector plates are modeled by creating areas between web keypoints and keypoints at the flange edge. On the actual girders, stiffeners and plates are of constant width and rarely extend to the flange edge. It was confirmed through a sensitivity study that the finite element models are insensitive to this modeling assumption, which essentially fully welds the stiffeners and plates to the girder at the web and both flanges. Figure 4.2 displays oblique and cross-sectional views of bearing and intermediate web stiffeners.

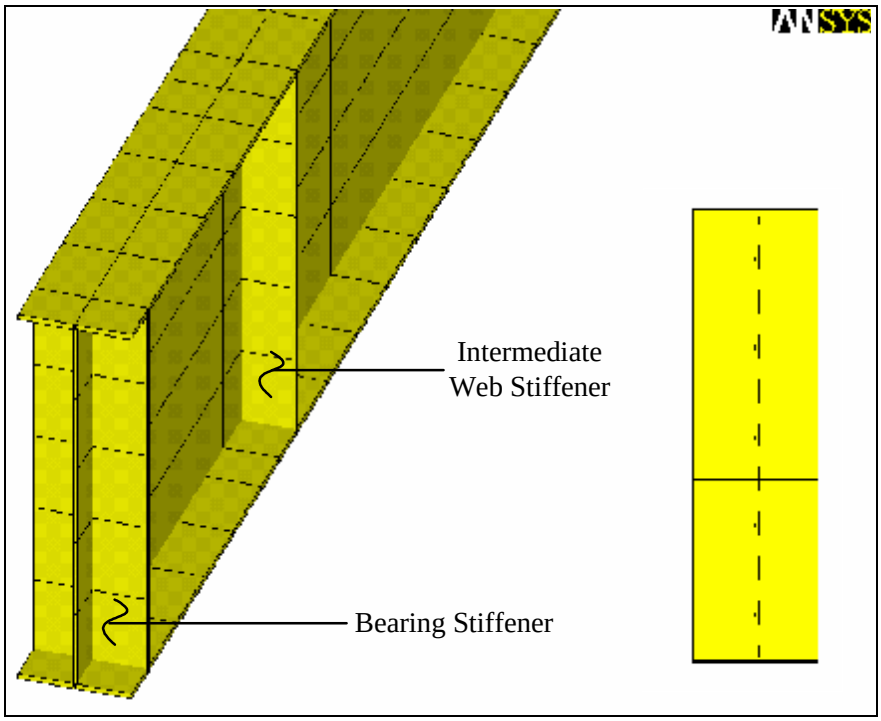

Figure 4.2: Bearing and Intermediate Web Stiffeners

4.3.1.3 Finite Elements

Eight-node shell elements (SHELL93) are utilized for each of the plate girder components, including: the girder, bearing stiffeners, intermediate web stiffeners and connector plates. The SHELL93 element has six degrees of freedom per node and includes shearing deformations (ANSYS 2003). Actual plate thicknesses are attained directly from the bridge construction plans and applied appropriately in the finite element models. A mesh refinement study conducted as a part of this research concluded that the finite element mesh of approximately one foot square to be viable for convergence. Aspect ratios were checked and considered acceptable at values less than five; values greater than three are rarely present in the models. Element representations are available in Figures 4.1 and 4.2.

4.3.2 Cross Frames

4.3.2.1 General

Three different cross frames are common to bridges in the study: intermediate cross frames, end bent diaphragms and interior bent diaphragms. According to the AASHTO LRFD Bridge Design Specifications (2004), the aforementioned cross frames must: transfer lateral wind loads from the bottom of the girder to the deck to the bearings, support bottom flange in negative moment regions, stabilize the top flange before the deck has cured, and distribute the all vertical dead and live loads applied to the bridge.

Each cross frame is modeled by creating lines between the girder keypoints existing at the intersection of the web and flange centerlines. On the actual girders, the cross frame connections are offset from the flange to web intersection to allow for the connection bolts. This simplifying assumption has been shown to have little effect on the predicted girder deflection. The other assumption is that the cross frame member stiffnesses are very small relative to the girders themselves; therefore, the member connections are modeled as pins and are free to rotate about the joint.

In the finite element models, each cross frame member is modeled as a single line element. The cross frame member section properties were acquired from the AISC Manual of Steel Construction and applied directly into ANSYS.

4.3.2.2 Intermediate Cross Frames

Intermediate cross frames are utilized on all ten measured bridges and were erected perpendicular to the girder centerlines. The intermediate cross frame members are typically steel angles or structural tees between three and five inches in size and are bolted to the

connector plates. X- and K-type cross frames are the two types associated with the studied bridges and are illustrated in Figures 4.3a and 4.3b respectively.

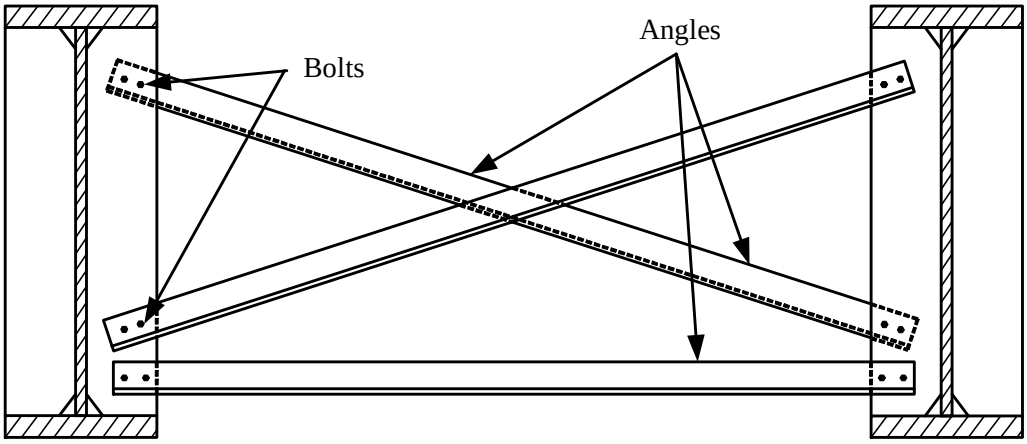

a) X-type

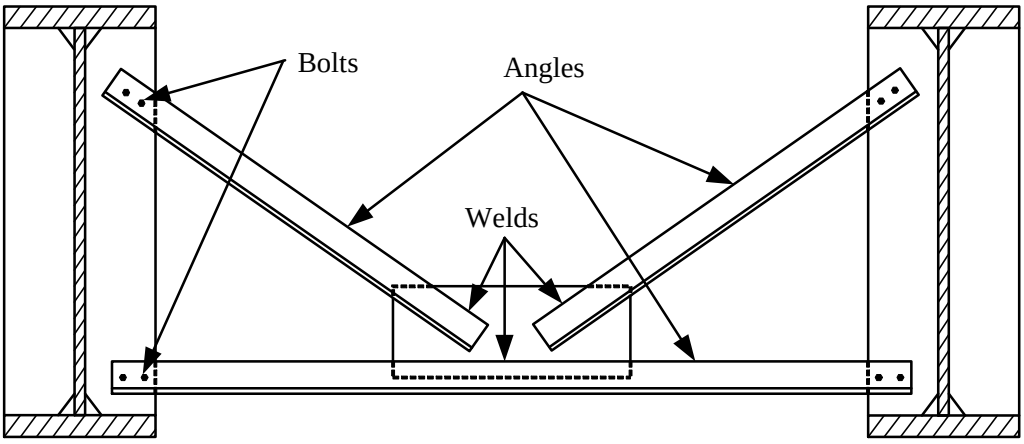

b) K-type

Figure 4.3: Intermediate Cross Frames

Intermediate cross frames are modeled with three-dimensional truss (LINK8) elements and three-dimensional beam (BEAM4) elements. LINK8 elements have two nodes with three degrees of freedom at each, whereas BEAM4 elements are defined with two or

three nodes and have six degrees of freedom at each (ANSYS 2003). LINK8 elements are utilized for each member of the X-type intermediate cross frame. For the K-type intermediate cross frame, BEAM4 elements are utilized for the bottom horizontal members and LINK8 elements are utilized for the diagonals. Figure 4.4 displays a characteristic ANSYS model with X-type intermediate cross frames.

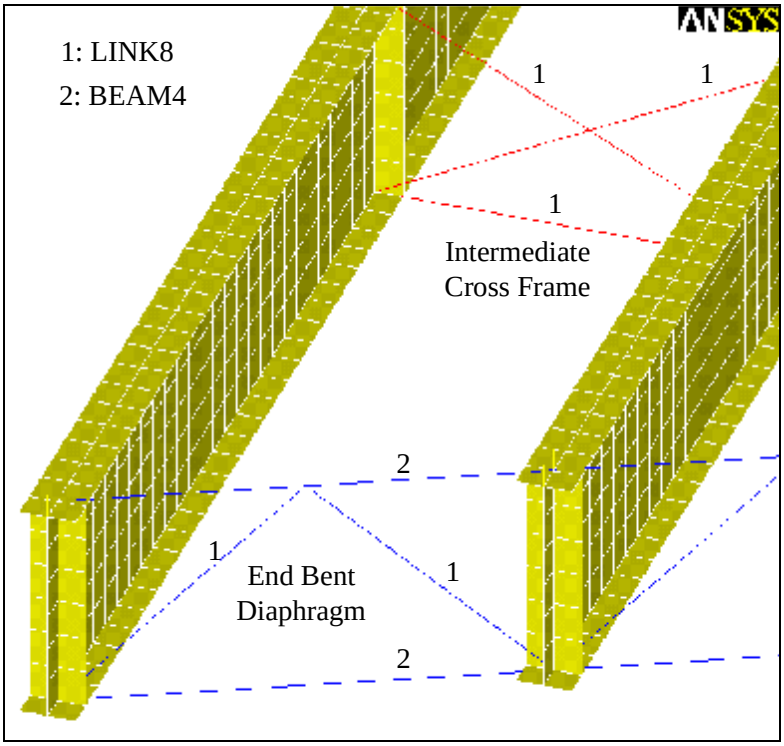

Figure 4.4: Finite Element Model with Cross Frames

4.3.2.3 End and Interior Bent Diaphragms

End bent diaphragms are utilized on nine of the ten measured bridges and were erected parallel to the abutment centerline. Bridge 14 includes integral end bents and, therefore, does not require end bent diaphragms. Figure 4.5 illustrates a typical end bent diaphragm with a large, horizontal steel channel section at the top and smaller steel angles or structural tees elsewhere. The other observed configuration included a short vertical member

between the bottom horizontal member and central gusset plate (as was the case for Bridge 10 and the Wilmington St Bridge). The end bent diaphragms brace the girder ends, at or near the bearing stiffeners.

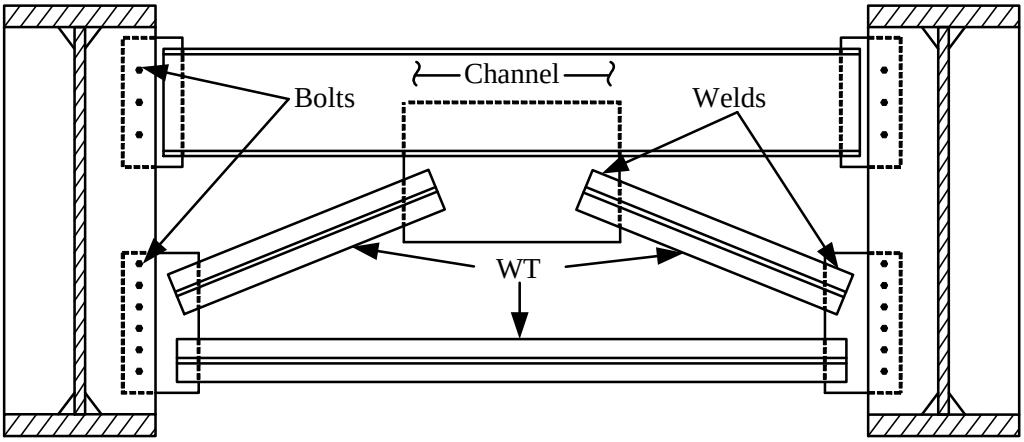

Figure 4.5: End Bent Diaphragm

Interior bent diaphragms are present on two of the three continuous span bridges (Bridge 14 and Bridge 1) and were also assembled parallel to the abutment centerline. In both cases, the diaphragms are exact duplicates of the intermediate cross frames, except that they are oriented differently and exist only at the interior supports. The other continuous span bridge (Bridge 10) utilizes intermediate cross frames directly at the interior bearing, perpendicular to the girder centerline; therefore, it does not utilize interior bent diaphragms.

End and interior bent diaphragms are modeled with LINK8 and BEAM4 elements. Typically, BEAM4 elements are utilized for horizontal members and LINK8 elements are utilized for diagonal and vertical members. Figure 4.4 illustrates an end bent diaphragm for a typical ANSYS finite element model.

4.3.3 Stay-in-Place Metal Deck Forms

4.3.3.1 General

A method to model the stay-in-place (SIP) metal deck forms, similar to the method previously developed by Helwig and Yura (2003), was incorporated into the finite element models. The method employs truss members (diagonal and chord members) between the girders to represent the SIP form's axial stiffness. The approach allows the models to capture the true ability of the SIP forms to transmit loads between girders.

4.3.3.2 Structural Behavior of SIP Forms

The SIP metal deck forms were initially thought to behave largely as a shear diaphragm spanning between the top girder flanges. Reasonable shear strength and stiffness properties were required for this study without conducting laboratory tests on the shear behavior of SIP systems. A research study by Jetann et al. (2002) provided shear properties of typical bridge SIP forms systems that account for the mitigating effect of the flexible connection of the SIP forms to the top girder flanges. This study provided the basis that was used to develop the shear properties to be used in the ANSYS models. It was later discovered that the SIP form systems largely behave as a tension-compression member that connects the top flanges of the girders (later discussed in detail). Details of the development of the SIP properties used in this study and their affect on the behavior of the bridge models will be later discussed.

The deflection behavior predicted by the ANSYS models of skewed bridges was found to be markedly different from that of a non-skewed bridge model. Figure 4.6 is a picture of the deflected shape predicted by ANSYS for a skewed bridge. According to the figure, the plate girders of skewed bridges tend to rotate out-of-plane in addition to the

downward deflection. This out-of-plane rotation varies in both magnitude and direction depending on the location along the girder span. This differs from the behavior of the non-skewed bridge model which was found to only deflect downward with little or no out-of-plane rotation. This rotation of the girder cross-sections would provide the mechanism necessary to activate the SIP forms as force distributing elements within the ANSYS models.

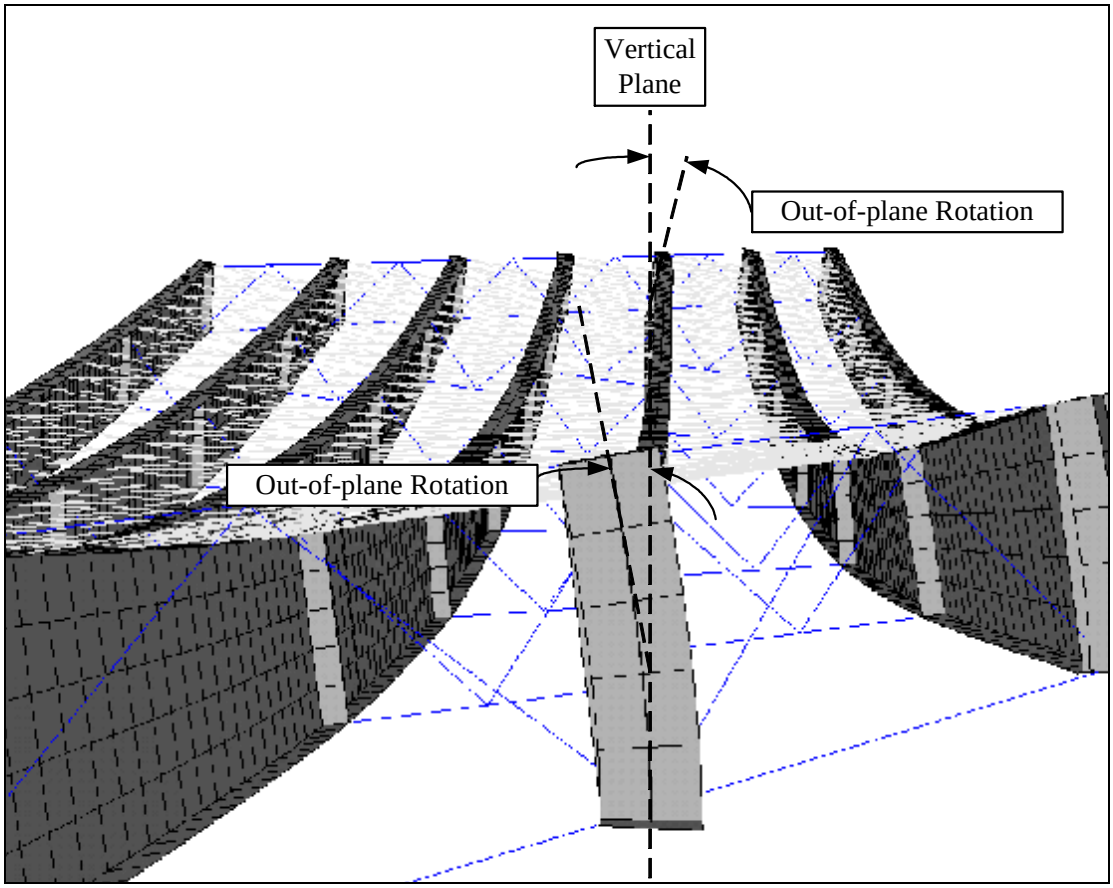

Figure 4.6- ANSYS Displaced Shape of a Skewed Bridge Model

4.3.3.3 Importance of SIP Forms in ANSYS Models

The weight of the SIP metal deck forms is accounted for in the design dead loads used for steel plate girder bridges. However, the ability of the SIP forms to transmit forces is not accounted for in steel bridge design. In an effort to investigate the load distribution

ability of the SIP forms, several intermediate ANSYS finite element models were created for the non-skewed (Eno River bridge) and skewed (US 29 bridge) both with and without SIP forms.

The mid-span deflections from the ANSYS models (with and without SIP forms) of the non-skewed bridge are plotted in Figure 4.7. It is clear from the figure that the inclusion of the SIP forms has little effect on the deflection behavior of the non-skewed bridge. This is due to the fact that the girders in the non-skewed bridge model only deflect downward and do not rotate out-of-plane significantly. This was not the case for the skewed bridge models.

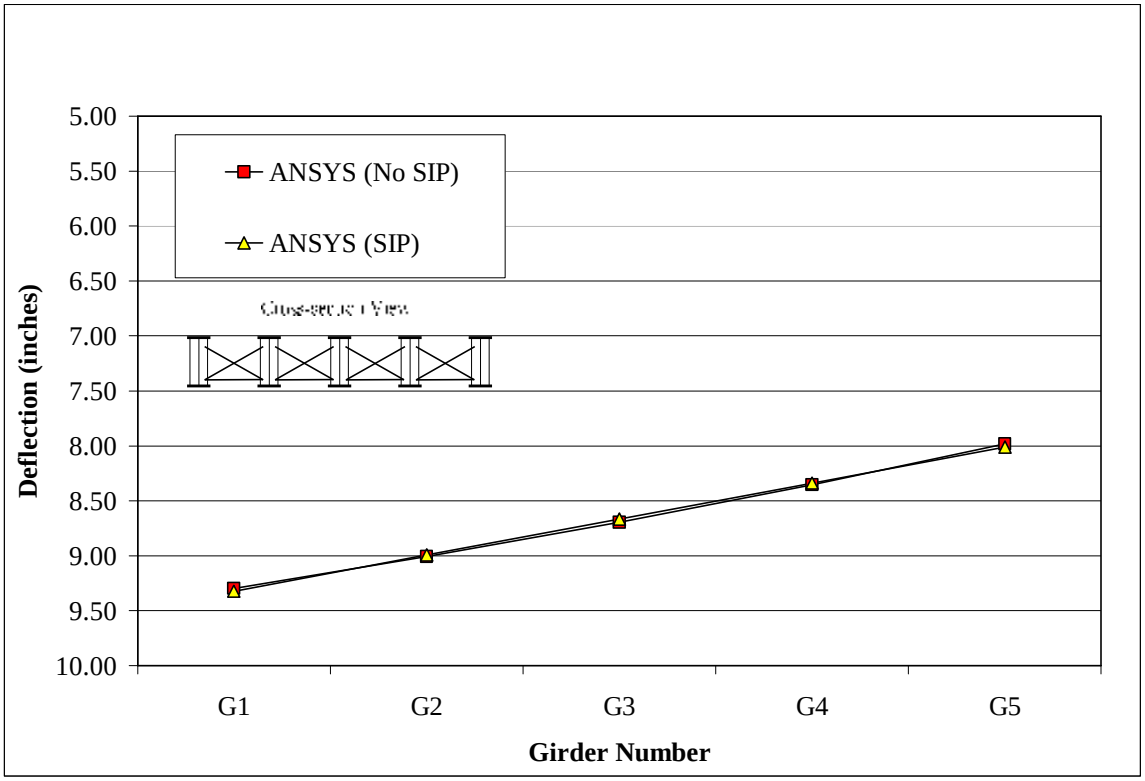

Figure 4.7- Non-skewed Bridge, ANSYS Models with and without SIP Forms

The effect of including the SIP forms in the ANSYS models for the skewed bridges much more prevalent than that of the non-skewed case. Figure 4.8 is a plot of the mid-span

deflections predicted by the ANSYS models for the skewed bridge both with and without SIP forms. The difference in deflection behavior of the two models is apparent. The ANSYS model without the SIP forms included predicts girder deflections that are largest for the interior girders giving the deflections a "v-shaped" profile. The opposite trend can easily be seen in the deflection profile of the ANSYS model with the SIP forms included. The predicted deflections for this model were largest for the exterior girders.

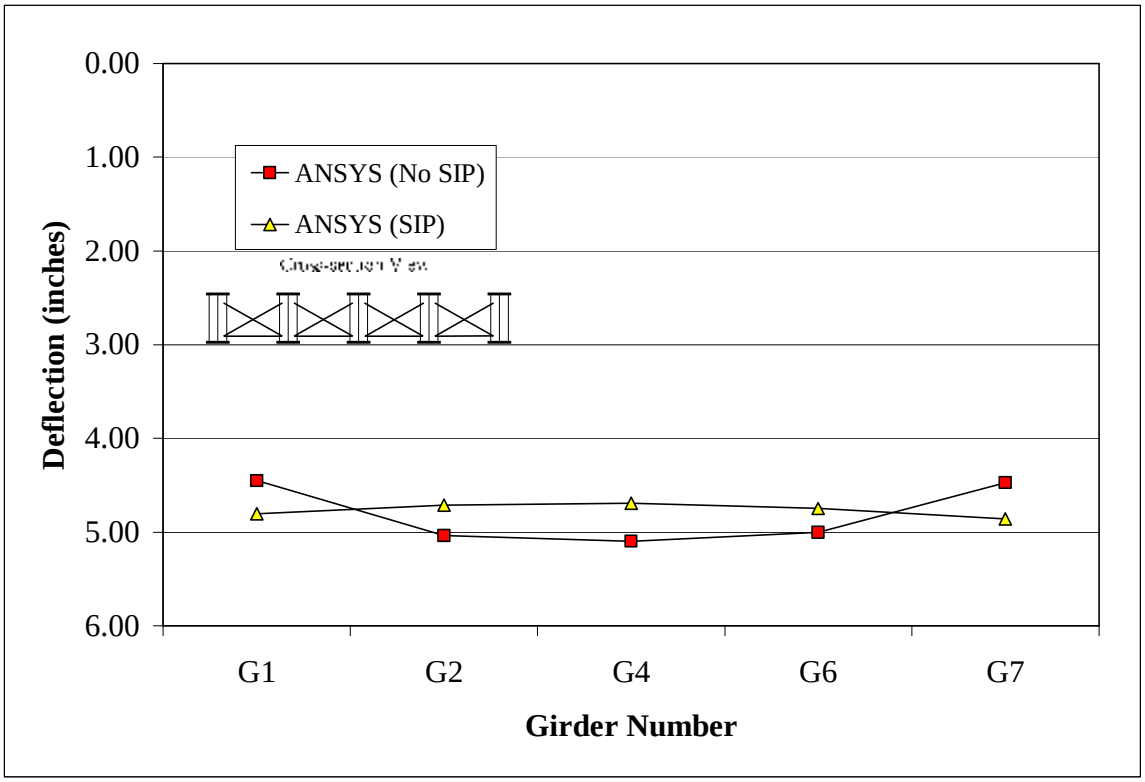

Figure 4.8- Skewed Bridge, ANSYS Models with and without SIP Forms

4.3.3.4 Modeling Methods of SIP forms

The SIP metal deck forms were initially modeled using four node shell elements (SHELL63). This was found to be inefficient in terms of the number of degrees of freedom (DOF's) it added to the models (Helwig, 2003). It was also difficult to properly assign shear strength and stiffness properties to the SHELL63 elements that account for the mitigating

affect of the flexible connection used between the SIP forms and the girders. It was determined that a more efficient modeling technique was needed to represent the SIP forms.

Another method used to model the SIP forms was based the technique developed by Helwig and Yura (2003) and employed by Egilmez et al. (2003). This method involved using truss elements (struts and diagonals) spanning between the top girder flanges. The truss elements used were two node three dimensional LINK8 elements and were connected to the girder flanges by coupling all of the translational DOF's (global x, y, and z directions) between the edges of the top flanges and the truss elements. This method of connecting the truss elements to the girder flanges differed from the technique used in Egilmez et al. (2003) but was believed to more accurately represent the true geometry of the connection. Egilmez et al. (2003) connected the truss elements to the intersection of the top flange and the girder web. Figure 4.9 illustrates this modeling technique which used much fewer DOF's than the previous method.

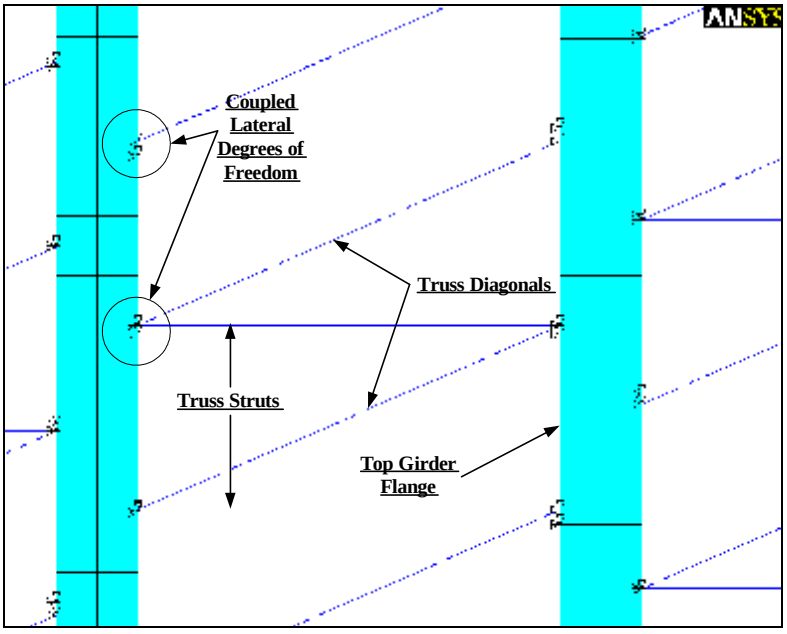

Figure 4.9- Plan View of Truss Modeling SIP Forms between Girder Flanges

The section properties of the strut and diagonal members of this SIP system was based on a truss analogy example obtained from the Diaphragm Design Manual (SDI, 1991). This example showed how to create a single diagonal truss with the same shear stiffness as an SIP diaphragm system.

A sensitivity study was performed to investigate how the in-plane (plane of the SIP form panels) shear stiffness of the SIP forms was affected by the presence of the truss diagonals. Preliminary ANSYS models were run with and without the diagonal to determine the affect on deflection behavior. The deflection magnitudes and behavior was very similar (within 1 percent) between the models with and without the diagonals. This indicates that the SIP forms predominantly behave as a tension-compression member spanning between the top girder flanges. However, it was determined that the diagonals were necessary to accurately represent the SIP forms to allow any shear forces to be transmitted from one girder to another in the plane of the SIP forms.

Another study was performed to determine how the orientation of the diagonal affects the behavior of the bridge models. In one preliminary model, the diagonal members were oriented similar to that in Figure 4.9. The same model was then reanalyzed with diagonal members in the opposite direction and again with diagonals in both directions thus forming an x-brace. Figure 4.10 is a plot of the mid-span deflections from both of the models.

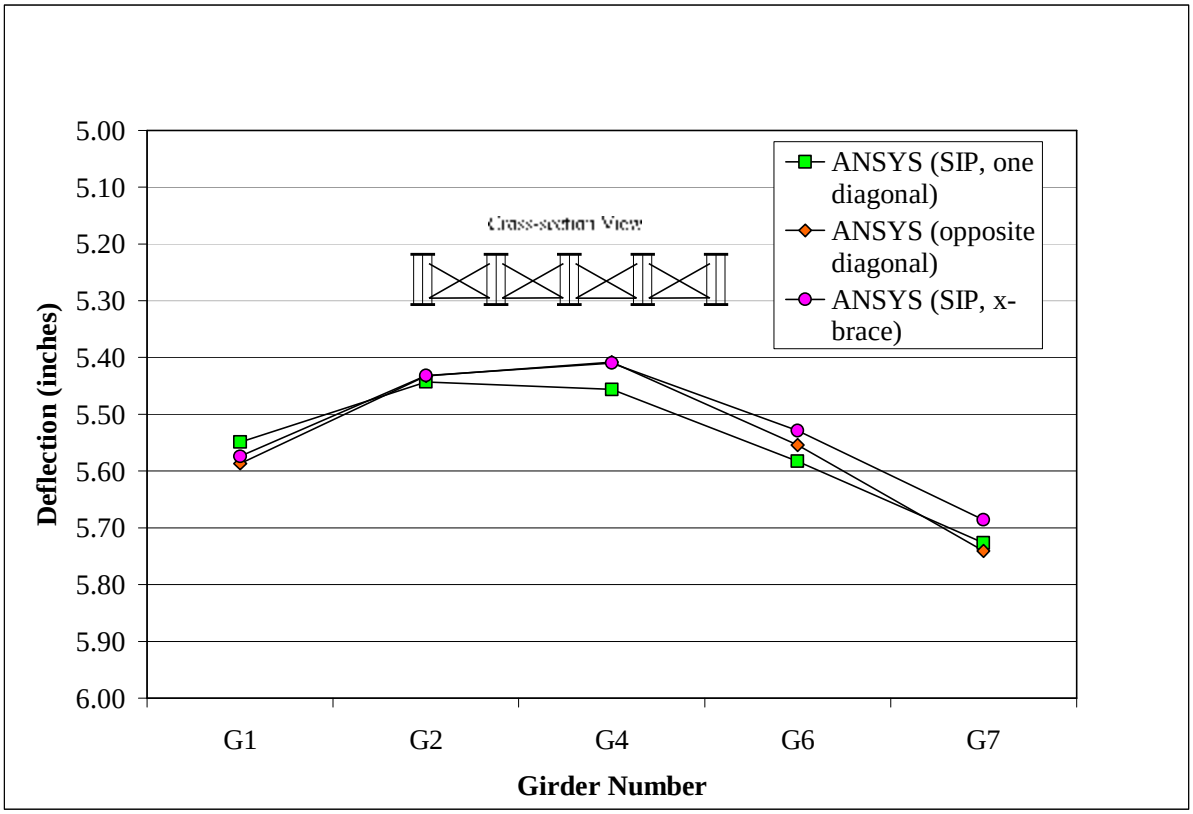

Figure 4.10- Affect of SIP Diagonal Member Direction in ANSYS Model

According to the above figure, the deflection magnitude and behaviors are very similar in both models. However, it was determined that an x-brace (two-diagonal) system would more adequately represent the shear stiffness of the SIP forms and more accurately account for the direction of in-plane shear transfer. The section properties used in the preliminary models with the x-brace SIP system were based on the same section properties that were obtained for the single diagonal SIP systems. In order to more accurately represent the shear stiffness of the SIP system with an x-brace system, a more rational approach to was needed to developing the section properties of the x-brace system.

4.3.3.5 SIP Properties

In order to accurately represent the SIP forms, properties had to be assigned to the truss elements that would allow accurate tension and compression behavior along with adequate in-plane shear stiffness.

The axial stiffness of the SIP system was determined to be dependent upon three components: the form panel stiffness, the screw connection stiffness, and the stiffness of the supporting angle. These three stiffnesses were combined using an equivalent spring model that represents the axial stiffness of the entire system (panel, screws, and supporting angles). Figure 4.11a illustrates the connection detail of the SIP forms to the girder flanges assumed for each ANSYS model. Figure 4.11b contains an illustration of the equivalent spring model used to combine the axial stiffness of each component in the SIP form system to represent the system axial stiffness.

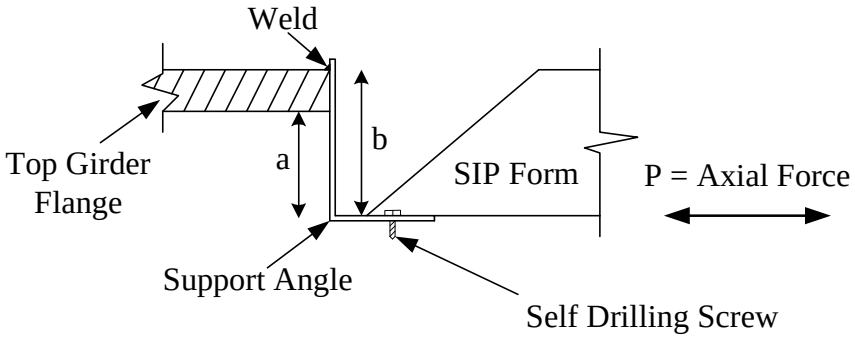

a) Connection Detail Assumed for Each Bridge

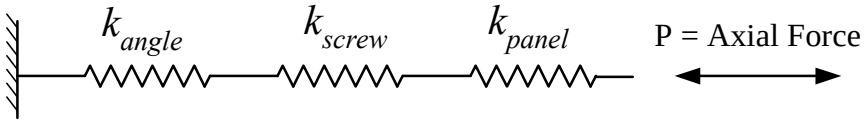

b) Equivalent Spring Model

Figure 4.11- SIP Form System Axial Stiffness

The following sections contain a discussion of how each component of the SIP form system stiffness was derived. Appendix G contains an example of the calculations used to derive the properties of a typical SIP form system.

The axial stiffness of an individual SIP panel was found by calculating the axial stiffness of a long slender rod with a cross-sectional area equivalent to that of a form panel. Figure 4.12 is an illustration of a typical cross-sectional profile of an SIP form panel. The SIP profile varied for each bridge included in this study, therefore the axial stiffness for the SIP form panels also varied.

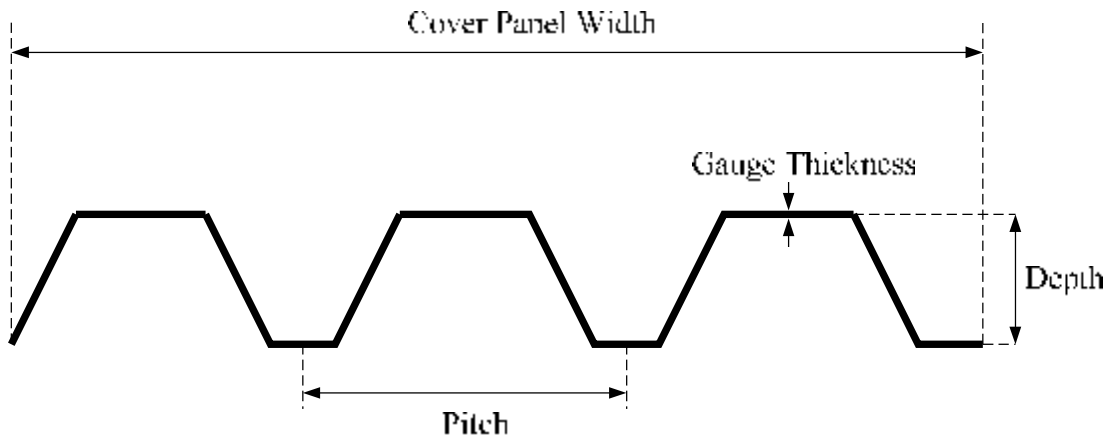

Figure 4.12- Typical SIP Form Cross-sectional Profile

A sample calculation of the cross-sectional area of a typical SIP form and its axial stiffness is located in Appendix G.

Each SIP panel was assumed to have three screws No. 12 self drilling screws on each end that attach the panel to the support angle. The shear stiffness of these screws was calculated using an expression developed in the Diaphragm Design Manual (SDI, 1991).

Appendix M contains this expression along with a sample calculation for the shear stiffness of the screws.

For the purposes of this study, all SIP forms were assumed to be connected to the same size angle (3.5"×2", thickness = 10 gauge) as illustrated in Figure 4.13a. The connection eccentricity between the axial force and the plane of the girder flange was maximized to simulate the most flexible case. Two different analytical models were created to simulate both tension and compression forces in the connection (see Figure 4.13b).

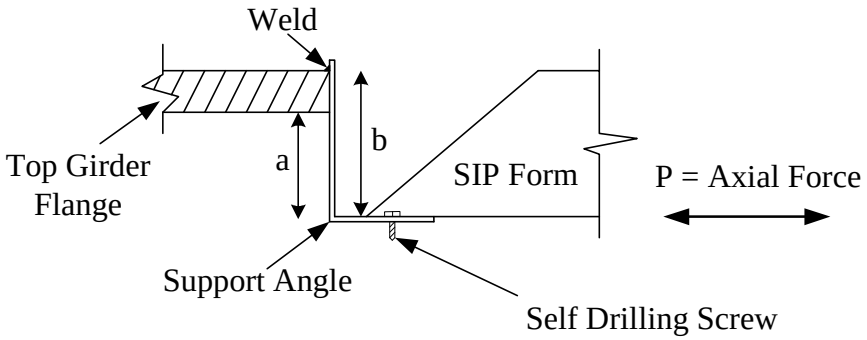

a) Connection Detail Assumed for Each Bridge

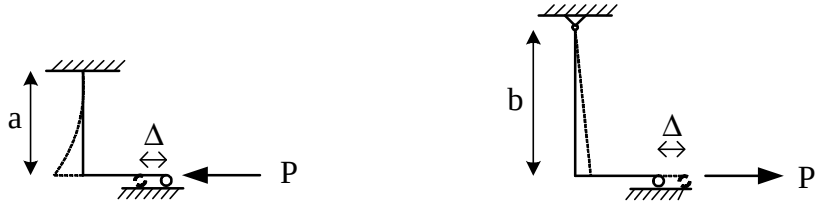

b) Analytical Models used in SAP2000

Figure 4.13- Support Angle Stiffness Analysis

Both of these analytical models were analyzed using the program SAP2000 to obtain stiffness per unit length of the support angle. The leftmost analytical model illustrated in

Figure 4.13b produced a much larger stiffness than the other model and thus was used in the calculation of the SIP system axial stiffness. The stiffness of each connection was calculated by dividing the applied axial force by the lateral displacement predicted by the SAP2000 models. A sample calculation of how the axial stiffness of the supporting angle was obtained from the SAP2000 results is located in Appendix MG.

Jetann et al. (2002) performed experimental tests that measured the diaphragm shear strength of bridge SIP form systems that utilized several different connection details. These form systems contained multiple SIP form panels connected together along their lengths with self-drilling screws and connected to the girder flanges via a connection detail similar to that shown in Figure 4.13a. A value of shear stiffness (G'=11 kips/inch) was measured for the SIP form system with the SIP connection detail similar to what has been utilized by the bridges in this study and was used as the basis for the shear properties in the ANSYS finite element models. This shear stiffness was used in conjunction with an example for a truss analogy obtained from the Diaphragm Design Manual to calculate the shear stiffness of the SIP form system. This example shows how to obtain an equivalent truss model from a shear diaphragm (SIP form system) with known dimensions and shear stiffness. Figure 4.14 is an illustration of the truss analogy.

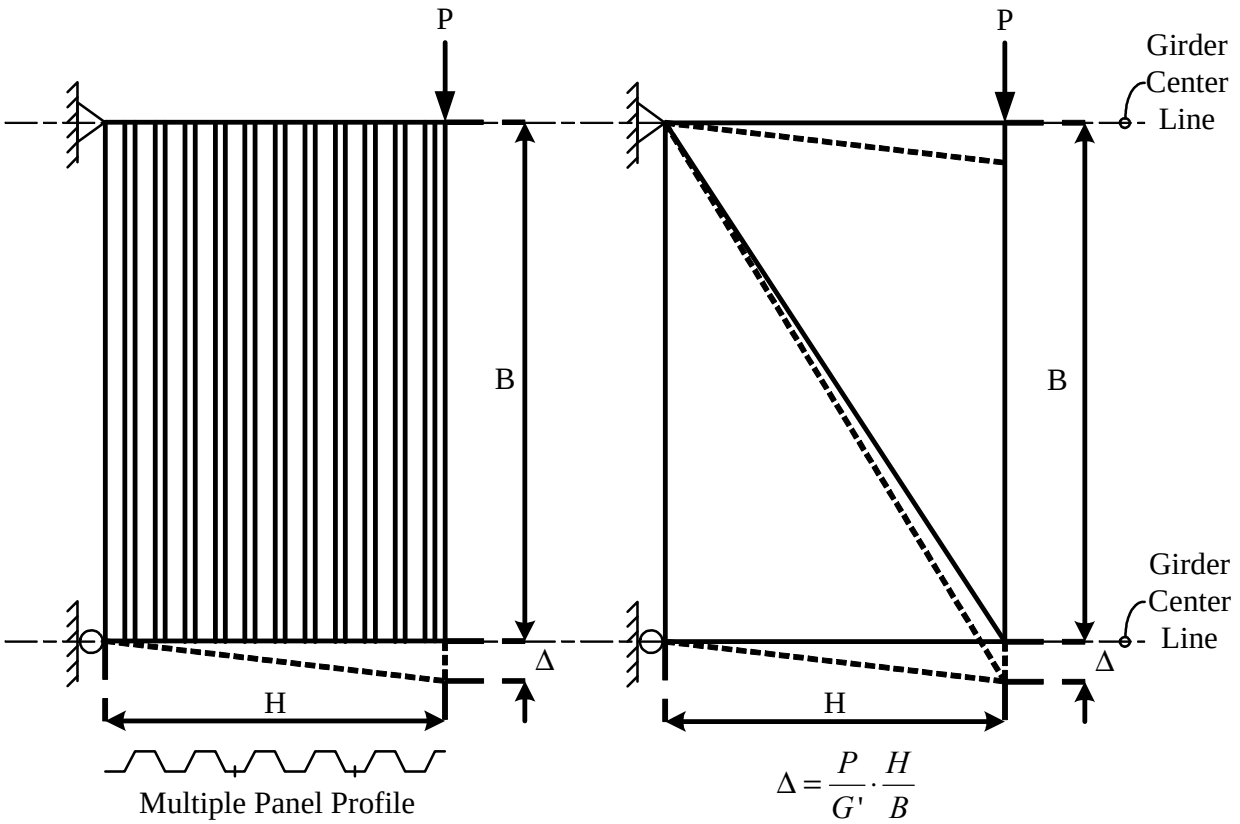

a) SIP Diaphragm System

b) Analogous Truss Model

Figure 4.14- Truss Analogy (SDI 1991)

The deflection of the analogous truss (see Figure 4.14b) can be obtained using the dimensions of the truss and the shear stiffness of the diaphragm via the relationship in Figure 4.14b. However, this example is only for a truss with a single diagonal. It was previously discussed that the SIP truss system used in the ANSYS models would employ two diagonals i.e., an x-frame truss. In order to obtain similar shear stiffness for the x-frame truss, models were created in SAP2000 based on the analytical model illustrated in Figure 4.15. A sample calculation of the properties used in the modeling of the x-brace system is contained in Appendix M.

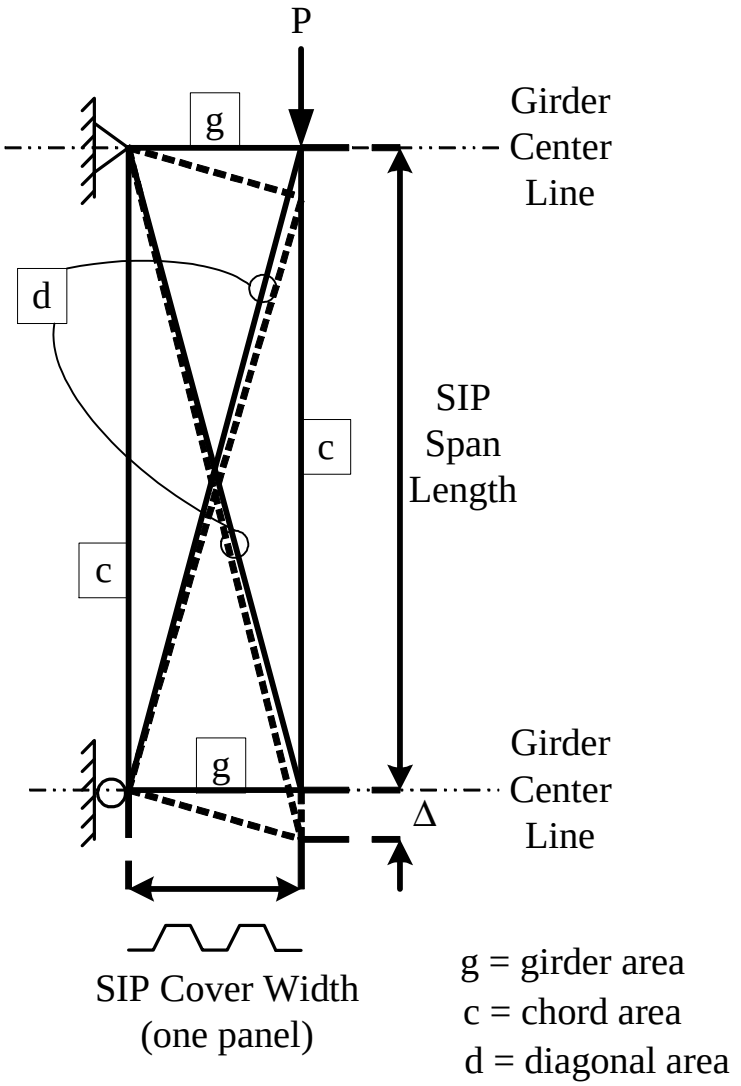

Figure 4.15- Analytical Truss Model of SIP Form System

Once the sizes of the diagonals were determined, all of the members of SIP truss system were known and could be implemented into the ANSYS models. Figure 4.16 is a plan view picture of an ANSYS model with the SIP truss system in place.

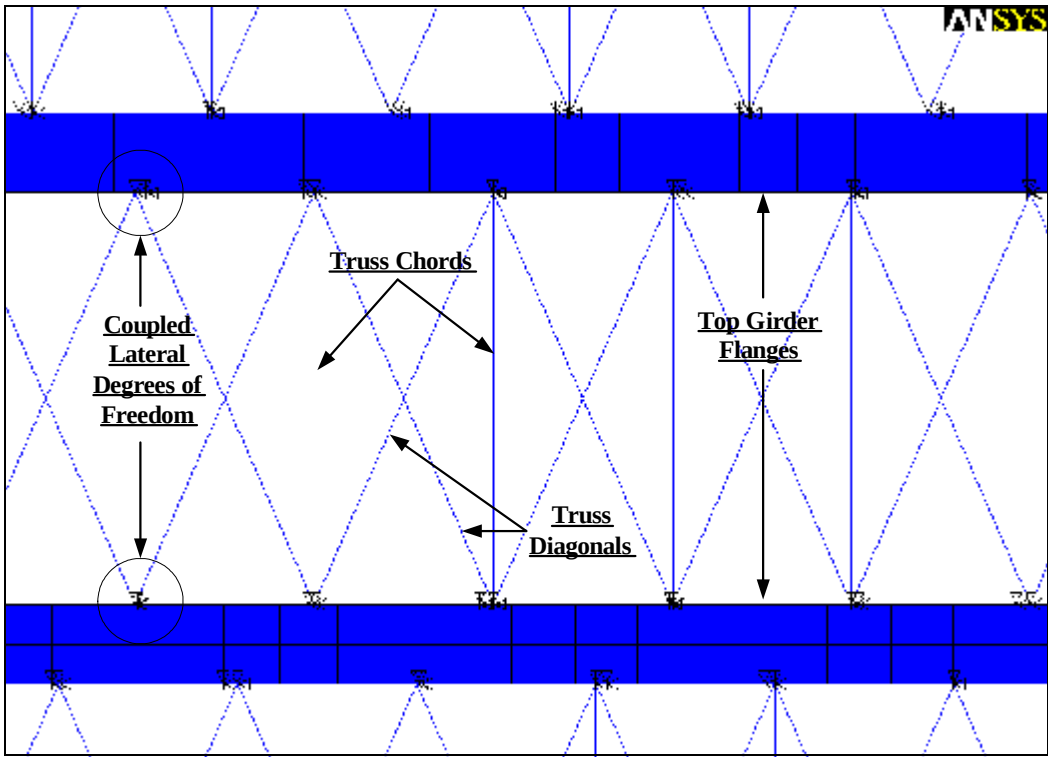

Figure 4.16- Plan View Picture of SIP X-frame Truss Models

4.3.4 Concrete Deck and Rigid Links

4.3.4.1 General

Finite element bridge models with concrete decks are required for composite analysis. Composite analysis was only conducted on structures with sequenced pours, i.e. continuous span bridges.

4.3.4.2 Modeling Procedure

The concrete deck is modeled utilizing the same procedure as used for the plate girders. First, keypoints are created an offset distance above the top girder flange, at the centerline of the concrete slab. Areas are then generated to join the keypoints and create the simulated slab. Rigid link elements are then created between the existing keypoints of the

slab and the existing keypoints of the girder (at the intersection of the web and top flange). The modeling approach is presented in Figure 4.17.

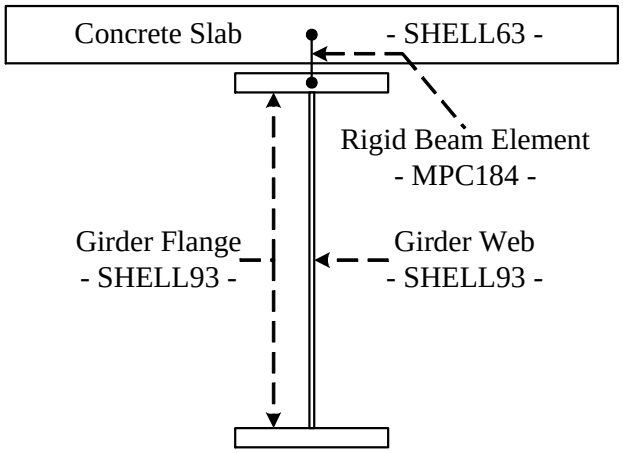

Figure 4.17: Schematic of Applied Method to Model the Concrete Slab

Four node shell (SHELL63) elements are utilized for the entire slab in the bridge models and two node rigid beam (MPC184) elements represent the links between the girders and slab to simulate composite behavior. For both element types, each node has six degrees of freedom. The thickness properties applied to the slab elements are attained directly from the bridge construction plans. The resulting shell element stiffness bears no consideration to the steel reinforcement or its possible bond development with the concrete. Figure 4.18 depicts a finite element model in which a bridge segment has been modeled as a composite section, complete with concrete slab elements. Note that the SIP forms are absent for clarity.

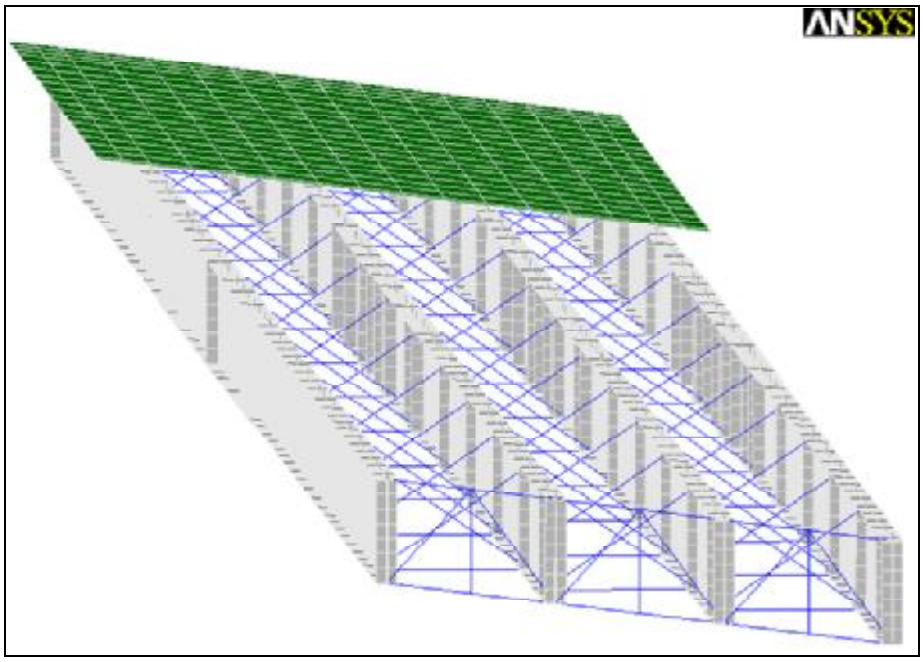

Figure 4.18: Finite Element Model Including a Segment of Concrete Deck Elements

4.3.4.3 Partial Composite Action

Partial composite action develops on a portion of the span length as the deck concrete is placed from one end of the bridge to the other. The longer the duration of the deck casting, the more composite action develops. To represent the onset of partial composite action in the ANSYS models, a step-by-step sequence of loadings simulating the progression of the concrete deck placement was incorporated. The stiffness along the bridge span was also varied in each loading sequence by applying different elastic properties to the concrete deck. This was done to simulate the early gain in stiffness of the wet concrete. The deflections from each of these loading stages were then added together using the method of superposition. Figure 4.19 illustrates the typical procedure used in the ANSYS models to mimic the progressive loading and development of composite action that occurs during an approximate 8 hour deck casting. Equation 2.1 was used to calculate the elastic modulus of

concrete for the varying degrees of concrete stiffness at each time interval during the concrete deck placement.

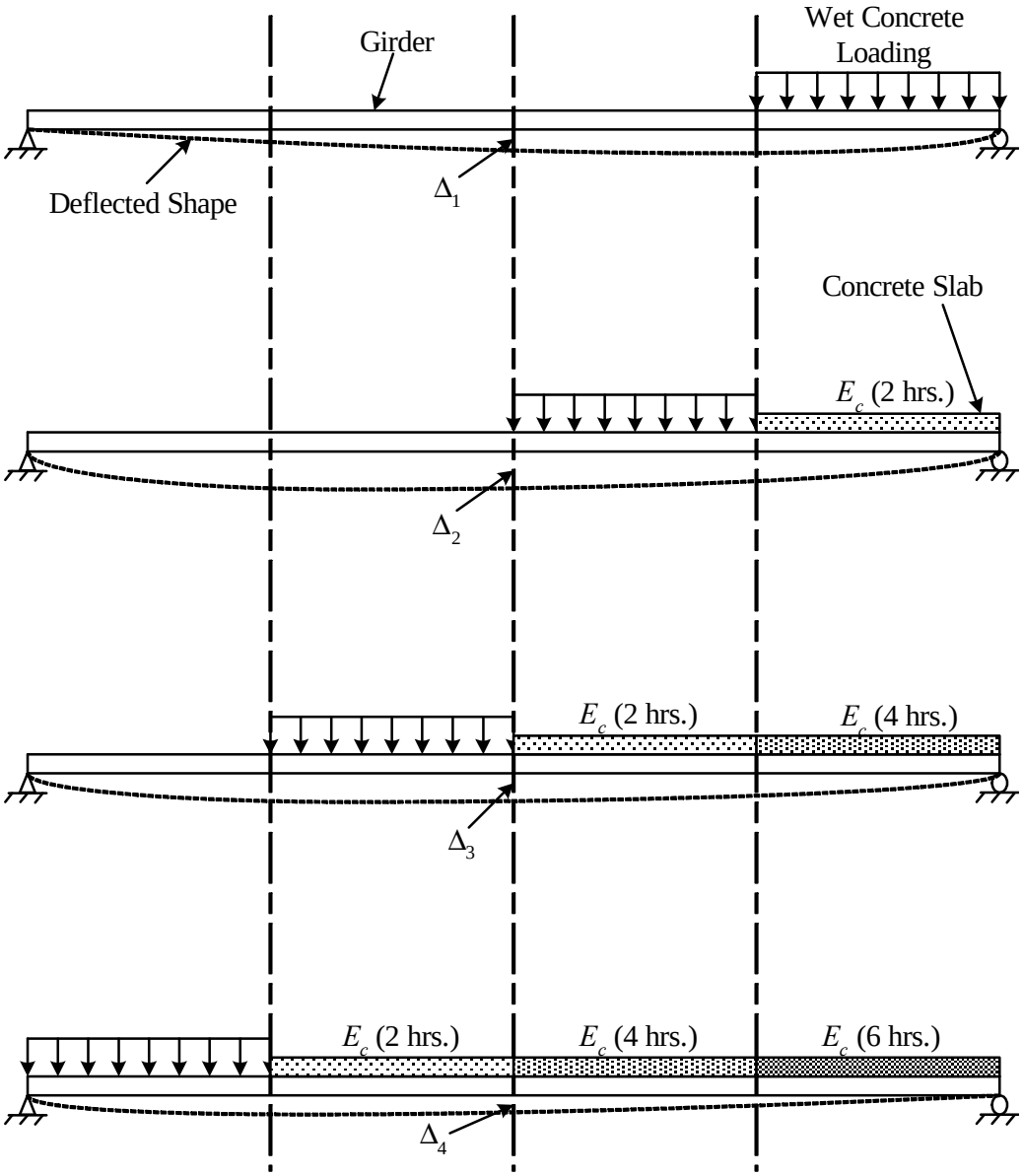

Figure 4.19- Method of Superposition Used to Mimic the Onset of Composite Action

The first loading case illustrated in Figure 4.19 represents the point when the wet has reached the one-quarter point along the span of the bridge. At this point, no composite action is considered to have developed thus the first segment of the concrete deck slab was not modeled. The second loading case is when the wet concrete has reached mid-span and the concrete on the first quarter span has gained stiffness equivalent to that of two hours (calculated using Equation 2.1). The loading was continuously incremented in the ANSYS models according to Figure 4.19 and the deflections were recorded for each stage. The total deflection resulting from load sequencing was obtained by superimposing all of the deflections from each stage.

4.3.4.4 Full Composite Action

To ensure that the preliminary ANSYS bridge models were providing realistic results, two of the bridges were modeled with the entire concrete deck slab modeled to represent full composite action. Full composite action between the steel girders and the concrete deck slab occurs when the concrete has reached adequate stiffness to safely support the service loads of a bridge. To represent this in the ANSYS models, the deck slab was given an elastic modulus equivalent to a normal strength concrete at 28 days calculated using equation 4.1.

The calculated loads were applied to the girders in the ANSYS models as previously discussed with the deck slab modeled as fully composite. This is not a realistic loading case because all deflections resulting from the concrete deck pour would have already occurred by the time the deck slab and girders are fully composite. However, this was done to create a "theoretical" minimum deflection that could be used as a lower bound for the ANSYS bridge models. The upper bound deflections would be provided by the completely non-composite loading case where the loads were applied to the girders without modeling the concrete deck

slab. In both cases where full composite action was modeled, the field measured deflections were found to be within the aforementioned upper and lower bounds. Therefore, it was determined that the previously discussed modeling techniques were suitable for this research.

4.3.5 Load Calculation and Application

Calculations of the dead load provided by the deck concrete were performed based on field measured dimensions of the concrete deck slabs. These dimensions included the depth of the concrete slab between each girder and the overhang width for each exterior girder. Loads were calculated for each interior girder based on the slab thicknesses and tributary widths equal to the girder spacing obtained from the construction plans. The tributary width for the exterior girders included the overhang width and one-half of the typical girder spacing. These loads were represented with uniform pressures applied to the surface areas of the top girder flanges in the ANSYS models.

4.4 Modeling Procedure

The large majority of finite element bridge models were created utilizing the MATLAB preprocessor program. The following discussion includes: automated model generation utilizing the MATLAB preprocessor program, MATLAB limitations, additional modeling performed manually, model adjustments specific to individual bridges, and MATLAB modeling validation. Note: the same basic modeling technique is followed to manually created complete bridge models within ANSYS.

4.4.1 Automated Model Generation Using MATLAB

4.4.1.1 General

The MATLAB preprocessor program is comprised of thirty eight files designed to collect data from bridge input files and generate two corresponding output files. A complete

collection of these files can be found in the appendix of Fisher (2006). Two things were required to ensure an appropriate transition from MATLAB to ANSYS. First, it was imperative that the program adequately "write" commands to the output files so that ANSYS could process them. Second, the code files were programmed to output a specifically ordered command list to ensure the proper modeling technique.

4.4.1.2 Required Input

The MATLAB program requires many specific characteristics of each bridge as input, including:

- Skew angle
- Number of girders
- Girder spacing
- Slab overhang lengths (separately for each side)
- Girder span length (one for each span for continuous span bridges)
- Bridge type (simple span, two-span continuous, three-span continuous)
- Build-up concrete thickness
- Slab thickness
- Elastic Modulus and Poisson's ratio of steel and concrete
- Field measurement locations
- Construction joint locations
- Number of girder sections and the z-coordinate location at which the section ends
- Width and thickness of the top and bottom flanges for each girder section
- Height and thickness of the web

- Number of bearing and intermediate web stiffeners, their thicknesses, and their z-coordinate location along the span
- Connector plate thickness, their spacing, and the z-coordinate location of the first one
- Type of intermediate cross frame, end bent diaphragm and interior bent diaphragm
- Areas and moments of inertia for all cross frame members
- SIP forms spacing
- SIP member areas
- SIP node couple tolerance

4.4.1.3 Generated Output

The MATLAB preprocessor program writes commands to two output files that are compatible with ANSYS. One output file is comprised of the commands to model the entire bridge. The second includes the commands issued to model the SIP forms. As the output files are thousands of ANSYS command lines apiece, creating partitioned output files helped keep the information organized.

The output is generated to emulate a specific modeling procedure, listed as follows:

- Material property sets are defined for the steel and concrete.
- Finite element types are defined. (SHELL93, BEAM4, LINK8, etc)
- Real constant sets are defined, including: plate thicknesses, truss areas, beam moments of inertia, etc.
- Keypoints are created for the girders, web stiffeners and connector plates.

- Areas are generated between the keypoints to represent the girders, web stiffeners and connector plates.
- Keypoints and areas are created for the concrete slab.
- Attributes are applied to all of the modeled areas (attributes include the element type and real constant set); then they are sized appropriately and meshed to create the girder and slab elements.
- Rigid link lines are generated between the slab keypoints and the girder keypoints.
- Lines are created between existing and newly originated keypoints to generate all three cross frame types, as applicable.
- Attributes are applied to the modeled lines; then they are sized and meshed to create the rigid link and cross frame elements.
- SIP metal deck forms are directly generated with nodes and elements, thus requiring no sizing or meshing.
- Nodes of the SIP form are coupled laterally to existing top flange nodes and checked to ensure finite element compatibility.

4.4.2 Additional Manual Modeling Steps

To complete each model, the loading conditions must be applied. First, the support boundary conditions are defined. The nodes along the bottom of the bearing stiffeners, which is the centerline of actual bearing, are restrained appropriately to simulate field boundary conditions. Pinned (or fixed) supports require restraints in all three translational directions and in rotational directions about the girder's vertical and longitudinal axes. Roller (or expansion) supports are similarly modeled except that the nodes are allowed to translate along the girder's longitudinal axis.

In addition to manually changing certain aspects of the finite element models, there is one component that must be inspected for consistency. As the SIP metal deck forms' nodes are coupled to existing nodes of the top flanges, it is possible for other flange nodes to be located within the specified tolerance, resulting in a three-node couple rather than the desired two-node couple. If such coupled sets exist, a separate MATLAB file should be run to correct this problem. The generated output is copied from the MATLAB command window and pasted into the ANSYS command prompt window. Generally, an estimated 20 percent of the models created by the program require the coupled node sets to be revised.

4.5 Summary of Modeling Assumptions

The assumptions used in the creation of the finite element bridge models were made as an overall effort to make the models practical to construct while maintaining as much detail about the bridge geometry as possible. The following list is an overview of the assumptions used in the development of the ANSYS finite element bridge models:

- The centerline distances between the top and bottom girder flanges were calculated using the cross-sectional dimensions of the mid-span location of the bridges (the largest cross-section).
- The geometry of the stiffener and cross-frame connector plates was simplified to facilitate a more accurate represent of their connection to the girder flanges by using the outer edge flange nodes as the corner nodes of the stiffener/connector plates. This resulted in a tapered vertical outer edge of the stiffener/connector plates in cases where the top flange and bottom flanges were of different width.
- The girders were assumed to be supported along the line of nodes that were coincident between the bottom flange and the bottom edge of the bearing stiffeners as

opposed to an area of the bottom flanges that is supported with pot bearings or elastomeric bearing pads.

- The cross-frame members were assumed to behave as tension-compression members that were connected to the intersections of the girder flanges and the web. The actual point of connection is offset from the centerline of the girder web and from the centerline of the girder flanges.
- All bridges were assumed to have the same SIP form connection to the top girder flanges. The properties of the individual form panels were based on each individual bridge but the same supporting angle and screw type was assumed for each bridge.
- The dead loads of the deck concrete was assumed to act as uniform pressures applied to the top girder flanges of the finite element models.
- It was assumed that the load values applied to the finite element models were only accurate estimations of what occurred in the field based on calculations using the field measurements of the in-place deck slab thickness.
- The affect of geometric non-linearity (affect of large displacements and strains) was assumed to be negligible in each bridge. The results from one bridge model indicated that using this option in ANSYS had virtually no affect on the predicted deflections.
- The procedure used to model partial composite action along the bridge span did not account for the affect of rebar embedded in the deck concrete. The elastic modulus of fresh concrete was used in conjunction with the nominal dimensions of the deck slab obtained from the construction plans to simulate partial composite action in the finite element models.

4.6 Deflection Results of ANSYS Models

The ten bridges monitored during this research were initially modeled with and without the SIP metal deck forms. The model deflections were tabulated and graphed and are included in the following subsections. The tables incorporate total super-imposed deflections for the continuous span bridges at each location of predicted maximum deflection; only the mid-span deflections are included for the simple span structures. A complete deflection summary for all ten models is available in Appendices C-L.

4.6.1 No SIP Forms

Table 4.1 presents the girder deflection results for the ANSYS bridge models not including the SIP forms.

Table 4.1: ANSYS Predicted Deflections (No SIP Forms, Inches)

	Span Location	Girder A	Girder B	Girder C	Girder D	Girder E	Girder F	Girder G
Eno	Mid-Span	8.98	8.70	8.40	8.07	7.71		
Bridge 8	Midspan	3.98	4.16	4.28	4.29	4.17	3.99	na
Avondale	Mid-Span	5.39	5.54	-	5.79	-	5.72	5.57
US-29	Mid-Span	4.04	4.59	-	4.55	-	4.55	4.04
Camden NB	Mid-Span	3.82	3.81	3.87	-	3.79	3.80	na
Camden SB	Mid-Span	3.22	3.28	-	3.46	-	3.29	3.22
Wilmington St	Midspan	2.74	3.41	3.60	3.56	3.72	na	na
Bridge 14	4/10 Span A	1.00	1.03	1.05	1.04	1.00	na	na
	6/10 Span B	1.35	1.36	1.37	1.36	1.34	na	na
Bridge 10	4/10 Span B	1.79	1.78	1.82	1.92	na	na	na
	6/10 Span C	1.26	1.18	1.14	1.15	na	na	na
Bridge 1	4/10 Span A	1.56	1.55	-	1.55	-	1.53	1.53
	4/10 Span B	3.79	3.79	-	3.81	-	3.79	3.79
	35/100 Span C	1.39	1.41	-	1.43	-	1.46	1.47

Mid-span deflections of the simple span models and “span B” deflections of the continuous span models in Table 4.1 have been plotted in Figure 4.20. The deflected shapes

of the continuous span models appear essentially straight. Contrastingly, the interior girders of Bridge 8 deflect more than the exterior girders. Unequal exterior girder loads on the Wilmington St Bridge model result in a slanted deflected shape, but the three leftmost girders (A-B-C) follow the general trend of Bridge 8.

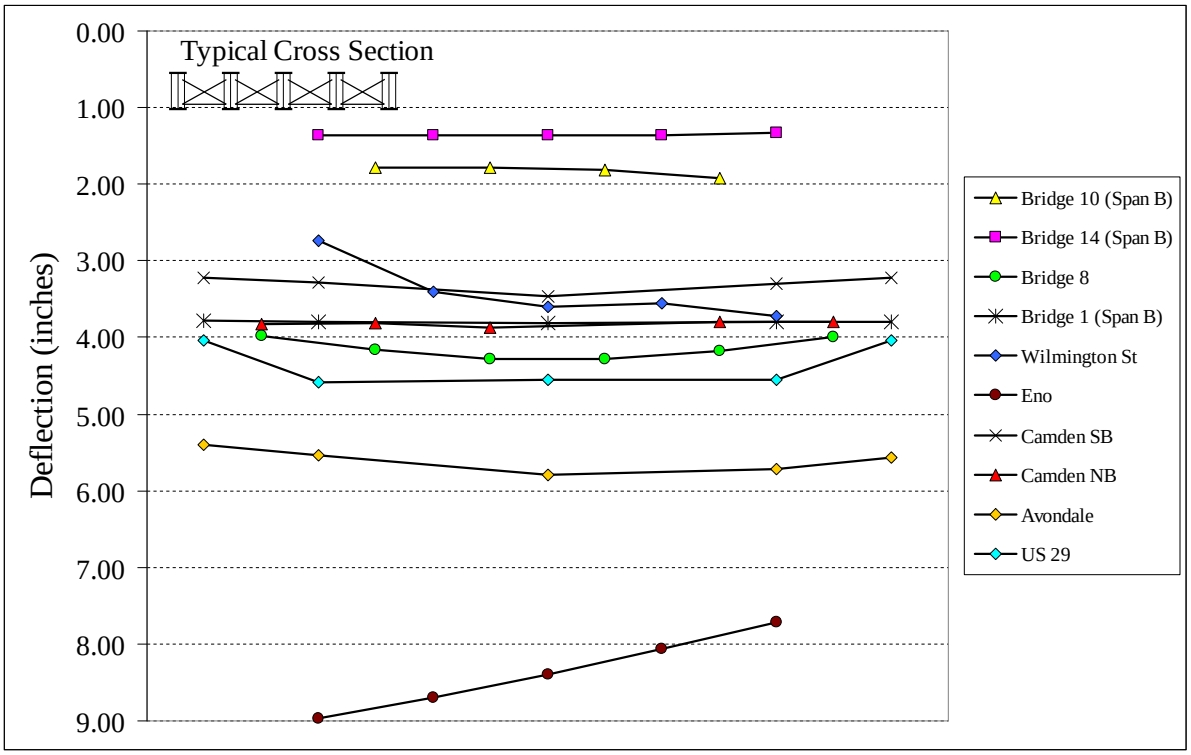

Figure 4.20: ANSYS Deflection Plot (No SIP Forms)

4.6.2 Including SIP Forms

Table 4.2 presents ANSYS girder deflections for models including the SIP forms. Once more, mid-span and "span B" deflections in Table 4.2 have been plotted in Figure 4.21. Similar deflected shapes have remained for the continuous span models, but differences exist in the deflected shapes of the simple span models. Although the interior girders of Bridge 8 continue to deflect more than the exterior girders, the deflected shape has flattened

considerably. The most obvious deviation is apparent in the Wilmington St Bridge model as the shape has effectively flipped with the middle girder deflecting less than the exterior girders.

Table 4.2: ANSYS Predicted Deflections (Including SIP Forms, Inches)

	Span Location	Girder A	Girder B	Girder C	Girder D	Girder E	Girder F	Girder G
Eno	Mid-Span	8.79	8.69	8.59	8.46	8.46	na	na
Bridge 8	Midspan	4.11	4.14	4.17	4.17	4.14	4.11	na
Avondale	Mid-Span	5.36	5.38	-	5.49	-	5.57	5.69
US-29	Mid-Span	4.53	4.42	-	4.46	-	4.48	4.51
Camden NB	Mid-Span	3.94	3.62	3.50	-	3.64	3.94	na
Camden SB	Mid-Span	3.39	3.14	-	3.07	-	3.11	3.335
Wilmington St	Midspan	3.20	3.02	3.03	3.28	3.86	na	na
Bridge 14	4/10 Span A	1.02	1.03	1.04	1.03	1.01	na	na
	6/10 Span B	1.36	1.35	1.35	1.35	1.35	na	na
Bridge 10	4/10 Span B	1.74	1.72	1.80	1.97	na	na	na
	6/10 Span C	1.30	1.17	1.11	1.11	na	na	na
Bridge 1	4/10 Span A	1.58	1.55	-	1.53	-	1.52	1.54
	4/10 Span B	3.82	3.80	-	3.78	-	3.79	3.81
	35/100 Span C	1.35	1.38	-	1.42	-	1.48	1.52

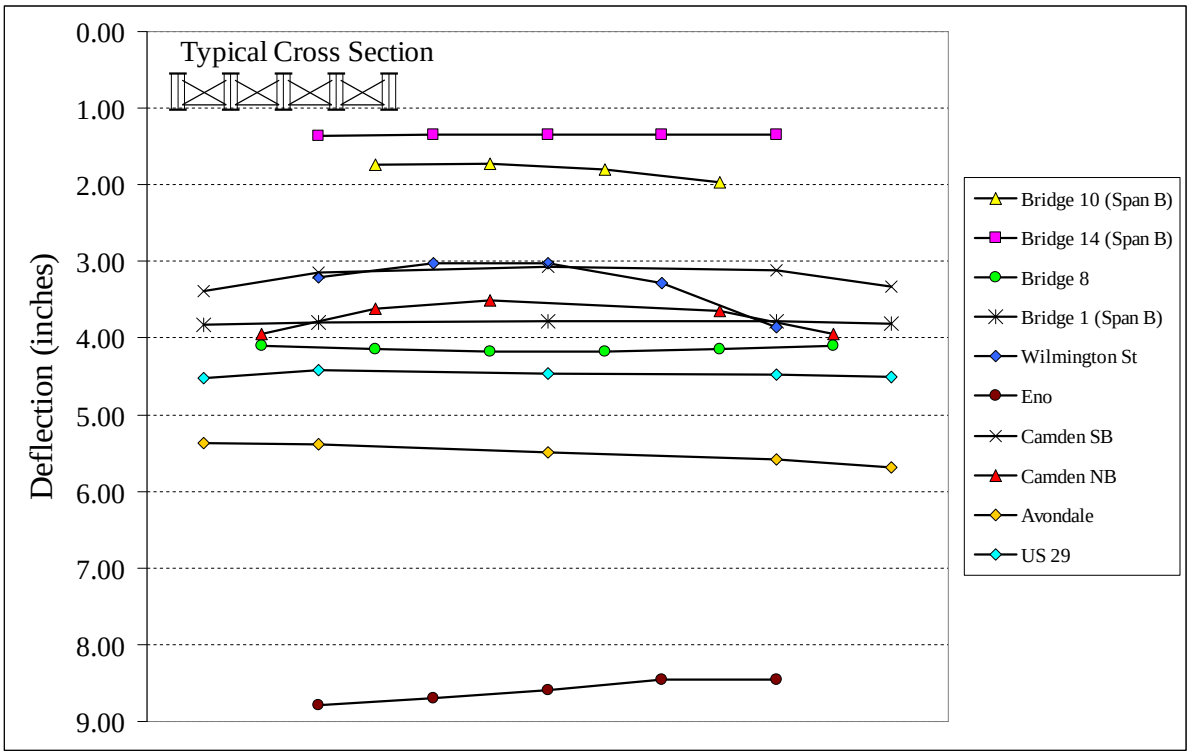

Figure 4.21: ANSYS Deflection Plot (Including SIP Forms)

4.7 Summary

Finite element bridge models have been generated in ANSYS to simulate the dead load deflection response of skewed and non-skewed steel plate girder bridges. The modeling technique includes the following detailed bridge components: plate girders (girder, bearing stiffeners, intermediate web stiffeners, and connector plates), cross frames (intermediate cross frames, end bent diaphragms and interior bent diaphragms), SIP metal deck forms, and the concrete deck. In generating the finite element models, several assumptions were made regarding the detailed bridge geometries in an effort to maintain a practical modeling technique. The resulting method was then applied to all ten field measured bridges. Each bridge was created with and without the SIP forms and the results have been discussed.

To greatly reduce the time and effort spent modeling, a preprocessor program was developed in MATLAB and utilized to generate the finite element models in ANSYS. The program processes a single input file (modified by the user) and creates two individual output files. The output files contain model generation commands that are copied and pasted into ANSYS. Following a few additional adjustments, a detailed finite element model is ready for analysis.

Development of the MATLAB program to quickly generate finite element models proved very beneficial to the research project. Utilizing the preprocessor program, an extensive parametric study was conducted to analyze hundreds of very detailed finite element models. Section 5 presents a discussion on the parametric study and the development of the simplified method.

5.0 Investigation of Simplified Modeling Techniques

5.1 Introduction

As part of this research, SAP2000 was used to create analytical models of five steel plate girder bridges. The primary propose of the modeling was to develop a modeling technique that was not as complex as the previously presented three-dimensional ANSYS models. The developed modeling techniques were compared to the ANSYS results and the field measured results.

5.2 General

Structural Analysis Program (SAP) is a finite element analysis program developed by the Computer and Structure Inc. (CSI). CSI has been developed several version of SAP and it has become one of the oldest finite element programs currently on the market. By using the interface command, SAP is also one of the simplest structure analytical programs that have been used from the engineer all over the world. SAP2000 is the latest release of the SAP series of computer program. In this report, SAP2000 version 9 was used to create all bridge models.

SAP2000 version 9 accommodate user to work easier and faster with new enhanced graphical user interface, such as object creation by point, line, area extrusions into line, area and solid, convenient unit conversion, allowing properties assignments during on screen object creation , and etc. In addition, SAP2000 version 9 was chosen to be used in this study because of the new function of the shell element allowed the user create orthotropic shell element. By using different modification factors multiply to the stiffness of the shell element, the user can create the shell element that has different stiffness in different direction. This function was used to model the SIP forms that will be discuss later.

To create bridge models, all material properties used to create models in this report were linear elastic. All modeled steel members, the elastic modulus was 29000 ksi and the Poisson's ratio was equal to 0.3. The yield strength of the steel member was assigned according to the real yield strength of the member in the bridge plan. Since the vertical deflections of the bridge structure were recorded due to the vertical dead load of the concrete deck only, the modification factor for the dead load in SAP2000 was set equal to zero.

The remaining sections in this section will outline the modeling techniques developed and each component of the model. Four techniques, two-dimensional grillage model, three dimensional model, three-dimensional with frame SIP, three-dimensional with shell SIP, will be discussed first, then the components of models will be in the following sections. These components included steel plate girder, cross frame, stay-in-place form, load calculation, and the composite action between concrete deck and steel plate girders. The results from the models will also be presented at the end of this section.

5.3 Types of Models

Four simplified modeling methods were created in this study. The development of the modeling methods started from the basic two-dimensional grillage model. Each steel plate girder was modeled as single girder frame element. The cross-frame members were transferred to the simulated beam modeled as a single frame element. Figure 5-1 shows the sample of the two-dimensional grillage model of Eno River Bridge. The method used to transfer the cross frame to the frame element will be discussed later.

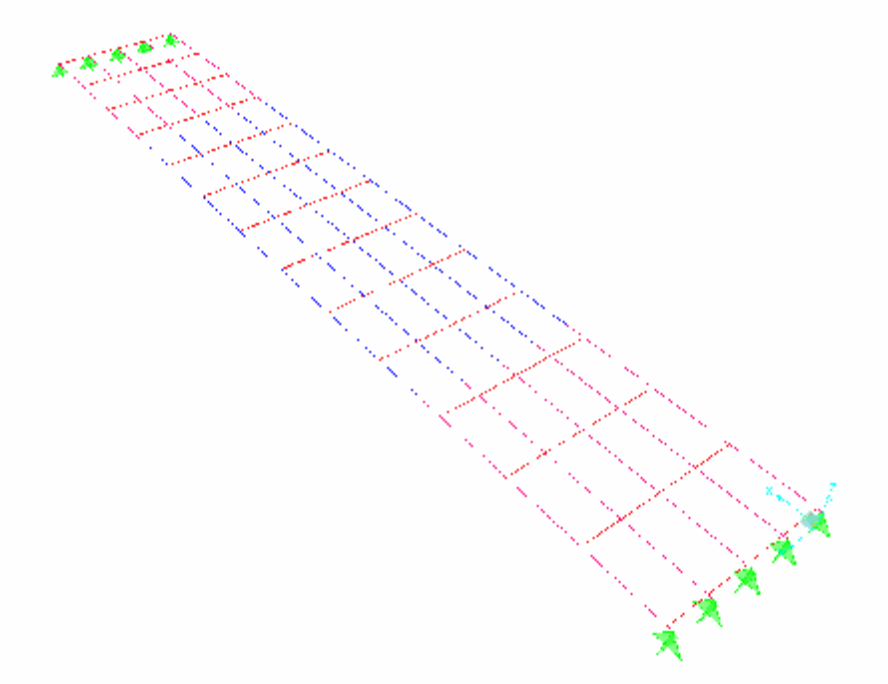

Figure 5-1 Two-Dimensional Grillage Model of Eno River Bridge

The three-dimensional analytical model was developed in the next step. Instead of using a single frame element simulated as the entire cross frame, the three-dimensional cross frame was created. The rigid links were connected to the frame elements to simulate the three-dimensional cross frame connected to the girders as shown in Figure 5-2.

SIP forms were included in the third modeling method. To represent the load transferring ability of the SIP form, tension-compression frame elements were used to create the simulated SIP forms. To represent the load transferring between girders and SIP forms, the frame elements as SIP form were connected to the girders by using rigid link elements as shown in Figure 5-3.

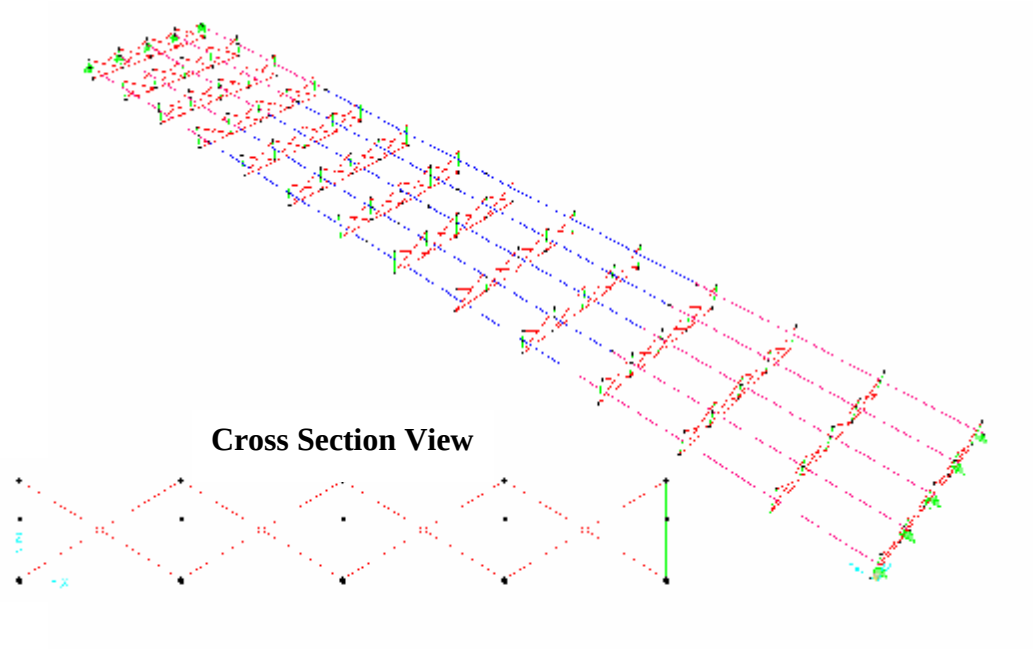

Figure 5-2 Three-Dimensional Model of Eno River Bridge

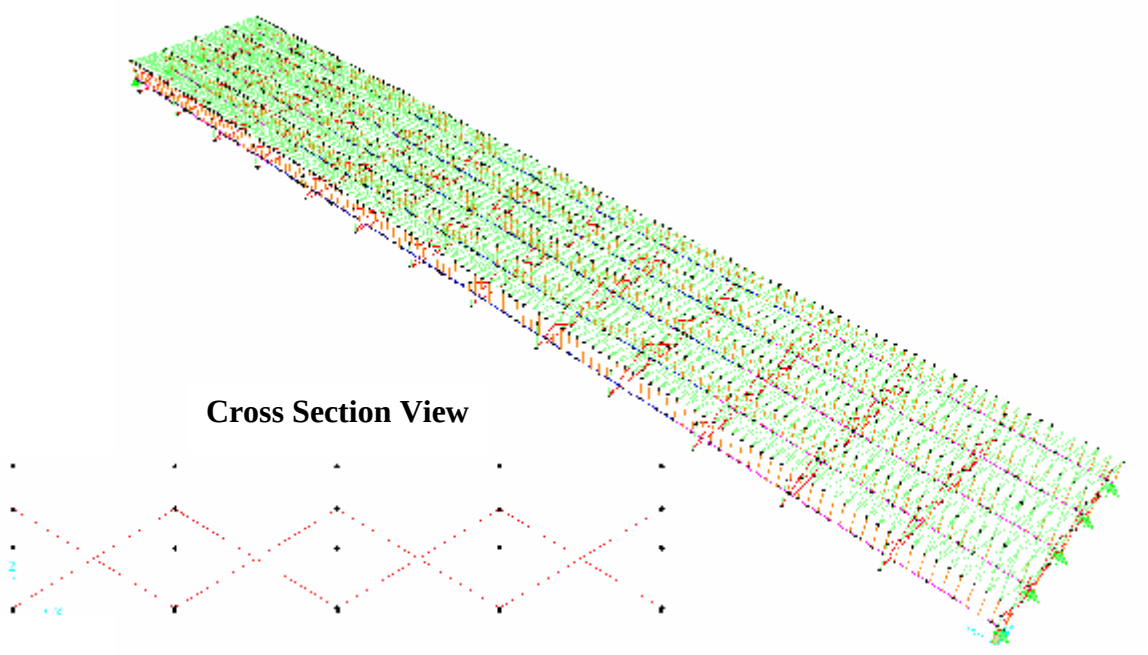

Figure 5-3 Three-Dimensional with SIP Frame Element Model of Eno River Bridge

The last step of the modeling method was developed by creating shell elements as the SIP forms. The compression and tension-transferring load ability composite with flexural

behavior of the SIP forms were calculated and transferred to the shell element properties. Again, the shell element was connected to the rigid link element to represent the composite action between SIP forms and girders. Figure 5-4 shows the picture of the three-dimensional model included shell elements as SIP forms.

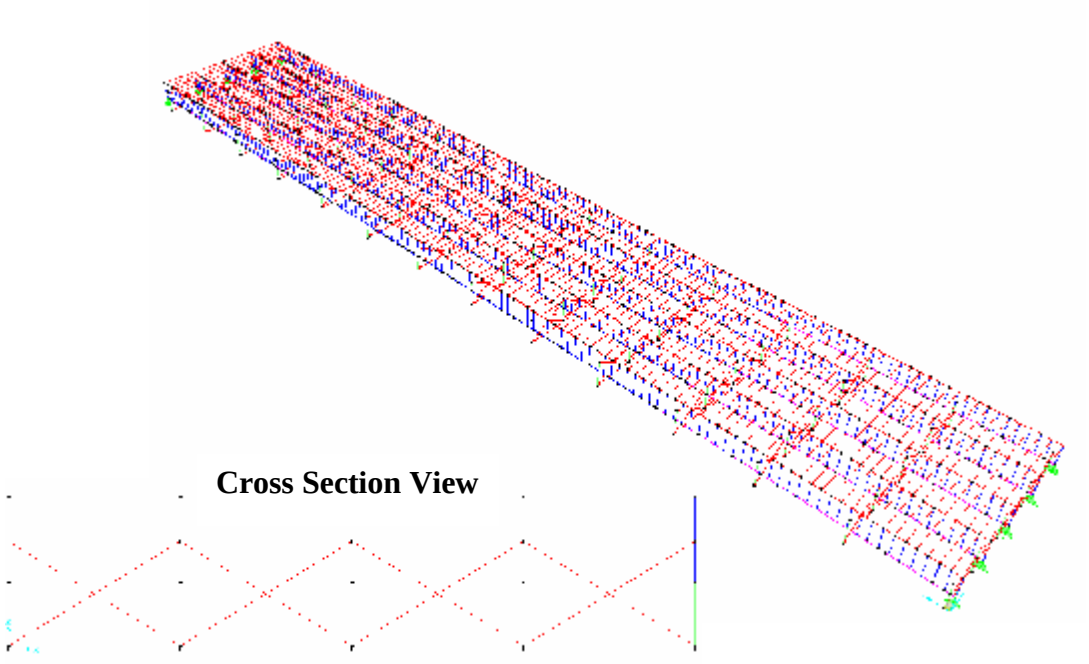

Figure 5-4 Three-Dimensional with SIP Shell Element Model of Eno River Bridge

5.4 Model's Component

5.4.1 Steel Plate Girders

The steel plate girder was created by using nodes to outline the length of the girder. By assigning nodes at both end-support points, the reference points of the edge of the girder were made. Since most of the steel plate girders were designed to increase the cross section at the mid location along span in order to increase the moment capacity; nodes need to be assigned at the change-section point. In addition, SAP2000 Version 9 is able to report the deflections only at nodes; nodes also need to be assigned at the same location as measured

points. Frame elements were used to connect each node together as the girder. (see Figure 5-5) Girder sections obtained from the bridge plan were assigned to the frame elements. By assuming that the frame element was laid out at the location of the centroid of the real steel plate girder sections, the location of the frame element will be used to refer to the locations of the cross frame and length of the rigid link elements in the following section.

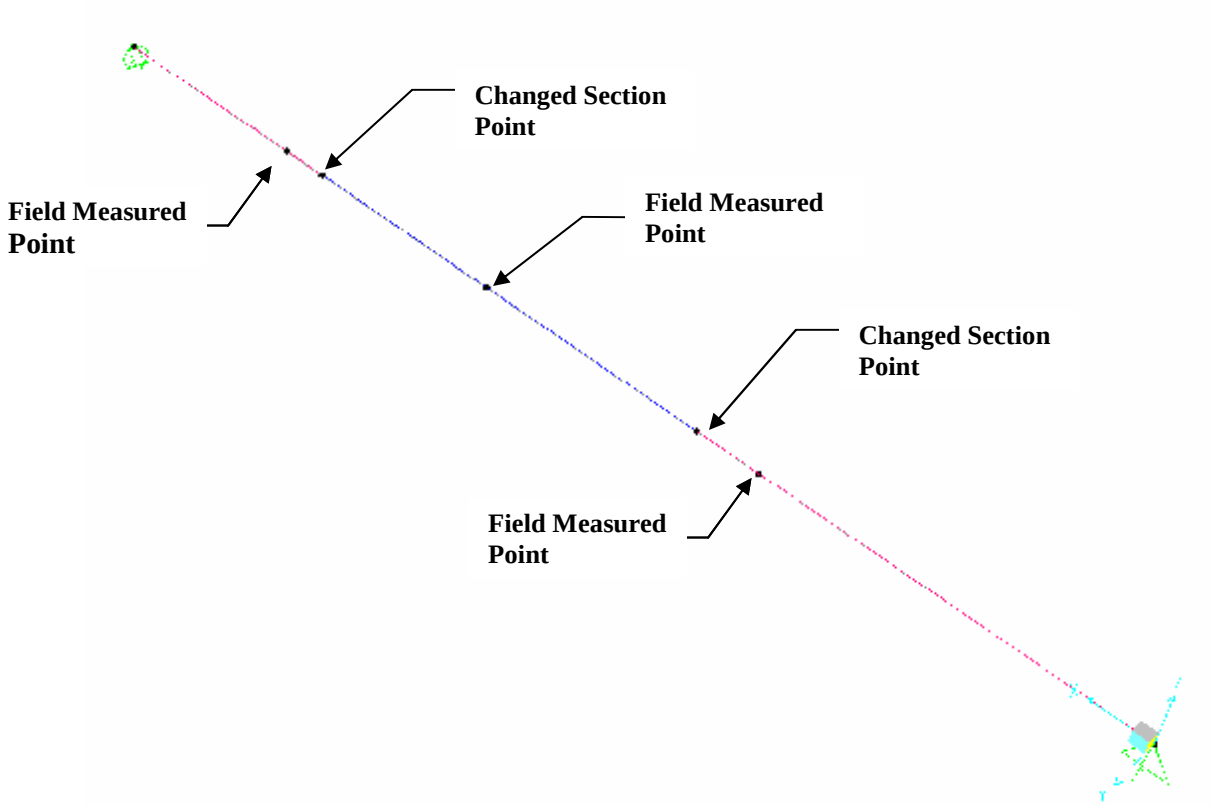

Figure 5-5 Single Girder Model

This modeling method was developed to be used for any girder configuration. To verify this modeling technique, the simple span girder was given the constant section for entire the model and subjected to uniformly distribution loads in order to compare the vertical deflection with the results from the hand analysis based on beam theory. In addition,

steel plate girder SAP model that has an unequal cross section along the span was also verified by comparing the results with the results from the ANSYS finite element model.

Ratios were used to compare the results from the analytical models to the results from the SAP models. As a result, the ratio between SAP2000 without shear deformation and the hand analysis based on beam theory was approximately one. (approximately zero percent difference). For the cross section changed along span of the girder, the ratio between result from SAP2000 model and ANSYS finite element model was 1.012 (approximately 2% different). Therefore, it was concluded that the accuracy of the girder modeling technique used in SAP2000 was adequate to use for the bridge models.

5.4.2 Cross Frames & Diaphragms

Intermediate cross frames and end bent diaphragms were modeled by using frame elements. The frame elements as cross frame were rigidly connected to the girder at the same location of the cross-frame laid out in the bridge plan. Two types of the modeling techniques were created to model the cross frame, two-dimensional simulated beam and three-dimensional cross frame, as explained in the following sections.

5.4.2.1 Two-Dimensional Simulated Beam

For the first developed modeling technique, the entire cross frame was transferred to a single beam element connected to bridge girders as shown in Figure 5-6. To calculate the cross section of the simulated beam element, SAP analytical truss model was created to compare with the hand analysis. By using the same geometry of the cross frame, truss model was created by restrained both nodes on the left sides and symmetrically loaded on nodes on the right side. The vertical deflection of the node on the right side was recorded and used to be the reference deflection value for the hand analysis.

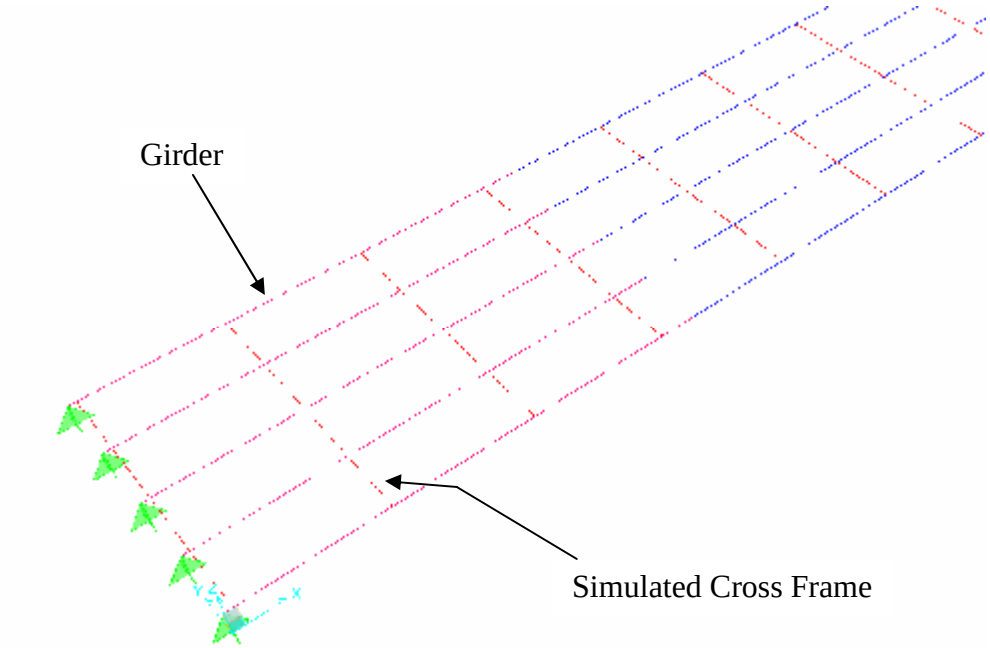

Figure 5-6 SAP, Simulated Beam as Cross Frames

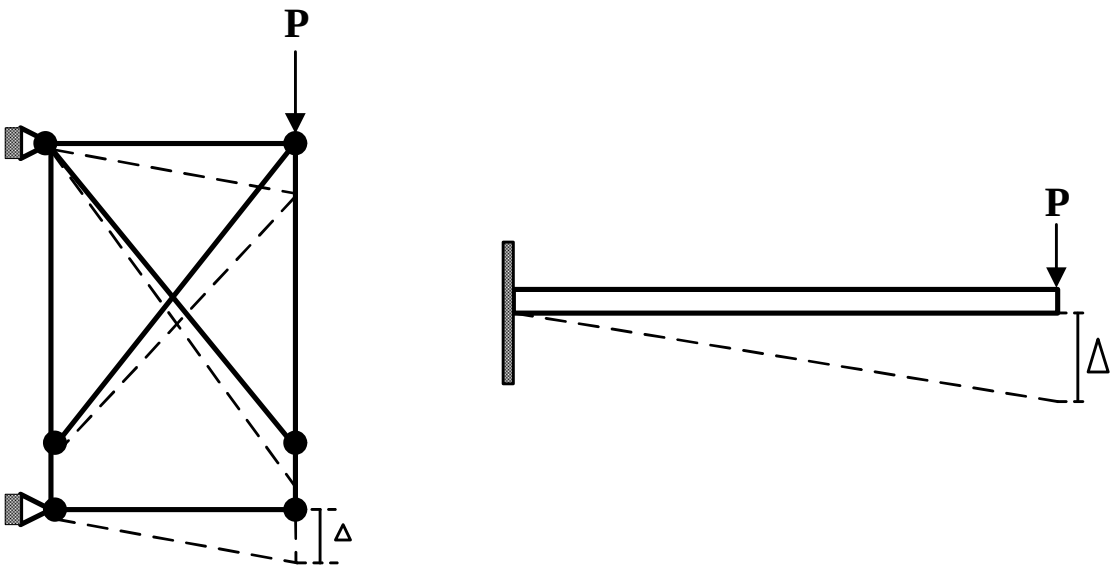

a) Cross-Frame Model, SAP

b.) Simulated Cross Beam, Beam Theory

Figure 5-7 Simulated Beam Element Compared with SAP Cross Frame Analysis

For simulated beam hand analysis, a fixed-end simulated beam was subjected to the same load condition to compare the vertical deflection with the results from the truss models. The length of the simulated beam was set equal to the width of the real cross frame. (Figure 5-7) The analysis based on beam theory was made in order to get the cross section of the beam. Cross section of the simulated beam obtained by adjusting the cross section until the analysis gave the same deflection.

5.4.2.2 Three-Dimensional Simulated Cross Frame

Frame elements were used to create the three-dimensional simulated cross-frame. The cross frames were typically consisted of L-shape steel angles, whereas the end bent diaphragms were consisted of C or MC shape and WT shape steel members. In order to represent the model behavior similar to the real bridge structure, the same cross sections of the cross-frame members were used to create the model. To represent the force and moment transferring behavior of the cross-frame, rigid link elements were used to connect the frame element to the girder (see Figure 5-8). The detail of the rigid link was explained as followed.

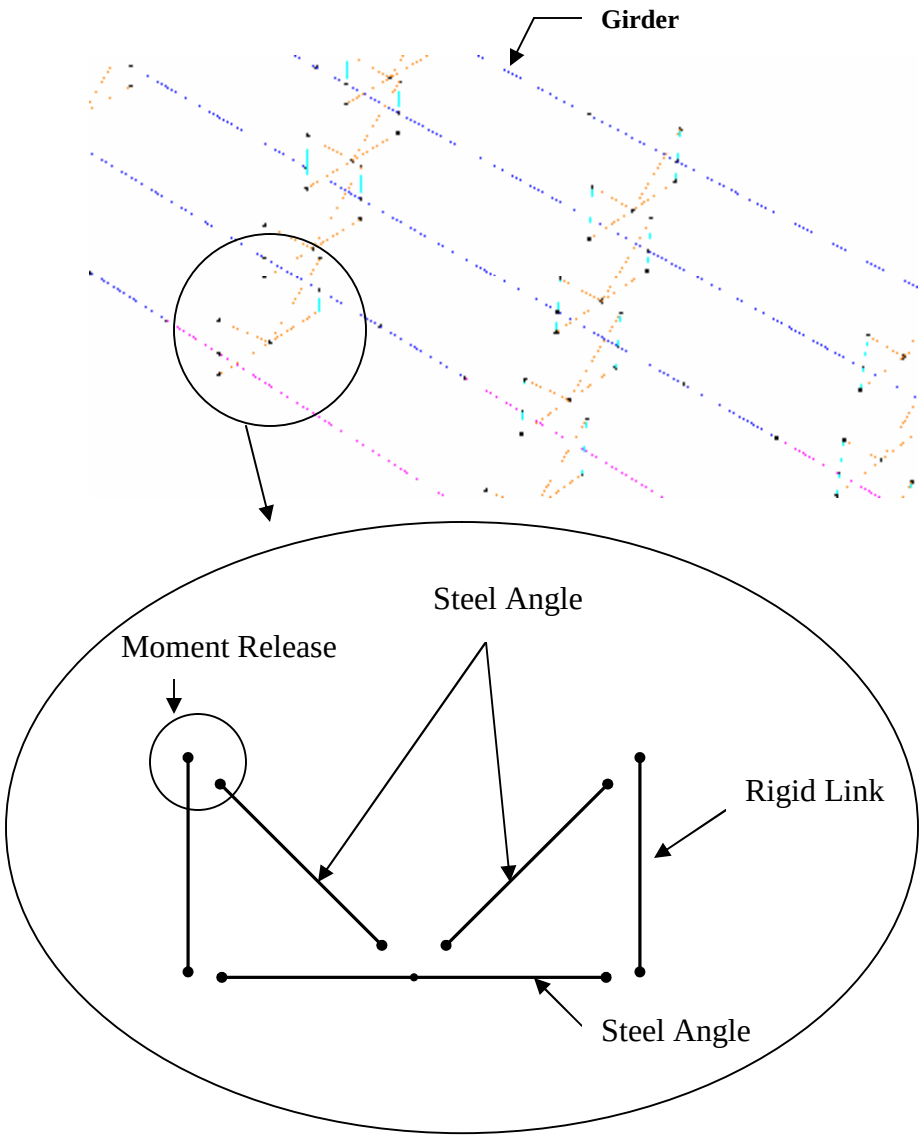

Figure 5-8 SAP, Simulated Cross-Frame

5.4.2.3 Rigid Link Element 1 (RL1)

Frame element was used to create the rigid link element. By assigning the large flexure rigidity to the element, fame element was assumed to be ideally rigid and transfer forces from element to adjacent element perfectly. Flexure rigidity or the product between elastic modulus and moment of inertia of the member is one of the most significant factors

affecting the vertical deflection behavior of the bridge model. It was believed by the author that increasing the stiffness of the rigid link element improves the stiffness of the model.

Regarding the previous research recommendations (Jetann, 2002), large elastic modulus of the member was chosen to be the variable factor of creating the rigid link element instead of varying the cross-section of the member. Jetann explained that large section of the rigid link might over improved the lateral bracing length and increased stiffness of the structures. However, SAP2000 program has a limitation for the difference of the bending stiffness of the adjacent elements. Too large of a different stiffness between the elements can cause an analytical error. In this study, the flexural rigidity of rigid link element was larger than the flexural rigidity of cross-frame member approximately fifty times. This approach was verified by a sensitivity study that will be discussed later in this section.

Length of the rigid link was creating regarding to the length from centroid of the girder to the center of the connection between girder and cross frame as shown in the Figure 5-9. Since there are two kinds of rigid link element in this study, the rigid link connected between cross frames and girders was named “Rigid Link 1” (RL1). “Rigid Link 2” (RL2) that used to connect between girders and SIP form will be discussed in the following section.

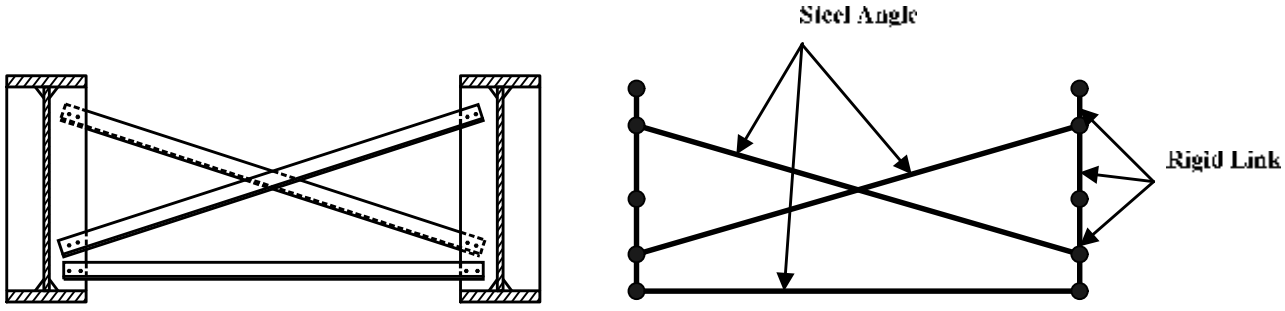

Figure 5-9 Simulated Cross Frame Compared with Actual Cross Frame

5.4.3 Stay-in-Place Metal Deck Form

5.4.3.1 General

Other portions of this research have revealed a significant effect of the stay-in-place form to the vertical deflection behavior of the bridge structure. Based on the study by Helwig (2002), reasonable strength and stiffness of SIP form was selected without conducting additional laboratory tests. This study provided the basis that was used to develop the shear properties to be used in the SAP models. First, the models were developed by using tension-compression only members that connect the top flanges of the girders. It was later discovered that the SIP form systems largely behaves as tension-compression composite with flexure behavior member. Details of the development of the SIP properties used in this study and their effect on the behavior of bridge models will be later discussed.

The deflection behavior predicted by SAP models of skewed bridges was found to be markedly different from the measured. Figure 5-10 is a picture of skewed bridge model with deflections on a node on the top of one of the rigid link elements. According to the figure, the plate girders of skewed bridges tend to rotate in addition to the downward deflection. U1 is represented the lateral deflection, whereas U3 represented the vertical deflection at the node. The lateral deflection on the node showed that the girders of the skewed bridge were rotated. This differs from the behavior of the non-skewed bridge model that was found only deflect downward with small or no rotation. This rotation of the girder cross-sections would provide the mechanism necessary to activate the SIP forms as force distributing elements within the SAP models.

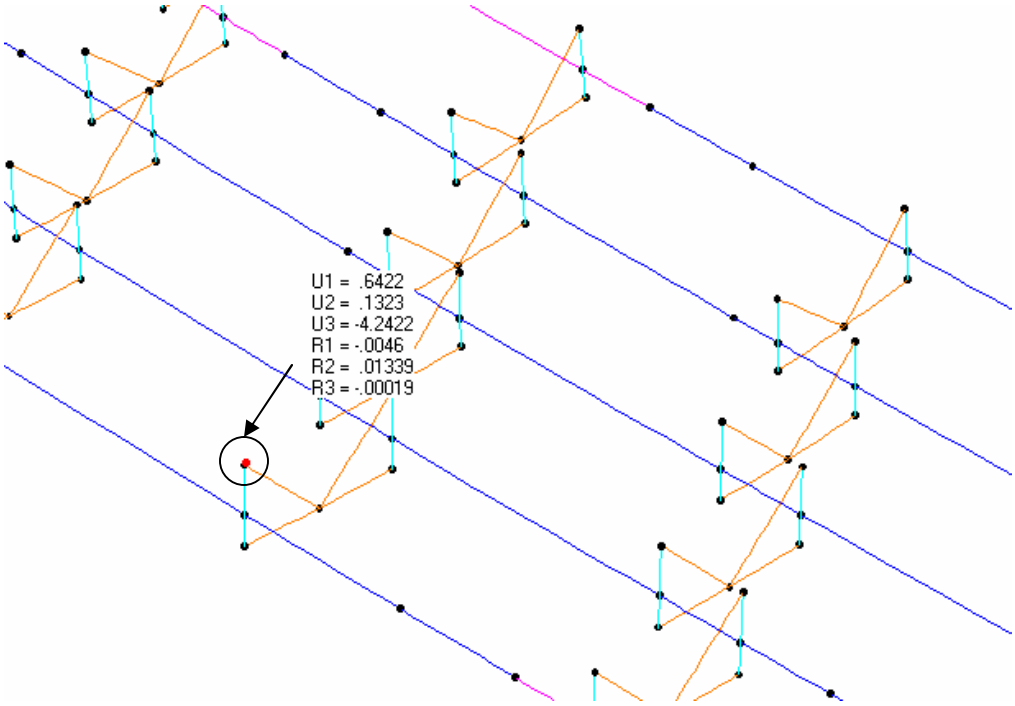

Note* unit is in inch

Figure 5-10 Displacement of Skewed Bridge Model

5.4.3.2 Importance of Stay-in-Place Metal Deck Form

Vertical load from weight of the SIP form was included to the design dead loads applied to the models in order to predict the vertical deflection. However, the force transferring behavior of the SIP was not included in the steel bridge design. In an effort to investigate the effect of SIP form to the vertical deflection behavior of the bridge models, the comparison of the non-skewed (Eno River Bridge) and skewed (Wilmington Street Bridge) bridge with and without SIP was conducted.

The vertical deflections from SAP models at the mid-span of non-skewed bridge were plotted in the Figure 5-11. It shows that the SIP form has no significant effect to the vertical deflection behavior of the non-skewed bridge. Since the girder of the non-skewed bridge has

no rotation and deflects downward only, the force transferring behavior of the SIP form does not account to the model.

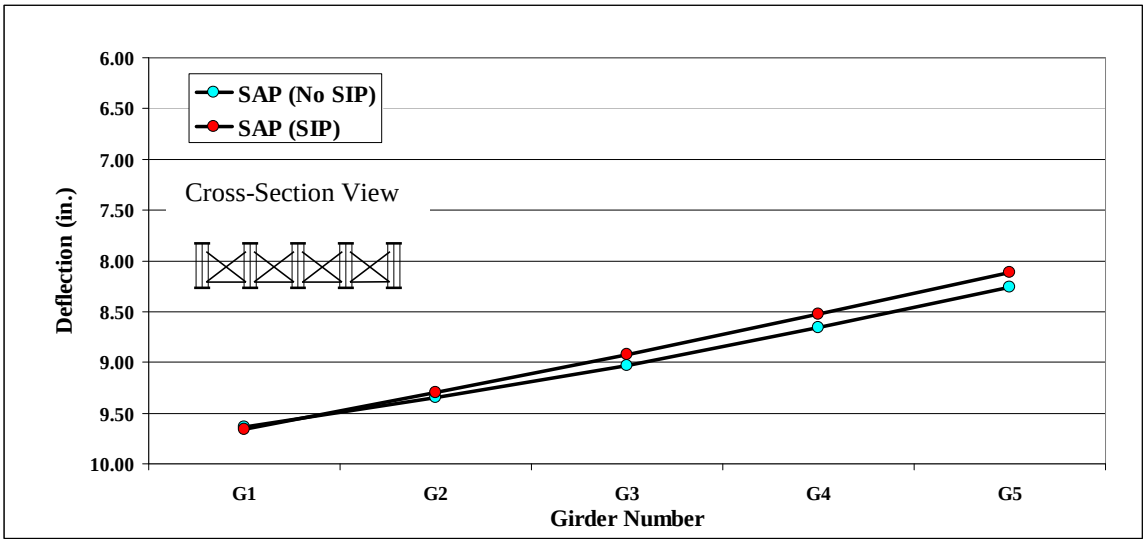

Figure 5-11 Non-skewed Bridge, Vertical Deflections from SAP Models with and Without SIP Forms at Mid Span

The effect of including SIP to the bridge model is significant in skewed bridge. Figure 5-12 shows the mid-span deflections predicted by SAP of the Wilmington Street Bridge model with and without SIP form. The difference in deflection behavior of the two models is apparent. The opposite trend of the deflected shape is obviously seen. Without SIP, the girder of the bridge deflected followed the trend of the vertical load. Since Wilmington Street Bridge has an unequal over hang, the results from the model without SIP form showed that the exterior girders in one side deflect less than the other one. In addition, the mid girder deflected more due to more proportion tributary width of the concrete deck. When SIP forms were included in the model, the deflection shape of the model with SIP form is inverted compared with the results from the model without SIP.

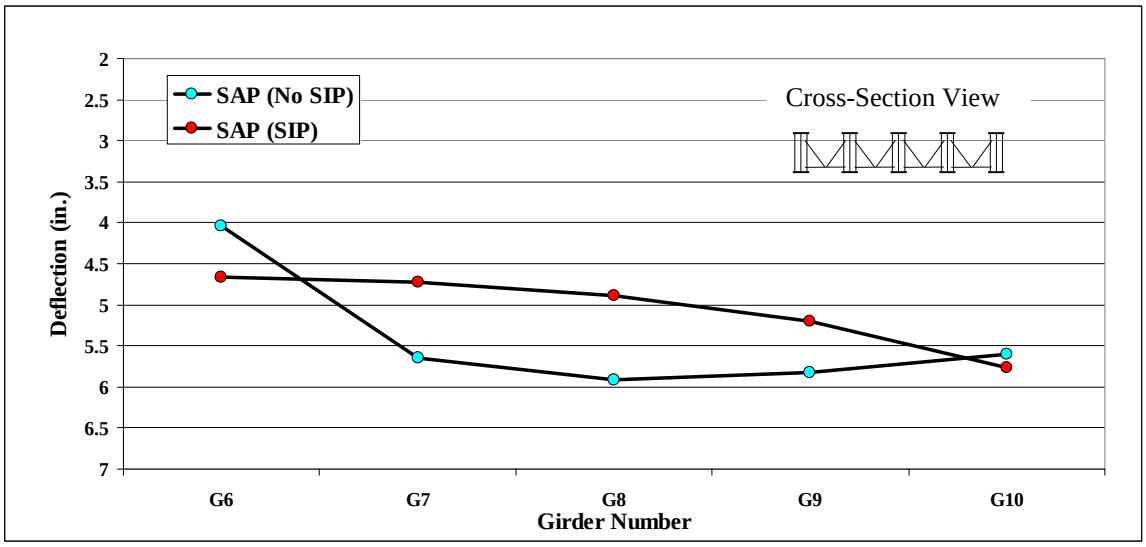

Figure 5-12 Skewed Bridge, Vertical Deflections from SAP Models with and without SIP Forms at Mid Span (Wilmington St. Bridge)

5.4.3.3 Stay-in-Place Modeling Method

To include SIP forms in the bridge models, two modeling method were created in this study; Tension-Compression frame element and Tension-Compression and Bending Shell Element.

One method utilized frame elements configured as an x-braced truss to represent the tension and compression behavior of the SIP. In this study, the frame element was connected to the rigid link connected to the girder as shown in Figure 5-13. The section properties of strut and diagonal members were assigned to the frame element using the SIP truss analogy previously presented in this report.

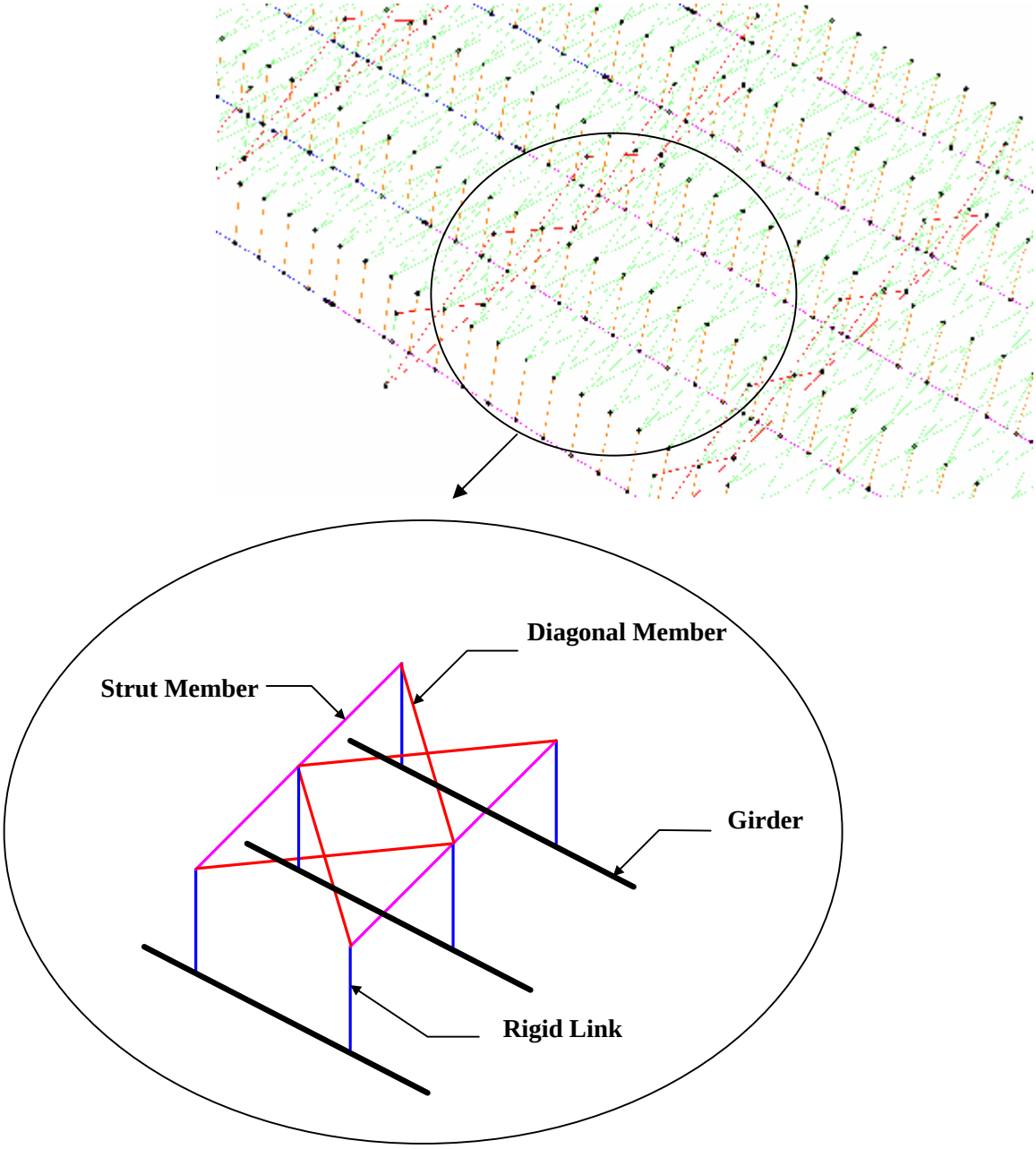

Figure 5-13 Frame Elements as SIP Forms

Another method utilized shell elements to represent the tension, compression and bending behavior of the SIP form. Shell element was connected to the rigid link element to transfer forces among each girder. The width of each shell element was set to equal to the

cover width of the SIP form, while the length of SIP form was assumed equal to the girder spacing of bridge structure as shown in Figure 5-14.

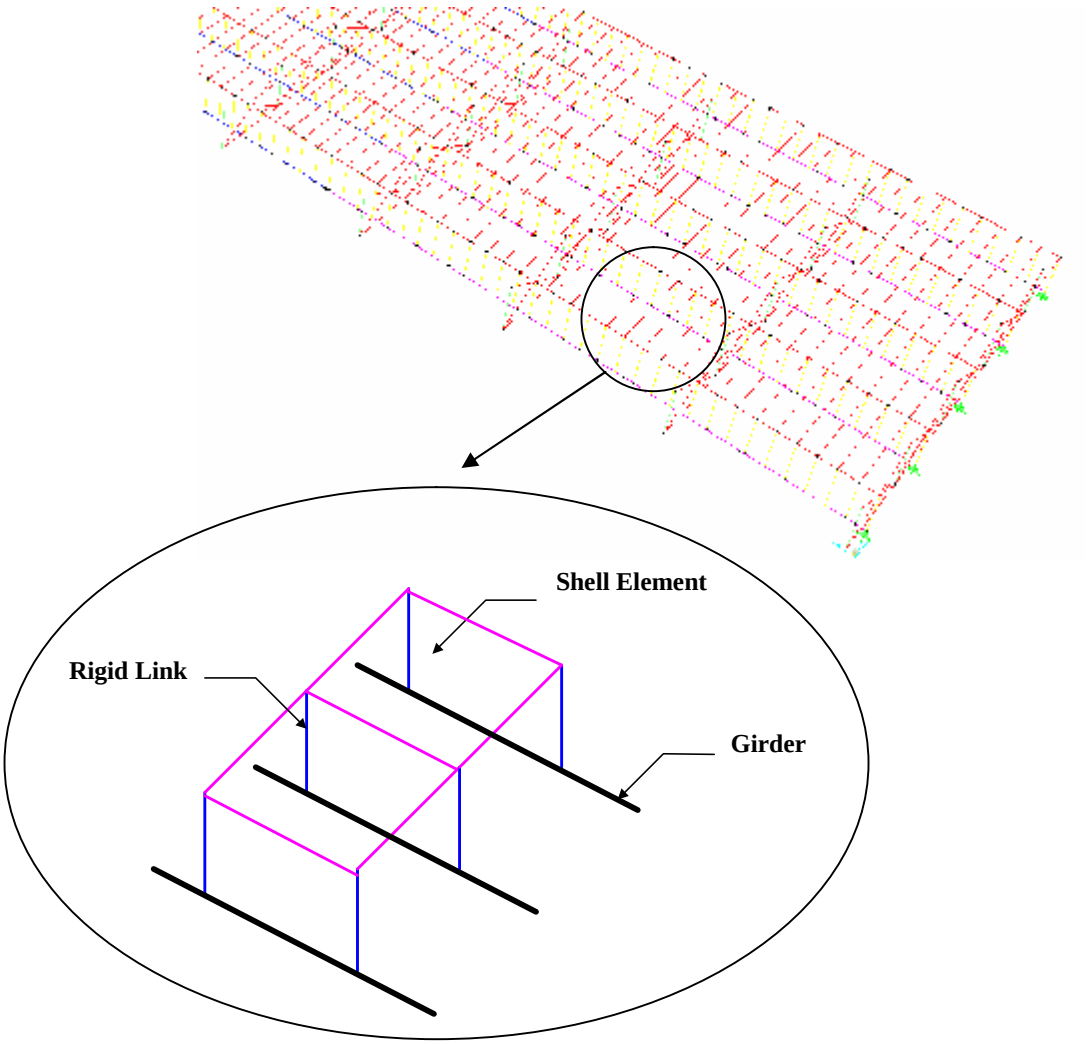

Figure 5-14 Shell Elements as SIP Forms

Shell elements in SAP2000 separates the calculation for stiffness into two categories; axial plus shear stiffness and bending stiffness. Therefore, two kinds of thickness need to be assigned. Thickness (th) is required to calculate axial and shear stiffness and thickness of bending (thb) is required for bending stiffness calculation. The sample of thickness calculation was performed in Appendix F.

The real SIP forms are a non-isotropic plate. To represent behavior of the SIP form more accurately, SIP forms properties were divided into three components, axial stiffness, shear stiffness and bending stiffness in order to obtain the different section properties of the orthotropic shell element.

SAP2000 assigned the local axis to the shell element compared with the SIP form as shown in the Figure 5-15. The axial stiffness of the SIP form model in the direction 1-1 was calculated by using the modification factor in direction 1-1 (f_{11}) multiply to the axial stiffness calculated from thickness (th) of the shell element. Therefore, factor f_{11} was a proportion between the thickness of the shell element (th) and the real thickness of SIP form. For the direction 2-2, three-dimensional SIP form analytical model was created in SAP2000 to compare with the shell element analytical model. The simulated SIP form model was subjected to the point load to record the deflection in the direction 2-2. By applying the same load condition, the elastic modulus of the shell element was varied to receive the same deflection. Figure 5-16 shows the pictures of the simulated SIP form analytical model compared with the shell element analytical model subjected to the applied point loads. The proportion between elastic modulus of shell element and elastic modulus of SIP form was used as the modification factor in direction2-2 (f_{22}).

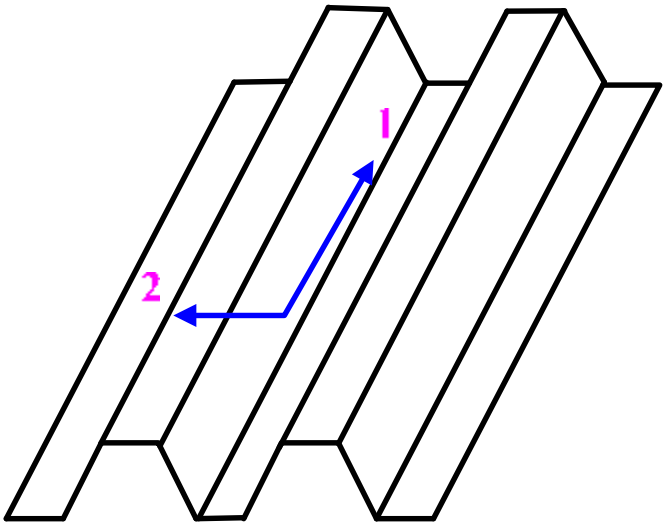

Figure 5-15 SAP Local Axis Direction 1-2 Compared with SIP Form

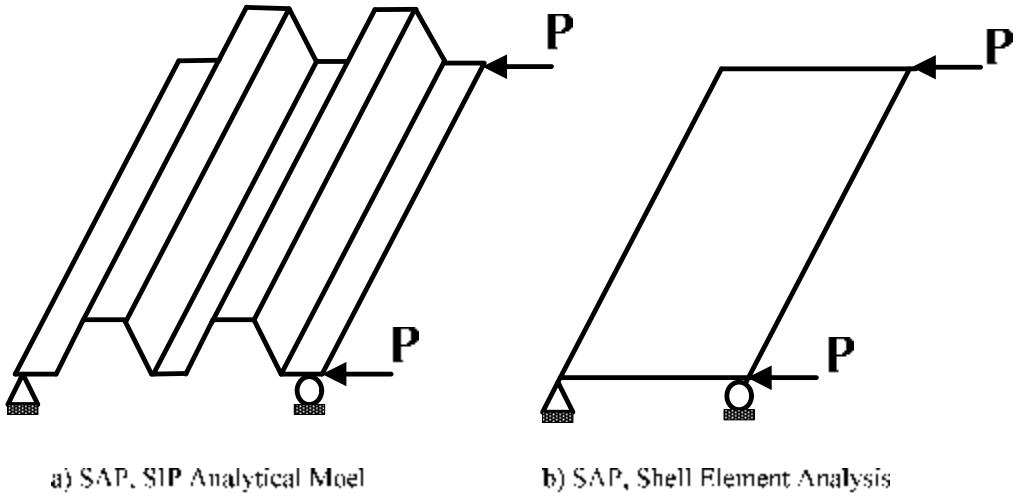

Figure 5-16 SAP Models of Simulated SIP form and Shell Element under Applied Load

Jetann et al. (2002) performed experimental tests that measured the diaphragm shear strength of SIP form systems that utilized several different connection details. A value of shear stiffness (G'=11 kips/inch) was measured for the SIP form system with the SIP connection detail similar to what has been found using by the bridges in this study and was

used as the basis for the shear properties in the SAP models. The shear stiffness was used in hand analysis to obtain the reference vertical deflection.

By using SAP to 2000 create a shell element in the truss frame and apply the vertical load as shown in the Figure 5-17, the appropriate shear modulus was assigned to the element to obtain the vertical deflection similar to the deflection from hand analysis. The proportion between the shear modulus obtained from SAP2000 analysis and the shear modulus of the regular steel plate was used to be modification factor for shear stiffness (f_{12}).

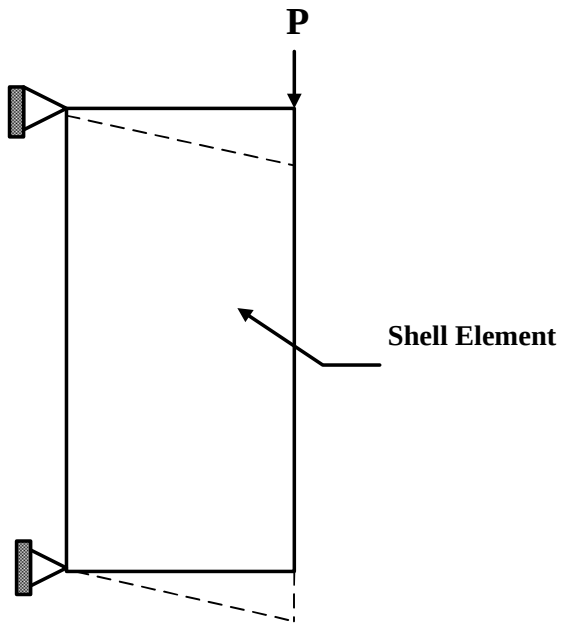

Figure 5-17 SAP, Shell Element Analysis for f_{12}

With regard to the bending stiffness, Figure 5-18 shows the direction of m_{11}, m_{22} and m_{12} of the orthotropic shell element. Since m11 is calculated based on the cross section of the shell element similar to what we used for the calculation of the thickness of bending, the modification factor m11 is set equal to one. For m22 and m12, the bending stiffness in direction 2-2 and torsional stiffness is varied on the thickness of member to the third (t^3), so

the proportion to the third of the thickness of bending (thb) and the real thickness of SIP was used in the modeling. A sample of the calculation and summary tables of SIP form properties used in the modeling are presented in Appendix N.

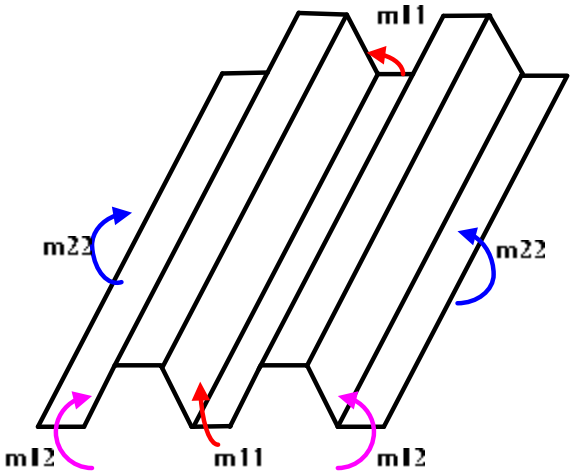

Figure 5-18 SAP, Moment Direction

The rigid link elements were also used to connect the shell element to girders. This connection was named as “RL2”. Because of the limitation of the different bending stiffness of the elements connected to each other in SAP2000, different stiffness from RL1 was assign to the RL2 used to connect girders and SIP form in order to prevent the calculation analytical error. Similar approach to RL1 but the flexural rigidity compared to girder instead of member of cross frame, the flexural rigidity of RL2 larger than girder’s about fifty times was used in this study. Figure 5-19 shows the location of RL1 and RL 2 in the bridge model.

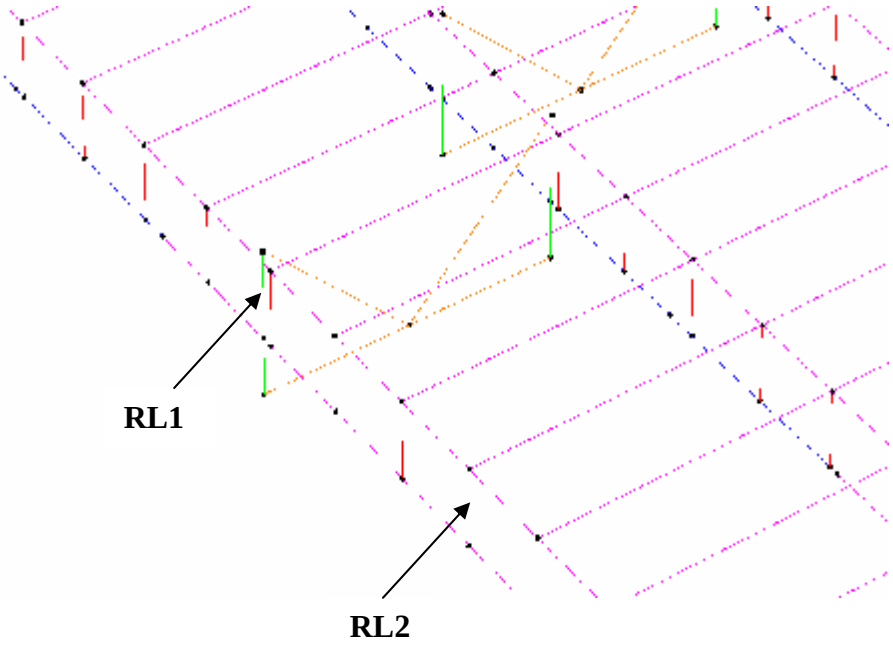

Figure 5-19 Location of RL1 and RL2

5.5 Composite Action

Since concrete deck placement in Bridge 10 had two stages. It was believed that the composite action between concrete deck and girders in the first pour affected the vertical deflection behavior of the bridge girders in the second pour. To represent the composite action between the concrete deck and girders in SAP modeling, plate girders were subjected to the vertical loads in two steps. First, the girders were loaded by wet concrete weight only on the first pour location. Second, the additional moment of inertial due to the cross section area from concrete deck were added to the girders on the first pour location. Then, the girders were subjected to the vertical load only on the second pour position. The vertical deflections from stage one and stage two loading were recorded and super imposed in order to obtain the total vertical deflections of the bridge models.

5.6 Load Calculation and Application

Calculation of the dead load due to the weight of concrete deck was performed base on the field measurement of the thickness of the concrete bridge deck. These dimensions included the depth of the concrete slab between each girder and the overhang width for each exterior girder. Loads were calculated for each interior girder based on the slab thicknesses and tributary widths equal to the girder spacing obtained from the construction plans. The tributary width for the exterior girders included the overhang width and one-half of the typical girder spacing. Steel bars, SIP forms, screeding machine and Labor were not included in the non-composite dead load. These loads were applied to the girders as line loads loaded on the top of the frame elements in SAP models.

5.7 Simple Span Bridge Modeling Results and Comparison

5.7.1 Modeling Results for the Eno River Bridge

Table 5-1 contains the summary of the mid-span deflection predicted by SAP with different modeling methods of Eno River Bridge. The deflections in Table 5-1 have been plotted to show the deflected shapes of mid-span cross-section of each modeling method. (see Figure 5-20). Appendix C contains all of the relevant results, pictures and graphs for the Eno River Bridge. The SAP prediction with different modeling methods plotted in Figure 5-20 illustrates that the cross-sectional deflected shape of Eno River Bridge is approximately linear across its cross-section with the largest deflection occurring at exterior girder one from each of the three modeling methods. However, deflected shape from two-dimensional grillage modeling method is flat along the cross section.

Table 5-1 Summary of Mid-Span SAP Deflections of Eno River Bridge (inches.)

Girder	2D	3D (No SIP)	3D (Frame SIP)	3D (Shell SIP)
G1	8.99	9.64	9.66	9.66
G2	8.99	9.35	9.30	9.30
G3	8.99	9.03	8.92	8.92
G4	8.99	8.66	8.53	8.53
G5	8.99	8.26	8.11	8.11

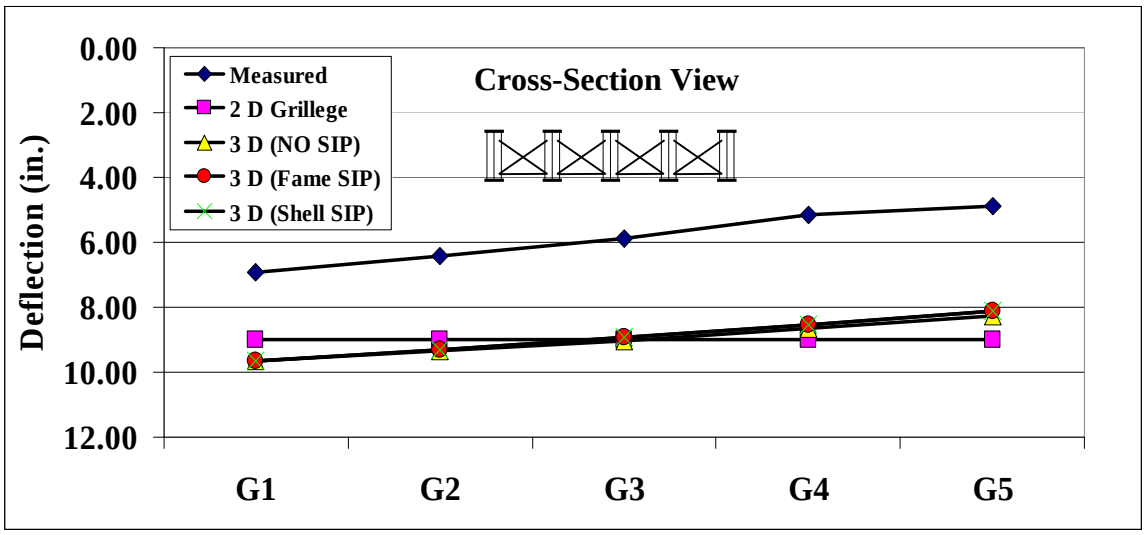

Figure 5-20 Plot of Mid-Span SAP Deflections of Eno River Bridge

5.7.2 Different SAP Modeling Results of US29

Table 5-2 contains a summary of the quarter-span deflection predicted by SAP with different modeling methods of US29. Appendix F contains all of the relevant results, pictures and graphs for US29. The deflections in Table 5-2 have been plotted to show the deflected shapes of mid-span cross-section of each modeling method. (see Figure 5-21). The SAP prediction with different modeling methods plotted in Figure 5-21 illustrates that the predicted cross-sectional deflected shape of the US29 Bridge is a bowl shape with the largest deflection occurring at the middle girder from each of the three modeling methods. However,

deflected shape from three-dimensional model with the shell SIP method is flat along the cross section.

Table 5-2 Summary of Mid-Span SAP Deflections of US29 (inch.)

Girder	3D (No SIP)	3D (Frame SIP)	3D (Shell SIP)
G1	5.02	5.16	5.38
G2	5.68	5.65	5.54
G3	5.78	5.78	5.64
G4	5.68	5.68	5.50
G5	35.02	5.13	5.35

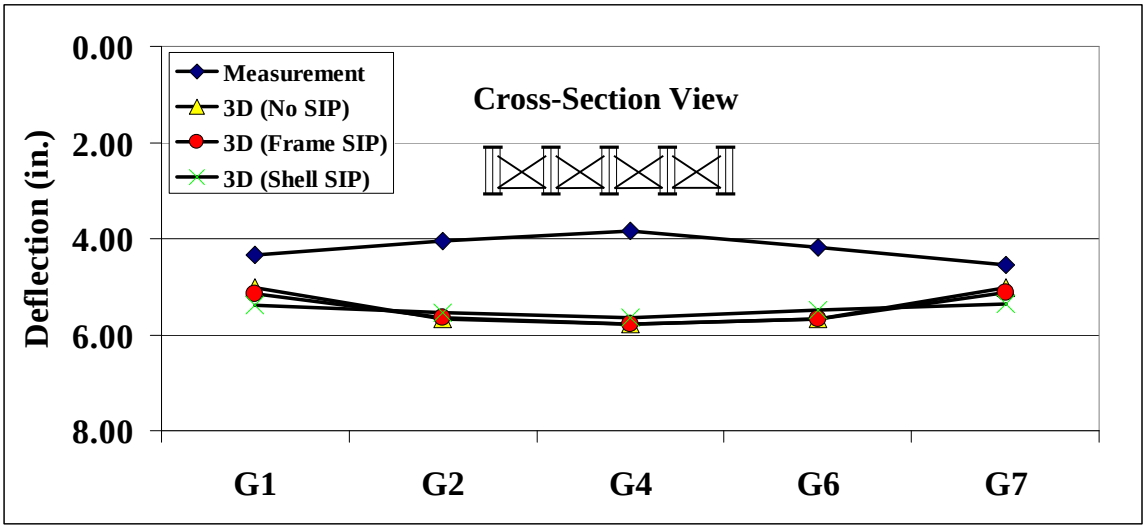

Figure 5-21 Plot of Mid-Span SAP Deflections of US29

5.7.3 SAP Three-Dimensional Model Deflections (Shell SIP) V.S. Measured Deflections & ANSYS (SIP) Deflections

Bridge models were developed by including SIP forms by using orthotropic shell element. This approach was done in an effort to develop a more simplified modeling method for skewed bridge structures. In this section, comparisons of the SAP predicted deflections with the measured deflection and the ANSYS finite element models (with SIP) are presented.

These comparisons are made to illustrate the accuracy of the SAP modeling method. Figure 5-22 contains plots with the SAP deflections including SIP forms versus measured and ANSYS (included SIP) deflections for the simple span bridges.

As illustrated in Figure 5-22, there is a good agreement in the deflected shapes predicted by SAP for the Eno River Bridge, Bridge 8 and Wilmington Street Bridge. The deflected shape in Eno River Bridge is similar to the results from the model without SIP. It emphasizes that SIP forms are not active in non-skewed bridge. However, by including SIP forms in skewed bridge, it is obviously seen that the deflected shape in US 29 and Wilmington Street Bridge are changed. Instead of having a "Bowl" shape, the deflected shapes of Wilmington Street Bridge is "Inverted Bowl" shape same as the measured. For the US 29, the deflected shape flattens out when the SIP forms are included. Similar to US 29 model behavior, deflected shape of Bridge 8 is flattened by minimizing interior girder deflections and increasing the exterior girder deflections.

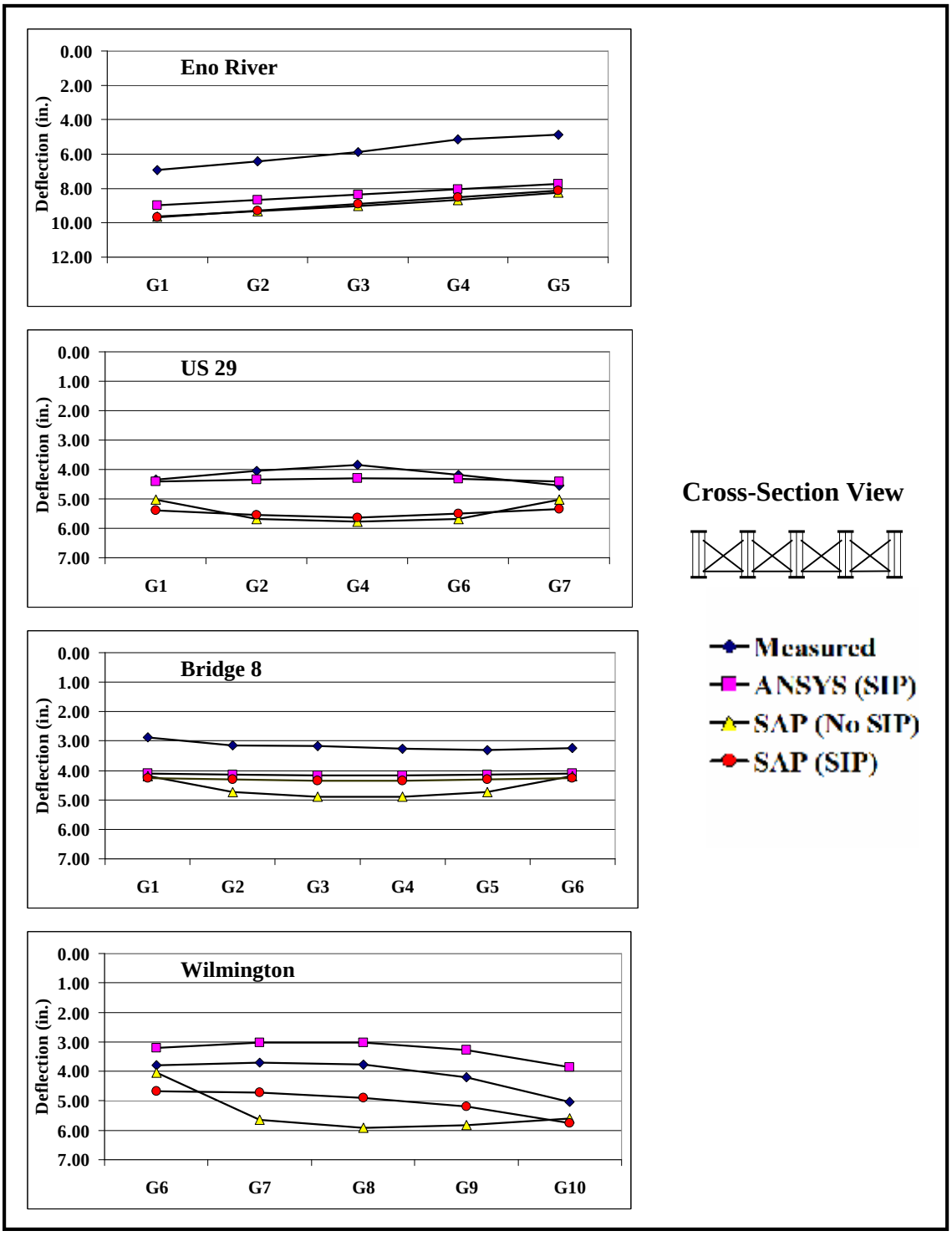

Figure 5-22 SAP Deflections (SIP) vs. Measured and ANSYS Deflections at Mid Span

According to Figure 5-22, deflections from the models including SIP forms to be more effective. The average ratios of Wilmington Street Bridge is approximately thirty percent for interior girders compared to sixty-eight percent different form results of the model without SIP. For Bridge 8, there is slightly effect of including SIP in the model to the exterior girder. The average difference is approximately thirty-three percent compared to thirty-eight percent from model not including SIP for the exterior girder. The effect of SIP form becomes greater in interior girders, from forty-six percent different decreases to thirty-one percent. Similar to what occur in Bridge 8, the deflections of interior girders of US 29 are more accurate to the measured result after included SIP form.

Table 5-3 Ratios of SAP2000 (Shell SIP) to Field Measurement Deflections

Bridges	Location	Girder A	Girder B	Girder C	Girder D	Girder E	Girder F
Eno	1/4	1.18	1.20	1.23	1.25	1.28	NA
	1/2	**1.39**	**1.45**	**1.52**	**1.66**	**1.66**	**NA**
	3/4	1.16	1.19	1.22	1.24	1.28	NA
US 29	1/4	1.24	1.37	1.37	1.35	1.15	NA
	1/2	**1.24**	**1.37**	**1.47**	**1.32**	**1.17**	**NA**
	3/4	1.21	1.38	1.46	1.29	1.16	NA
Bridge 8	1/4	1.34	1.33	1.30	1.30	1.28	1.31
	1/2	**1.47**	**1.37**	**1.37**	**1.34**	**1.31**	**1.31**
	3/4	1.30	1.29	1.34	1.26	1.29	1.25
Wilmington St.	1/4	1.32	1.35	1.36	1.32	1.23	NA
	1/2	**1.23**	**1.28**	**1.29**	**1.24**	**1.14**	**NA**
	3/4	1.25	1.32	1.33	1.25	1.17	NA

Compared to ANSYS results, SAP models by including SIP forms have a very good agreement in the deflected shapes in every bridge. The deflected shapes from SAP seem to shift down from deflected shapes from ANSYS. According to Table 5-4, the average ratios seem to be constant along each girder. The effect of SIP forms in all of the skewed bridges is

apparent. The results from SAP modeling indicated that SIP forms participate in the transverse distribution of the applied vertical load in skewed bridges. However, SIP forms do not significantly contribute to the distribution of vertical load in non-skewed bridges. This is illustrated in the analysis of the Eno River Bridge where there was no significant difference between the predicted deflections of the models with and without the SIP forms.

Table 5-4 Ratios of SAP2000 (Shell SIP) to ANSYS (SIP) Deflections

Bridges	Location	Girder A	Girder B	Girder C	Girder D	Girder E	Girder F
Eno	1/4	1.09	1.08	1.08	1.06	1.05	NA
	1/2	**1.08**	**1.07**	**1.07**	**1.06**	**1.05**	**NA**
	3/4	1.08	1.08	1.08	1.07	1.06	NA
US 29	1/4	1.24	1.30	1.33	1.30	1.23	NA
	1/2	**1.22**	**1.28**	**1.31**	**1.27**	**1.22**	**NA**
	3/4	1.23	1.29	1.32	1.28	1.23	NA
Bridge 8	1/4	1.01	1.02	1.02	1.02	1.02	1.01
	1/2	**1.04**	**1.04**	**1.04**	**1.04**	**1.04**	**1.04**
	3/4	1.01	1.01	1.02	1.02	1.02	1.02
Wilmington St.	1/4	1.43	1.59	1.62	1.60	1.66	NA
	1/2	**1.46**	**1.57**	**1.61**	**1.58**	**1.49**	**NA**
	3/4	1.53	1.62	1.67	1.65	1.48	NA

5.8 Continuous Bridge Modeling Results and Comparison

The comparison plots between SAP, ANSYS and measured deflections at different locations along the span of bridge 10 are presented in Figure 5-23. The SAP model results plotted in Figure 5-23 were developed with SIP forms but without the composite action. The results of the ANSYS modeling are included for comparison.

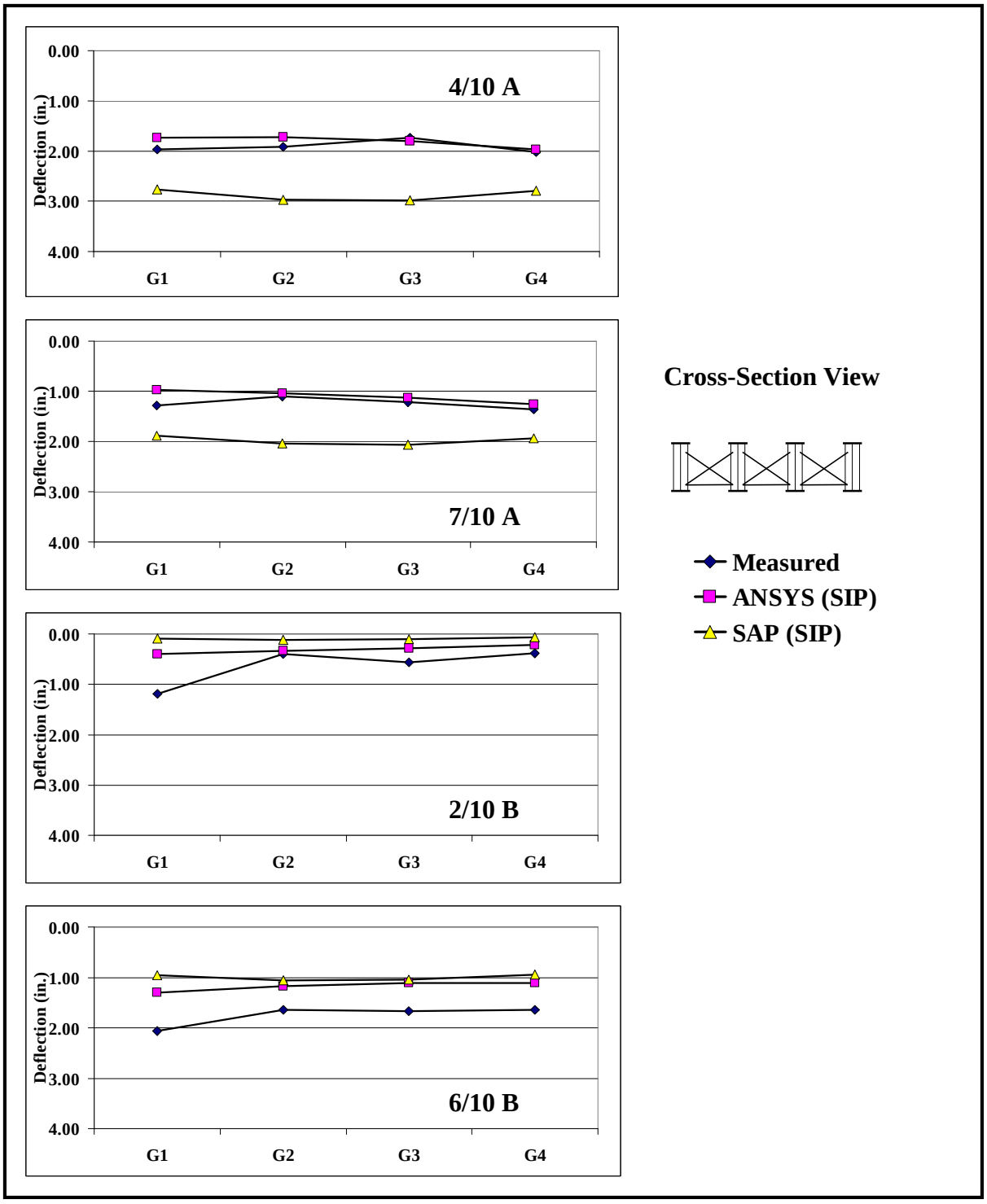

Figure 5-23 SAP Deflections (SIP) vs. Measure and ANSYS Deflections at Each Location of Bridge 10

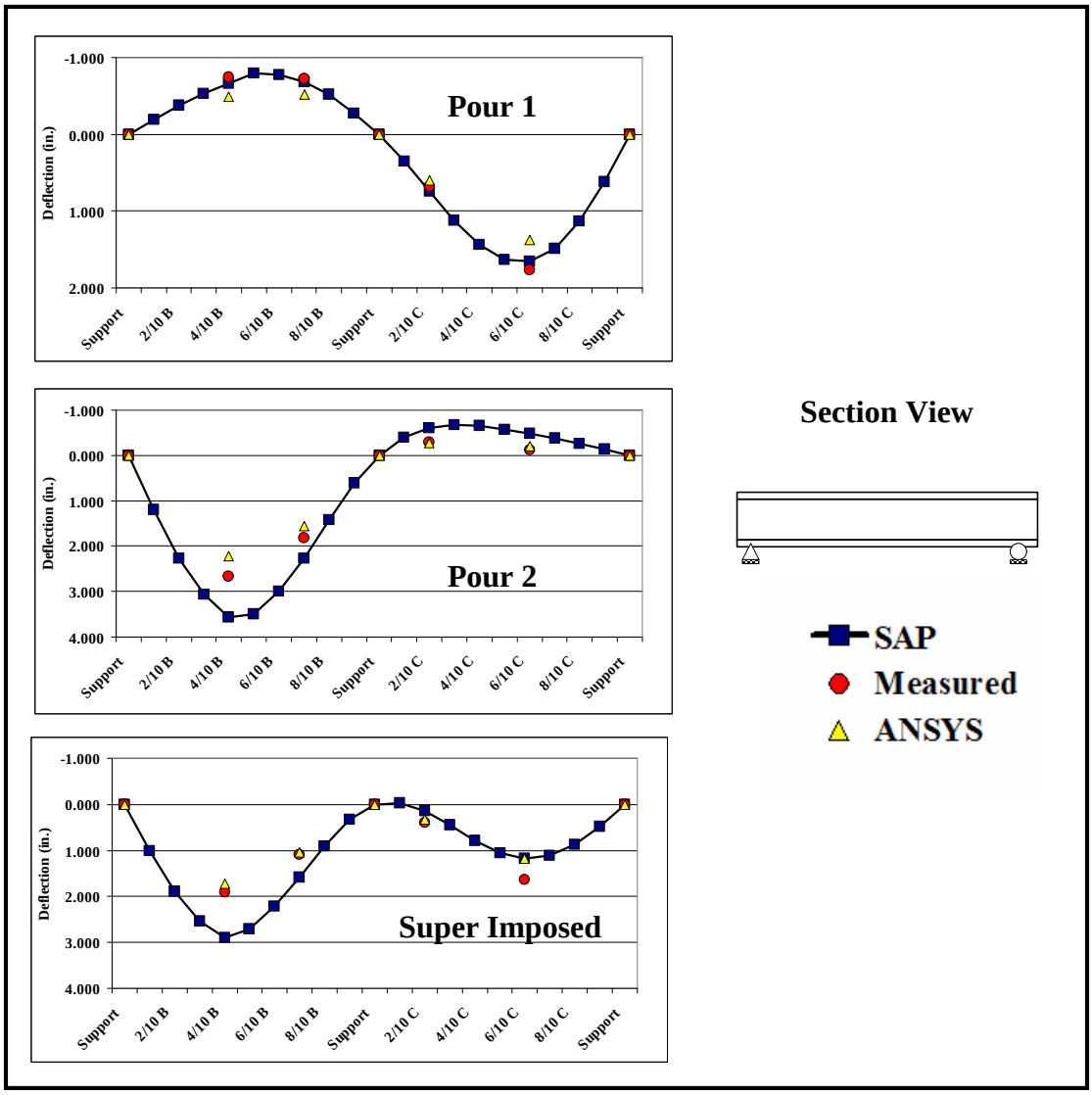

Figure 5-24 SAP Deflections (SIP) vs. Measured and ANSYS Deflections along Girder 2

Since Bridge 10 is a continuous span bridge, the vertical deflection behavior observed in the field was more complex than the simple span bridges. The deflected shapes and measured magnitudes in Span A are markedly different from the field measured and the ANSYS modeling results. The field measured and ANSYS deflected shapes were "Inverted Bowl" shapes, whereas the predicted deflected shape from SAP is a "Bowl" shape. However, there is a good agreement between SAP and ANSYS in span B. The shapes from both

predicted models are linear along the cross section but the shapes are still different from the measured.

The composite action was simulated in Bridge 10. Figure 5-24 represents the plot showing the effect of including composite action in the model compared to the measurement and ANSYS results in interior girder (Girder 2). According to Figure 5-24, SAP modeling method has a very good agreement with both ANSYS and measured deflected shapes in pour one. However, the composite action modeling method used in pour two made the model less stiff than ANSYS model and the real bridge structure. After the deflections were super imposed, the deflections from the SAP models are much larger than ANSYS and the measured results in Span A, whereas the deflection in Span B are smaller than the measured and almost equal to the result from ANSYS.

5.9 Summary

It is apparent that the finite elements models created using SAP2000 are less complex than the previously described models created using ANSYS. Using a single frame element in SAP2000 to create the entire steel plate girder can reduce time for creating the model compared to using the combination of shell elements as done in ANSYS. By creating the simplified SAP2000 models with and without SIP forms, the results emphasized the importance of SIP forms. Including SIP form in skewed bridge models significantly improved accuracy of the prediction. However, the SIP forms had no significant effect to non-skewed bridge. From the comparisons of modeling the SIP forms using shell element with and without flexural behavior, the results were more accurate with the flexural behavior included. Orthotropic shell element function in SAP2000 is recommended for representing the different stiffness in the different directions of the SIP forms. SAP simplified modeling

methods developed in this study have a reasonable agreement with the field measured and ANSYS modeling results in single span bridges. However, in the continuous, two-span bridge, the simplified SAP2000 modeling method is not effective.

6.0 Parametric Study and Development of the Simplified Procedure

6.1 Introduction

Utilizing the modeling technique and MATLAB preprocessor program described in Section 4, a parametric study was conducted to establish relationships between various bridge parameters and dead load deflections of skewed and non-skewed steel plate girder bridges. The controlling parameters were further investigated to develop a simplified procedure to predict the girder deflections. This section discusses detailed information of the parametric study and developing the simplified procedure. Despite the development's focus on simple span bridges with equal exterior-to-interior girder load ratios, discussions on the deflection behavior of simple span bridges with unequal exterior-to-interior girder load ratios and continuous span bridges with equal exterior-to-interior girder load ratios are included.

6.2 General

Steel plate girder deflected shapes are described herein by the exterior girder deflection and the differential deflection between adjacent girders. Together, they can define the entire deflected shape at a given location along the span (i.e. deflections in cross-section). Figure 6.1 presents an example of the exterior girder deflection and differential deflection as defined in this report.

Also, the exterior-to-interior girder load ratio is defined in percent by dividing the exterior girder load by the interior girder load. For instance, the interior and exterior girders of Bridge 8 are loaded at 1.42 k/ft and 1.19 k/ft, respectively; thus, the exterior-to-interior girder load ratio is 84 percent. Last, a negative differential deflection between girders corresponds to an observed "hat" shape in cross-section (see deflections of the Wilmington

St Bridge), whereas, a positive differential deflection corresponds to an observed "bowl" shape (see deflections of Bridge 8).

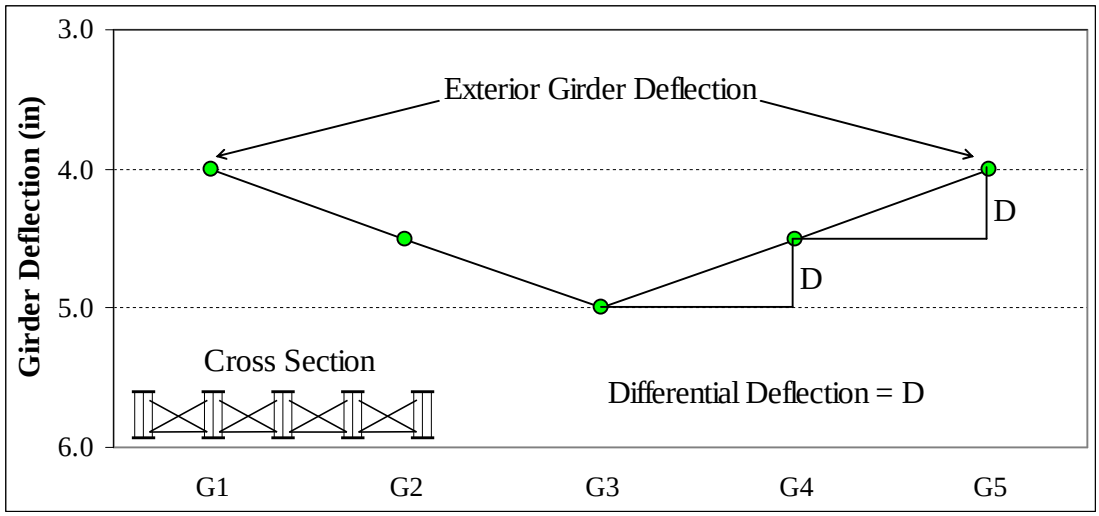

Figure 6.1: Exterior Girder Deflection and Differential Deflection

6.3 Parametric Study

Five bridge parameters were investigated, either directly or indirectly, to help develop the simplified procedure for predicting dead load deflections of steel plate girder bridges. They are as follows: number of girders within the bridge span, cross frame stiffness, exterior-to-interior girder load ratio, skew offset of the bridge, and girder spacing-to-span ratio. Each parameter was investigated independently to discover any relationship that existed with the deflection of the girder.

6.3.1 Number of Girders

The number of girders within the span was investigated by creating ten finite element models using the Bridge 8 structure. Five girder arrangements were checked at two different skew offsets. The number of girders ranged from four to eight, whereas the skew offsets

were set at 0 and 50 degrees. Figures 6.2 and 6.3 present the deflection results of the ANSYS models at the zero and fifty degree offsets, respectively.

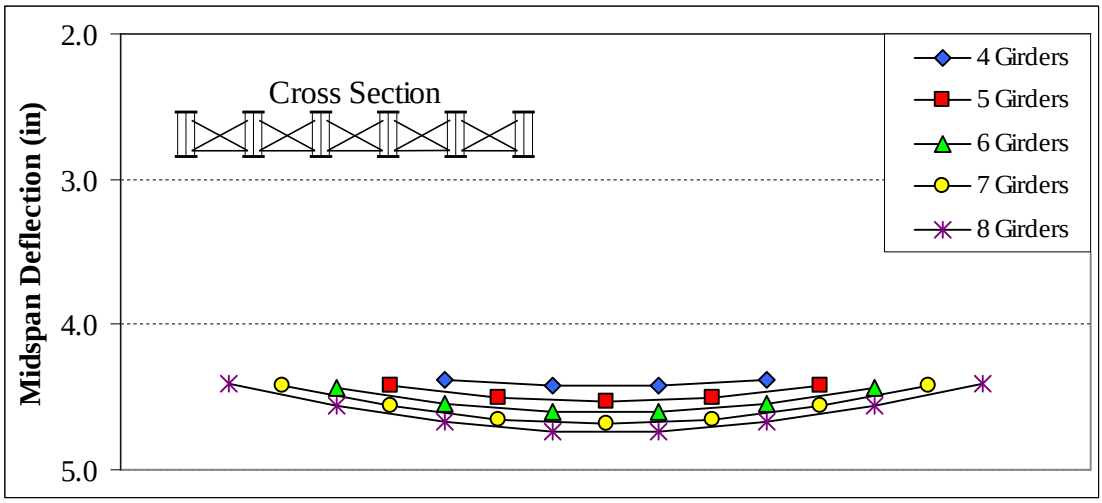

Figure 6.2: Bridge 8 at 0 Degree Skew Offset – Number of Girders Investigation

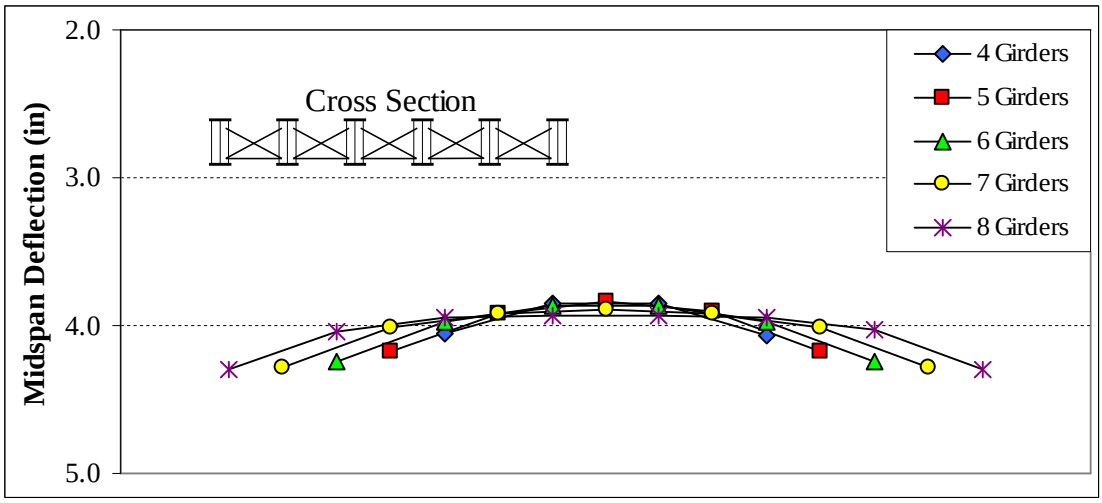

Figure 6.3: Bridge 8 at 50 Degrees Skew Offset – Number of Girders Investigation

For models at the 0 degree skew offset, exterior girder deflections range from 4.38 to 4.44, a 1 percent difference of only 0.06 inches. At the 50 degree skew offset, the difference is 0.24 inches (from 4.06 to 4.30), which is an approximate 6 percent difference. For

comparison, the differential deflection was averaged across the girders in each model. At the 0 degree skew offset, the differential deflection decreased only 0.07 inches as the number of girders was increased. Similarly, the decrease was 0.09 inches for the 50 degree skew offset models. Therefore, regardless of skew offset, the changes in exterior girder deflection and differential deflection are negligible.

6.3.2 Cross Frame Stiffness

Fourteen finite element models were generated to examine the effect of intermediate cross frame stiffness on deflection behavior. Bridge 8 was replicated with ten models: five select cross frame stiffnesses at 0 and 50 degree skew offsets. The cross frame stiffness was adjusted to represent one-tenth, one-quarter, one-half, one, and two times the original stiffness. Bridge 8 was chosen for this analysis because it has the maximum girder spacing, thus simulating the most extreme circumstances. Figures 6.4 and 6.5 represent the deflected shape of Bridge 8 at the 0 and 50 degree skew offsets, respectively, as cross frame stiffness is adjusted.

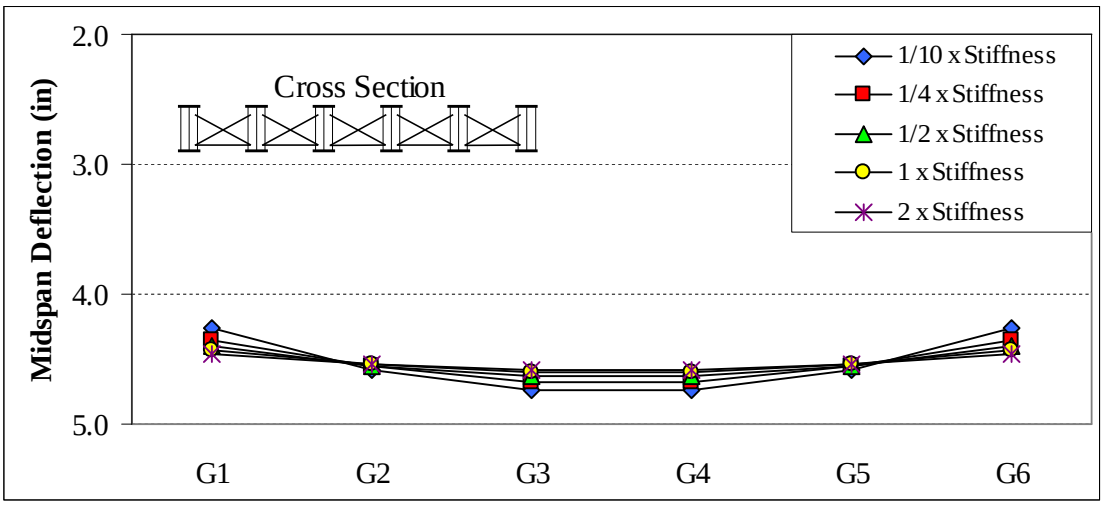

Figure 6.4: Bridge 8 at 0 Degree Skew Offset – Cross Frame Stiffness Investigation

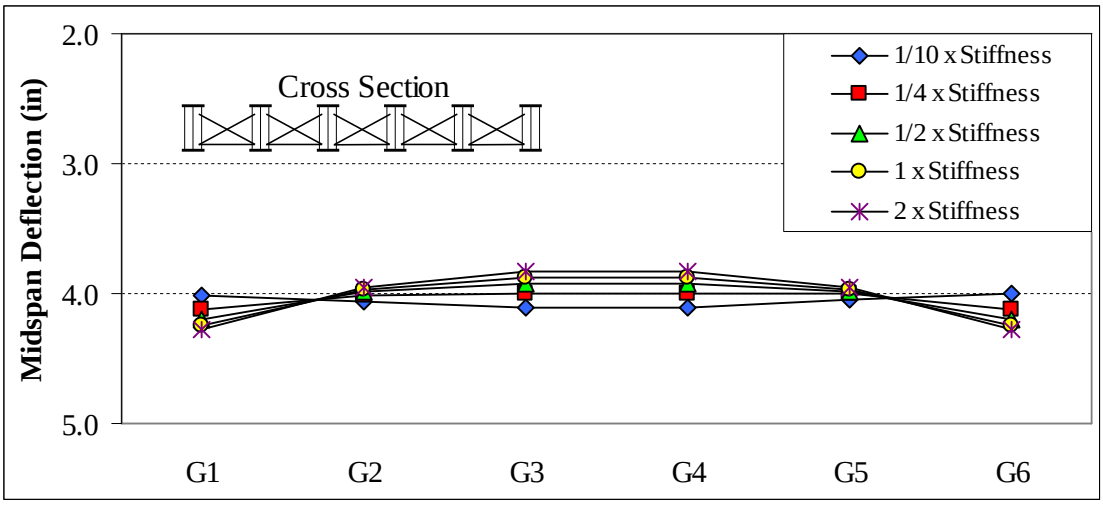

Figure 6.5: Bridge 8 at 50 Degrees Skew Offset – Cross Frame Stiffness Investigation

Additionally, the Eno Bridge was modeled four times, with stiffnesses adjusted to the extreme cases of one-tenth and two times the original stiffness at the 0 and 50 degree offsets. In this particular analysis, K-type intermediate cross frames replaced X-type cross frames in the Eno Bridge models to verify the insignificance of cross frame type. Note that Eno was stage-constructed, thus unequal exterior-to-interior girder load ratios were present. Figures 6.6 and 6.7 represent the deflected shape of the Eno Bridge at the 0 and 50 degree offsets, respectively, for the two cross frame stiffnesses.

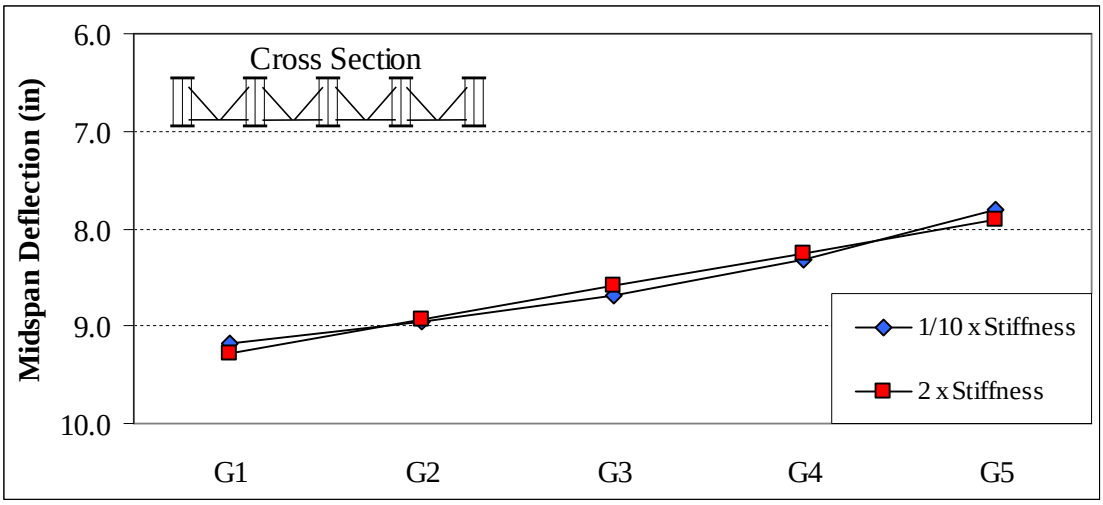

Figure 6.6: Eno at 0 Degree Skew Offset – Cross Frame Stiffness Investigation

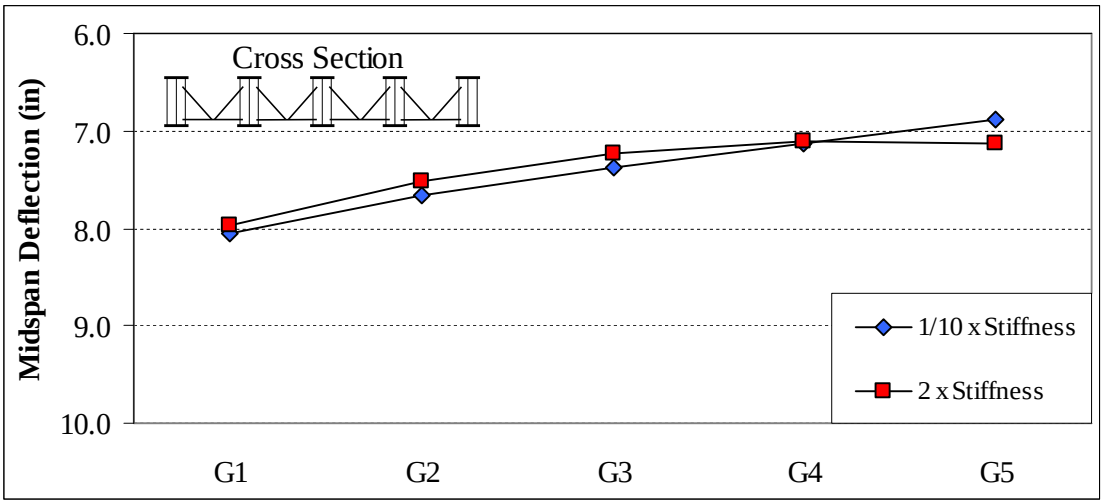

Figure 6.7: Eno at 50 Degrees Skew Offset – Cross Frame Stiffness Investigation

The plotted results in all four figures indicate that variable cross frame stiffnesses have little effect on the non-composite deflection behavior of steel plate girder bridges. The maximum difference between exterior girder deflections at the two extreme cross frame stiffnesses was 0.28 inches, a 6.5 percent difference (girder 6 of Bridge 8 at the 50 degree offset). The differential deflections appear to react slightly to stiffness adjustments, but not

considerably enough. Note that in Figure 6.5, the differential deflection is positive for the 1/10 stiffness, whereas the other differentials are negative. In reality, steel angles are not manufactured small enough to achieve that cross frame stiffness.

6.3.3 Exterior-to-Interior Girder Load Ratio

Twenty-seven finite element models were generated to investigate how the exterior-to-interior girder load ratio affects steel plate girder deflection behavior. Three bridges (Camden SB, Eno, and Wilmington St) were modeled at 0, 50 and 60 degree skew offsets with equal exterior-to-interior girder load ratios of 50, 75 and 100 percent. The analysis revealed very similar results for all three bridges, therefore, only the Camden SB Bridge is discussed. Figures 6.8 and 6.9 represent the deflected shape of the Camden SB Bridge for the different exterior-to-interior girder load ratios at 0 and 50 degree skew offsets, respectively.

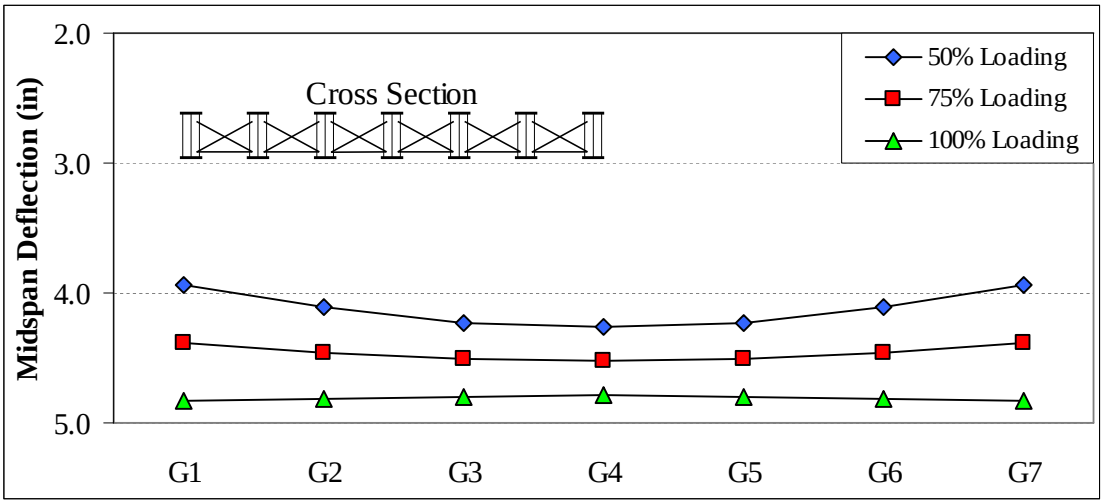

Figure 6.8: Camden SB at 0 Degree Skew Offset – Exterior-to-Interior Girder Load Ratio Investigation

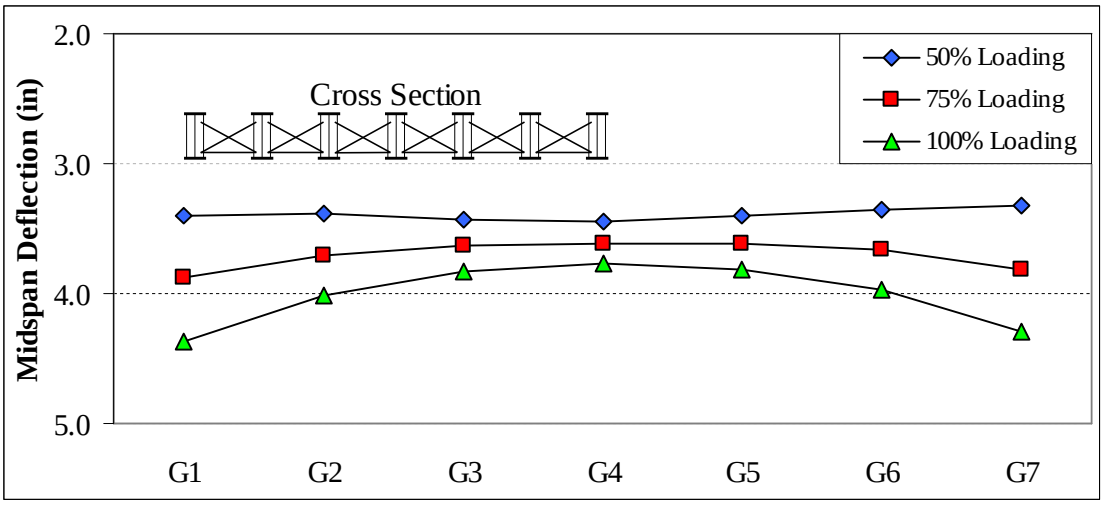

Figure 6.9: Camden SB at 50 Degree Skew Offset – Exterior-to-Interior Girder Load Ratio Investigation

It is apparent from the plots that exterior girder deflections and differential deflections between adjacent girders are both influenced by increased or decreased exterior-to-interior girder load ratios. For instance, doubling the exterior-to-interior girder load ratio in the 50 degree skew offset model causes girder 1 (an exterior girder) to deflect about 1 (0.98) additional inch and girder 4 (middle interior girder) to defect an additional 0.33 inches (see Figure 6.8). The girder deflection behavior is affected because the exterior girders help carry the interior girder load by way of transverse load distribution. The relationship between exterior-to-interior girder load ratios and the deflection behavior required further investigation and a discussion is included.

6.3.4 Skew Offset

The skew offset parameter was analyzed by creating thirty-five finite element models. Each simple span bridge was modeled at skew offsets of 0, 25, 50, 60 and 75 degrees. After the analysis, it was evident that all seven bridges exhibited a common deflection behavior as

the skew offset was increased. To illustrate the effect of skew offset, deflections are displayed in Figure 6.10 for Bridge 8 and in Figure 6.11 for the Eno Bridge.

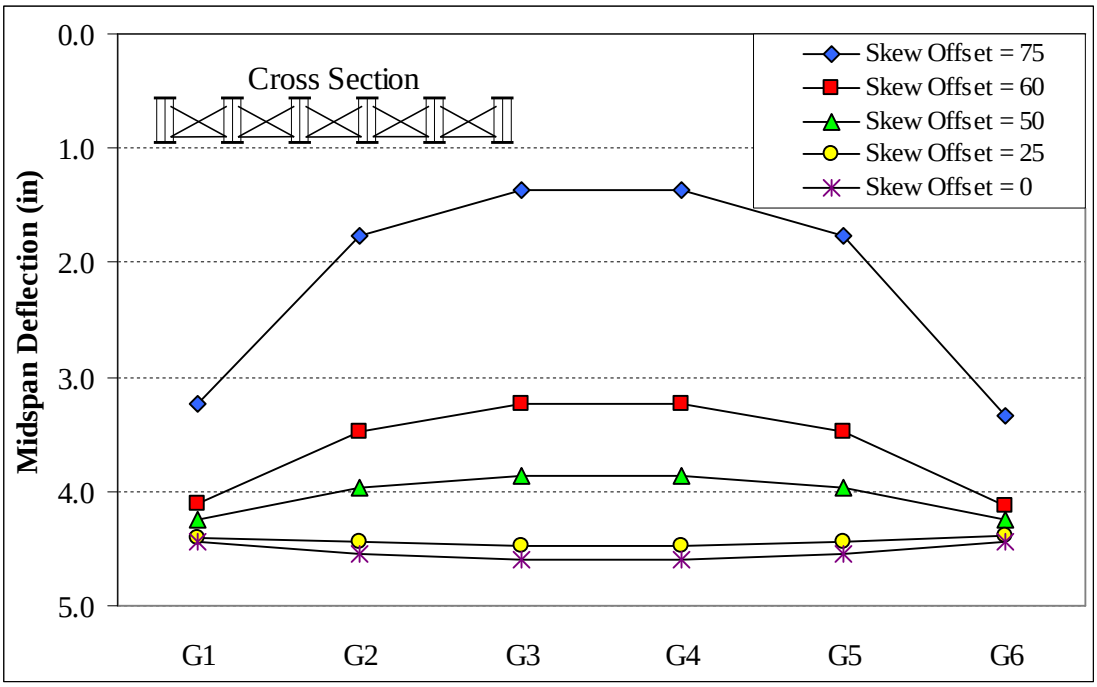

Figure 6.10: Bridge 8 Mid-span Deflections at Various Skew Offsets

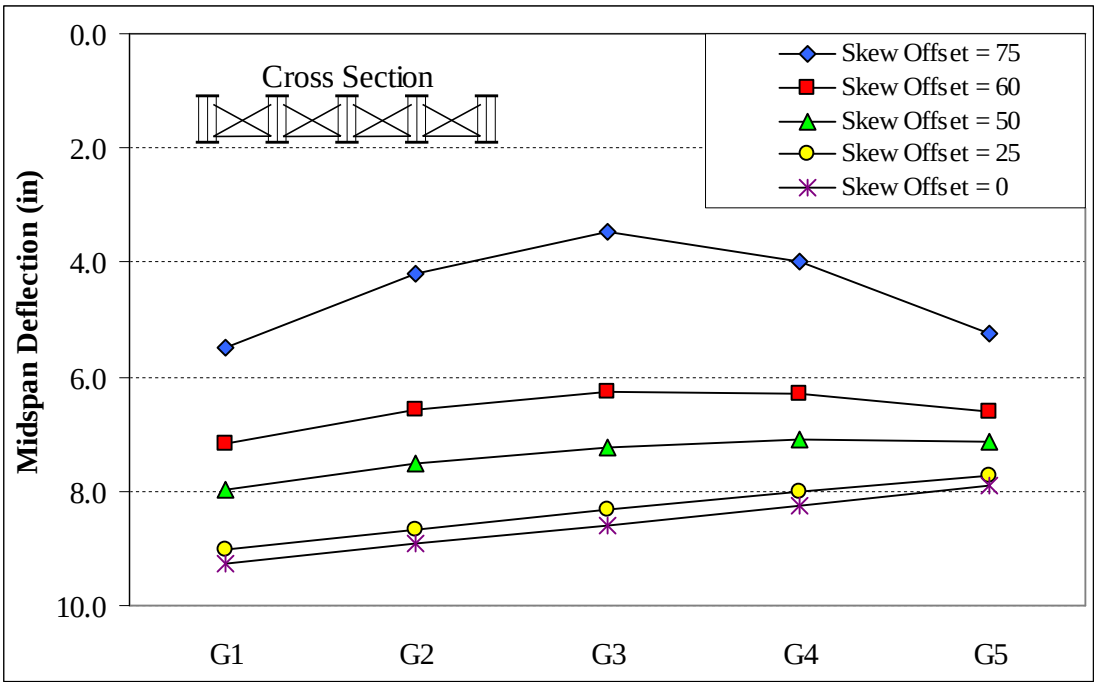

Figure 6.11: Eno Bridge Mid-span Deflections at Various Skew Offsets

Figures 6.10 and 6.11 reveal a unique relationship between skew offset and girder deflection behavior. As the skew offset is increased, the exterior girders deflect less and the differential deflections become more negative. This relationship between skew offset and girder deflection behavior was further investigated.

6.3.5 Girder Spacing- to-Span Ratio

As four bridge parameters were investigated directly, an additional parameter was studied indirectly. The girder spacing-to-span ratio is a unitless parameter unique to each of the seven simple span bridges (see Table 6.1).

Table 6.1: Girder Spacing-to-Span Ratios

	Girder Spacing (ft)	Span Length (ft)	Spacing/Span Ratio
Eno	9.65	235.96	0.041
Wilmington St	8.25	149.50	0.055
Camden NB	8.69	144.25	0.060
Camden SB	8.69	144.25	0.060
US-29	7.74	123.83	0.063
Bridge 8	11.29	153.04	0.074
Avondale	11.19	142.96	0.078

To determine possible relationships between the girder spacing-to-span ratio and girder deflections, fourteen finite element models were generated: two models per bridge at 0 and 50 degree skew offsets, with an exterior-to-interior girder load ratio of 75 percent. As deflection magnitudes are primarily dependent on the magnitude of load, only differential deflections were compared to the girder spacing-to-span ratios. The results at 0 degree skew offset are plotted in Figure 6.12.

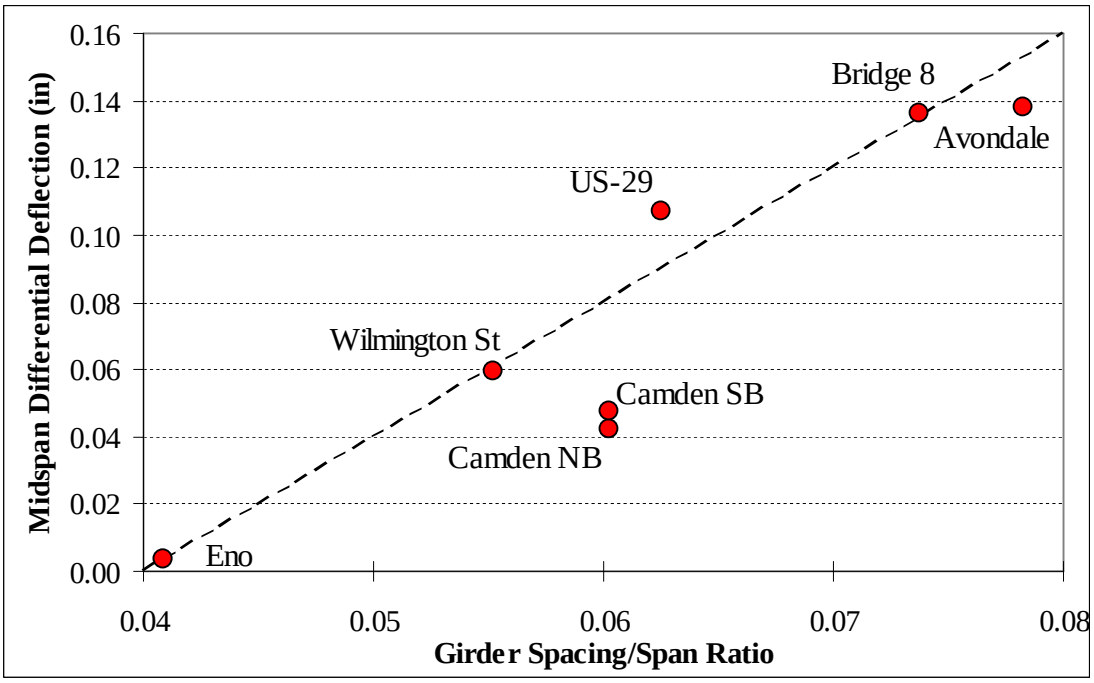

Figure 6.12: Differential Deflection vs. Girder Spacing-to-Span Ratio

In Figure 6.12, the differential deflection value appears to increase in a linear fashion (displayed as a dashed line) as the girder spacing-to-span ratio is increased. The resulting relationship is considerable and investigated further.

6.3.6 Conclusions

Sections 6.3.1 – 6.3.5 present the results of a parametric study, conducted to determine the controlling bridge parameters affecting non-composite deflection behavior. Of the five parameters analyzed, the exterior-to-interior girder load ratio, skew offset, and the girder spacing-to-span ratio certainly influence girder deflections. Test results from the two studies involving number of girders within the span and cross frame stiffness did not produce significant changes in deflection behavior. Therefore, these two parameters are not included in the simplified procedure. Table 6.2 presents a matrix to summarize the entire parametric study and includes each parameter's range of values. Note that checked cells indicate

referenced tests and shaded cells indicate repeated configurations. The number of girders within the span was not investigated against the girder spacing-to-span ratio as only one bridge (Bridge 8) was modeled with a varying number of girders. The results provided evidence that the number of girders within the span does not affect deflection behavior. Therefore, additional studies were not conducted for other bridge models.

Table 6.2: Parametric Study Matrix

	Skew	Spacing/Span Ratio	Number of Girders	Exterior Girder Loading	Cross Frame Stiffness
Skew	√	√	√	√	√
Spacing/Span Ratio		√	-	√	√
Number of Girders			√	√	√
Exterior Girder Loading				√	√
Cross Frame Stiffness					√
Range of Values	0 - 75 degrees	0.04 - 0.08	4 - 8	50% - 100%	0.1 - 2.0

6.4 Simplified Procedure Development

Developing the simplified procedure for predicting dead load steel plate girder deflections required a reasonable starting point. The traditional single girder line (SGL) prediction of an interior girder was deemed a reasonable base deflection on which to develop the simplified procedure for two reasons. First, SGL predictions involve simple calculations and are included in the majority of bridge design software. Second, an interior SGL prediction corresponds to an exterior SGL prediction with the exterior-to-interior girder load ratio at 100 percent and 0 degree skew offset, allowing for direct adjustments accordingly.

From the base prediction, a two-step approach was established to predict the deflection behavior. The first step is to predict the exterior girder deflections by adjusting the base prediction, while accounting for trends discovered in the parametric study. The second step is to utilize the predicted differential deflection, according to those same trends, to predict the interior girder deflections.

To implement this approach, specific relationships were established between the controlling parameters (skew offset, exterior-to-interior girder load ratio, and girder spacing-to-span ratio) and the girder deflection behavior by investigating the trends presented in Section 6.3. First, the effect of skew offset and exterior-to-interior girder load ratio on exterior girder deflections is addressed. Then, a discussion is presented regarding the differential deflection predictions, as influenced by all three key parameters.

6.4.1 Exterior Girder Deflections

6.4.1.1 Skew Offset

To investigate the skew offset, the exterior girder deflections at the 0 degree skew offset were divided by the corresponding deflection at the other skew offsets. The resulting ratio defined the change in deflection as the skew offset was increased. It is apparent in Figure 6.13 that plots of deflection ratio vs. skew offset followed a tangent function for each bridge. The A and B variables of the general tangent function, $A\tan(Bq)$, were then adjusted to best fit the tangent function through the plots. Results indicated that values of 0.1 and 1.2 for A and B were appropriate up to around 65 degrees skew offset. Figure 6.13 includes plots of all seven simple span bridges and the fitted tangent function. Note that the tangent function is vertically offset one unit and aligned with the deflection ratio plots.

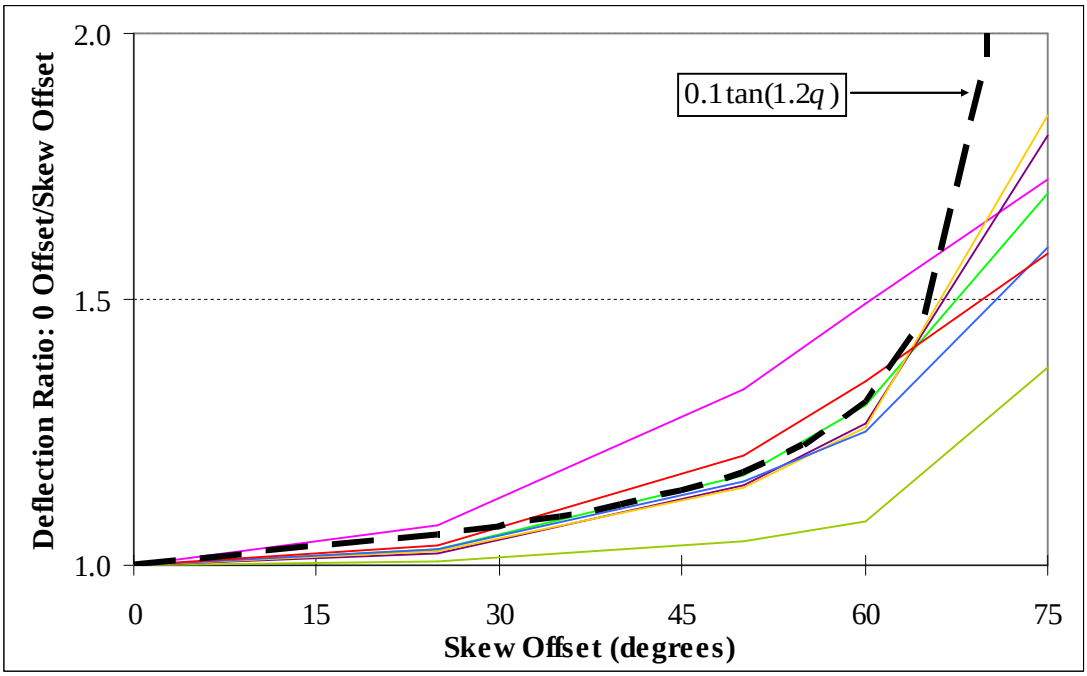

Figure 6.13: Exterior Girder Deflection as Related to Skew Offset

6.4.1.2 Exterior-to-Interior Girder Load Ratio

The exterior-to-interior girder load ratio was further studied by isolating the individual exterior girder deflections. Plotting the deflections vs. the exterior-to-interior girder load ratio revealed a linear relationship at all considered skew offset values (0, 50 and 60). Figure 6.14 presents the results for the Camden SB Bridge.

In the 0 degree skew offset model, the exterior girder deflection increases about 22 percent as the exterior-to-interior girder load ratio is increased from 50 to 100 percent, as shown in Figure 6.14. For Eno and Camden SB, the increase is 25 and 28 percent, respectively. It is apparent that the effect of exterior-to-interior girder load ratio on exterior girder deflections is dependent on additional variables.

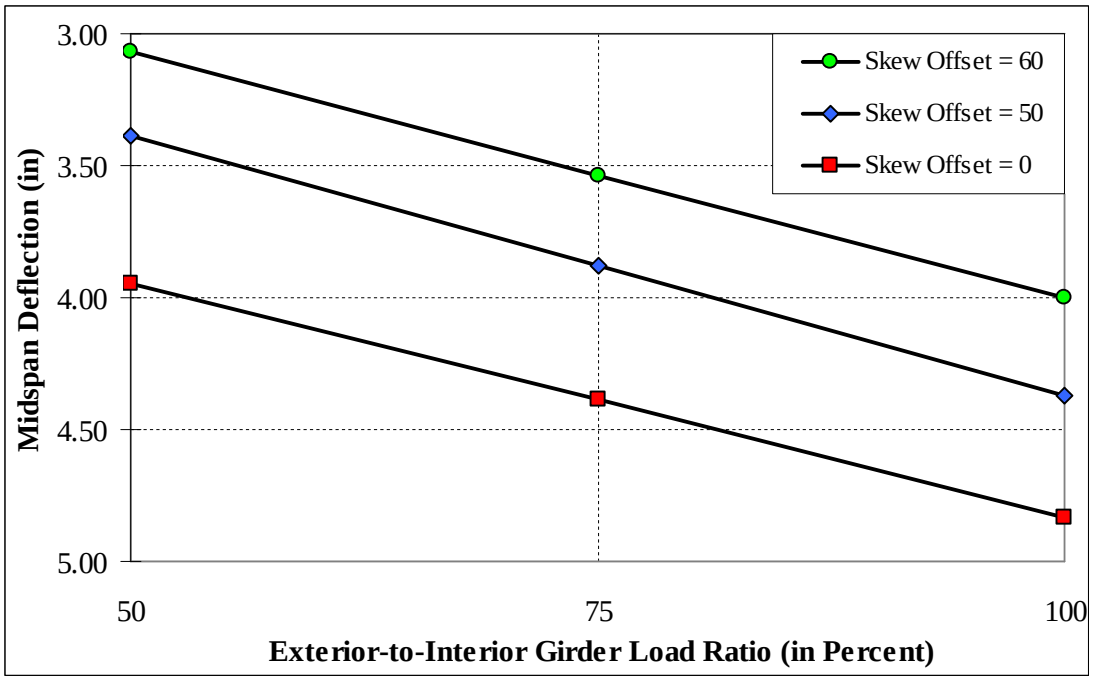

Figure 6.14: Exterior Girder Deflections as Related to Exterior-to-Interior Girder Load Ratio

To resolve the discrepancy, a multiplier variable was adapted into a spreadsheet analysis. The spreadsheet accounted for both the tangent relationship of the skew offset and the linear relationship of the exterior-to-interior girder load ratio. The multiplier was changed manually to match ANSYS modeling deflection results for every bridge, at various skew offsets, with a 75 percent exterior-to-interior girder load ratio. The multiplier values were tabulated and graphed vs. skew offset (see Figure 6.15).

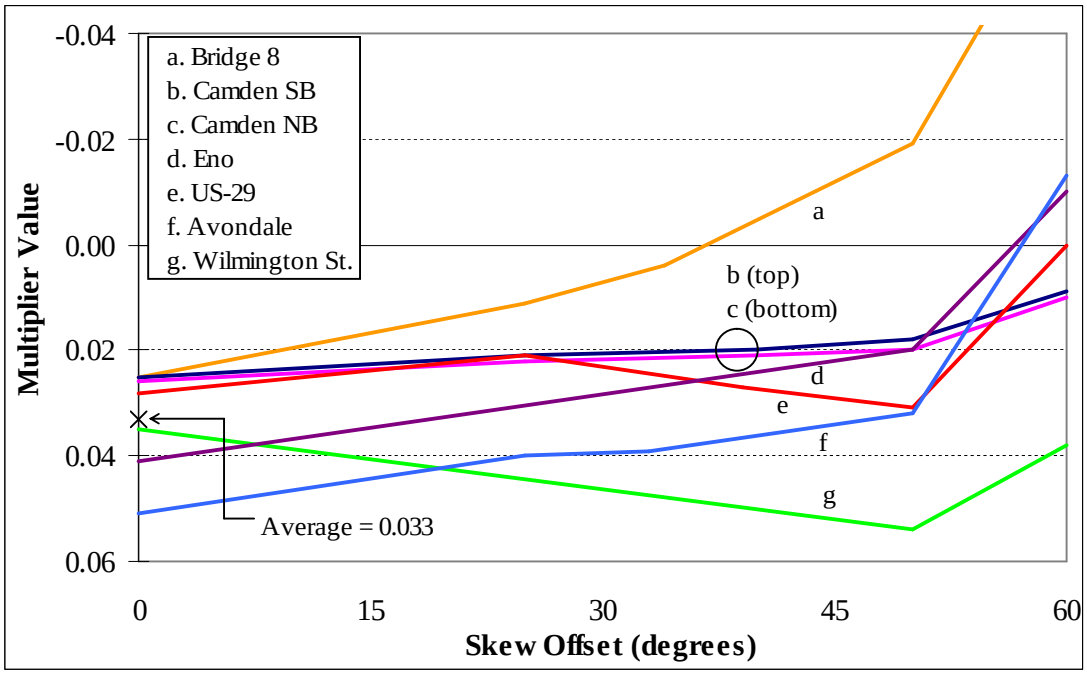

Figure 6.15: Multiplier Analysis Results for Determining Exterior Girder Deflection

For the non-skewed models, the multiplier value averaged to 0.033 (labeled in Figure 6.15), and therefore, was set to 0.03 at 0 degree skew offset for all bridges. Because different behaviors transpired as the skew offset was increased, linear trend lines were plotted through each data set and their slopes were compared to other parameters. An applicable relationship exists between the trend line slope and girder spacing, as presented in Figure 6.16. The dashed line represents a fitted linear trend line between 2.5 and 3.5 meter girder spacing, with a slope of 0.001. The trend line slope value of 0.0002 is used at girder spacing less than or equal to 8.2 feet.

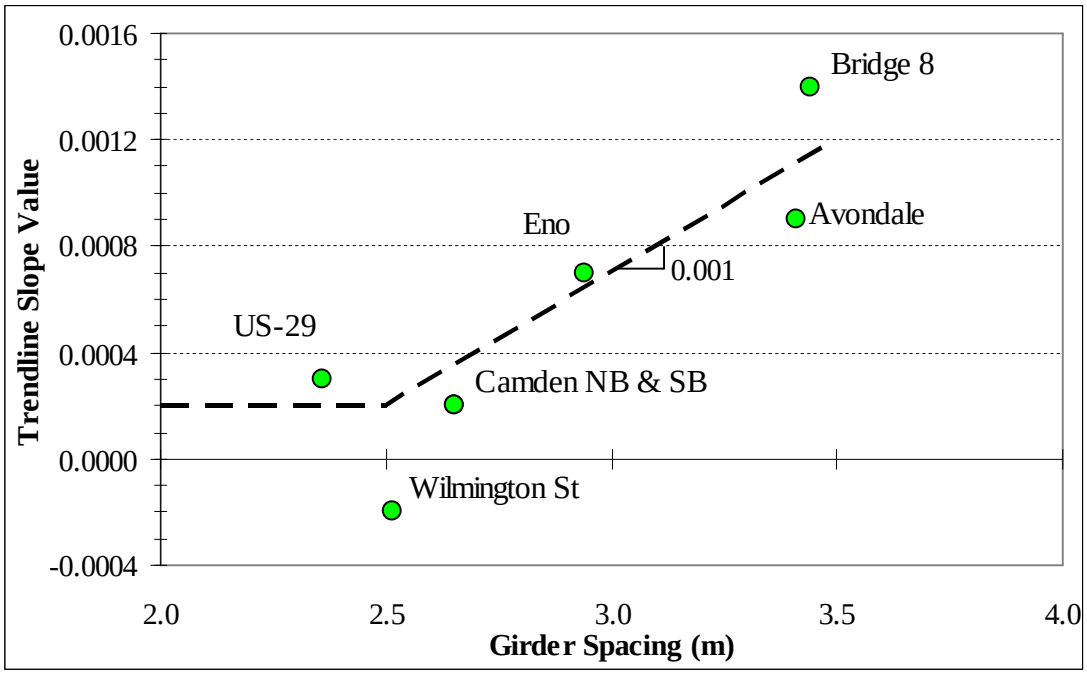

Figure 6.16: Multiplier Trend Line Slopes as Related to Girder Spacing

Therefore, the exterior girder deflection may be adjusted according the exterior-to-interior girder load ratio by also considering the girder spacing. The girder spacing determines the trend line slope value, which determines the multiplier value at a given skew offset. The multiplier is applied directly to the exterior-to-interior girder load ratio to restrain its effect on the exterior girder deflection.

6.4.1.3 Conclusive Results

A final equation to predict the exterior girder deflection was developed from the findings presented in the previous sections. The result is presented in Equation 6.1, accounting for skew offset and exterior-to-interior girder load ratio. This equation is applicable to bridge structures with a skew offset angle, q, less than or equal to sixty five degrees.

$$d_{EXT} = [d_{SGL\_INT} - F(100 - L)][1 - 0.1\tan(1.2q)] \quad \text{(eq. 6.1)}$$

where: d_{SGL_INT} = interior girder SGL predicted deflection at locations along the span (in)

$F = 0.03 - a(q)$

where: $a = 0.0002$ if $(g <= 8.2)$

$a = 0.0002 + 0.000305\,(g - 8.2)$ if $(8.2 < g <= 11.5)$

where: g = girder spacing (ft)

L = exterior-to-interior girder load ratio (in percent, ex: 65 %)

q = skew offset (degrees) = |skew - 90|

6.4.2 Differential Deflections

6.4.2.1 Skew Offset

The previously described procedure was repeated to determine the influence of skew offset on differential deflections. Instead of deflection ratios, the actual differential deflection values were reviewed; again, 0.1 and 1.2 for A and B were deemed appropriate for the tangent function up to a skew offset of about 65 degrees. The plot in Figure 6.17 displays the fitted tangent function (vertically offset down 0.05 units) and the differential deflections for all seven simple span bridges as the skew offset is increased.

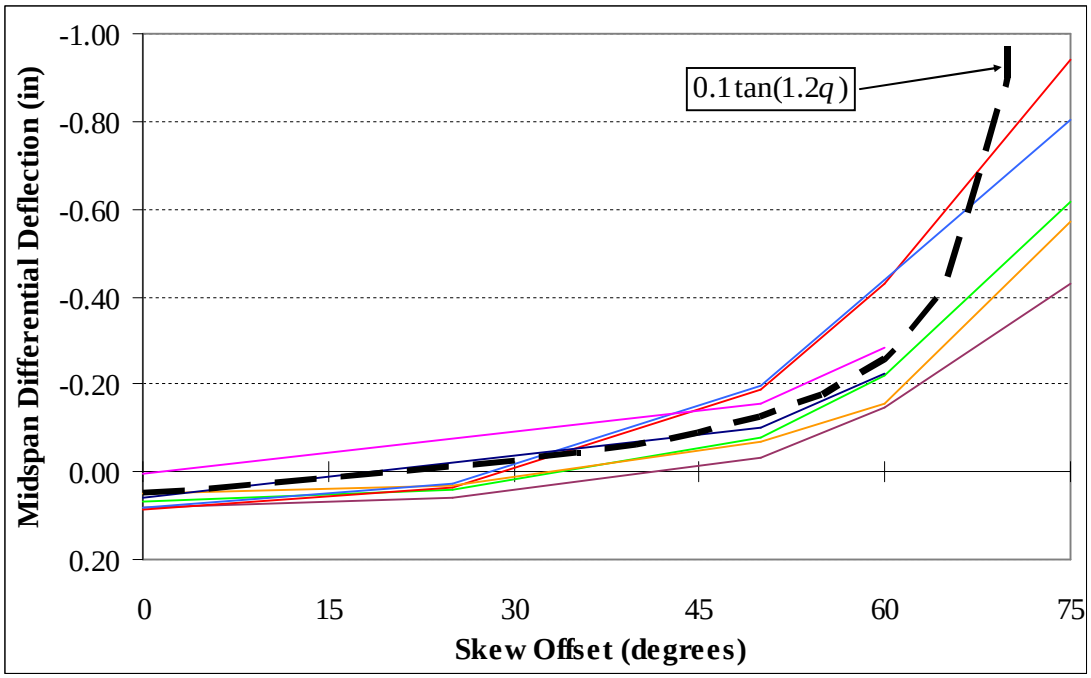

Figure 6.17: Differential Deflections as Related to Skew Offset

6.4.2.2 Exterior-to-Interior Girder Load Ratio

Differential deflections were plotted vs. exterior-to-interior girder load ratios at various skew offsets to determine the relationship. Again, linear trends were observed in all three bridges (Eno, Wilmington St, and Camden SB), as shown for the Camden SB Bridge in Figure 6.18. As the exterior-to-interior girder load ratio is decreased, the differential deflection increases (i.e. produces more of a "bowl" shape).

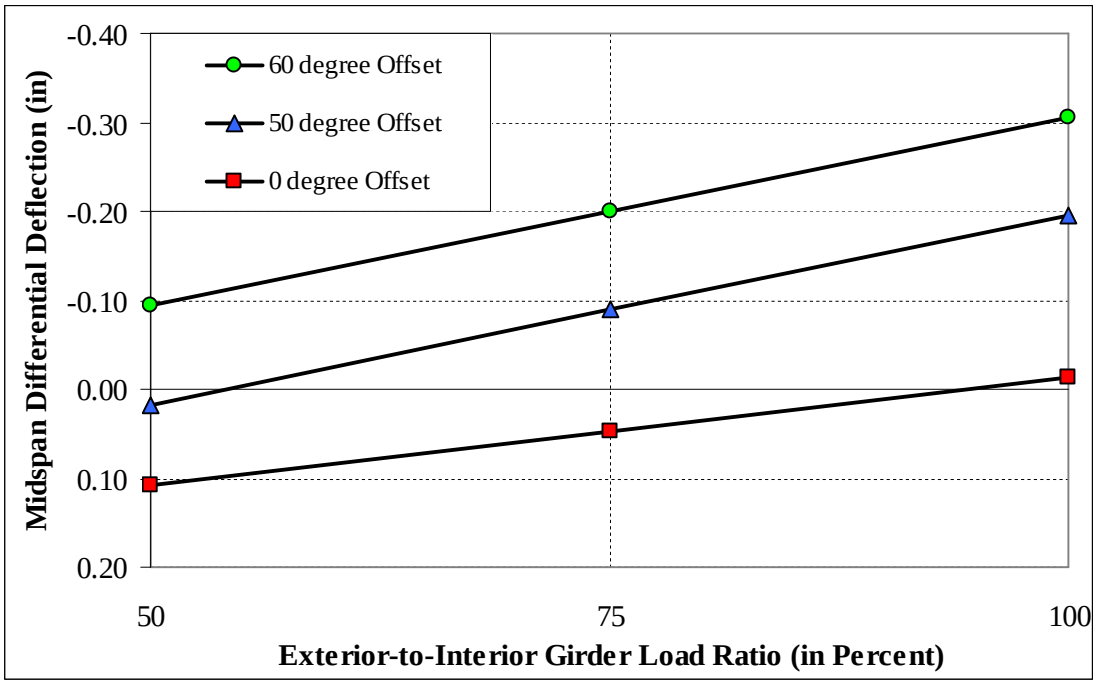

Figure 6.18: Differential Deflections as Related to Exterior-to-Interior Girder Load Ratio

For the three bridges, the change in differential deflection was analyzed vs. the girder spacing-to-span ratio, for 0 degree skew offset models, as the exterior-to-interior girder load ratio was decreased from 100 to 50 percent. Consequently, the differential deflection varied more for higher girder spacing-to-span ratios, following the trend displayed in Figure 6.12. Figure 6.19 presents the differential deflection increase vs. the girder spacing-to-span ratio for the three bridges, resulting from the decreased exterior-to-interior girder load ratio. Included is a linear trend line, fit to account for expected data point values for the other four simple span bridges (again, according to Figure 6.12). The slope value for the trend line was rounded up to ten (from about 9.3) because subsequent spreadsheet analysis revealed minimal change to the final differential deflection prediction as the slope value was varied.

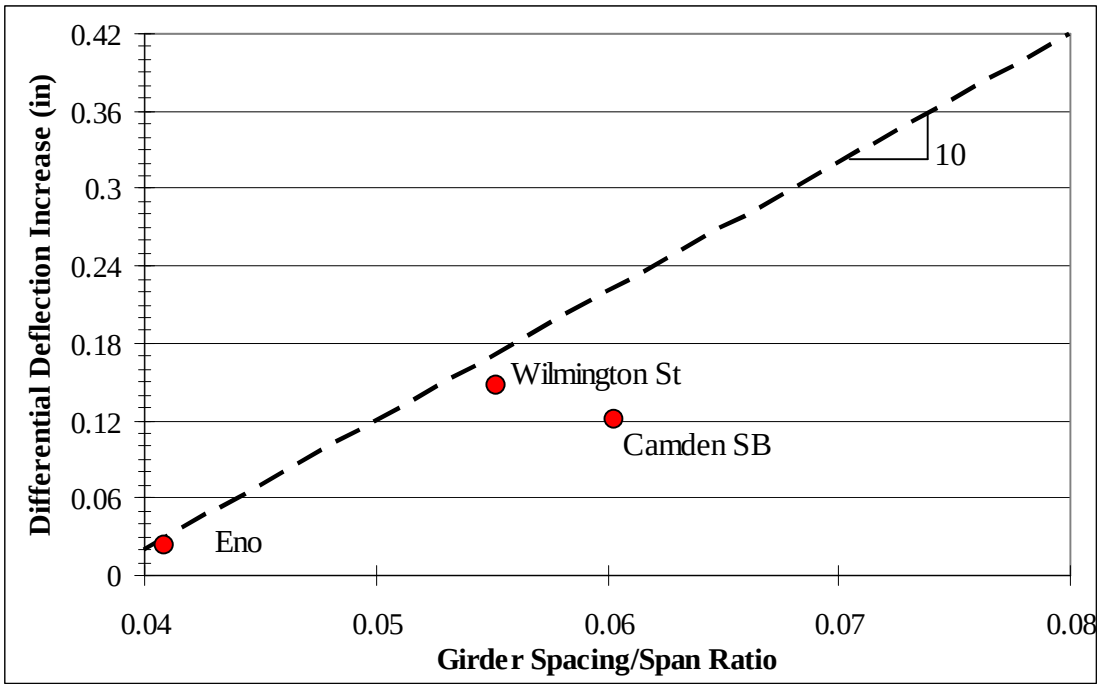

Figure 6.19: Differential Deflections as Related to Girder Spacing-to-Span Ratio

Therefore, the amount of change in differential deflection, as the exterior-to-interior girder load ratio increases or decreases, is dependant upon the girder spacing-to-span ratio. Also, the minimal effect of changing the slope value applied in the equation reveals the minor, but considerable, influence of exterior-to-interior girder load ratio on differential deflection.

6.4.2.3 Girder Spacing-to-Span Ratio

Previously, Figure 6.12 presented the differential deflections vs. girder spacing-to-span ratios for 0 degree offset models. The results for the 50 degree offset models are displayed in Figure 6.20. The linear trend apparent in Figure 6.12 is no longer present in Figure 6.20, therefore, the effect of the girder spacing-to-span ratio is dependant on additional variables.

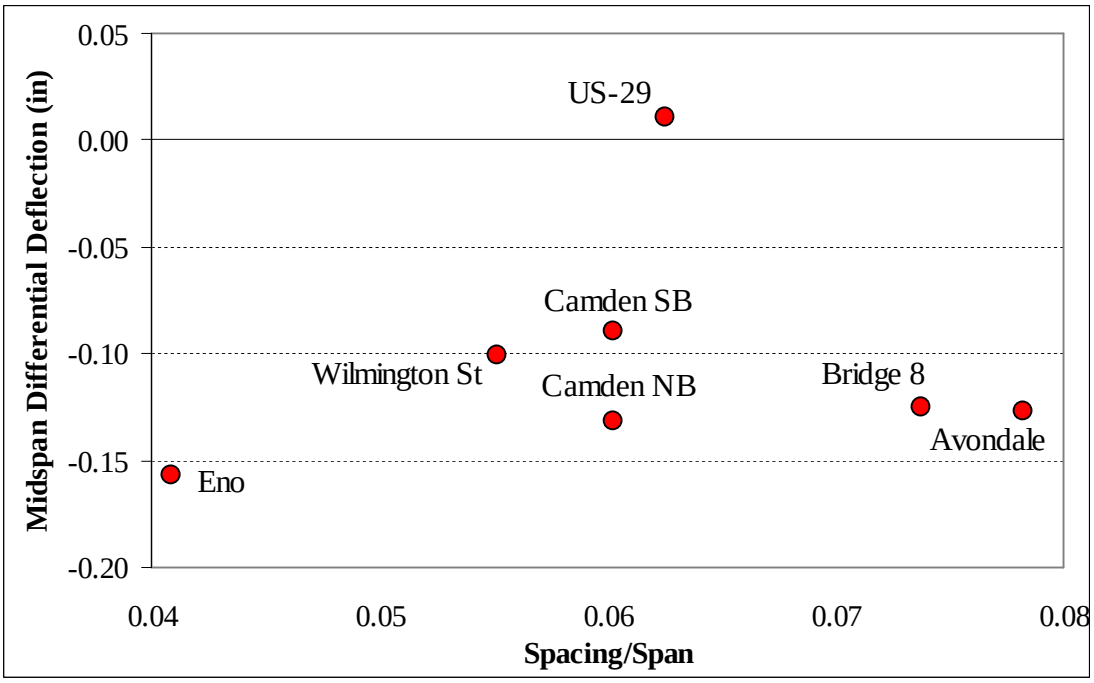

Figure 6.20: Differential Deflections at 50 Degrees Skew Offset as Related to the Girder Spacing-to-Span Ratio

Again, a multiplier variable was adapted into a spreadsheet analysis. Differential deflections were predicted in the spreadsheet, accounting for the skew offset and the exterior-to-interior girder load ratios, previously discussed. As previously described for the exterior girder deflection, the multiplier values were manually changed and the resulting multiplier values were graphed vs. skew offset (see Figure 6.21).

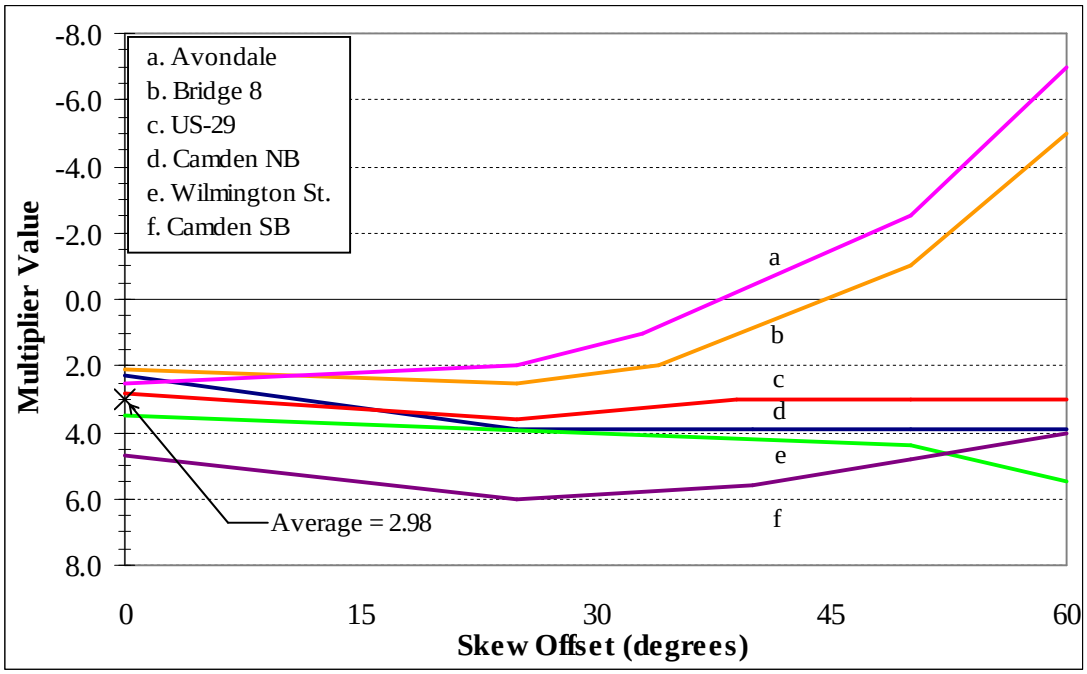

Figure 6.21: Multiplier Analysis Results for Determining Differential Deflection

Eno Bridge data is absent in Figure 6.21 on account of the inconsiderable effect of manually changing the multiplier value (i.e. small changes in differential deflection were observed for high ranges of multiplier values). For the non-skewed models of the remaining bridges, the multiplier value averaged to 2.98 (labeled in Figure 6.21), therefore set to 3.0 for all bridges. Distinct behaviors emerge as the skew offset is increased and, therefore, linear trend lines were plotted through the data sets and their slopes were set against other parameters. A useful relationship is present between the trend line slope and the girder spacing-to-span ratio, as presented in Figure 6.22. The dashed line represents a fitted linear trend line between the ratios of 0.05 and 0.08, with a slope of 8.0. The trend line slope value of -0.08 is used at ratio values less than or equal to 0.06.

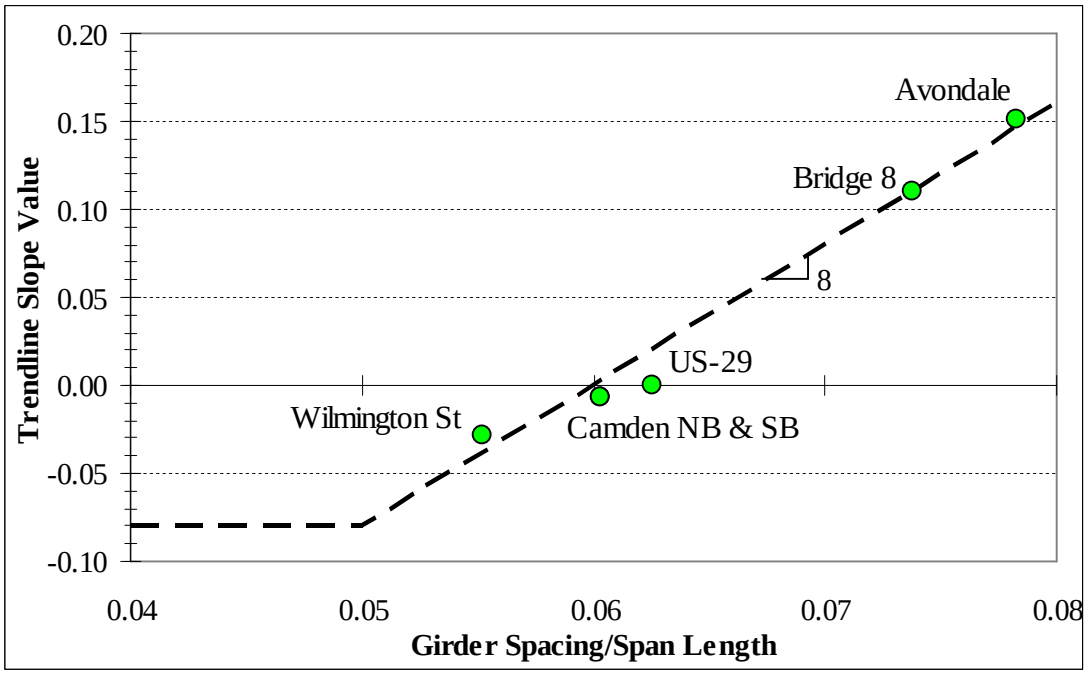

Figure 6.22: Multiplier Trend Line Slopes as Related to Girder Spacing-to-Span Ratio

Therefore, the differential deflection may account for the girder spacing-to-span ratio by reanalyzing the girder spacing-to-span ratio as the skew offset is increased. The ratio determines the trend line slope value, which determines the multiplier at a given skew offset, starting at 3.0 for non-skewed bridges. The multiplier is applied directly to the girder spacing-to-span ratio to determine its effect on the differential deflection.

6.4.2.4 Conclusive Results

A final equation to predict the differential deflection between adjacent girders was developed from the findings presented in the previous sections. The result is presented in Equation 6.2, accounting for skew offset, exterior-to-interior girder load ratio, and girder spacing-to-span ratio. This equation is applicable to bridge structures with a skew offset angle, q, less than or equal to sixty five degrees.

$$\boldsymbol{D_{INT}} = \boldsymbol{x}\left[a\left(\boldsymbol{S} - \mathbf{0.04}\right)\left(\mathbf{1} + \boldsymbol{z}\right) - \mathbf{0.1}\,\boldsymbol{tan}\left(\mathbf{1.2}q\right)\right] \qquad \text{(eq. 6.2)}$$

where: $\boldsymbol{x} = (d_{SGL\_INT})/(d_{SGL\_M})$

where: d_{SGL_M} = SGL predicted girder deflection at midspan (in)

$a = 3.0 - \boldsymbol{b}(q)$

where: $\boldsymbol{b} = -0.08$ if $(\boldsymbol{S} <= 0.05)$

$\boldsymbol{b} = -0.08 + 8(\boldsymbol{S} - 0.05)$ if $(0.05 < \boldsymbol{S} <= 0.08)$

where: $\boldsymbol{S}$ = girder spacing-to-span ratio

$\boldsymbol{z} = (10(S - 0.04) + 0.02)(2 - \boldsymbol{L}/50)$

q = skew offset (degrees) = |skew - 90|

The applied scalar variable, x, scales the differential deflection by accounting for the location along the span. The maximum differential deflection occurs at the maximum deflection location (i.e. the mid-span for simple span bridges). As the span approaches the support, the differential deflection is scaled proportional to the girder deflection at that location. For instance, the differential deflection at the quarter span is scaled by the ratio of quarter span deflection to mid-span deflection. The deflections used to calculate the scalar, x, should be obtained from simple SGL predictions.

To illustrate the scalar application, Figure 6.23 presents an example situation. Twentieth point deflections were calculated for a simple span bridge with a uniformly distributed load according to the AISC Manual of Steel Construction. The deflections were

divided by the mid-span deflection and the ratios (i.e. the scalar variable) were plotted for half the span. Also included is an illustration of the span configuration. Note that the example is for girders with constant cross-section.

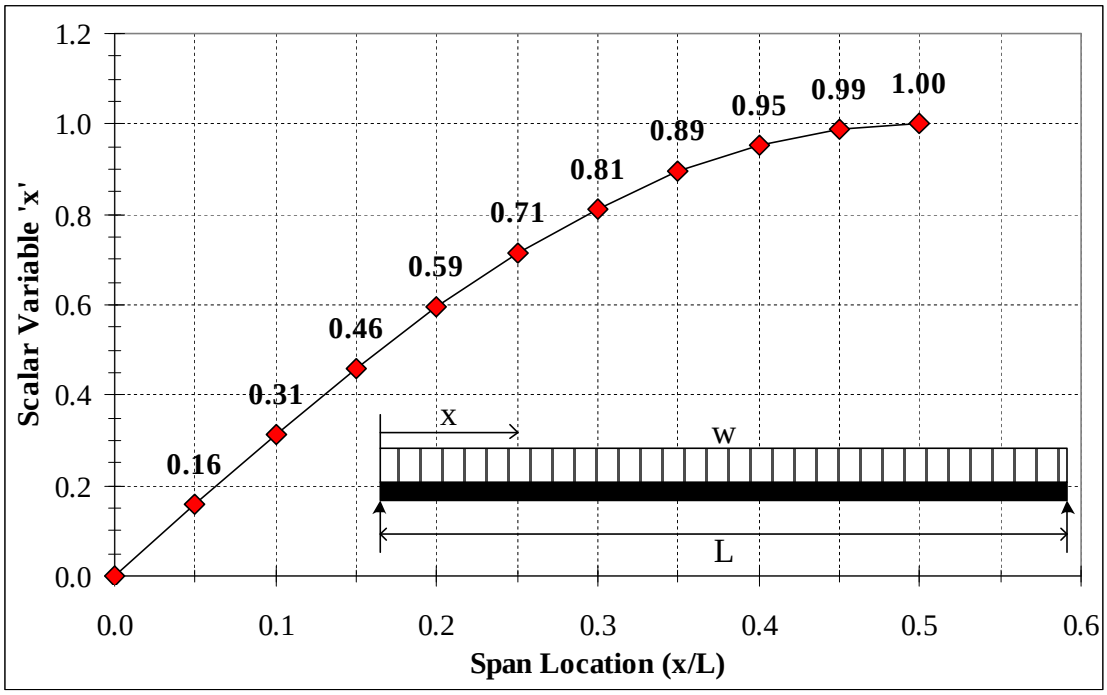

Figure 6.23: Scalar Values for Simple Span Bridge with Uniformly Distributed Load

A final note regarding the application of the differential deflection: through multiple spreadsheet analyses, it was apparent that the differential deflection should only be applied twice to adjacent girders. Therefore, in a seven girder bridge (girders labeled A-G), the girder A deflection is calculated with Equation 6.1, and then the deflections of girders B and C are calculated by adding the differential deflection predicted via Equation 6.2. Finally, the girder D deflection will simply equal that of girder C and the deflections of girders E, F, and G will equal to the deflections of girders C, B, and A respectively. The resulting predicted

deflected shape is symmetrical about a vertical axis through the middle of the cross-section. See the subsequent section and/or Appendix B for further explanation.

6.4.3 Example

To illustrate the entire simplified procedure, the deflections predicted by the simplified procedure were calculated and plotted for the US-29 Bridge in Figure 6.24, along with the SGL predicted deflections. First, the exterior girder deflection (δ_{EXT} = 4.73 inches) was calculated according to the interior SGL deflection (δ_{SGL_i} = 6.76 inches). Next, the differential deflection (D_{INT}) was calculated as -0.085 inches and added twice to predict the adjacent girder deflections (as denoted in Figure 6.24). The predicted differential deflection is not added to the girder 3 prediction, and, therefore, the deflections of girders 3, 4 and 5 are equal (4.56 inches). Additionally, note that the deflected shape predicted by the simplified procedure is symmetrical about an imaginary vertical axis through girder 4. A more in depth example is presented in Appendix B with sample calculations.

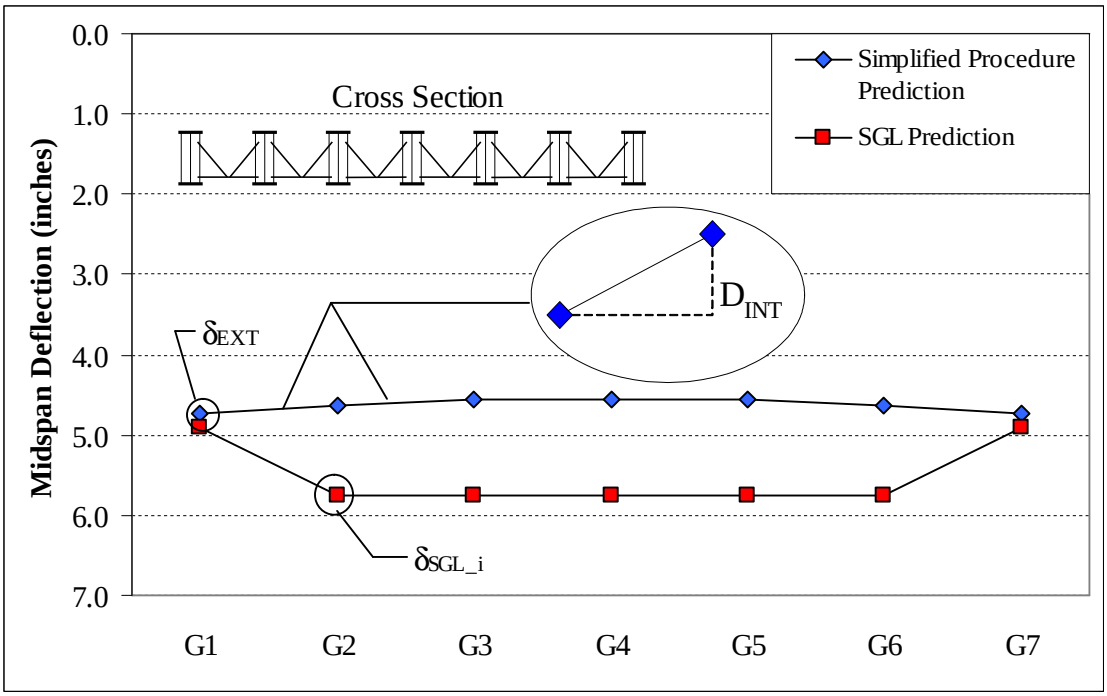

Figure 6.24: Deflections Predicted by the Simplified Procedure vs. SGL Predicted Deflections for the US-29 Bridge

6.4.4 Conclusions

The simplified development procedure involved generating two empirical equations. The first equation utilizes the traditional interior SGL prediction and adjusts the magnitude by considering the skew offset, the exterior-to-interior girder load ratio, and the girder spacing. The second equation predicts the differential deflection by accounting for the skew offset, the exterior-to-interior girder load ratio, the girder spacing-to-span ratio, and the span location. The detailed procedure is addressed in Section 7 and a flow chart is presented in Appendix A.

6.5 Additional Considerations

Thus far, the developed equations have exclusively accounted for simple span bridges with equal exterior-to-interior girder load ratios. Additional limited studies were conducted

to consider continuous span bridges with equal exterior-to-interior girder load ratios and simple span bridges with unequal exterior-to-interior girder load ratios.

6.5.1 Continuous Span Bridges

The effect of skew offset on deflection behavior was investigated for both two-span continuous bridges (Bridge 10 and Bridge 14) to determine if the developed equations are applicable to continuous span structures. Eight finite element models were generated: one model for each structure at 0, 25, 50, and 60 degree skew offsets. The resulting deflections were monitored at the locations of predicted maximum deflection (see Section 3.3.2). Figures 6.25 and 6.26 present deflections for Bridge 10, whereas Figures 6.27 and 6.28 present deflections for Bridge 14.

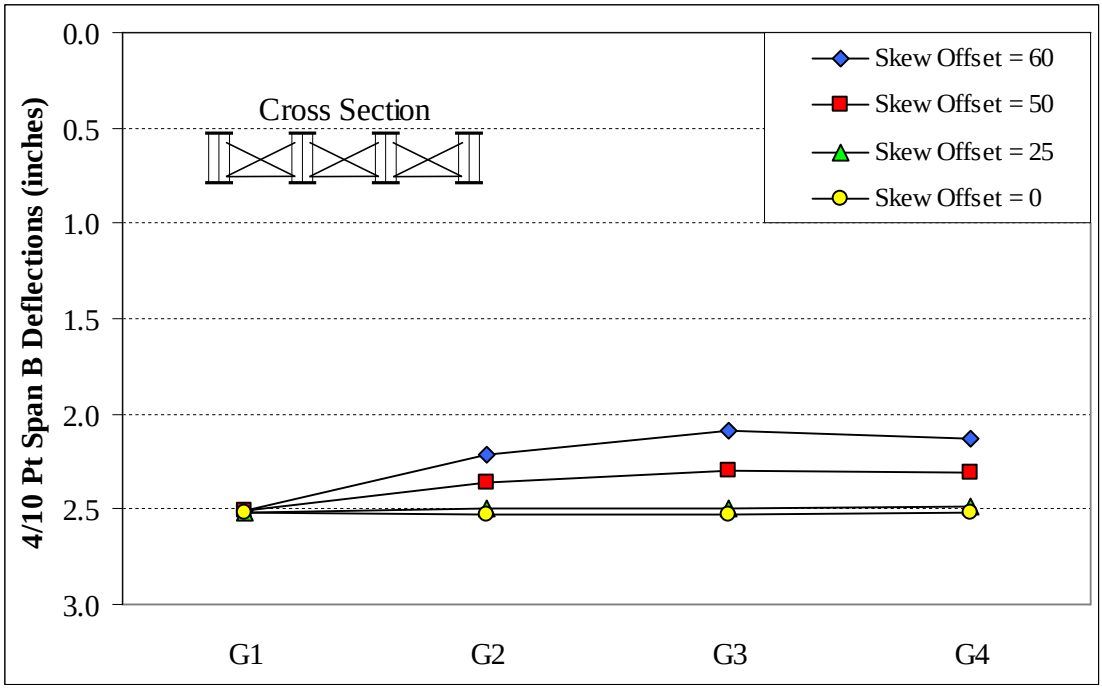

Figure 6.25: Bridge 10 – Span B Deflections at Various Skew Offsets

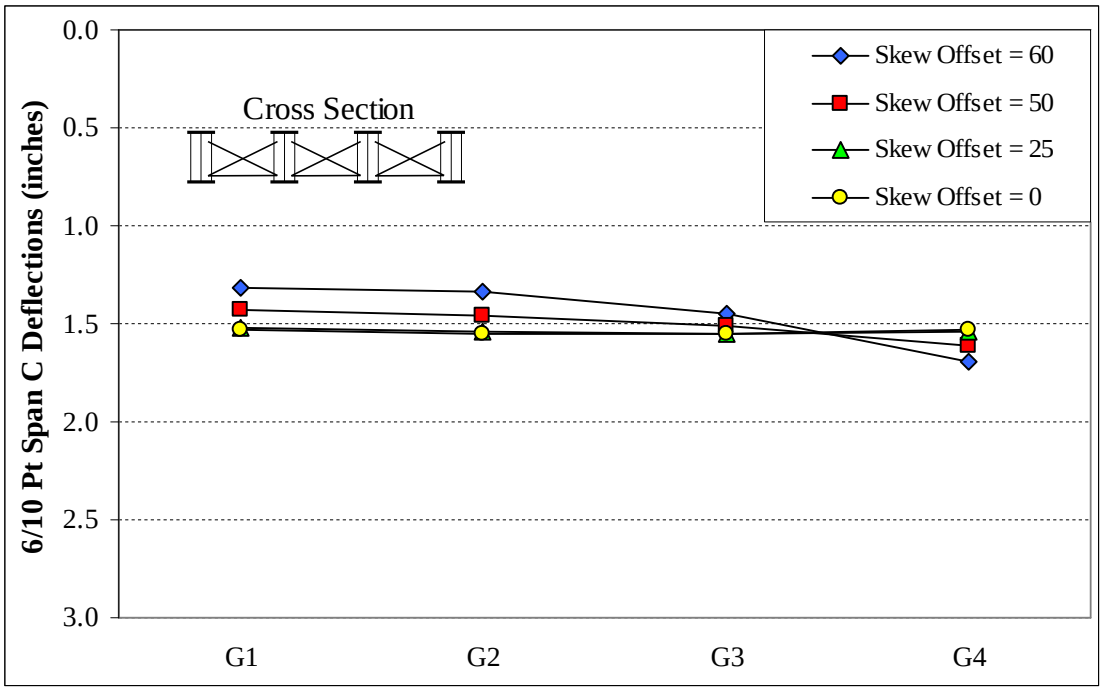

Figure 6.26: Bridge 10 – Span C Deflections at Various Skew Offsets

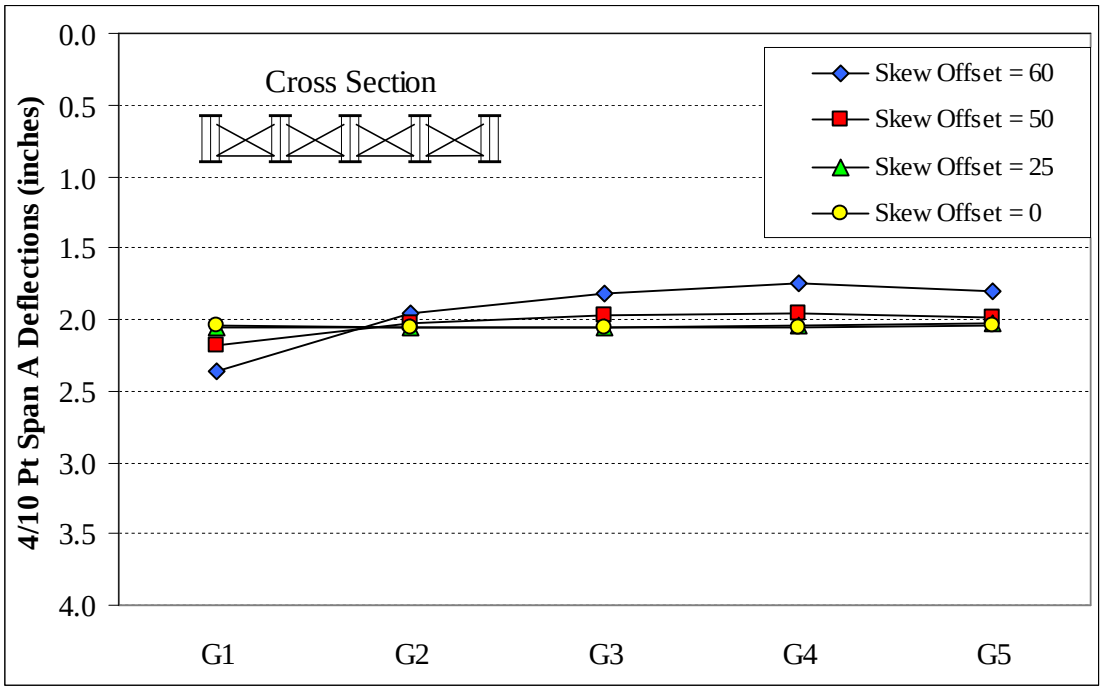

Figure 6.27: Bridge 14 – Span A Deflections at Various Skew Offsets

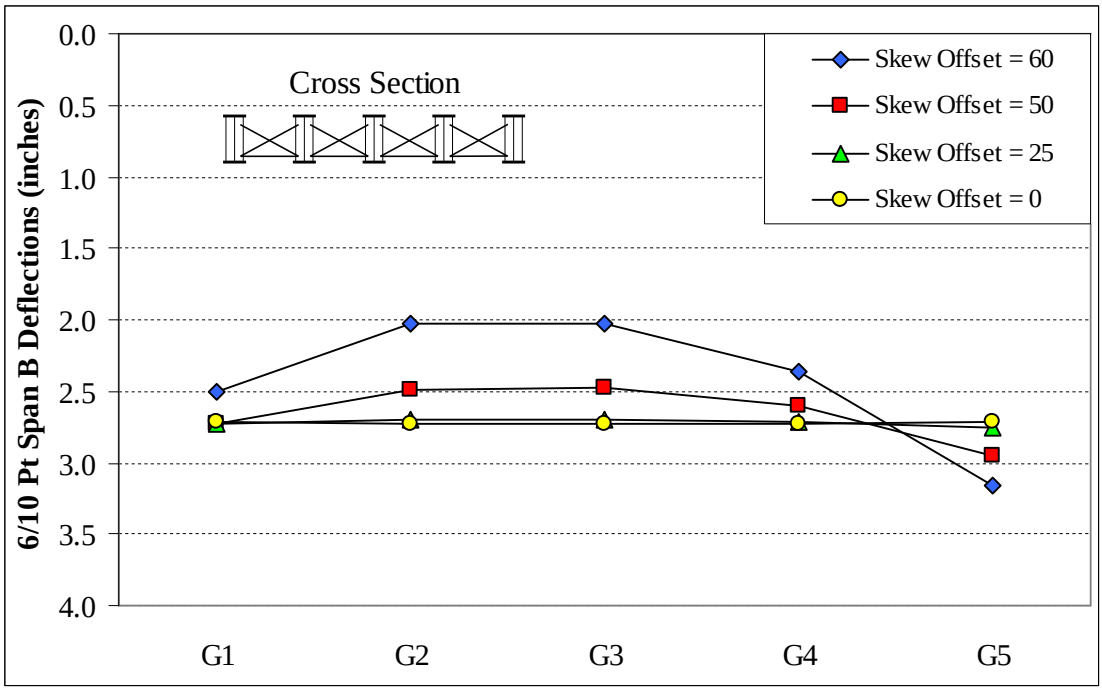

Figure 6.28: Bride 14 – Span B Deflections at Various Skew Offsets

The illustrated behavior is dislike those observed for the simple span bridges, in which all girders deflected less as skew was increased (see Figure 6.10). For the continuous span bridges, one exterior girder deflects more as the skew offset is increased, while the other exterior girder deflects less. This behavior is caused by the interaction of a given span with the adjacent span.

Two prediction methods were investigated for two-span continuous bridges. They are: the traditional SGL method and an alternate SGL method. The alternate SGL method utilizes the exterior SGL deflections by connecting them with a straight line (i.e. the method predicts equal deflections for each girder, which is equal to the exterior SGL deflection); hence it is labeled the SGL straight line method (SGLSL method). A detailed procedure is addressed in Section 7 and a flow chart is presented in Appendix A. Note that the observed

deflection behavior for continuous span bridges was inconsistent with simple span bridge behavior; therefore, the developed simplified procedure was not applicable.

6.5.2 Unequal Exterior-to-Interior Girder Load Ratios

Unequal exterior-to-interior girder load ratios were considered for the Eno Bridge and the Wilmington St Bridge. Eight finite element models were analyzed to check both bridges at skew offsets of 0, 25, 50, and 60 degrees. For the Eno Bridge, the exterior-to-interior girder load ratio for girders 1 and 5 were 94 percent and 74 percent, respectively (a 20 percent difference). For the Wilmington St Bridge, the ratio for girders 1 and 5 were 66 and 90 percent, respectively (a 24 percent difference). The results were graphed and it is apparent in Figures 6.29 (Eno) and 6.30 (Wilmington St) that an alternative procedure must be applied to aptly predict deflections for bridges with unequal exterior-to-interior girder load ratios.

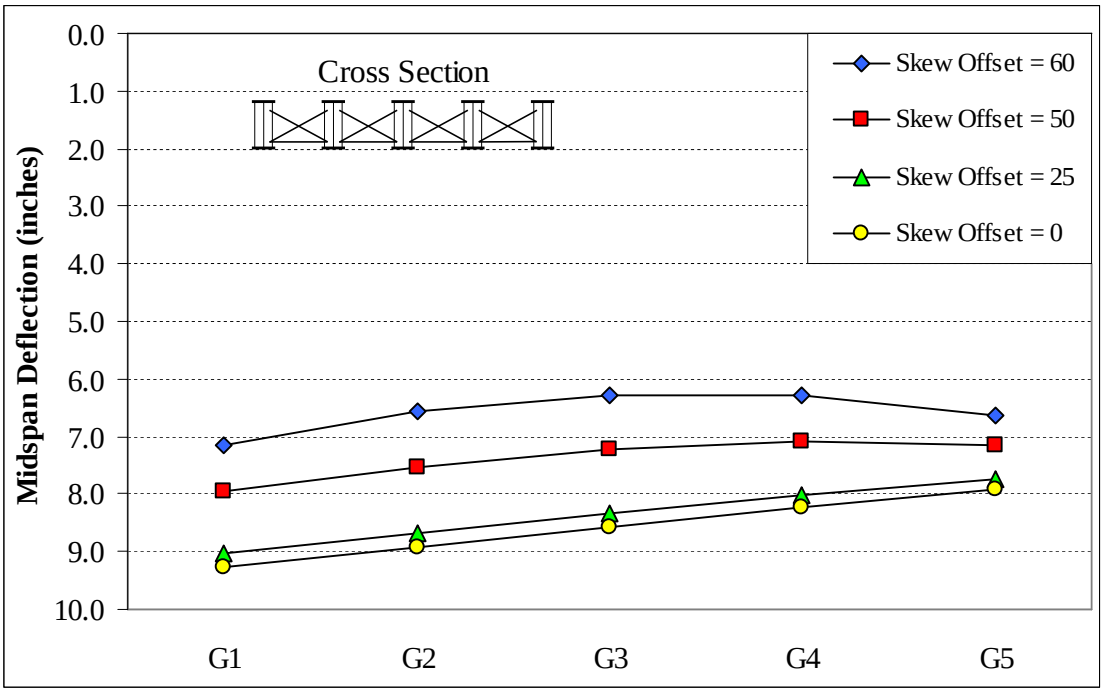

Figure 6.29: Unequal Exterior-to-Interior Girder Load Ratio – Eno Bridge

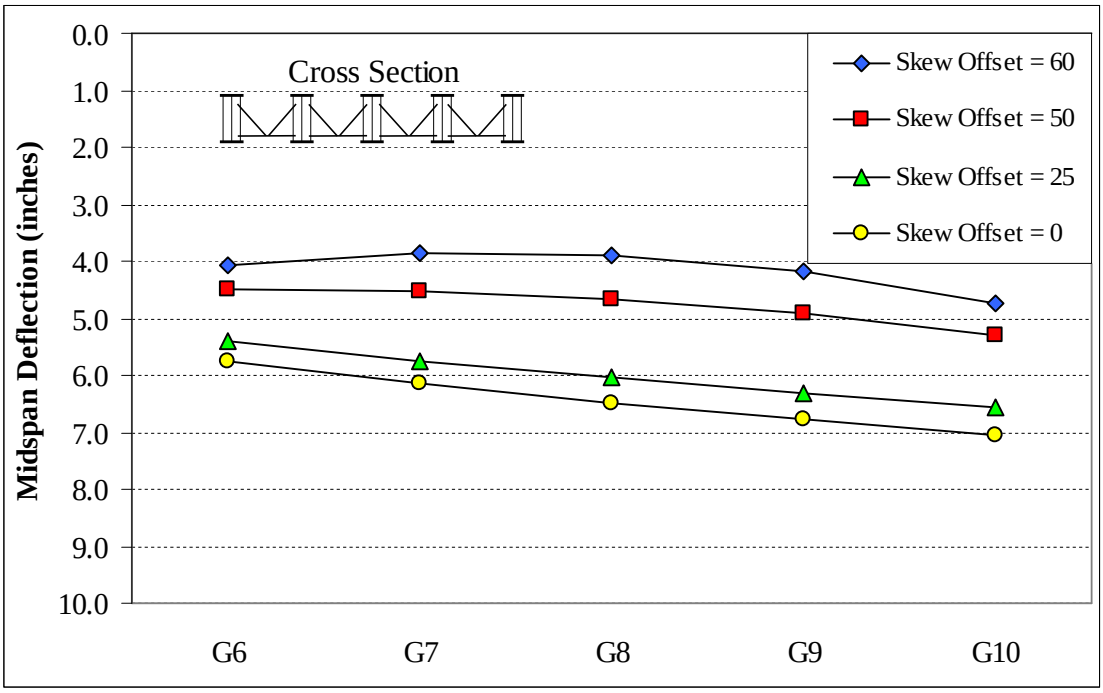

Figure 6.30: Unequal Exterior-to-Interior Girder Load Ratio – Wilmington St Bridge

Several methods were investigated to predict deflections in bridges with unequal exterior-to-interior girder load ratios, all of which utilized the developed equations of the simplified procedure. The most appropriate technique involves calculating the exterior girder deflection (Equation 6.1) for the higher exterior-to-interior girder load ratio. Additionally, the exterior girder deflection and differential deflection (Equation 6.2) are calculated according the lower exterior-to-interior girder load ratio. The results are combined to predict a linear deflection behavior for simple span bridges with unequal exterior-to-interior girder load ratios. The procedure is tagged the alternative simplified procedure (ASP) and the details are discussed in Section 7 and a flow chart is presented in Appendix A.

6.6 Summary

An extensive parametric study was conducted to determine which bridge parameters influence steel plate girder deflections. During the study, about 200 finite element bridge models were built and analyzed, each with 200,000 – 250,000 degrees of freedom. It was discovered that skew offset, exterior-to-interior girder load ratio, and the girder spacing-to-span ratio all play key roles in the deflection behavior. Further investigation established relationships between the controlling parameters and the girder deflections. A bi-linear approach was developed to predict the non-composite dead load deflections for simple span bridges with equal exterior-to-interior girder load ratios (i.e. equal overhang dimensions). Additional limited studies were performed to account for continuous span bridges with equal exterior-to-interior girder load ratios and simple span bridges with unequal exterior-to-interior girder load ratios. Section 7 presents the results and comparisons of all observed deflection behaviors, including: field measurements, SGL analysis, ANSYS modeling, the

developed simplified procedure, alternative SGL analysis (for continuous span bridges) and the alternative simplified procedure (for unequal exterior-to-interior girder load ratios).

7.0 Comparisons of Results

7.1 Introduction

The primary objective of this research is to develop a procedure to more accurately predict dead load deflections in skewed and non-skewed steel plate girder bridges. To show that this objective has been accomplished, multiple comparisons between field measured deflections, ANSYS predicted deflections, single girder line (SGL) predictions and other methods developed as a part of this research are presented. The detailed comparisons of the girder deflections presented in this section establish the necessity for an improved prediction method. The comparisons are presented in the following order:

- Field measured deflections are compared to SGL predicted deflections and ANSYS predicted deflections.
- ANSYS predicted deflections are compared to simplified procedure predictions and SGL predictions for simple span bridges with equal exterior-to-interior girder load ratios.
- ANSYS predicted deflections are compared to alternative simplified procedure (ASP) predictions and SGL predictions for simple span bridges with unequal exterior-to-interior girder load ratios.
- ANSYS predicted deflections are compared to SGL straight line (SGLSL) predictions and SGL predictions for continuous span bridges with equal exterior-to-interior girder load ratios.
- The newly developed predictions are compared to the field measured deflections for comparison, and to "close the loop".

7.2 General

To compare deflection results, multiple statistical analyses have been performed on calculated deflection ratios throughout this section. The following statistics are included: average, minimum, maximum, standard deviation, and coefficient of variance. The latter two are included to evaluate the precision of the prediction methods. A low standard deviation and coefficient of variance signify a low variability in the data set (i.e. good precision). In the presented tables, the coefficient of variance is labeled COV and the standard deviation is St. Dev.

To illustrate the statistical analyses, several box plots have been incorporated. In the plots, the boxes represent the average ratio plus or minus one standard deviation; therefore, the darkest center band represents the average and standard deviation is expanded vertically up and down. The smaller (or tighter) the box, the better the precision in the data set. The plots also include 'tails' to designate the maximum and minimum ratio values.

In developing the simplified procedure to predict deflections, it was apparent that the deflection behavior of simple span bridges differs from that of continuous span bridges. Therefore, the results and comparisons are discussed individually for simple and continuous span bridges.

Finally, this section includes several deflection ratio tables with generic girder labels ('Girders A') and non-numeric data entries ('-' or 'na'). A detailed discussion of these is included in Section 3.6.

7.3 Comparisons of Field Measured Deflections to Predicted Single Girder Line and ANSYS Deflections

Field measured deflections were compared to the predicted SGL and ANSYS deflections for all ten studied bridges. Initially, the field measured deflections were

compared individually to the predicted SGL and ANSYS deflections by calculating the ratios of the predicted to measured deflections. The ratios were calculated for mid-span deflections in the simple span bridges and at similar maximum deflection locations in the continuous span bridges. The ensuing statistical analysis contrasted the ratios to determine which deflections more accurately matched those measured in the field. The results are discussed herein.

7.3.1 Predicted Single Girder Line Deflections vs. Field Measured Deflections

Comparisons between the field measured deflections and predicted SGL deflections were made for all ten studied bridges. The details of the SGL predictions and the comparisons for simple and continuous span bridges are presented.

7.3.1.1 Single Girder Line Deflection Predictions

The structural analysis program SAP2000 was utilized to predict SGL deflections. Single girders were modeled with frame elements between nodes located at specific locations of cross-sectional variance, load bearing support, and field measurement location. Exact geometry was applied to the frame elements to accurately represent the bending properties of the steel plate girders. Additionally, the self weight of the frame elements was not included, and the effect of shearing deformation was included. Finally, non-composite dead loads were calculated from nominal dimensions presented in the construction plans, and applied to the SGL models for correlation. The deflection results confirmed the SGL models' ability to match the dead load deflections included in the bridge plans; thus, the models were deemed applicable for analysis.

7.3.1.2 Simple Span Bridges

Throughout the research study, it was apparent that the SGL predicted deflections were significantly greater than the field measured mid-span deflections for simple span bridges. Figure 7.1 displays such an example for the Wilmington St Bridge. From the figure, the measured mid-span deflection of G7 is approximately 3.5 inches less than predicted by the SGL method.

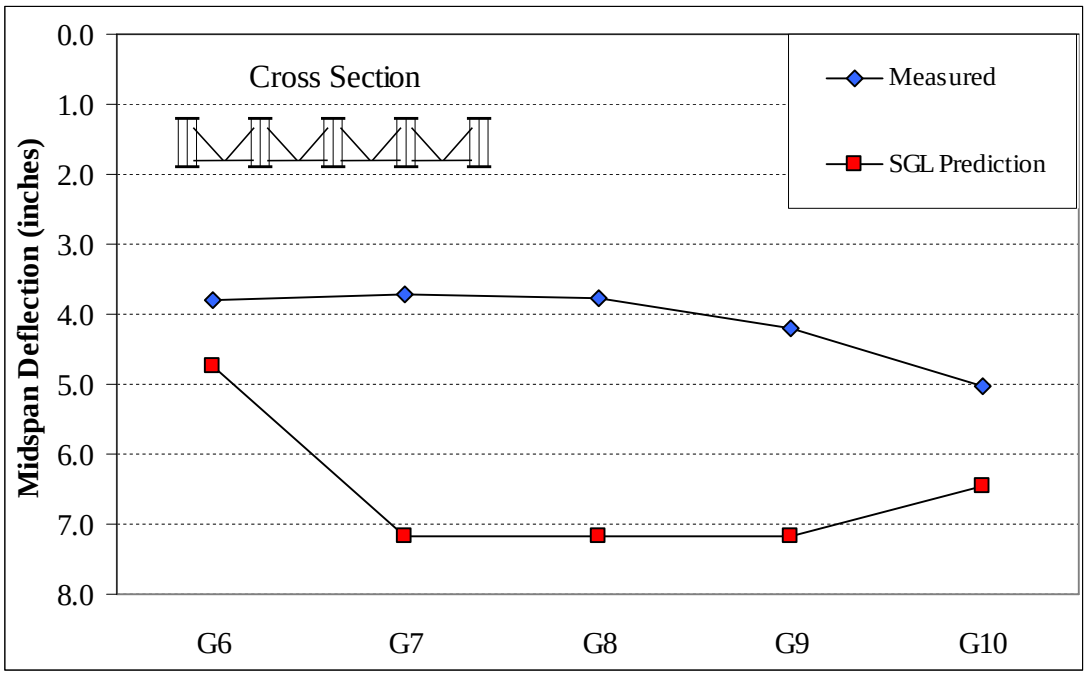

Figure 7.1: SGL Predicted Deflections vs. Field Measured Deflections for the Wilmington St Bridge

To gauge the amount of over prediction, the ratios of the predicted SGL deflections to field measured deflections were calculated for each girder of the seven simple span bridges included in this study. The results are tabulated in Table 7.1; the bridges are listed in the order of increasing skew offset.

Table 7.1: Ratios of SGL Predicted Deflections to Field Measured Deflections for Simple Span Bridges at Mid-span

	Girder A	Girder B	Girder C	Girder D	Girder E	Girder F	Girder G
Eno	1.07	1.19	1.23	1.29	0.99	na	na
Bridge 8	1.33	1.46	1.45	1.41	1.39	1.19	na
Avondale	1.16	1.30	-	1.26	-	1.20	1.02
US-29	1.10	1.39	-	1.45	-	1.34	1.05
Camden NB	0.99	1.53	-	1.45	1.54	1.02	na
Camden SB	1.06	1.62	-	1.54	-	1.62	1.09
Wilmington St	1.25	1.94	1.90	1.71	1.28	na	na

Only two data entries are slightly less than 1.0, revealing SGL deflections less than the field measured deflections (Girder A for Camden NB and Girder E of Eno). The deflection ratios tend to be greater for the interior girders than for the exterior girders. In Table 7.1, the average ratios are 1.12 and 1.46 for the exterior and interior girders respectively.

7.3.1.3 Continuous Span Bridges

For the continuous span bridges, SGL models predict deflections greater and less than field measured deflections, with no clear trend (see Table 7.2). Figure 7.2 illustrates the SGL over prediction of span A and under prediction of span B in Bridge 1. The variance in behavior is likely due to the interaction of the adjacent continuous span.

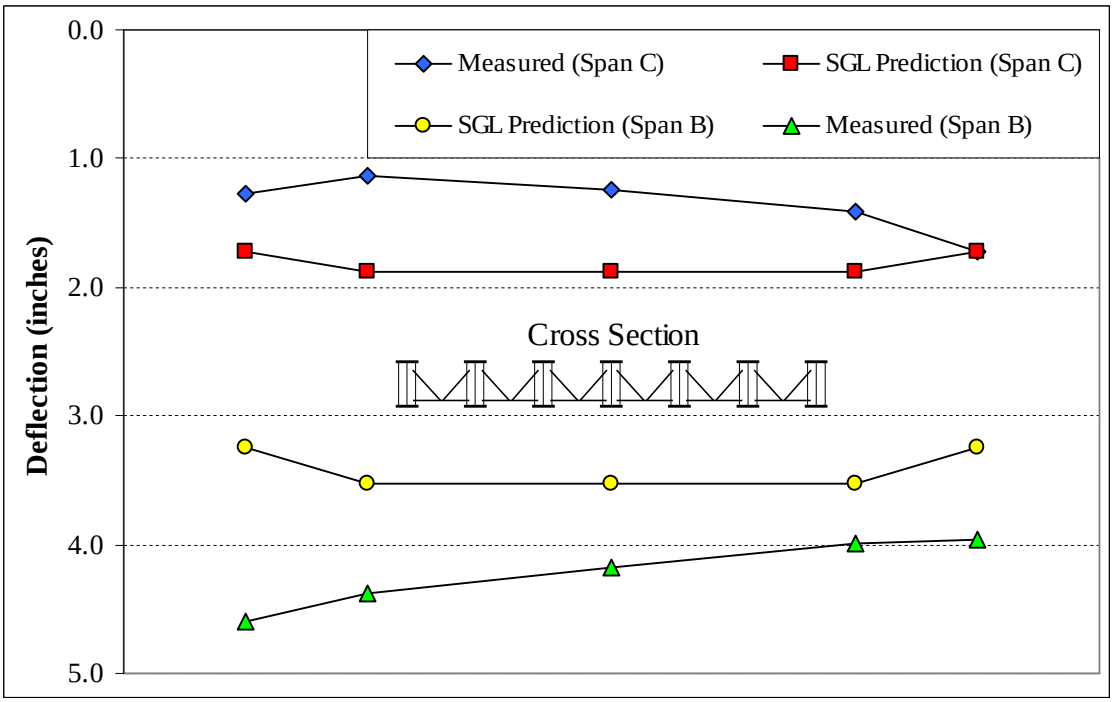

Figure 7.2: SGL Predicted Deflections vs. Field Measured Predictions for Bridge 1 (Spans B and C)

The ratios of the predicted SGL deflections to field measured deflections were calculated for each girder of the three continuous span bridges. The results are tabulated in Table 7.2. For both two-span continuous bridges (Bridges 14 and 10), SGL deflections over predict the field measured deflections for one span and under predicts them for the other. For Bridge 1, Girders F and G are under predicted in all three spans, Girders A and B are under predicted in two of the three spans, and the middle girder (D) is under predicted only is Span B. Overall, the SGL deflections appear to predict deflections equally well for both the exterior and interior girders, with average ratios of 0.96 and 1.04 respectively.

Table 7.2: Ratios of SGL Predicted Deflections to Field Measured Deflections for Continuous Span Bridges

	Span Location	Girder A	Girder B	Girder C	Girder D	Girder E	Girder F	Girder G
Bridge 14	4/10 Span A	1.13	1.28	1.05	1.20	1.92	na	na
	6/10 Span B	0.84	0.87	0.76	0.84	0.79	na	na
Bridge 10	4/10 Span B	1.10	1.27	1.40	1.07	na	na	na
	6/10 Span C	0.69	0.98	0.96	0.87	na	na	na
Bridge 1	4/10 Span A	0.80	0.99	-	1.11	-	0.96	0.78
	4/10 Span B	0.78	0.88	-	0.92	-	0.97	0.91
	35/100 Span C	1.05	1.24	-	1.16	-	0.99	0.77

7.3.2 ANSYS Predicted Deflections vs. Field Measured Deflections

ANSYS finite element models were generated for all ten studied bridges in an effort to improve predicted dead load deflections (the modeling technique is presented in Section 4). Comparisons of the field measured deflections to the ANSYS predicted deflections are discussed herein.

7.3.2.1 Simple Span Bridges

The predicted ANSYS deflections are greater than the field measured deflections at mid-span in all but one of the simple span bridges. The under prediction is possibly due to partial composite behavior of the concrete deck slab during the concrete placement and/or temperature effects due to the curing of the concrete. Figure 7.3 presents the field measured deflections and the ANSYS predicted deflections at mid-span for the US-29 Bridge.

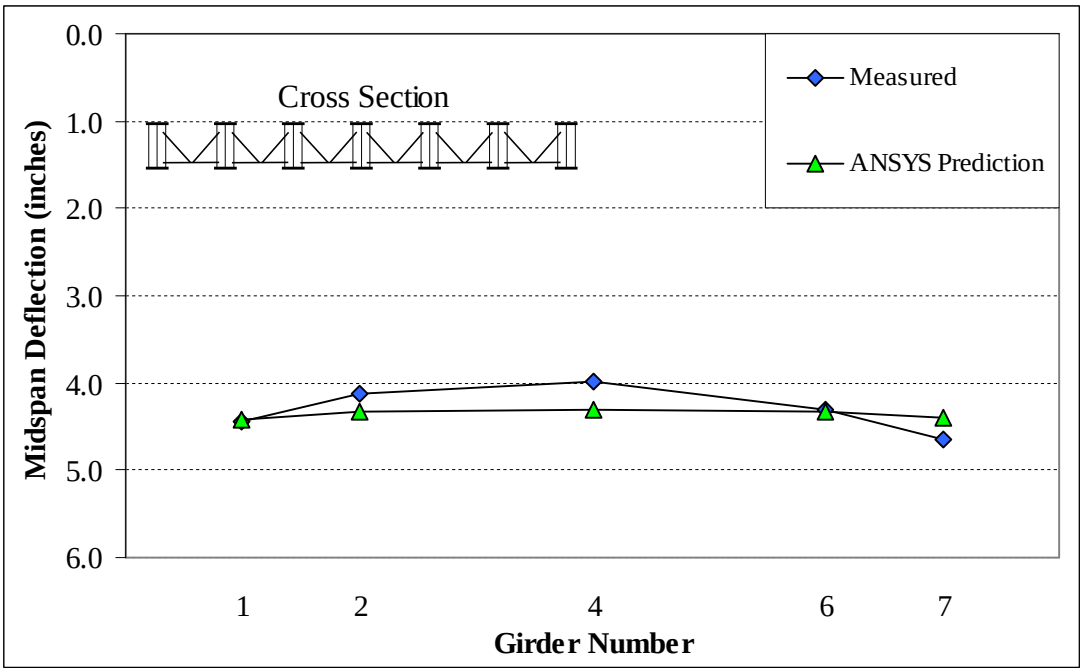

Figure 7.3: ANSYS Predicted Deflections vs. Field Measured Deflections for the US-29 Bridge

A summary of the ratios of the ANSYS predicted deflections to field measured deflections is presented in Table 7.3. The ANSYS deflections for the Wilmington St Bridge under predict the field measured deflections by an average of 20 percent for the exterior and interior girders. Overall, the average deflection ratios for the exterior and interior girders are 1.11 and 1.07 respectively. Note that the bridges are listed in the order of increasing skew offset.

Table 7.3: Ratios of ANSYS Predicted Deflections to Field Measured Deflections for Simple Span Bridges at Mid-span

	Girder A	Girder B	Girder C	Girder D	Girder E	Girder F	Girder G
Eno	1.08	1.11	1.14	1.17	1.22	na	na
Bridge 8	1.42	1.32	1.32	1.28	1.26	1.27	na
Avondale	1.12	1.09	-	1.08	-	1.04	1.04
US-29	1.02	1.07	-	1.12	-	1.04	0.97
Camden NB	1.24	1.10	-	1.01	1.11	1.28	na
Camden SB	1.14	1.01	-	0.94	-	1.00	1.15
Wilmington St	0.84	0.82	0.80	0.78	0.77	na	na

7.3.2.2 Continuous Span Bridges

For the continuous span bridges, the ANSYS predicted deflections were sometimes greater than and other times less than the field measured deflections. For instance, the ANSYS deflections were greater than the field measured deflections in span B of Bridge 14, and less in span A. Figure 7.4 includes the ANSYS predicted deflections and field measured deflections of spans B and C of Bridge 1.

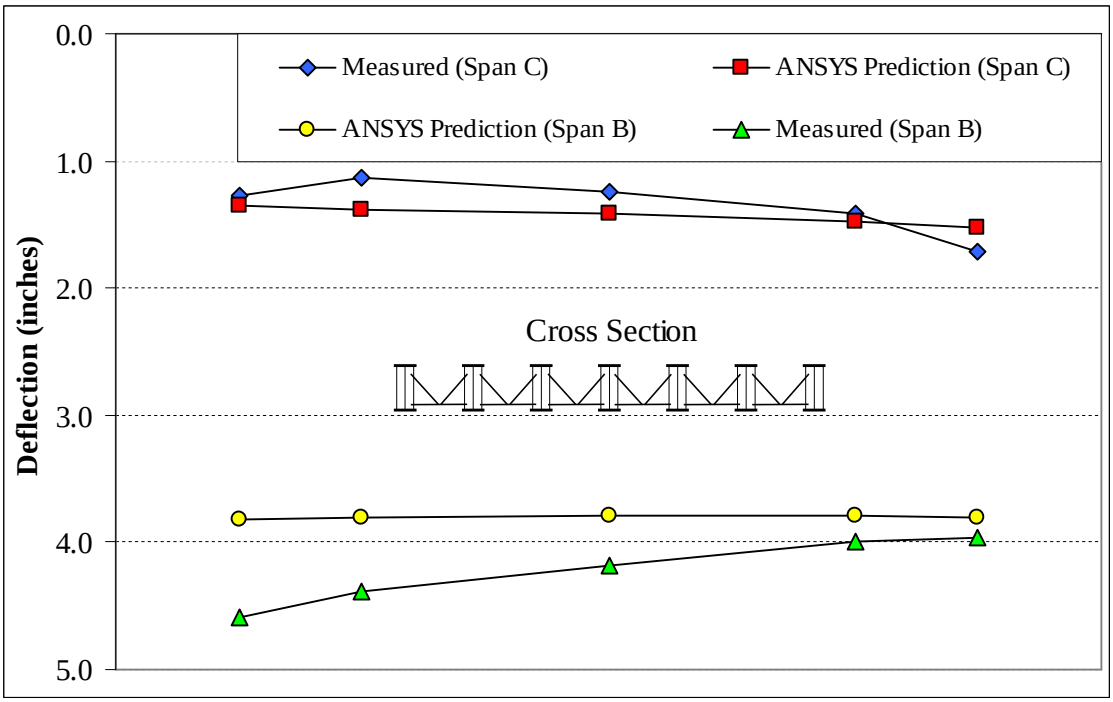

Figure 7.4: ANSYS Predicted Deflections vs. Field Measured Deflections for Bridge 1 (Spans B and C)

The ratios of ANSYS deflections to field measured deflections were calculated for each girder in the three continuous span bridges. The results are tabulated in Table 7.4. Though the averages of the ratios are close to 1.0 for the exterior and interior girders (0.95 and 0.97 respectively), they alone are inadequate to asses the deflection correlations between ANSYS and the field measurements because the over predictions and under predictions, in effect, cancel each other out. A statistical analysis was performed to further investigate the correlations.

Table 7.4: Ratios of ANSYS Predicted Deflections to Field Measured Deflections for Continuous Span Bridges

	Span Location	Girder A	Girder B	Girder C	Girder D	Girder E	Girder F	Girder G
Bridge 14	4/10 Span A	1.17	1.30	1.08	1.22	1.97	na	na
	6/10 Span B	0.88	0.93	0.82	0.90	0.82	na	na
Bridge 10	4/10 Span B	0.88	0.90	1.04	0.98	na	na	na
	6/10 Span C	0.63	0.72	0.67	0.68	na	na	na
Bridge 1	4/10 Span A	0.79	0.90	-	1.00	-	0.86	0.76
	4/10 Span B	0.83	0.87	-	0.91	-	0.95	0.96
	35/100 Span C	1.07	1.22	-	1.18	-	1.05	0.88

7.3.3 Single Girder Line Predicted Deflections vs. ANSYS Predicted Deflections

To thoroughly investigate the advantage of ANSYS modeling over traditional SGL analysis, statistical analyses were completed to compare the previously presented ratios. Box plots were created to illustrate a direct comparison of ANSYS and SGL deflection ratios. The results are presented first for simple span bridges and then for continuous span bridges.

7.3.3.1 Simple Span Bridges

The deflection ratios in Tables 7.1 and 7.3 were combined to conduct a statistical analysis for simple span bridges and the results are presented in Table 7.5. The results establish the advantage of ANSYS modeling over SGL analysis for the interior girders. The average ratio was lowered from 1.46 to 1.07 (39 percent more accurate) and the standard deviation was lowered from 0.20 to 0.15. It is apparent that the SGL analysis predicts exterior girder deflections more accurately than ANSYS. The average ratio was more accurate by 1 percent (from 1.12 to 1.11), and the SGL analysis exhibits better precision with a considerably lower standard deviation and coefficient of variance. A comparison is presented graphically in Figure 7.5 to confirm the observations.

Table 7.5: Statistical Analysis of Deflection Ratios at Mid-span for Simple Span Bridges

	Exterior Girders		Interior Girders	
	ANSYS/ Measured	SGL/ Measured	ANSYS/ Measured	SGL/ Measured
Average	**1.11**	**1.12**	**1.07**	**1.46**
Min	0.77	0.99	0.78	1.19
Max	1.42	1.33	1.32	1.94
St. Dev.	0.18	0.11	0.15	0.20
COV	0.16	0.10	0.14	0.14

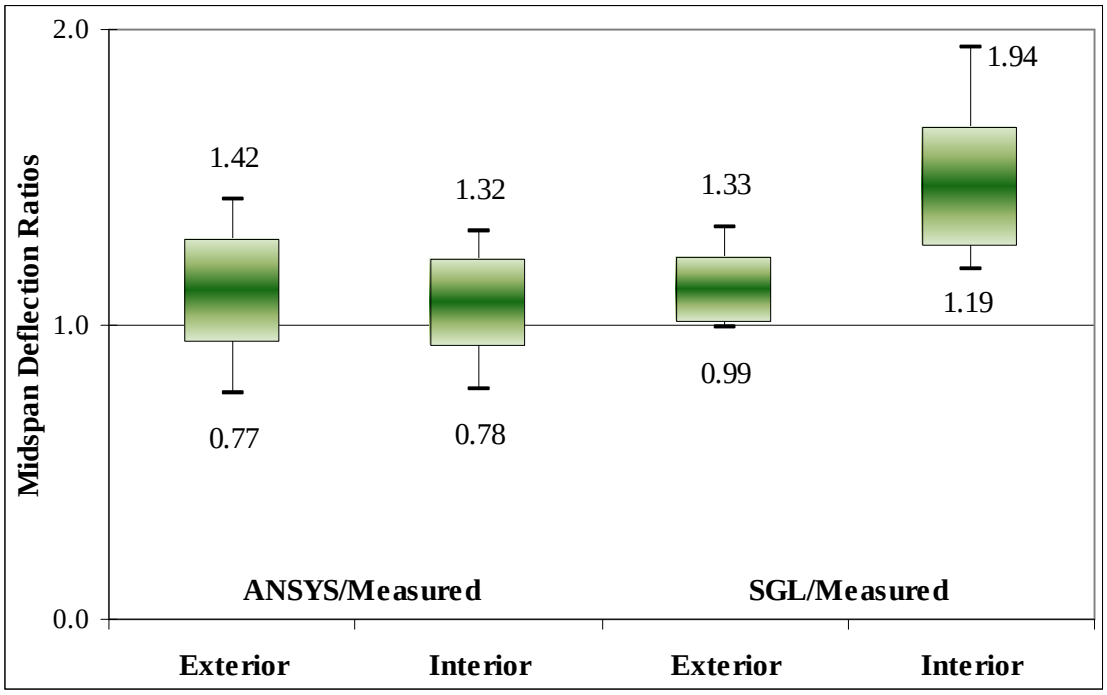

Figure 7.5: ANSYS Predicted Deflections vs. SGL Predicted Deflections for Simple Span Bridges

7.3.3.2 Continuous Span Bridges

The deflection ratios in Tables 7.2 and 7.4 were combined to conduct a statistical analysis for continuous span bridges and the results are presented in Table 7.6. Comparable numbers in Table 7.6 reveal no clear advantage of one analysis over the other. For the

exterior girders, the ANSYS and SGL average deflection ratios are 0.95 and 0.96 respectively. Similarly, for the interior girders, the average deflection ratios are 0.97 and 1.04 respectively. Correspondingly, Figure 7.6 displays similar vertical spreads centered at similar average deflection ratios. Note that the large maximum deflection ratios for the exterior girders (1.97 and 1.92 for ANSYS and SGL respectively) result from small deflection magnitudes. For instance, the maximum deflection ratio for the ANSYS predicted deflections (1.97) correlates to an ANSYS prediction of 0.98 inches and a field measurement of 0.51 inches (a 0.47 inch difference).

Table 7.6: Statistical Analysis of Deflection Ratios for Continuous Span Bridges

	Exterior Girders		Interior Girders	
	ANSYS/ Measured	SGL/ Measured	ANSYS/ Measured	SGL/ Measured
Average	**0.95**	**0.96**	**0.97**	**1.04**
Min	0.63	0.69	0.67	0.76
Max	1.97	1.92	1.30	1.40
St. Dev.	0.33	0.31	0.17	0.17
COV	0.34	0.32	0.17	0.17

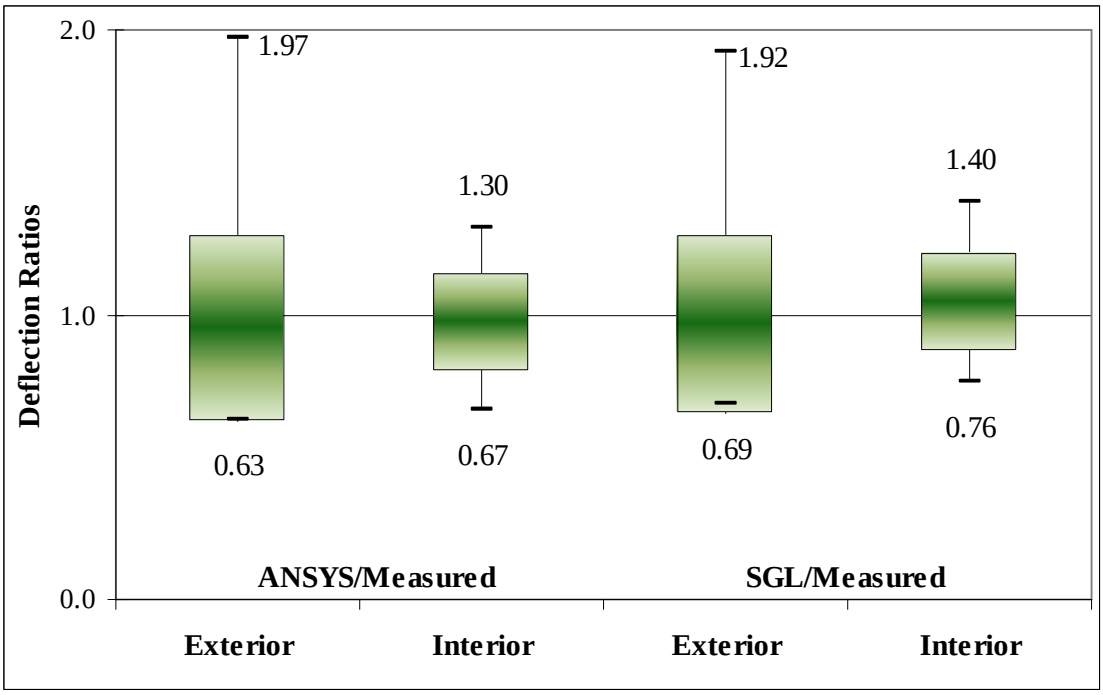

Figure 7.6: ANSYS Predicted Deflections vs. SGL Predicted Deflections for Continuous Span Bridges

7.3.4 Summary

Field measured deflections of the ten bridges included in this research were compared to SGL and ANSYS predicted deflections. Deflection plots quickly revealed the greater accuracy of ANSYS model predictions to the SGL analysis predictions in matching deflected shapes, for both simple and continuous span bridges. To compare the predictions, deflection ratios (SGL to field measured and ANSYS to field measured) were calculated for each bridge. A statistical analysis was performed on the ratios and the following conclusions were reached:

- ANSYS predicted deflections more closely match field measured deflections than SGL predicted deflections for the interior girders of the simple span bridges.

- SGL predicted deflections more closely match field measured deflections than the ANSYS predicted deflections for the exterior girders of the simple span bridges.
- ANSYS modeling and the SGL method appear to predict field measured deflections equally well for the girders of the continuous span bridges.

7.4 Comparisons of ANSYS Predicted Deflections to Simplified Procedure Predictions and SGL Predictions for Simple Span Bridges with Equal Exterior-to-Interior Girder Load Ratios

7.4.1 General

The simplified procedure developed to predict dead load deflections utilizes two equations, as discussed in Section 5. The equations were derived from an extensive parametric study conducted to determine the key parameters affecting bridge deflection behavior. To ensure the equations' ability to predict deflections, comparisons were made between the simplified procedure predictions and ANSYS predicted deflections at mid-span. Additionally, SGL predictions were included to demonstrate the degree of improved accuracy.

For the comparisons discussed herein, the collection of ANSYS models included simple span bridges with equal exterior-to-interior girder load ratios (i.e. the two exterior girders were evenly loaded per bridge). These models incorporated multiple skew offsets, different of exterior-to-interior girder load ratios, and several girder spacing-to-span ratios. Girder loads were consistently altered during the parametric study; therefore, new SGL models were created for direct comparisons to the ANSYS predicted deflections and simplified procedure predictions.

7.4.2 Comparisons

Mid-span deflection ratios were calculated to compare the ANSYS deflections to the simplified procedure predictions and the SGL predictions. The ratios were calculated as the prediction method's deflections divided by the ANSYS predicted deflections. Accordingly, the ratios greater than 1.0 refer to an over prediction, and those less than 1.0 refer to an under prediction.

The calculated ratios were then broken down by various skew offsets to highlight the effect of skew offset on the behavior of the bridge. A statistical analysis was performed and the results are presented in Table 7.7 for both prediction methods at four skew offsets (0, 25, 50 and 60). Note that the results are presented individually for the exterior and interior girders and the simplified procedure reference is denoted as SP.

Table 7.7: Statistical Analysis Comparing SP Predictions to SGL Predictions at Various Skew Offsets

0 Degree Skew Offset	Exterior Girders		Interior Girders	
	SP/ ANSYS	SGL/ ANSYS	SP/ ANSYS	SGL/ ANSYS
Average	**1.00**	**0.86**	**1.00**	**1.12**
Min	0.95	0.76	0.93	1.04
Max	1.05	0.96	1.06	1.20
St. Dev.	0.03	0.07	0.04	0.05
COV	0.03	0.08	0.04	0.05
25 Degree Skew Offset	Exterior Girders		Interior Girders	
	SP/ ANSYS	SGL/ ANSYS	SP/ ANSYS	SGL/ ANSYS
Average	**1.03**	**0.89**	**1.00**	**1.16**
Min	0.98	0.78	0.96	1.08
Max	1.09	0.99	1.07	1.25
St. Dev.	0.04	0.09	0.03	0.06
COV	0.04	0.10	0.03	0.05
50 Degree Skew Offset	Exterior Girders		Interior Girders	
	SP/ ANSYS	SGL/ ANSYS	SP/ ANSYS	SGL/ ANSYS
Average	**1.08**	**1.01**	**1.07**	**1.40**
Min	1.02	0.87	0.99	1.22
Max	1.15	1.13	1.17	1.55
St. Dev.	0.05	0.10	0.06	0.09
COV	0.05	0.10	0.05	0.07
60 Degree Skew Offset	Exterior Girders		Interior Girders	
	SP/ ANSYS	SGL/ ANSYS	SP/ ANSYS	SGL/ ANSYS
Average	**1.00**	**1.10**	**1.02**	**1.68**
Min	0.92	0.96	0.89	1.39
Max	1.08	1.25	1.15	1.96
St. Dev.	0.05	0.12	0.08	0.15
COV	0.05	0.11	0.08	0.09

As the skew offset is increased, it is apparent that the SGL predictions diminish, especially for the interior girders. For the interior girders, the average SGL deflection ratio

diverges from the ideal ratio of 1.0, while the average SP deflection ratio remains close to 1.0 (see Figure 7.7). For the interior and exterior girders, the average, standard deviation, and coefficient of variance all increase as the skew offset is increased. At the 60 degree skew offset, the average interior girder deflection ratio (1.68) signifies that the average interior SGL prediction is more than two-thirds greater than the corresponding ANSYS deflection. Additionally, the maximum interior girder deflection ratio is 1.96; this signifies an interior SGL prediction almost double that of the corresponding ANSYS deflection.

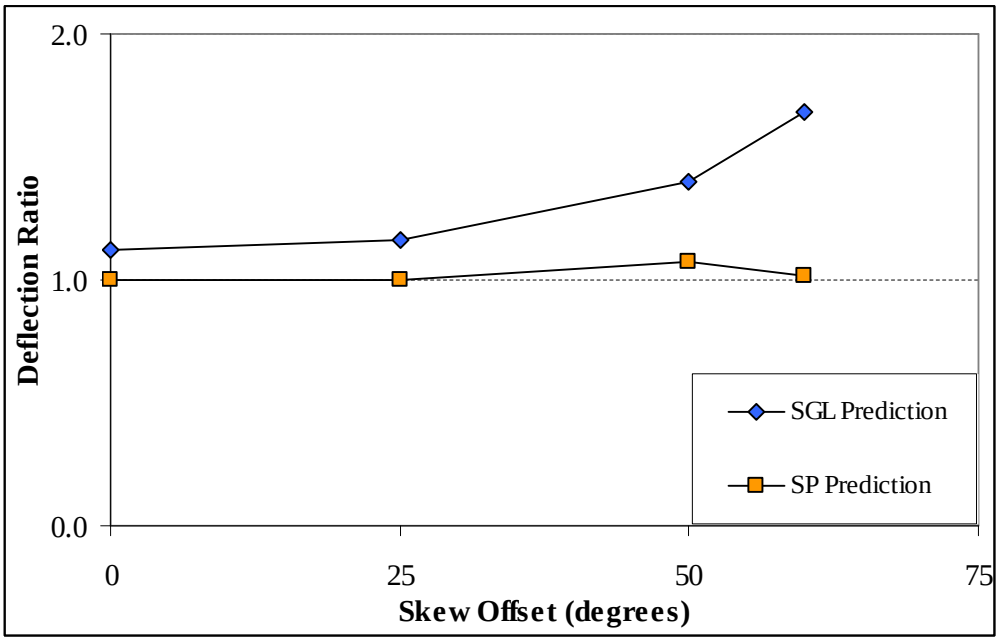

Figure 7.7: Effect of Skew Offset on Deflection Ratio for Interior Girders of Simple Span Bridges

Overall, the simplified procedure predictions more closely match the ANSYS predicted deflections than the SGL predictions. The standard deviations and coefficients of variance are less at all skew offsets, for the exterior and interior girders. Additionally, the

ratio averages at all four skew offsets are consistently close to 1.0 for the exterior and interior girders.

The results in Table 7.7 are displayed in the subsequent box plots to compare mid-span deflection ratios of the SGL predictions to the simplified procedure predictions. Comparisons for the exterior girders are presented in Figures 7.8 and 7.9 and for the interior girders in Figures 7.10 and 7.11. Additionally, the mid-span deflection ratios from the four skew offsets were combined to evaluate the overall prediction improvement and the resulting plot is presented in Figure 7.12.

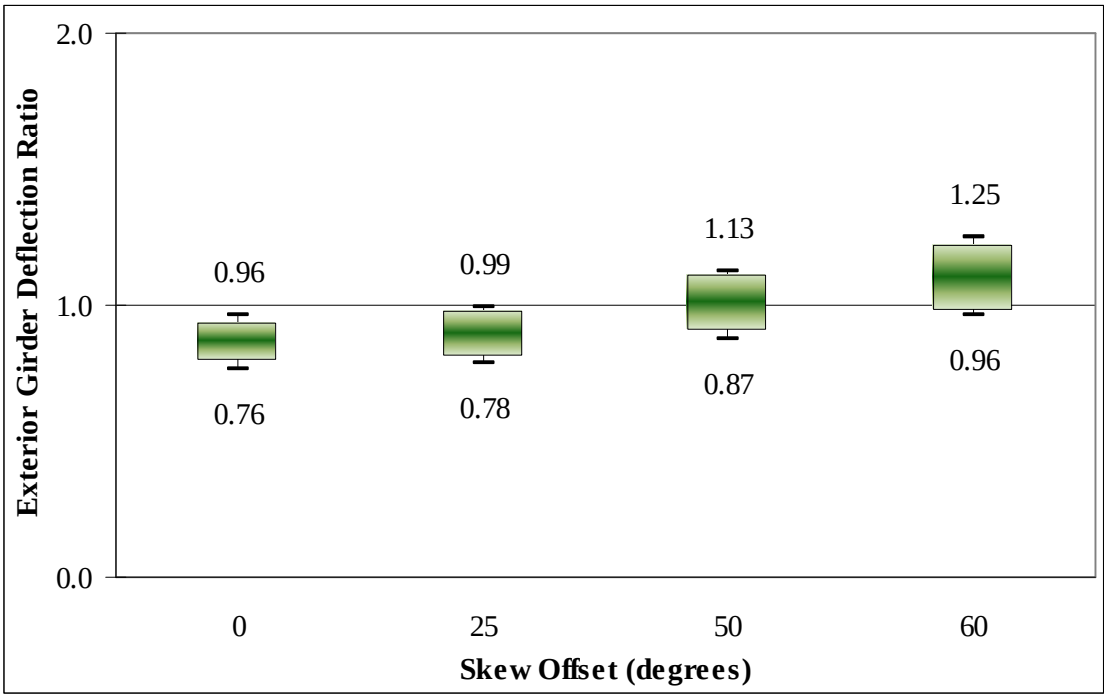

Figure 7.8: Exterior Girder SGL Predictions at Various Skew Offsets

Figure 7.9: Exterior Girder Simplified Procedure Predictions at Various Skew Offsets

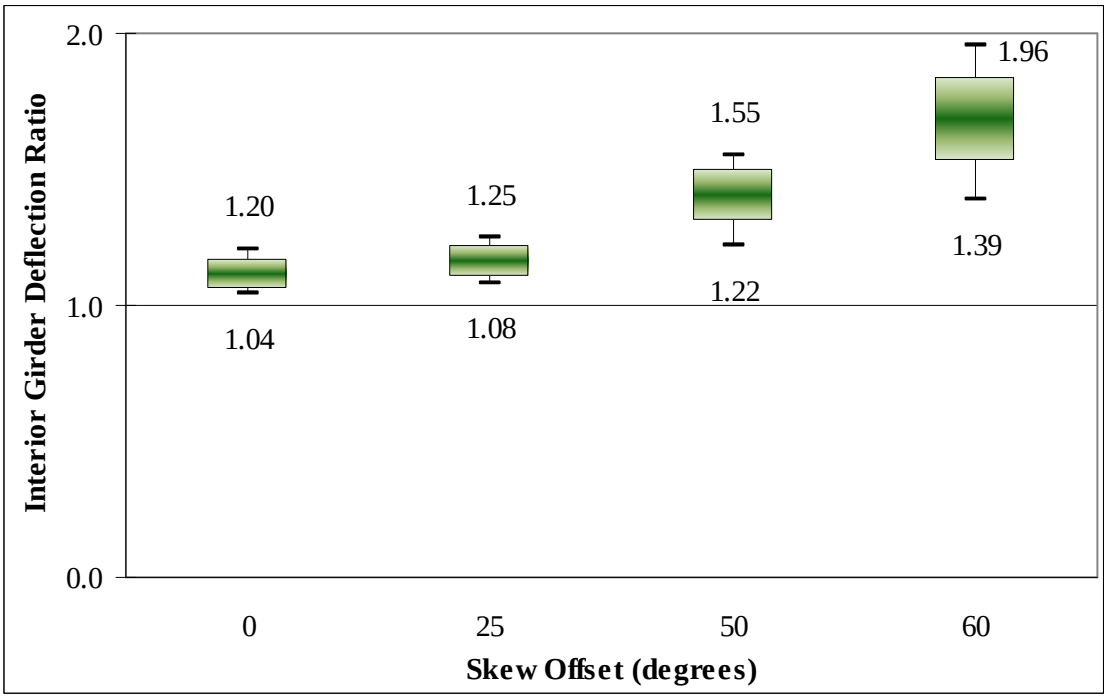

Figure 7.10: Interior Girder SGL Predictions at Various Skew Offsets

Figure 7.11: Interior Girder Simplified Procedure Predictions at Various Skew Offsets

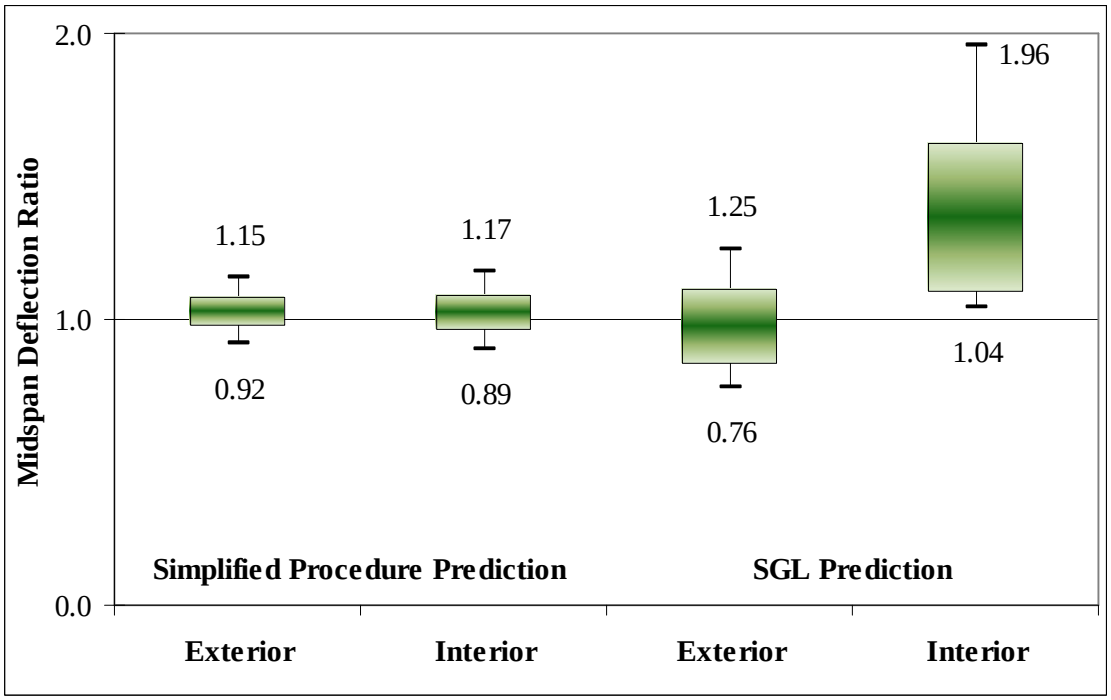

Figure 7.12: Simplified Procedure Predictions vs. SGL Predictions

Figures 7.7 – 7.12 present further evidence that the simplified procedure predicts ANSYS deflections considerably better than traditional SGL predictions. In all cases, the vertical spreads are tighter and centered closer (or as close) to the ideal ratio of 1.0.

As an example to illustrate the improved predictions, Figure 7.13 presents the mid-span deflection results for the Camden SB Bridge at 0 and 50 degree skew offsets. Again, SGL predictions do not change as skew offset is increased, as apparent in the figure. Note that in Figure 7.13, the number in parentheses beside the data set name refers to the skew offset and the simplified procedure prediction is denoted as 'SP Prediction'. It is clear in the figure that the simplified procedure predicts ANSYS deflections significantly better than the SGL method. The deflected shapes predicted by the simplified procedure closely match the ANSYS deflected shapes for both skew offsets.

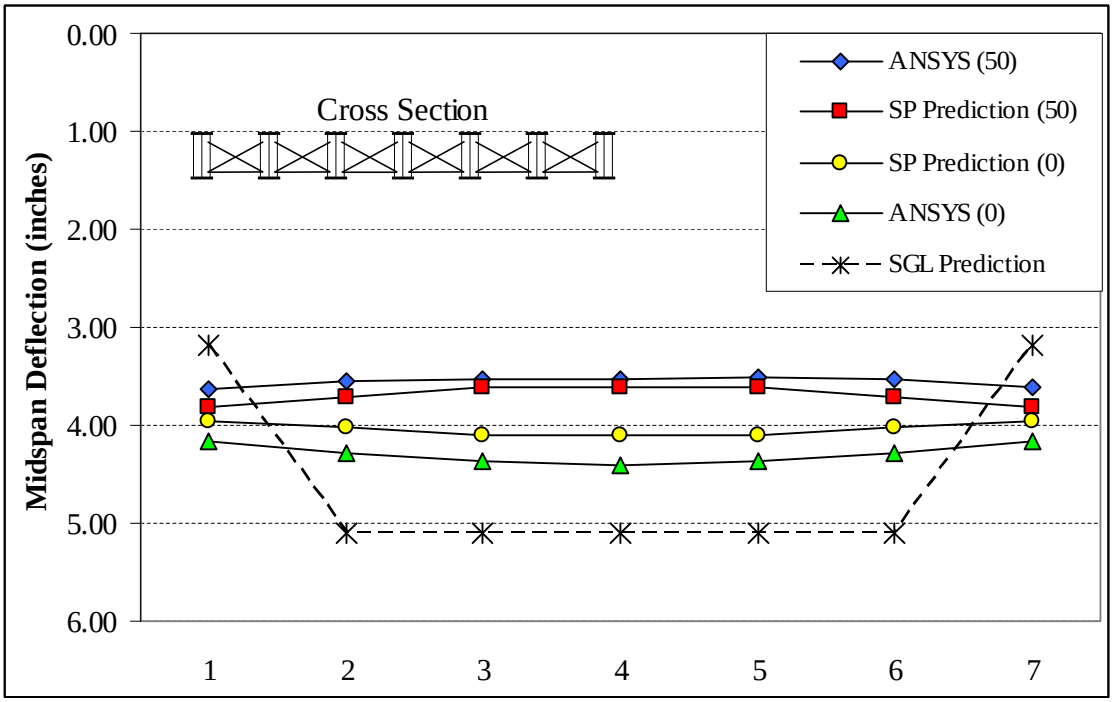

Figure 7.13: ANSYS Deflections vs. Simplified Procedure and SGL Predictions for the Camden SB Bridge

7.4.3 Summary

ANSYS predicted deflections were compared to simplified procedure predictions and SGL predictions for simple span bridges with equal exterior-to-interior girder load ratios. A statistical analysis was performed on mid-span deflection ratios and the results were tabulated and plotted to demonstrate the improved accuracy of predicting dead load deflections by the simplified procedure. The primary conclusion is that deflections predicted by the simplified procedure are more accurate than SGL predicted deflections for exterior and interior girders at all skew offsets.

7.5 Comparisons of ANSYS Predicted Deflections to Alternative Simplified Procedure Predictions and SGL Predictions for Simple Span Bridges with Unequal Exterior-to-Interior Girder Load Ratios

7.5.1 General

The two equations developed for the simplified procedure are utilized for the alternative simplified procedure (ASP). The ASP method modifies the simplified procedure to predict deflections for simple span bridges with unequal exterior-to-interior girder load ratios. The result is a straight line prediction between the two exterior girder deflections.

To establish the ability of the ASP method to accurately capture deflection behavior, the predictions were compared to ANSYS predicted deflections at mid-span. The Eno Bridge and the Wilmington St Bridge were modeled with unequal exterior-to-interior girder load ratios at skew offsets of 0, 25, 50 and 60 degrees. Additionally, SGL models of the two bridges were subjected to corresponding loads and analyzed for direct comparison with the ASP predictions and ANSYS predicted deflections. All comparisons are discussed herein.

7.5.2 Comparisons

The ASP and SGL predicted deflections were divided by the ANSYS predicted deflections at mid-span for comparison. The corresponding ratios for all the models were combined and a statistical analysis was performed. It is apparent from the results (presented in Table 7.8) that the ASP predictions more closely match the exterior and interior ANSYS predicted deflections than the SGL predictions. For the interior girders, the average ASP deflection ratio (1.01) is closer than the SGL ratio (1.32) to the ideal ratio of 1.0 and better precision is exhibited. The average deflection ratios of the two prediction methods are comparable for the exterior girders, but the ASP method results in a lower standard deviation and coefficient of variance. The data in Table 7.8 is displayed graphically as box plots in Figure 7.14 to further validate the ASP prediction method.

Table 7.8: Statistical Analysis Comparing ASP Predictions to SGL Predictions

	Exterior Girders		Interior Girders	
	ASP/ ANSYS	SGL/ ANSYS	ASP/ ANSYS	SGL/ ANSYS
Average	**0.98**	**1.02**	**1.01**	**1.32**
Min	0.83	0.83	0.91	1.04
Max	1.09	1.37	1.12	1.85
St. Dev.	0.07	0.15	0.05	0.25
COV	0.07	0.15	0.05	0.19

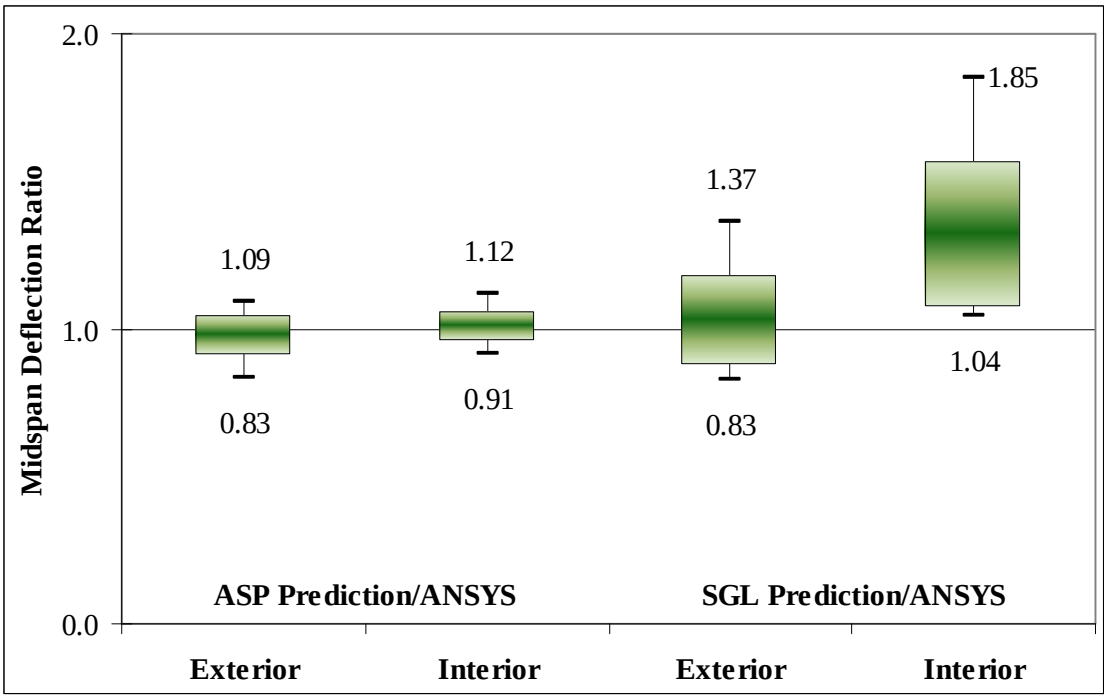

Figure 7.14: ASP Predictions vs. SGL Predictions for Simple Span Bridges with Unequal Exterior-to-Interior Girder Load Ratios

To illustrate the improved predictions, ANSYS predicted deflections at mid-span were plotted against the corresponding ASP and SGL predictions for the Wilmington St Bridge at 50 degrees skew offset and for the Eno Bridge at 0 degree skew offset (see Figure 7.15). Note that the Wilmington St data sets are labeled 'W' in parentheses, whereas the Eno data sets are labeled 'E'. The plots clearly display the ability of the ASP method to predict deflections for simple span bridges with unequal exterior-to-interior girder load ratios. The predictions are very accurate to the skewed and non-skewed ANSYS models, and the deflected shapes are much improved from the SGL predictions.

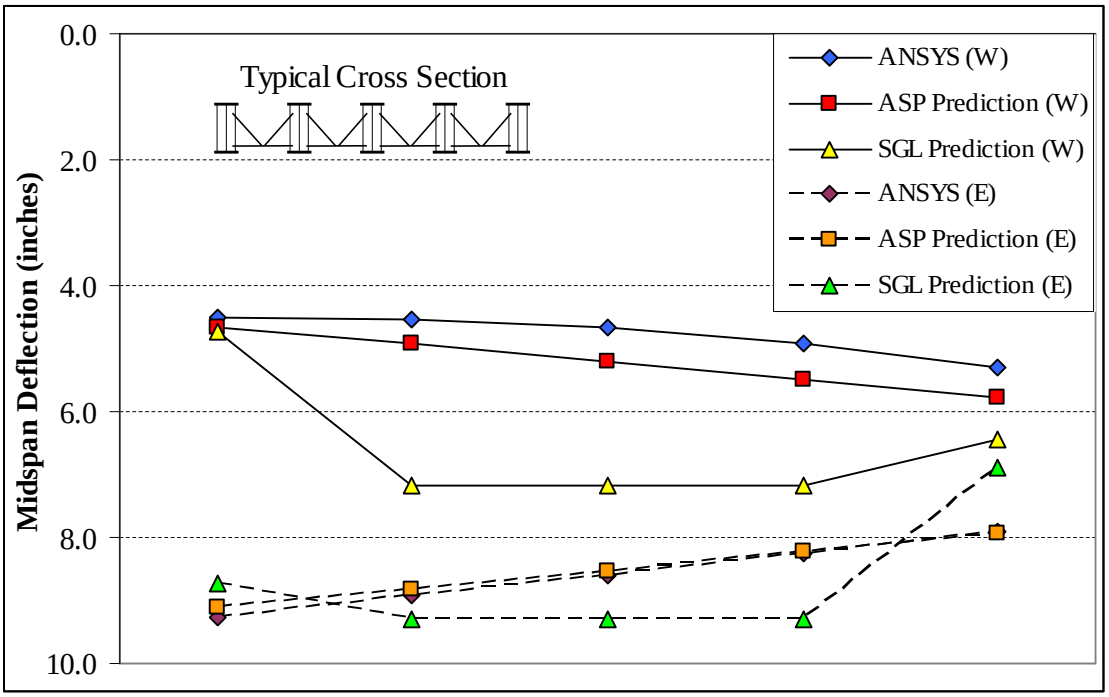

Figure 7.15: ANSYS Deflections vs. ASP and SGL Predictions for the Eno and Wilmington St Bridges

7.5.3 Summary

ANSYS deflections were compared to ASP and SGL predictions for simple span bridges with unequal exterior-to-interior girder load ratios by calculating deflection ratios at mid-span. The ratios were subjected to a statistical analysis and the results pointed to significant advantages in utilizing ASP predictions. In direct comparison with SGL predictions, the ASP predictions were much more precise and deflected shapes more closely matched the ANSYS predicted deflections.

7.6 Comparisons of ANSYS Deflections to SGL Straight Line Predictions and SGL Predictions for Continuous Span Bridges with Equal Exterior-to-Interior Girder Load Ratios

7.6.1 General

Traditional SGL predictions are utilized for the SGL straight line (SGLSL) predictions. The SGLSL method simply predicts all girder deflections equal to the exterior SGL prediction. The SGLSL method is believed to more accurately predict ANSY deflections for two reasons: exterior SGL predictions adequately match ANSYS predicted deflections, and deflected shapes for continuous span bridges are commonly flat (i.e. equal girder deflections in cross-section).

To establish the ability of the SGLSL method to accurately predict girder deflections, the predictions were compared to ANSYS predicted deflections and corresponding SGL predictions. Bridge 14 and Bridge 10 were modeled at skew offsets of 0, 25, 50 and 60 degrees, and the equal exterior-to-interior girder load ratios were 96 and 89 percent respectively. The comparisons are discussed herein.

7.6.2 Comparisons

SGLSL and SGL predicted deflections were divided by ANSYS predicted deflections to directly compare the methods. The corresponding ratios for all the models were combined and a statistical analysis was performed. Note that since the two methods predict identical exterior girder deflections, the exterior and interior girder ratios have been combined for this analysis. The results are presented in Table 7.9. It is apparent that SGLSL predictions are slightly more accurate than SGL predictions. The average is closer to 1.0 (1.02 compared to 1.06) and the standard deviation and coefficient of variance is lower for the SGLSL predictions. The data in Table 7.9 is displayed graphically in Figure 7.16 as a box plot.

Based on the behavior of simple span bridges, the SGL/ANSYS deflection ratios would likely deviate from 1.0 as the exterior-to-interior girder load ratio is decreased. In this analysis, both continuous span bridges have exterior-to-interior girder load ratios of 89 percent, or higher, resulting in relatively flat SGL predictions (see Figure 7.17). Further, it is likely that SGLSL/ANSYS deflection ratios would remain closer to 1.0 as the load is decreased as most ANSYS deflected shapes are essentially flat.

Table 7.9: Statistical Analysis Comparing SGL Predictions to SGLSL Predictions

	SGL Prediction/ ANSYS	SGLSL Prediction/ ANSYS
Average	**1.06**	**1.02**
Min	0.86	0.86
Max	1.40	1.34
St. Dev.	0.10	0.08
COV	0.10	0.08

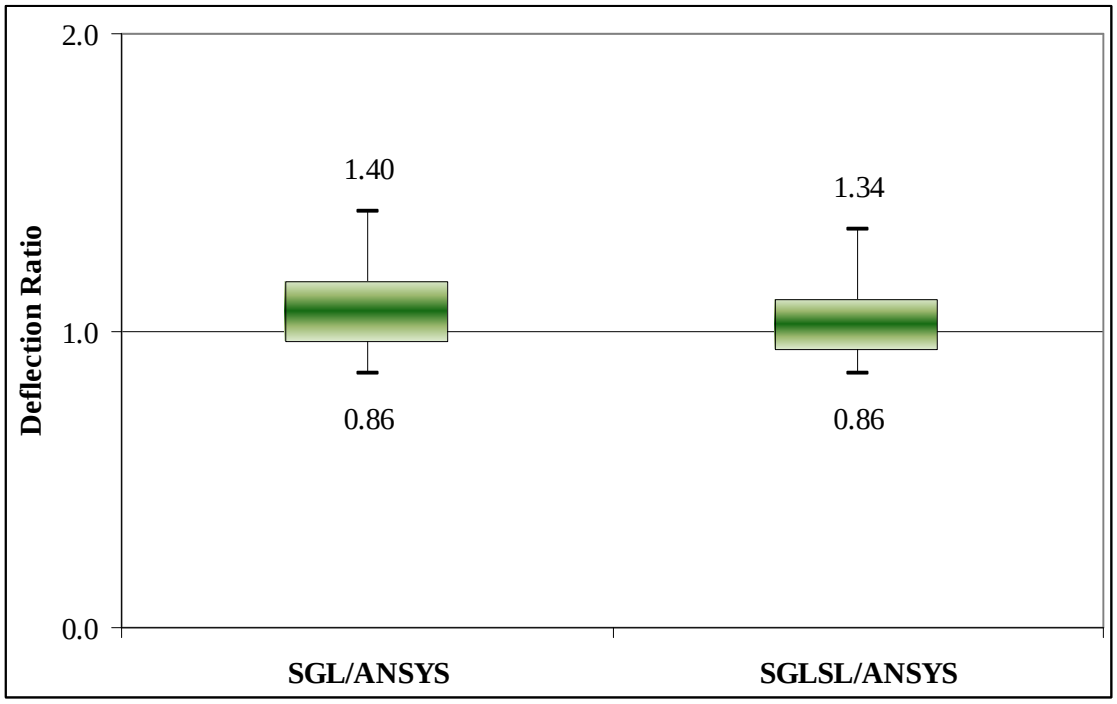

Figure 7.16: SGL Predictions vs. SGLSL Predictions for Continuous Span Bridges with Equal Exterior-to-Interior Girder Load Ratios

ANSYS predicted deflections, SGL predictions and SGLSL predictions have been plotted for Bridge 10 at 0 and 50 degrees skew offsets to further compare the prediction methods (see Figure 7.17). Note that the ANSYS data sets list the corresponding skew offsets (in degrees) in parentheses. The figure plainly illustrates the improved predictions of the SGLSL method. The SGLSL predicted deflected shape matches the ANSYS deflections better than the SGL prediction at both skew offsets. Additionally, the SGLSL interior girder predictions are closer to the ANSYS deflections at the skew offsets.

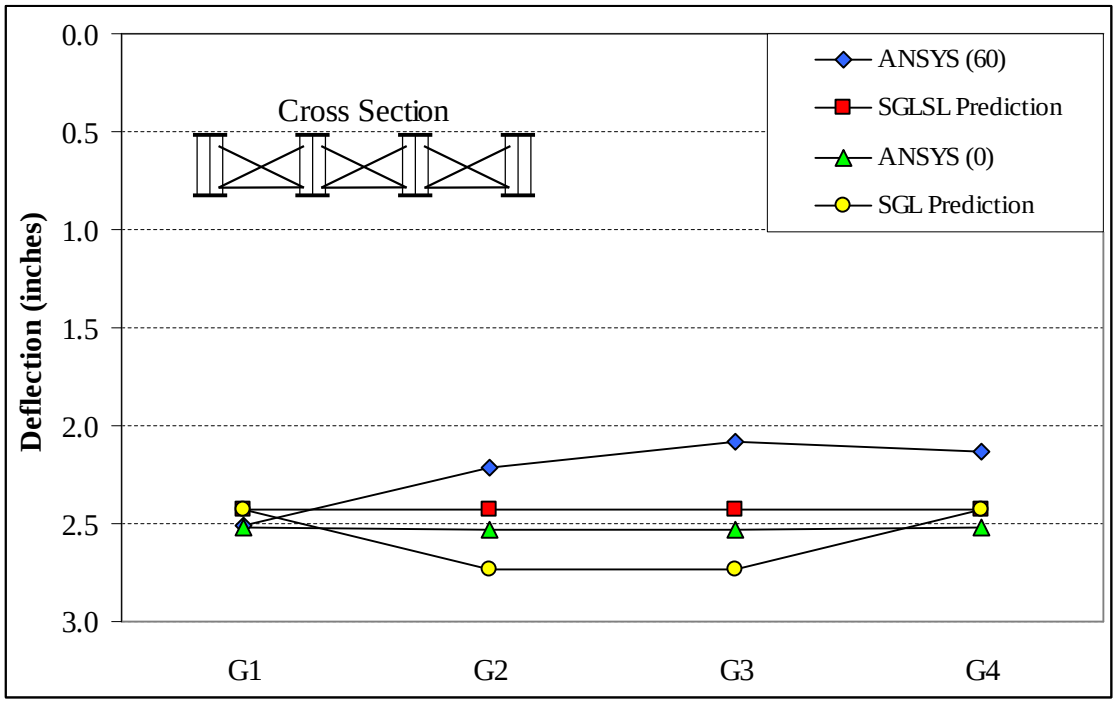

Figure 7.17: ANSYS Deflections vs. SGL and SGLSL Predictions for Bridge 10

7.6.3 Summary

ANSYS deflections were compared to SGL and SGLSL predictions for continuous span bridges with equal exterior-to-interior girder load ratios. Deflection ratios were calculated and subjected to a statistical analysis. It was revealed that the SGLSL method appears to match ANSYS predicted deflections more closely than the traditional SGL method. Further, it is believed that the advantage of SGLSL over SGL would be more prevalent in models with smaller exterior-to-interior girder load ratios.

7.7 Comparisons of Prediction Methods to Field Measured Deflections

7.7.1 General

Sections 7.4 – 7.6 present comparisons of three developed prediction methods to ANSYS predicted deflections for various bridge configurations. In each case, the newly

developed predictions were directly compared to the traditional SGL predictions, and in each case, the new predictions matched ANSYS predicted deflections more closely than the SGL predictions. The final investigation compares the developed prediction methods back to deflections that were measured in the field. SGL predictions, addressed in Section 7.3, are included and all comparisons are discussed herein.

7.7.2 Simplified Procedure Predictions vs. Field Measured Deflections

Five studied bridges met the criterion for the simplified procedure, which was developed for simple span bridges with equal exterior-to-interior girder load ratios. The simplified procedure predictions at mid-span were divided by the corresponding field measured deflections and the results are presented in Table 7.10. Note that the five bridges are listed in order of increasing skew offset and the simplified procedure is denoted as SP. It is apparent that the simplified procedure generally over predicts the field measured deflections. The five individual under predictions are restricted to various interior girders of seven-girder bridges.

Table 7.10: Mid-span Deflection Ratios of SP Predictions to Field Measured Deflections

	Girder A	Girder B	Girder C	Girder D	Girder E	Girder F	Girder G
Bridge 8	1.49	1.35	1.31	1.27	1.28	1.33	na
Avondale	1.24	1.16	-	1.09	-	1.07	1.08
US-29	1.07	1.12	-	1.15	-	1.08	1.02
Camden NB	1.03	0.92	-	0.80	0.92	1.06	na
Camden SB	1.10	0.97	-	0.85	-	0.97	1.12

The ratios in Table 7.10 were combined with the related SGL ratios in Table 7.1 and a statistical analysis was performed. The results are tabulated in Table 7.11 and plotted in Figure 7.18. It is apparent that the simplified procedure predicts interior girder deflections

more accurately than the SGL method. Although the standard deviation and coefficient of variance is slightly higher, the average ratio is much closer to 1.0 (1.08 compared to 1.43). The SGL method more accurately predicts the exterior girder deflections; the average is closer to 1.0 (1.10 compared to 1.15) and the precision is better. Overall, the interior girder deflections are predicted significantly better by the simplified procedure, whereas the exterior girder deflections are approximately predicted equally as well.

Table 7.11: Statistical Analysis Comparing SP Predictions to SGL Predictions

	Exterior Girders		Interior Girders	
	SP Prediction/ Measured	SGL Prediction/ Measured	SP Prediction/ Measured	SGL Prediction/ Measured
Average	**1.15**	**1.10**	**1.08**	**1.43**
Min	1.02	0.99	0.80	1.20
Max	1.49	1.33	1.35	1.62
St. Dev.	0.15	0.10	0.17	0.12
COV	0.13	0.09	0.15	0.08

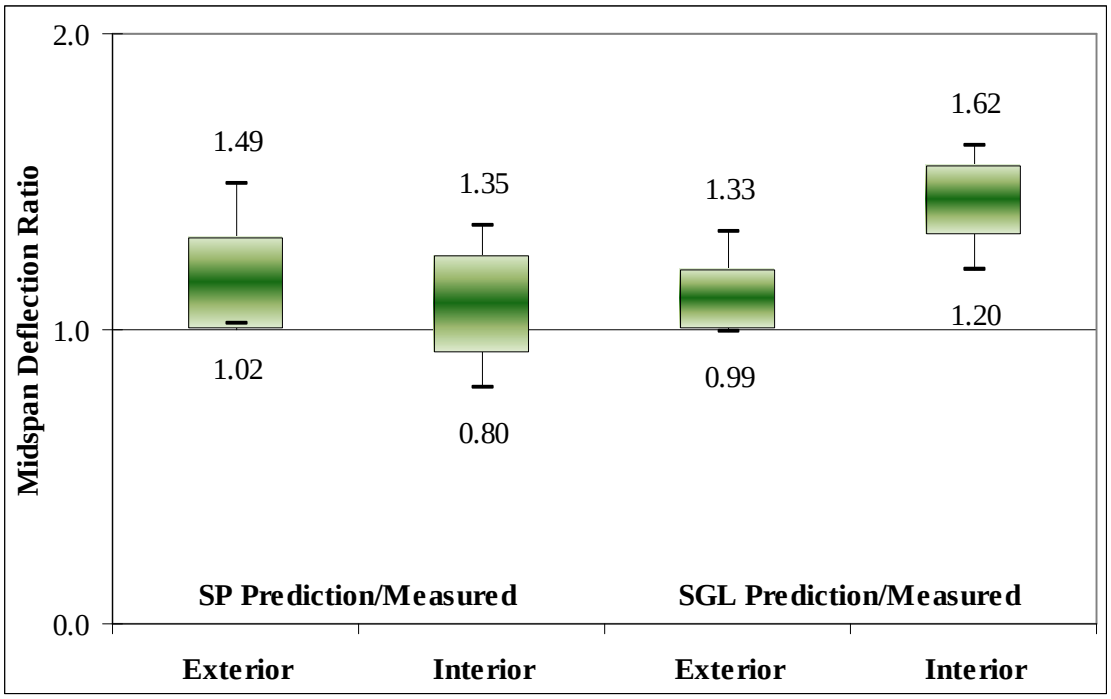

Figure 7.18: SP Predictions vs. SGL Predictions for Comparison to Field Measured Deflections

As an example to illustrate the prediction improvements made by the simplified procedure, the US-29 Bridge (skew offset = 44 degrees) has been plotted in Figure 7.19. Illustrated is the ability of the simplified procedure to accurately predict field measured deflections for the exterior and interior girders.

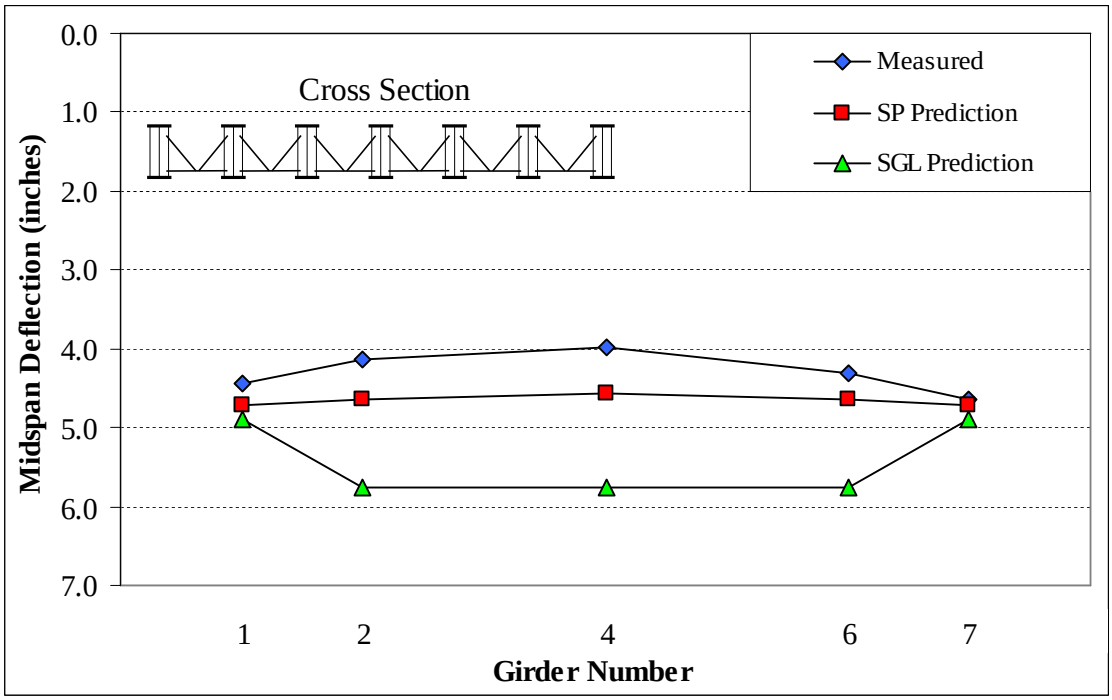

Figure 7.19: Field Measured Deflections vs. SP and SGL Predictions for US-29

7.7.3 Alternative Simplified Procedure Predictions vs. Field Measured Deflections

The alternative simplified procedure (ASP) was developed for simple span bridges with unequal exterior-to-interior girder load ratios – only the Eno and Wilmington St Bridges met this criterion. The ASP predictions at mid-span were divided by the corresponding field measured deflections and the results are presented in Table 7.12.

Table 7.12: Mid-span Deflection Ratios of ASP Predictions to Field Measured Deflections

	Girder A	Girder B	Girder C	Girder D	Girder E
Eno	1.12	1.13	1.13	1.14	1.14
Wilmington St	1.32	1.43	1.47	1.39	1.21

For the Eno and Wilmington St Bridges, the ASP predictions have over predicted the field measured deflections. The ratios in Table 7.12 were combined with the related SGL

ratios in Table 7.1 and a statistical analysis was performed. Table 7.13 and Figure 7.20 present the statistics results and it is apparent that the ASP method predicts deflections more accurately than the SGL method. The ratio averages are comparable for the exterior girders, but the ASP ratio is much closer to 1.0 for the interior girders (1.28 compared to 1.54). Additionally, the standard deviations and coefficients of variance of the exterior and interior girders are significantly lower for the ASP predictions.

Table 7.13: Statistical Analysis Comparing ASP Predictions to SGL Predictions

	Exterior Girders		Interior Girders	
	ASP Prediction/ Measured	SGL Prediction/ Measured	ASP Prediction/ Measured	SGL Prediction/ Measured
Average	**1.20**	**1.15**	**1.28**	**1.54**
Min	1.12	0.99	1.13	1.19
Max	1.32	1.28	1.47	1.94
St. Dev.	0.09	0.14	0.17	0.35
COV	0.08	0.12	0.13	0.22

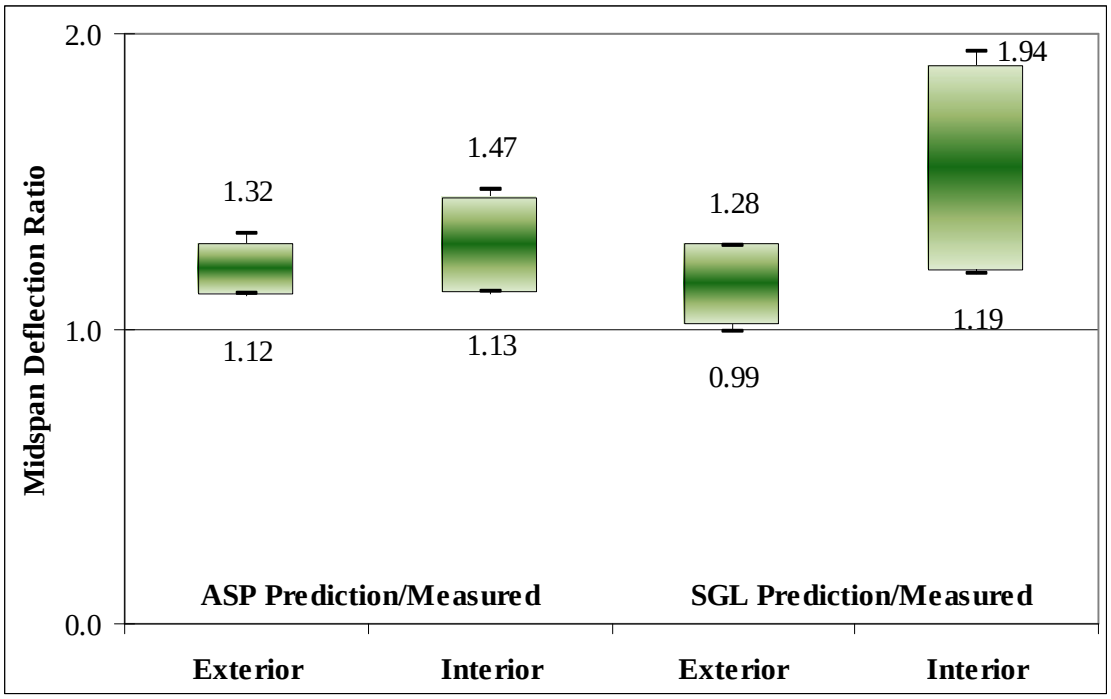

Figure 7.20: ASP Predictions vs. SGL Predictions for Comparison to Field Measured Deflections

The Wilmington St Bridge (skew offset = 62 degrees) is presented in Figure 7.21 to illustrate the improvements made by the ASP method in predicting field measured deflections. Most significant is the closely matching deflected shapes.

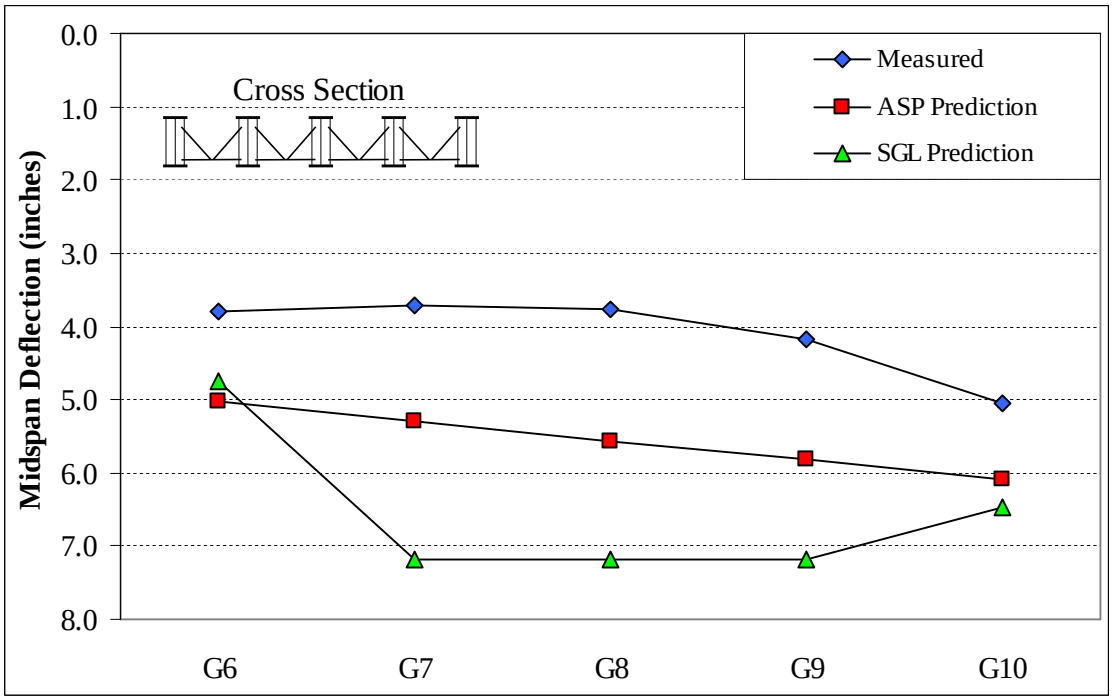

Figure 7.21: Field Measured Deflections vs. ASP and SGL Predictions for the Wilmington St Bridge

7.7.4 SGL Straight Line Predictions vs. Field Measured Deflections

The SGL straight line (SGLSL) method was implemented to predict the deflections of continuous span bridges with equal exterior-to-interior girder load ratios. Although only Bridge 14 and Bridge 10 (two-span continuous bridges) were included in the parametric study, Bridge 1 (three-span continuous bridge) has been included in this investigation. Corresponding predictions were divided by the field measured deflections at each span location for all three bridges and the results are presented in Table 7.14. It is apparent that under predictions and over predictions are consistent within a given span. The SGLSL method entirely over predicts one span in each of the three continuous span bridges, and under predicts the others.

Table 7.14: Deflection Ratios of SGLSL Predictions to Field Measured Deflections

	Span Location	Girder A	Girder B	Girder C	Girder D	Girder E	Girder F	Girder G
Bridge 14	4/10 Span A	1.15	1.27	1.03	1.18	1.96	na	na
	6/10 Span B	0.86	0.92	0.80	0.89	0.81	na	na
Bridge 10	4/10 Span B	1.12	1.15	1.26	1.09	na	na	na
	6/10 Span C	0.64	0.80	0.80	0.80	na	na	na
Bridge 1	4/10 Span A	0.73	0.84	-	0.95	-	0.82	0.71
	4/10 Span B	0.71	0.74	-	0.78	-	0.81	0.82
	35/100 Span C	1.36	1.53	-	1.40	-	1.23	1.01

The ratios in Table 7.14 were combined with the related SGL ratios in Table 7.2 and a statistical analysis was performed (see Table 7.15 and Figure 7.22 for results). Note that the two methods predict identical exterior girder deflections, and, therefore, the exterior and interior girder ratios have been combined. It is apparent from the results that only a slight advantage exists in predicting girder deflections by the SGLSL method. The two methods exhibit very similar precision, but the SGLSL average ratio is essentially 1.0, whereas the SGL ratio is slightly higher at 1.04.

Table 7.15: Statistical Analysis Comparing SGLSL Predictions to SGL Predictions

	SGLSL Prediction/ Measured	SGL Prediction/ Measured
Average	**1.00**	**1.04**
Min	0.64	0.64
Max	1.96	1.96
St. Dev.	0.29	0.30
COV	0.29	0.29

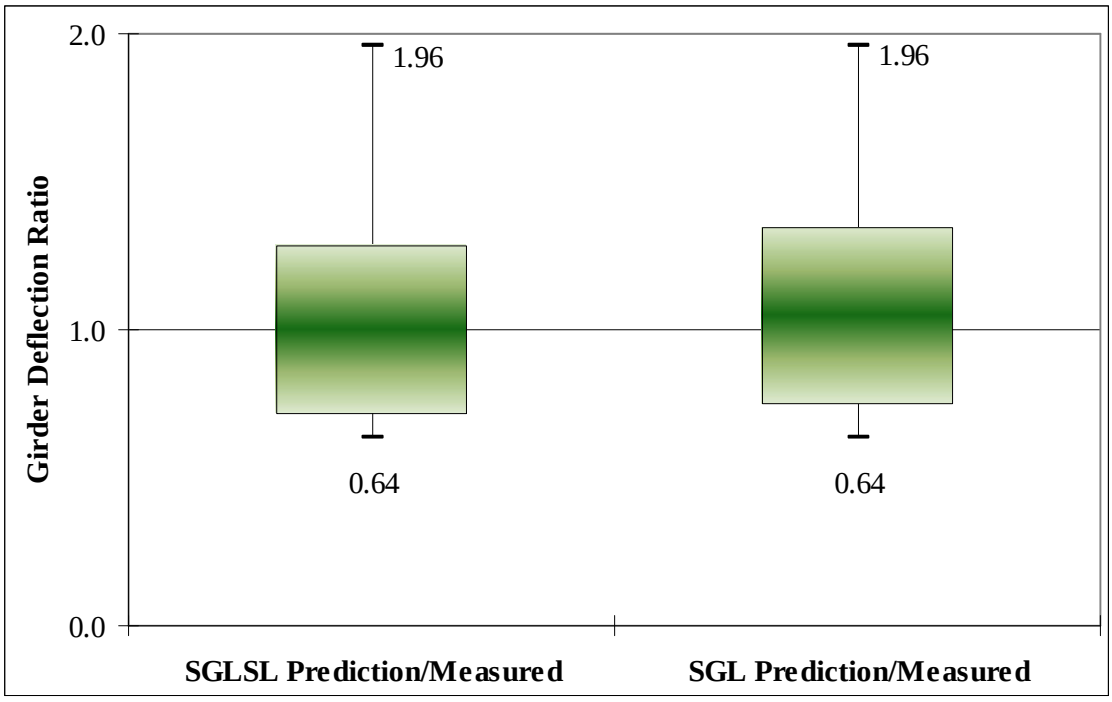

Figure 7.22: SGLSL Predictions vs. SGL Predictions for Comparison to Field Measured Deflections

As an example to compare the similar prediction methods, the span B deflections of Bridge 10 (skew offset = 57 degrees) have been plotted in Figure 7.23. The only variation between the two prediction methods is the improved interior girder predictions by the SGLSL method.

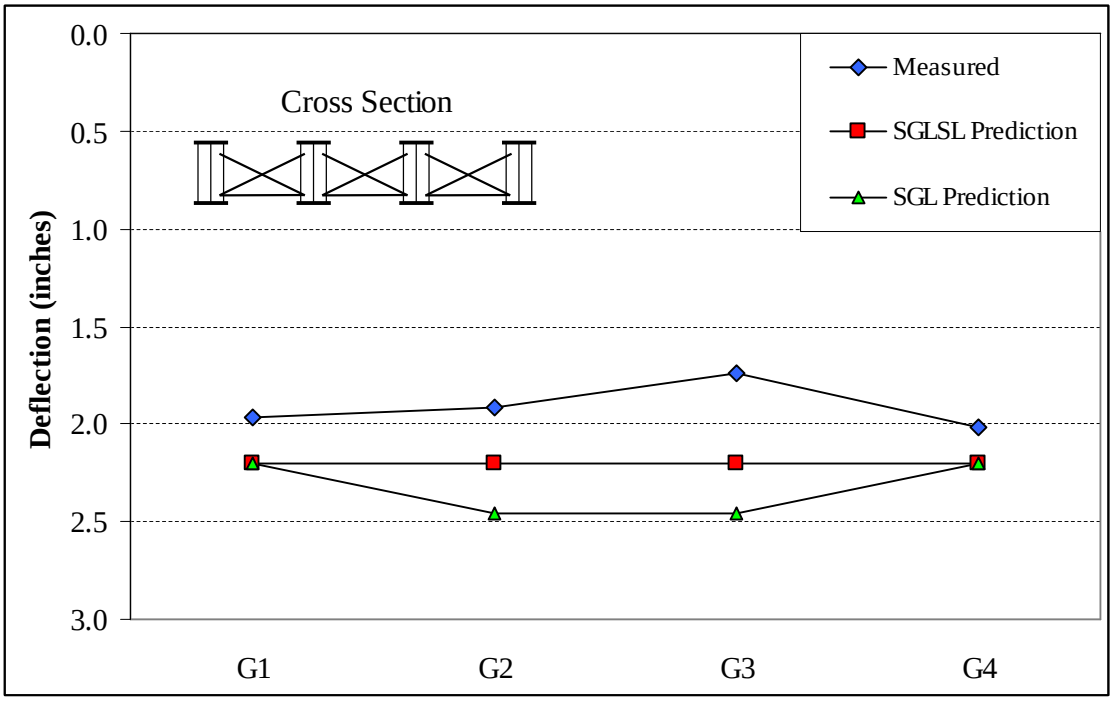

Figure 7.23: Field Measured Deflections vs. SGLSL and SGL Predictions for Bridge 10 (Span B)

7.8 Summary

Comparisons have been made between field measured deflections, ANSYS predicted deflections, SGL predicted deflections, and deflections predicted by three newly developed procedures. Girder deflections for simple span bridges have been predicted by the simplified procedure and the alternative simplified procedure for bridges with equal and unequal exterior-to-interior girder load ratios, respectively. Additionally, deflections of continuous span bridges with equal exterior-to-interior girder load ratios have been predicted by the SGL straight line method. According to multiple statistical analyses, it has been concluded that all three new prediction methods predict dead load deflections in steel plate girder bridges more accurately than traditional SGL analysis.

To verify this conclusion, the SGL method was shown not to accurately predict field measured deflections for either bridge type. Finite element models, created in ANSYS, proved to capture the deflection behavior more accurately than the traditional SGL method. Next, the three new prediction methods were individually compared to the SGL method, as related to ANSYS predicted deflections. Each method demonstrated the ability to predict ANSYS simulated deflections more accurately than the SGL approach. Finally, deflections predicted by the newly developed methods were compared to the field measured deflections.

Following are two tables and ten figures to present the deflection data for all ten measured bridges. Table 7.16 includes various deflection ratios for field measured deflections, SGL predicted deflections, ANSYS predicted deflections, and newly predicted deflections. Similarly, Table 7.17 includes the differences in magnitudes for the aforementioned deflections. Finally, Figures 7.24 – 7.33 present the field measured deflections, SGL predicted deflections, ANSYS predicted deflections, and deflections predicted by the newly developed procedures to compare the girder deflections discussed in this section.

Table 7.16 Summary of Girder Deflection Ratios

	SGL/Measured		SGL/ANSYS		ANSYS/Measured		New Prediction*/Measured		New Prediction*/ANSYS	
Bridge	**Exterior**	**Interior**	**Exterior**	**Interior**	**Exterior**	**Interior**	**Exterior**	**Interior**	**Exterior**	**Interior**
Eno	1.03	1.24	0.90	1.08	1.15	1.14	1.13	1.13	0.99	0.99
Bridge 8	1.26	1.42	0.94	1.10	1.34	1.29	1.41	1.30	1.05	1.01
Avondale	1.09	1.25	1.01	1.17	1.08	1.07	1.16	1.10	1.07	1.03
US-29	1.08	1.39	1.08	1.29	1.00	1.08	1.04	1.12	1.05	1.04
Camden NB	1.01	1.51	0.80	1.41	1.26	1.07	1.04	0.88	0.83	0.82
Camden SB	1.07	1.59	0.94	1.62	1.15	0.98	1.11	0.93	0.97	0.95
Wilmington St	1.26	1.85	1.58	2.31	0.80	0.80	1.27	1.43	1.58	1.79
Bridge 14 - A	1.56	1.20	0.99	1.01	1.57	1.20	1.56	1.16	0.99	0.97
Bridge 14 - B	0.83	0.90	0.98	1.02	0.85	0.88	0.83	0.87	0.98	0.98
Bridge 10 - B	1.10	1.35	1.19	1.40	0.93	0.97	1.10	1.21	1.19	1.25
Bridge 10 - C	0.72	0.90	1.10	1.30	0.65	0.69	0.72	0.80	1.10	1.16
Bridge 1 - A	0.72	0.94	0.93	1.02	0.77	0.92	0.72	0.87	0.93	0.94
Bridge 1 - B	0.76	0.84	0.85	0.93	0.90	0.91	0.76	0.78	0.85	0.85
Bridge 1 - C	1.18	1.50	1.21	1.32	0.97	1.14	1.18	1.38	1.21	1.21
Average	**1.05**	**1.28**	**1.04**	**1.28**	**1.03**	**1.01**	**1.07**	**1.07**	**1.06**	**1.07**
Min	0.72	0.84	0.80	0.93	0.65	0.69	0.72	0.78	0.83	0.82
Max	1.56	1.85	1.58	2.31	1.57	1.29	1.56	1.43	1.58	1.79
St. Dev.	0.23	0.30	0.20	0.35	0.25	0.16	0.25	0.22	0.19	0.24
COV	0.22	0.23	0.19	0.28	0.24	0.16	0.23	0.20	0.18	0.22

Table 7.17 Summary of Girder Deflection Magnitude Differences

	SGL - Measured		SGL - ANSYS		ANSYS - Measured		New Prediction* - Measured		New Prediction* - ANSYS	
Bridge	**Exterior**	**Interior**	**Exterior**	**Interior**	**Exterior**	**Interior**	**Exterior**	**Interior**	**Exterior**	**Interior**
Eno	0.28	1.77	-0.81	0.72	1.09	1.05	0.99	0.99	-0.10	-0.06
Bridge 8	0.78	1.36	-0.27	0.42	1.04	0.94	1.25	0.97	0.20	0.03
Avondale	0.43	1.29	0.03	0.94	0.40	0.36	0.79	0.53	0.39	0.17
US-29	0.36	1.62	0.38	1.31	-0.03	0.31	0.19	0.47	0.21	0.16
Camden NB	0.02	1.69	-0.79	1.45	0.81	0.24	0.13	-0.41	-0.68	-0.65
Camden SB	0.22	1.88	-0.21	1.93	0.43	-0.06	0.33	-0.22	-0.10	-0.17
Wilmington St	1.18	3.29	2.07	4.07	-0.89	-0.78	1.14	1.67	2.03	2.45
Bridge 14 - A	0.31	0.17	-0.01	0.01	0.32	0.16	0.31	0.13	-0.01	-0.03
Bridge 14 - B	-0.27	-0.16	-0.03	0.03	-0.24	-0.18	-0.27	-0.21	-0.03	-0.02
Bridge 10 - B	0.21	0.64	0.34	0.70	-0.14	-0.06	0.21	0.38	0.34	0.44
Bridge 10 - C	-0.54	-0.17	0.11	0.34	-0.65	-0.51	-0.54	-0.33	0.11	0.18
Bridge 1 - A	-0.56	-0.11	-0.11	0.03	-0.45	-0.14	-0.56	-0.23	-0.11	-0.09
Bridge 1 - B	-1.04	-0.66	-0.58	-0.27	-0.46	-0.39	-1.04	-0.94	-0.58	-0.55
Bridge 1 - C	0.24	0.62	0.30	0.45	-0.06	0.17	0.24	0.47	0.30	0.30
Average	**0.11**	**0.95**	**0.03**	**0.87**	**0.08**	**0.08**	**0.23**	**0.23**	**0.14**	**0.15**
Min	-1.04	-0.66	-0.81	-0.27	-0.89	-0.78	-1.04	-0.94	-0.68	-0.65
Max	1.18	3.29	2.07	4.07	1.09	1.05	1.25	1.67	2.03	2.45
St. Dev.	0.57	1.09	0.70	1.11	0.62	0.51	0.67	0.69	0.63	0.72
COV	4.94	1.15	22.61	1.28	7.39	6.40	2.97	2.94	4.42	4.68

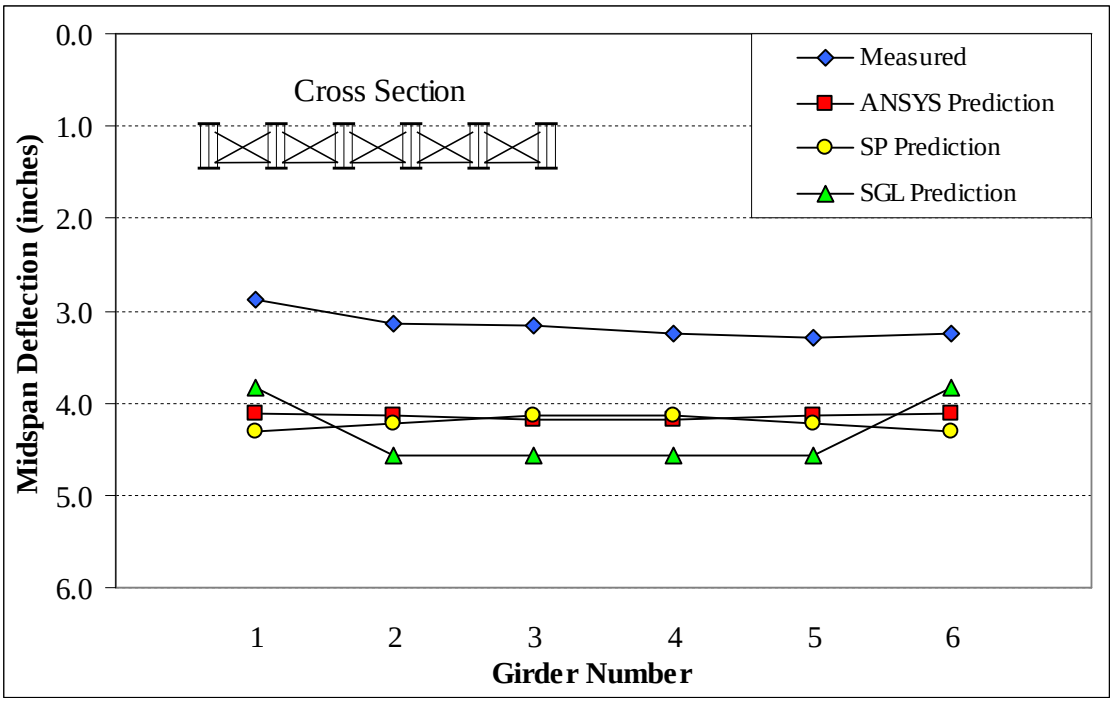

Figure 7.24: Field Measured Deflections vs. Predicted Deflections for Bridge 8

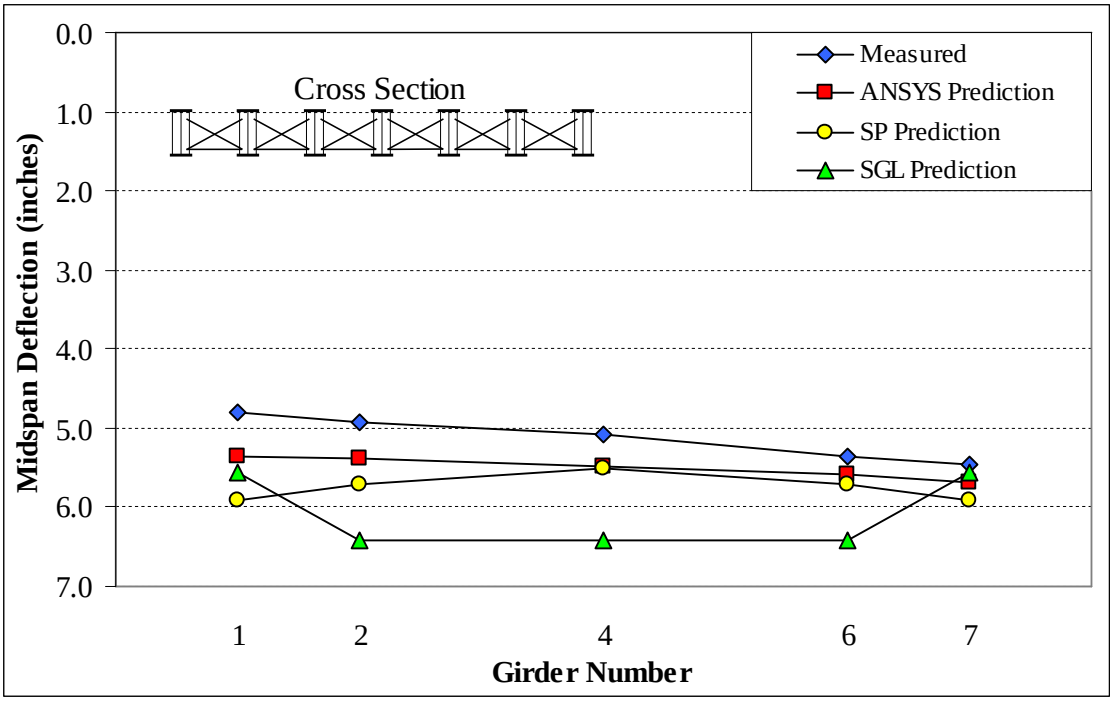

Figure 7.25: Field Measured Deflections vs. Predicted Deflections for the Avondale Bridge

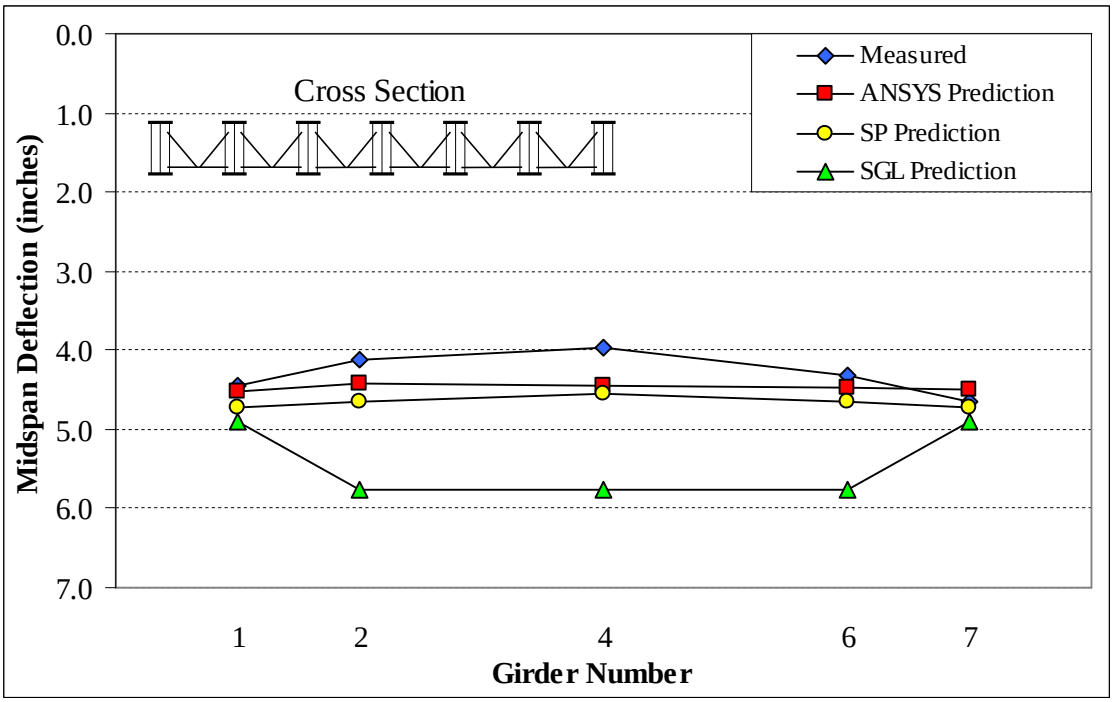

Figure 7.26: Field Measured Deflections vs. Predicted Deflections for the US-29 Bridge

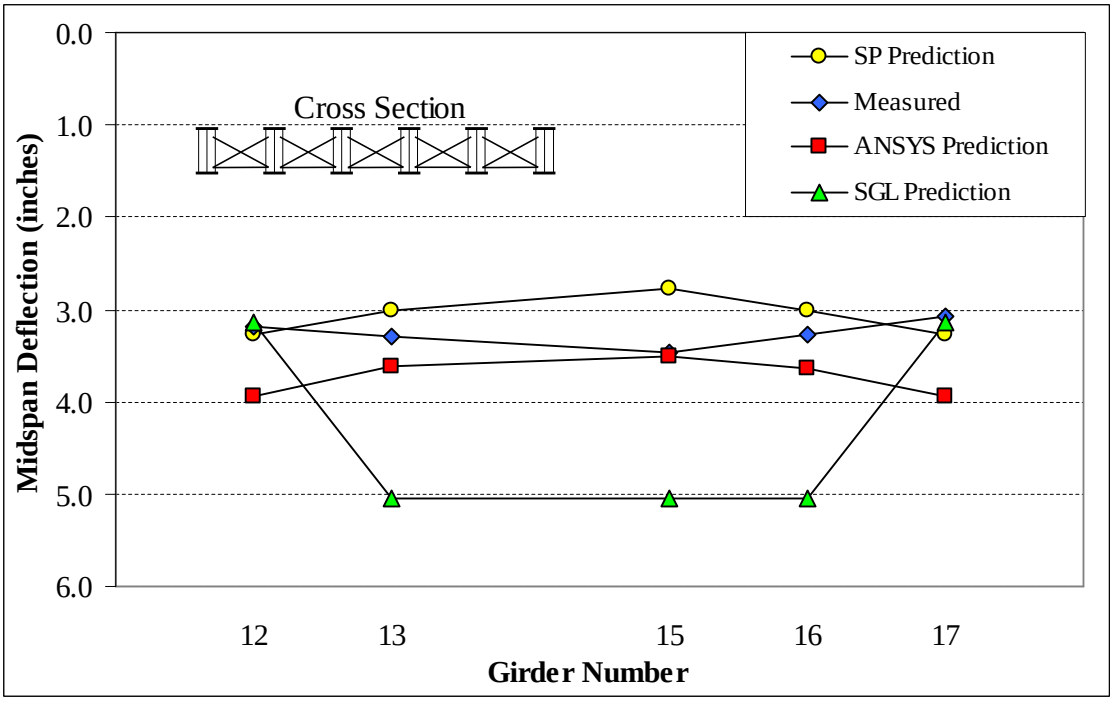

Figure 7.27: Field Measured Deflections vs. Predicted Deflections for the Camden NB Bridge

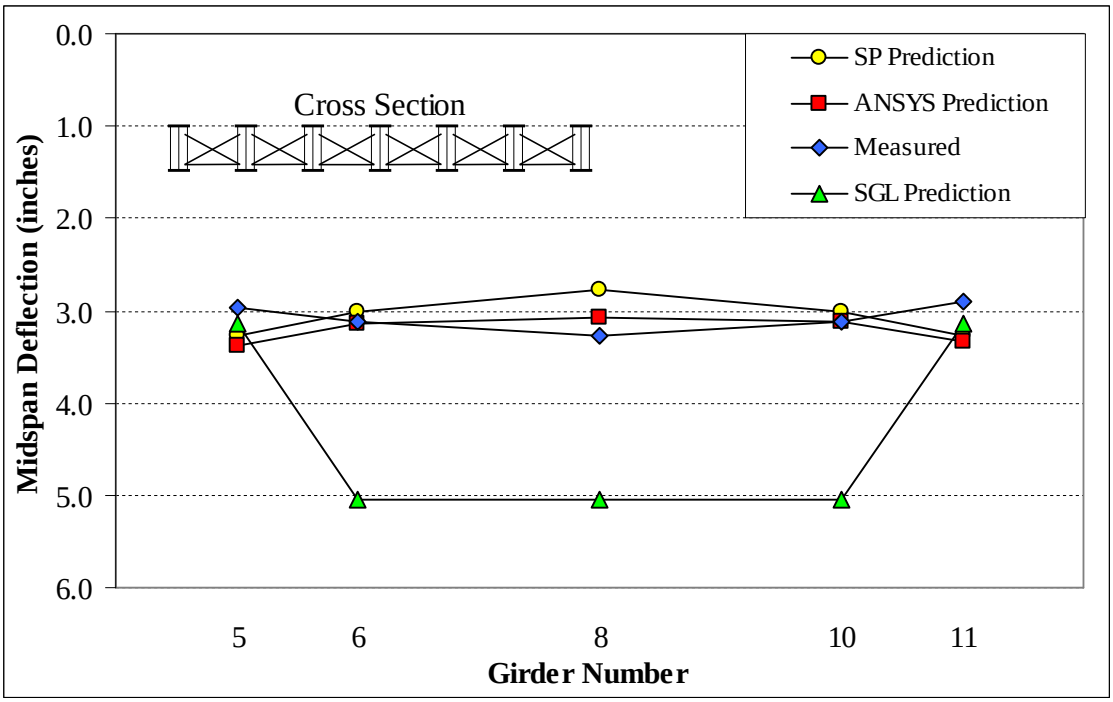

Figure 7.28: Field Measured Deflections vs. Predicted Deflections for the Camden SB Bridge

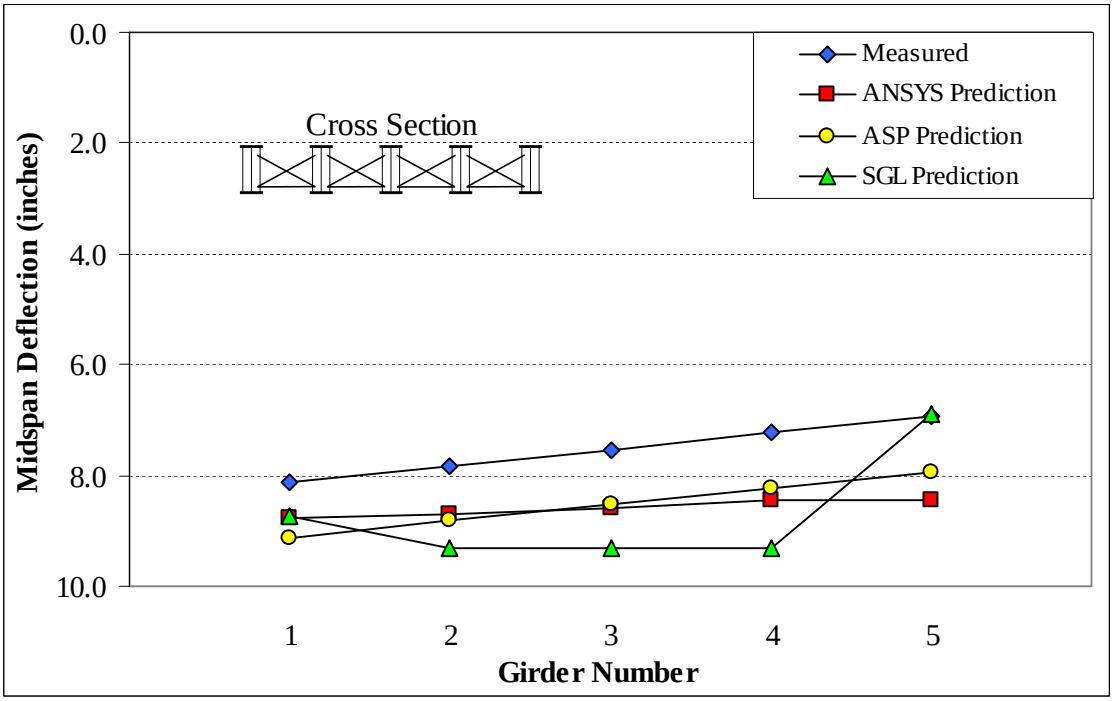

Figure 7.29: Field Measured Deflections vs. Predicted Deflections for the Eno Bridge

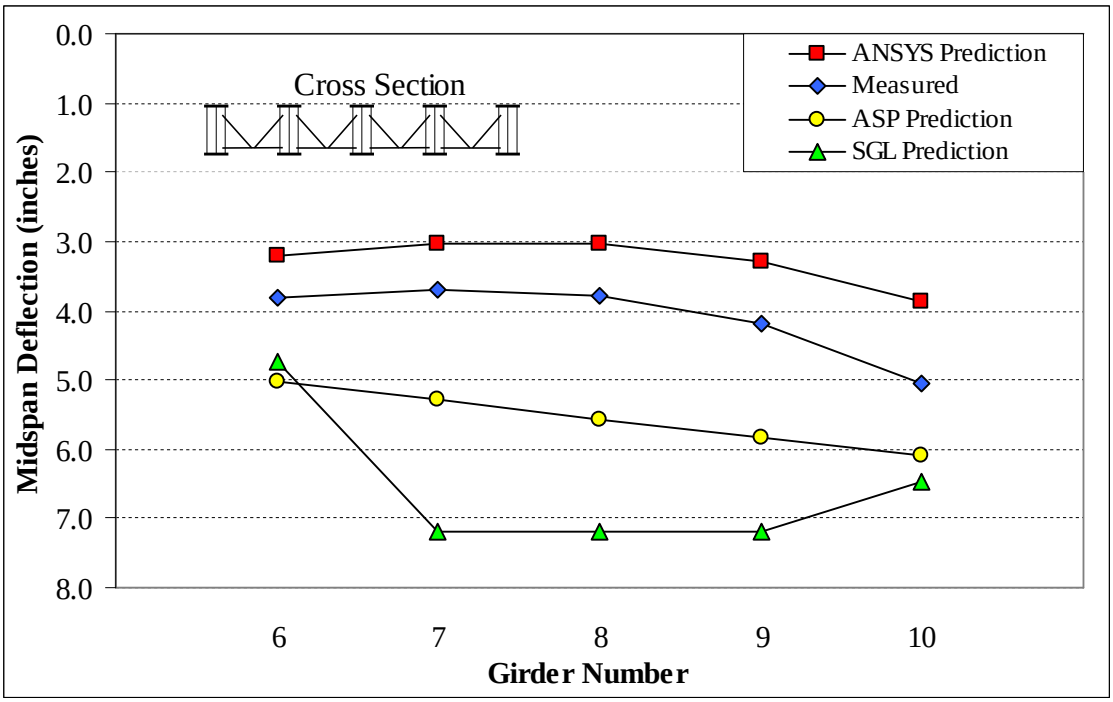

Figure 7.30: Field Measured Deflections vs. Predicted Deflections for the Wilmington St Bridge

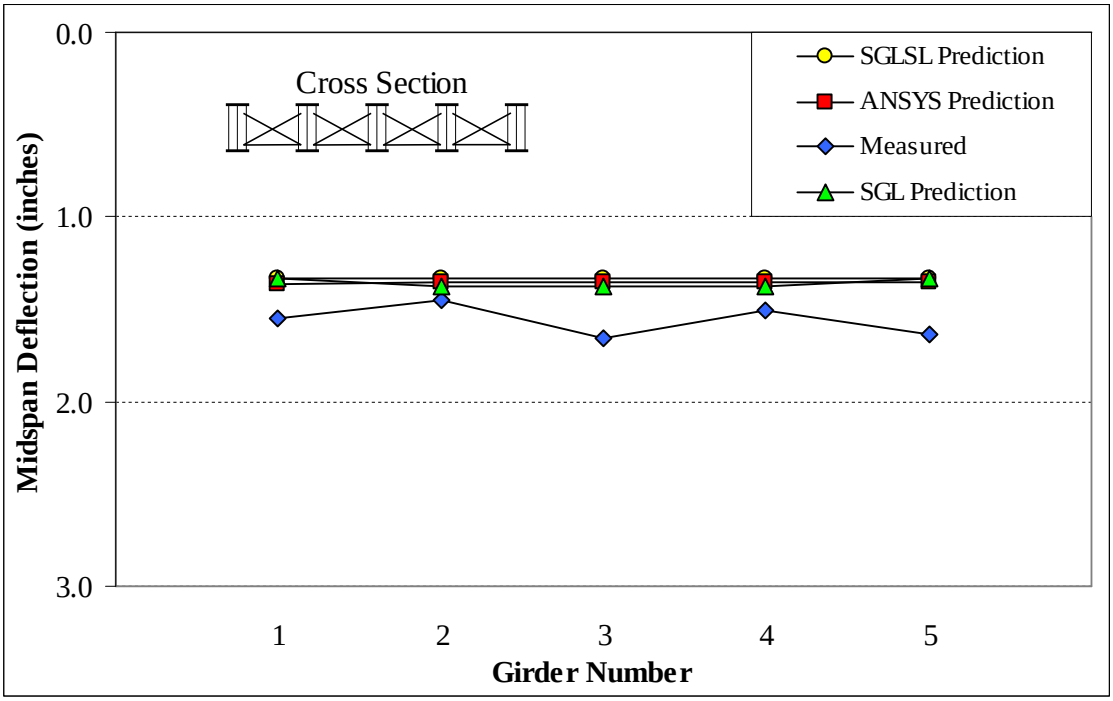

Figure 7.31: Field Measured Deflections vs. Predicted Deflections for Bridge 14 (Span B)

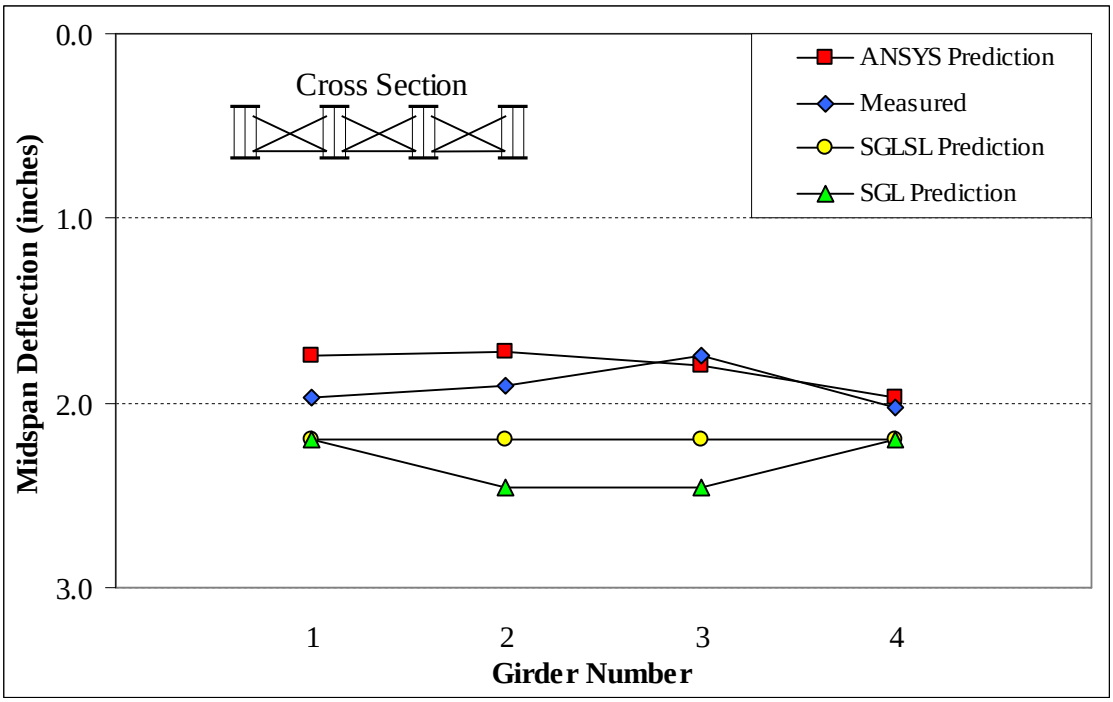

Figure 7.32: Field Measured Deflections vs. Predicted Deflections for Bridge 10 (Span B)

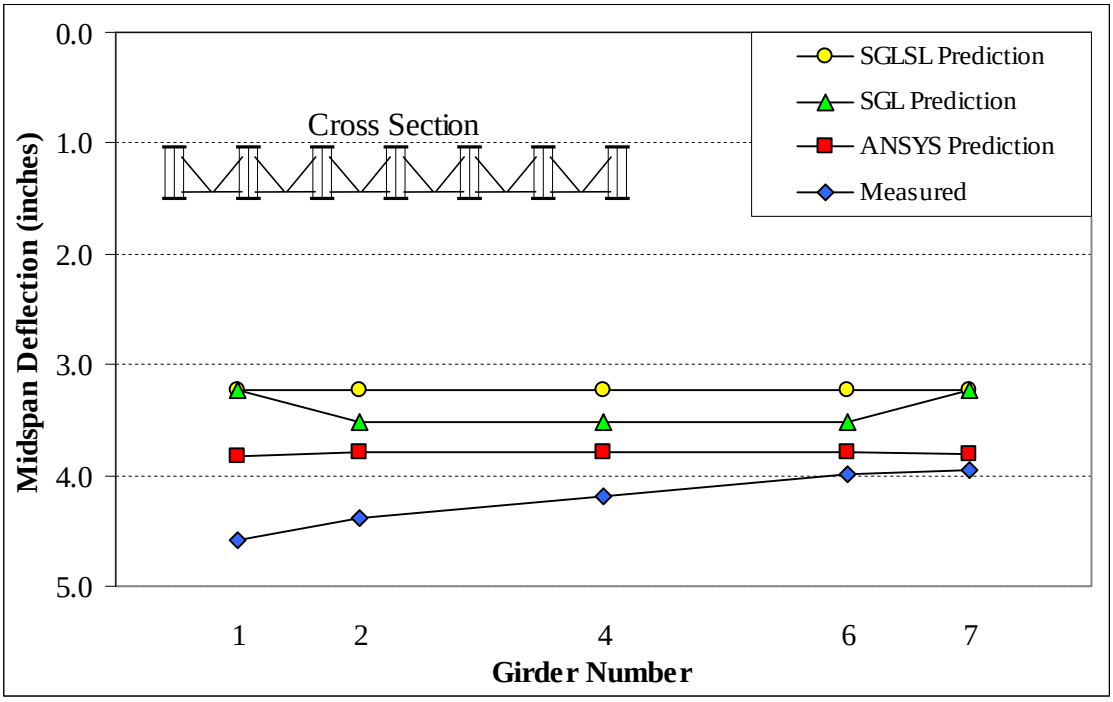

Figure 7.33: Field Measured Deflections vs. Predicted Deflections for Bridge 1 (Span B)

8.0 Observations, Conclusions, and Recommendations

8.1 Summary

A simplified procedure has been developed to predict dead load deflections of skewed and non-skewed steel plate girder bridges for use by the North Carolina Department of Transportation (NCDOT). The research was funded to mitigate costly construction delays and maintenance and safety issues in future projects that result from inaccurate deflection predictions via the traditional single girder line (SGL) analysis.

Ten steel plate girder bridges were monitored and field measured deflections were recorded to capture true girder deflection behavior during concrete deck construction. A three-dimensional finite element bridge modeling technique was established and the simulated girder deflections correlated well with field measured deflections. In combination with a preprocessor program developed by the author, the finite element modeling technique was utilized to conduct a parametric study, in which the effects of skew angle, girder spacing, span length, cross frame stiffness, number of girders within the span, and exterior-to-interior girder load ratio on girder deflection behavior were investigated. The results were analyzed and the simplified procedure was developed to predict deflections in steel plate girder bridges. The procedure utilizes empirically derived modifications which are applied to the traditional SGL predictions to account for the effects of skew angle, girder spacing, span length, and exterior-to-interior girder load ratio. Predictions via the simplified procedure were compared to field measured deflections and SGL predictions to validate the procedure.

8.2 Observations

The observations discussed herein relate to field measurements, finite element modeling, automated model generation, the parametric study, the development of the simplified procedure, and comparisons of the deflection results.

- The field measured deflections for the five bridges included in this research did not correlate well with the SGL predicted deflections.
- Incorporating the SIP metal deck forms into the finite element models resulted in distinctly different simulated deflection behavior.
- SGL predictions over predict field measured deflections for the interior and exterior girders of simple span bridges by approximately 12 and 46 percent, respectively.
- ANSYS finite element models predict field measured deflections more accurately than SGL predictions. The interior and exterior girders of simple span bridges are over predicted by approximately 11 and 7 percent respectively.
- SGL predictions and ANSYS predictions match field measured deflections equally well for interior and exterior girders of continuous span bridges.
- Predictions from the simplified procedure for simple span bridges with equal exterior-to-interior girder load ratios over predict field measured deflections by 8 and 15 percent for the interior and exterior girders, respectively.
- Predictions from the alternative simplified procedure (ASP) for simple span bridges with unequal exterior-to-interior girder load ratios over predict field measured deflections by 28 and 20 percent for the interior and exterior girders, respectively.

- On average, predictions from the SGL straight line (SGLSL) method match the field measured deflections for the exterior and interior girders of continuous span bridges with equal exterior-to-interior girder load ratios.

8.3 Conclusions

The conclusions discussed herein relate to field measurements, finite element modeling, automated model generation, the parametric study, the development of the simplified procedure, and comparisons of the deflection results.

- The traditional SGL method does not accurately predict dead load deflections of steel plate girder bridges.
- Finite element models created according to the technique presented in this report are capable of predicting deflections for skewed and non-skewed steel plate girder bridges.
- Finite element models with SIP forms generate more accurate results, and should be included in the finite element models.
- Skew, the exterior-to-interior girder load ratio, and the girder spacing-to-span ratio affect girder dead load deflections for simple span bridges.
- Cross frame stiffness and the number of girders within the span do not have a significant effect on girder dead load deflections for simple span bridges.
- The simplified procedure (SP), alternative simplified procedure (ASP), and SGL straight line (SGLSL) method can accurately predict girder dead load deflections.

8.4 Recommended Simplified Procedures

The recommended simplified procedures to predict the dead load deflections are presented for simple span bridges with equal exterior-to-interior girder load ratios, simple span bridges with unequal exterior-to-interior girder load ratios, and continuous span bridges with equal exterior-to-interior girder load ratios. The three procedures utilize the equations presented in the following sections to predict the exterior girder deflections and the differential deflections between adjacent girders. A flowchart illustrating the procedures is included in Appendix A and detailed sample calculations are presented in Appendix B.

8.4.1 Simple Span Bridges with Equal Exterior-to-Interior Girder Load Ratios

The following simplified procedure was developed in Section 6 for simple span bridges with equal exterior-to-interior girder load ratios. Note that the procedure is applied to half of the bridge cross-section and the predictions are then mirrored about an imaginary vertical axis through: the middle girder of a bridge with an odd number of girders or the middle of a bridge with an even number of girders. For instance, the procedure would be utilized to calculate the predicted deflections of girders 1, 2, 3, and 4 in a seven girder bridge. The predictions would then be symmetric about an imaginary vertical axis through girder 4. As a result, the predicted deflection of girder 5 would equal that of girder 3, girder six would equal girder 2, and so on (see Figure 8.1).

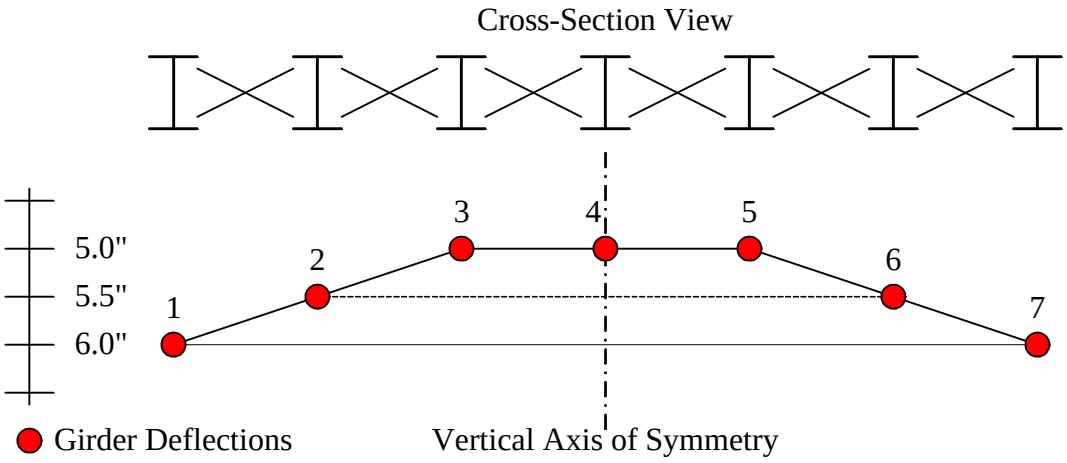

Figure 8.1: Simplified Procedure (SP) Application

- Step 1: Calculate the interior girder SGL prediction, d_{SGL_INT}, at desired locations along the span (ex. 1/10 points), and at mid-span, d_{SGL_M}.
- Step 2: Calculate the predicted exterior girder deflection at each location along the span using the following:

$$d_{EXT} = [d_{SGL\_INT} - F(100 - L)][1 - 0.1\tan(1.2q)] \quad \text{(eq. 8.1)}$$

where: d_{SGL_INT} = interior girder SGL predicted deflection at locations along the span (in)

$F = 0.03 - a(q)$

where: $a = 0.0002$ if $(g <= 8.2)$

$a = 0.0002 + 0.000305\,(g - 8.2)$ if $(8.2 < g <= 11.5)$

where: g = girder spacing (ft)

L = exterior-to-interior girder load ratio (in percent, ex: 65 %)

q = skew offset (degrees) = |skew - 90| Note: Applicable for $q \leq 65$

- Step 3: Calculate the predicted differential deflection between adjacent girders at each location along the span using the following:

$$D_{INT} = x\left[a\left(S - 0.04\right)\left(1 + z\right) - 0.1\tan\left(1.2q\right)\right] \quad \text{(eq. 8.2)}$$

where: $x = (d_{SGL\_INT})/(d_{SGL\_M})$

where: d_{SGL_M} = SGL predicted girder deflection at midspan (in)

$a = 3.0 - b(q)$

where: $b = -0.08$ if $(S <= 0.05)$

$b = -0.08 + 8(S - 0.05)$ if $(0.05 < S <= 0.08)$

where: S = girder spacing-to-span ratio

$z = (10(S - 0.04) + 0.02)(2 - L/50)$

q = skew offset (degrees) = |skew - 90| Note: Applicable for $q \leq 65$

- Step 4: Calculatethe predicted interior girder deflections at each location along the span using the following:

$$d_{INT\_i} = d_{EXT} + y * D_{INT} \quad \text{(eq. 8.3)}$$

where: $y = 1$ (first interior girder)

$y = 2$ (other interior girders)

8.4.2 Simple Span Bridges with Unequal Exterior-to-Interior Girder Load Ratios

The following recommendation utilizes the alternative simplified procedure (ASP) developed in Section 6 for simple span bridges with unequal exterior-to-interior girder load ratios. Note that 'high ratio' and 'low ratio' refers to the greater and lesser of the two exterior-to-interior girder load ratios respectively. Additionally, the procedure is applicable for a difference in exterior-to-interior girder load ratios of more than 10 percent. For instance, if one exterior girder load is 78 percent of the interior girder load and the other exterior girder load is 90 percent (difference of 12 percent), this method is applicable. If the

second exterior girder load is only 86 percent (difference of 8 percent) the simplified procedure (SP) is applied, as previously discussed.

- Step 1: Calculate the interior girder SGL prediction, d_{SGL_INT}, at desired locations along the span (ex. 1/10 points), and at mid-span, d_{SGL_M}.
- Step 2: Calculate the predicted exterior girder deflections, d_{EXT}, at each location along the span for both the 'high ratio' and 'low ratio' using Equation 8.1.

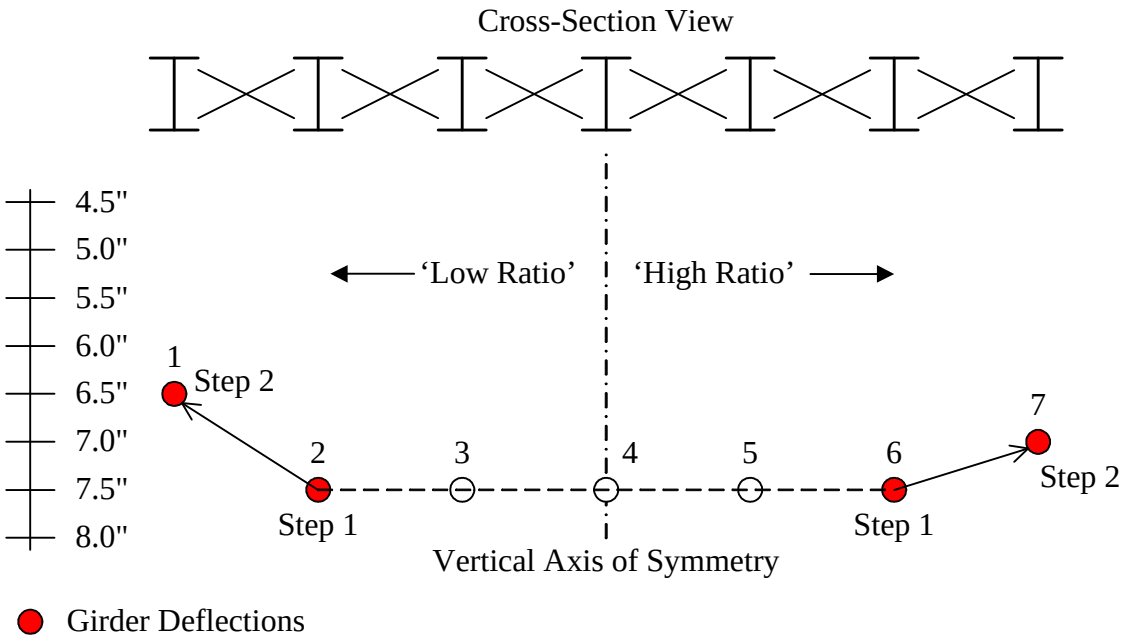

Figure 8.2: Steps 1 and 2 of the Alternative Simplified Procedure (ASP)

- Step 3: Calculate the predicted differential deflection, D_{INT}, between adjacent girders for the 'low ratio' according to Equation 8.2.
- Step 4: Calculate the predicted interior girder deflections, d_{INT_i}, for the 'low ratio,' to the middle girder for an odd number of girders and to the center girders for an even number of girders, according to Equation 8.3.

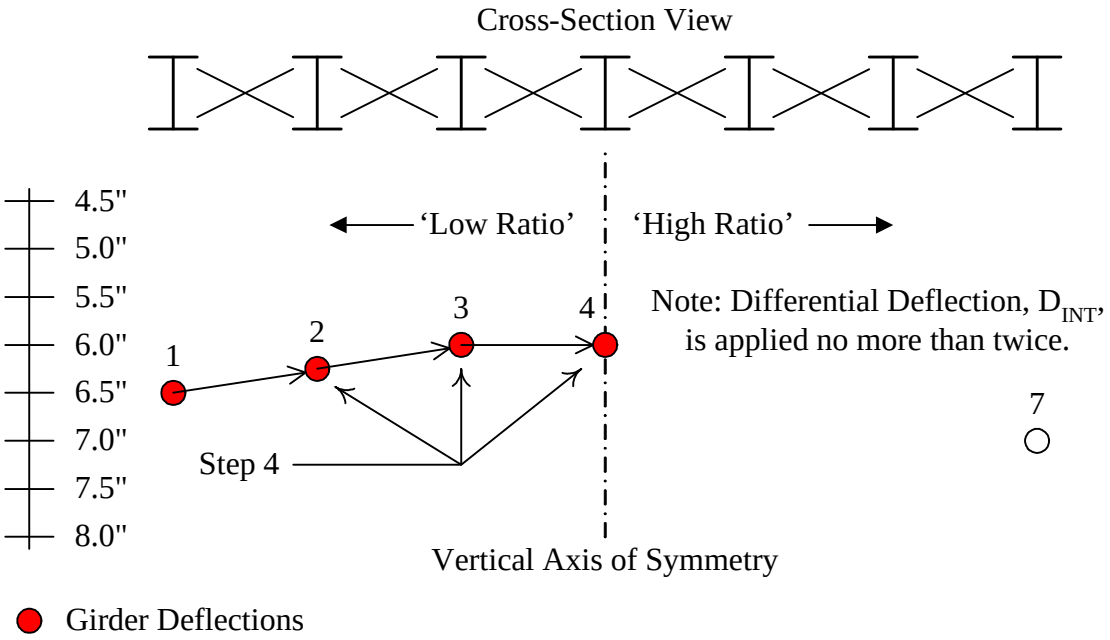

Figure 8.3: Step 4 of the Alternative Simplified Procedure (ASP)

- Step 5: Calculate the 'slope' of a line through the predicted exterior girder deflection for the 'high ratio' (girder 7 in the Figures) and the predicted center girder deflection for the 'low ratio' (girder 4 in the Figures).
- Step 6: Interpolate and extrapolate deflections to predict the entire deflected shape along the straight line referenced in Step 5.

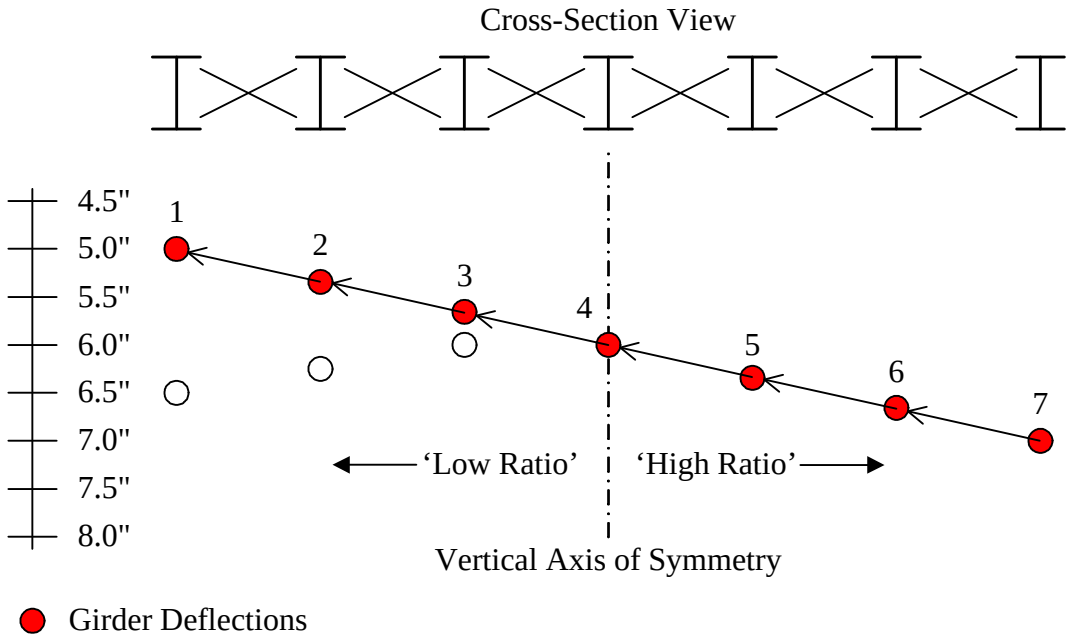

Figure 8.4: Step 6 of the Alternative Simplified Procedure (ASP)

8.4.3 Continuous Span Bridges with Equal Exterior-to-Interior Girder Load Ratios

The following SGL straight line (SGLSL) method was developed in Section 6 for continuous span bridges with equal exterior-to-interior girder load ratios.

- Step 1: Calculate the exterior girder SGL predictions, d_{SGL_EXT}, at desired locations along the span (ex. 1/20 points).
- Step 2: Use the predicted exterior girder SGL deflections as the interior girder deflections, resulting in a straight line prediction (see Figure 8.5).

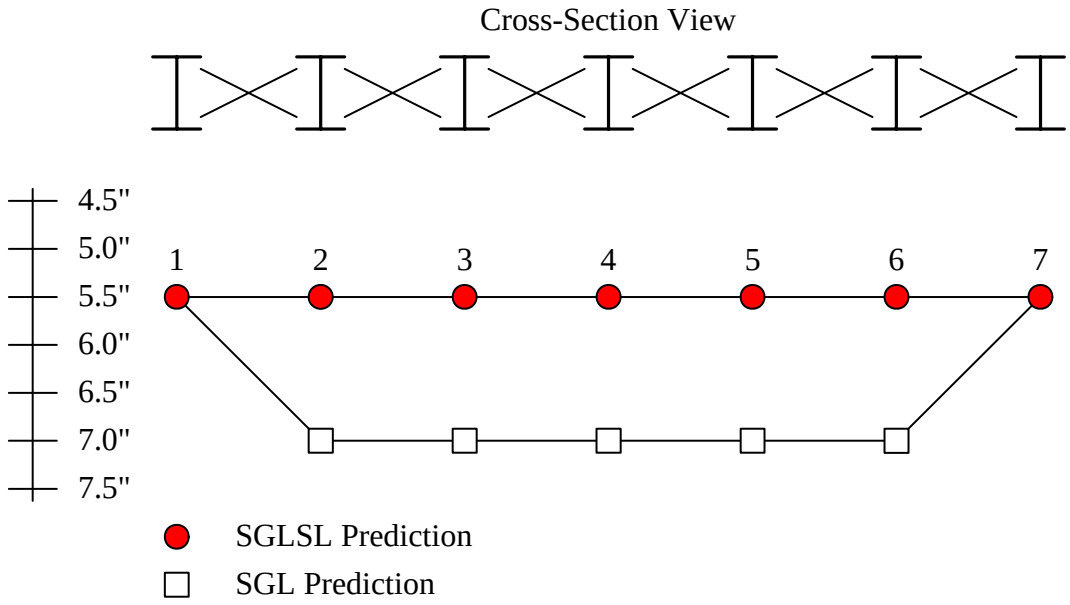

Figure 8.5: SGL Straight Line (SGLSL) Application

8.5 Implementation Plan

The NCDOT plans to implement the new design procedures for all steel girder structures immediately, regardless of skew. The Engineering Development group of NCDOT's Structure Design Unit plans to distribute the new formulas immediately for use by their in-house engineering staff on designs performed in-house. Distribution of the formulas to Private Engineering Firms will proceed as soon as practical, but no later than the December 2006 letting. In the meantime, previously let projects may have their cambers recomputed and the plans revised. This will be done on a case-by-case basis, and most likely will be required for structures with long-spans or severe skews.

Initially, engineers will receive a policy memo requiring the use of the new procedures for steel superstructure bridges. Attached to this will be a short summary of why the research was commissioned and the research findings, along with a simple spreadsheet for use in performing the calculations. Once the new policy has been released, a one-hour

training session will be held for Department personnel. For the benefit of consulting engineers, the summary and the spreadsheet will be placed on the NCDOT website. While the full report will not be placed on the website, there will be instructions as to where to find the full copy of the research. To further educate private engineering firm personnel and to explain the history and development of the new formulas, DOT will present the research findings in October of 2006 via a regularly scheduled, joint ACEC-DOT educational seminar series.

8.6 Future Considerations

Future research can be directed to improve upon the recommendations concluded in this research. Additional steel plate girder bridges should be monitored in the field to further validate the measured deflections to finite element models. Consequently, increased variance in measured bridge parameters would provide further validation to the simplified procedure and allow for future improvements. Additional bridges should include the possible bridge configurations: simple span bridges with equal and unequal exterior-to-interior girder load ratios and continuous span bridges with equal and unequal exterior-to-interior girder load ratios.

9.0 References

AASHTO (1996). *Standard Specifications for Highway Bridges*, 16th Ed., Washington D.C.

AASHTO/NSBA (2002). *Guidelines for Design for Constructability, G 12.1-2002, Draft for Ballot*, American Association of State Highway and Transportation Officials/National Steel Bridge Alliance.

ACI (1992). *Guide for Widening Highway Bridges, ACI committee 345*, American Concrete Institute Structural Journal.

ANSYS 7.1 Documentation (2003), Swanson Analysis System, Inc.

Austin, M.A., Creighton, S., Albrecht, P. (1993). "XBUILD: Preprocessor for Finite Element Analysis of Steel Bridges," *Journal of Computing in Civil Engineering*, ASCE, January, 54-70.

Bakht, B. (1988). "Analysis of Some Skew Bridges as Right Bridges," *Journal of Structural Engineering*, ASCE, 114(10), 2307-2322.

Barefoot, J.B., Barton, F.W., Baber, T.T., McKeel, W.T. (1997). "Development of Finite Element Models to Predict Dynamic Bridge Response," *Research Report No. VTRC 98-R8*, Virginia Transportation Research Council, Charlottesville, VA.

Berglund, E.M., Schultz, A.E. (2001). "Analysis Tools and Rapid Screening Data for Assessing Distortional Fatigue in Steel Bridge Girders," *Research Report No. MN/RC-2002-06*, Department of Civil Engineering, University of Minnesota, Minneapolis, MN.

Bishara, A.G., Elmir, W.E. (1990). "Interaction Between Cross Frames and Girders," *Journal of Structural Engineering*, ASCE, 116(5), 1319-1333.

Bishara, A.G. (1993). "Cross Frames Analysis and Design," *FHWA/OH-93/004*, Federal Highway Administration, Washington, D.C. and Ohio Department of Transportation, Columbus, OH.

Bishara, A.G., Liu, M.C., El-Ali, N.D. (1993). "Wheel Load Distribution on Simply Supported Skew I-Beam Composite Bridges," *Journal of Structural Engineering*, ASCE, 119(2), 399-419.

Brockenbrough, R.L. (1986). "Distribution Factors for Curved I-Girder Bridges," *Journal of Structural Engineering*, ASCE, 112(10), 2200-2215.

Buckler, J.G., Barton, F.W., Gomez, J.P., Massarelli, P.J., McKeel, W.T. (2000). "Effect of Girder Spacing on Bridge Deck Response," *Research Report No. TRC 01-R6*, Virginia Transportation Research Council, Charlottesville, VA.

Chen, S.S., Daniels, J.H., Wilson, J.L. (1986). "Computer Study of Redundancy of a Single Span Welded Two-Girder Bridge," Interim Report, Lehigh University, Bethlehem, PA.

Currah, R.M. (1993). "Shear Strength and Shear Stiffness of Permanent Steel Bridge Deck Forms," M.S. Thesis, Department of Civil Engineering, University of Texas, Austin, TX.

Ebeido, T., Kennedy, J.B. (1995). "Shear Distribution in Simply Supported Skew Composite Bridges," *Canadian Journal of Civil Engineering*, National Research Council of Canada, 22(6), 1143-1154.

Ebeido, T., Kennedy, J.B. (1996). "Girder Moments in Simply Supported Skew Composite Bridges," *Canadian Journal of Civil Engineering*, National Research Council of Canada, 23(4), 904-916.

Egilmez, O.O., Jetann, C.A., Helwig, T.A. (2003). "Bracing Behavior of Permanent Metal Deck Forms," *Proceedings of the Annual Technical Session and Meeting*, Structural Stability Research Council.

Fisher, S.F. (2006). "Development of a Simplified Method to Predict Dead Load Deflections of Skewed and Non-Skewed Steel Plate Girder Bridges," M.S. Thesis, Department of Civil Engineering, North Carolina State University, Raleigh, NC.

Fu, K.C., Lu, F. (2003). "Nonlinear Finite-Element Analysis for Highway Bridge Superstructures," *Journal of Bridge Engineering*, ASCE, 8(3), 173-179.

Gupta, Y.P., Kumar, A. (1983). "Structural Behaviour of Interconnected Skew Slab-Girder Bridges," *Journal of the Institution of Engineers (India), Civil Engineering Division*, 64, 119-124.

Hays, C.O., Sessions, L.M., Berry, A.J. (1986). "Further Studies on Lateral Load Distribution Using FEA," *Transportation Research Record 1072*, Transportation Research Board, Washington D.C.

Helwig, T. (1994). "Lateral Bracing of Bridge Girders by Metal Deck Forms," Ph.D. Dissertation, Department of Civil Engineering, The University of Texas at Austin, Austin, TX.

Helwig, T., Wang, L. (2003). "Cross-Frame and Diaphragm Behavior for Steel Bridges with Skewed Supports," *Research Report No. 1772-1, Project No. 0-1772*, Department of Civil and Environmental Engineering, University of Houston, Houston, TX.

Helwig, T., and Yura, J. (2003), "Strength Requirements for Diaphragm Bracing of Beams," Draft manuscript to be submitted.

Hilton, M.H. (1972). "Factors Affecting Girder Deflections During Bridge Deck Construction," *Highway Research Record*, HRB, 400, 55-68.

Imbsen, R.A. and Nutt, R.V. (1978). "Load Distribution Study on Highway Bridges Using STRUDL FEA," *Proceedings of the Conference on Computing in Civil Engineering*, ASCE, New York, NY.

Jetann, C.A., Helwig, T.A., Lowery, R. (2002). "Lateral Bracing of Bridge Girders by Permanent Metal Deck Forms," *Proceedings of the Annual Technical Session and Meeting*, Structural Stability Research Council.

Keating, P.B., Alan, R.C. (1992). "Evaluation and Repair of Fatigue Damage to Midland County Bridges," *Draft, TX-92/1331-1*.

Mabsout, M.E., Tarhini, K.M., Frederick, G.R., Tayar, C. (1997a). "Finite-Element Analysis of Steel Girder Highway Bridges," *Journal of Bridge Engineering*, ASCE, 2(3), 83-87.

Mabsout, M.E., Tarhini, K.M., Frederick, G.R., Kobrosly, M. (1997b). "Influence of Sidewalks and Railings on Wheel Load Distribution in Steel Girder Bridges," *Journal of Bridge Engineering*, ASCE, 2(3), 88-96.

Mabsout, M.E., Tarhini, K.M., Frederick, G.R., Kesserwan, A. (1998). "Effect of Continuity on Wheel Load Distribution in Steel Girder Bridges," *Journal of Bridge Engineering*, ASCE, 3(3), 103-110.

Martin, T.M., Barton, F.W., McKeel, W.T., Gomez, J.P., Massarelli, P.J. (2000). "Effect of Design Parameters on the Dynamic Response of Bridges," *Research Report No. TRC 00-R23*, Virginia Transportation Research Council, Charlottesville, VA.

Melhem, H., Hu, K., Niazi, K. (1996). "Concrete Dead Load Deflections of Continuous Steel Girder Composite Bridges," *Research Report No. K-Tran: KSU 95-6*, Department of Civil Engineering, Kansas State University, Manhattan, KS.

Norton, E.K. (2001). "Response of a Skewed Composite Steel-Concrete Bridge Floor System to Placement of Deck Slab," M.S. Thesis Proposal, Department of Civil and Environmental Engineering, The Pennsylvania State University, University Park, PA.

Norton, E.K., Linzell, D.G., Laman, J.A. (2003). "Examination of Response of a Skewed Steel Bridge Superstructure During Deck Placement," *Transportation Research Record 1845*, Transportation Research Board, Washington D.C.

Nutt, R.V., Zokaie, T., Schamber, R.A. (1987). "Distribution of Wheel Loads on Highway Bridges," *NCHRP Project No. 12-26*, National Cooperative Highway Research Program, Transportation Research Board, National Research Council, Washington D.C.

Padur, D.S., Wang, X., Turer, A., Swanson, J.A., Helmicki, A.J., Hunt, V.J. (2002). "Non Destructive Evaluation/Testing Methods – 3D Finite Element Modeling of Bridges," *American Society for Nondestructive Testing*, NDE/NDT for Highways and Bridges, Cincinnati, OH.

Paoinchantara, N. (2005). "Measurement and Simplified Modeling Method of the Non-Composite Deflections of Steel Plate Girder Bridges," M.S. Thesis, Department of Civil Engineering, North Carolina State University, Raleigh, NC.

Paracha, S. (1997). "Computer Simulation of the Time Dependent Deflections of a Continuous Composite Girder During Casting of Concrete Deck," M.S. Thesis, Department of Civil Engineering, Kansas State University, Manhattan, KS.

Plaut, R. (1993). "Requirements for Lateral Bracing of Columns With Two Spans," *Journal of Structural Engineering*, ASCE, 119(10), 2913-2931.

Sahajwani, K. (1995). "Analysis of Composite Steel Bridges With Unequal Girder Spacings," M.S. Thesis, Department of Civil and Environmental Engineering, University of Houston, Houston, TX.

Schilling, C.G. (1982). "Lateral-Distribution Factors for Fatigue Design," *Journal of the Structural Division*, ASCE, 108(ST9), 2015-2033.

Shi, J. (1997). "Brace Stiffness Requirements of Skewed Bridge Girders," M.S. Thesis, Department of Civil and Environmental Engineering, University of Houston, Houston, TX.

Soderberg, E.G. (1994). "Strength and Stiffness of Stay-in-Place Metal Deck Form Systems," M.S. Thesis, Department of Civil Engineering, University of Texas, Austin, TX.

Steel Deck Institute (1991). Diaphragm Design Manual, second edition.

Swett, G.D. (1998). "Constructability Issues With Widened and Stage Constructed Steel Plate Girder Bridges," M.S. Thesis, Department of Civil and Environmental Engineering, University of Washington, Seattle, WA.

Swett, G.D., Stanton, J.F., Dunston, P.S. (2000). "Methods for Controlling Stresses and Distortions in Stage-Constructed Steel Bridges," *Transportation Research Record 1712*, Transportation Research Board, Washington D.C.

Tabsh, S., Sahajwani, K. (1997). "Approximate Analysis of Irregular Slab-on-Girder Bridges," *Journal of Bridge Engineering*, ASCE, 2(1), 11-17.

Tarhini, K.M., Frederick, G.R. (1992). "Wheel Load Distribution in I-Girder Highway Bridges," *Journal of Structural Engineering*, ASCE, 118(5), 1285-1294.

Tarhini, K.M., Mabsout, M., Harajli, M., Tayar, C. (1995). "Finite Element Modeling Techniques of Steel Girder Bridges," *Proceedings of the Conference on Computing in Civil Engineering*, ASCE, New York, NY.

Whisenhunt, T.W. (2004). "Measurement and Finite Element Modeling of the Non-Composite Deflections of Steel Plate Girder Bridges," M.S. Thesis, Department of Civil Engineering, North Carolina State University, Raleigh, NC.

Winter, G. (1958). "Lateral Bracing of Columns and Beams," *Journal of the Structural Division*, ASCE, 84(ST2), Proceedings Paper 1561, 1-22.

Yam, L. C. P., Chapman, J.C. (1972). "The Inelastic Behavior of Continuous Composite Beams of Steel and Concrete." *Proc., Inst. Civ. Eng., Struct. Build*., 53, 487-501.

Appendix A

Simplified Procedure Flow Chart

This appendix contains a flow chart outlining the simplified procedures developed to predict dead load deflections of skewed and non-skewed steel plate girder bridges.

The flow chart can be utilized for the following: simple span bridges with equal exterior-to-interior girder load ratios, simple span bridges with unequal exterior-to-interior girder load ratios, and continuous span bridges with equal exterior-to-interior girder load ratios.

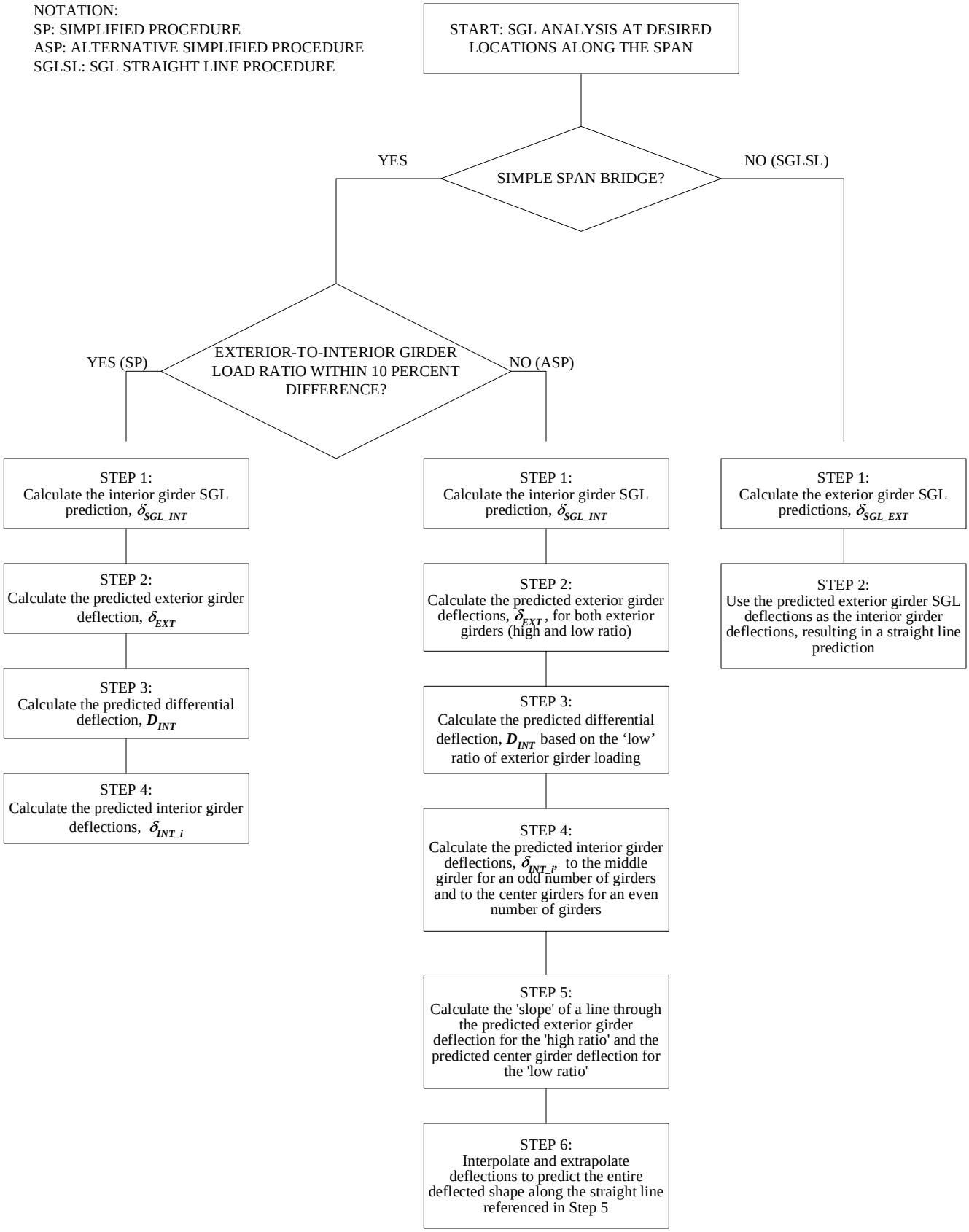
NOTATION:
SP: SIMPLIFIED PROCEDURE
ASP: ALTERNATIVE SIMPLIFIED PROCEDURE
SGLSL: SGL STRAIGHT LINE PROCEDURE
START: SGL ANALYSIS AT DESIRED LOCATIONS ALONG THE SPAN
SIMPLE SPAN BRIDGE?
YES
NO (SGLSL)
EXTERIOR-TO-INTERIOR GIRDER LOAD RATIO WITHIN 10 PERCENT DIFFERENCE?
YES (SP)
NO (ASP)
STEP 1: Calculate the interior girder SGL prediction, δ_{SGL_INT}
STEP 2: Calculate the predicted exterior girder deflection, δ_{EXT}
STEP 3: Calculate the predicted differential deflection, D_{INT}
STEP 4: Calculate the predicted interior girder deflections, δ_{INT_i}
STEP 1: Calculate the interior girder SGL prediction, δ_{SGL_INT}
STEP 2: Calculate the predicted exterior girder deflections, δ_{EXT}, for both exterior girders (high and low ratio)
STEP 3: Calculate the predicted differential deflection, D_{INT} based on the 'low' ratio of exterior girder loading
STEP 4: Calculate the predicted interior girder deflections, δ_{INT_i}, to the middle girder for an odd number of girders and to the center girders for an even number of girders
STEP 5: Calculate the 'slope' of a line through the predicted exterior girder deflection for the 'high ratio' and the predicted center girder deflection for the 'low ratio'
STEP 6: Interpolate and extrapolate deflections to predict the entire deflected shape along the straight line referenced in Step 5
STEP 1: Calculate the exterior girder SGL predictions, δ_{SGL_EXT}
STEP 2: Use the predicted exterior girder SGL deflections as the interior girder deflections, resulting in a straight line prediction

A.1 Simple Span Bridges with Equal Exterior-to-Interior Girder Load Ratios

The following simplified procedure was developed in Section 5 for simple span bridges with equal exterior-to-interior girder load ratios. Note that the procedure is applied to half of the bridge cross-section and the predictions are then mirrored about an imaginary vertical axis through: the middle girder of a bridge with an odd number of girders or the middle of a bridge with an even number of girders. For instance, the procedure would be utilized to calculate the predicted deflections of girders 1, 2, 3, and 4 in a seven girder bridge. The predictions would then be symmetric about an imaginary vertical axis through girder 4. As a result, the predicted deflection of girder 5 would equal that of girder 3, girder six would equal girder 2, and so on (see Figure A.1).

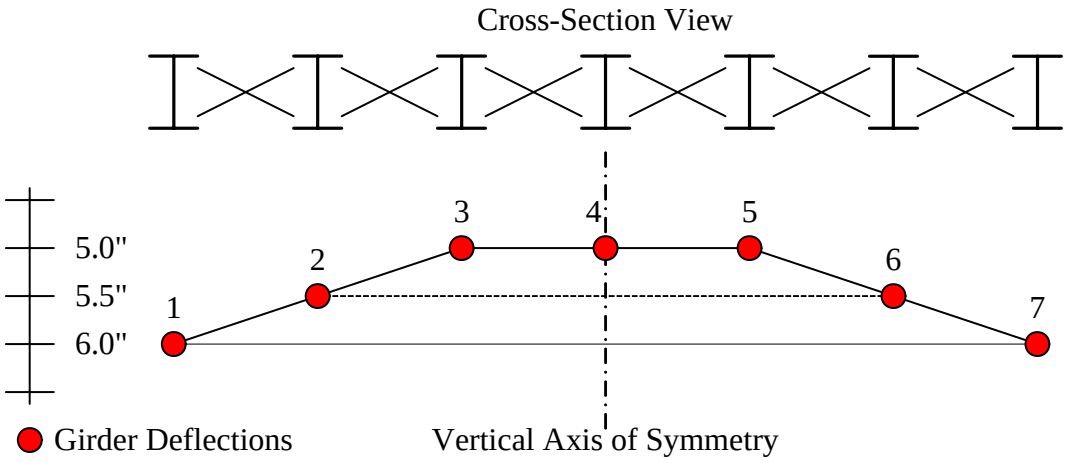

Figure A.1: Simplified Procedure (SP) Application

- Step 1: Calculate the interior girder SGL prediction, δ_{SGL_INT}, at desired locations along the span (ex. 1/10 points), and at midspan, δ_{SGL_M}.

- Step 2: Calculate the predicted exterior girder deflection at each location along the span using the following:

$$\delta_{EXT} = [\delta_{SGL\_INT} - \Phi(100 - L)][1 - 0.1\tan(1.2\theta)] \quad \text{(eq. A.1)}$$

where: δ_{SGL_INT} = interior girder SGL predicted deflection at locations along the span (in)

$\Phi = 0.03 - a(\theta)$

where: $a = 0.0002$ if $(g <= 8.2)$

$a = 0.0002 + 0.000305\,(g - 8.2)$ if $(8.2 < g <= 11.5)$

where: g = girder spacing (ft)

L = exterior-to-interior girder load ratio (in percent, ex: 65 %)

θ = skew offset (degrees) = |skew - 90| Note: Applicable for $\theta \leq 65$

- Step 3: Calculate the predicted differential deflection between adjacent girders at each location along the span using the following:

$$D_{INT} = x[\alpha(S - 0.04)(1 + z) - 0.1\tan(1.2\theta)] \quad \text{(eq. A.2)}$$

where: $x = (\ _{SGL\_INT})/(\ _{SGL\_M})$

where: $_{SGL\_M}$ = SGL predicted girder deflection at midspan (in)

b

where: $b = -0.08$ if $(S <= 0.05)$

$b = -0.08 + 8(S - 0.05)$ if $(0.05 < S <= 0.08)$

where: S = girder spacing-to-span ratio

$z = (10(S - 0.04) + 0.02)(2 - L/50)$

= skew offset (degrees) = |skew - 90| Note: Applicable for _

- Step 4: Calculate the predicted interior girder deflections at each location along the span using the following:

$$\delta_{INT\_i} = \delta_{EXT} + y * D_{INT} \qquad \text{(eq. A.3)}$$

where: $y = 1$ (first interior girder)
$y = 2$ (other interior girders)

A.2 Simple Span Bridges with Unequal Exterior-to-Interior Girder Load Ratios

The following recommendation utilizes the alternative simplified procedure (ASP) developed in Section 5 for simple span bridges with unequal exterior-to-interior girder load ratios. Note that 'high ratio' and 'low ratio' refers to the greater and lesser of the two exterior-to-interior girder load ratios respectively. Additionally, the procedure is applicable for a difference in exterior-to-interior girder load ratios of more than 10 percent. For instance, if one exterior girder load is 78 percent of the interior girder load and the other exterior girder load is 90 percent (difference of 12 percent), this method is applicable. If the second exterior girder load is only 86 percent (difference of 8 percent) the simplified procedure (SP) is applied, as previously discussed.

- Step 1: Calculate the interior girder SGL prediction, δ_{SGL_INT}, at desired locations along the span (ex. 1/10 points), and at midspan, δ_{SGL_M}.
- Step 2: Calculate the predicted exterior girder deflections, δ_{EXT}, at each location along the span for both the 'high ratio' and 'low ratio' using Equation A.1.

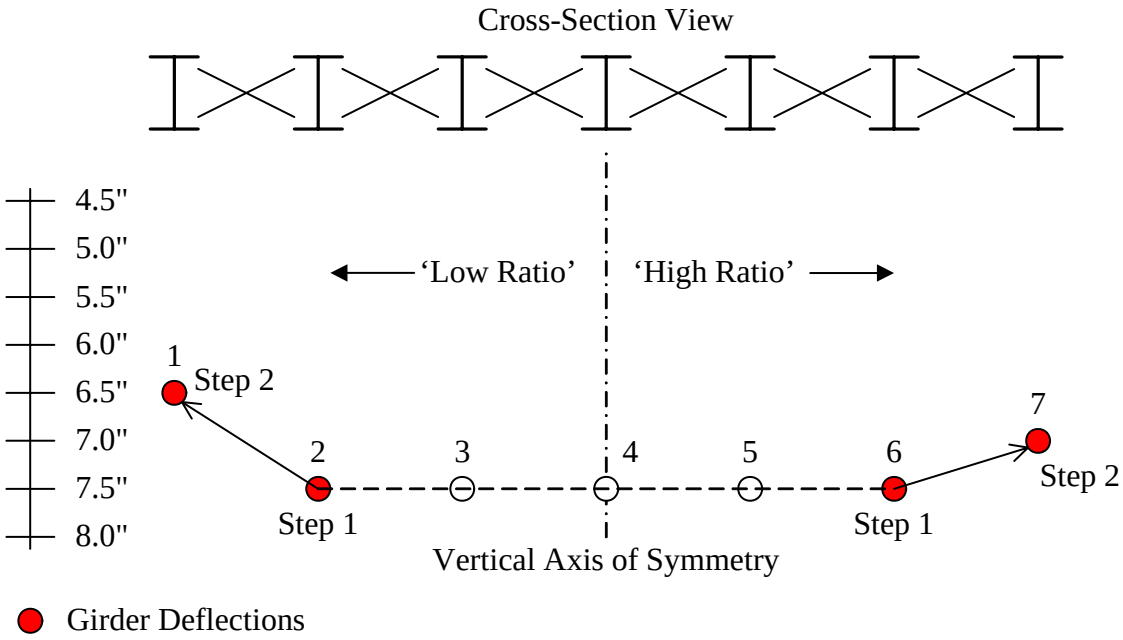

Figure A.2: Steps 1 and 2 of the Alternative Simplified Procedure (ASP)

- Step 3: Calculate the predicted differential deflection, D_{INT}, between adjacent girders for the 'low ratio' according to Equation A.2.
- Step 4: Calculate the predicted interior girder deflections, δ_{INT_i}, for the 'low ratio,' to the middle girder for an odd number of girders and to the center girders for an even number of girders, according to Equation A.3.

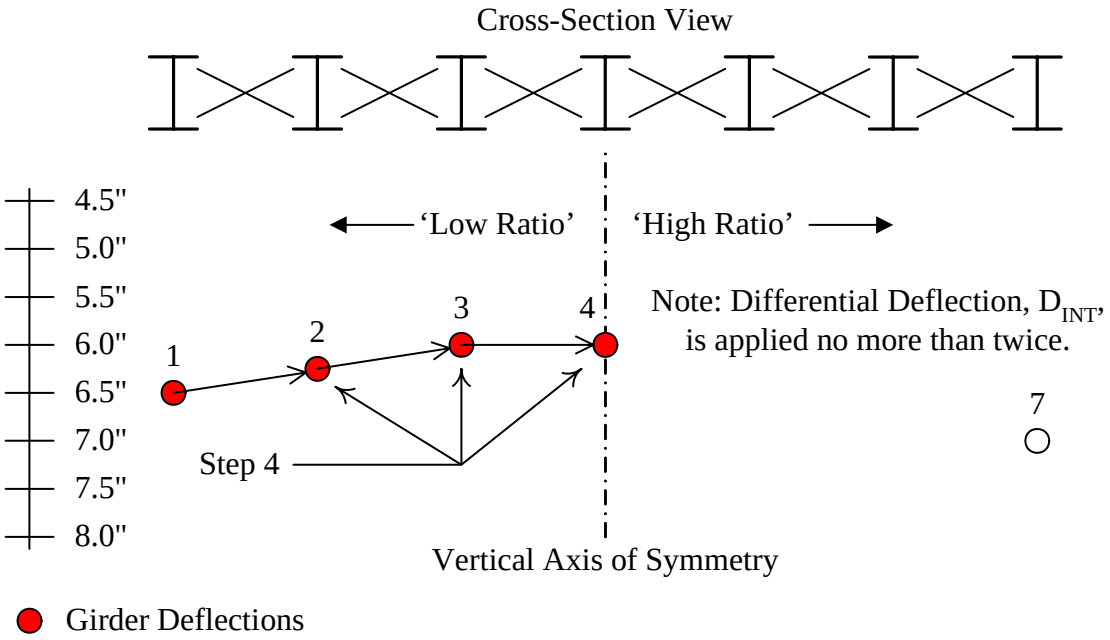

Figure A.3: Step 4 of the Alternative Simplified Procedure (ASP)

- Step 5: Calculate the 'slope' of a line through the predicted exterior girder deflection for the 'high ratio' (girder 7 in the Figures) and the predicted center girder deflection for the 'low ratio' (girder 4 in the Figures).
- Step 6: Interpolate and extrapolate deflections to predict the entire deflected shape along the straight line referenced in Step 5.

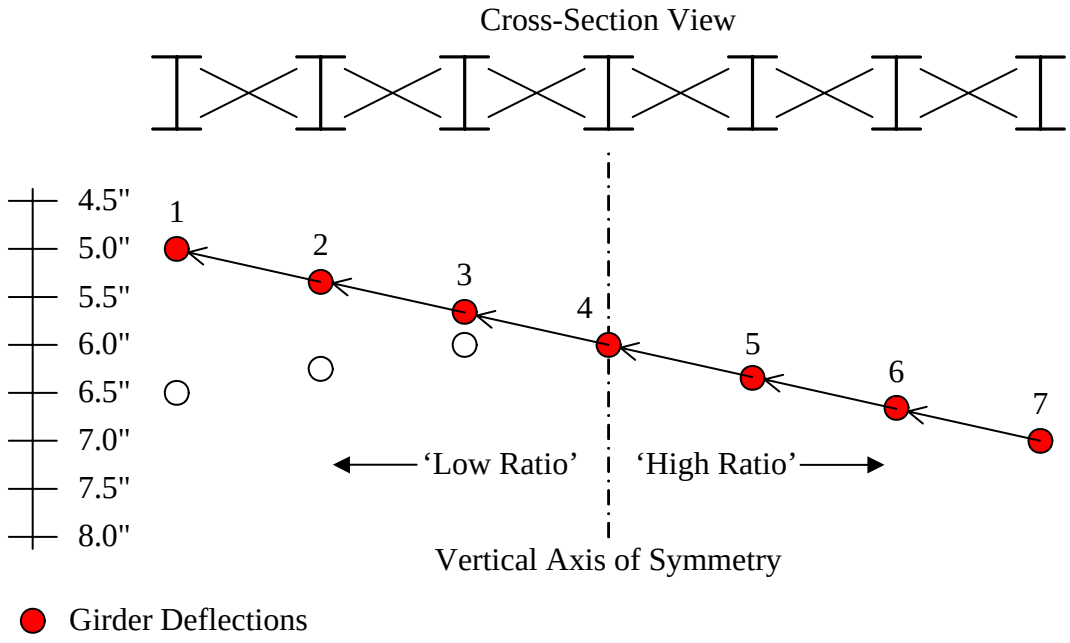

Figure A.4: Step 6 of the Alternative Simplified Procedure (ASP)

A.3 Continuous Span Bridges with Equal Exterior-to-Interior Girder Load Ratios

The following SGL straight line (SGLSL) method was developed in Section 5 for continuous span bridges with equal exterior-to-interior girder load ratios.

- Step 1: Calculate the exterior girder SGL predictions, δ_{SGL_EXT}, at desired locations along the span (ex. 1/20 points).
- Step 2: Use the predicted exterior girder SGL deflections as the interior girder deflections, resulting in a straight line prediction (see Figure A.5).

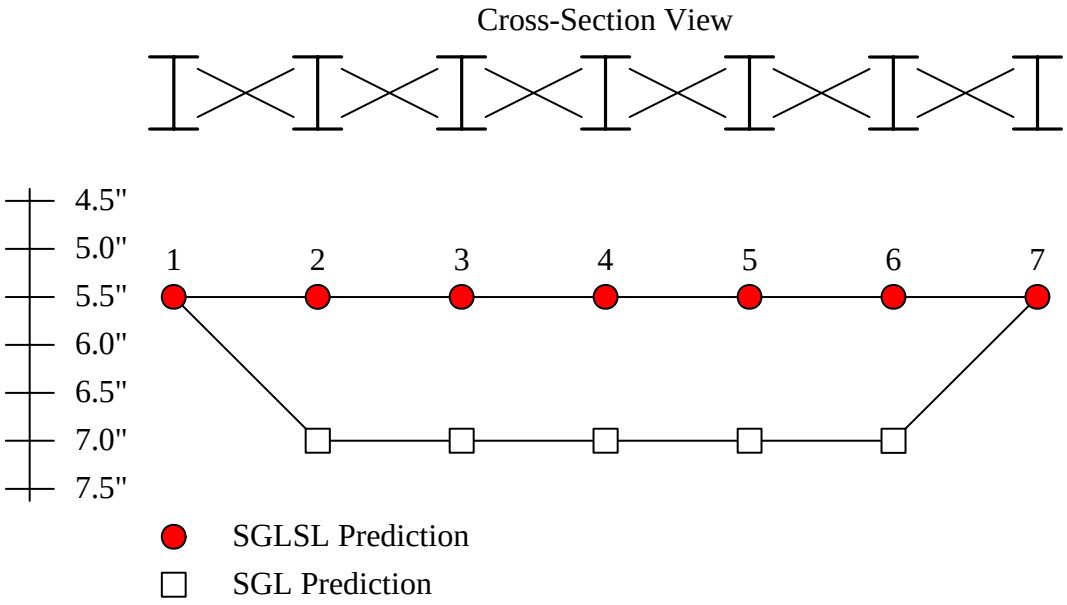

Figure A.5: SGL Straight Line (SGLSL) Application

Appendix B

Sample Calculations of the Simplified Procedure

This appendix contains a step-by-step sample calculation of the simplified procedure developed to predict dead load deflections in steel plate girder bridges. In this sample, deflections are predicted for the US-29 Bridge (simple span). Two cases were considered: equal exterior-to-interior girder load ratios and unequal exterior-to-interior girder load ratios.

Single girder line (SGL) analysis is utilized for the base prediction on which the simplified procedure predicts deflections. In this appendix, the girders are assumed to have constant cross-section and the SGL deflections are predicted for a prismatic beam with a uniformly distributed dead load, determined from tributary width assumptions.

Sample Calculations of the Simplified Procedure for the US-29 Bridge

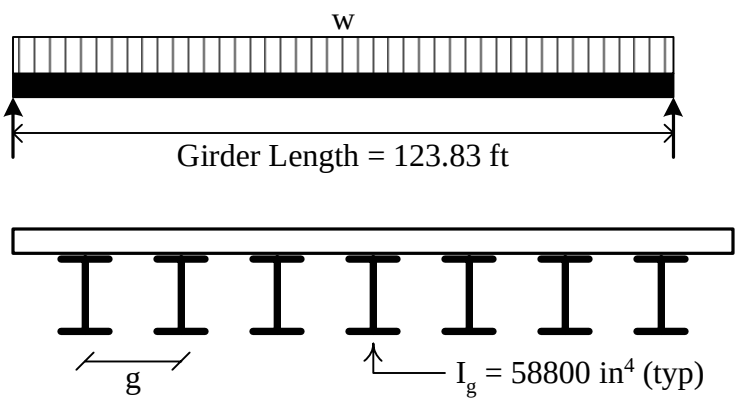

Given

Number of Girders = 7

Skew Angle = 46 degrees

Constant, E_s = 30,000 ksi

Girder Spacing, g = 7.75 ft

Interior girder load, w_i = 2 k/ft

Case I: Equal Exterior-to-Interior Girder Load Ratios, $w_1 = w_7 = 1.7$ k/ft

Case II: Unequal Exterior-to-Interior Girder Load Ratios, $w_1 = 1.7$ k/ft, $w_7 = 1.3$ k/ft

Case I Calculations

Equivalent Skew Offset: $\theta = |90 - skew| = |90 - 46| = 44$ **degrees**

Girder Spacing to Span Ratio: $S = g/L = 7.75/123.83 = 0.063$

½ Span: $$\delta_{SGL\_INT} = \frac{5wl^4}{384EI} = \frac{5(2)(123.83)^4}{384(1.225*10^7)} = 0.50\ ft = 6.00 \text{ in}$$

$$\delta_{EXT} = [\delta_{SGL\_INT} - \Phi(100 - L)][1 - 0.1\tan(1.2\theta)]$$

$$= [6.00 - 0.018(100 - 85)][1 - 0.1\tan(1.2*44)] = 4.93 \text{ in}$$

where: $\Phi = 0.03 - a(\theta) = 0.03 - 0.0002(44) = 0.018$

Note: $a = 0.0002 \quad (g \le 8.2\ ft)$

$$L = \frac{w_{EXT}}{w_{INT}} = \frac{1.7}{2.0} = 85\%$$

$$D_{INT} = x[\alpha(S - 0.04)(1 + z) - 0.1\tan(1.2\theta)]$$

$$= 1.0[1.94(0.063 - 0.04)(1 + 0.074) - 0.1\tan(1.2*44)] = -0.08 \text{ in}$$

where: $x = \delta_{SLG\_INT} / \delta_{SGL\_M} = 6.0/6.0 = 1.0$

Case I (cont.)

where: $\alpha = 3.0 - b(\theta) = 3.0 - .024(44) = 1.94$

Note: $b = -0.08 + 8(S - 0.05) = -0.08 + 8(0.063 - 0.05) = 0.021$

$(0.05 < S \le 0.08)$

$$z = (10(S - 0.04) + 0.02)(2 - L/50)$$

$$= (10(0.063 - 0.04) + 0.02)(2 - 85/50) = 0.074$$

¼ Span: $\delta_{SGL\_INT} = \dfrac{57wl^4}{6144EI} = \dfrac{57(2)(123.83)^4}{6144(1.225*10^7)} = 0.36\ ft = 4.27$ in

$\delta_{EXT} = [4.27 - 0.018(100 - 85)][1 - 0.1\tan(1.2*44)] = 3.43$ in

$D_{INT} = 0.71[1.94(0.063 - 0.04)(1 + 0.074) - 0.1\tan(1.2*44)] = -0.06$ in

where: $x = \delta_{SLG\_INT} / \delta_{SGL\_M} = 4.27/6.0 = 0.71$

Results (inches):

		G1	G2	G3	G4	G5	G6	G7
SGL	¼ Span	3.63	4.27	4.27	4.27	4.27	4.27	4.27
	½ Span	5.10	6.00	6.00	6.00	6.00	6.00	5.10
Simplified Procedure	¼ Span	3.43	3.37	3.32	3.32	3.32	3.37	3.43
	½ Span	4.93	4.85	4.77	4.77	4.77	4.85	4.93

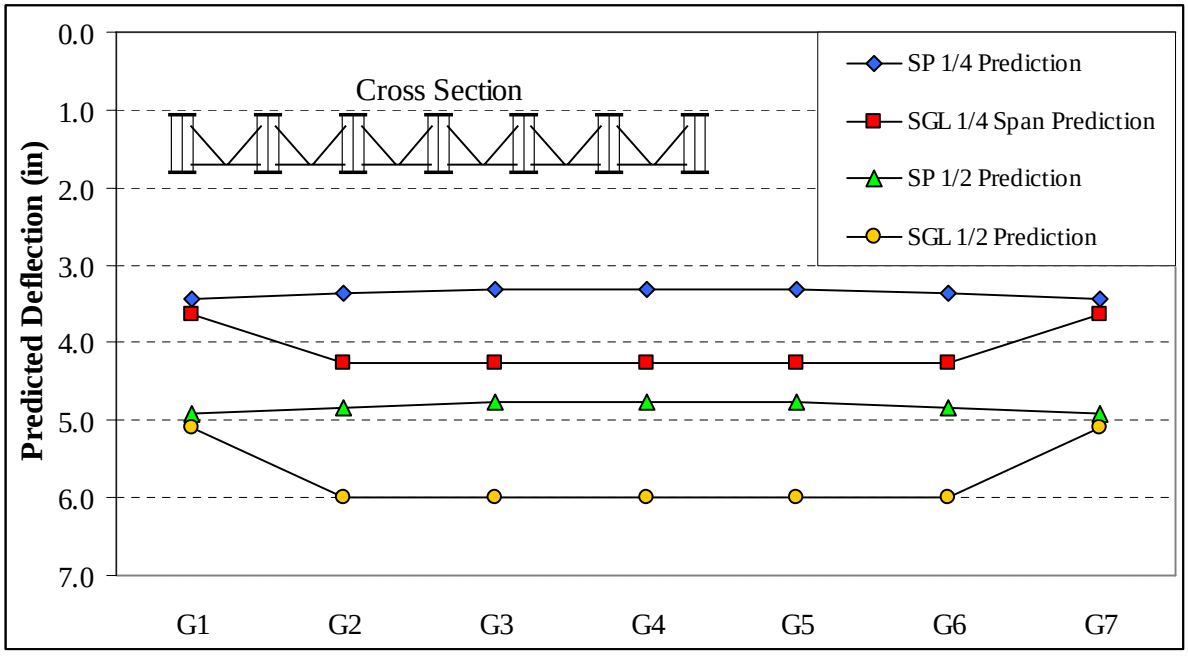

Case II (Midspan Only)

65% Load ('Light Load'):

$$\delta_{EXT} = [6.00 - 0.018(100 - 65)][1 - 0.1\tan(1.2 * 44)] = 4.57 \text{ in}$$

where: $$L = \frac{w_{EXT}}{w_{INT}} = \frac{1.3}{2.0} = 65\%$$

$$D_{INT} = 1.0[1.94(0.063 - 0.04)(1 + 0.172) - 0.1\tan(1.2 * 44)] = -0.08 \text{ in}$$

where: $$z = (10(0.063 - 0.04) + 0.02)(2 - {}^{65}\!/_{50}) = 0.172$$

Girder 4 Deflection (middle): $$\delta_4 = \delta_{EXT} + 2(D_{INT}) = 4.57 + 2(-0.08) = 4.41 \text{ in}$$

Recall, Girder 1 Deflection: $$\delta_1 = \delta_{EXT} = 4.93 \text{ in}$$ (from Case I)

Predict other girder deflections with straight line passing through δ_1 and δ_4

$$Slope = Differential = \frac{\delta_4 - \delta_1}{4 - 1} = \frac{4.41 - 4.93}{4 - 1} = -0.173$$

Results (inches):

	G1	G2	G3	G4	G5	G6	G7
SGL	5.10	6.00	6.00	6.00	6.00	6.00	3.90
ASP	4.93	4.76	4.58	4.41	4.24	4.06	3.89

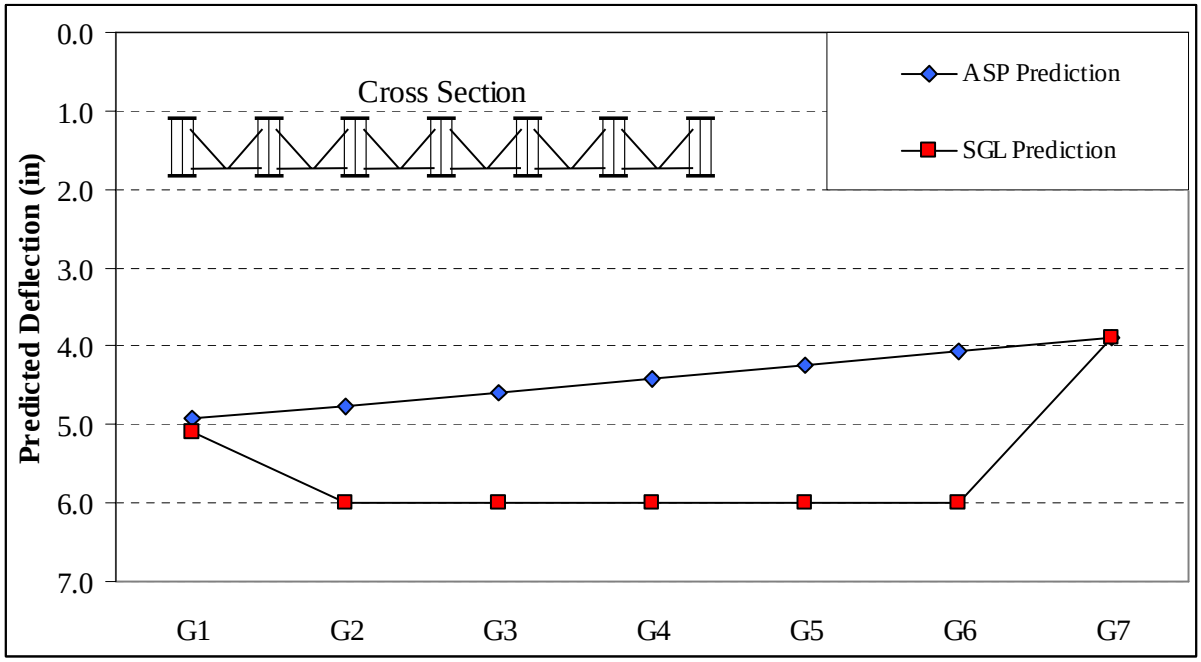

Appendix C

Deflection Summary for the Eno River Bridge

This appendix contains a detailed description of the Eno River Bridge including bridge geometry, material data, cross-frame type and size, and dead loads calculated from slab geometry. Tables and graphs of the field measured non-composite girder deflections are included.

A summary of the ANSYS finite element model created for the Eno River Bridge is also included in this appendix. This summary includes a picture of the ANSYS model, details about the elements used in the model generation, the loads applied to the model, and tables and graphs of the deflections predicted by the model.

FIELD MEASUREMENT SUMMARY

PROJECT NUMBER: U-2102 (Guess Road over Eno River, Stage 2)
MEASUREMENT DATE: February 28, 2003

BRIDGE DESCRIPTION

TYPE	One Span Simple	
LENGTH	236.02 ft (71.94 m)	
NUMBER OF GIRDERS	5	
GIRDER SPACING	9.65 ft (2.94 m)	
SKEW	90 deg	
OVERHANG	3.41 ft (G1)	(from web centerline)
BEARING TYPE	Pot Bearing	

MATERIAL DATA

STRUCTURAL STEEL	**Grade**	**Yield Strength**
Girder:	HPS70W (HPS485W)	70 ksi (485 MPa)
Other:	AASHTO M270	50 ksi (345 MPa)

CONCRETE UNIT WEIGHT	120 pcf (nominal)
	117 pcf (measured)
SIP FORM WEIGHT	3 psf (nominal)

GIRDER DATA

LENGTH	236.02 ft (71.94 m)
TOP FLANGE WIDTH	20.08 in (510 mm)
BOTTOM FLANGE WIDTH	22.84 in (580 mm)
WEB THICKNESS	0.55 in (14 mm)
WEB DEPTH	101.58 in (2580 mm)

FLANGES	**Thickness**	**Begin**	**End**
Top:	1.10 in (28 mm)	0.00	118.01 ft (35.97 m)
Bottom:	1.18 in (30 mm)	0.00	58.76 ft (17.91 m)
	1.97 in (50 mm)	58.76 ft (17.91 m)	118.01 ft (35.97 m)

STIFFENERS	
Longitudinal:	PL 0.63" × 6.30" (16 mm × 160 mm)
Bearing:	PL 1.10" × 11.02" (28 mm × 280 mm)
Intermediate:	PL 0.79" × NA (20 mm × NA, connector plate)
	PL 0.47" × 4.724" (12 mm × 120 mm)

CROSS-FRAME DATA

	Type	**Diagonals**	**Horizontals**
END	K	L 5×5×5/16	MC 12×31 (top)
			L 5×5×5/16 (bottom)
INTERMEDIATE	X	L 5×5×5/16	L 5×5×5/16 (bottom)

FIELD MEASUREMENT SUMMARY

Project Number: U-2102 (Guess Road over Eno River, Stage 2)
Measurement Date: February 28, 2003

Girder Centerline:

Measurement Location:

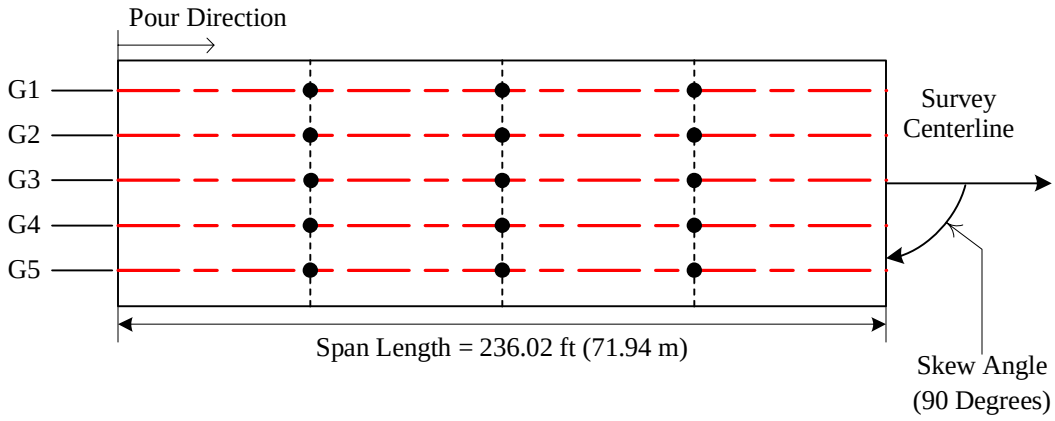

(a) Plan View (Not to Scale)

Girder:

String Pots:

Expansion Support:

Fixed Support:

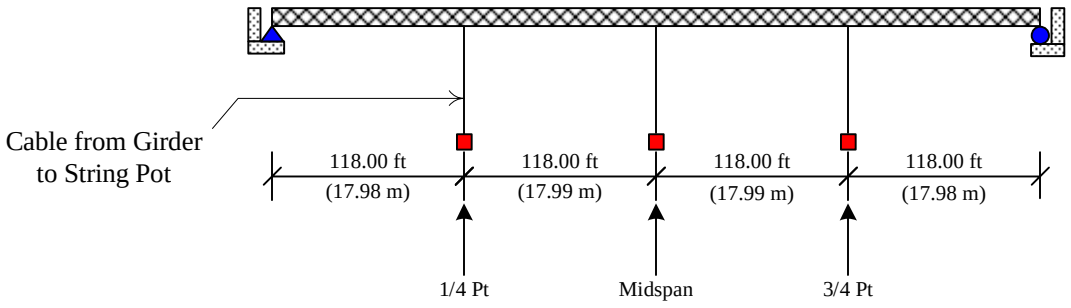

(b) Elevation View (Not to Scale)

Plan and Elevation View of the Eno Bridge (Durham, NC)

FIELD MEASUREMENT SUMMARY

PROJECT NUMBER: U-2102 (Guess Road over Eno River, Stage 2)
MEASUREMENT DATE: February 28, 2003

DECK LOADS

	Concrete*		Deck Slab**		Ratio
Girder	**lb/ft**	**N/mm**	**lb/ft**	**N/mm**	
G1	770.19	11.24	891.47	13.01	0.86
G2	814.04	11.88	992.20	14.48	0.82
G3	803.76	11.73	992.20	14.48	0.81
G4	848.99	12.39	992.20	14.48	0.86
G5	604.36	8.82	670.83	9.79	0.90

*calculated with measured slab thicknesses
**includes slab, buildups, and stay-in-place forms (nominal)

SLAB DATA

THICKNESS 9.06 in (nominal)

BUILD-UP 2.95 in (nominal)

REBAR	**Size**	**Spacing**
LONGITUDINAL	(metric)	(nominal)
Top:	#13	460 mm
Bottom:	#16	220 mm
TRANSVERSE		
Top:	#16	150 mm
Bottom:	#16	150 mm

GIRDER DEFLECTIONS (data in inches, full span concrete deflections less bearing settlement)

MEASURED

	1/4 Span Loading			1/2 Span Loading		
Point	**1/4**	**1/2**	**3/4**	**1/4**	**1/2**	**3/4**
G1	0.96	0.63	0.66	3.00	2.95	2.44
G2	0.91	0.56	0.59	2.74	2.58	2.21
G3	0.87	0.43	0.56	2.51	2.18	2.01
G4	0.82	0.35	0.55	2.29	1.67	1.83
G5	0.76	0.41	0.50	2.05	1.61	1.61
	3/4 Span Loading			**Full Span Loading**		
Point	**1/4**	**1/2**	**3/4**	**1/4**	**1/2**	**3/4**
G1	5.53	6.34	5.56	5.91	6.94	6.01
G2	5.22	5.83	5.04	5.57	6.41	5.64
G3	4.90	5.36	4.72	5.23	5.88	5.28
G4	4.61	4.61	4.46	4.93	5.14	4.98
G5	4.26	4.38	4.14	4.54	4.89	4.57

MEASURED BEARING

	Total Settlement		
Point	**End 1**	**End 2**	**Avg.**
G1	0.07	0.11	0.09
G2	0.09	0.12	0.11
G3	0.08	0.14	0.11
G4	0.07	0.11	0.09
G5	0.07	0.18	0.12

PREDICTED AND SURVEYED

	Original			Revision		
Point	**1/4**	**1/2**	**3/4**	**1/4**	**1/2**	**3/4**
G1	---	10.00	---	---	9.65	---
G2	---	11.10	---	---	9.25	---
G3	---	11.10	---	---	8.74	---
G4	---	11.10	---	---	8.27	---
G5	---	7.52	---	---	7.52	---
	Adjusted Revision* **			**Surveyed**		
Point	**1/4**	**1/2**	**3/4**	**1/4**	**1/2**	**3/4**
G1	---	8.33	---	5.62	7.71	5.70
G2	---	7.59	---	3.36	6.82	4.70
G3	---	7.08	---	4.85	7.01	4.57
G4	---	7.07	---	5.14	7.19	4.91
G5	---	6.77	---	3.50	6.73	3.50

***predicted revision multiplied by the ratio of deck concrete to total slab weigh

FIELD MEASUREMENT SUMMARY

PROJECT NUMBER: U-2102 (Guess Road over Eno River, Stage 2)
MEASUREMENT DATE: February 28, 2003

GIRDER DEFLECTIONS
CROSS SECTION VIEW

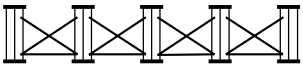

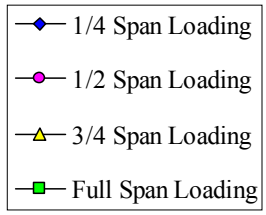

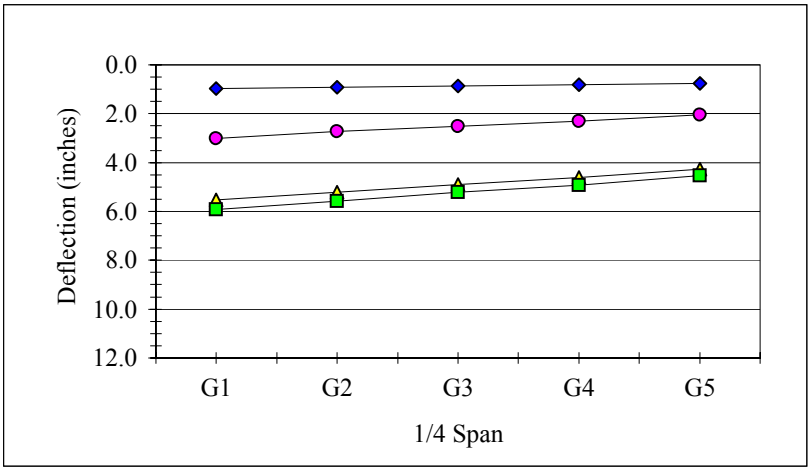

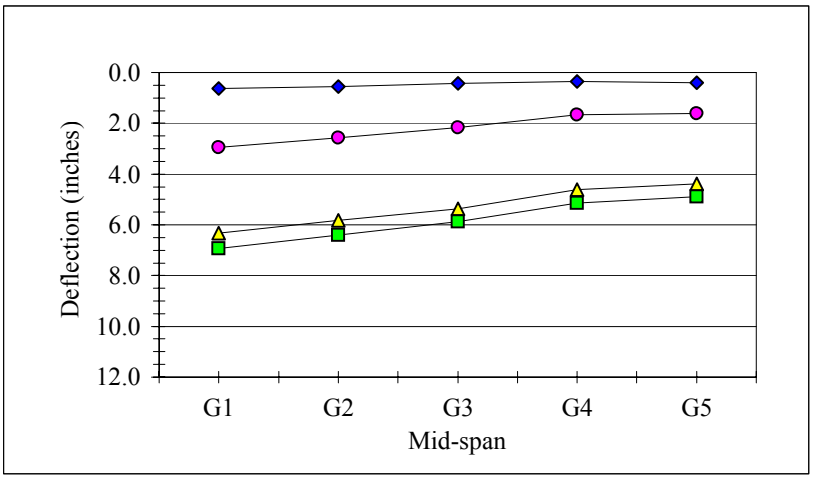

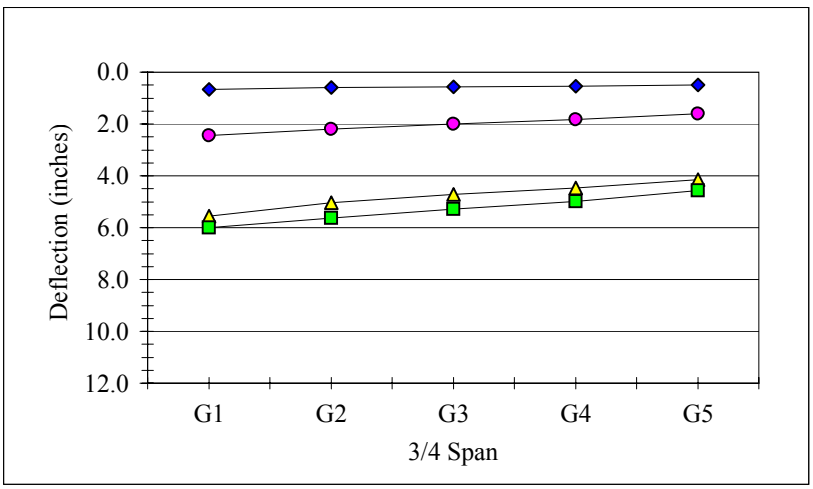

FIELD MEASUREMENT SUMMARY

PROJECT NUMBER: U-2102 (Guess Road over Eno River, Stage 2)
MEASUREMENT DATE: February 28, 2003

SLAB THICKNESS
CROSS SECTION VIEW

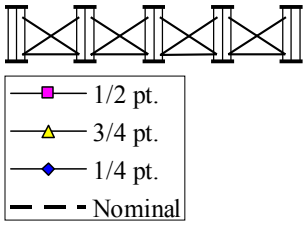

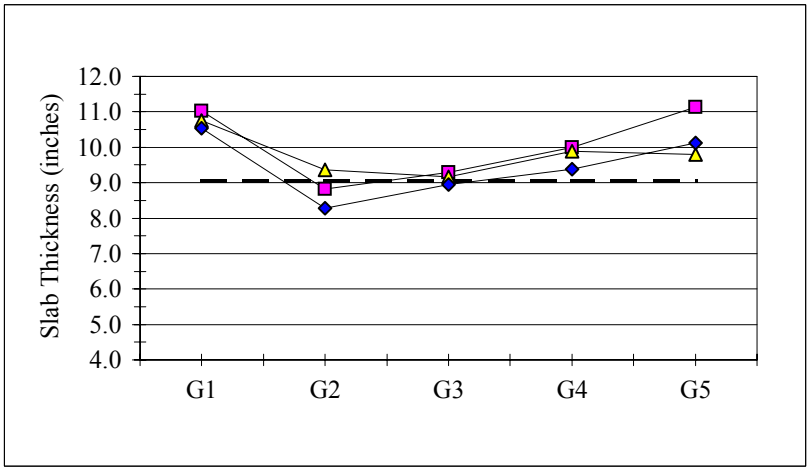

*GIRDER DEFLECTIONS
ELEVATION VIEW

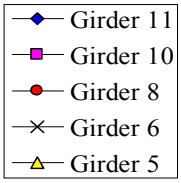

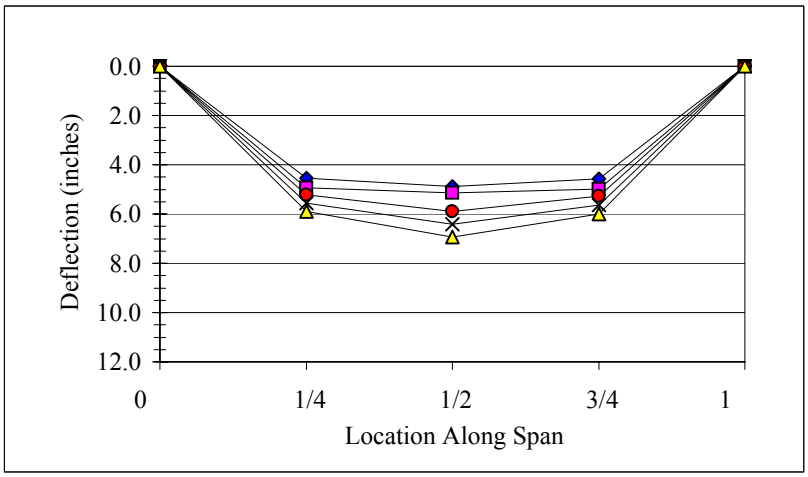

GIRDER DEFLECTIONS
CROSS SECTION VIEW

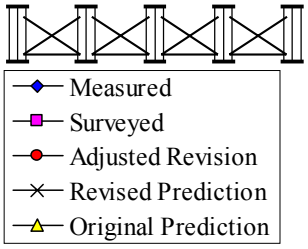

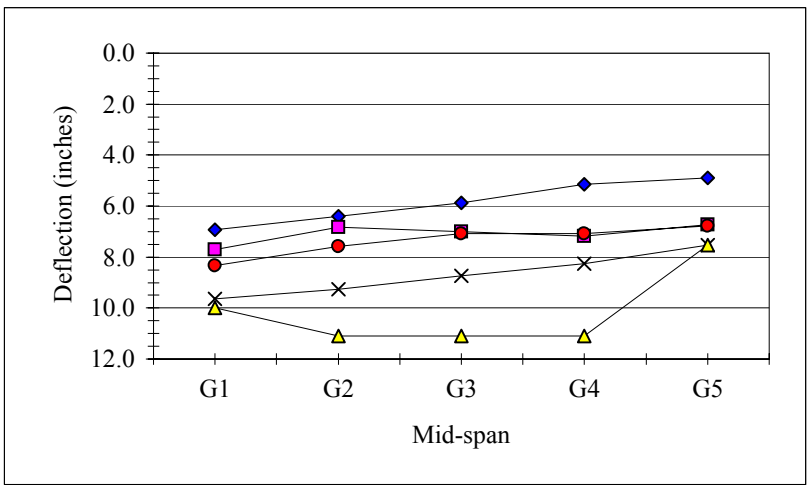

ANSYS FINITE ELEMENT MODELING SUMMARY

PROJECT NUMBER: U-2102 (Guess Road over Eno River, Stage 2)

MODEL PICTURE (Steel only, oblique view)

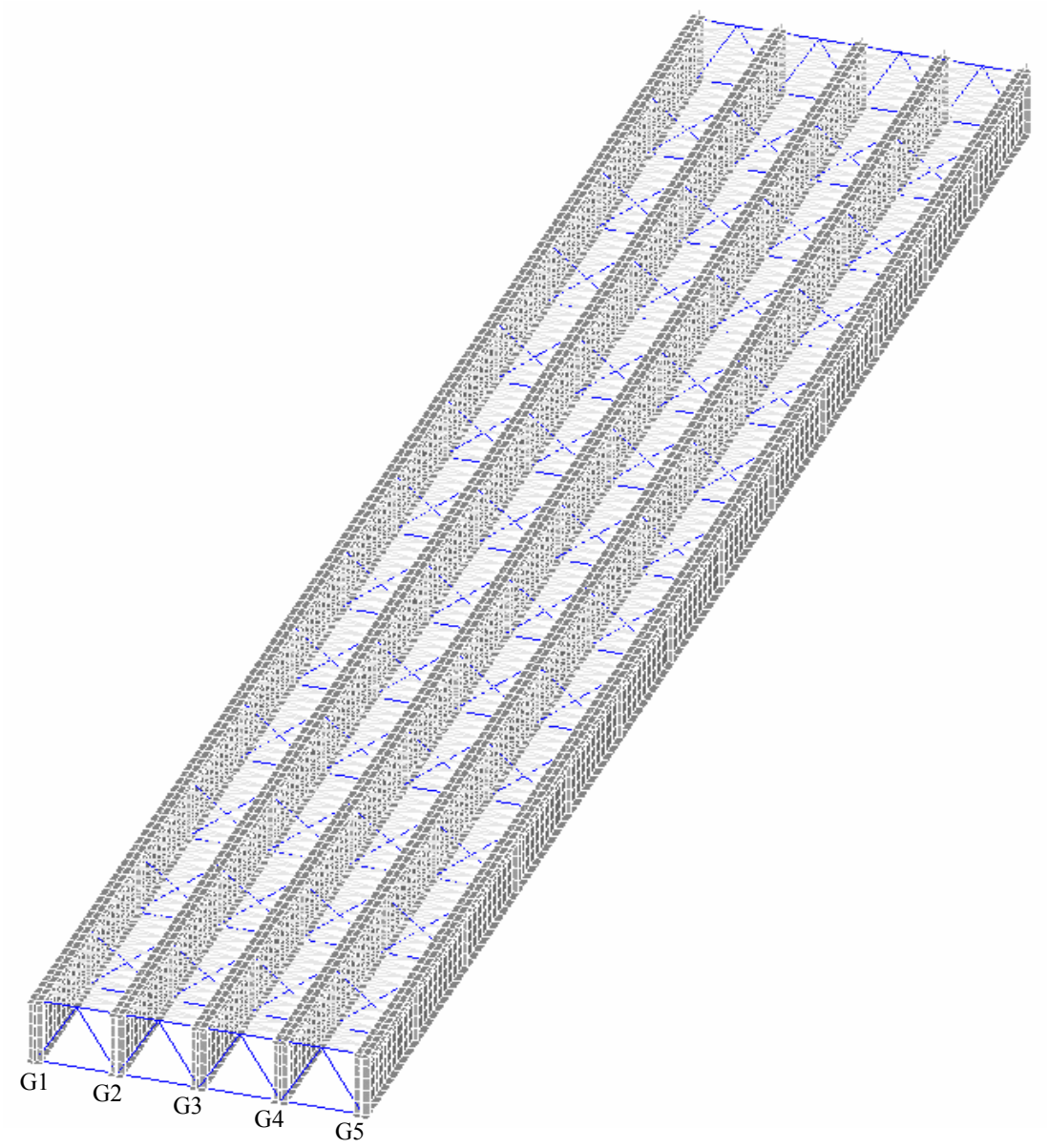

ANSYS FINITE ELEMENT MODELING SUMMARY

PROJECT NUMBER: U-2102 (Guess Road over Eno River, Stage 2)

MODEL DESCRIPTION

COMPONENT	**Element Type**
Girder:	SHELL93
Connector Plates:	SHELL93
Stiffener Plates:	SHELL93
Cross-frame Members:	LINK8 (diagonal)
	LINK8 (horizontal)
End Diaphragm:	LINK8 (diagonal)
	BEAM4 (diagonal)
Stay-in-place Deck Forms:	LINK8
Concrete Slab:	SHELL63
Shear Studs:	MPC184

APPLIED LOADS

Girder	*Load	
	lb/ft	N/mm
G1	770.19	11.24
G2	814.04	11.88
G3	803.76	11.73
G4	848.99	12.39
G5	604.36	8.82

*applied as a uniform pressure to area of top flange

GIRDER DEFLECTIONS

	ANSYS (load step 1)			ANSYS (load step 2)		
Point	**1/4**	**1/2**	**3/4**	**1/4**	**1/2**	**3/4**
G1	1.10	**1.27**	0.79	2.41	**3.21**	2.11
G2	1.07	**1.23**	0.77	2.33	**3.10**	2.03
G3	1.03	**1.19**	0.74	2.25	**3.00**	1.96
G4	1.00	**1.14**	0.72	2.17	**2.89**	1.89
G5	0.96	**1.10**	0.69	2.09	**2.78**	1.82
	ANSYS (load step 3)			**ANSYS (load step 4)**		
Point	**1/4**	**1/2**	**3/4**	**1/4**	**1/2**	**3/4**
G1	2.08	**3.20**	2.41	0.76	**1.24**	1.09
G2	2.02	**3.09**	2.33	0.73	**1.20**	1.05
G3	1.95	**2.99**	2.25	0.71	**1.16**	1.02
G4	1.89	**2.89**	2.17	0.69	**1.12**	0.98
G5	1.82	**2.78**	2.09	0.67	**1.08**	0.94
	***Adjusted Measured			ANSYS (no SIP)		
Point	**1/4**	**1/2**	**3/4**	**1/4**	**1/2**	**3/4**
G1	5.91	**8.33**	6.01	6.42	**8.98**	6.42
G2	5.57	**7.83**	5.64	6.22	**8.70**	6.23
G3	5.23	**7.34**	5.28	6.01	**8.40**	6.01
G4	4.93	**6.92**	4.98	5.78	**8.07**	5.78
G5	4.54	**6.36**	4.57	5.51	**7.71**	5.51
	ANSYS (SIP)			****ANSYS (p.c., SIP)		
Point	**1/4**	**1/2**	**3/4**	**1/4**	**1/2**	**3/4**
G1	6.42	**8.98**	6.43	6.35	**8.92**	6.39
G2	6.20	**8.67**	6.21	6.15	**8.62**	6.18
G3	5.99	**8.37**	5.99	5.95	**8.33**	5.97
G4	5.78	**8.06**	5.77	5.74	**8.04**	5.76
G5	5.56	**7.76**	5.55	5.54	**7.75**	5.54

***For mid-span only, calculated by dividing ANSYS (SIP) by average ratio of ANSYS (SIP)/Measured Deflections (see above)

****superimposed from load steps 1-4 for partial composite action

RATIOS

	ANSYS (SIP)/Measured		
Point	**1/4**	****1/2**	**3/4**
G1	1.09	1.08	1.07
G2	1.11	1.11	1.10
G3	1.15	1.14	1.13
G4	1.17	1.17	1.16
G5	1.22	1.22	1.21

**avg. of 1/4 and 3/4

ANSYS FINITE ELEMENT MODELING SUMMARY

PROJECT NUMBER: U-2102 (Guess Road over Eno River, Stage 2)

*GIRDER DEFLECTIONS
CROSS SECTION VIEW

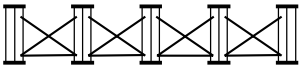

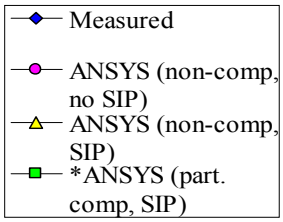

*using adjusted mid-span deflections (see page B-7)

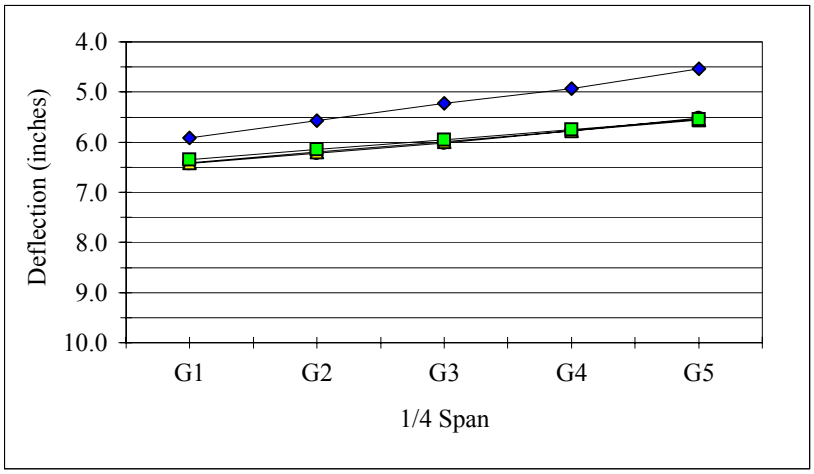

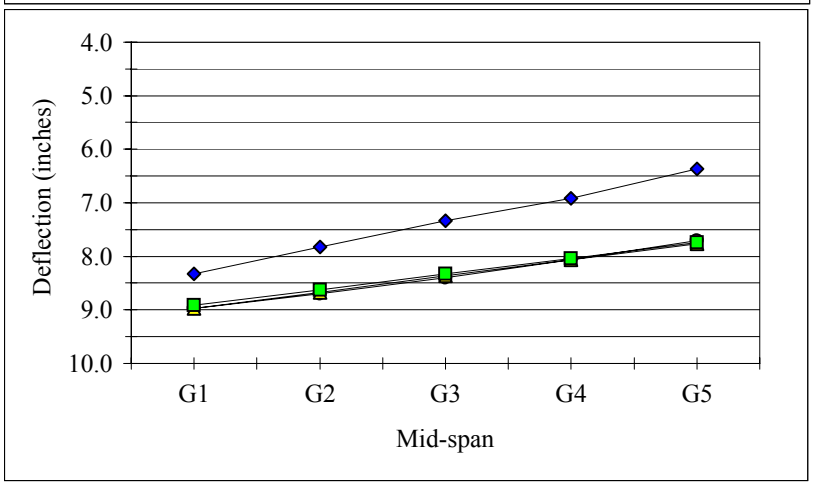

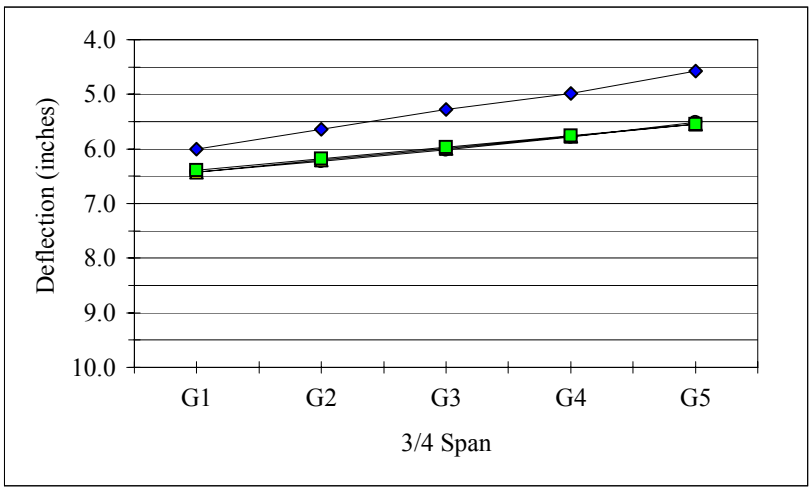

SAP 2000 MODELING SUMMARY

PROJECT NUMBER: U-2102 (Guess Road over Eno River, Stage 2)

MODEL PICTURE (Steel only, isometric view)

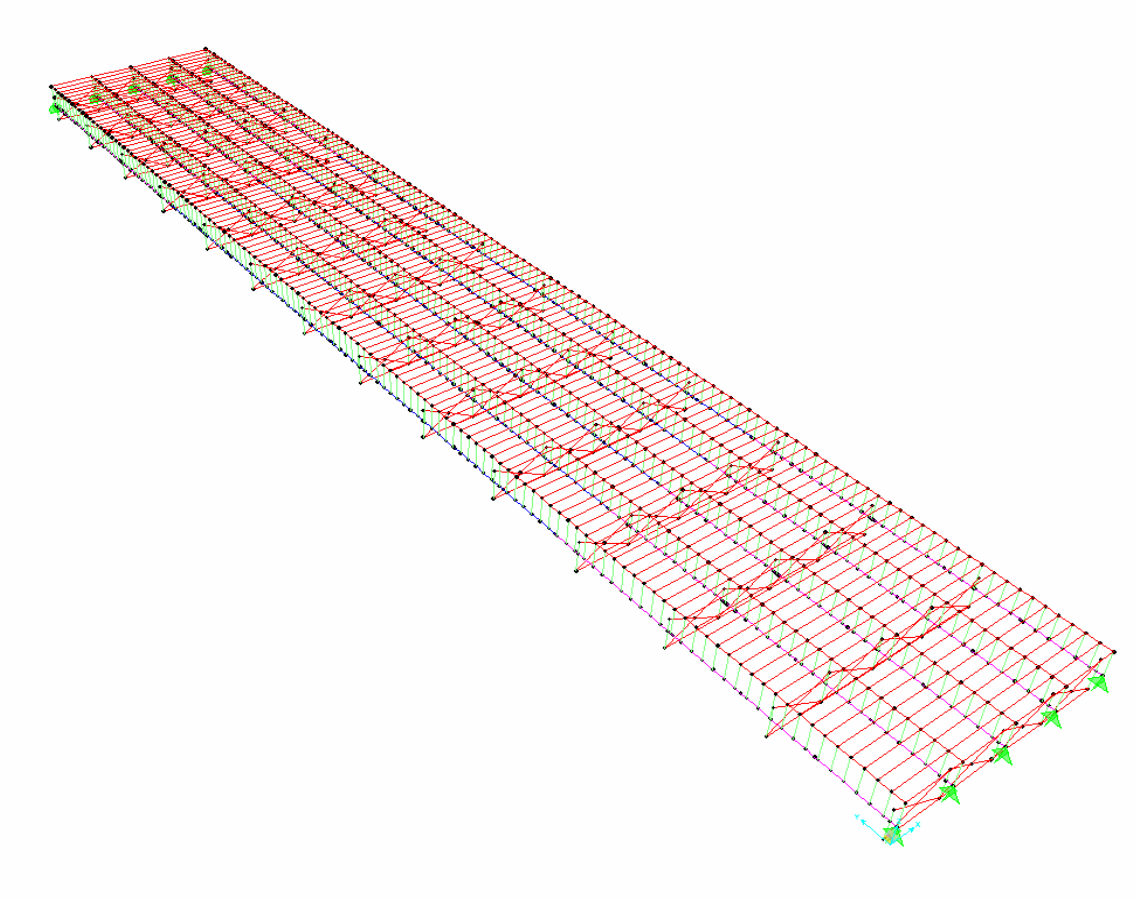

SAP2000 MODELING SUMMARY

PROJECT NUMBER: U-2102 (Guess Road over Eno River, Stage 2)

MODEL DESCRIPTION

COMPONENT	**Element Type**
Girder:	Frame Element
Cross Frame Members:	Frame Element
Stay-in-Place Deck Forms:	Area Element* (Shell Element)
	Frame Element
Rigid Link:	Frame Element

* See Shell Properties in Appendix F

GIRDER DEFLECTIONS

SAP				**Single Girder Line**		
Point	**1/4**	**1/2**	**3/4**	**1/4**	**1/2**	**3/4**
G1	6.94	9.64	6.94	6.49	9.00	6.49
G2	6.74	9.35	6.74	6.86	9.52	6.86
G3	6.51	9.03	6.51	6.77	9.40	6.77
G4	6.24	8.66	6.24	7.15	9.93	7.15
G5	5.94	8.26	5.94	5.09	7.07	5.09
SAP (Shell SIP)				**ANSYS (SIP)**		
Point	**1/4**	**1/2**	**3/4**	**1/4**	**1/2**	**3/4**
G1	6.97	9.66	6.96	6.42	8.98	6.43
G2	6.71	9.30	6.72	6.20	8.67	6.21
G3	6.44	8.92	6.46	5.99	8.37	5.99
G4	6.14	8.53	6.18	5.78	8.06	5.77
G5	5.83	8.11	5.87	5.56	7.76	5.55

SAP (Frame SIP)			
Point	**1/4**	**1/2**	**3/4**
G1	6.96	9.66	6.95
G2	6.70	9.30	6.72
G3	6.43	8.92	6.48
G4	6.14	8.53	6.24
G5	5.84	8.11	5.99

SAP 2000 MODELING SUMMARY

PROJECT NUMBER: U-2102 (Guess Road over Eno River, Stage 2)

*GIRDER DEFLECTIONS
CROSS SECTION VIEW

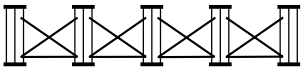

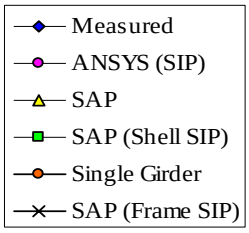

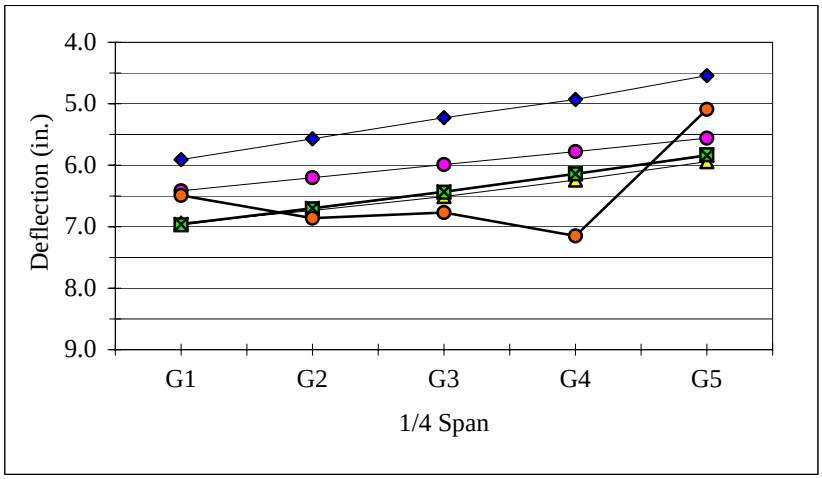

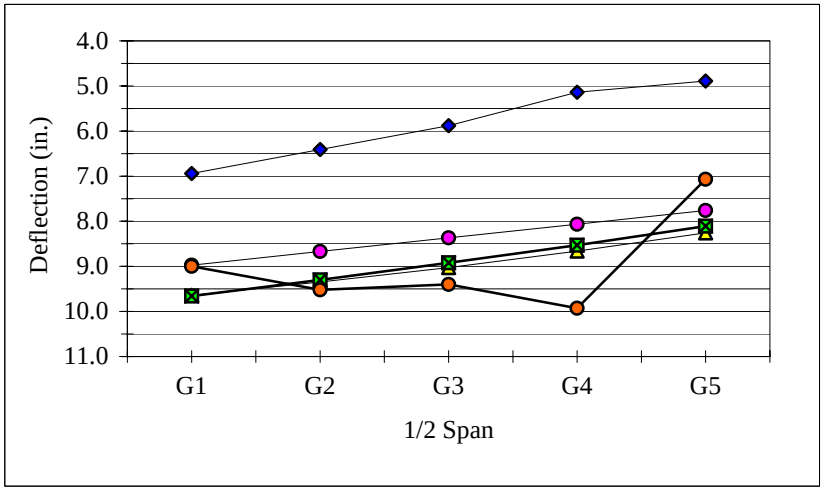

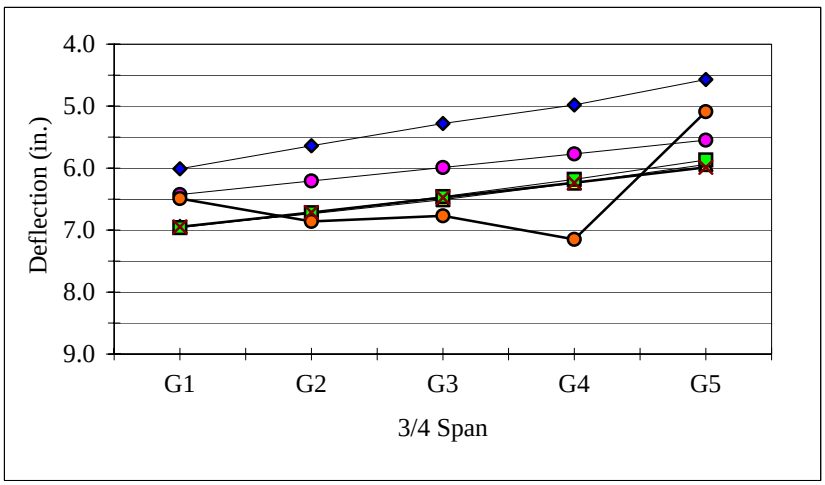

Appendix D

Deflection Summary for Bridge 8

This appendix contains a detailed description of Bridge 8 including bridge geometry, material data, cross frame type and size, and dead loads calculated from slab geometry. Illustrations detailing the bridge geometry and field measurement locations are included, along with tables and graphs of the field measured non-composite girder deflections.

A summary of the ANSYS finite element model created for Bridge 8 is also included in this appendix. This summary includes a picture of the ANSYS model, details about the elements used in the model generation, the loads applied to the model, and tables and graphs of the deflections predicted by the model.

FIELD MEASUREMENT SUMMARY

PROJECT NUMBER: R-2547 (EB Bridge on US 64 Bypass over Smithfield Rd.)
MEASUREMENT DATE: August 24, 2004

BRIDGE DESCRIPTION

TYPE	One Span Simple	
LENGTH	153.04 ft (46.648 m)	
NUMBER OF GIRDERS	6	
GIRDER SPACING	11.29 ft (3.440 m)	
SKEW	60 deg	
OVERHANG	2.85 ft (870 mm)	(from web centerline)
BEARING TYPE	Elastomeric Pad	

MATERIAL DATA

STRUCTURAL STEEL	**Grade**	**Yield Strength**
Girder:	AASHTO M270	50 ksi (345 MPa)
Other:	AASHTO M270	50 ksi (345 MPa)

CONCRETE UNIT WEIGHT	150 pcf (nominal)
SIP FORM WEIGHT	4.69 psf (CSI Catalog)

GIRDER DATA

LENGTH	153.04 ft (46.648 m)
WEB THICKNESS	0.63 in (16 mm)
WEB DEPTH	68.03 in (1728 mm)
TOP FLANGE WIDTH	17.99 in (457 mm)
BOTTOM FLANGE WIDTH	17.99 in (457 mm)

	Flange Thickness	**Begin**	**End**
Top:	2.00 in (51 mm)	0.00	153.04 ft (46.648 m)
Bottom:	2.00 in (51 mm)	0.00	40.98 ft (12.490 m)
	3.00 in (76 mm)	40.98 ft (12.490 m)	112.07 ft (34.158 m)
	2.00 in (51 mm)	112.07 ft (34.158 m)	153.04 ft (46.648 m)

CROSS-FRAME DATA

	Diagonals	**Horizontals**	**Verticals**
END BENT (Type K)	WT 4 x 14	C 15 x 33.9 (top) WT 4 x 14 (bottom)	NA
MIDDLE BENT	NA	NA	NA
INTERMEDIATE (Type X)	L 3 x 3 x 3/8"	L 3 x 3 x 3/8" (bottom)	NA

FIELD MEASUREMENT SUMMARY

PROJECT NUMBER: R-2547 (EB Bridge on US 64 Bypass over Smithfield Rd.)
MEASUREMENT DATE: August 24, 2004

STIFFENERS

Longitudinal:	NA
Bearing:	PL 0.87" × 7.09" (22 mm × 180 mm)
Intermediate:	PL 0.63" × NA (16 mm × NA, connector plate)
	No Intermediate Siffeners
Middle Bearing:	NA
End Bent Connector:	PL 0.87" × NA (22 mm × NA, connector plate)

SLAB DATA

THICKNESS	9.25 in (235 mm)	nominal
BUILD-UP	3.74 in (95 mm)	nominal
LONGITUDINAL REBAR	SIZE (metric)	SPACING (nominal)
Top:	#13	17.72 in (450 mm)
Bottom:	#16	8.27 in (210 mm)
TRANSVERSE REBAR		
Top:	#16	5.51 in (140 mm)
Bottom:	#16	5.51 in (140 mm)

DECK LOADS

Girder	Concrete[1]		Slab[2]		Ratio
	lb/ft	N/mm	lb/ft	N/mm	
G1	1186.80	17.32	1256.69	18.34	0.94
G2	1414.97	20.65	1517.76	22.15	0.93
G3	1414.97	20.65	1517.76	22.15	0.93
G4	1414.97	20.65	1517.76	22.15	0.93
G5	1414.97	20.65	1517.76	22.15	0.93
G6	1186.80	17.32	1256.69	18.34	0.94

[1] Calculated with nominal slab thicknesses

[2] Includes slab, buildups, and stay-in-place forms (nominal)

FIELD MEASUREMENT SUMMARY

Project Number: R-2547 (EB Bridge on US 64 Bypass over Smithfield Rd.)
Measurement Date: August 24, 2004

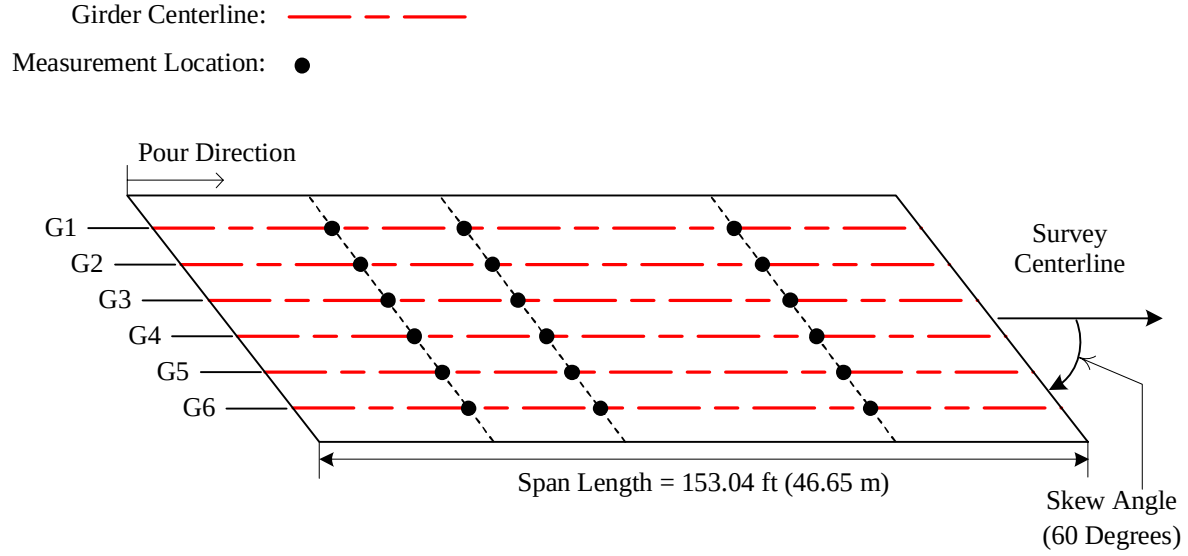

(a) Plan View (Not to Scale)

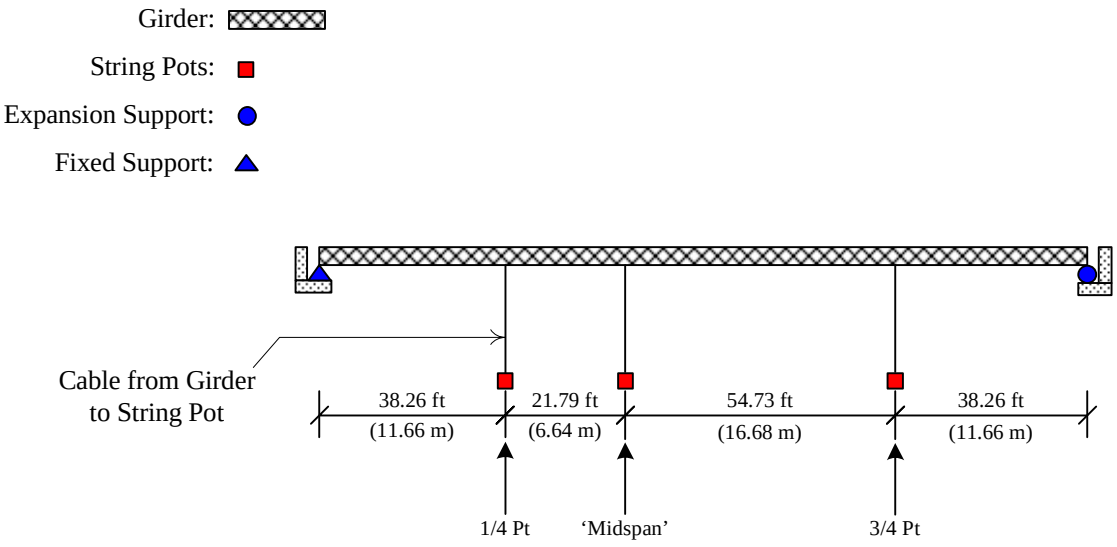

(b) Elevation View (Not to Scale)

Plan and Elevation View of Bridge 8 (Knightdale, NC)

FIELD MEASUREMENT SUMMARY

PROJECT NUMBER: R-2547 (EB Bridge on US 64 Bypass over Smithfield Rd.)
MEASUREMENT DATE: August 24, 2004

BEARING SETTLEMENTS (data in inches)

	Pour 1 Settlement		
Point	**End 1**	**End 2**	**Avg.**
G1	0.09	0.10	0.09
G2	0.13	0.11	0.12
G3	---	0.12	0.12
G4	0.04	0.04	0.04
G5	0.07	0.09	0.08
G6	0.08	0.10	0.09

GIRDER DEFLECTIONS (data in inches)
MEASURED

	1/4 Span Loading			Midspan[3] Loading		
Point	**1/4**	**Midspan**	**3/4**	**1/4**	**Midspan**	**3/4**
G1	0.50	0.45	0.28	1.22	1.44	0.98
G2	0.49	0.64	0.29	1.16	1.49	0.95
G3	0.59	0.68	0.26	1.21	1.43	0.85
G4	0.57	0.75	0.32	1.11	1.36	0.97
G5	0.60	0.82	0.32	1.07	1.35	0.87
G6	0.62	0.81	0.34	1.02	1.31	0.86
	3/4 Span Loading			**Full Span Loading**		
Point	**1/4**	**Midspan**	**3/4**	**1/4**	**Midspan**	**3/4**
G1	2.15	2.75	2.24	2.29	2.89	2.38
G2	2.19	2.94	2.19	2.35	3.14	2.40
G3	2.25	2.94	2.09	2.43	3.17	2.34
G4	2.24	3.02	2.22	2.42	3.26	2.49
G5	2.26	3.05	2.13	2.43	3.30	2.42
G6	2.23	3.03	2.17	2.34	3.24	2.45

[3] Midspan measurement location was 5.02 m offset from actual midspan.

PREDICTIONS[4] (Single Girder-Line Model in SAP 2000)

Point	**1/4**	**Midspan**	**3/4**
G1	3.01	4.03	3.01
G2	3.59	4.81	3.59
G3	3.59	4.81	3.59
G4	3.59	4.81	3.59
G5	3.59	4.81	3.59
G6	3.01	4.03	3.01

[4] Using nominal slab thicknesses

FIELD MEASUREMENT SUMMARY

PROJECT NUMBER: R-2547 (EB Bridge on US 64 Bypass over Smithfield Rd.)
MEASUREMENT DATE: August 24, 2004

GIRDER DEFLECTIONS
CROSS SECTION VIEW

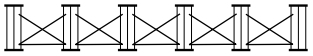

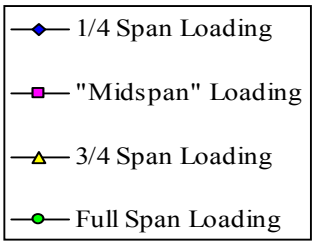

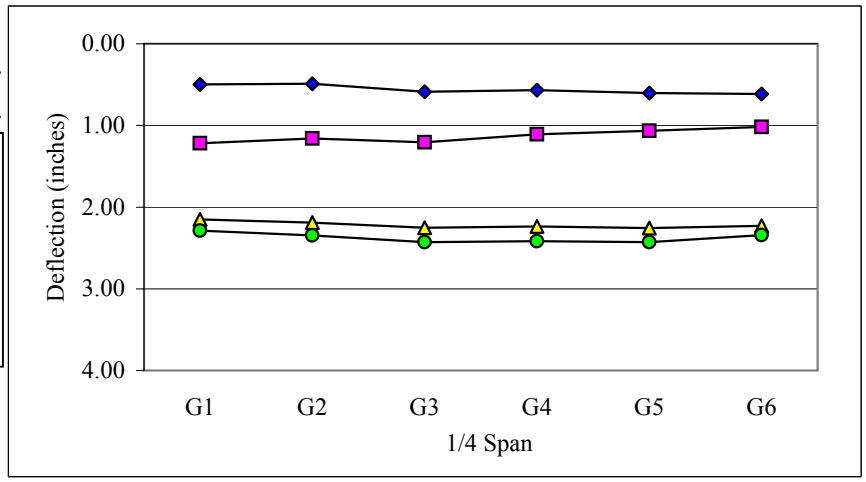

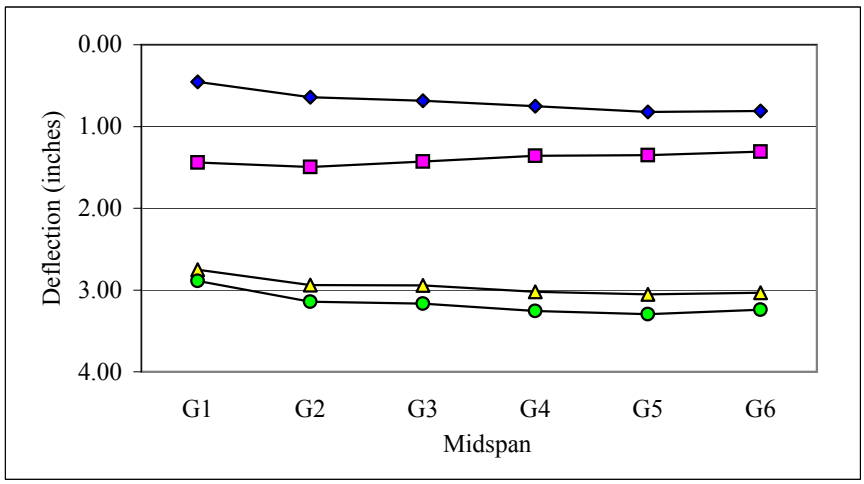

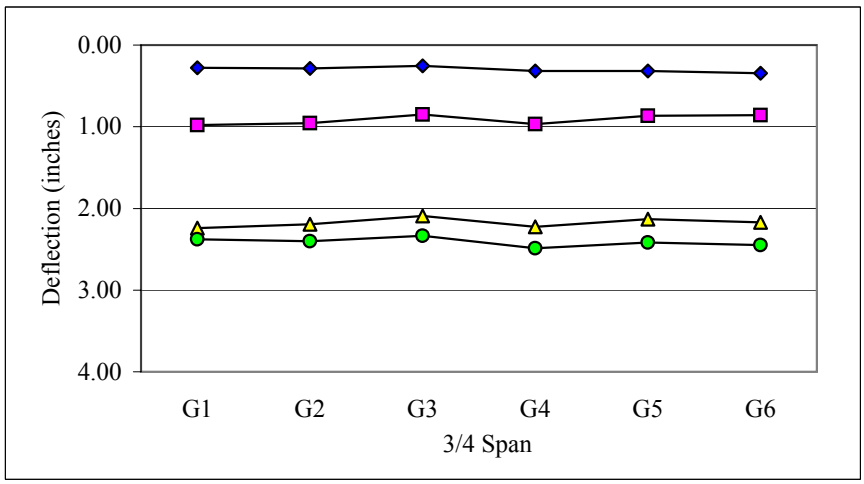

FIELD MEASUREMENT SUMMARY

PROJECT NUMBER: R-2547 (EB Bridge on US 64 Bypass over Smithfield Rd.)
MEASUREMENT DATE: August 24, 2004

GIRDER DEFLECTIONS
CROSS SECTION VIEW

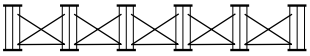

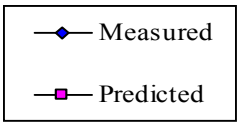

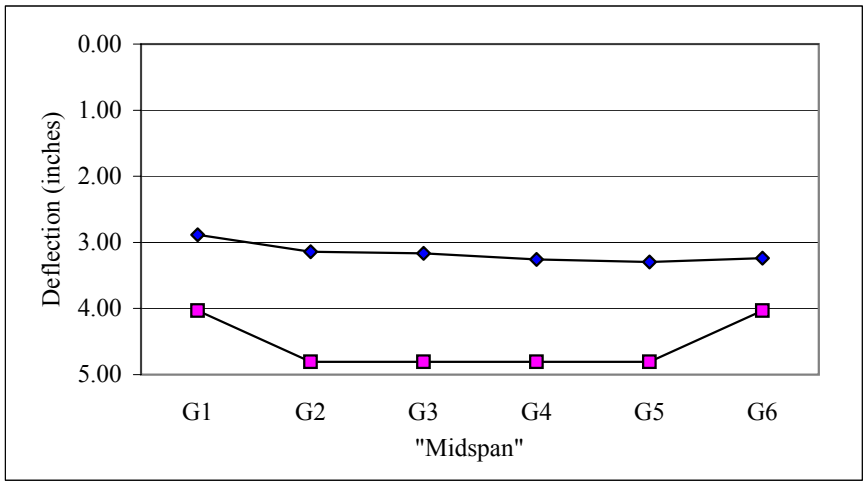

GIRDER DEFLECTIONS
ELEVATION VIEW

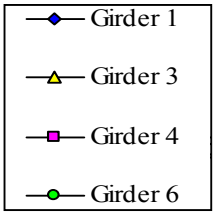

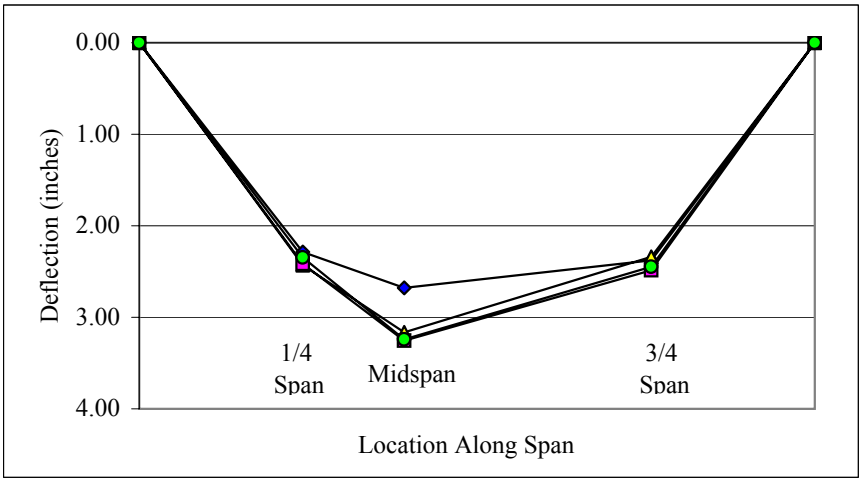

ANSYS FINITE ELEMENT MODELING SUMMARY

PROJECT NUMBER: R-2547 (EB Bridge on US 64 Bypass over Smithfield Rd.)

MODEL PICTURE: (Steel Only, Oblique View)

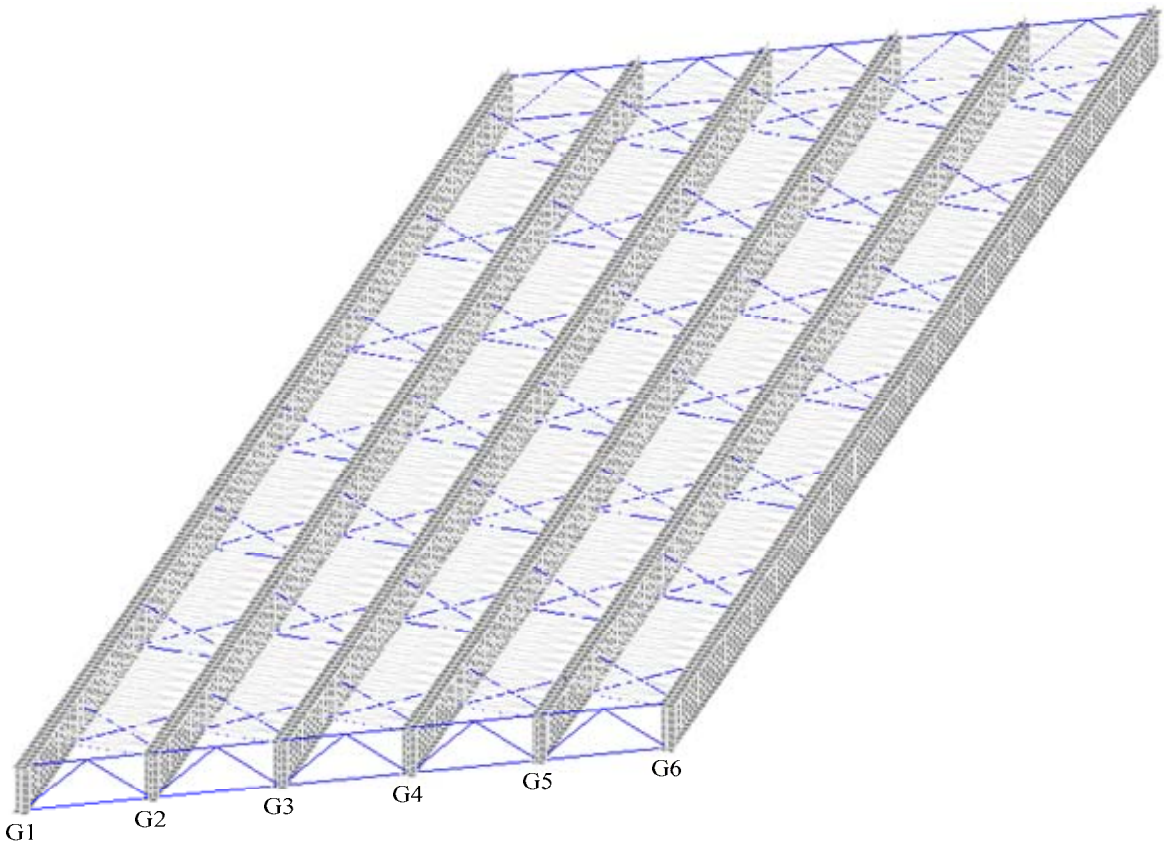

ANSYS FINITE ELEMENT MODELING SUMMARY

PROJECT NUMBER: R-2547 (EB Bridge on US 64 Bypass over Smithfield Rd.)

MODEL DESCRIPTION

COMPONENT	**Element Type**
Girder:	SHELL93
Connector Plates:	SHELL93
Stiffener Plates:	SHELL93
Cross-frame Members:	LINK8 (diagonal)
	LINK8 (horizontal)
End Diaphragm:	BEAM4 (horizontal)
	LINK8 (diagonal)
Stay-in-place Deck Forms:	LINK8
Concrete Slab:	SHELL63
Shear Studs:	MPC184

APPLIED LOADS

Girder	*Load	
	lb/ft	N/mm
G1	1186.80	17.32
G2	1414.97	20.65
G3	1414.97	20.65
G4	1414.97	20.65
G5	1414.97	20.65
G6	1186.80	17.32

*applied as a uniform pressure to area of top flange

GIRDER DEFLECTIONS

	ANSYS			ANSYS (SIP)		
Point	**1/4**	**Midspan**	**3/4**	**1/4**	**Midspan**	**3/4**
G1	2.94	3.98	2.94	3.03	4.11	3.04
G2	3.07	4.16	3.09	3.06	4.14	3.07
G3	3.16	4.28	3.17	3.08	4.17	3.09
G4	3.17	4.29	3.16	3.09	4.17	3.08
G5	3.09	4.17	3.07	3.06	4.14	3.05
G6	2.95	3.99	2.94	3.04	4.11	3.02
	Measured			**Predicted**		
Point	**1/4**	**Midspan**	**3/4**	**1/4**	**Midspan**	**3/4**
G1	2.29	2.89	2.38	3.01	4.03	3.01
G2	2.35	3.14	2.40	3.59	4.81	3.59
G3	2.43	3.17	2.34	3.59	4.81	3.59
G4	2.42	3.26	2.49	3.59	4.81	3.59
G5	2.43	3.30	2.42	3.59	4.81	3.59
G6	2.34	3.24	2.45	3.01	4.03	3.01

ANSYS FINITE ELEMENT MODELING SUMMARY

PROJECT NUMBER: R-2547 (EB Bridge on US 64 Bypass over Smithfield Rd.)

GIRDER DEFLECTIONS
CROSS SECTION VIEW

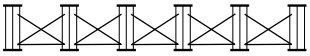

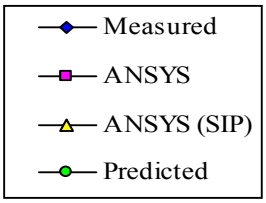

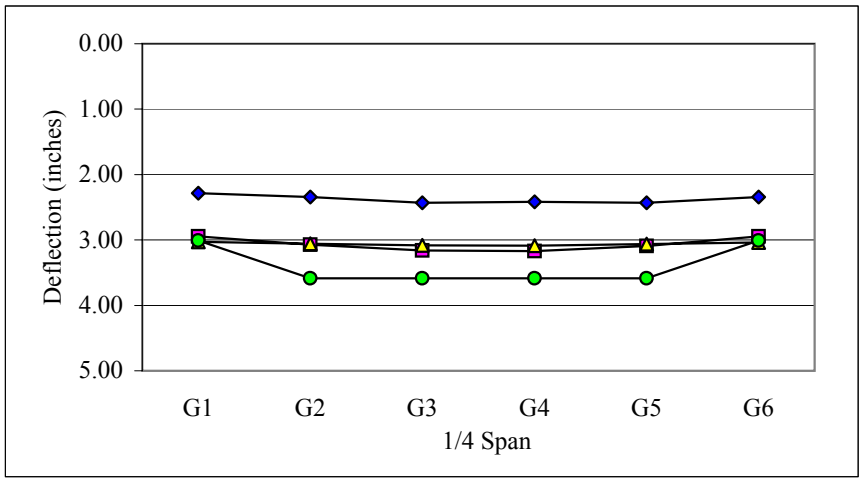

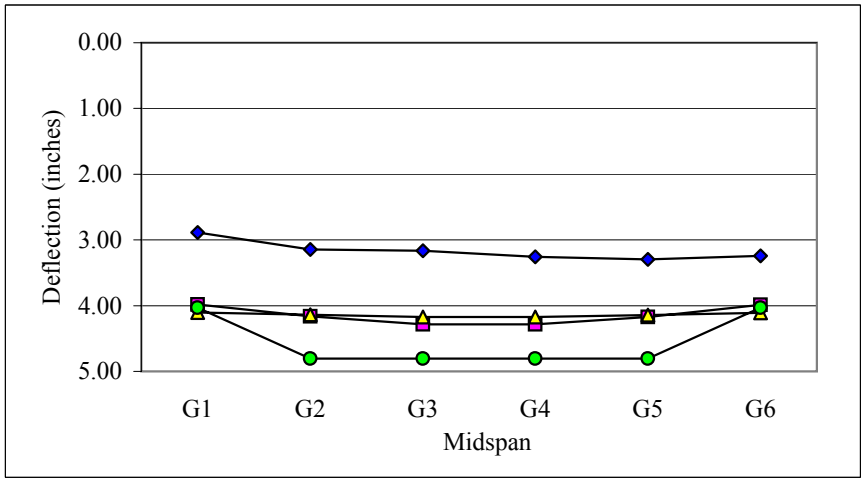

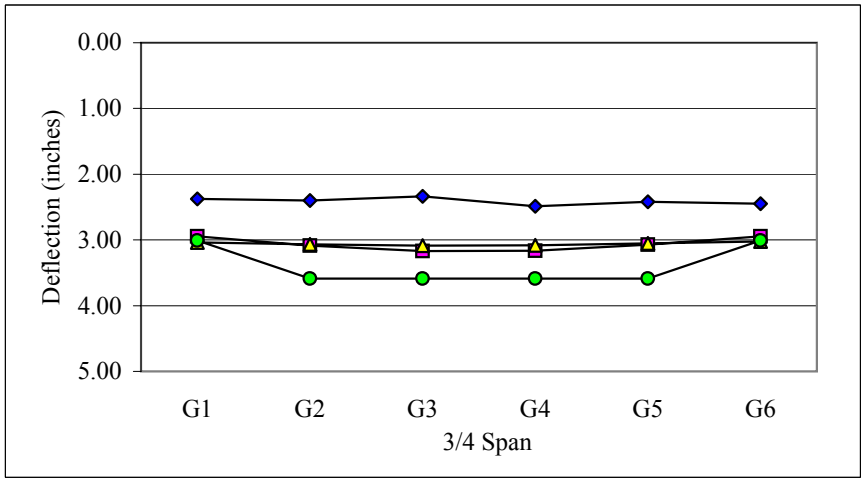

SAP 2000 MODELING SUMMARY

PROJECT NUMBER: R-2547 (EB Bridge on US 64 Bypass over Smithfield Rd.)

MODEL PICTURE (Steel only, isometric view)

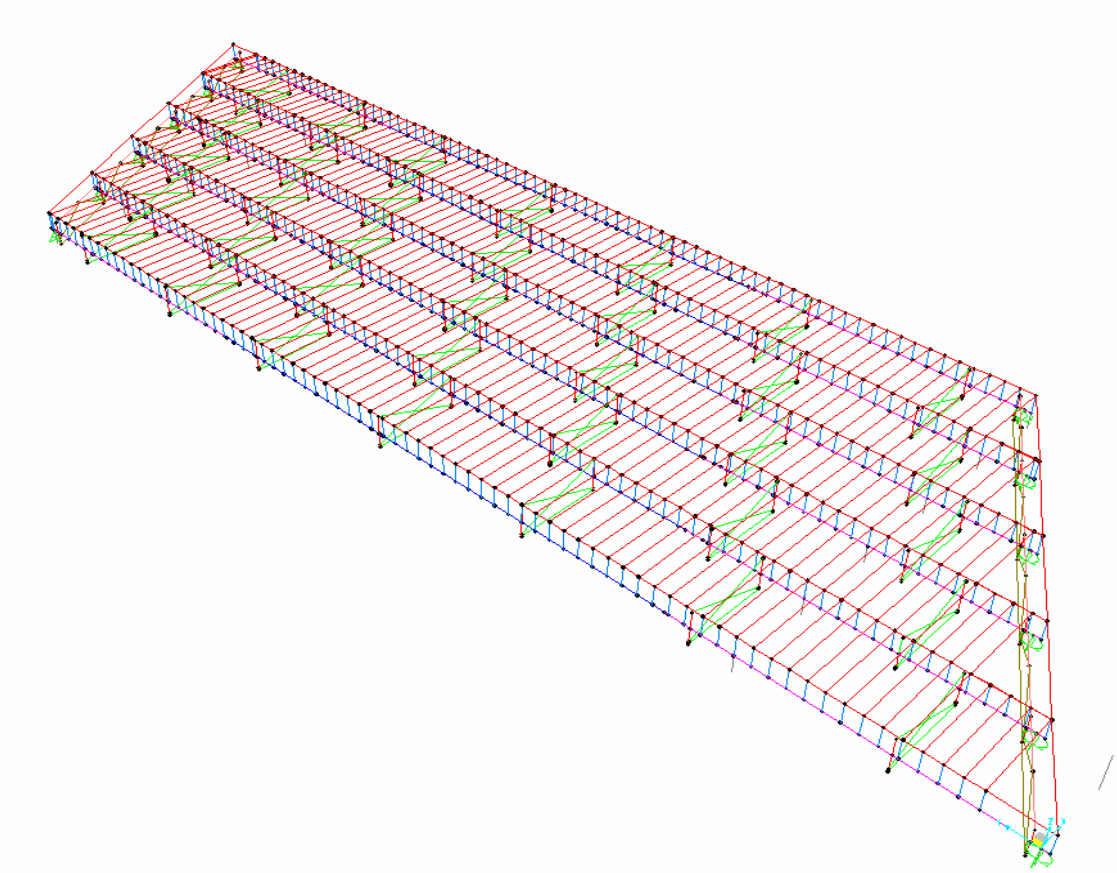

SAP2000 MODELING SUMMARY

PROJECT NUMBER: R-2547 (EB Bridge on US 64 Bypass over Smithfield Rd.)

MODEL DESCRIPTION

COMPONENT	**Element Type**
Girder:	Frame Element
Cross Frame Members:	Frame Element
Stay-in-place Deck Forms:	Area Element* (Shell Element)
Rigid Link:	Frame Element

* See Area Properties in Appendix F

GIRDER DEFLECTIONS

SAP				**Single Girder Model**		
Point	**1/4**	**1/2**	**3/4**	**1/4**	**1/2**	**3/4**
G1	3.02	4.18	3.02	2.95	4.08	2.95
G2	3.42	4.73	3.42	3.52	4.87	3.52
G3	3.54	4.90	3.55	3.52	4.87	3.52
G4	3.54	4.90	3.55	3.52	4.87	3.52
G5	3.42	4.73	3.42	3.52	4.87	3.52
G6	3.02	4.18	3.02	2.95	4.08	2.95
SAP (SIP)				**ANSYS (SIP)**		
Point	**1/4**	**1/2**	**3/4**	**1/4**	**1/2**	**3/4**
G1	3.07	4.25	3.08	3.03	4.11	3.04
G2	3.12	4.31	3.11	3.06	4.14	3.07
G3	3.15	4.35	3.14	3.08	4.17	3.09
G4	3.14	4.35	3.14	3.09	4.17	3.08
G5	3.12	4.31	3.12	3.06	4.14	3.05
G6	3.07	4.26	3.07	3.04	4.11	3.02

SAP 2000 MODELING SUMMARY

PROJECT NUMBER: R-2547 (EB Bridge on US 64 Bypass over Smithfield Rd.)

*GIRDER DEFLECTIONS
CROSS SECTION VIEW

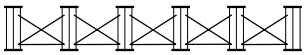

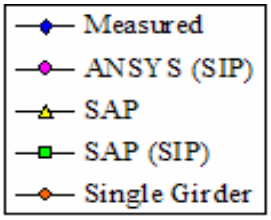

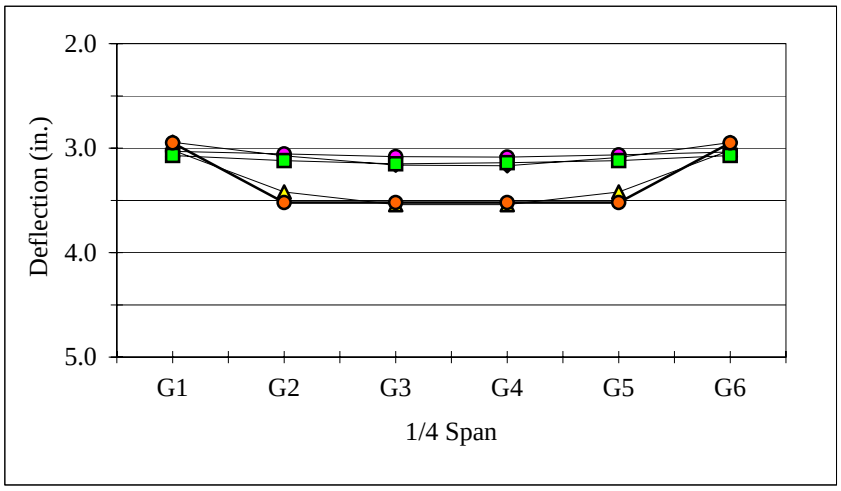

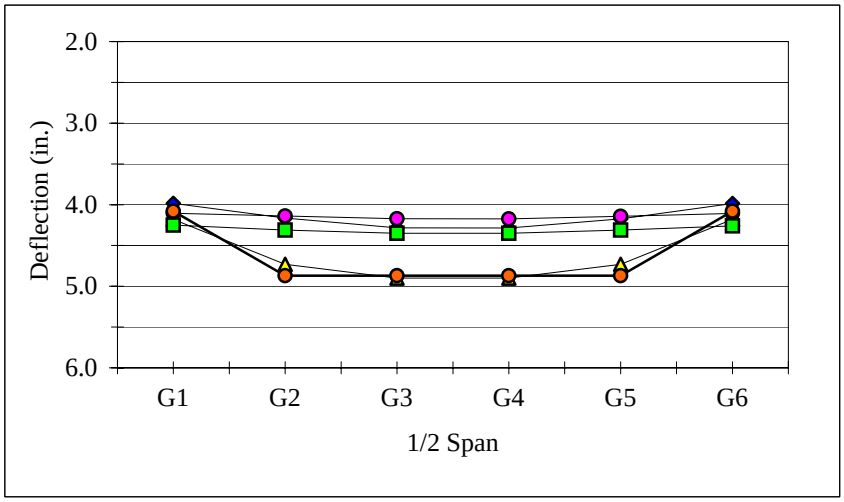

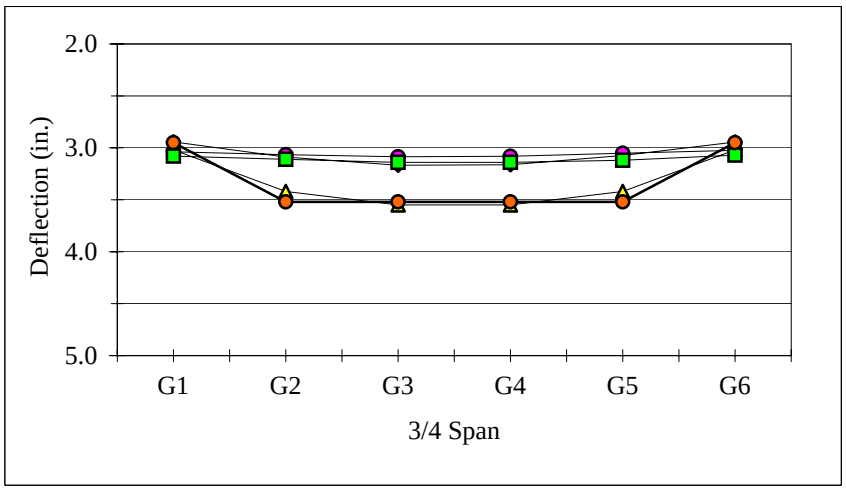

Appendix E

Deflection Summary for the Avondale Bridge

This appendix contains a detailed description of the Avondale Bridge including bridge geometry, material data, cross-frame type and size, and dead loads calculated from slab geometry. Tables and graphs of the field measured non-composite girder deflections are included.

A summary of the ANSYS finite element model created for the Avondale Bridge is also included in this appendix. This summary includes a picture of the ANSYS model, details about the elements used in the model generation, the loads applied to the model, and tables and graphs of the deflections predicted by the model.

FIELD MEASUREMENT SUMMARY

PROJECT NUMBER: I-306DB (I-85 over Avondale Drive)
MEASUREMENT DATE: September 4, 2003

BRIDGE DESCRIPTION

TYPE	Three Span Simple	(center span measured)
LENGTH	143.96 ft (43.58 m)	
NUMBER OF GIRDERS	7	
GIRDER SPACING	11.19 ft (3.41 m)	
SKEW	53 deg	
OVERHANG	3.41 ft (1.04 m)	(deck curved in plan)
BEARING TYPE	Elastomeric Pad	

MATERIAL DATA

STRUCTURAL STEEL	**Grade**	**Yield Strength**
Girder:	AASHTO M270	50 ksi (345 MPa)
Other:	AASHTO M270	50 ksi (345 MPa)

CONCRETE UNIT WEIGHT	150 pcf (nominal)
SIP FORM WEIGHT	3 psf (nominal)

GIRDER DATA

LENGTH	143.96 ft (43.58 m)
TOP FLANGE WIDTH	14.96 in (380 mm)
BOTTOM FLANGE WIDTH	20.08 in (510 mm)
WEB THICKNESS	0.63 in (16 mm)
WEB DEPTH	64.96 in (1650 mm)

FLANGES	**Thickness**	**Begin**	**End**
Top:	1.10 in (28 mm)	0.00	41.01 ft (12.50 m)
	1.26 in (32 mm)	41.01 ft (12.50 m)	71.48 ft (21.79 m)
Bottom:	1.10 in (28 mm)	0.000	18.05 ft (5.50 m)
	1.38 in (35 mm)	18.05 ft (5.50 m)	41.010 ft (12.50 m)
	1.77 in (45 mm)	41.01 ft (12.50 m)	71.48 ft (21.79 m)

STIFFENERS	
Longitudinal:	NONE
Bearing:	PL 1.10" × 7.09" (28 mm × 180 mm)
Intermediate:	PL 0.63" × NA (16 mm × NA, connector plate)
End Bent Connector:	NONE

CROSS-FRAME DATA

	Type	**Diagonals**	**Horizontals**
END	K	WT 5×15	C15×40 (top) WT 5×15 (bottom)
INTERMEDIATE	X	L 3½×3½×⅜	L 3½×3½×⅜ (bottom)

FIELD MEASUREMENT SUMMARY

Project Number: I-306DB (I-85 over Avondale Drive)
Measurement Date: September 4, 2003

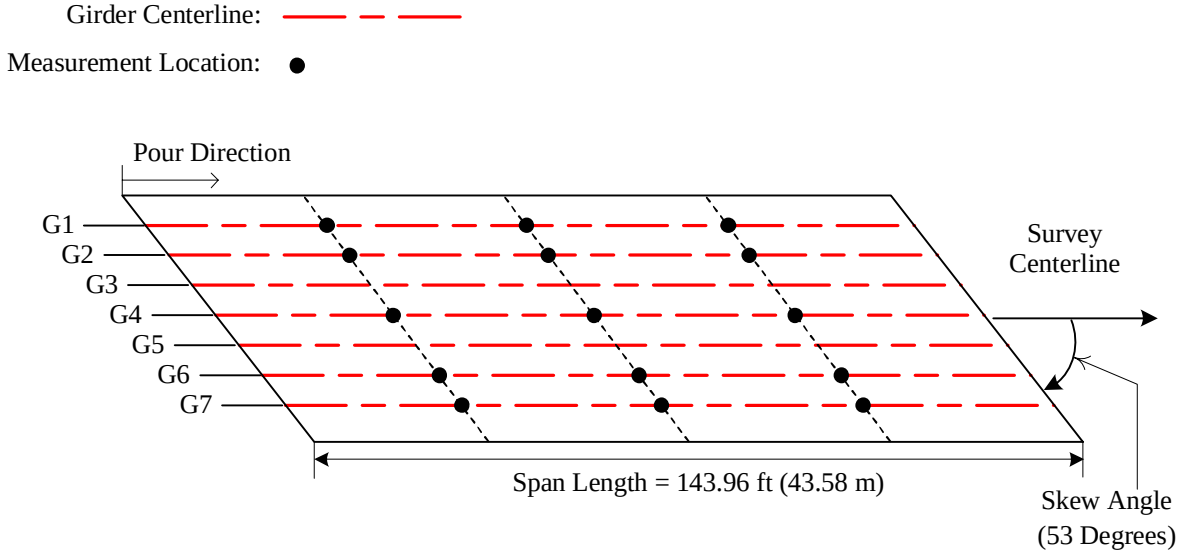

(a) Plan View (Not to Scale)

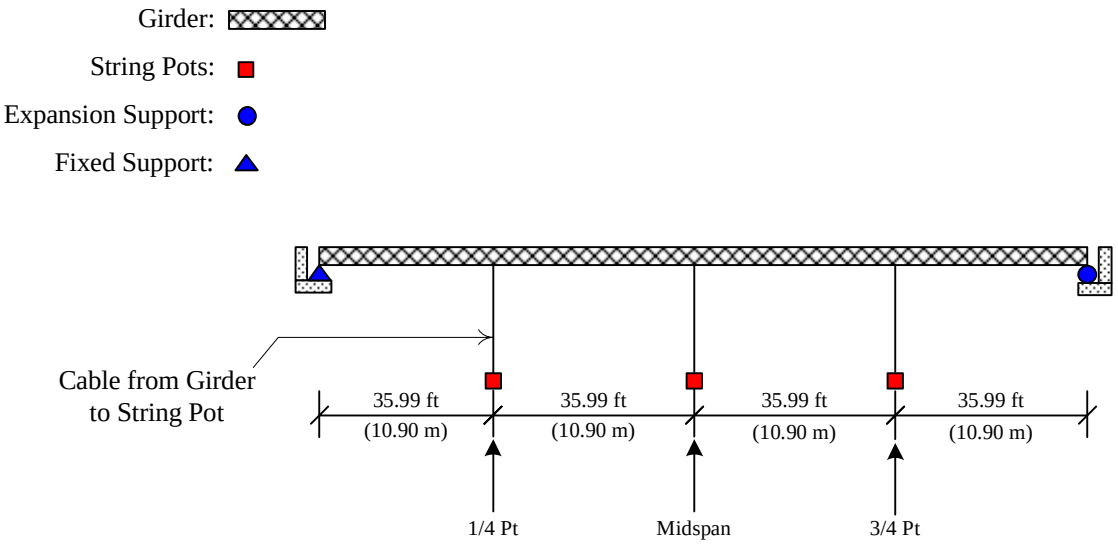

(b) Elevation View (Not to Scale)

Plan and Elevation View of the Avondale Bridge (Durham, NC)

FIELD MEASUREMENT SUMMARY

PROJECT NUMBER: I-306DB (I-85 over Avondale Drive)
MEASUREMENT DATE: September 4, 2003

DECK LOADS

	Concrete*		Deck Slab**		Ratio
Girder	lb/ft	N/mm	lb/ft	N/mm	
G1	1173.4	17.12	1243.7	18.15	0.94
G2	1348.8	19.68	1526.6	22.28	0.88
G4	1369.7	19.99	1526.6	22.28	0.90
G6	1438.1	20.99	1526.6	22.28	0.94
G7	1183.6	17.27	1209.0	17.64	0.98

*calculated with measured slab thicknesses
**includes slab, buildups, and stay-in-place forms (nominal)

SLAB DATA

THICKNESS 9.06 in (nominal)

BUILD-UP 2.56 in (nominal)

REBAR LONGITUDINAL	Size (metric)	Spacing (nominal)
Top:	#13	340 mm
Bottom:	#16	210 mm
TRANSVERSE		
Top:	#16	140 mm
Bottom:	#16	140 mm

GIRDER DEFLECTIONS (data in inches, full span concrete deflections less bearing settlement)

MEASURED

	1/4 Span Loading			1/2 Span Loading		
Point	1/4	1/2	3/4	1/4	1/2	3/4
G1	0.88	1.05	0.63	2.32	2.96	1.88
G2	0.86	1.13	0.67	2.29	3.07	1.96
G4	0.85	1.20	0.68	2.37	3.23	2.04
G6	0.89	1.11	0.73	2.62	3.50	2.15
G7	0.85	1.08	0.73	2.78	3.67	2.26
	3/4 Span Loading			Full Span Loading		
Point	1/4	1/2	3/4	1/4	1/2	3/4
G1	3.54	4.79	3.31	3.39	4.79	3.28
G2	3.47	4.85	3.34	3.42	4.94	3.37
G4	3.54	4.97	3.43	3.54	5.08	3.49
G6	3.69	5.15	3.65	3.72	5.36	3.71
G7	3.86	5.46	3.91	3.80	5.47	3.87

MEASURED BEARING

	Total Settlement		
Point	End 1	End 2	Avg.
G1	0.39	---	0.39
G2	0.32	---	0.32
G4	---	---	---
G6	---	---	---
G7	---	---	---

PREDICTED AND SURVEYED

	Original			Revision		
Point	1/4	1/2	3/4	1/4	1/2	3/4
G1	---	5.59	---	---	6.10	---
G2	---	6.73	---	---	6.38	---
G4	---	6.73	---	---	6.65	---
G6	---	6.73	---	---	6.46	---
G7	---	5.75	---	---	6.22	---
	Adjusted Revision***			Surveyed		
Point	1/4	1/2	3/4	1/4	1/2	3/4
G1	---	5.76	---	---	6.10	---
G2	---	5.64	---	---	5.90	---
G4	---	5.97	---	---	6.41	---
G6	---	6.08	---	---	6.61	---
G7	---	6.09	---	---	6.81	---

***predicted revision multiplied by the ratio of deck concrete to total slab weigh

FIELD MEASUREMENT SUMMARY

PROJECT NUMBER: I-306DB (I-85 over Avondale Drive)
MEASUREMENT DATE: September 4, 2003

GIRDER DEFLECTIONS
CROSS SECTION VIEW

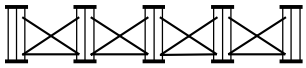

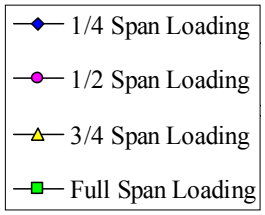

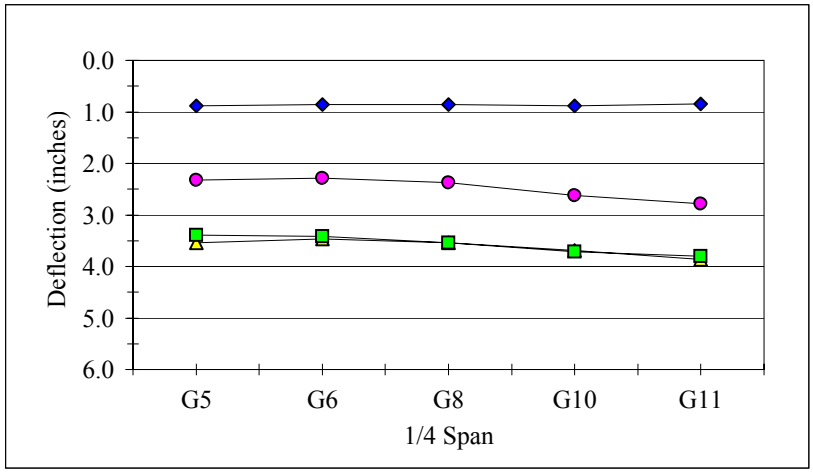

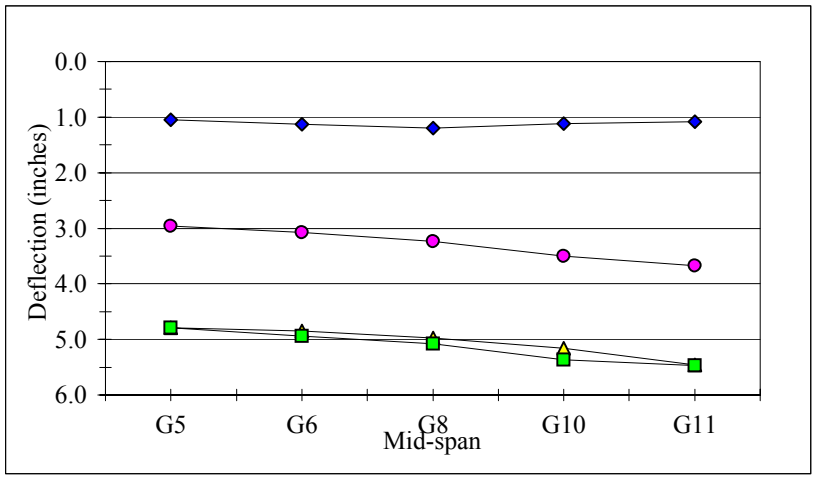

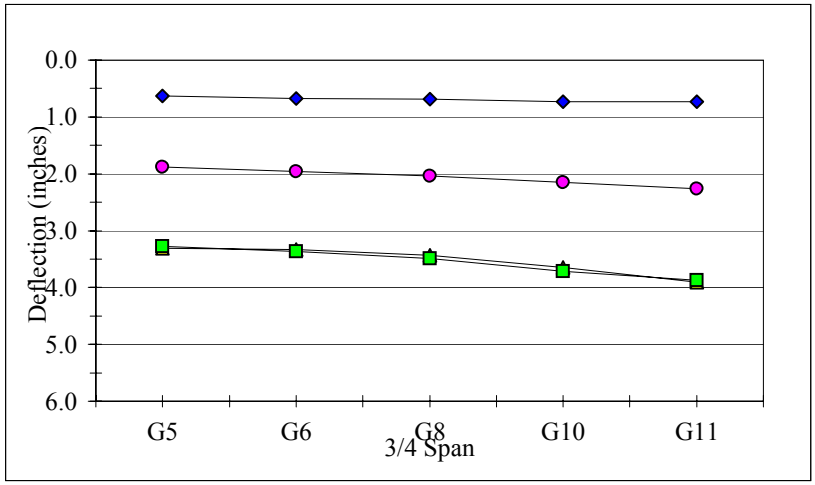

FIELD MEASUREMENT SUMMARY

PROJECT NUMBER: I-306DB (I-85 over Avondale Drive)
MEASUREMENT DATE: September 4, 2003

SLAB THICKNESS
CROSS SECTION VIEW

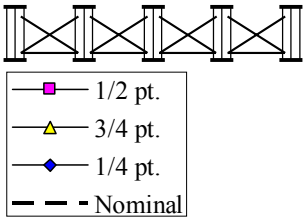

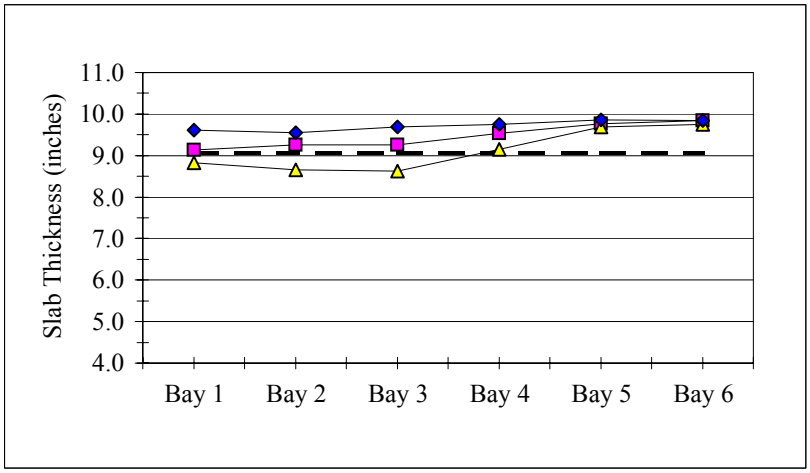

GIRDER DEFLECTIONS
ELEVATION VIEW

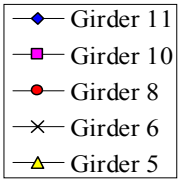

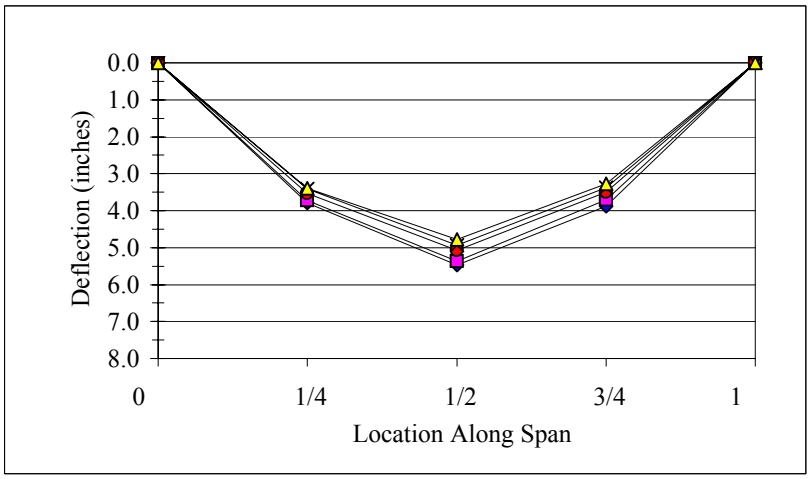

GIRDER DEFLECTIONS
CROSS SECTION VIEW

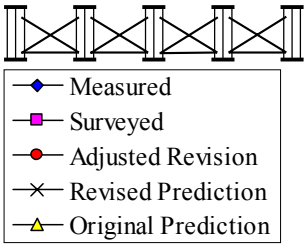

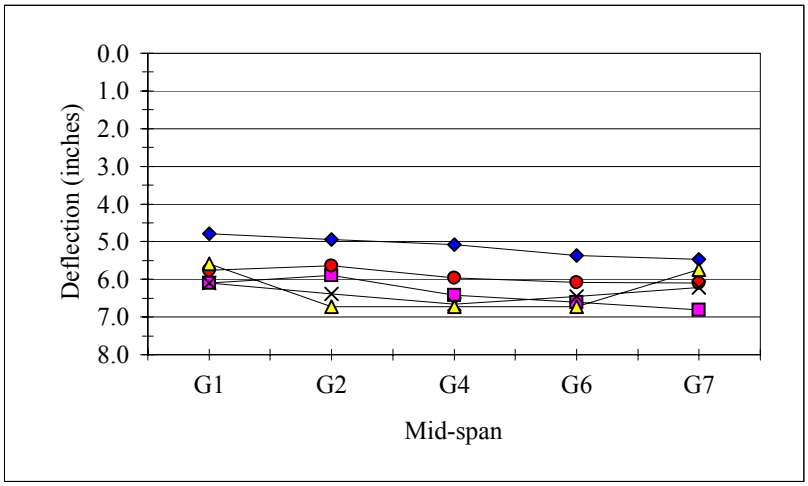

ANSYS FINITE ELEMENT MODELING SUMMARY

PROJECT NUMBER: I-306DB (I-85 over Avondale Drive)

MODEL PICTURE (Steel only, oblique view)

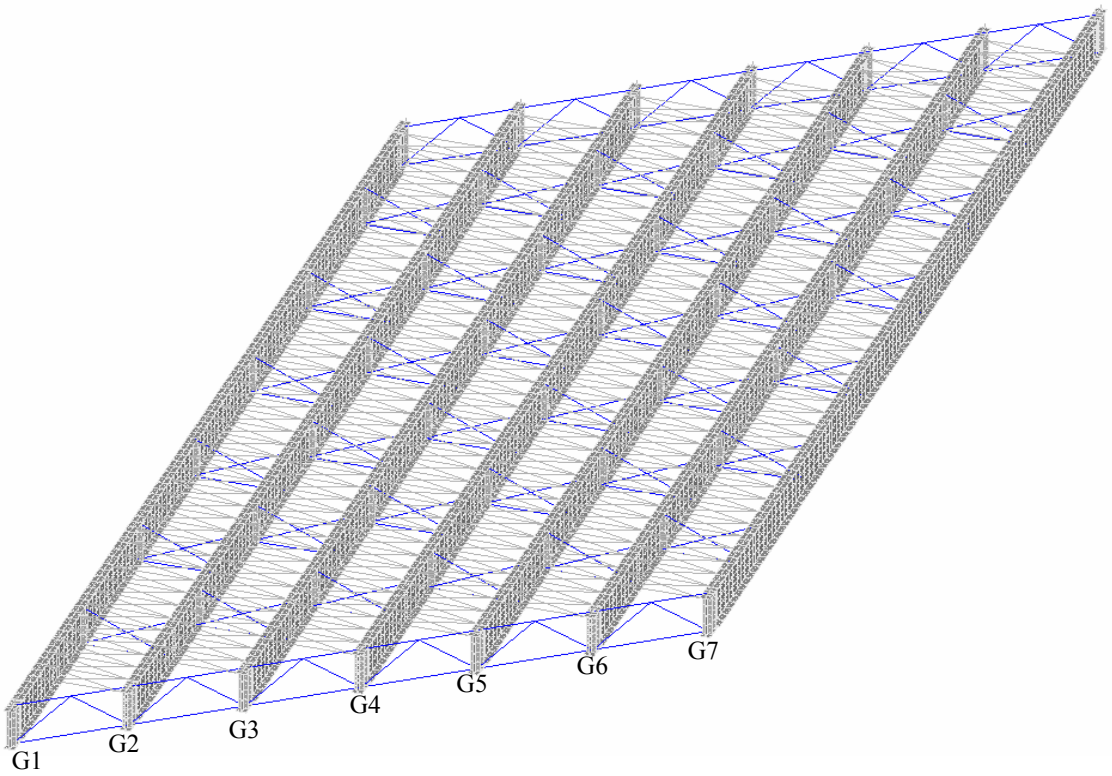

ANSYS FINITE ELEMENT MODELING SUMMARY

PROJECT NUMBER: I-306DB (I-85 over Avondale Drive)

MODEL DESCRIPTION

COMPONENT	**Element Type**
Girder:	SHELL93
Connector Plates:	SHELL93
Stiffener Plates:	SHELL93
Cross-frame Members:	LINK8 (diagonal)
	LINK8 (horizontal)
End Diaphragm:	LINK8 (diagonal)
	BEAM4 (diagonal)
Stay-in-place Deck Forms:	LINK8
Concrete Slab:	SHELL63
Shear Studs:	MPC184

APPLIED LOADS

Girder	***Load**	
	lb/ft	**N/mm**
G1	1173.4	17.12
G2	1348.8	19.68
G3	1359.3	19.84
G4	1369.7	19.99
G5	1403.9	20.49
G6	1438.1	20.99
G7	1183.6	17.27

*applied as a uniform pressure to area of top flange

GIRDER DEFLECTIONS

	ANSYS (load step 1)			**ANSYS (load step 2)**		
Point	**1/4**	**1/2**	**3/4**	**1/4**	**1/2**	**3/4**
G1	0.68	**0.78**	0.48	1.47	**1.96**	1.27
G2	0.68	**0.77**	0.48	1.46	**1.93**	1.25
G4	0.69	**0.78**	0.48	1.48	**1.96**	1.27
G6	0.71	**0.80**	0.50	1.50	**2.00**	1.30
G7	0.71	**0.83**	0.52	1.52	**2.04**	1.33
	ANSYS (load step 3)			**ANSYS (load step 4)**		
Point	**1/4**	**1/2**	**3/4**	**1/4**	**1/2**	**3/4**
G1	1.29	**1.97**	1.48	0.45	**0.74**	0.65
G2	1.26	**1.95**	1.46	0.44	**0.73**	0.65
G4	1.26	**1.96**	1.48	0.44	**0.74**	0.66
G6	1.28	**1.98**	1.49	0.45	**0.74**	0.67
G7	1.31	**2.01**	1.51	0.46	**0.76**	0.66
	Measured			**ANSYS (no SIP)**		
Point	**1/4**	**1/2**	**3/4**	**1/4**	**1/2**	**3/4**
G1	3.39	**4.79**	3.28	3.85	**5.39**	3.85
G2	3.42	**4.94**	3.37	3.96	**5.54**	3.95
G4	3.54	**5.08**	3.49	4.14	**5.79**	4.13
G6	3.72	**5.36**	3.71	4.07	**5.72**	4.09
G7	3.80	**5.47**	3.87	3.98	**5.57**	3.98
	ANSYS (SIP)			***ANSYS (p.c., SIP)**		
Point	**1/4**	**1/2**	**3/4**	**1/4**	**1/2**	**3/4**
G1	3.85	**5.38**	3.83	3.89	**5.45**	3.88
G2	3.84	**5.36**	3.82	3.83	**5.38**	3.85
G4	3.92	**5.48**	3.90	3.87	**5.44**	3.89
G6	3.97	**5.57**	3.98	3.93	**5.53**	3.95
G7	4.03	**5.67**	4.05	4.00	**5.63**	4.03

*superimposed from load steps 1-4 for partial composite action

ANSYS FINITE ELEMENT MODELING SUMMARY

PROJECT NUMBER: I-306DB (I-85 over Avondale Drive)

GIRDER DEFLECTIONS
CROSS SECTION VIEW

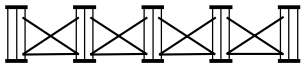

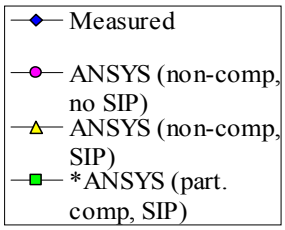

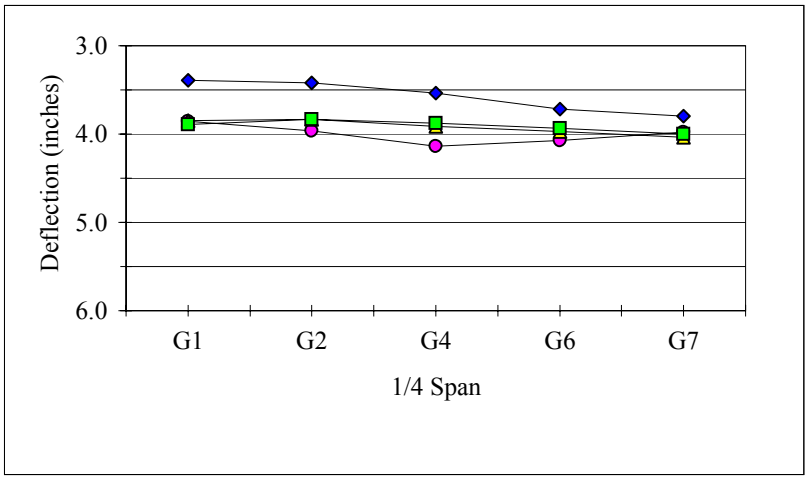

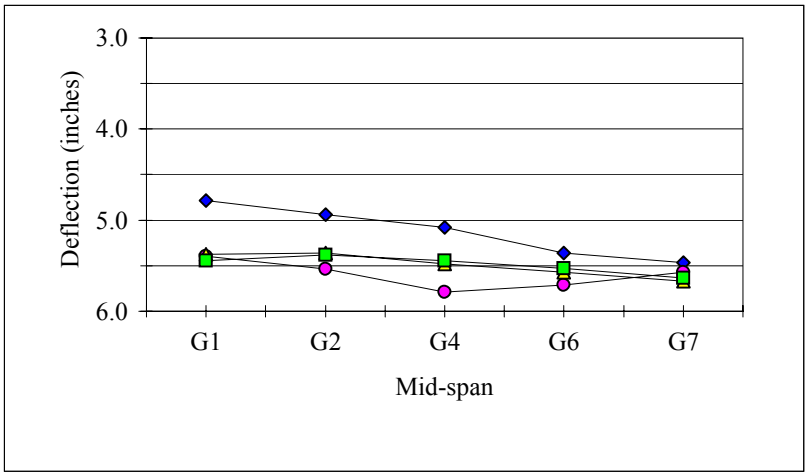

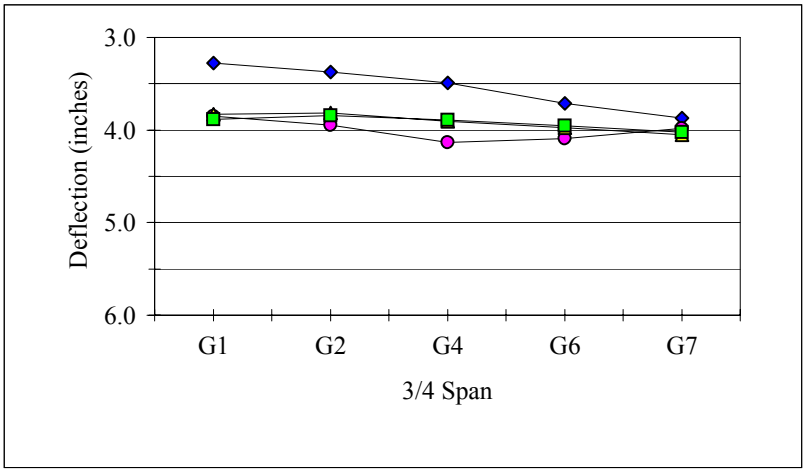

Appendix F

Deflection Summary for the US 29 Bridge

This appendix contains a detailed description of the US 29 bridge including bridge geometry, material data, cross-frame type and size, and dead loads calculated from slab geometry. Tables and graphs of the field measured non-composite girder deflections are included.

A summary of the ANSYS finite element model created for the US 29 bridge is also included in this appendix. This summary includes a picture of the ANSYS model, details about the elements used in the model generation, the loads applied to the model, and tables and graphs of the deflections predicted by the model.

FIELD MEASUREMENT SUMMARY

PROJECT NUMBER: R-0984B (US 29 over NC 150, southbound)
MEASUREMENT DATE: May 6, 2004

BRIDGE DESCRIPTION

TYPE	One Span Simple	
LENGTH	123.83 ft (34.74 m)	
NUMBER OF GIRDERS	7	
GIRDER SPACING	7.75 ft (2.36 m)	
SKEW	46 deg	
OVERHANG	2.29 ft (symmetric)	(from web centerline)
BEARING TYPE	Elastomeric Pad	

MATERIAL DATA

STRUCTURAL STEEL	**Grade**	**Yield Strength**
Girder:	AASHTO M270	50 ksi (345 MPa)
Other:	AASHTO M270	50 ksi (345 MPa)

CONCRETE UNIT WEIGHT	150 pcf (nominal)
SIP FORM WEIGHT	3 psf (nominal)

GIRDER DATA

LENGTH	123.83 ft (34.74 m)
TOP FLANGE WIDTH	15 in (381 mm)
BOTTOM FLANGE WIDTH	15 in (381 mm)
WEB THICKNESS	0.5 in (13 mm)
WEB DEPTH	52 in (1321 mm)

FLANGES	**Thickness**	**Begin**	**End**
Top:	0.75 in (19.05 mm)	0.00	61.92 ft (18.872 m)
Bottom:	0.75 in (19.05 mm)	0.00	26.92 ft (8.20 m)
	1.38 in (34.93 mm)	26.92 ft (8.20 m)	61.92 ft (18.87 m)

STIFFENERS	
Longitudinal:	NONE
Bearing:	PL 0.75" × 7.25" (19 mm × 184 mm)
Intermediate:	PL 0.375" × NA (10 mm × NA, connector plate)
End Bent Connector:	PL 0.375" × NA (10 mm × NA, connector plate)

CROSS-FRAME DATA

	Type	**Diagonals**	**Horizontals**
END	K	WT 4×9	C 15×33.9 (top) WT 4×9 (bottom)
INTERMEDIATE	K	L 3½×3½×5/16	L 3½×3½×5/16 (bottom)

FIELD MEASUREMENT SUMMARY

Project Number: R-094B (US 29 Over NC 150, Southbound)
Measurement Date: May 6, 2004

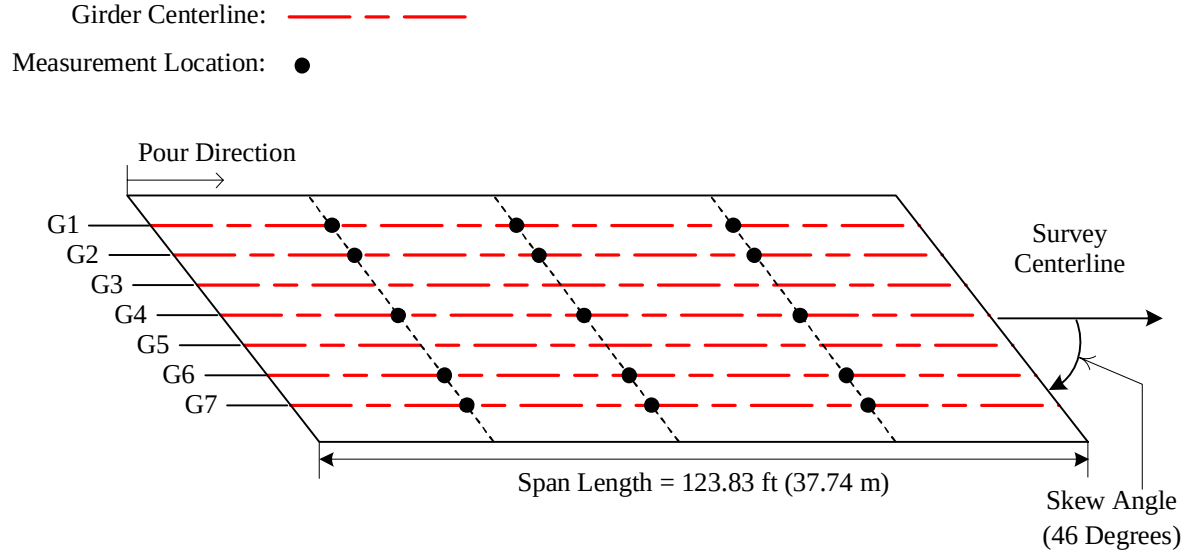

(a) Plan View (Not to Scale)

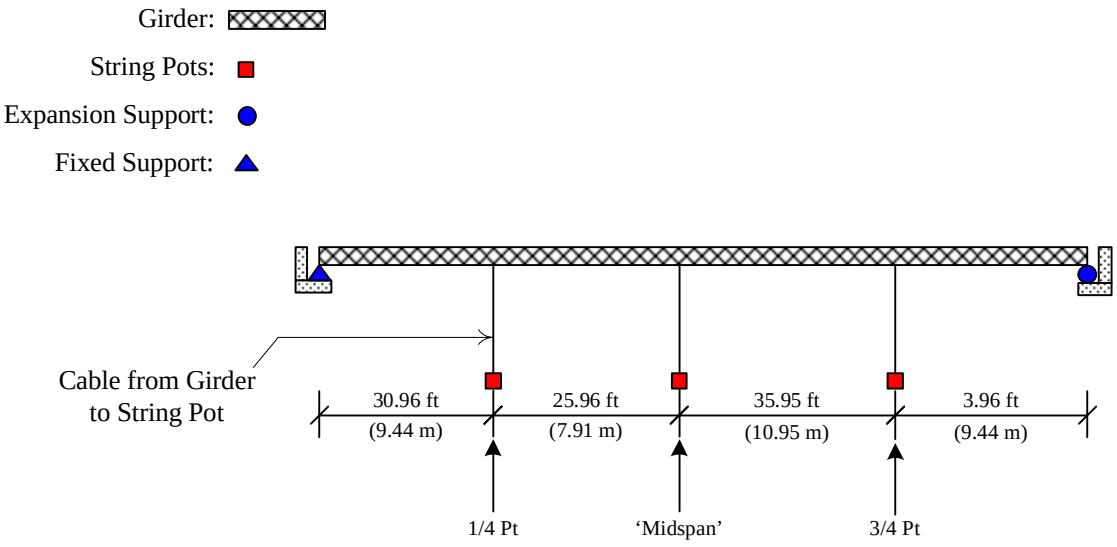

(b) Elevation View (Not to Scale)

Plan and Elevation View of the US-29 Bridge (Reidsville, NC)

FIELD MEASUREMENT SUMMARY

PROJECT NUMBER: R-0984B (US 29 over NC 150, southbound)
MEASUREMENT DATE: May 6, 2004

DECK LOADS

	Concrete*		Deck Slab**		Ratio
Girder	**lb/ft**	**N/mm**	**lb/ft**	**N/mm**	
G1	746.40	10.89	794.64	11.60	0.94
G2	866.40	12.64	926.04	13.51	0.94
G4	866.40	12.64	926.04	13.51	0.94
G6	866.40	12.64	926.04	13.51	0.94
G7	746.40	10.89	794.64	11.60	0.94

*calculated with measured slab thicknesses
**includes slab, buildups, and stay-in-place forms (nominal)

SLAB DATA

THICKNESS 8.25 in (nominal)

BUILD-UP 2.50 in (nominal)

REBAR	**Size**	**Spacing**
LONGITUDINAL	(US)	(nominal)
Top:	#4	18 in
Bottom:	#5	10 in
TRANSVERSE		
Top:	#5	7 in
Bottom:	#5	7 in

GIRDER DEFLECTIONS (data in inches, full span concrete deflections less bearing settlement)

MEASURED

	1/4 Span Loading			1/2 Span Loading		
Point	**1/4**	**1/2**	**3/4**	**1/4**	**1/2**	**3/4**
G1	0.07	-0.10	0.05	0.95	1.87	1.62
G2	0.02	-0.04	0.11	0.83	1.69	1.40
G4	0.43	0.21	0.29	0.93	1.62	1.37
G6	0.31	0.64	0.64	0.91	1.85	1.62
G7	0.57	0.93	0.79	1.21	2.08	1.85
	3/4 Span Loading			**Full Span Loading**		
Point	**1/4**	**1/2**	**3/4**	**1/4**	**1/2**	**3/4**
G1	2.73	4.03	3.02	3.21	4.44	3.29
G2	2.47	3.61	2.66	2.98	4.13	2.97
G4	2.47	3.36	2.50	3.10	3.98	2.91
G6	2.67	3.70	2.83	3.09	4.31	3.18
G7	3.12	4.12	3.13	3.44	4.65	3.39

MEASURED BEARING

	Total Settlement		
Point	**End 1**	**End 2**	**Avg.**
G1	0.13	0.07	0.10
G2	0.13	0.04	0.09
G4	0.11	0.16	0.14
G6	0.14	0.13	0.13
G7	0.11	0.08	0.09

PREDICTED AND SURVEYED

	Original			Revision		
Point	**1/4**	**1/2**	**3/4**	**1/4**	**1/2**	**3/4**
G1	3.79	5.18	3.79	3.90	5.40	3.90
G2	4.76	6.50	4.76	4.48	6.24	4.48
G4	4.76	6.50	4.76	4.48	6.24	4.48
G6	4.76	6.50	4.76	4.48	6.24	4.48
G7	3.79	5.18	3.79	3.90	5.40	3.90
	Adjusted Revision* **			**Surveyed**		
Point	**1/4**	**1/2**	**3/4**	**1/4**	**1/2**	**3/4**
G1	3.66	5.07	3.66	---	---	---
G2	4.19	5.84	4.19	---	---	---
G4	4.19	5.84	4.19	---	---	---
G6	4.19	5.84	4.19	---	---	---
G7	3.66	5.07	3.66	---	---	---

***predicted revision multiplied by the ratio of deck concrete to total slab weigh

FIELD MEASUREMENT SUMMARY

PROJECT NUMBER: R-0984B (US 29 over NC 150, southbound)
MEASUREMENT DATE: May 6, 2004

GIRDER DEFLECTIONS
CROSS SECTION VIEW

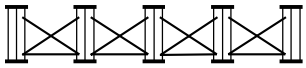

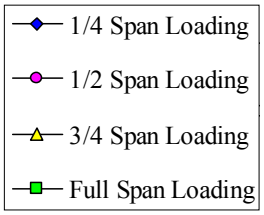

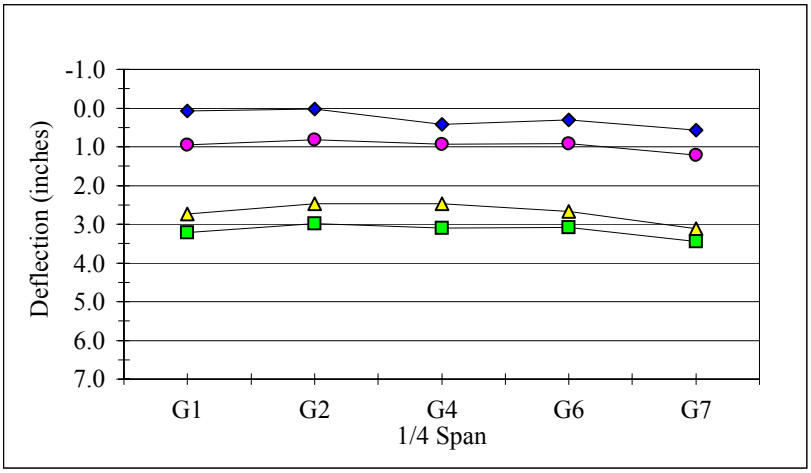

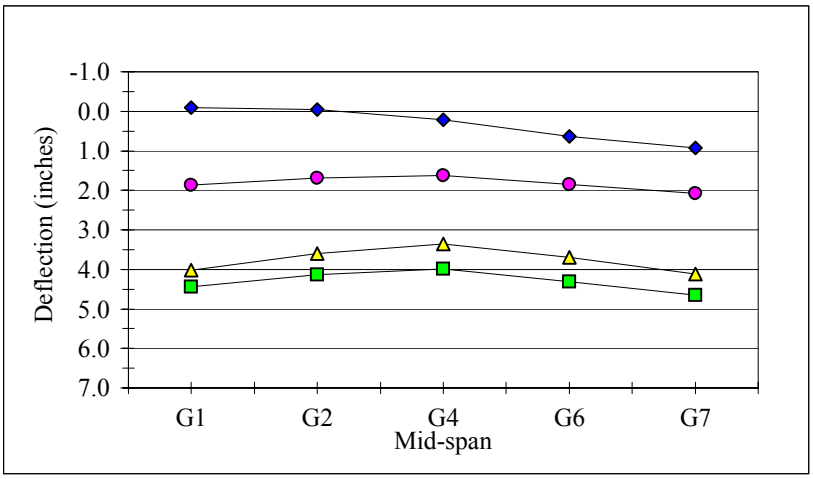

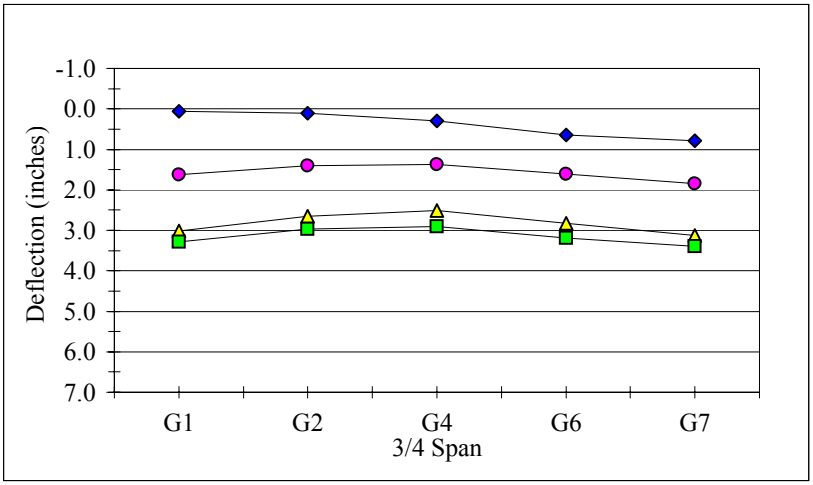

FIELD MEASUREMENT SUMMARY

PROJECT NUMBER: R-0984B (US 29 over NC 150, southbound)
MEASUREMENT DATE: May 6, 2004

SLAB THICKNESS
CROSS SECTION VIEW

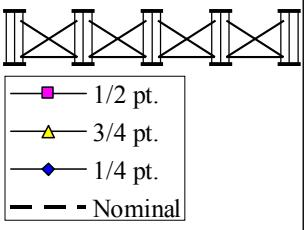

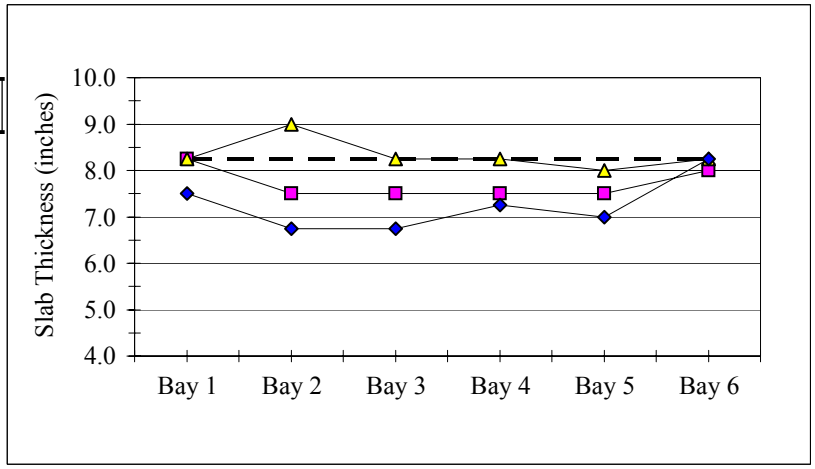

GIRDER DEFLECTIONS
ELEVATION VIEW

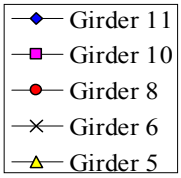

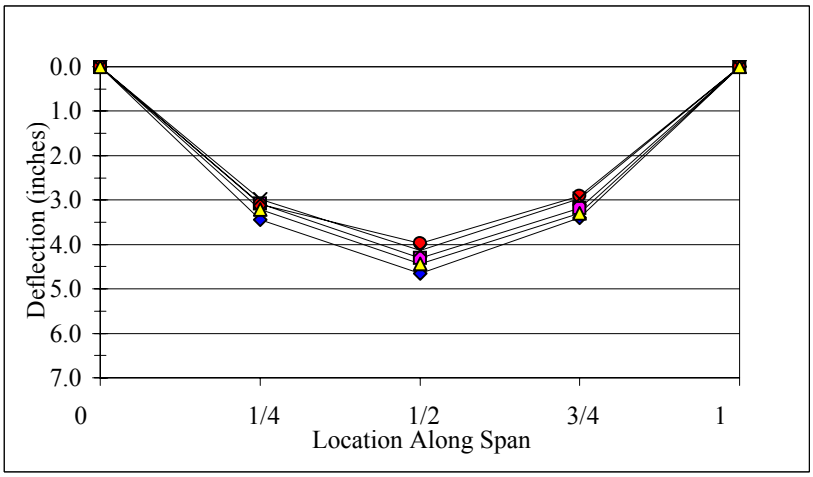

GIRDER DEFLECTIONS
CROSS SECTION VIEW

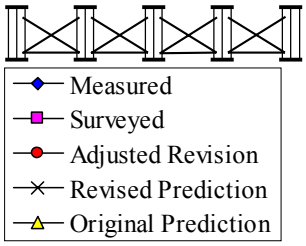

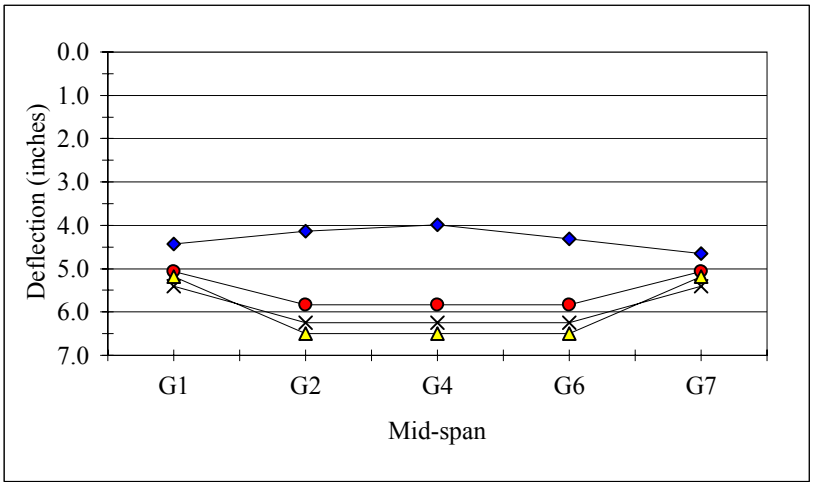

ANSYS FINITE ELEMENT MODELING SUMMARY

PROJECT NUMBER: R-0984B (US 29 over NC 150, southbound)

MODEL PICTURE (Steel only, oblique view)

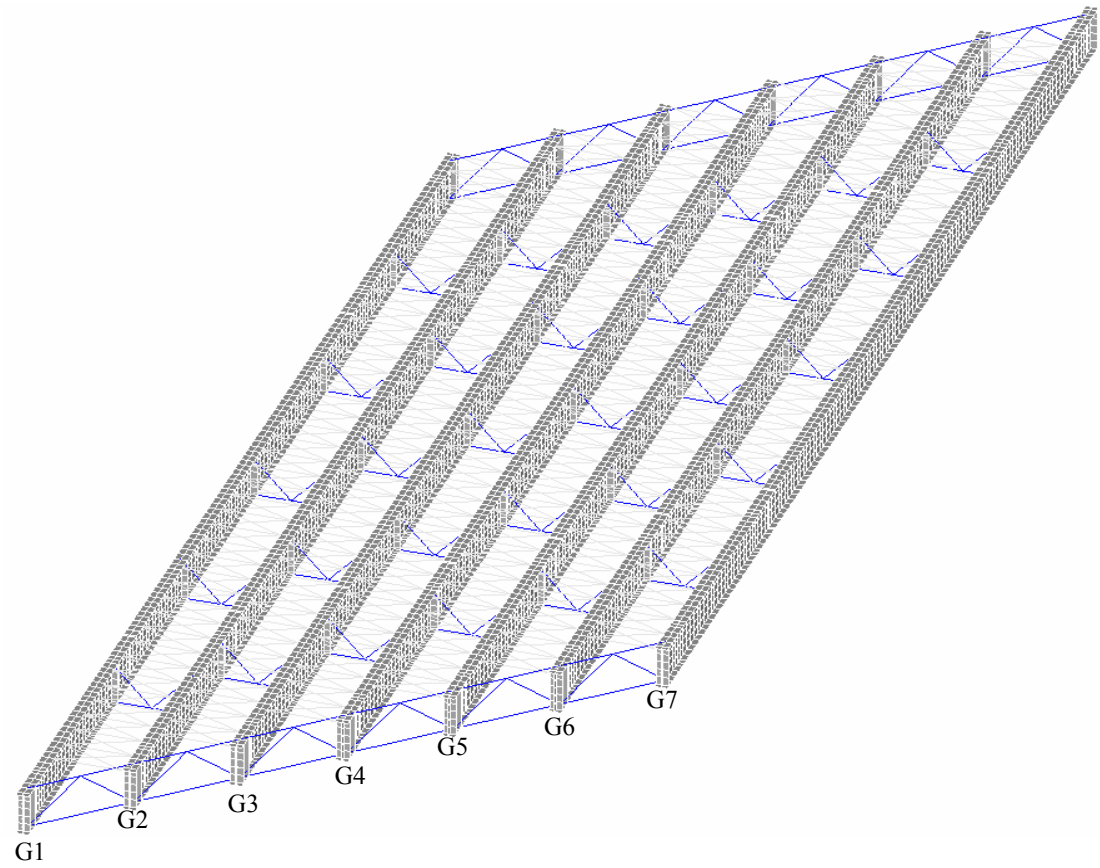

ANSYS FINITE ELEMENT MODELING SUMMARY

PROJECT NUMBER: R-0984B (US 29 over NC 150, southbound)

MODEL DESCRIPTION

COMPONENT	**Element Type**
Girder:	SHELL93
Connector Plates:	SHELL93
Stiffener Plates:	SHELL93
Cross-frame Members:	LINK8 (diagonal)
	LINK8 (horizontal)
End Diaphragm:	LINK8 (diagonal)
	BEAM4 (diagonal)
Stay-in-place Deck Forms:	LINK8
Concrete Slab:	SHELL63
Shear Studs:	MPC184

APPLIED LOADS

Girder	***Load**	
	lb/ft	**N/mm**
G1	746.40	10.89
G2	866.40	12.64
G3	866.40	12.64
G4	866.40	12.64
G5	866.40	12.64
G6	866.40	12.64
G7	746.40	10.89

*applied as a uniform pressure to area of top flange

GIRDER DEFLECTIONS

	ANSYS (load step 1)			**ANSYS (load step 2)**		
Point	**1/4**	**1/2**	**3/4**	**1/4**	**1/2**	**3/4**
G1	---	---	---	---	---	---
G2	---	---	---	---	---	---
G4	---	---	---	---	---	---
G6	---	---	---	---	---	---
G7	---	---	---	---	---	---
	ANSYS (load step 3)			**ANSYS (load step 4)**		
Point	**1/4**	**1/2**	**3/4**	**1/4**	**1/2**	**3/4**
G1	---	---	---	---	---	---
G2	---	---	---	---	---	---
G4	---	---	---	---	---	---
G6	---	---	---	---	---	---
G7	---	---	---	---	---	---
	Measured			**ANSYS (no SIP)**		
Point	**1/4**	**1/2**	**3/4**	**1/4**	**1/2**	**3/4**
G1	3.11	**4.33**	3.19	2.88	**4.04**	2.88
G2	2.90	**4.05**	2.89	3.23	**4.59**	3.28
G4	2.96	**3.84**	2.77	3.22	**4.55**	3.24
G6	2.95	**4.18**	3.05	3.24	**4.55**	3.23
G7	3.35	**4.55**	3.30	2.89	**4.04**	2.88
	ANSYS (SIP)			***ANSYS (p.c., SIP)**		
Point	**1/4**	**1/2**	**3/4**	**1/4**	**1/2**	**3/4**
G1	3.10	**4.41**	3.16	---	---	---
G2	3.06	**4.33**	3.09	---	---	---
G4	3.04	**4.30**	3.07	---	---	---
G6	3.07	**4.32**	3.07	---	---	---
G7	3.14	**4.40**	3.13	---	---	---

*superimposed from load steps 1-4 for partial composite action

ANSYS FINITE ELEMENT MODELING SUMMARY

PROJECT NUMBER: R-0984B (US 29 over NC 150, southbound)

GIRDER DEFLECTIONS
CROSS SECTION VIEW

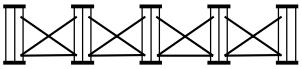

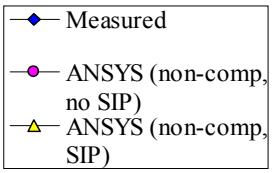

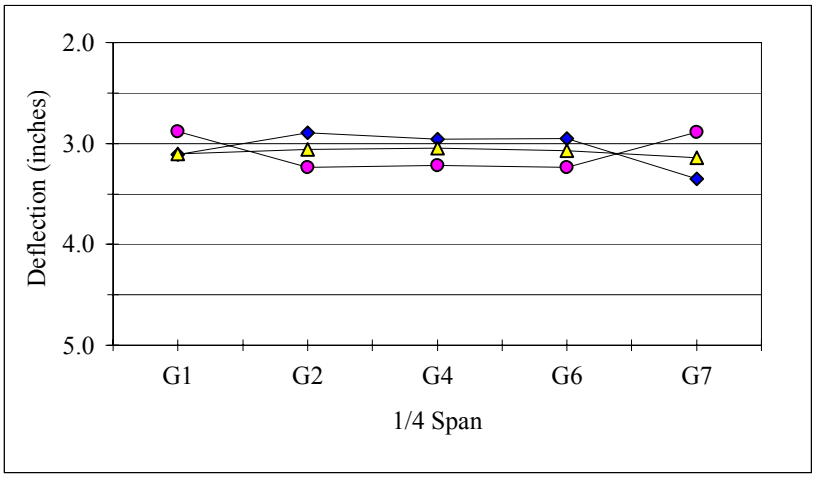

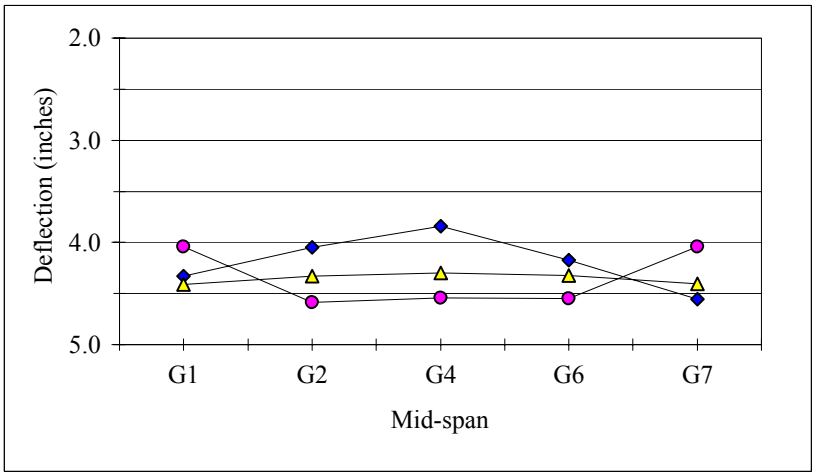

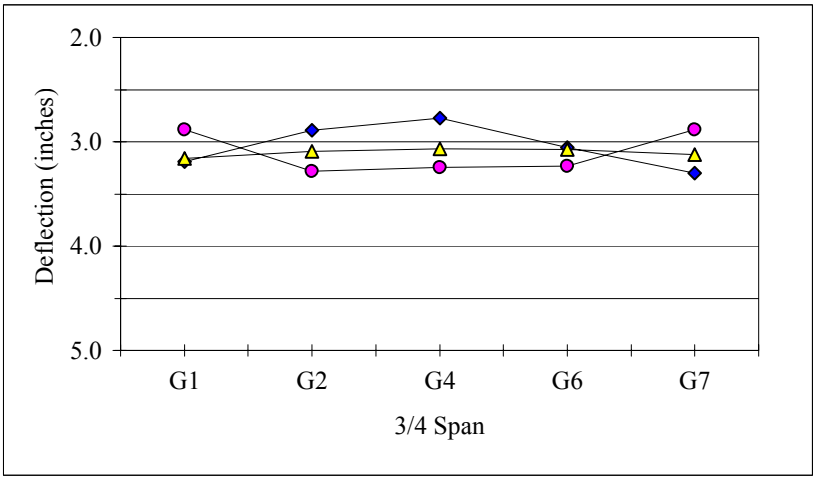

SAP 2000 MODELING SUMMARY

PROJECT NUMBER: R-0984B (US 29 over NC 150, southbound)

MODEL PICTURE (Steel only, oblique view)

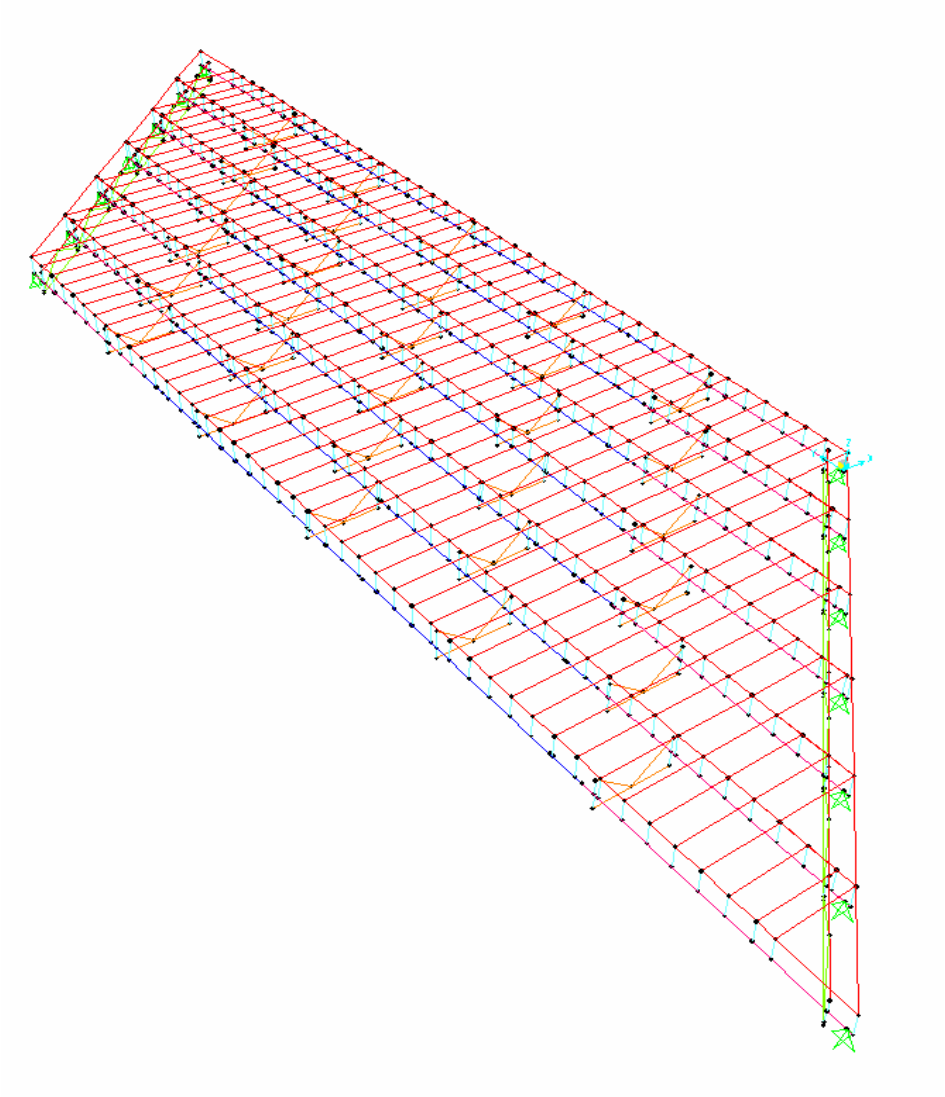

SAP 2000 MODELING SUMMARY

PROJECT NUMBER: R-0984B (US 29 over NC 150, southbound)

MODEL DESCRIPTION

COMPONENT	**Element Type**
Girder:	Frame Element
Cross Frame Members:	Frame Element
Stay-in-place Deck Forms:	Area Element* (Shell Element)
	Frame Element
Rigid Link:	Frame Element

* See Shell Properties in Appendix F

GIRDER DEFLECTIONS

SAP				**Single Girder Line**		
Point	**1/4**	**1/2**	**3/4**	**1/4**	**1/2**	**3/4**
G1	3.61	5.02	3.61	3.63	5.03	3.63
G2	4.08	5.68	4.08	4.22	5.84	4.22
G4	4.16	5.78	4.16	4.22	5.84	4.22
G6	4.08	5.68	4.08	4.22	5.84	4.22
G7	3.61	5.02	3.61	3.63	5.03	3.63
SAP (SIP)				**ANSYS (SIP)**		
Point	**1/4**	**1/2**	**3/4**	**1/4**	**1/2**	**3/4**
G1	3.86	5.38	3.87	3.10	4.41	3.16
G2	3.98	5.54	3.99	3.06	4.33	3.09
G4	4.04	5.64	4.06	3.04	4.30	3.07
G6	3.98	5.50	3.95	3.07	4.32	3.07
G7	3.86	5.35	3.84	3.14	4.40	3.13

SAP (Frame SIP)			
Point	**1/4**	**1/2**	**3/4**
G1	3.71	5.16	3.61
G2	4.07	5.65	4.08
G3	4.17	5.78	4.16
G4	4.09	5.68	4.08
G5	3.71	5.13	3.68

SAP 2000 MODELING SUMMARY

PROJECT NUMBER: R-0984B (US 29 over NC 150, southbound)

GIRDER DEFLECTIONS
CROSS SECTION VIEW

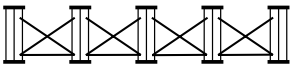

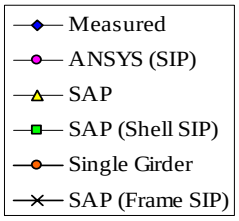

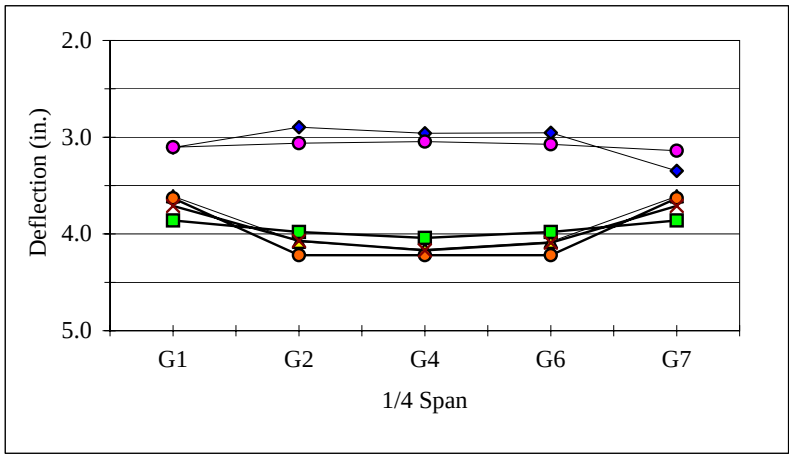

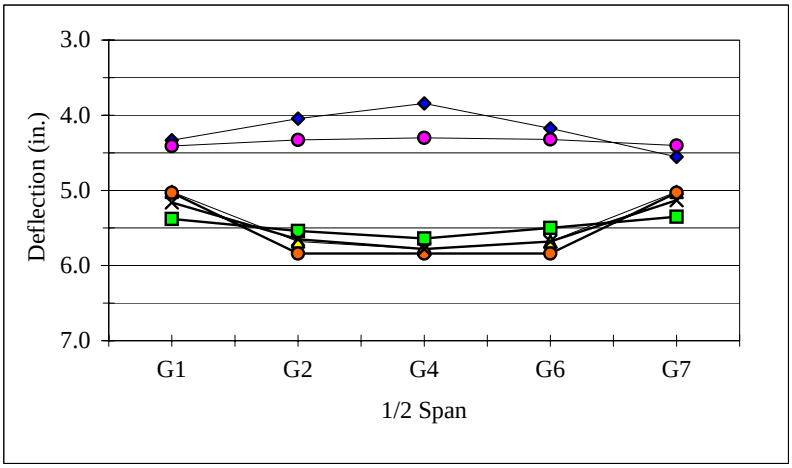

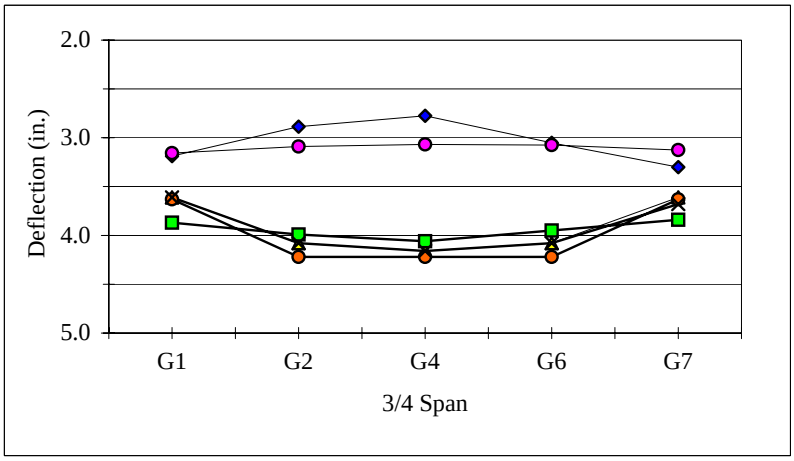

Appendix G

Deflection Summary for the Camden NBL Bridge

This appendix contains a detailed description of the Camden NBL Bridge including bridge geometry, material data, cross-frame type and size, and dead loads calculated from slab geometry. Tables and graphs of the field measured non-composite girder deflections are included.

A summary of the ANSYS finite element model created for the Camden NBL Bridge is also included in this appendix. This summary includes a picture of the ANSYS model, details about the elements used in the model generation, the loads applied to the model, and tables and graphs of the deflections predicted by the model.

FIELD MEASUREMENT SUMMARY

PROJECT NUMBER: I-306DC (I-85 over Camden Avenue, Northbound Lanes)
MEASUREMENT DATE: November 4, 2003

BRIDGE DESCRIPTION

TYPE	Three Span Simple	(center span measured)
LENGTH	144.25 ft (43.97 m)	
NUMBER OF GIRDERS	6	
GIRDER SPACING	8.69 ft (2.65 m)	
SKEW	150 deg	
OVERHANG	none	
BEARING TYPE	Elastomeric Pad	

MATERIAL DATA

STRUCTURAL STEEL	**Grade**	**Yield Strength**
Girder:	AASHTO M270	50 ksi (345 MPa)
Other:	AASHTO M270	50 ksi (345 MPa)

CONCRETE UNIT WEIGHT	150 pcf (nominal)
SIP FORM WEIGHT	3 psf (nominal)

GIRDER DATA

LENGTH	144.25 ft (43.97 m)
TOP FLANGE WIDTH	16.14 in (410 mm)
BOTTOM FLANGE WIDTH	18.90 in (480 mm)
WEB THICKNESS	0.63 in (16 mm)
WEB DEPTH	66.14 in (1680 mm)

FLANGES	**Thickness**	**Begin**	**End**
Top:	0.98 in (25 mm)	0.00	36.03 ft (10.98 m)
	1.18 in (30 mm)	36.03 ft (10.98 m)	72.12 ft (21.98 m)
Bottom:	1.10 in (28 mm)	0.00	36.03 ft (10.98 m)
	1.77 in (45 mm)	36.03 ft (10.98 m)	72.12 ft (21.98 m)

STIFFENERS	
Longitudinal:	NONE
Bearing:	PL 0.71" × 6.65" (18 mm × 169 mm)
Intermediate:	PL 0.39" × NA (10 mm × NA, connector plate)
End Bent Connector:	PL 0.55" × NA (14 mm × NA, connector plate)

CROSS-FRAME DATA

	Type	**Diagonals**	**Horizontals**
END	K	WT 7×17	MC 18×42.7 (top) WT 7×17 (bottom)
INTERMEDIATE	X	L 3½×3½×⅜	L 3½×3½×⅜ (bottom)

FIELD MEASUREMENT SUMMARY

Project Number: I-306DC (I-85 over Camden Avenue, Northbound Lanes)
Measurement Date: November 4, 2003

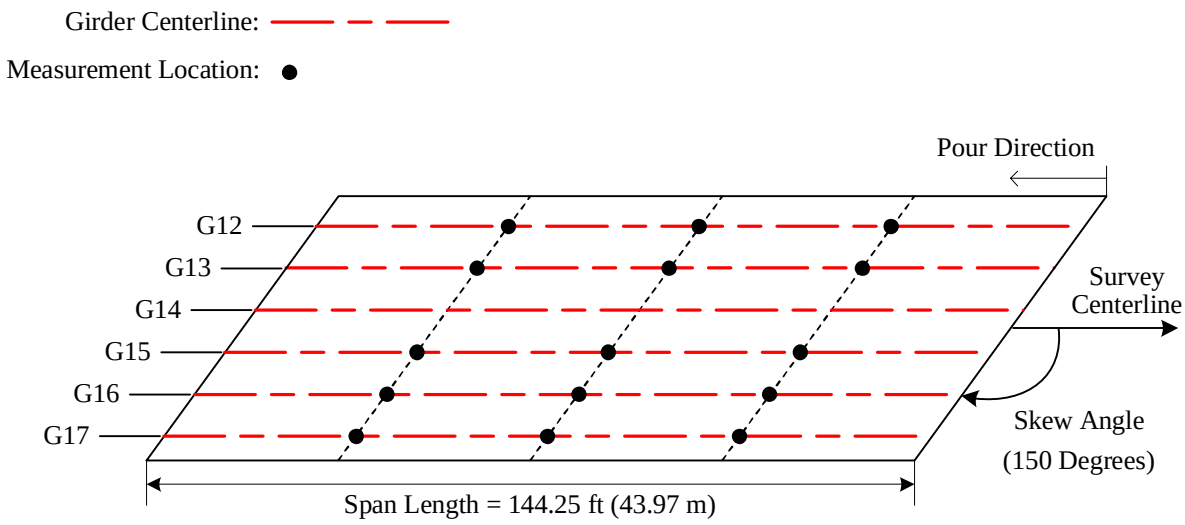

(a) Plan View (Not to Scale)

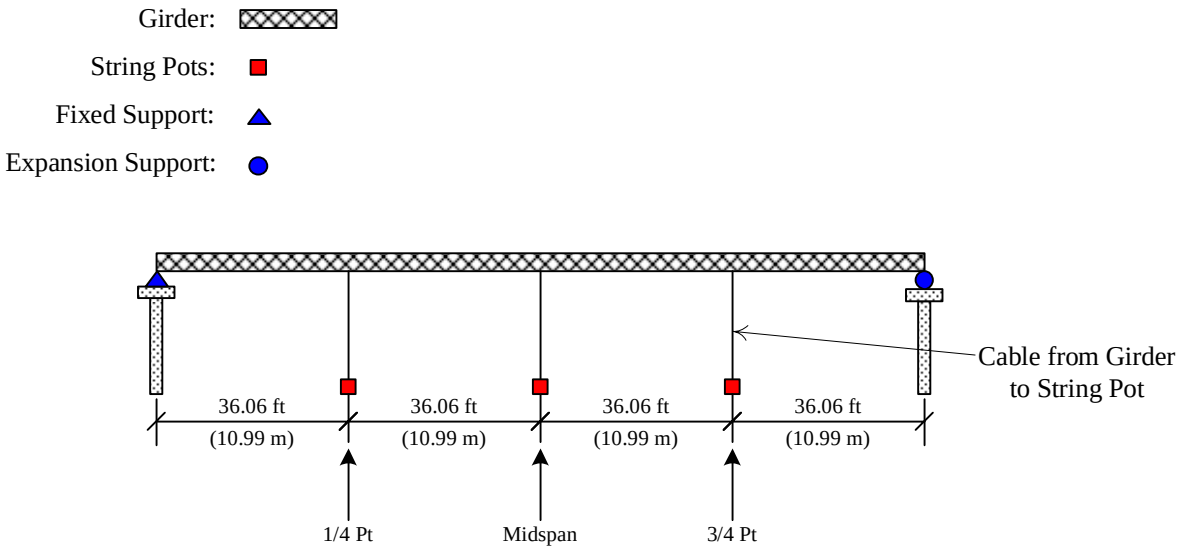

(b) Elevation View (Not to Scale)

Plan and Elevation View of the Camden SB Bridge (Durham, NC)

FIELD MEASUREMENT SUMMARY

PROJECT NUMBER: I-306DC (I-85 over Camden Avenue, Northbound Lanes)
MEASUREMENT DATE: November 4, 2003

DECK LOADS

	Concrete*		Deck Slab**		Ratio
Girder	lb/ft	N/mm	lb/ft	N/mm	
G12	674.3	9.84	689.9	10.07	0.98
G13	1068.1	15.59	1103.3	16.10	0.97
G15	1062.8	15.51	1103.3	16.10	0.96
G16	1040.3	15.18	1103.3	16.10	0.94
G17	671.7	9.80	689.9	10.07	0.97

*calculated with measured slab thicknesses
**includes slab, buildups, and stay-in-place forms (nominal)

SLAB DATA

THICKNESS 8.86 in (nominal)

BUILD-UP 2.56 in (nominal)

REBAR	Size	Spacing
LONGITUDINAL	(metric)	(nominal)
Top:	#10	340 mm
Bottom:	#15	230 mm
TRANSVERSE		
Top:	#15	160 mm
Bottom:	#15	160 mm

GIRDER DEFLECTIONS (data in inches, full span concrete deflections less bearing settlement)

MEASURED

	1/4 Span Loading			1/2 Span Loading		
Point	1/4	1/2	3/4	1/4	1/2	3/4
G12	0.53	0.88	0.78	1.02	1.66	1.37
G13	0.45	0.82	0.75	0.93	1.59	1.33
G15	0.32	0.64	0.61	0.75	1.36	1.19
G16	0.25	0.54	0.54	0.62	1.14	1.02
G17	0.22	0.44	0.43	0.55	0.93	0.80
	3/4 Span Loading			Full Span Loading		
Point	1/4	1/2	3/4	1/4	1/2	3/4
G12	2.19	3.05	2.21	2.31	3.18	2.23
G13	2.14	3.06	2.24	2.40	3.29	2.29
G15	1.96	2.95	2.19	2.46	3.47	2.43
G16	1.70	2.66	2.00	2.28	3.28	2.29
G17	1.48	2.32	1.73	2.11	3.08	2.16

MEASURED BEARING

	Total Settlement		
Point	End 1	End 2	Avg.
G12	0.14	0.08	0.11
G13	---	---	---
G15	0.10	0.14	0.12
G16	0.04	0.23	0.13
G17	0.11	0.04	0.07

PREDICTED AND SURVEYED

	Original			Revision		
Point	1/4	1/2	3/4	1/4	1/2	3/4
G12	3.88	5.39	3.88	3.23	4.49	3.23
G13	3.88	5.39	3.88	3.44	4.80	3.44
G15	3.84	5.39	3.84	3.41	4.76	3.41
G16	3.68	4.33	3.68	3.07	4.33	3.07
G17	2.13	2.99	2.13	2.60	3.62	2.60
	Adjusted Revision***			Surveyed		
Point	1/4	1/2	3/4	1/4	1/2	3/4
G12	3.16	4.39	3.16	2.06	3.44	2.33
G13	3.34	4.65	3.34	2.23	3.02	2.19
G15	3.28	4.59	3.28	2.36	3.42	2.52
G16	2.90	4.08	2.90	1.99	3.18	2.47
G17	2.53	3.53	2.53	1.97	2.96	2.29

***predicted revision multiplied by the ratio of deck concrete to total slab weigh

FIELD MEASUREMENT SUMMARY

PROJECT NUMBER: I-306DC (I-85 over Camden Avenue, Northbound Lanes)
MEASUREMENT DATE: November 4, 2003

GIRDER DEFLECTIONS
CROSS SECTION VIEW

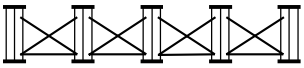

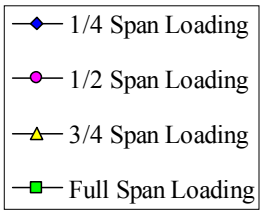

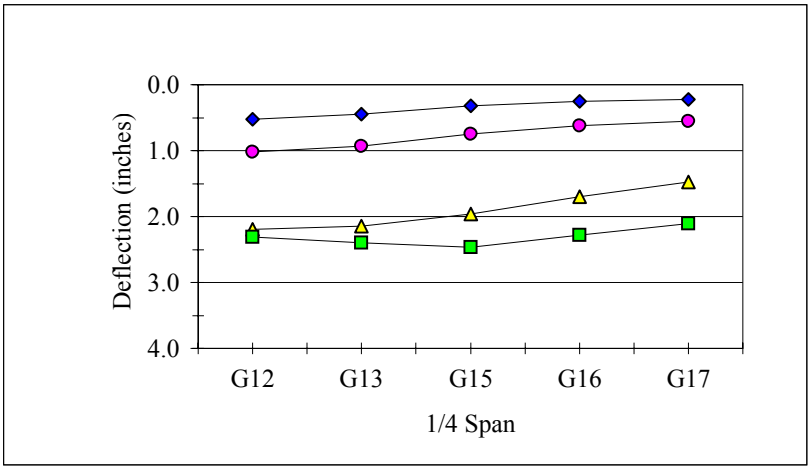

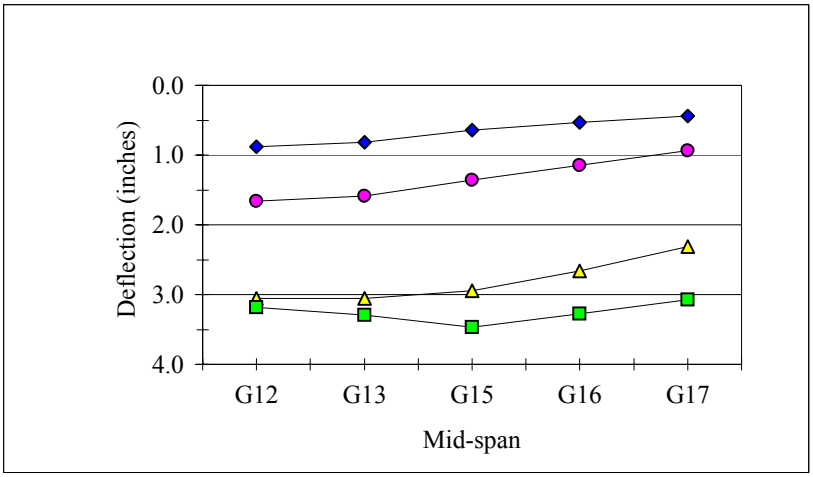

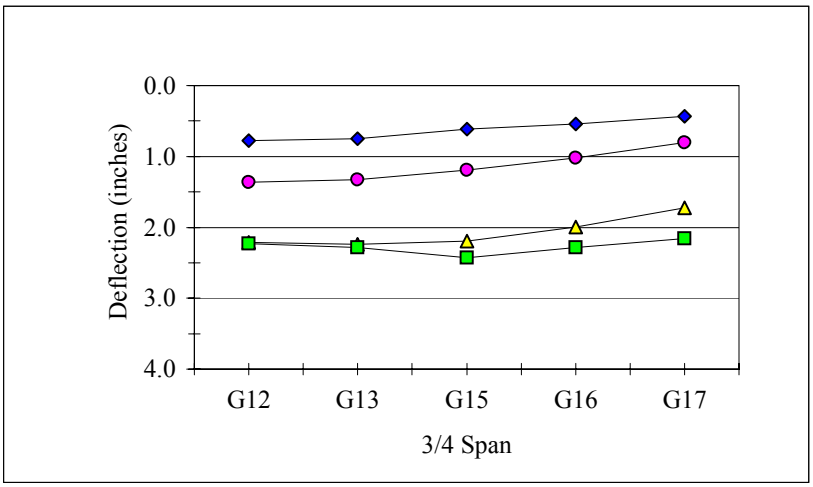

FIELD MEASUREMENT SUMMARY

PROJECT NUMBER: I-306DC (I-85 over Camden Avenue, Northbound Lanes)
MEASUREMENT DATE: November 4, 2003

SLAB THICKNESS
CROSS SECTION VIEW

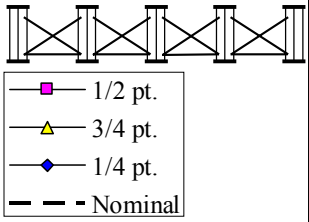

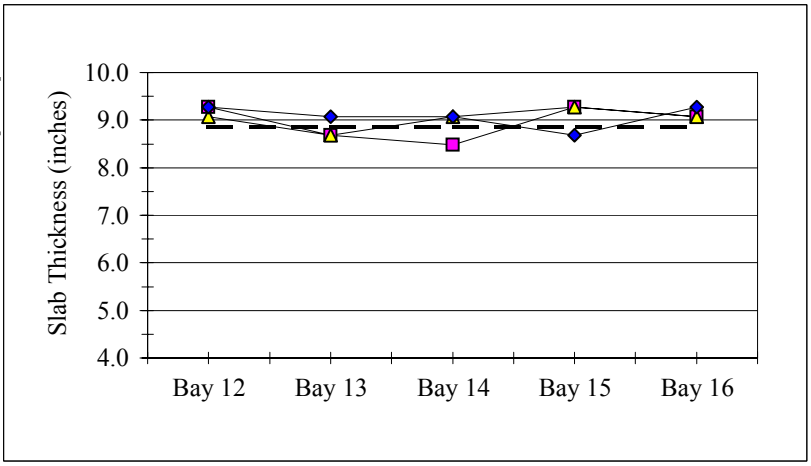

GIRDER DEFLECTIONS
ELEVATION VIEW

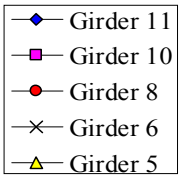

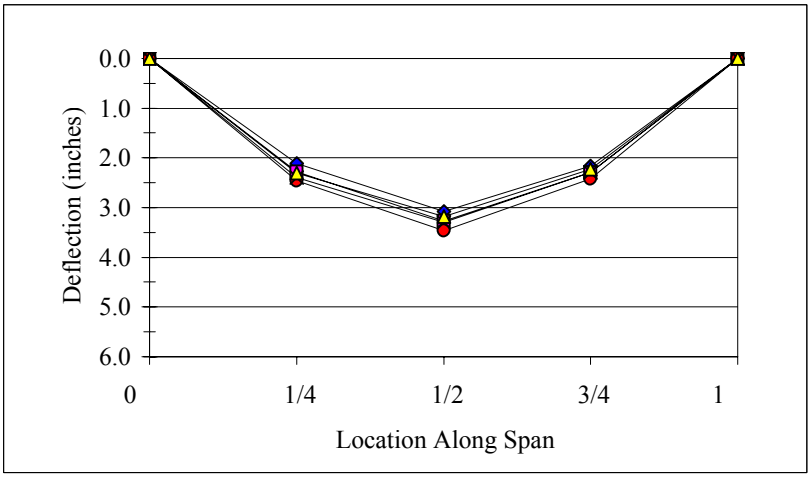

GIRDER DEFLECTIONS
CROSS SECTION VIEW

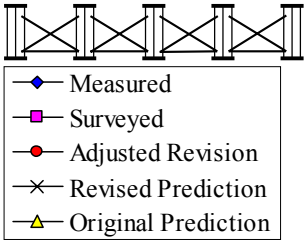

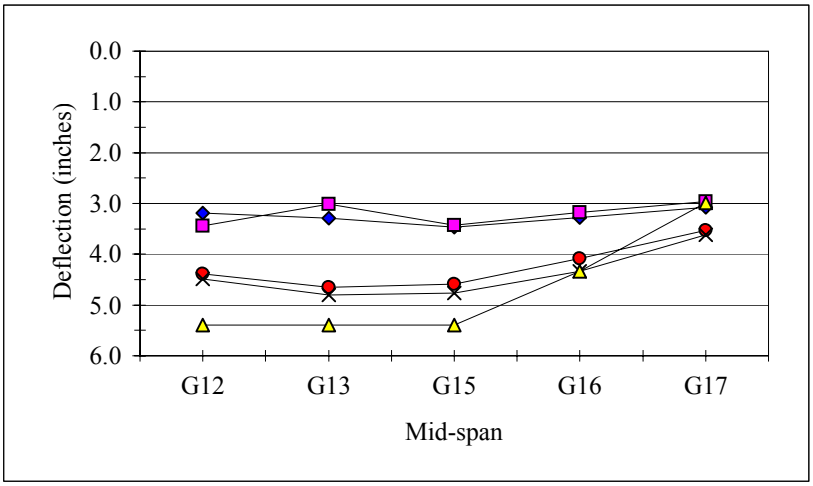

ANSYS FINITE ELEMENT MODELING SUMMARY

PROJECT NUMBER: I-306DC (I-85 over Camden Avenue, Northbound Lanes)

MODEL PICTURE (Steel only, isometric view)

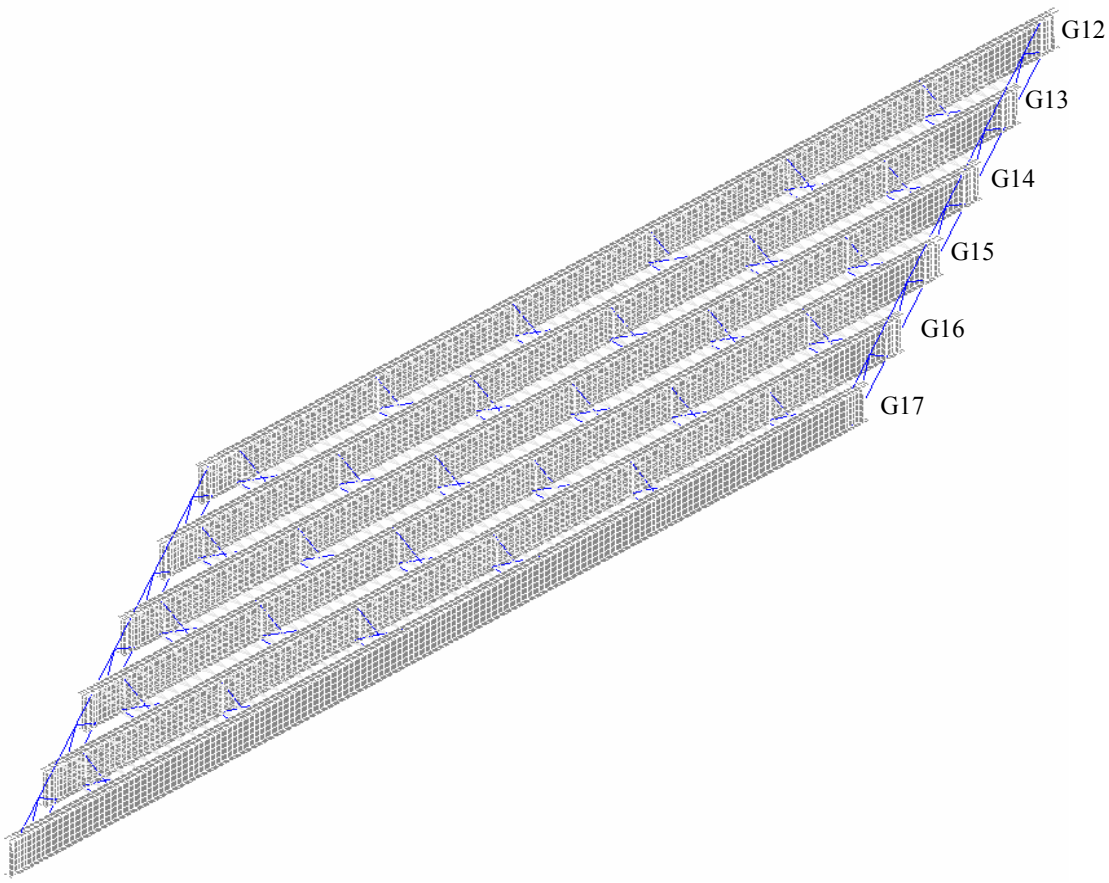

ANSYS FINITE ELEMENT MODELING SUMMARY

PROJECT NUMBER: I-306DC (I-85 over Camden Avenue, Northbound Lanes)

MODEL DESCRIPTION

COMPONENT	**Element Type**
Girder:	SHELL93
Connector Plates:	SHELL93
Stiffener Plates:	SHELL93
Cross-frame Members:	LINK8 (diagonal)
	LINK8 (horizontal)
End Diaphragm:	LINK8 (diagonal)
	BEAM4 (diagonal)
Stay-in-place Deck Forms:	LINK8
Concrete Slab:	SHELL63
Shear Studs:	MPC184

APPLIED LOADS

Girder	*Load	
	lb/ft	N/mm
G12	674.3	9.84
G13	1068.1	15.59
G14	1065.4	15.55
G15	1062.8	15.51
G16	1040.3	15.18
G17	671.7	9.80

*applied as a uniform pressure to area of top flange

GIRDER DEFLECTIONS

	ANSYS (load step 1)			ANSYS (load step 2)		
Point	**1/4**	**1/2**	**3/4**	**1/4**	**1/2**	**3/4**
G12	0.38	**0.61**	0.51	0.97	**1.45**	1.06
G13	0.33	**0.54**	0.48	0.85	**1.32**	1.00
G15	0.29	**0.48**	0.44	0.80	**1.25**	0.95
G16	0.30	**0.48**	0.43	0.83	**1.28**	0.96
G17	0.32	**0.51**	0.45	0.88	**1.37**	1.04
	ANSYS (load step 3)			**ANSYS (load step 4)**		
Point	**1/4**	**1/2**	**3/4**	**1/4**	**1/2**	**3/4**
G12	1.03	**1.35**	0.87	0.45	**0.51**	0.31
G13	0.95	**1.26**	0.81	0.43	**0.48**	0.29
G15	0.95	**1.26**	0.80	0.45	**0.50**	0.30
G16	0.99	**1.31**	0.84	0.48	**0.54**	0.33
G17	1.05	**1.42**	0.94	0.50	**0.60**	0.37
	Measured			**ANSYS (no SIP)**		
Point	**1/4**	**1/2**	**3/4**	**1/4**	**1/2**	**3/4**
G12	2.31	**3.18**	2.23	2.74	**3.82**	2.72
G13	2.40	**3.29**	2.29	2.75	**3.81**	2.71
G15	2.46	**3.47**	2.43	2.76	**3.87**	2.78
G16	2.28	**3.28**	2.29	2.69	**3.79**	2.73
G17	2.11	**3.08**	2.16	2.70	**3.80**	2.73
	ANSYS (SIP)			***ANSYS (p.c., SIP)**		
Point	**1/4**	**1/2**	**3/4**	**1/4**	**1/2**	**3/4**
G12	2.84	**3.93**	2.77	2.82	**3.92**	2.75
G13	2.57	**3.61**	2.59	2.56	**3.60**	2.58
G15	2.52	**3.50**	2.50	2.50	**3.49**	2.49
G16	2.60	**3.63**	2.59	2.59	**3.60**	2.56
G17	2.76	**3.94**	2.85	2.75	**3.90**	2.80

*superimposed from load steps 1-4 for partial composite action

ANSYS FINITE ELEMENT MODELING SUMMARY

PROJECT NUMBER: I-306DC (I-85 over Camden Avenue, Northbound Lanes)

GIRDER DEFLECTIONS
CROSS SECTION VIEW

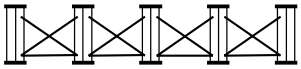

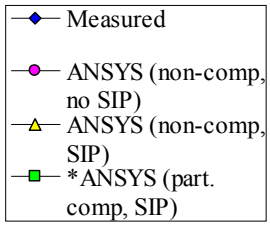

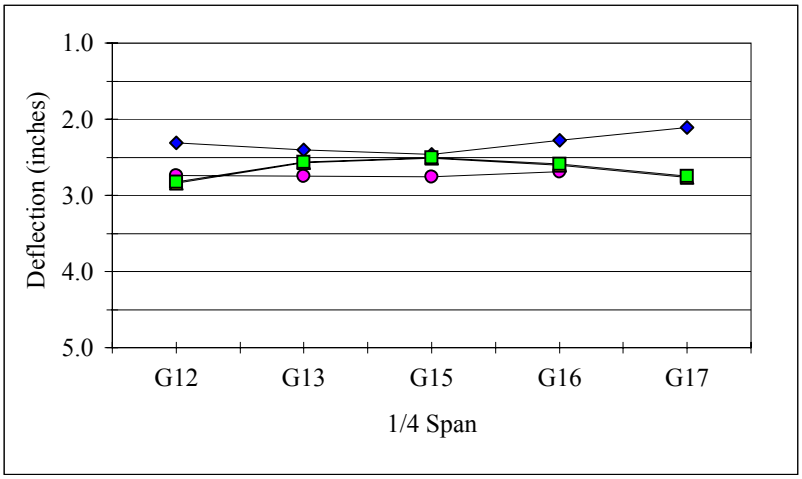

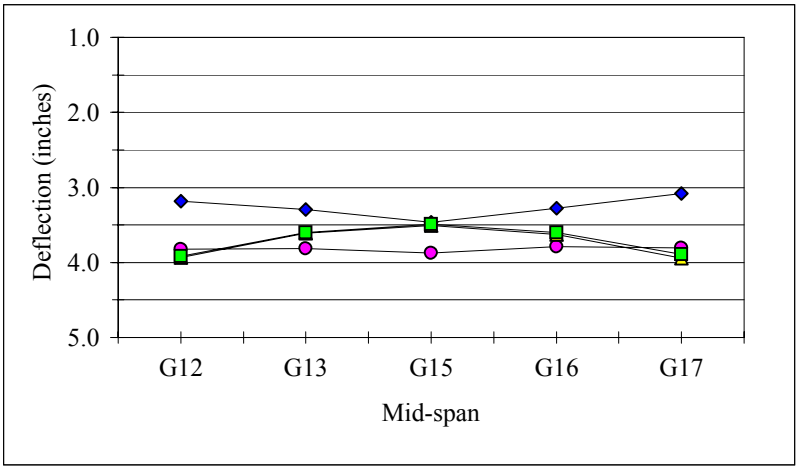

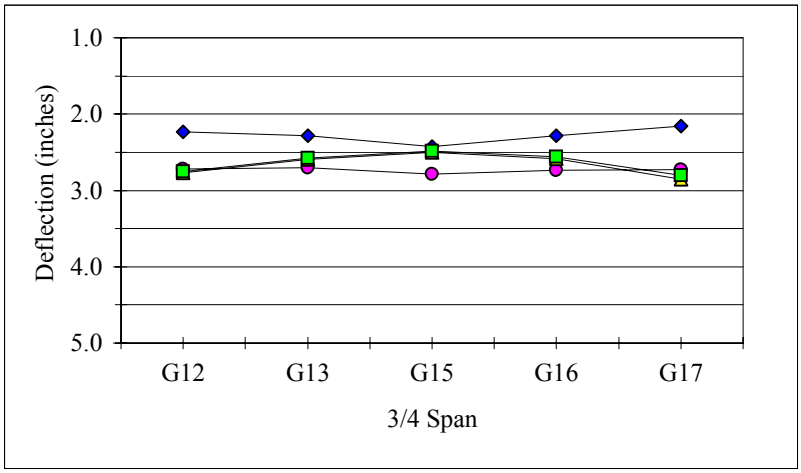

Appendix H

Deflection Summary for the Camden SBL Bridge

This appendix contains a detailed description of the Camden SBL Bridge including bridge geometry, material data, cross-frame type and size, and dead loads calculated from slab geometry. Tables and graphs of the field measured non-composite girder deflections are included.

A summary of the ANSYS finite element model created for the Camden SBL Bridge is also included in this appendix. This summary includes a picture of the ANSYS model, details about the elements used in the model generation, the loads applied to the model, and tables and graphs of the deflections predicted by the model.

FIELD MEASUREMENT SUMMARY

PROJECT NUMBER: I-306DC (I-85 over Camden Avenue, Southbound Lanes)
MEASUREMENT DATE: October 22, 2003

BRIDGE DESCRIPTION

TYPE	Three Span Simple	(center span measured)
LENGTH	144.25 ft (43.97 m)	
NUMBER OF GIRDERS	6	
GIRDER SPACING	8.69 ft (2.65 m)	
SKEW	150 deg	
OVERHANG	none	
BEARING TYPE	Elastomeric Pad	

MATERIAL DATA

STRUCTURAL STEEL	**Grade**	**Yield Strength**
Girder:	AASHTO M270	50 ksi (345 MPa)
Other:	AASHTO M270	50 ksi (345 MPa)

CONCRETE UNIT WEIGHT	150 pcf (nominal)
SIP FORM WEIGHT	3 psf (nominal)

GIRDER DATA

LENGTH	144.25 ft (43.97 m)
TOP FLANGE WIDTH	16.14 in (410 mm)
BOTTOM FLANGE WIDTH	18.90 in (480 mm)
WEB THICKNESS	0.63 in (16 mm)
WEB DEPTH	66.14 in (1680 mm)

FLANGES	**Thickness**	**Begin**	**End**
Top:	0.98 in (25 mm)	0.00	36.03 ft (10.98 m)
	1.18 in (30 mm)	36.03 ft (10.98 m)	72.12 ft (21.98 m)
Bottom:	1.10 in (28 mm)	0.00	36.03 ft (10.98 m)
	1.77 in (45 mm)	36.03 ft (10.98 m)	72.12 ft (21.98 m)

STIFFENERS	
Longitudinal:	NONE
Bearing:	PL 0.71" × 6.65" (18 mm × 169 mm)
Intermediate:	PL 0.39" × NA (10 mm × NA, connector plate)
End Bent Connector:	PL 0.55" × NA (14 mm × NA, connector plate)

CROSS-FRAME DATA

	Type	**Diagonals**	**Horizontals**
END	K	WT 7×17	MC 18×42.7 (top) WT 7×17 (bottom)
INTERMEDIATE	X	L 3½×3½×⅜	L 3½×3½×⅜ (bottom)

FIELD MEASUREMENT SUMMARY

Project Number: I-306DC (I-85 over Camden Avenue, Southbound Lanes)
Measurement Date: October 22, 2003

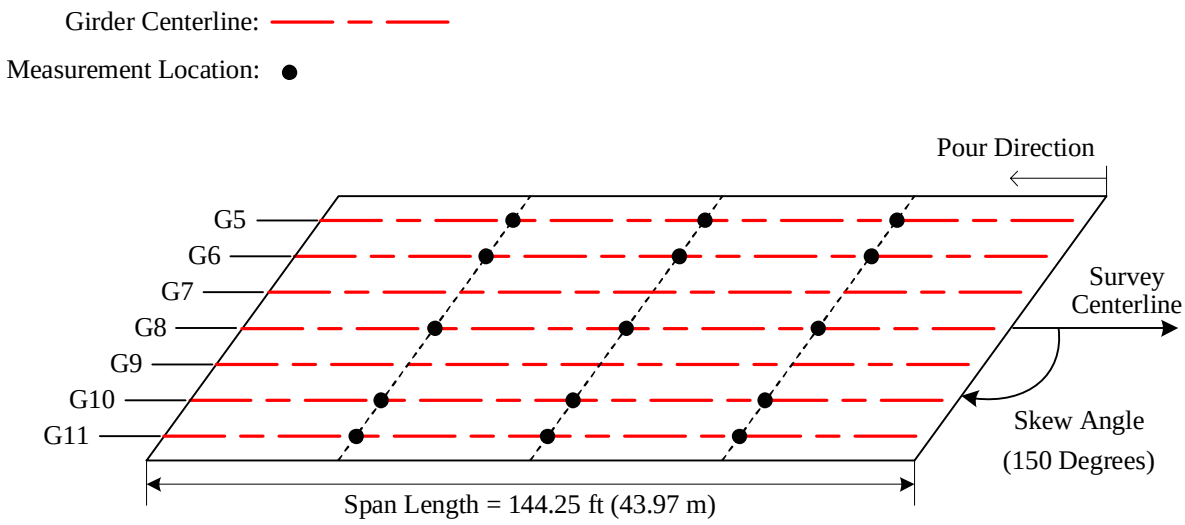

(a) Plan View (Not to Scale)

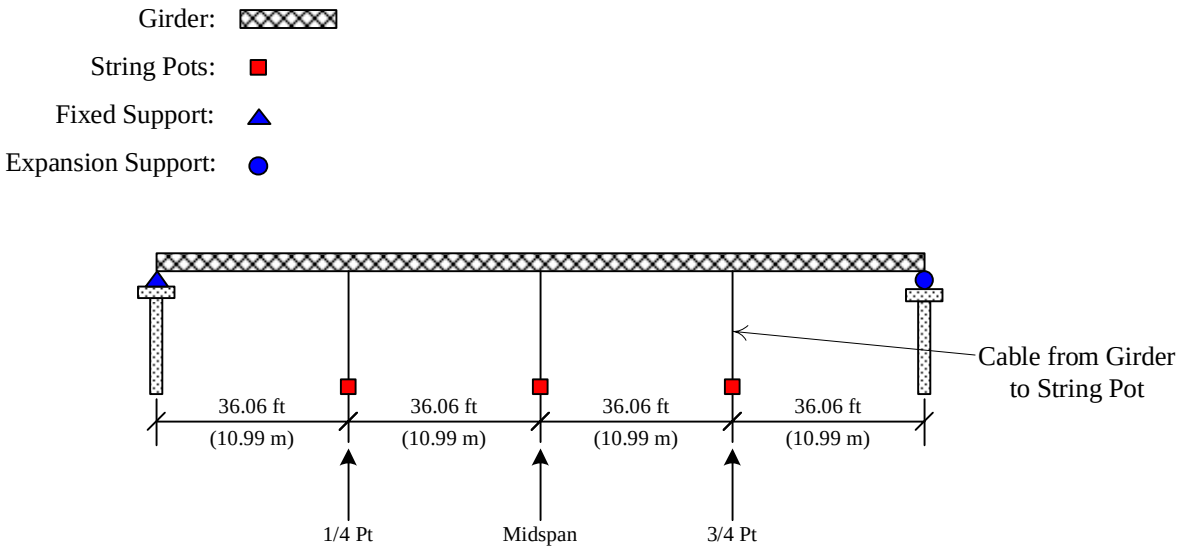

(b) Elevation View (Not to Scale)

Plan and Elevation View of the Camden SB Bridge (Durham, NC)

FIELD MEASUREMENT SUMMARY

PROJECT NUMBER: I-306DC (I-85 over Camden Avenue, Southbound Lanes)
MEASUREMENT DATE: October 22, 2003

DECK LOADS

	Concrete*		Deck Slab**		Ratio
Girder	**lb/ft**	**N/mm**	**lb/ft**	**N/mm**	
G5	648.8	9.47	689.9	10.07	0.94
G6	1028.0	15.00	1103.3	16.10	0.93
G8	1044.0	15.24	1103.3	16.10	0.95
G10	1053.4	15.37	1103.3	16.10	0.95
G11	649.8	9.48	689.9	10.07	0.94

*calculated with measured slab thicknesses
**includes slab, buildups, and stay-in-place forms (nominal)

SLAB DATA

THICKNESS 8.86 in (nominal)

BUILD-UP 2.56 in (nominal)

REBAR	**Size**	**Spacing**
LONGITUDINAL	(metric)	(nominal)
Top:	#10	340 mm
Bottom:	#15	230 mm
TRANSVERSE		
Top:	#15	160 mm
Bottom:	#15	160 mm

GIRDER DEFLECTIONS (data in inches, full span concrete deflections less bearing settlement)

MEASURED

	1/4 Span Loading			1/2 Span Loading		
Point	**1/4**	**1/2**	**3/4**	**1/4**	**1/2**	**3/4**
G5	0.18	0.21	0.17	0.66	0.84	0.60
G6	0.26	0.29	0.22	0.89	1.03	0.66
G8	0.45	0.50	0.43	1.21	1.48	1.02
G10	0.52	0.58	0.31	1.30	1.62	0.98
G11	0.53	0.69	0.45	1.27	1.70	1.15
	3/4 Span Loading			**Full Span Loading**		
Point	**1/4**	**1/2**	**3/4**	**1/4**	**1/2**	**3/4**
G5	1.63	2.17	1.47	2.06	2.97	2.07
G6	1.77	2.33	1.54	2.18	3.11	2.15
G8	2.02	2.75	1.93	2.25	3.27	2.37
G10	2.02	2.79	1.35	2.12	3.11	1.46
G11	1.98	2.89	2.05	1.90	2.90	2.07

MEASURED BEARING

	Total Settlement		
Point	**End 1**	**End 2**	**Avg.**
G5	0.23	0.31	0.27
G6	0.194	0.162	0.18
G8	0.230	0.243	0.24
G10	---	---	---
G11	---	---	---

PREDICTED AND SURVEYED

	Original			Revision		
Point	**1/4**	**1/2**	**3/4**	**1/4**	**1/2**	**3/4**
G5	2.30	3.19	2.30	2.74	3.82	2.74
G6	3.84	5.39	3.84	3.23	4.49	3.23
G8	3.76	5.28	3.76	3.43	4.80	3.43
G10	3.88	5.39	3.88	2.83	3.98	2.83
G11	3.76	5.28	3.76	2.83	3.98	2.83
	Adjusted Revision* **			**Surveyed**		
Point	**1/4**	**1/2**	**3/4**	**1/4**	**1/2**	**3/4**
G5	2.57	3.59	2.57	2.37	3.47	2.41
G6	3.01	4.18	3.01	2.54	3.68	2.54
G8	3.24	4.55	3.24	2.52	3.86	2.64
G10	2.71	3.80	2.71	2.26	3.44	1.55
G11	2.67	3.75	2.67	2.17	3.16	2.13

***predicted revision multiplied by the ratio of deck concrete to total slab weigh

FIELD MEASUREMENT SUMMARY

PROJECT NUMBER: I-306DC (I-85 over Camden Avenue, Southbound Lanes)
MEASUREMENT DATE: October 22, 2003

GIRDER DEFLECTIONS
CROSS SECTION VIEW

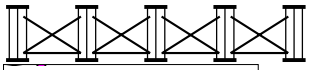

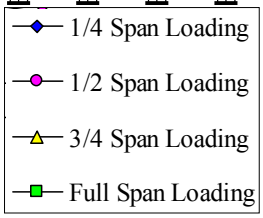

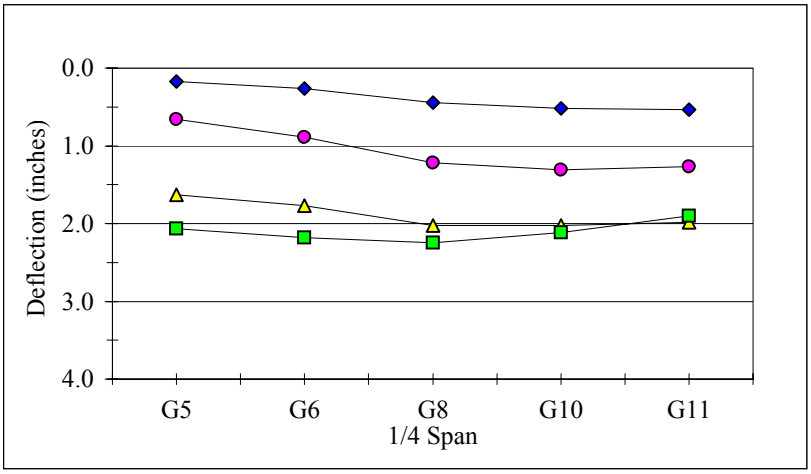

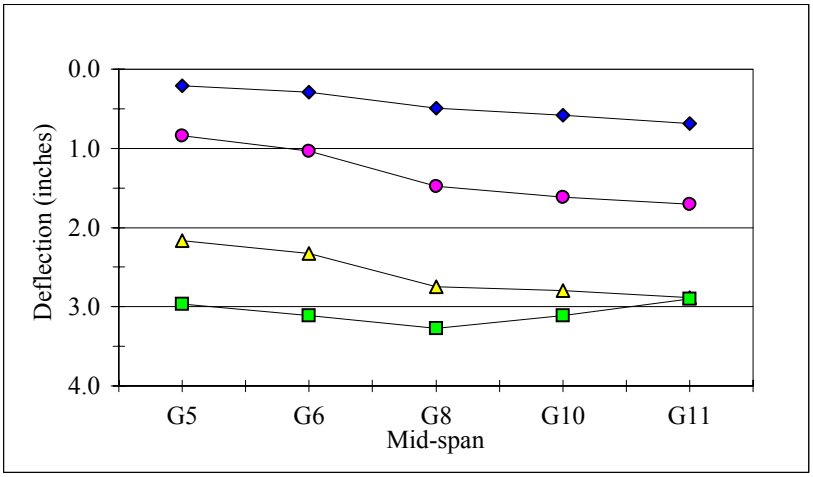

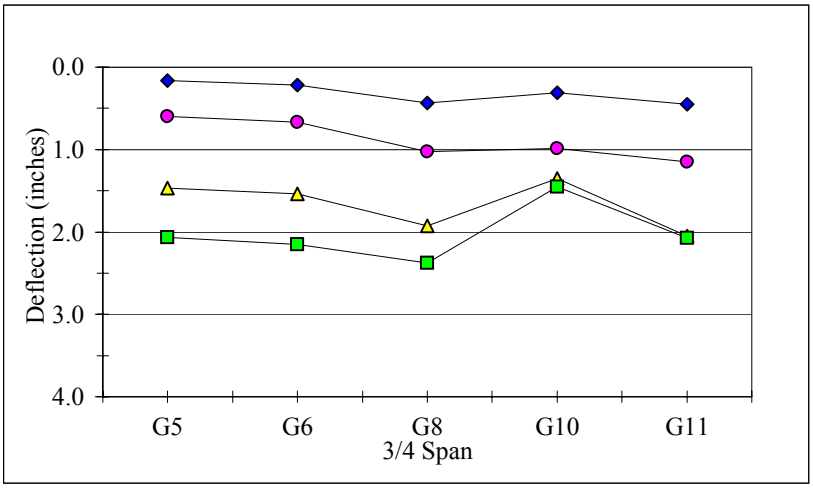

FIELD MEASUREMENT SUMMARY

PROJECT NUMBER: I-306DC (I-85 over Camden Avenue, Southbound Lanes)
MEASUREMENT DATE: October 22, 2003

SLAB THICKNESS
CROSS SECTION VIEW

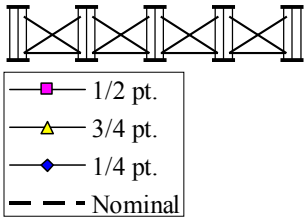

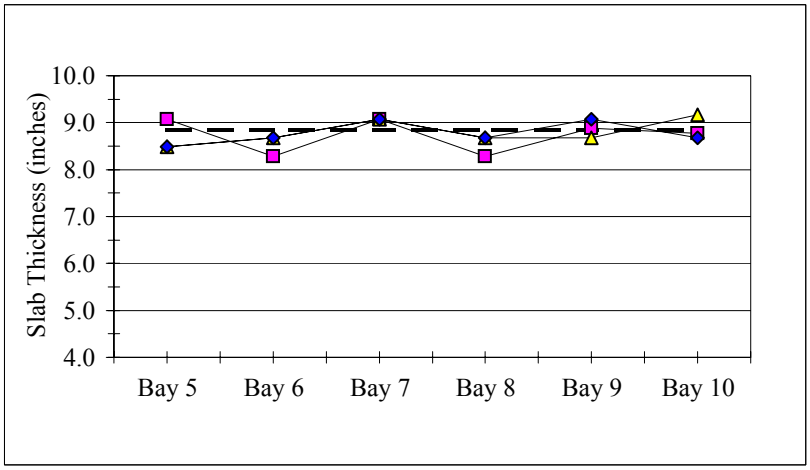

GIRDER DEFLECTIONS
ELEVATION VIEW

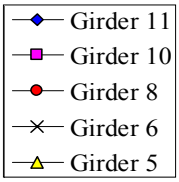

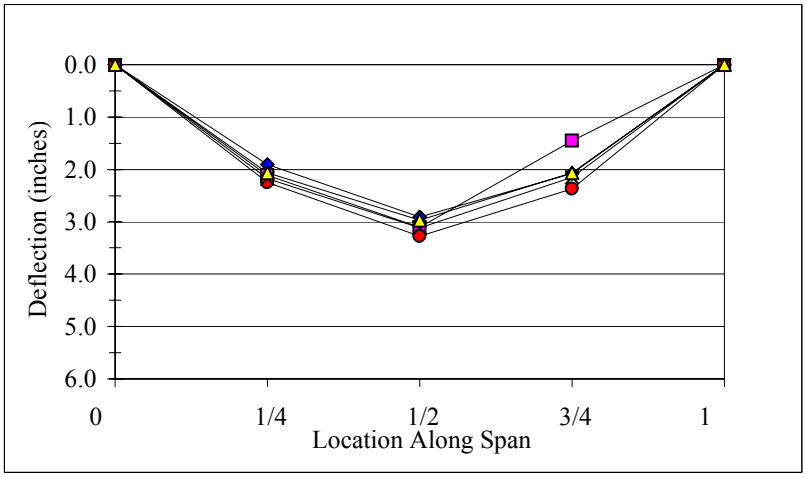

GIRDER DEFLECTIONS
CROSS SECTION VIEW

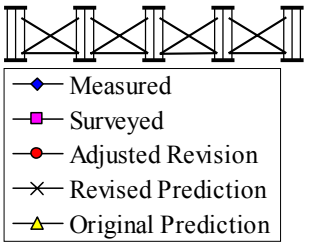

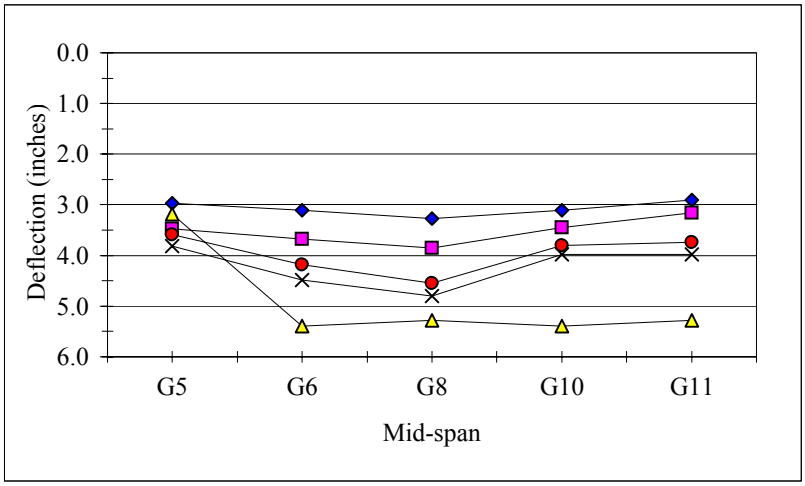

ANSYS FINITE ELEMENT MODELING SUMMARY

PROJECT NUMBER: I-306DC (I-85 over Camden Avenue, Southbound Lanes)

MODEL PICTURE (Steel only, isometric view)

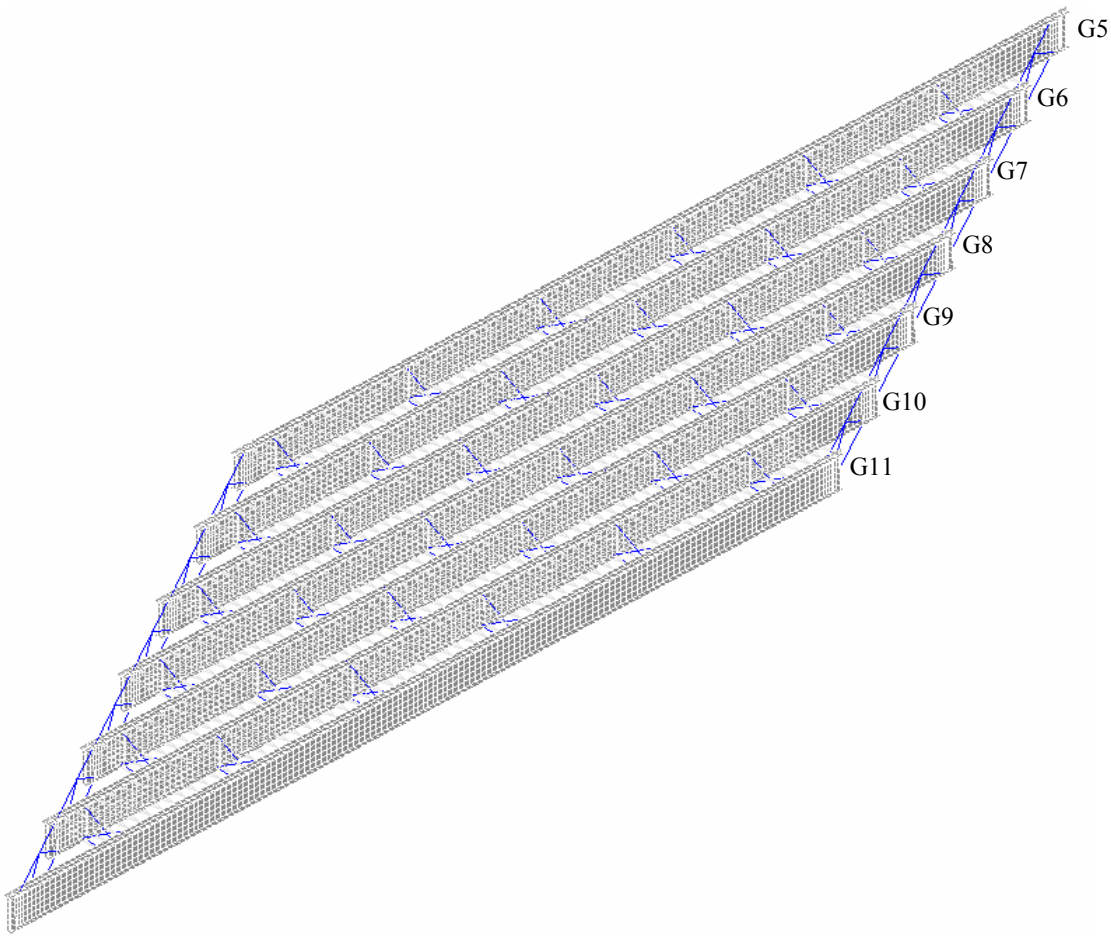

ANSYS FINITE ELEMENT MODELING SUMMARY

PROJECT NUMBER: I-306DC (I-85 over Camden Avenue, Southbound Lanes)

MODEL DESCRIPTION

COMPONENT	**Element Type**
Girder:	SHELL93
Connector Plates:	SHELL93
Stiffener Plates:	SHELL93
Cross-frame Members:	LINK8 (diagonal)
	LINK8 (horizontal)
End Diaphragm:	LINK8 (diagonal)
	BEAM4 (diagonal)
Stay-in-place Deck Forms:	LINK8
Concrete Slab:	SHELL63
Shear Studs:	MPC184

APPLIED LOADS

Girder	***Load**	
	lb/ft	**N/mm**
G5	648.8	9.47
G6	1028.0	15.00
G7	1036.0	15.12
G8	1044.0	15.24
G9	1048.7	15.30
G10	1053.4	15.37
G11	649.8	9.48

*applied as a uniform pressure to area of top flange

GIRDER DEFLECTIONS

	ANSYS (load step 1)			**ANSYS (load step 2)**		
Point	**1/4**	**1/2**	**3/4**	**1/4**	**1/2**	**3/4**
G5	0.38	**0.43**	0.26	0.90	**1.18**	0.74
G6	0.37	**0.41**	0.24	0.84	**1.11**	0.70
G8	0.39	**0.42**	0.25	0.83	**1.11**	0.69
G10	0.41	**0.46**	0.28	0.85	**1.15**	0.74
G11	0.42	**0.50**	0.32	0.88	**1.23**	0.82
	ANSYS (load step 3)			**ANSYS (load step 4)**		
Point	**1/4**	**1/2**	**3/4**	**1/4**	**1/2**	**3/4**
G5	0.80	**1.23**	0.89	0.27	**0.45**	0.39
G6	0.73	**1.15**	0.85	0.25	**0.43**	0.39
G8	0.68	**1.10**	0.84	0.23	**0.41**	0.39
G10	0.67	**1.09**	0.83	0.23	**0.40**	0.37
G11	0.70	**1.14**	0.88	0.24	**0.41**	0.38
	****Adjusted Measured**			**ANSYS (no SIP)**		
Point	**1/4**	**1/2**	**3/4**	**1/4**	**1/2**	**3/4**
G5	2.06	**2.97**	2.07	2.29	**3.22**	2.28
G6	2.18	**3.11**	2.15	2.35	**3.28**	2.30
G8	2.25	**3.27**	2.37	2.45	**3.46**	2.45
G10	2.12	**3.11**	2.12	2.31	**3.29**	2.36
G11	1.90	**2.90**	2.07	2.26	**3.22**	2.29
	ANSYS (SIP)			*****ANSYS (p.c., SIP)**		
Point	**1/4**	**1/2**	**3/4**	**1/4**	**1/2**	**3/4**
G5	2.44	**3.39**	2.35	2.36	**3.29**	2.29
G6	2.24	**3.15**	2.23	2.19	**3.09**	2.19
G8	2.16	**3.06**	2.18	2.14	**3.04**	2.17
G10	2.19	**3.12**	2.23	2.16	**3.09**	2.22
G11	2.28	**3.33**	2.41	2.24	**3.29**	2.39

**only adjustment is the 3/4 span deflection of girder 10, (set equal to 1/4 span deflection of girder 10)

***superimposed from load steps 1-4 for partial composite action

ANSYS FINITE ELEMENT MODELING SUMMARY

PROJECT NUMBER: I-306DC (I-85 over Camden Avenue, Southbound Lanes)

GIRDER DEFLECTIONS*
CROSS SECTION VIEW

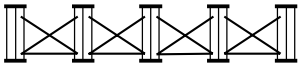

Measured
ANSYS (non-comp, no SIP)
ANSYS (non-comp, SIP)
*ANSYS (part. comp, SIP)

*using adjusted 3/4 span deflections (see page D-7)

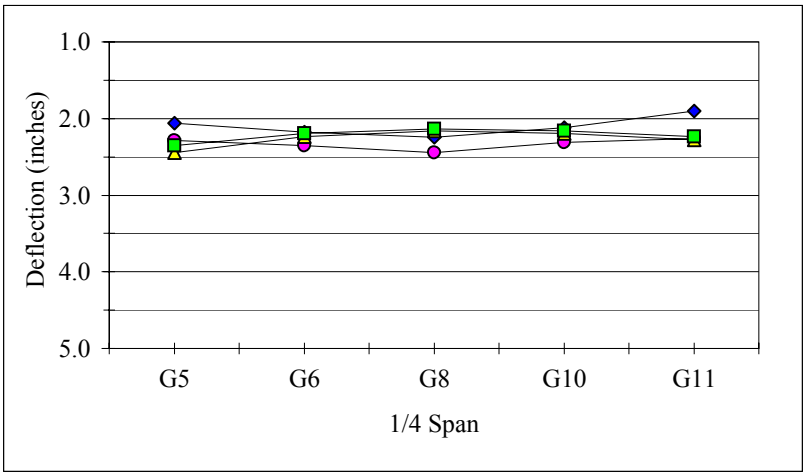

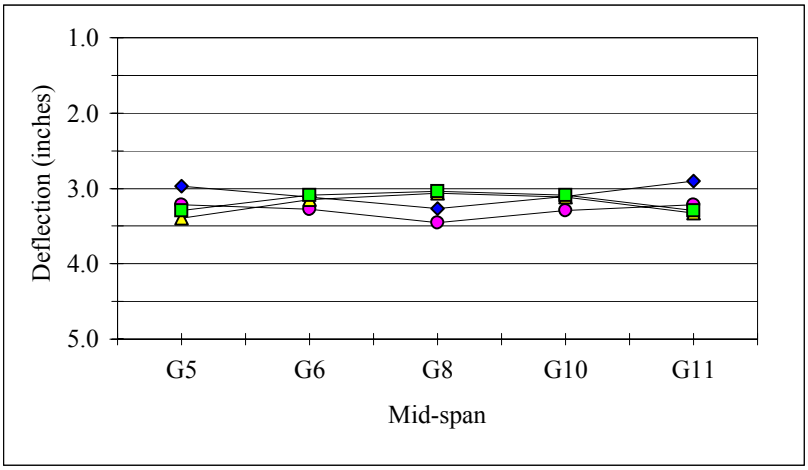

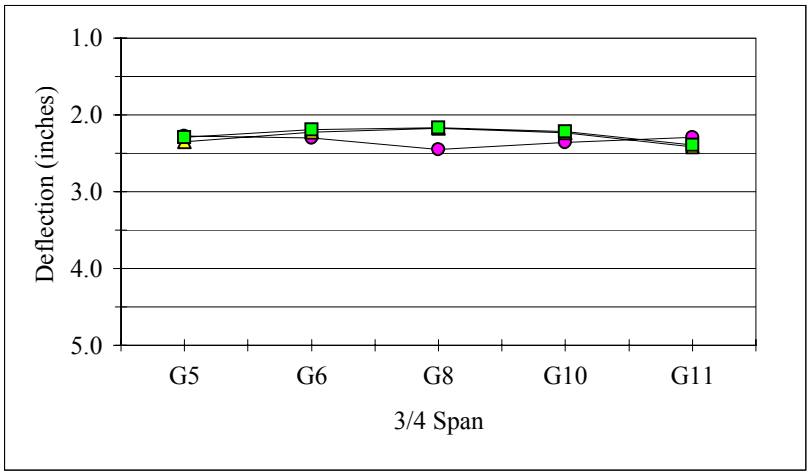

Appendix I

Deflection Summary for the Wilmington St Bridge

This appendix contains a detailed description of the Wilmington St Bridge including bridge geometry, material data, cross frame type and size, and dead loads calculated from slab geometry. Illustrations detailing the bridge geometry and field measurement locations are included, along with tables and graphs of the field measured non-composite girder deflections.

A summary of the ANSYS finite element model created for the Wilmington St Bridge is also included in this appendix. This summary includes a picture of the ANSYS model, details about the elements used in the model generation, the loads applied to the model, and tables and graphs of the deflections predicted by the model.

FIELD MEASUREMENT SUMMARY

PROJECT NUMBER: B-3257 (South Wilmington Street Bridge)
MEASUREMENT DATE: November 1, 2004

BRIDGE DESCRIPTION

TYPE	One Span Simple
LENGTH	149.50 ft (44.85 m)
NUMBER OF GIRDERS	5
GIRDER SPACING	8.25 ft (2.475 m)
SKEW	152 deg
OVERHANG	3.042 ft (Overhang Side)
	1 ft (ADJ to Stage I side)
BEARING TYPE	Pot Bearing

MATERIAL DATA

STRUCTURAL STEEL	**Grade**	**Yield Strength**
Girder:	AASHTO M270	50 ksi (345 MPa)
Other:	AASHTO M270	50 ksi (345 MPa)

CONCRETE UNIT WEIGHT	118 pcf (measured)
SIP FORM WEIGHT	3 psf (nominal)

GIRDER DATA

LENGTH	149.50 ft (44.85 m)
WEB THICKNESS	0.5 in (13 mm)
WEB DEPTH	54 in (1371.6 mm)
TOP FLANGE WIDTH	16 in (406.4 mm)
BOTTOM FLANGE WIDTH	20 in (508.0 mm)

	Flange Thickness	**Begin**	**End**
Top:	1 in (25.4 mm)	0.00	31.25 ft (9.375 m)
	1.375 in (34.93 mm)	31.25 ft (9.375 m)	118.25 ft (35.475 m)
	1 in (25.4 mm)	118.25 ft (35.475 m)	149.5 ft (44.85 m)
Bottom:	1.125 ft (28.575 mm)	0.00	31.25 ft (9.375 m)
	1.875 in (34.93 mm)	31.25 ft (9.375 m)	118.25 ft (35.475 m)
	1.125 ft (28.575 mm)	118.25 ft (35.475 m)	149.5 ft (44.85 m)

CROSS-FRAME DATA

	Diagonals	**Horizontals**	**Verticals**
END BENT (Type K)	WT 4×12	C 15×50 (top) WT 4×12 (bottom)	NA
MIDDLE BENT	NA	NA	NA
INTERMEDIATE (Type K)	L 3×3×5/16	L 3×3×5/16 (bottom)	NA

FIELD MEASUREMENT SUMMARY

PROJECT NUMBER: B-3257 (South Wilmington Street Bridge)
MEASUREMENT DATE: November 1, 2004

STIFFENERS

Longitudinal:	NA
Bearing:	PL 1" × 7" (25.4 mm × 177.8 mm)
Intermediate:	PL 0.5 " x NA (12.7 mm x NA, connector Plate)
	No Intermediate Siffeners
Middle Bearing:	NA
End Bent Connector:	PL 0.5 " x NA (12.7 mm x NA, connector Plate)

SLAB DATA

THICKNESS	8.5 in (215.9 mm)	nominal
BUILD-UP	2.5 in (63.5 mm)	nominal

LONGITUDINAL REBAR	SIZE (US)	SPACING (nominal)
Top:	#4	18.0 in (457.2 mm)
Bottom:	#5	10.0 in (254.0 mm)
TRANSVERSE REBAR		
Top:	#5	7.0 in (177.8 mm)
Bottom:	#5	7.0 in (177.8 mm)

DECK LOADS

Girder	Concrete[1]		Slab[2]		Ratio
	lb/ft	N/mm	lb/ft	N/mm	
G6	518.71	7.57	549.54	8.02	0.94
G7	800.33	11.68	861.32	12.57	0.93
G8	769.50	11.23	831.17	12.13	0.93
G9	800.33	11.68	861.32	12.57	0.93
G10	743.46	10.85	774.30	11.30	0.96

[1] Calculated with measured slab thicknesses

[2] Includes slab, buildups, and stay-in-place forms (nominal)

FIELD MEASUREMENT SUMMARY

Project Number: B-3257 (South Wilmington Street Bridge)
Measurement Date: November 1, 2004

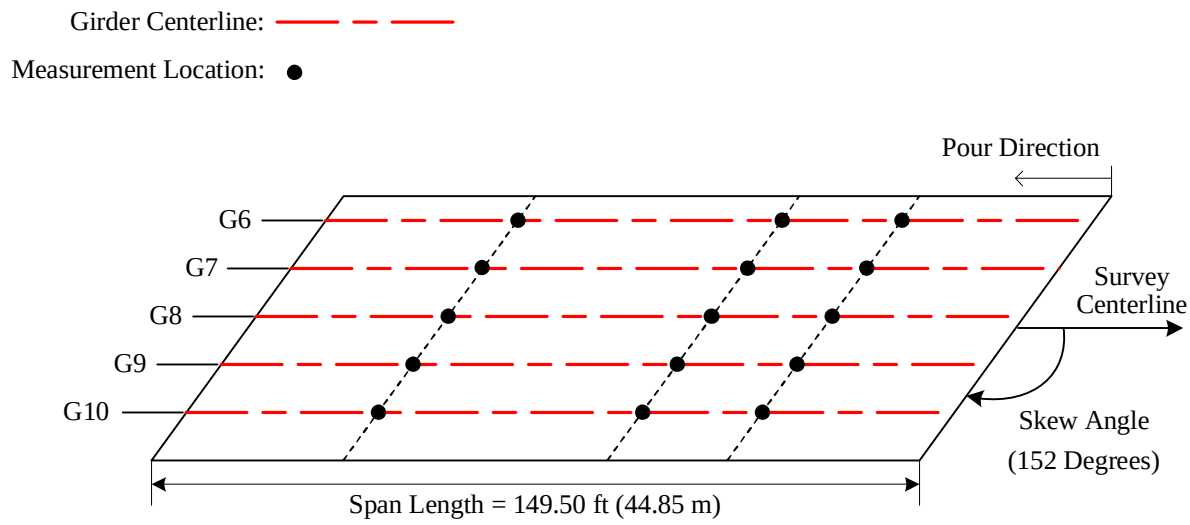

(a) Plan View (Not to Scale)

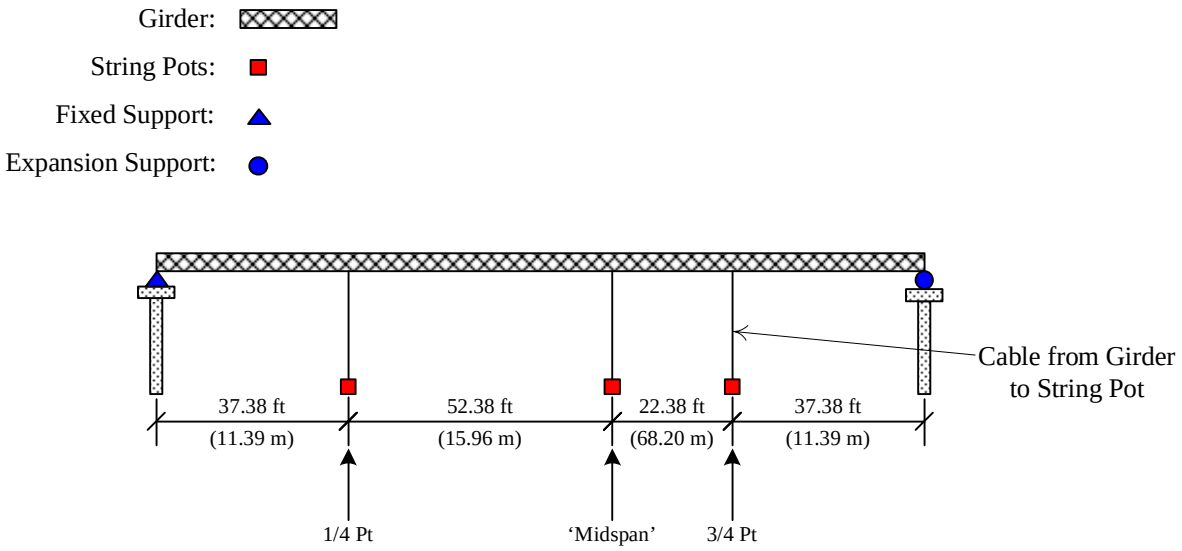

(b) Elevation View (Not to Scale)

Plan and Elevation View of the Wilmington St Bridge (Raleigh, NC)

FIELD MEASUREMENT SUMMARY

PROJECT NUMBER: B-3257 (South Wilmington Street Bridge)
MEASUREMENT DATE: November 1, 2004

BEARING SETTLEMENTS (data in inches)

	Pour 1 Settlement		
Point	**End 1**	**End 2**	**Avg.**
G6	---	---	---
G7	---	---	---
G8	---	---	---
G9	---	---	---
G10	---	---	---

GIRDER DEFLECTIONS (data in inches)
MEASURED

	1/4 Span Loading			Midspan[3] Loading		
Point	**1/4**	**Midspan**	**3/4**	**1/4**	**Midspan**	**3/4**
G6	1.52	2.01	1.30	2.28	3.01	2.13
G7	1.42	1.75	1.04	2.20	2.81	1.85
G8	1.36	1.65	0.94	2.15	2.80	1.79
G9	1.38	1.67	1.00	2.20	2.99	1.93
G10	1.59	1.93	1.04	2.60	3.46	2.15
	3/4 Span Loading			**Full Span Loading**		
Point	**1/4**	**Midspan**	**3/4**	**1/4**	**Midspan**	**3/4**
G6	2.68	3.88	2.93	2.64	3.80	2.83
G7	2.70	3.76	2.72	2.64	3.70	2.72
G8	2.72	3.84	2.80	2.72	3.78	2.80
G9	2.97	4.25	3.17	2.97	4.19	3.17
G10	3.66	5.10	3.64	3.62	5.04	3.70

[3] Midspan measurement location was 14.95 ft offset from actual midspan.

PREDICTIONS[4] (Single Girder-Line Model in SAP 2000)

Point	**1/4**	**Midspan**	**3/4**
G6	2.94	3.86	2.94
G7	4.53	5.96	4.53
G8	4.36	5.73	4.36
G9	4.53	5.96	4.53
G10	4.21	5.54	4.21

[4] Using measured slab thicknesses

FIELD MEASUREMENT SUMMARY

PROJECT NUMBER: B-3257 (South Wilmington Street Bridge)
MEASUREMENT DATE: November 1, 2004

GIRDER DEFLECTIONS
CROSS SECTION VIEW

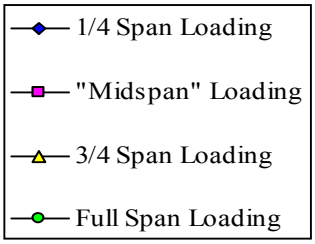

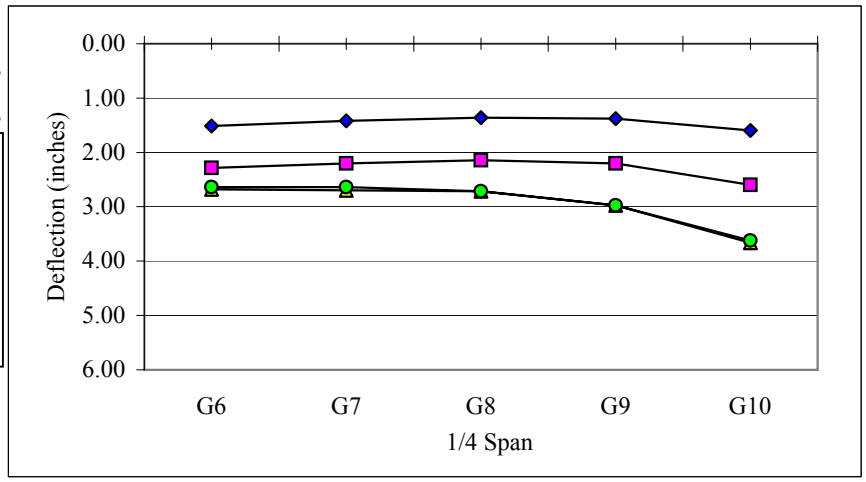

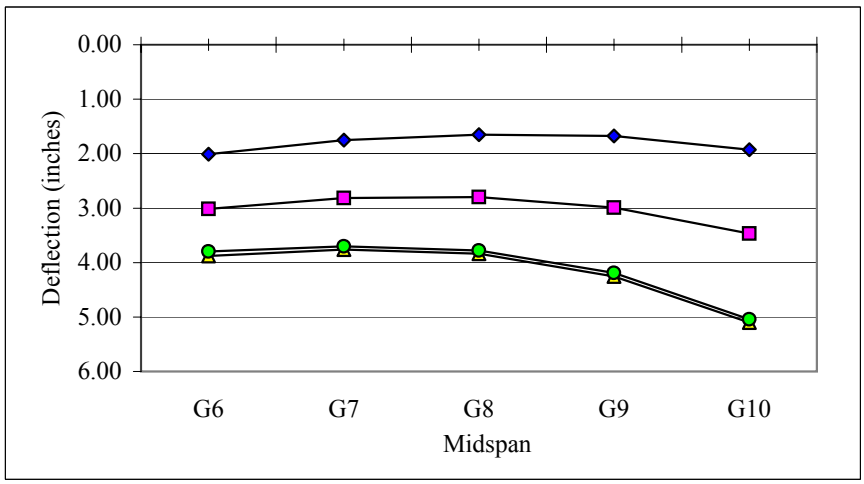

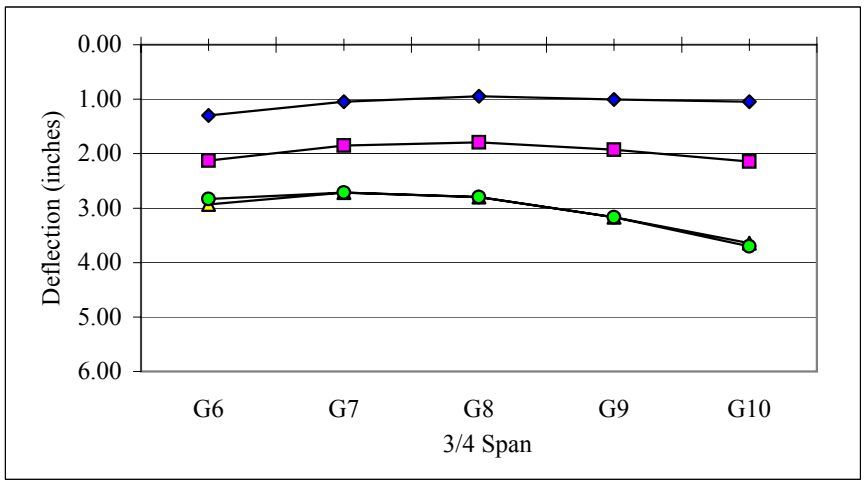

FIELD MEASUREMENT SUMMARY

PROJECT NUMBER: B-3257 (South Wilmington Street Bridge)
MEASUREMENT DATE: November 1, 2004

GIRDER DEFLECTIONS
CROSS SECTION VIEW

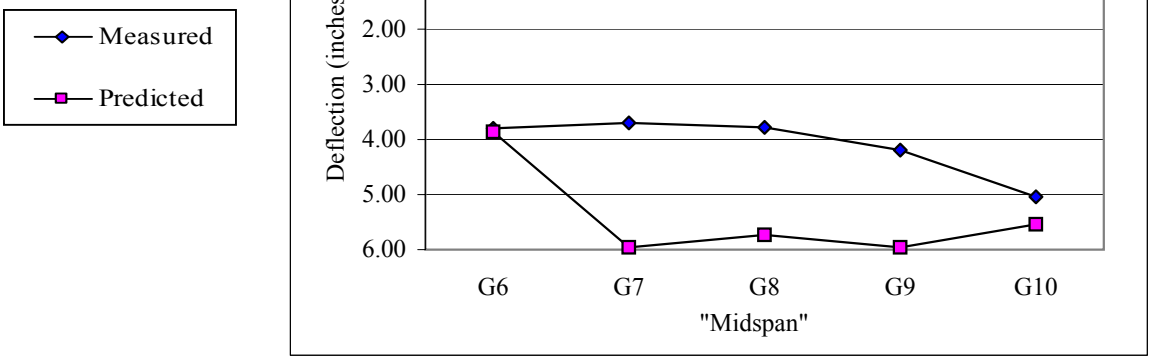

GIRDER DEFLECTIONS
ELEVATION VIEW

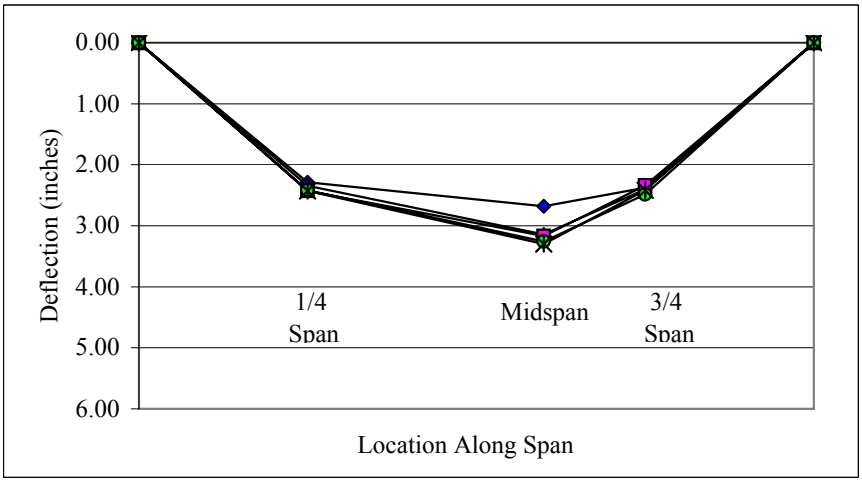

ANSYS FINITE ELEMENT MODELING SUMMARY

PROJECT NUMBER: B-3257 (South Wilmington Street Bridge)

MODEL DESCRIPTION: (Steel Only, Isometric View)

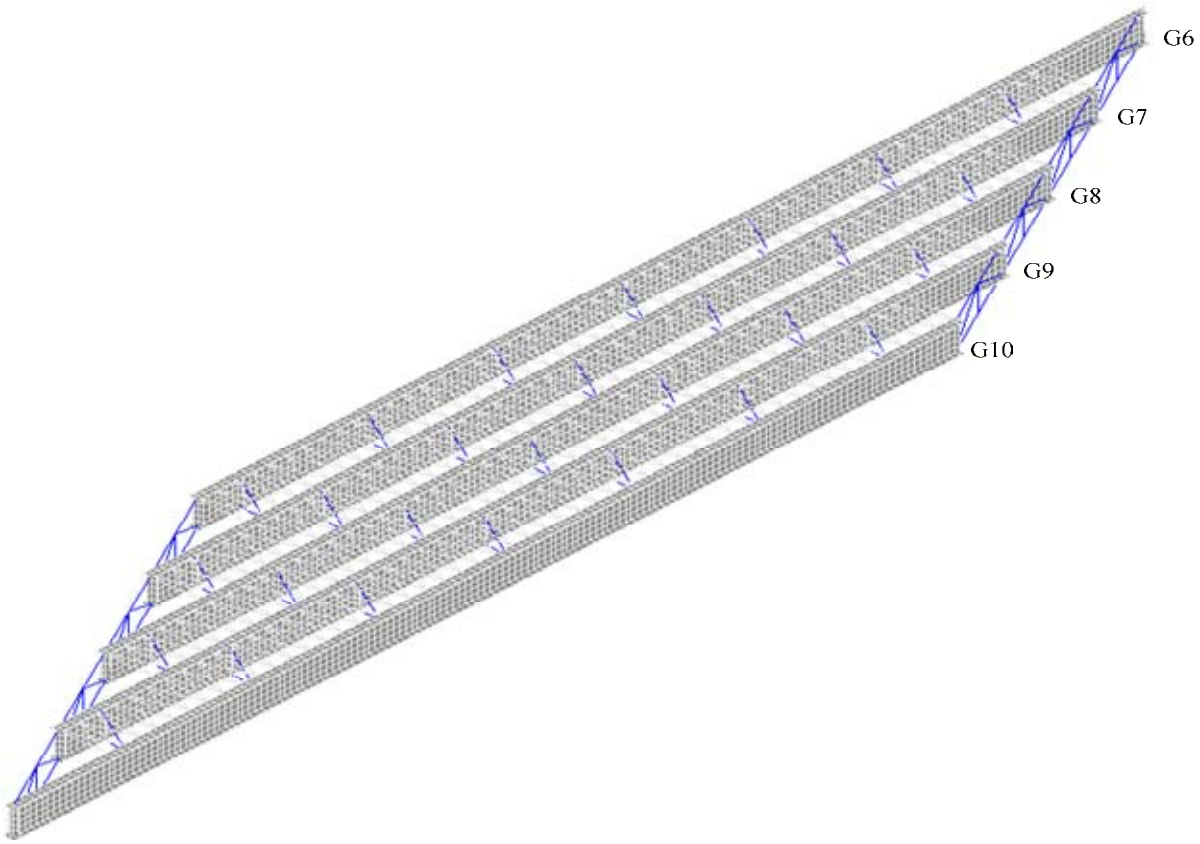

ANSYS FINITE ELEMENT MODELING SUMMARY

PROJECT NUMBER: B-3257 (South Wilmington Street Bridge)

MODEL DESCRIPTION

COMPONENT	**Element Type**
Girder:	SHELL93
Connector Plates:	SHELL93
Stiffener Plates:	SHELL93
Cross-frame Members:	LINK8 (diagonal)
	LINK8 (horizontal)
End Diaphragm:	BEAM4 (horizontal)
	LINK8 (diagonal)
Stay-in-place Deck Forms:	LINK8
Concrete Slab:	SHELL63
Shear Studs:	MPC184

APPLIED LOADS

Girder	*Load	
	lb/ft	N/mm
G6	447.17	6.52
G7	686.15	10.01
G8	655.73	9.57
G9	686.15	10.01
G10	619.68	9.04

*applied as a uniform pressure to area of top flange

GIRDER DEFLECTIONS

	ANSYS			ANSYS (SIP)		
Point	**1/4**	**Midspan**	**3/4**	**1/4**	**Midspan**	**3/4**
G6	2.05	2.74	2.03	2.44	3.20	2.32
G7	2.51	3.41	2.51	2.24	3.02	2.22
G8	2.63	3.60	2.65	2.27	3.03	2.22
G9	2.63	3.56	2.60	2.45	3.28	2.40
G10	2.77	3.72	2.77	2.68	3.86	2.92
	Measured			**Predicted**		
Point	**1/4**	**Midspan**	**3/4**	**1/4**	**Midspan**	**3/4**
G6	2.64	3.80	2.83	2.94	3.86	2.94
G7	2.64	3.70	2.72	4.53	5.96	4.53
G8	2.72	3.78	2.80	4.36	5.73	4.36
G9	2.97	4.19	3.17	4.53	5.96	4.53
G10	3.62	5.04	3.70	4.21	5.54	4.21

ANSYS FINITE ELEMENT MODELING SUMMARY

PROJECT NUMBER: B-3257 (South Wilmington Street Bridge)

GIRDER DEFLECTIONS
CROSS SECTION VIEW

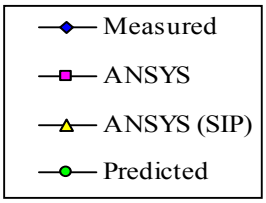

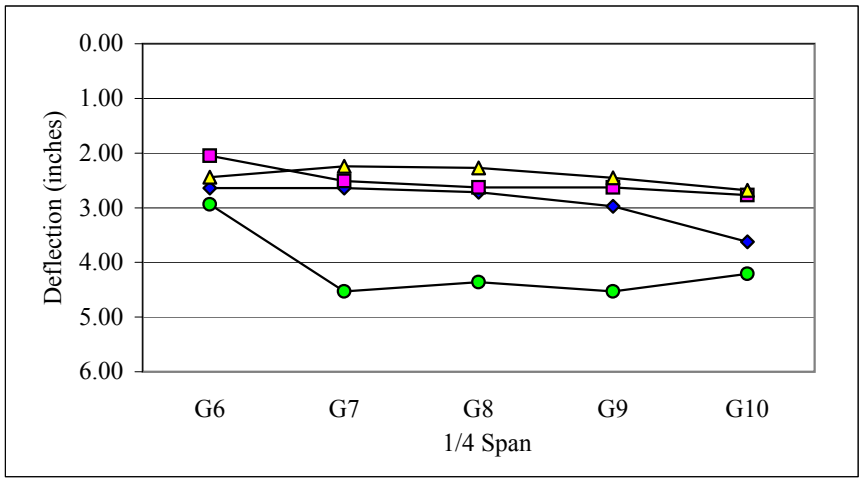

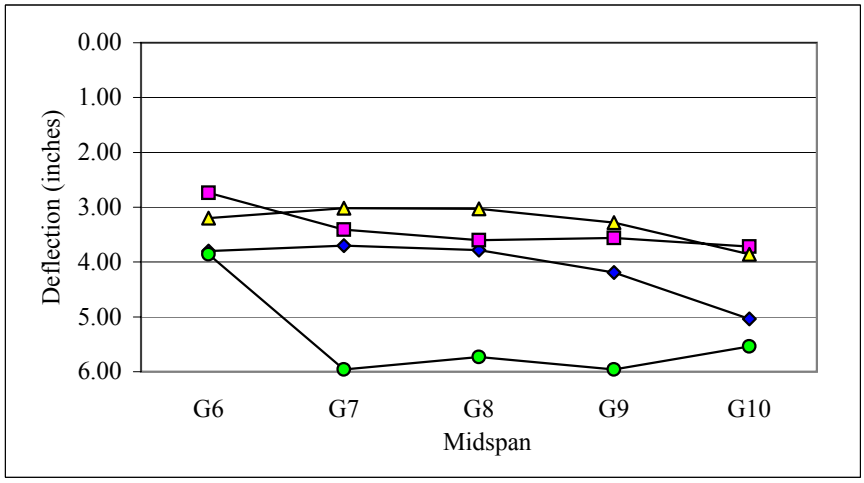

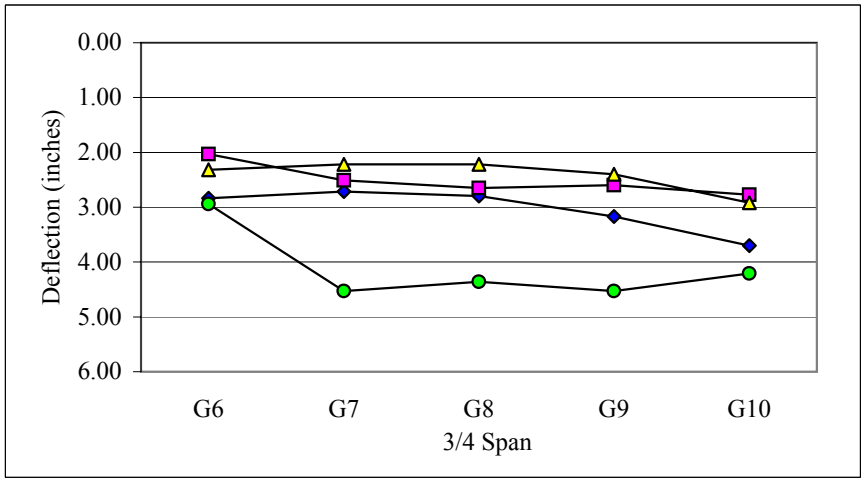

SAP 2000 MODELING SUMMARY

PROJECT NUMBER: B-3257 (South Wilmington Street Bridge)

MODEL PICTURE (Steel only, isometric view)

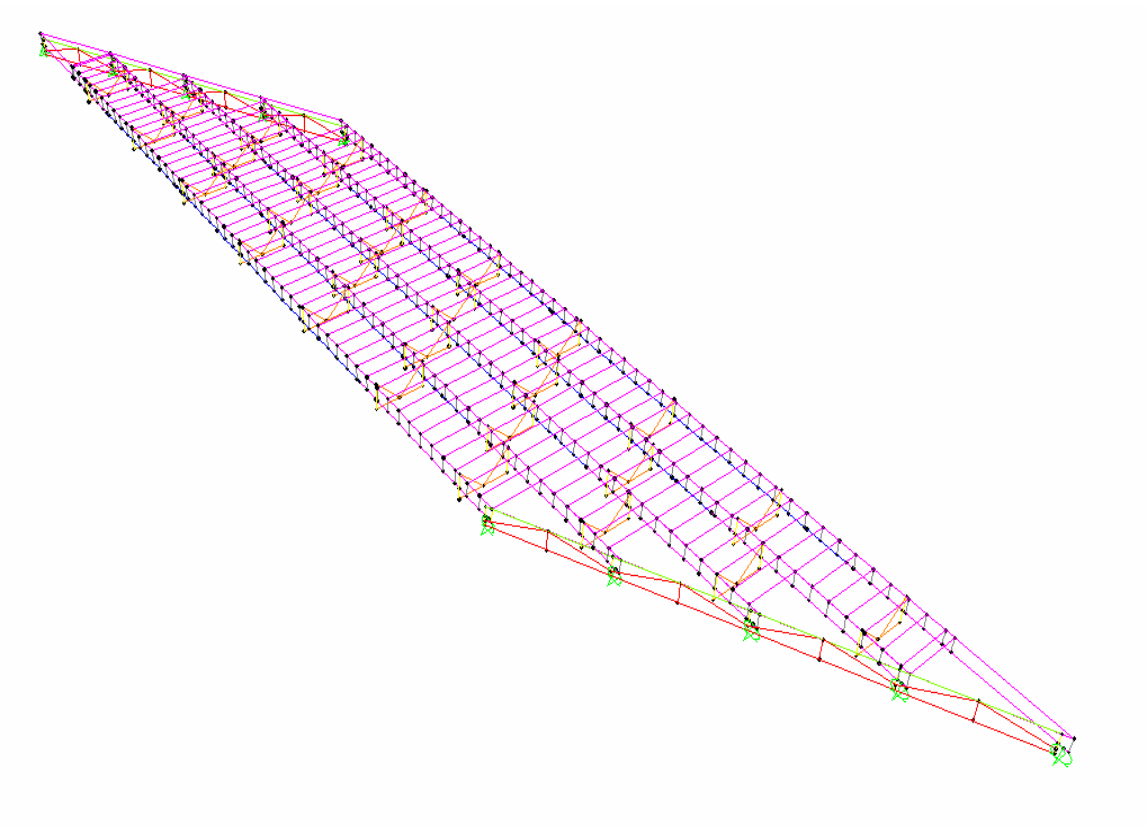

SAP 2000 MODELING SUMMARY

PROJECT NUMBER: B-3257 (South Wilmington Street Bridge)

MODEL DESCRIPTION

COMPONENT	**Element Type**
Girder:	Frame Element
Cross Frame Members:	Frame Element
Stay-in-place Deck Forms:	Area Element* (Shell Element)
Rigid Link:	Frame Element

* See Area Properties in Appendix F

GIRDER DEFLECTIONS

	SAP			**Single Girder Model**		
Point	**1/4**	**6/10**	**3/4**	**1/4**	**6/10**	**3/4**
G6	3.06	4.04	3.07	2.94	3.87	2.94
G7	4.27	5.64	4.28	4.53	5.97	4.53
G8	4.50	5.91	4.48	4.36	5.74	4.36
G9	4.42	5.83	4.43	4.53	5.97	4.53
G10	4.25	5.60	4.24	4.21	5.54	4.21
	SAP (SIP)			**ANSYS (SIP)**		
Point	**1/4**	**6/10**	**3/4**	**1/4**	**6/10**	**3/4**
G6	3.48	4.67	3.55	2.44	3.20	2.32
G7	3.56	4.73	3.59	2.24	3.02	2.22
G8	3.69	4.89	3.71	2.27	3.03	2.22
G9	3.92	5.20	3.95	2.45	3.28	2.40
G10	4.44	5.76	4.33	2.68	3.86	2.92

SAP 2000 MODELING SUMMARY

PROJECT NUMBER: B-3257 (South Wilmington Street Bridge)

*GIRDER DEFLECTIONS
CROSS SECTION VIEW

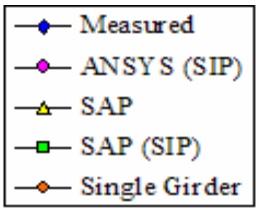

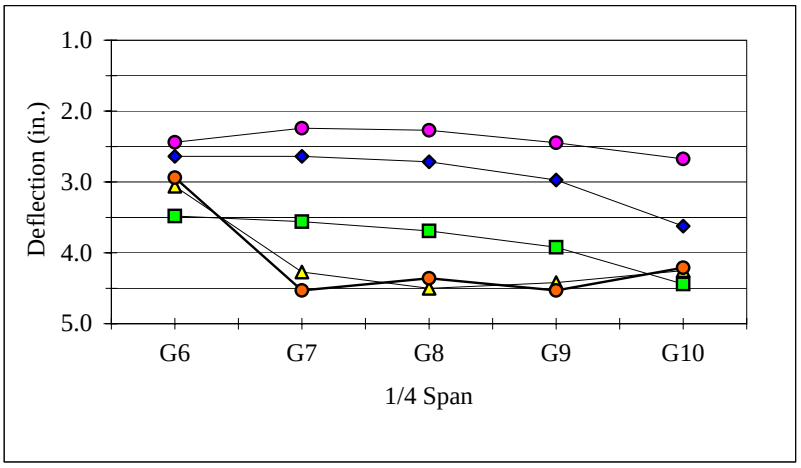

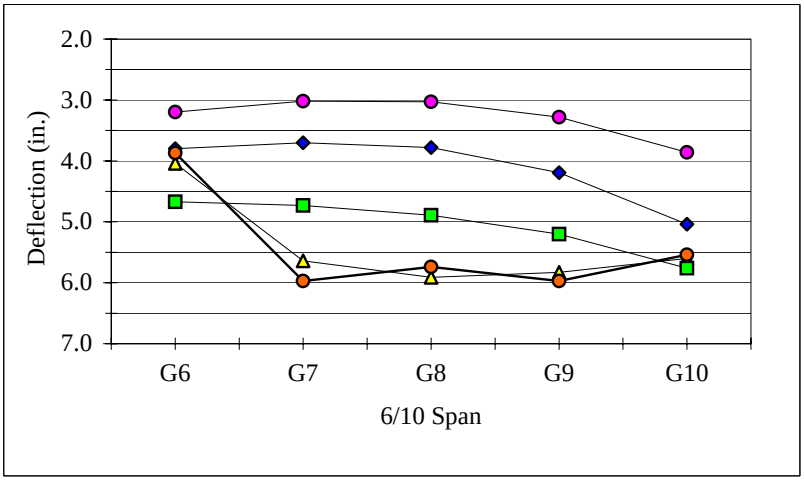

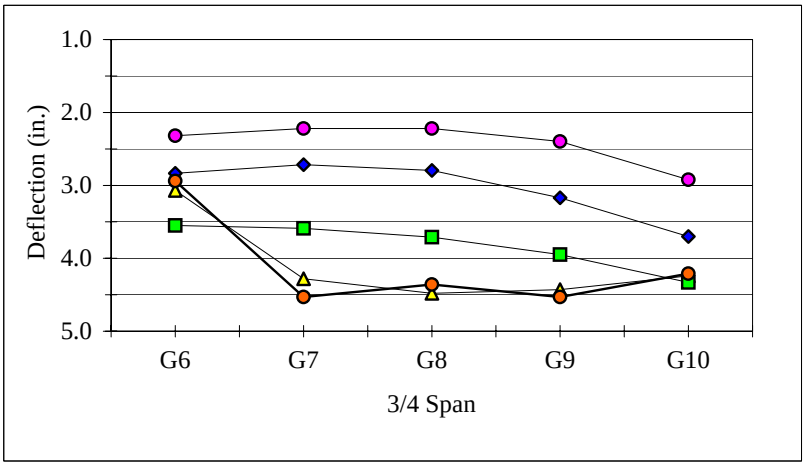

Appendix J

Deflection Summary for Bridge 14

This appendix contains a detailed description of Bridge 14 including bridge geometry, material data, cross frame type and size, and dead loads calculated from slab geometry. Illustrations detailing the bridge geometry and field measurement locations are included, along with tables and graphs of the field measured non-composite girder deflections.

A summary of the ANSYS finite element model created for Bridge 14 is also included in this appendix. This summary includes a picture of the ANSYS model, details about the elements used in the model generation, the loads applied to the model, and tables and graphs of the deflections predicted by the model.

FIELD MEASUREMENT SUMMARY

PROJECT NUMBER: R-2547 (Ramp (RPBDY1) Over US-64 Business)
MEASUREMENT DATE: June 29 & July 2, 2004

BRIDGE DESCRIPTION

TYPE	Two Span Continous	
LENGTH	208.26 ft (63.477 m)	
NUMBER OF GIRDERS	5	
GIRDER SPACING	9.97 ft (3.04 m)	
SKEW	65.6 deg	
OVERHANG	3.70 ft (1130 mm)	(from web centerline)
BEARING TYPE	Elastomeric Pad	

MATERIAL DATA

STRUCTURAL STEEL	**Grade**	**Yield Strength**
Girder:	AASHTO M270	50 ksi (345 MPa)
Other:	AASHTO M270	50 ksi (345 MPa)

CONCRETE UNIT WEIGHT	150 pcf (nominal)
SIP FORM WEIGHT	2.98 psf (CSI Catalog)

GIRDER DATA

LENGTH	101.92 ft (31.064 m)	"Span A"
	106.34 ft (32.413 m)	"Span B"

WEB THICKNESS	0.47 in (12 mm)
WEB DEPTH	62.99 in (1600 mm)
TOP FLANGE WIDTH	14.96 in (380 mm)
BOTTOM FLANGE WIDTH	17.72 in (450 mm)

	Flange Thickness	**Begin**	**End**
Top:	0.79 in (20 mm)	0.00	92.07 ft (28.064 m)
	1.18 in (30 mm)	92.07 ft (28.064 m)	111.76 ft (34.064 m)
	0.79 in (20 mm)	111.76 ft (34.064 m)	208.26 ft (63.477 m)
Bottom:	0.79 in (20 mm)	0.00	92.07 ft (28.064 m)
	1.38 in (35 mm)	92.07 ft (28.064 m)	111.76 ft (34.064 m)
	0.79 in (20 mm)	111.76 ft (34.064 m)	208.26 ft (63.477 m)

FIELD MEASUREMENT SUMMARY

PROJECT NUMBER: R-2547 (Ramp (RPBDY1) Over US-64 Business)
MEASUREMENT DATE: June 29 & July 2, 2004

STIFFENERS

Longitudinal:	N/A
Bearing:	PL 0.98" × 8.27" (25 mm × 210 mm)
Intermediate:	PL 0.63" × NA (16 mm × NA, connector plate) PL 0.47" × 5.12" (12 mm × 130 mm)
Middle Bearing:	PL 0.98" × 8.27" (25 mm × 210 mm)
End Bent Connector:	NA (Integral Bent)

CROSS-FRAME DATA

	Diagonals	**Horizontals**	**Verticals**
END BENT	NA	NA	NA
MIDDLE BENT (Type X)	L 4 x 4 x 5/8"	L 4 x 4 x 5/8" (Bottom)	NA
INTERMEDIATE (Type X)	L 4 x 4 x 5/8"	L 4 x 4 x 5/8" (Bottom)	NA

SLAB DATA

THICKNESS	8.86 in (225 mm)	nominal
BUILD-UP	2.95 in (75 mm)	nominal

Over Middle Bent:

LONGITUDINAL REBAR	SIZE (metric)	SPACING (nominal)
Top:	#16	4.33 in (110 mm)
Bottom:	#16	8.66 in (220 mm)
TRANSVERSE REBAR		
Top:	#16	5.91 in (150 mm)
Bottom:	#16	5.91 in (150 mm)

Otherwise:

LONGITUDINAL REBAR	SIZE (metric)	SPACING (nominal)
Top:	#16	21.65 in (550 mm)
Bottom:	#16	8.66 in (220 mm)
TRANSVERSE REBAR		
Top:	#16	5.91 in (150 mm)
Bottom:	#16	5.91 in (150 mm)

FIELD MEASUREMENT SUMMARY

Project Number: R-2547 (Ramp (RBPDY1) over US-64 Business)
Measurement Date: June 29 & July 2, 2004

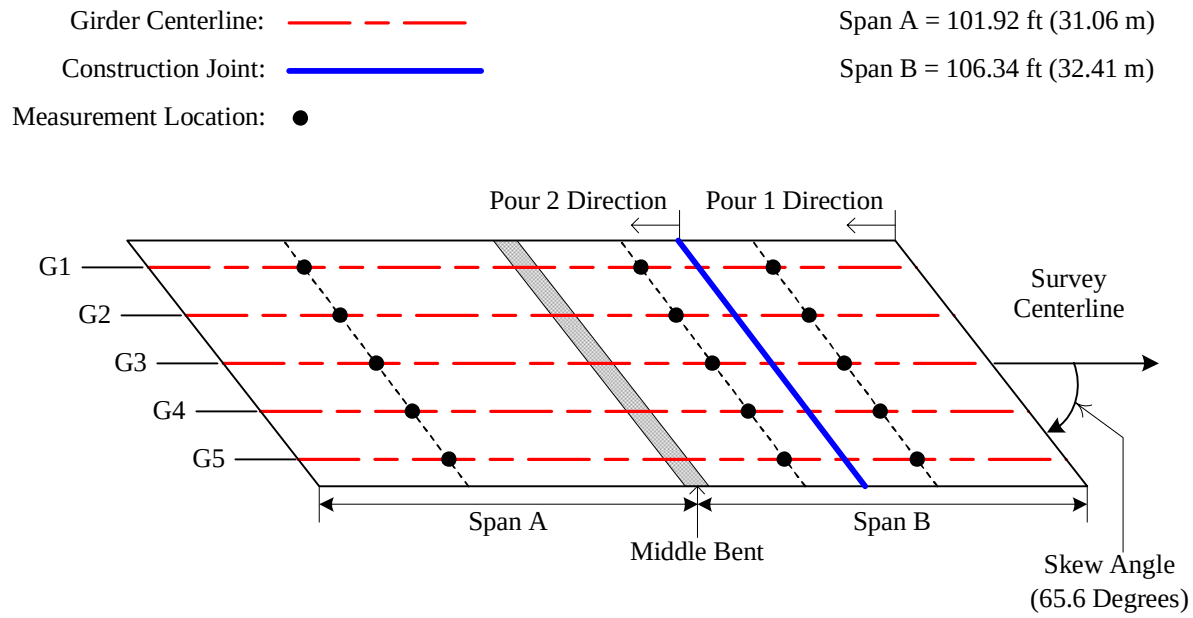

(a) Plan View (Not to Scale)

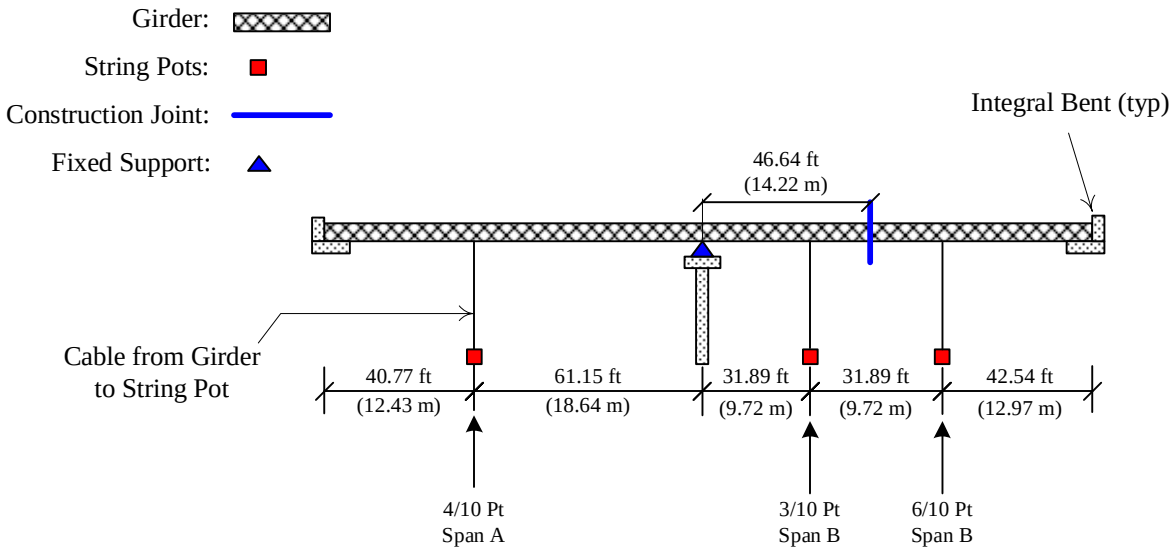

(b) Elevation View (Not to Scale)

Plan and Elevation View of Bridge 14 (Knightdale, NC)

FIELD MEASUREMENT SUMMARY

PROJECT NUMBER: R-2547 (Ramp (RPBDY1) Over US-64 Business)
MEASUREMENT DATE: June 29 & July 2, 2004

DECK LOADS

Girder	Concrete[1]		Slab[2]		Ratio
	lb/ft	N/mm	lb/ft	N/mm	
G1	1160.07	16.93	1229.28	17.94	0.94
G2	1204.61	17.58	1296.43	18.92	0.93
G3	1204.61	17.58	1296.43	18.92	0.93
G4	1204.61	17.58	1296.43	18.92	0.93
G5	1160.07	16.93	1229.28	17.94	0.94

[1] Calculated with nominal slab thicknesses

[2] Includes slab, buildups, and stay-in-place forms (nominal)

BEARING SETTLEMENTS[3] (data in inches, negative is deflection upwards)

Point	Pour 1 Settlement		
	End 1	Middle	End 2
G1	---	-0.03	---
G2	---	-0.03	---
G3	---	-0.02	---
G4	---	-0.03	---
G5	---	-0.05	---

Point	Pour 2 Settlement		
	End 1	Middle	End 2
G1	---	0.03	---
G2	---	0.01	---
G3	---	0.01	---
G4	---	0.01	---
G5	---	0.03	---

[3] Noticeably, the settlement totaled from the two pours was very close to zero.

GIRDER DEFLECTIONS (data in inches, negative is deflection upwards)
POUR 1 MEASURED

Point	7/10 Span B Loading			End of Span B		
	4/10 A	3/10 B	6/10 B	4/10 A	3/10 B	6/10 B
G1	-0.07	0.23	0.38	-0.49	0.96	1.42
G2	0.00	0.26	0.38	-0.37	0.91	1.34
G3	0.01	0.25	0.54	-0.25	0.90	1.46
G4	-0.07	0.20	0.41	-0.42	0.88	1.36
G5	-0.09	0.27	0.50	-0.40	1.04	1.57

FIELD MEASUREMENT SUMMARY

PROJECT NUMBER: R-2547 (Ramp (RPBDY1) Over US-64 Business)
MEASUREMENT DATE: June 29 & July 2, 2004

GIRDER DEFLECTIONS (data in inches, negative is deflection upwards)

POUR 2 MEASURED

	Middle Bent Loading			7/10 Span A Loading			5/10 Span A Loading		
Point	**4/10 A**	**3/10 B**	**6/10 B**	**4/10 A**	**3/10 B**	**6/10 B**	**4/10 A**	**3/10 B**	**6/10 B**
G1	0.28	0.63	0.52	0.11	0.43	0.38	0.43	0.30	0.29
G2	-0.19	0.48	0.50	0.14	0.30	0.37	0.38	0.18	0.28
G3	-0.18	0.49	0.58	0.17	0.31	0.44	0.37	0.19	0.35
G4	-0.25	0.50	0.52	0.27	0.30	0.35	0.42	0.18	0.28
G5	-0.10	0.49	0.43	0.29	0.25	0.26	0.37	0.13	0.18

	2/10 Span A Loading			Complete Loading		
Point	**4/10 A**	**3/10 B**	**6/10 B**	**4/10 A**	**3/10 B**	**6/10 B**
G1	1.19	0.14	0.16	1.36	0.07	0.13
G2	1.04	0.02	0.14	1.16	-0.05	0.11
G3	1.09	0.03	0.22	1.21	-0.02	0.20
G4	1.18	0.03	0.14	1.27	-0.02	0.15
G5	0.90	-0.02	0.04	0.91	-0.04	0.07

TOTAL MEASURED

	Super-Imposed Total		
Point	**4/10 A**	**3/10 B**	**6/10 B**
G1	0.87	1.03	1.55
G2	0.79	0.86	1.45
G3	0.97	0.88	1.66
G4	0.85	0.86	1.50
G5	0.51	1.00	1.64

PREDICTIONS[4] (Single Girder-Line Model in SAP 2000)

	Pour 1			Pour 2		
Point	**4/10 A**	**3/10 B**	**6/10 B**	**4/10 A**	**3/10 B**	**6/10 B**
G1	-0.45	0.93	1.39	1.43	-0.17	-0.09
G2	-0.47	0.97	1.44	1.49	-0.17	-0.17
G3	-0.47	0.97	1.44	1.49	-0.17	-0.17
G4	-0.47	0.97	1.44	1.49	-0.17	-0.17
G5	-0.45	0.93	1.39	1.43	-0.17	-0.09

	Super-Imposed Total		
Point	**4/10 A**	**3/10 B**	**6/10 B**
G1	0.98	0.76	1.30
G2	1.02	0.80	1.26
G3	1.02	0.80	1.26
G4	1.02	0.80	1.26
G5	0.98	0.76	1.30

[4] Using nominal slab thicknesses

FIELD MEASUREMENT SUMMARY

PROJECT NUMBER: R-2547 (Ramp (RPBDY1) Over US-64 Business)
MEASUREMENT DATE: June 29 & July 2, 2004

GIRDER DEFLECTIONS
CROSS SECTION VIEW

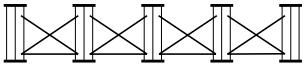

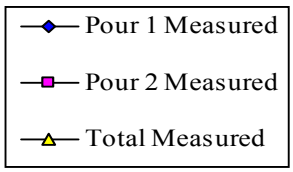

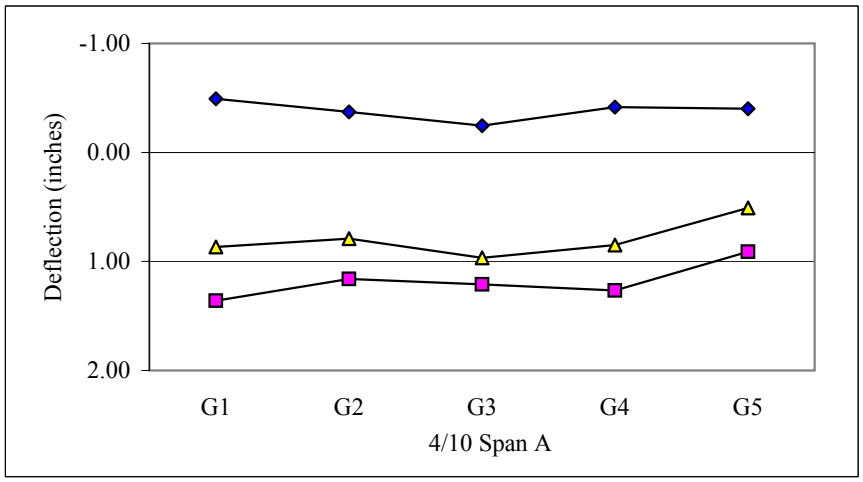

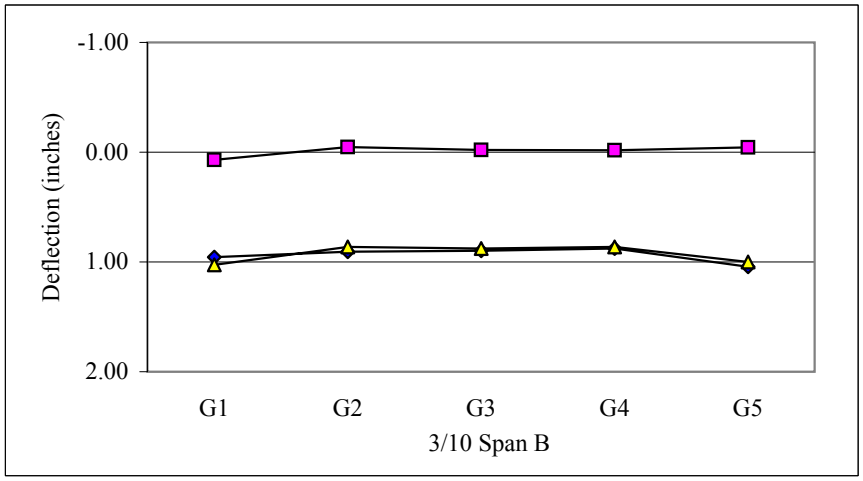

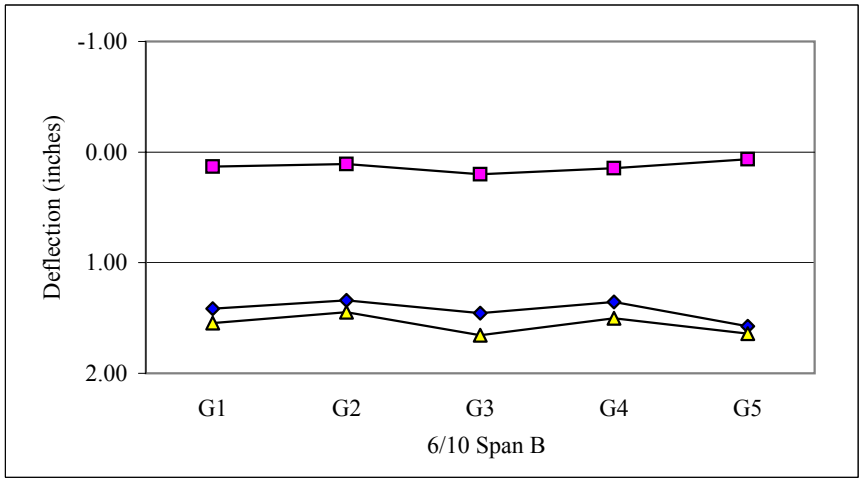

FIELD MEASUREMENT SUMMARY

PROJECT NUMBER: R-2547 (Ramp (RPBDY1) Over US-64 Business)
MEASUREMENT DATE: June 29 & July 2, 2004

GIRDER DEFLECTIONS
CROSS SECTION VIEW

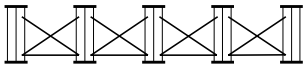

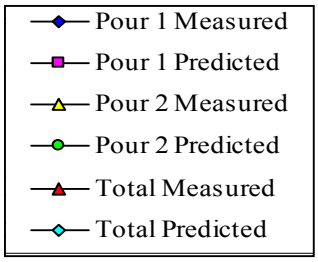

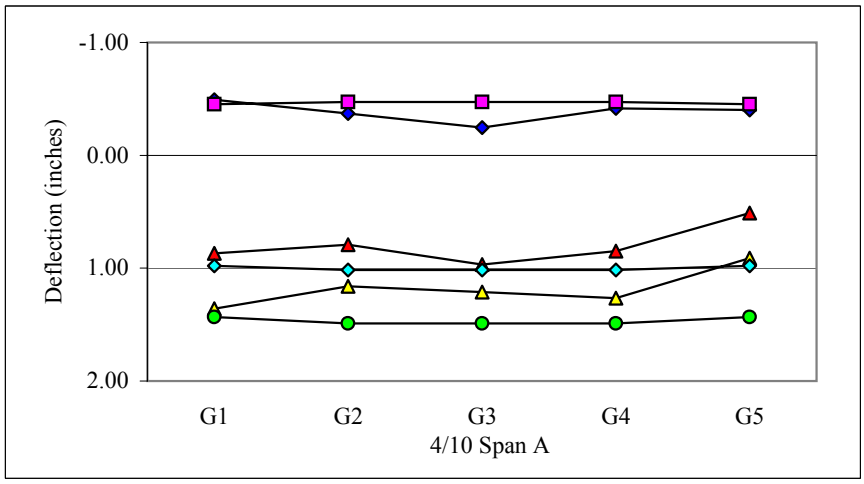

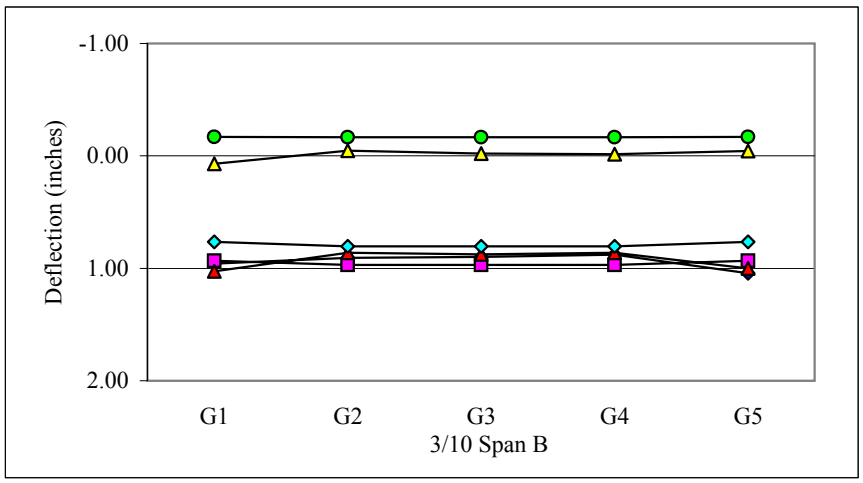

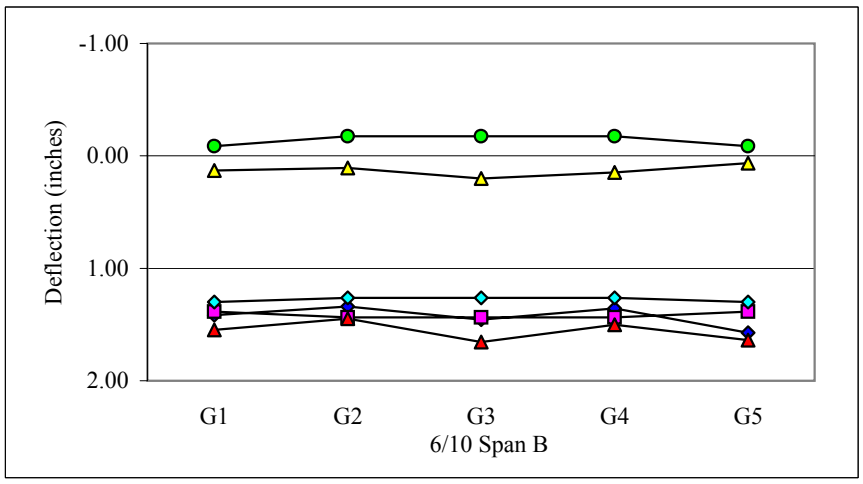

FIELD MEASUREMENT SUMMARY

PROJECT NUMBER: R-2547 (Ramp (RPBDY1) Over US-64 Business)
MEASUREMENT DATE: June 29 & July 2, 2004

GIRDER DEFLECTIONS
ELEVATION VIEW

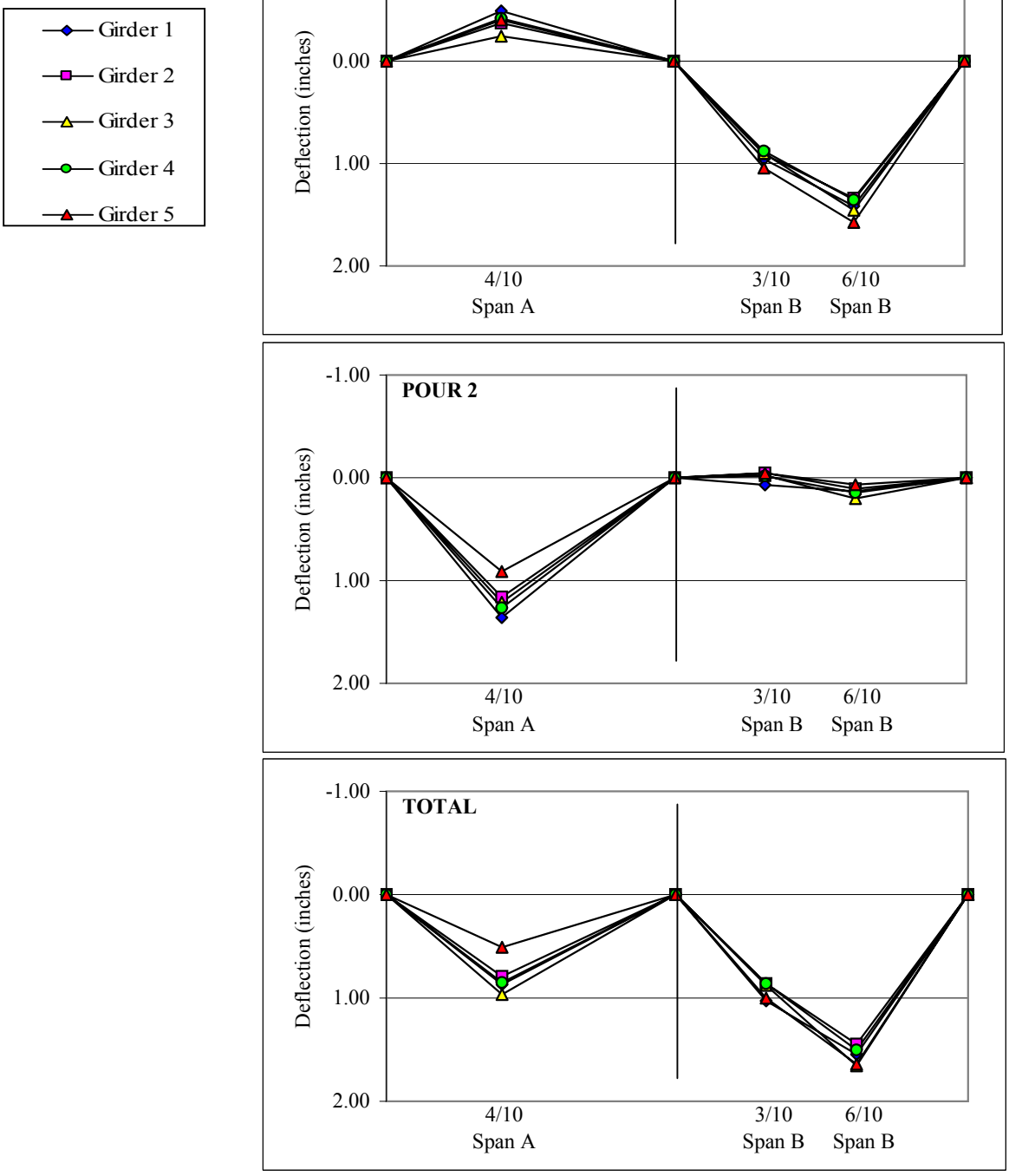

ANSYS FINITE ELEMENT MODELING SUMMARY

PROJECT NUMBER: R-2547 (Ramp (RPBDY1) Over US-64 Business)

MODEL PICTURE: (Steel Only, Oblique View)

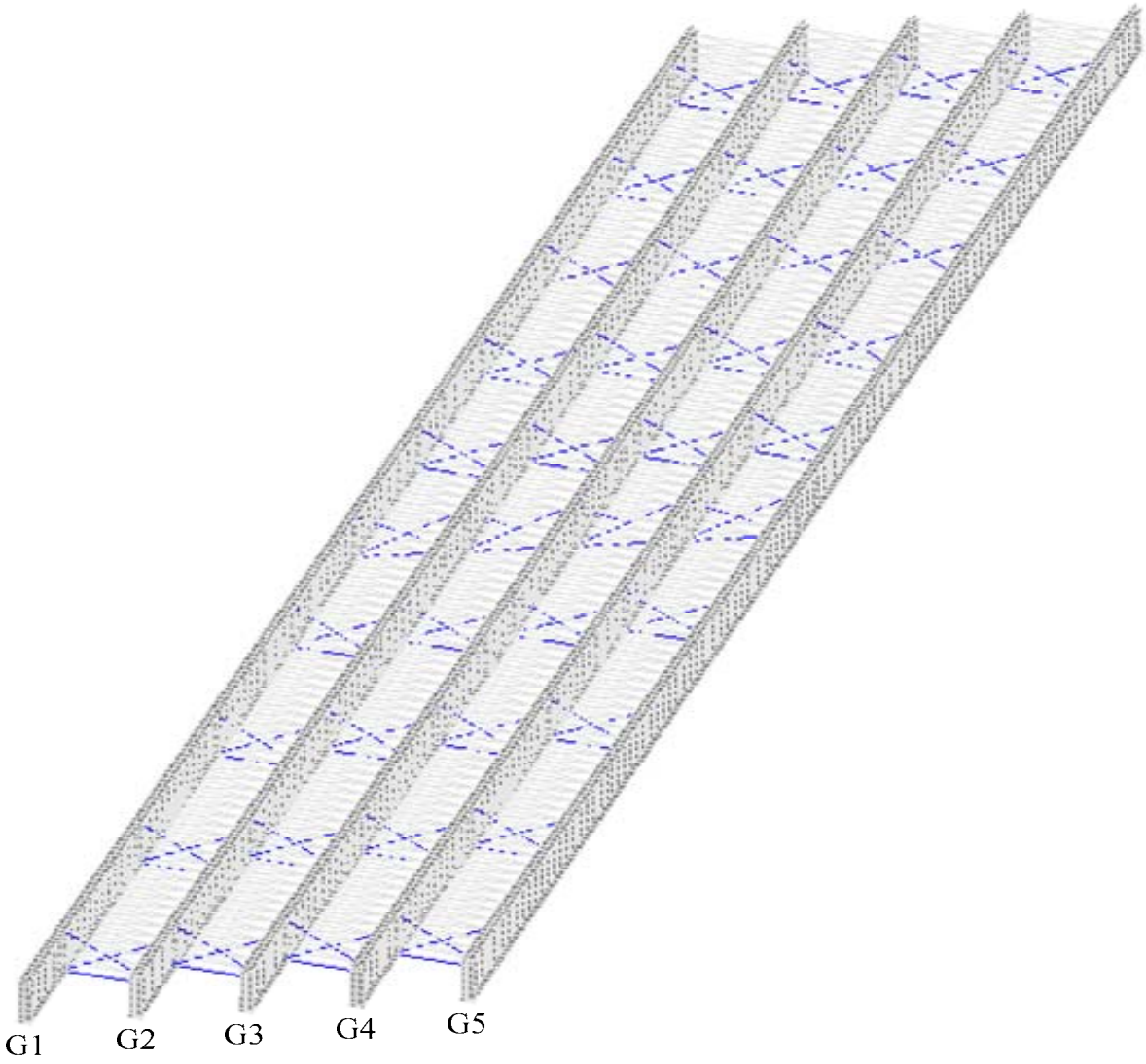

ANSYS FINITE ELEMENT MODELING SUMMARY

PROJECT NUMBER: R-2547 (Ramp (RPBDY1) Over US-64 Business)

MODEL DESCRIPTION

COMPONENT	**Element Type**
Girder:	SHELL93
Connector Plates:	SHELL93
Stiffener Plates:	SHELL93
Cross-frame Members:	LINK8 (diagonal)
	LINK8 (horizontal)
Middle Diaphragm:	LINK8 (diagonal)
	LINK8 (horizontal)
Stay-in-place Deck Forms:	LINK8
Concrete Slab:	SHELL63
Shear Studs:	MPC184

APPLIED LOADS

Girder	*Load	
	lb/ft	N/mm
G1	1229.3	17.94
G2	1296.4	18.92
G3	1296.4	18.92
G4	1296.4	18.92
G5	1229.3	17.94

*applied as a uniform pressure to area of top flange

	ANSYS Pour 1			ANSYS Pour 1 (SIP)			Pour 1 Measured		
Point	**4/10 A**	**3/10 B**	**6/10 B**	**4/10 A**	**3/10 B**	**6/10 B**	**4/10 A**	**3/10 B**	**6/10 B**
G1	-0.45	0.96	1.43	-0.45	0.97	1.43	-0.49	0.96	1.42
G2	-0.45	0.96	1.43	-0.44	0.96	1.42	-0.37	0.91	1.34
G3	-0.45	0.97	1.43	-0.44	0.95	1.42	-0.25	0.90	1.46
G4	-0.45	0.96	1.43	-0.44	0.96	1.42	-0.42	0.88	1.36
G5	-0.45	0.95	1.41	-0.46	0.96	1.42	-0.40	1.04	1.57
	ANSYS Pour 2			**ANSYS Pour 2 (SIP)**			**Pour 2 Measured**		
Point	**4/10 A**	**3/10 B**	**6/10 B**	**4/10 A**	**3/10 B**	**6/10 B**	**4/10 A**	**3/10 B**	**6/10 B**
G1	1.45	-0.15	-0.07	1.47	-0.16	-0.07	1.36	0.07	0.13
G2	1.48	-0.15	-0.07	1.47	-0.15	-0.07	1.16	-0.05	0.11
G3	1.50	-0.15	-0.07	1.48	-0.14	-0.06	1.21	-0.02	0.20
G4	1.49	-0.14	-0.07	1.48	-0.14	-0.06	1.27	-0.02	0.15
G5	1.45	-0.15	-0.07	1.46	-0.15	-0.07	0.91	-0.04	0.07
	ANSYS Total			**ANSYS Total (SIP)**			**Total Measured**		
Point	**4/10 A**	**3/10 B**	**6/10 B**	**4/10 A**	**3/10 B**	**6/10 B**	**4/10 A**	**3/10 B**	**6/10 B**
G1	1.00	0.81	1.35	1.02	0.81	1.36	0.87	1.03	1.55
G2	1.03	0.82	1.36	1.03	0.81	1.35	0.79	0.86	1.45
G3	1.05	0.82	1.37	1.04	0.81	1.35	0.97	0.88	1.66
G4	1.04	0.82	1.36	1.03	0.82	1.35	0.85	0.86	1.50
G5	1.00	0.81	1.34	1.01	0.82	1.35	0.51	1.00	1.64

Note: When ANSYS numbers were compared with ANSYS (SIP) numbers, there was 1% difference, therefore, ANSYS with SIP will not be shown on graphs.

ANSYS FINITE ELEMENT MODELING SUMMARY

PROJECT NUMBER: R-2547 (Ramp (RPBDY1) Over US-64 Business)

GIRDER DEFLECTIONS
CROSS SECTION VIEW

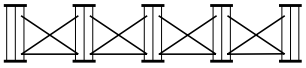

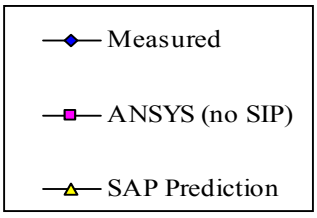

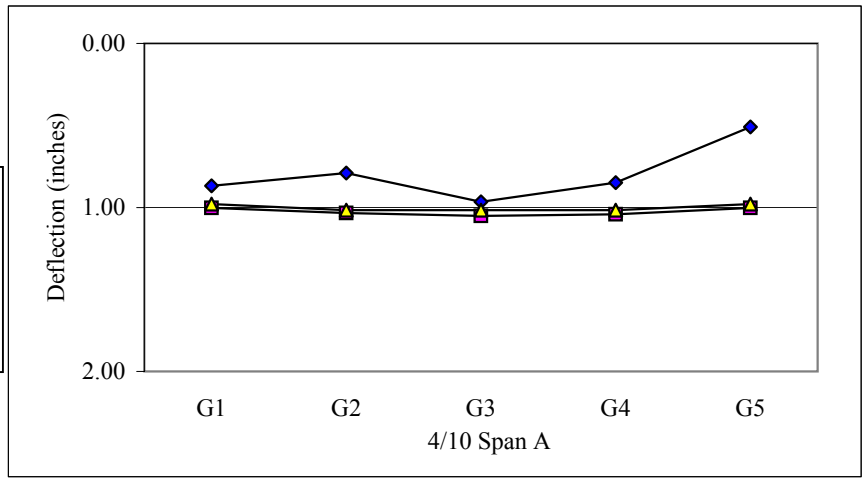

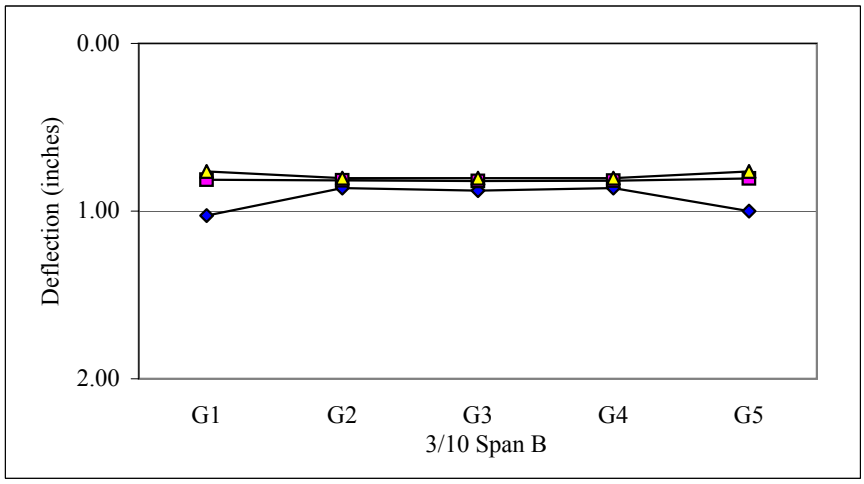

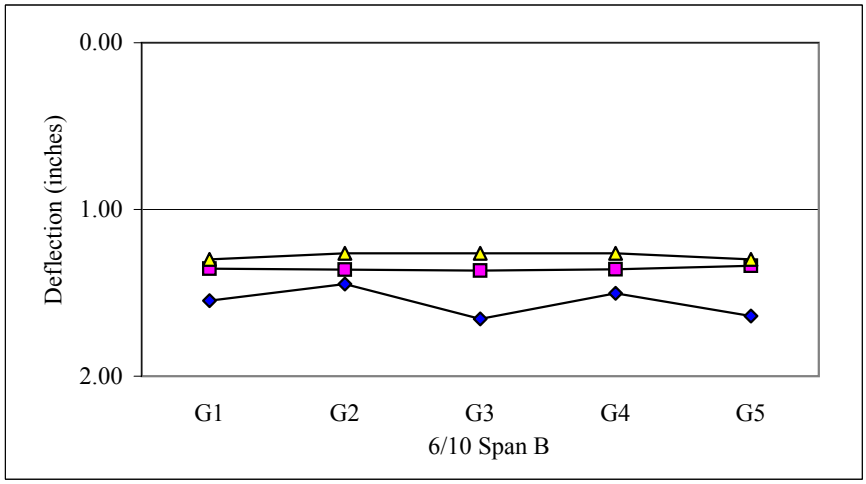

Appendix K

Deflection Summary for Bridge 10

This appendix contains a detailed description of Bridge 10 including bridge geometry, material data, cross frame type and size, and dead loads calculated from slab geometry. Illustrations detailing the bridge geometry and field measurement locations are included, along with tables and graphs of the field measured non-composite girder deflections.

A summary of the ANSYS finite element model created for Bridge 10 is also included in this appendix. This summary includes a picture of the ANSYS model, details about the elements used in the model generation, the loads applied to the model, and tables and graphs of the deflections predicted by the model.

FIELD MEASUREMENT SUMMARY

PROJECT NUMBER: R-2547 (Knightdale-Eagle Rock Rd. Over US-64 Bypass)
MEASUREMENT DATE: March 20 & March 29, 2004

BRIDGE DESCRIPTION

TYPE	Two Span Continous, Two Simple Spans (Continuous Spans Measured)	
LENGTH	300.19 ft (91.5 m)	
NUMBER OF GIRDERS	4	
GIRDER SPACING	9.51 ft (2.9 m)	
SKEW	147.1 deg	
OVERHANG	3.02 ft (920 mm)	(from web centerline)
BEARING TYPE	Elastomeric Pad	

MATERIAL DATA

STRUCTURAL STEEL	**Grade**	**Yield Strength**
Girder:	AASHTO M270	50 ksi (345 MPa)
Other:	AASHTO M270	50 ksi (345 MPa)

CONCRETE UNIT WEIGHT	150 pcf (nominal)
SIP FORM WEIGHT	2.57 psf (CSI Catalog)

GIRDER DATA

LENGTH	155.51 ft (47.4 m)	"Span B"	
	144.68 ft (44.1 m)	"Span C"	
WEB THICKNESS	0.55 in (14 mm)		
WEB DEPTH	75.79 in (1925 mm)		

	Flange Thickness	**Begin**	**End**
Top:	1.26 in (32 mm)	0.00	112.86 ft (34.4 m)
	1.26 in (32 mm)	112.86 ft (34.4 m)	132.55 ft (40.4 m)
	1.97 in (50 mm)	132.55 ft (40.4 m)	178.48 ft (54.4 m)
	1.26 in (32 mm)	178.48 ft (54.4 m)	199.80 ft (60.9 m)
	1.26 in (32 mm)	199.80 ft (60.9 m)	300.19 ft (91.5 m)
	Flange Width	**Begin**	**End**
	15.75 in (400 mm)	0.00	112.86 ft (34.4 m)
	18.50 in (470 mm)	112.86 ft (34.4 m)	132.55 ft (40.4 m)
	18.50 in (470 mm)	132.55 ft (40.4 m)	178.48 ft (54.4 m)
	18.50 in (470 mm)	178.48 ft (54.4 m)	199.80 ft (60.9 m)
	15.75 in (400 mm)	199.80 ft (60.9 m)	300.19 ft (91.5 m)

Bottom: Same as Top Flange

FIELD MEASUREMENT SUMMARY

PROJECT NUMBER: R-2547 (Knightdale-Eagle Rock Rd. Over US-64 Bypass)
MEASUREMENT DATE: March 20 & March 29, 2004

STIFFENERS

Longitudinal:	N/A
Bearing:	PL 0.79" × 7.09" (20 mm × 180 mm)
Intermediate:	PL 0.47" × NA (12 mm × NA, connector plate)
	PL 0.55" × 5.91" (14 mm × 150 mm)
Middle Bearing:	PL 1.10" × 8.27" (28 mm × 210 mm)
End Bent Connector:	PL 0.47" × NA (12 mm × NA)

CROSS-FRAME DATA

	Diagonals	**Horizontals**	**Verticals**
END BENT (Type K)	WT 4×12	MC 18×42.7 WT 4×12	WT 4×12
MIDDLE BENT	NA	NA	NA
INTERMEDIATE (Type X)	WT 4×12	WT 4×12 (bottom)	NA

SLAB DATA

THICKNESS	8.86 in (225 mm)	nominal
BUILD-UP	2.56 in (65 mm)	nominal

Over Middle Bent:

LONGITUDINAL REBAR	SIZE (metric)	SPACING (nominal)
Top:	#19	6.69 in (170 mm)
Bottom:	#16	9.45 in (240 mm)
TRANSVERSE REBAR		
Top:	#16	6.30 in (160 mm)
Bottom:	#16	6.30 in (160 mm)

Otherwise:

LONGITUDINAL REBAR	SIZE (metric)	SPACING (nominal)
Top:	#16	13.39 in (340 mm)
Bottom:	#16	9.45 in (240 mm)
TRANSVERSE REBAR		
Top:	#16	6.30 in (160 mm)
Bottom:	#16	6.30 in (160 mm)

FIELD MEASUREMENT SUMMARY

Project Number: R-2547 (Knightdale-Eagle Rock Rd. over US-64 Bypass)
Measurement Date: March 20 & March 29, 2004

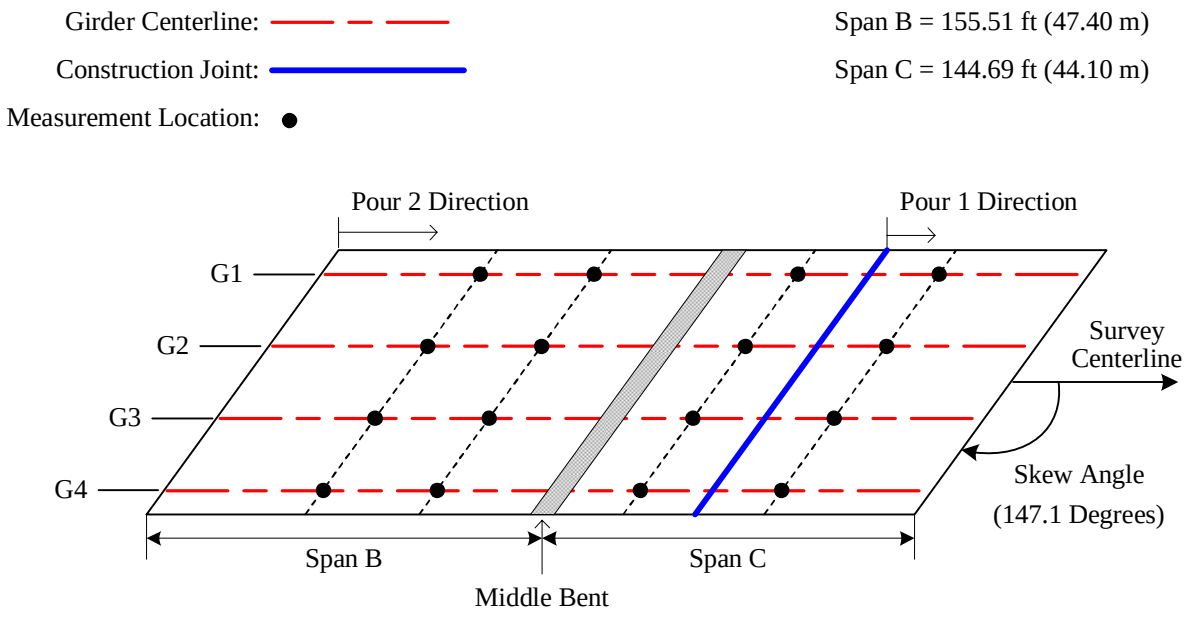

(a) Plan View (Not to Scale)

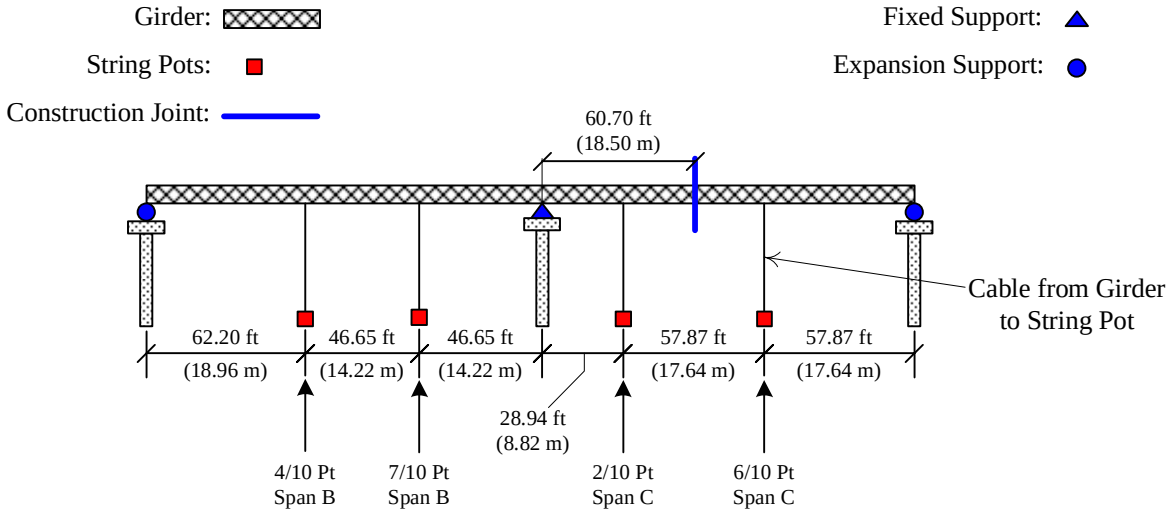

(b) Elevation View (Not to Scale)

Plan and Elevation View of Bridge 10 (Knightdale, NC)

FIELD MEASUREMENT SUMMARY

PROJECT NUMBER: R-2547 (Knightdale-Eagle Rock Rd. Over US-64 Bypass)
MEASUREMENT DATE: March 20 & March 29, 2004

DECK LOADS

Girder	Concrete[1]		Slab[2]		Ratio
	lb/ft	N/mm	lb/ft	N/mm	
G1	1014.81	14.81	1081.27	15.78	0.94
G2	1138.83	16.62	1227.91	17.92	0.93
G3	1138.83	16.62	1227.91	17.92	0.93
G4	1014.81	14.81	1081.27	15.78	0.94

[1] Calculated with nominal slab thicknesses

[2] Includes slab, buildups, and stay-in-place forms (nominal)

BEARING SETTLEMENTS[3] (data in inches, negative is deflection upwards)

Point	Pour 1 Settlement		
	End 1	Middle	End 2
G1	0.05	0.06	---
G2	0.03	0.07	---
G3	0.03	0.06	---
G4	0.01	0.06	---

Point	Pour 2 Settlement		
	End 1	Middle	End 2
G1	-0.09	-0.06	0.01
G2	-0.12	-0.08	0.00
G3	-0.14	-0.08	0.01
G4	-0.18	-0.09	0.00

[3] Noticeably, the settlement totaled from the two pours was very close to zero.

GIRDER DEFLECTIONS (data in inches, negative is deflection upwards)
POUR 1 MEASURED

Point	7/10 Span C Loading				8/10 Span C Loading			
	4/10 B	7/10 B	2/10 C	6/10 C	4/10 B	7/10 B	2/10 C	6/10 C
G1	-0.70	-0.60	1.23	1.51	-0.83	-0.71	1.32	1.75
G2	-0.60	-0.58	0.51	1.35	-0.73	-0.69	0.61	1.55
G3	-0.69	-0.60	0.61	1.26	-0.82	-0.64	0.73	1.51
G4	-0.73	-0.55	0.62	1.44	-0.88	-0.63	0.73	1.60

Point	End of Span C			
	4/10 B	7/10 B	2/10 C	6/10 C
G1	-0.87	-0.71	1.42	1.99
G2	-0.75	-0.73	0.67	1.76
G3	-0.83	-0.71	0.78	1.66
G4	-0.89	-0.63	0.71	1.68

FIELD MEASUREMENT SUMMARY

PROJECT NUMBER: R-2547 (Knightdale-Eagle Rock Rd. Over US-64 Bypass)
MEASUREMENT DATE: March 20 & March 29, 2004

GIRDER DEFLECTIONS (data in inches, negative is deflection upwards)
POUR 2 MEASURED

	3/10 Span B Loading				5/10 Span B Loading			
Point	**4/10 B**	**7/10 B**	**2/10 C**	**6/10 C**	**4/10 B**	**7/10 B**	**2/10 C**	**6/10 C**
G1	0.85	0.56	-0.08	0.20	2.08	1.39	-0.38	-0.12
G2	0.98	0.54	-0.15	-0.04	2.10	1.34	-0.43	-0.36
G3	1.08	0.70	-0.08	0.10	2.13	1.50	-0.36	-0.19
G4	1.46	0.79	-0.19	0.07	2.63	1.66	-0.49	-0.24
	7/10 Span B Loading				**Middle Bent Loading**			
Point	**4/10 B**	**7/10 B**	**2/10 C**	**6/10 C**	**4/10 B**	**7/10 B**	**2/10 C**	**6/10 C**
G1	2.91	2.02	-0.57	-0.32	3.28	2.41	-0.73	-0.50
G2	2.76	1.90	-0.62	-0.58	3.07	2.23	-0.75	-0.69
G3	2.77	2.09	-0.58	-0.40	3.01	2.34	-0.68	-0.51
G4	3.26	2.31	-0.76	-0.51	3.40	2.52	-0.86	-0.60

	Complete Loading			
Point	**4/10 B**	**7/10 B**	**2/10 C**	**6/10 C**
G1	2.83	2.00	-0.23	0.08
G2	2.66	1.83	-0.28	-0.12
G3	2.57	1.92	-0.22	0.00
G4	2.92	1.99	-0.33	-0.04

TOTAL MEASURED

	Super-Imposed Total			
Point	**4/10 B**	**7/10 B**	**2/10 C**	**6/10 C**
G1	1.97	1.29	1.18	2.07
G2	1.91	1.10	0.39	1.64
G3	1.74	1.21	0.56	1.66
G4	2.02	1.36	0.38	1.64

PREDICTIONS[4] (Single Girder-Line Model in SAP 2000)

	Pour 1				Pour 2			
Point	**4/10 B**	**7/10 B**	**2/10 C**	**6/10 C**	**4/10 B**	**7/10 B**	**2/10 C**	**6/10 C**
G1	-0.71	-0.74	0.82	1.81	2.88	2.03	-0.47	-0.38
G2	-0.80	-0.83	0.92	2.03	3.23	2.27	-0.53	-0.43
G3	-0.80	-0.83	0.92	2.03	3.23	2.27	-0.53	-0.43
G4	-0.71	-0.74	0.82	1.81	2.88	2.03	-0.47	-0.38

	Super-Imposed Total			
Point	**4/10 B**	**7/10 B**	**2/10 C**	**6/10 C**
G1	2.17	1.29	0.35	1.43
G2	2.43	1.44	0.39	1.60
G3	2.43	1.44	0.39	1.60
G4	2.17	1.29	0.35	1.43

[4] Using nominal slab thicknesses

FIELD MEASUREMENT SUMMARY

PROJECT NUMBER: R-2547 (Knightdale-Eagle Rock Rd. Over US-64 Bypass)
MEASUREMENT DATE: March 20 & March 29, 2004

GIRDER DEFLECTIONS
CROSS SECTION VIEW

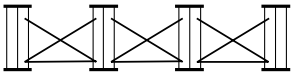

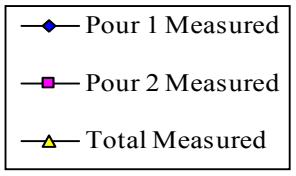

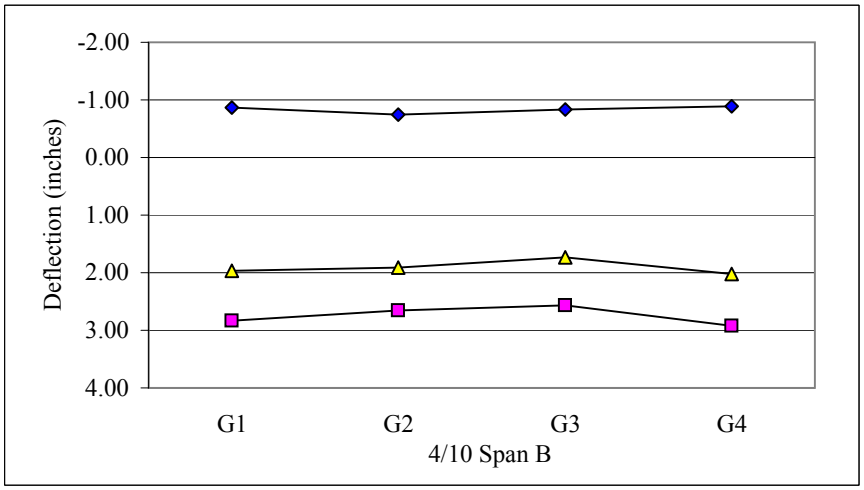

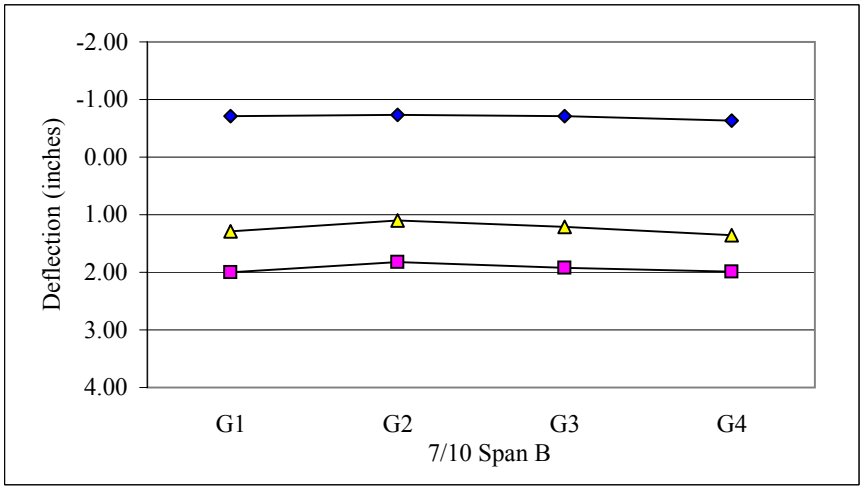

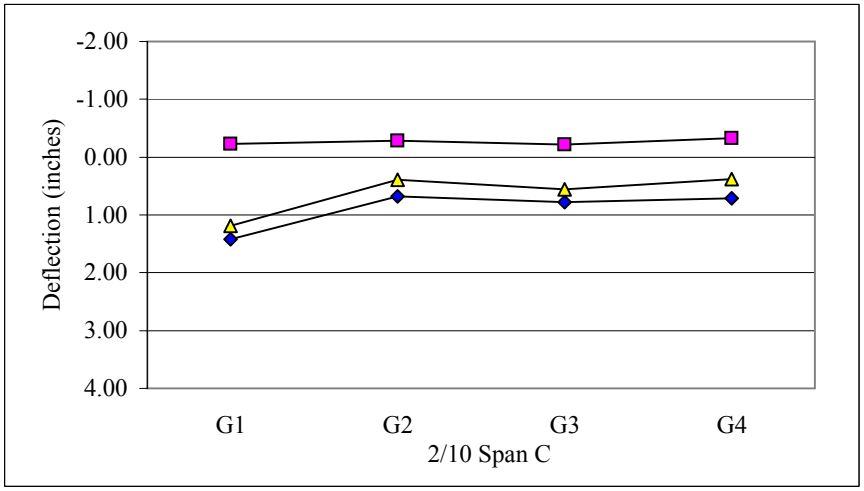

FIELD MEASUREMENT SUMMARY

PROJECT NUMBER: R-2547 (Knightdale-Eagle Rock Rd. Over US-64 Bypass)
MEASUREMENT DATE: March 20 & March 29, 2004

GIRDER DEFLECTIONS
CROSS SECTION VIEW

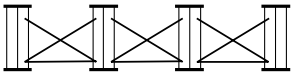

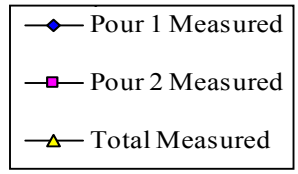

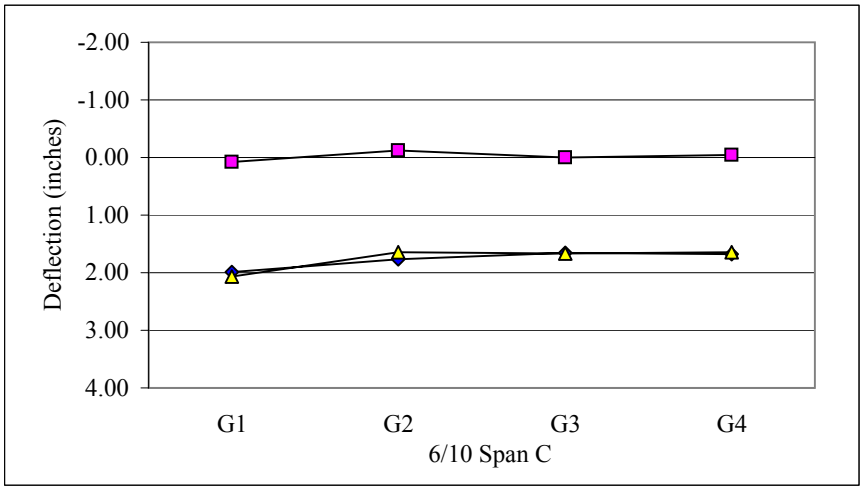

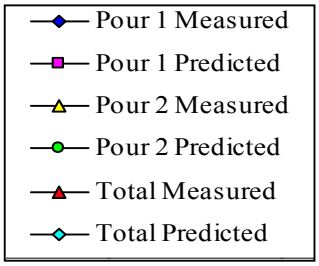

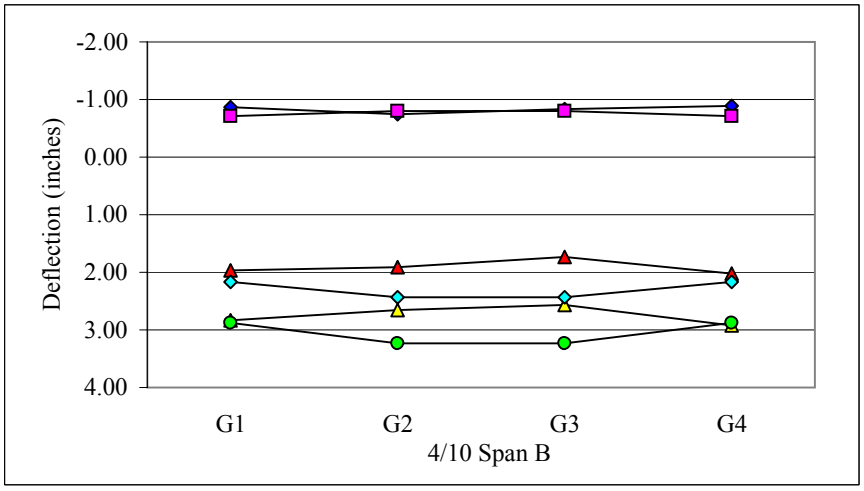

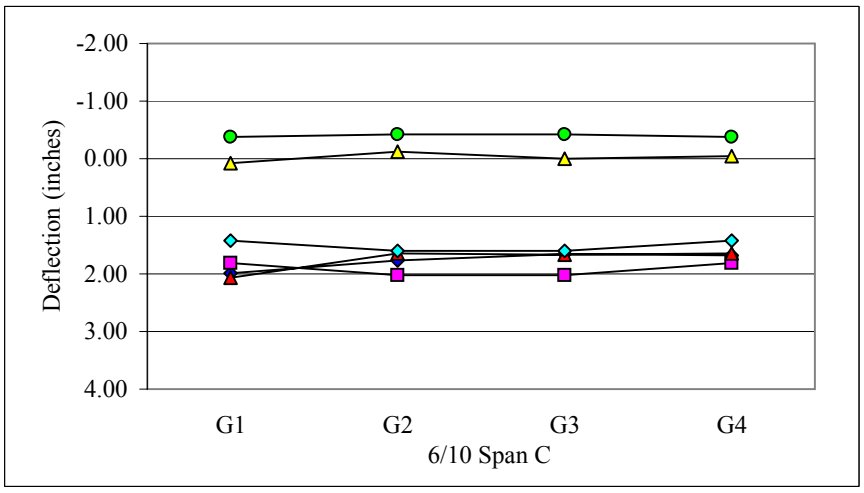

FIELD MEASUREMENT SUMMARY

PROJECT NUMBER: R-2547 (Knightdale-Eagle Rock Rd. Over US-64 Bypass)
MEASUREMENT DATE: March 20 & March 29, 2004

GIRDER DEFLECTIONS
ELEVATION VIEW

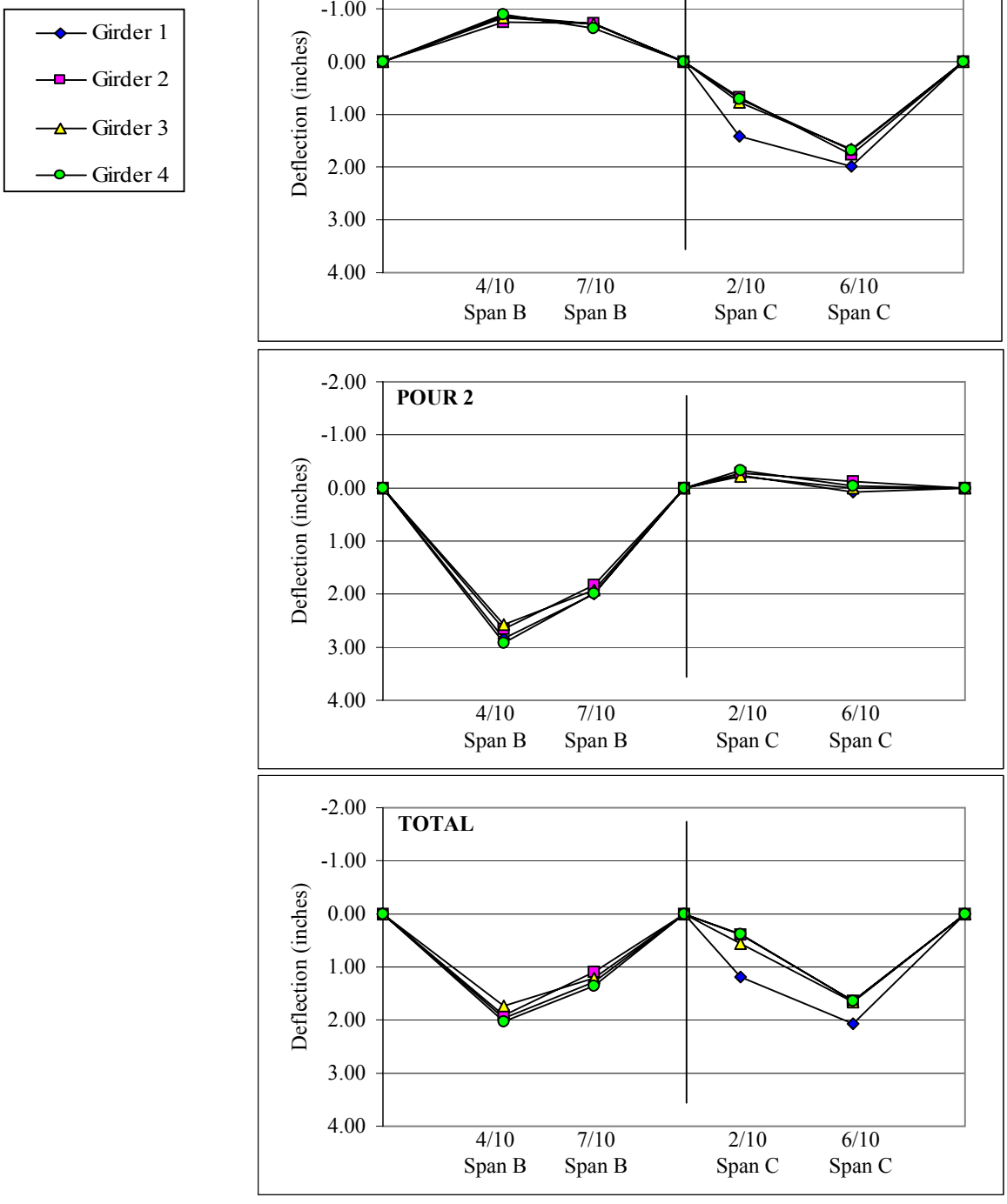

ANSYS FINITE ELEMENT MODELING SUMMARY

PROJECT NUMBER: R-2547 (Knightdale-Eagle Rock Rd. Over US-64 Bypass)

MODEL PICTURE: (Steel Only, Isometric View)

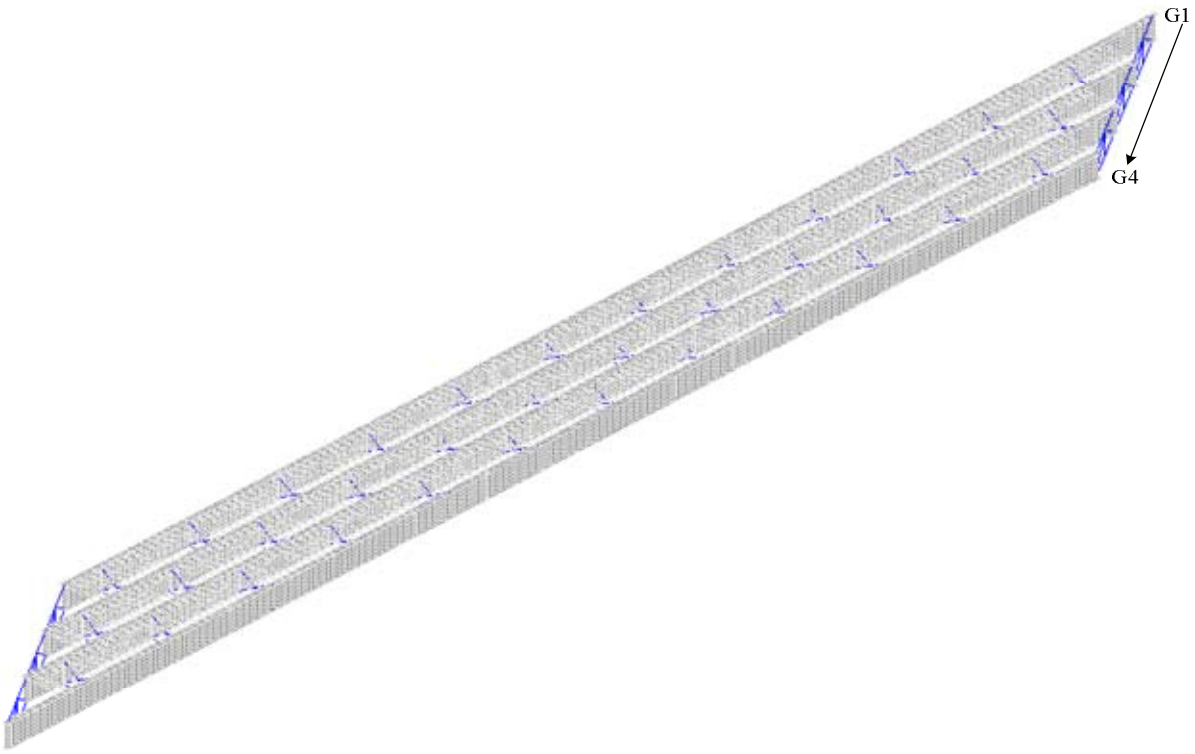

ANSYS FINITE ELEMENT MODELING SUMMARY

PROJECT NUMBER: R-2547 (Knightdale-Eagle Rock Rd. Over US-64 Bypass)

MODEL DESCRIPTION

COMPONENT	**Element Type**
Girder:	SHELL93
Connector Plates:	SHELL93
Stiffener Plates:	SHELL93
Cross-frame Members:	LINK8 (diagonal)
	LINK8 (horizontal)
End Diaphragm:	LINK8 (diagonal)
	LINK8 (vertical)
	BEAM4 (horizontal)
Stay-in-place Deck Forms:	LINK8
Concrete Slab:	SHELL63
Shear Studs:	MPC184

APPLIED LOADS

Girder	*Load	
	lb/ft	N/mm
G1	674.3	14.81
G2	1068.1	16.62
G3	1065.4	16.62
G4	1062.8	14.81

*applied as a uniform pressure to area of top flange

	ANSYS Pour 1 Loading				ANSYS Pour 1 Loading (SIP)			
Point	**4/10 B**	**7/10 B**	**2/10 C**	**6/10 C**	**4/10 B**	**7/10 B**	**2/10 C**	**6/10 C**
G1	-0.56	-0.59	0.68	1.49	-0.56	-0.60	0.69	1.51
G2	-0.49	-0.53	0.61	1.40	-0.49	-0.52	0.60	1.38
G3	-0.48	-0.50	0.59	1.37	-0.47	-0.49	0.58	1.34
G4	-0.50	-0.53	0.61	1.42	-0.48	-0.51	0.59	1.40
	ANSYS Pour 2 Loading				**ANSYS Pour 2 Loading (SIP)**			
Point	**4/10 B**	**7/10 B**	**2/10 C**	**6/10 C**	**4/10 B**	**7/10 B**	**2/10 C**	**6/10 C**
G1	2.34	1.63	-0.32	-0.22	2.30	1.57	-0.29	-0.20
G2	2.27	1.61	-0.28	-0.22	2.21	1.56	-0.27	-0.20
G3	2.30	1.63	-0.31	-0.23	2.27	1.61	-0.31	-0.22
G4	2.42	1.73	-0.36	-0.27	2.45	1.77	-0.38	-0.29
	ANSYS Total				**ANSYS Total (SIP)**			
Point	**4/10 B**	**7/10 B**	**2/10 C**	**6/10 C**	**4/10 B**	**7/10 B**	**2/10 C**	**6/10 C**
G1	1.79	1.04	0.36	1.26	1.74	0.98	0.40	1.30
G2	1.78	1.08	0.32	1.18	1.72	1.04	0.33	1.17
G3	1.82	1.13	0.29	1.14	1.80	1.12	0.28	1.11
G4	1.92	1.20	0.25	1.15	1.97	1.26	0.21	1.11
	Pour 1 Measured				**Pour 2 Measured**			
Point	**4/10 B**	**7/10 B**	**2/10 C**	**6/10 C**	**4/10 B**	**7/10 B**	**2/10 C**	**6/10 C**
G1	-0.87	-0.71	1.42	1.99	2.83	2.00	-0.23	0.08
G2	-0.75	-0.73	0.67	1.76	2.66	1.83	-0.28	-0.12
G3	-0.83	-0.71	0.78	1.66	2.57	1.92	-0.22	0.00
G4	-0.89	-0.63	0.71	1.68	2.92	1.99	-0.33	-0.04
	Total Measured							
Point	**4/10 B**	**7/10 B**	**2/10 C**	**6/10 C**				
G1	1.97	1.29	1.18	2.07				
G2	1.91	1.10	0.39	1.64				
G3	1.74	1.21	0.56	1.66				
G4	2.02	1.36	0.38	1.64				

ANSYS FINITE ELEMENT MODELING SUMMARY

PROJECT NUMBER: R-2547 (Knightdale-Eagle Rock Rd. Over US-64 Bypass)

GIRDER DEFLECTIONS
CROSS SECTION VIEW

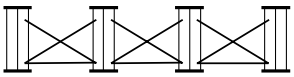

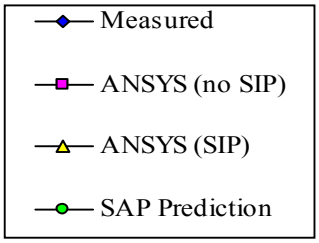

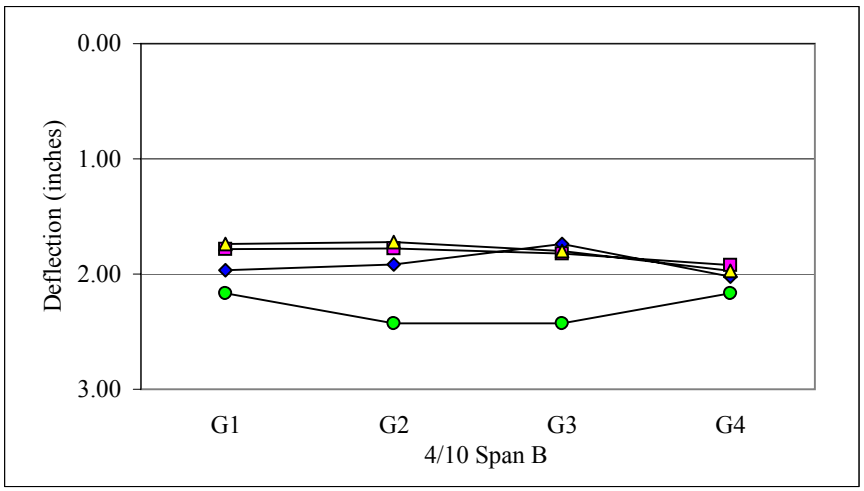

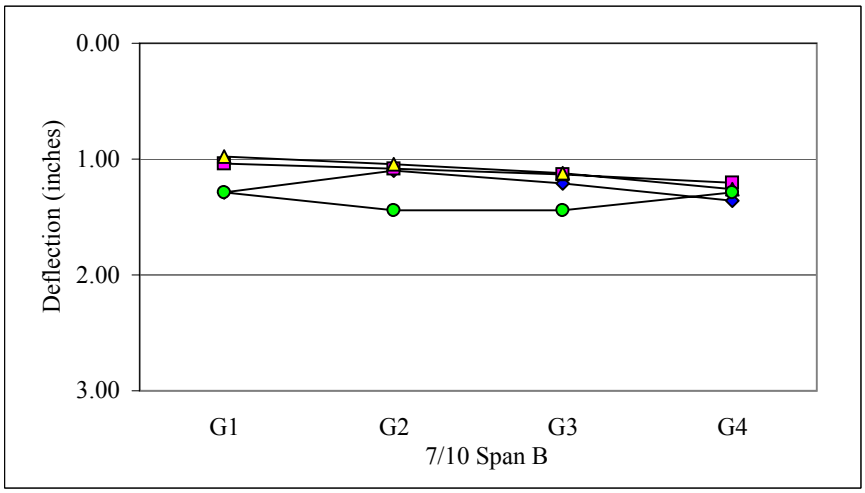

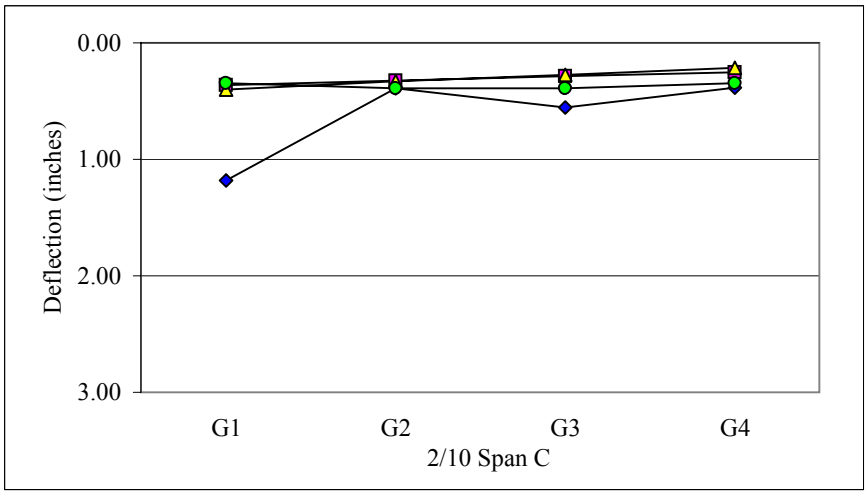

ANSYS FINITE ELEMENT MODELING SUMMARY

PROJECT NUMBER: R-2547 (Knightdale-Eagle Rock Rd. Over US-64 Bypass)

GIRDER DEFLECTIONS
CROSS SECTION VIEW

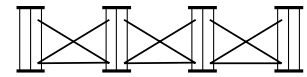

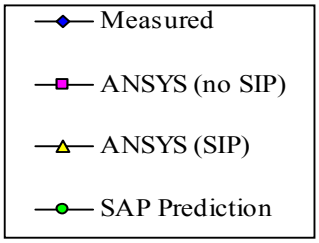

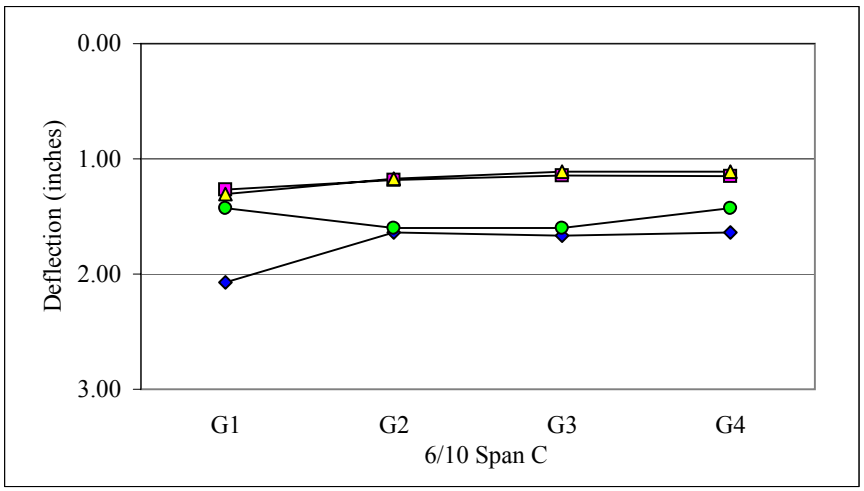

FIELD MEASUREMENT SUMMARY

PROJECT NUMBER: R-2547 (Knightdale-Eagle Rock Rd. Over US-64 Bypass)
MEASUREMENT DATE: March 20 & March 29, 2004

GIRDER DEFLECTIONS
CROSS SECTION VIEW

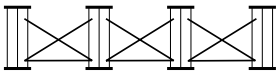

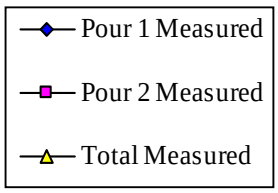

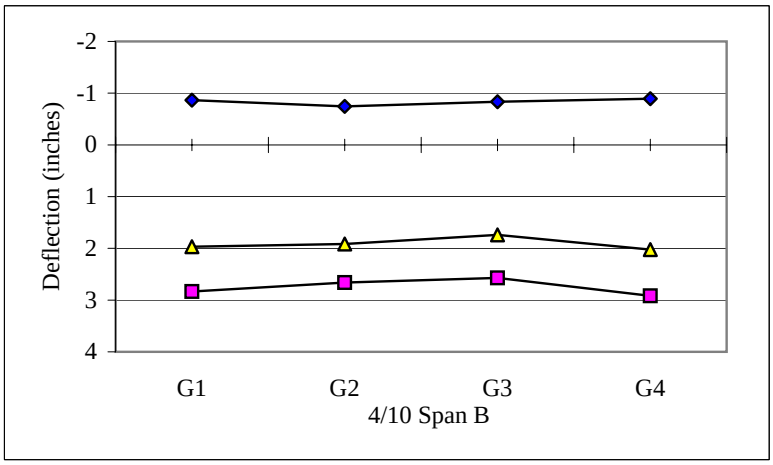

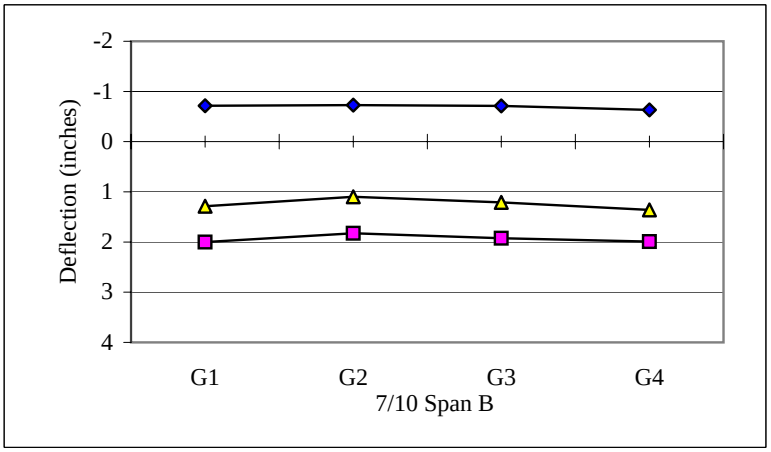

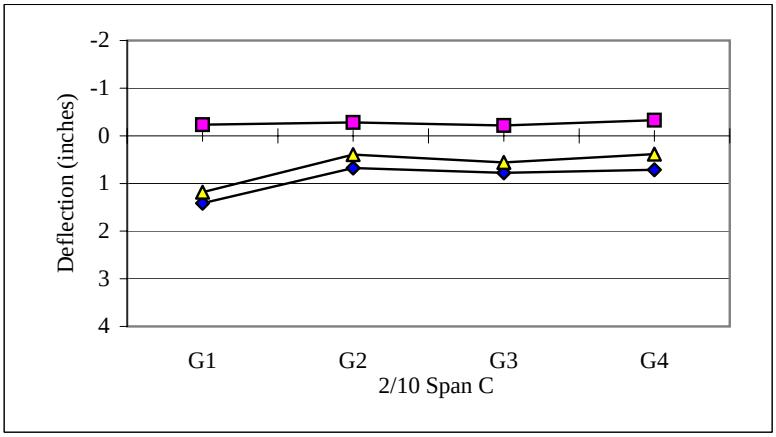

FIELD MEASUREMENT SUMMARY

PROJECT NUMBER: R-2547 (Knightdale-Eagle Rock Rd. Over US-64 Bypass)
MEASUREMENT DATE: March 20 & March 29, 2004

GIRDER DEFLECTIONS
CROSS SECTION VIEW

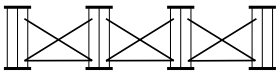

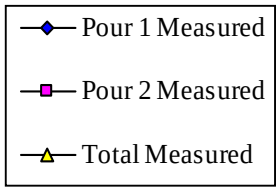

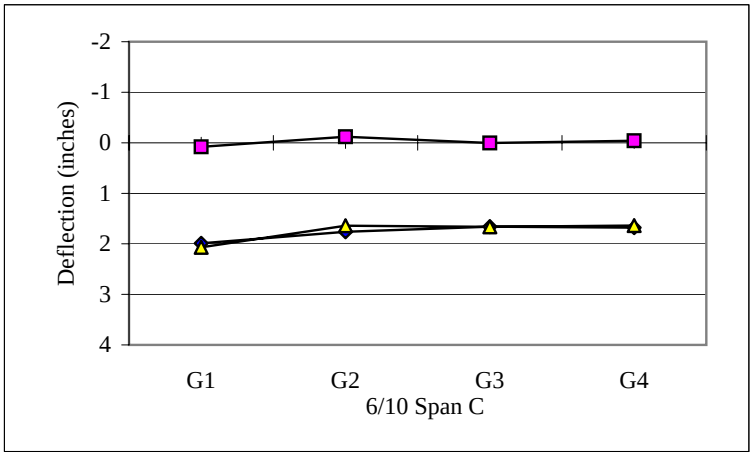

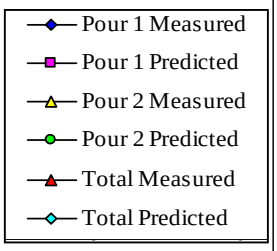

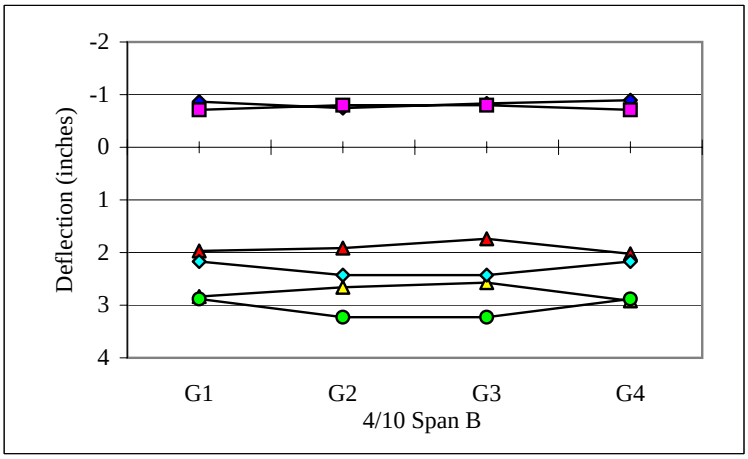

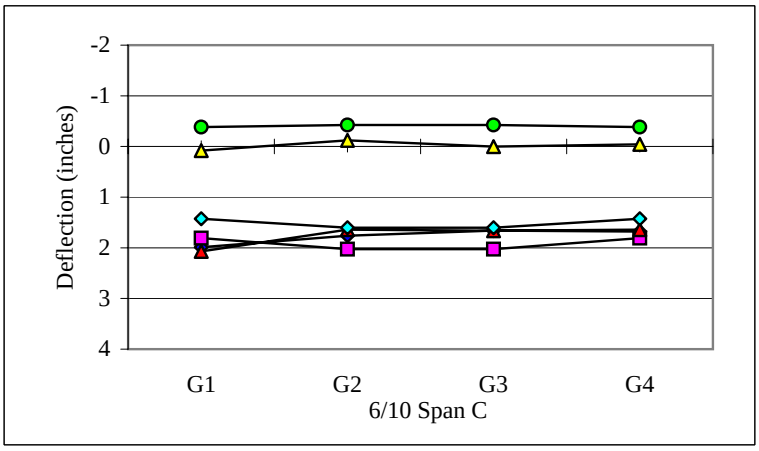

FIELD MEASUREMENT SUMMARY

PROJECT NUMBER: R-2547 (Knightdale-Eagle Rock Rd. Over US-64 Bypass)
MEASUREMENT DATE: March 20 & March 29, 2004

GIRDER DEFLECTIONS
ELEVATION VIEW

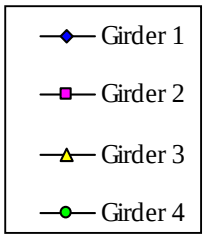

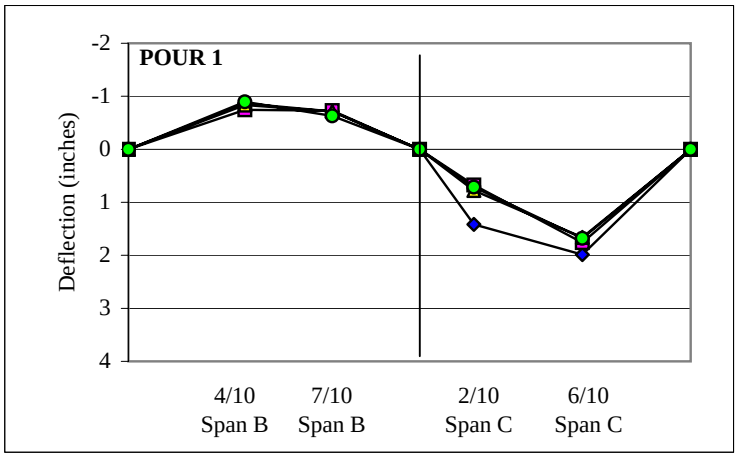

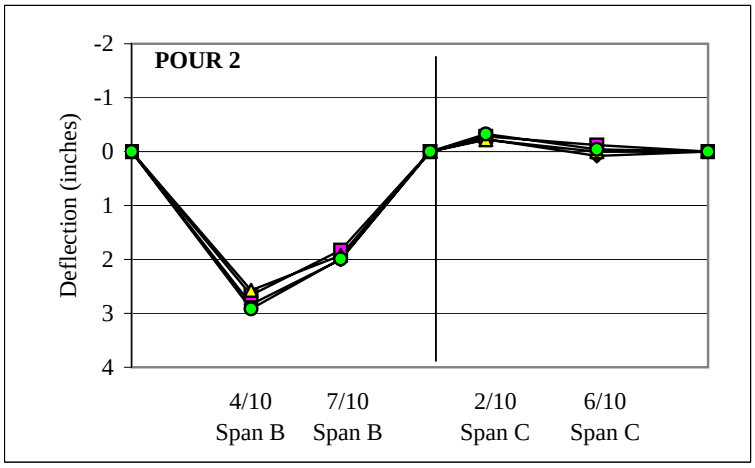

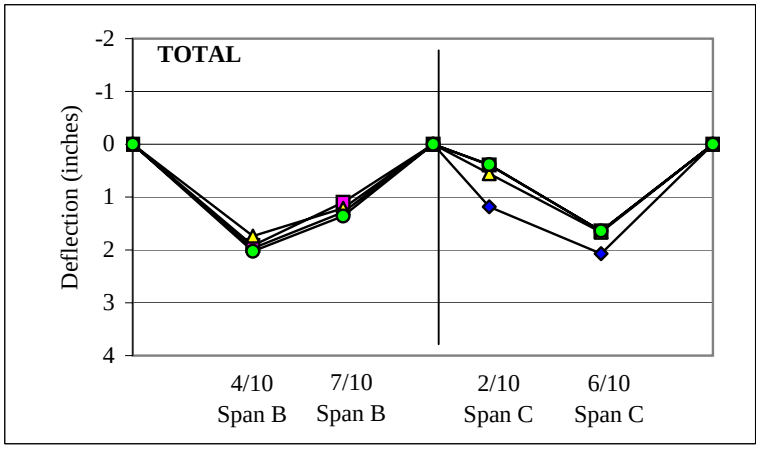

Appendix L

Deflection Summary for Bridge 1

This appendix contains a detailed description of Bridge 1 including bridge geometry, material data, cross frame type and size, and dead loads calculated from slab geometry. Illustrations detailing the bridge geometry and field measurement locations are included, along with tables and graphs of the field measured non-composite girder deflections.

A summary of the ANSYS finite element model created for Bridge 1 is also included in this appendix. This summary includes a picture of the ANSYS model, details about the elements used in the model generation, the loads applied to the model, and tables and graphs of the deflections predicted by the model.

FIELD MEASUREMENT SUMMARY

PROJECT NUMBER: R-2547 (Rogers Ln. Extension over US 64 Bypass)
MEASUREMENT DATE: October 19, October 26, & November 3, 2004

BRIDGE DESCRIPTION

TYPE	Three Span Continous	
LENGTH	585.98 ft (178.608 m)	
NUMBER OF GIRDERS	7	
GIRDER SPACING	9.68 ft (2.95 m)	
SKEW	57.6 deg	
OVERHANG	3.28 ft (1000 mm)	(from web centerline)
BEARING TYPE	Pot Bearing	

MATERIAL DATA

STRUCTURAL STEEL	**Grade**	**Yield Strength**
Girder:	AASHTO M270	50 ksi (345 MPa)
Other:	AASHTO M270	50 ksi (345 MPa)

CONCRETE UNIT WEIGHT	150 pcf (nominal)
SIP FORM WEIGHT	2.57 psf (CSI Catalog)

GIRDER DATA

LENGTH	164.09 ft (50.015 m)	"Span A"
	233.61 ft (71.205 m)	"Span B"
	188.28 ft (57.388 m)	"Span C"

WEB THICKNESS	0.63 in (16 mm)
WEB DEPTH	90.55 in (2300 mm)
TOP FLANGE WIDTH	19.69 in (500 mm)
BOTTOM FLANGE WIDTH	22.05 in (560 mm)

FLANGE THICKNESSES

Top	**Bottom**	**Begin**	**End**
0.87 in (22 mm)	0.98 in (25 mm)	0.00	104.92 ft (31.981 m)
1.38 in (35 mm)	1.38 in (35 mm)	104.92 ft (31.981 m)	147.69 ft (45.016 m)
2.17 in (55 mm)	2.36 in (60 mm)	147.69 ft (45.016 m)	180.50 ft (55.016 m)
1.38 in (35 mm)	1.38 in (35 mm)	180.50 ft (55.016 m)	223.03 ft (67.981 m)
0.87 in (22 mm)	1.18 in (30 mm)	223.03 ft (67.981 m)	343.27 ft (104.629 m)
1.38 in (35 mm)	1.38 in (35 mm)	343.27 ft (104.629 m)	378.02 ft (115.221 m)
2.76 in (70 mm)	2.76 in (70 mm)	378.02 ft (115.221 m)	417.39 ft (127.221 m)
1.38 in (35 mm)	1.38 in (35 mm)	417.39 ft (127.221 m)	464.66 ft (141.629 m)
0.87 in (22 mm)	1.18 in (30 mm)	464.66 ft (141.629 m)	585.98 ft (178.608 m)

FIELD MEASUREMENT SUMMARY

PROJECT NUMBER: R-2547 (Rogers Ln. Extension over US 64 Bypass)
MEASUREMENT DATE: October 19, October 26, & November 3, 2004

STIFFENERS

Longitudinal:	N/A
Bearing:	PL 0.98" × 9.06" (25 mm × 230 mm)
Intermediate:	PL 0.47" × NA (12 mm × NA, connector plate)
	PL 0.71" × 7.68" (18 mm × 195 mm)
Middle Bearing:	PL 1.57" × 9.06" (40 mm × 230 mm)
End Bent Connector:	PL 0.79" × NA (20 mm × NA, connector plate)

CROSS-FRAME DATA

	Diagonals	**Horizontals**	**Verticals**
END BENT (D1, Type K)	WT 5 x 15	C 15 x 33.9 (Top)	NA
		WT 5 x 15 (Bottom)	
MIDDLE BENT (D3, Type K)	L 4 x 4 x 1/2"	L 4 x 4 x 1/2" (Top)	NA
		L 4 x 4 x 1/2" (Bottom)	
INTERMEDIATE (D4, Type K)	L 4 x 4 x 1/2"	L 4 x 4 x 1/2" (Top)	NA
		L 4 x 4 x 1/2" (Bottom)	
INTERMEDIATE (D2, Type K)	L 4 x 4 x 1/2"	L 4 x 4 x 1/2" (Bottom)	NA

SLAB DATA

THICKNESS	8.86 in (225 mm)	nominal
BUILD-UP	3.54 in (90 mm)	nominal

Over Middle 2 Bents:

LONGITUDINAL REBAR	SIZE (metric)	SPACING (nominal)
Top:	#16	5.12 in (130 mm)
Bottom:	#16	9.45 in (240 mm)
TRANSVERSE REBAR		
Top:	#16	6.30 in (160 mm)
Bottom:	#16	6.30 in (160 mm)

Otherwise:

LONGITUDINAL REBAR	SIZE (metric)	SPACING (nominal)
Top:	#16	20.47 in (520 mm)
Bottom:	#16	9.45 in (240 mm)
TRANSVERSE REBAR		
Top:	#16	6.30 in (160 mm)
Bottom:	#16	6.30 in (160 mm)

FIELD MEASUREMENT SUMMARY

Project Number: R-2547 (Rogers Ln. Extension over US 64 Bypass)
Measurement Date: October 19, October 26, & November 3, 2004

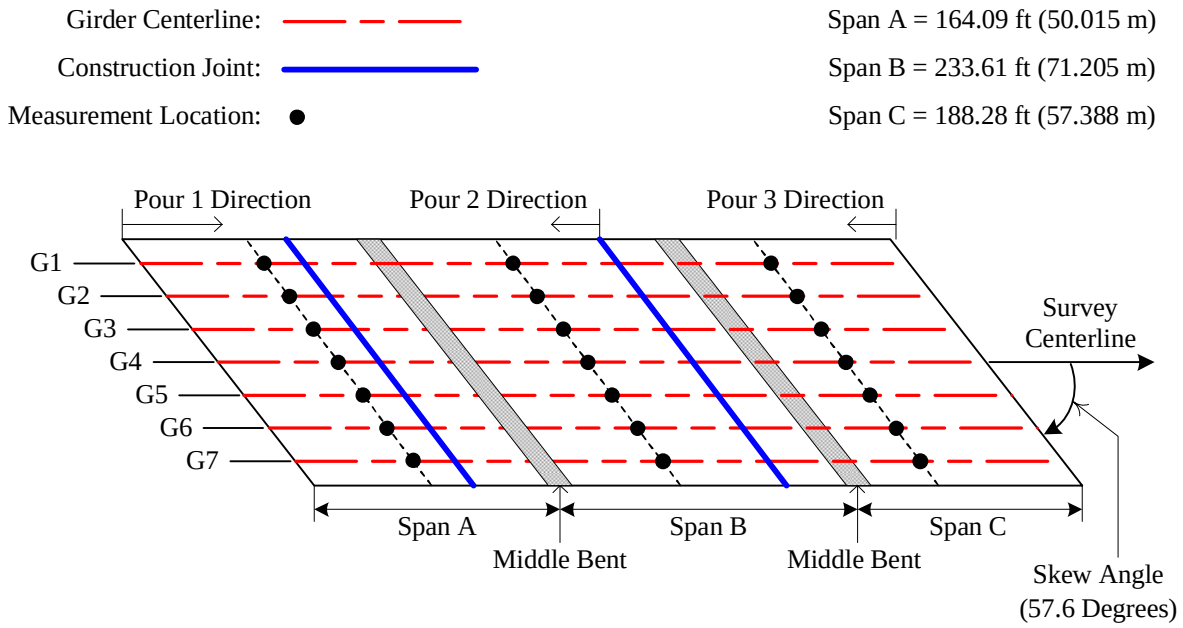

(a) Plan View (Not to Scale)

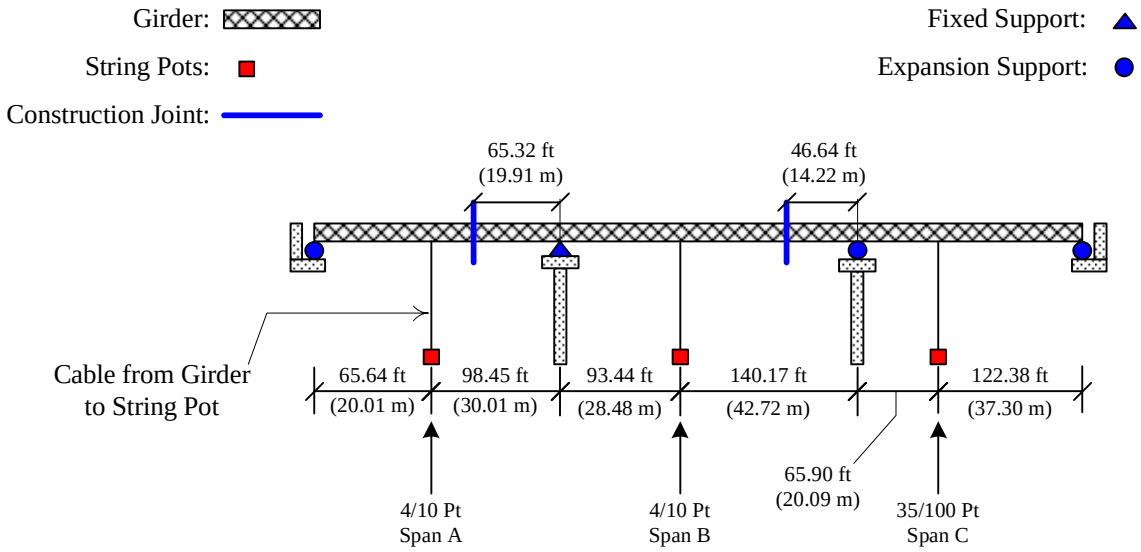

(b) Elevation View (Not to Scale)

Plan and Elevation View of Bridge 1 (Raleigh, NC)

FIELD MEASUREMENT SUMMARY

PROJECT NUMBER: R-2547 (Rogers Ln. Extension over US 64 Bypass)
MEASUREMENT DATE: October 19, October 26, & November 3, 2004

DECK LOADS

Girder	Concrete[1]		Slab[2]		Ratio
	lb/ft	N/mm	lb/ft	N/mm	
G1	1109.37	16.19	1177.89	17.19	0.94
G2	1183.37	17.27	1273.82	18.59	0.93
G4	1183.37	17.27	1273.82	18.59	0.93
G6	1183.37	17.27	1273.82	18.59	0.93
G7	1109.37	16.19	1177.89	17.19	0.94

[1] Calculated with nominal slab thicknesses

[2] Includes slab, buildups, and stay-in-place forms (nominal)

GIRDER DEFLECTIONS (data in inches, negative is deflection upwards)

POUR 1 MEASURED

	2/10 Span A Loading			6/10 Span A Loading		
Point	**4/10 A**	**4/10 B**	**35/100 C**	**4/10 A**	**4/10 B**	**35/100 C**
G1	0.60	-0.21	0.06	2.39	-0.99	0.25
G2	0.54	-0.20	0.06	2.23	-0.99	0.24
G4	0.46	-0.14	0.07	2.08	-0.95	0.30
G6	0.49	-0.19	0.07	2.14	-1.03	0.28
G7	0.54	-0.19	0.07	2.26	-1.01	0.29

POUR 2 MEASURED

	4/10 Span B Loading			2/10 Span B Loading			Middle Bent 1		
Point	**4/10 A**	**4/10 B**	**35/100 C**	**4/10 A**	**4/10 B**	**35/100 C**	**4/10 A**	**4/10 B**	**35/100 C**
G1	-0.56	2.87	-1.53	-1.18	5.79	-2.23	-1.47	6.80	-2.61
G2	-0.55	2.84	-1.52	-1.15	5.58	-2.26	-1.42	6.56	-2.66
G4	-0.57	2.86	-1.43	-1.10	5.41	-2.16	-1.34	6.32	-2.48
G6	-0.58	2.98	-1.41	-0.97	5.40	-2.15	-1.10	6.22	-2.42
G7	-0.57	3.05	-1.40	-0.90	5.44	-2.07	-0.94	6.15	-2.29

	8/10 Span A Loading			6/10 Span A Loading		
Point	**4/10 A**	**4/10 B**	**35/100 C**	**4/10 A**	**4/10 B**	**35/100 C**
G1	-0.95	6.49	-2.62	-0.69	6.33	-2.54
G2	-0.96	6.28	-2.63	-0.73	6.14	-2.58
G4	-0.95	6.05	-2.47	-0.74	5.96	-2.45
G6	-0.72	5.91	-2.38	-0.60	5.87	-2.38
G7	-0.71	5.82	-2.30	-0.58	5.80	-2.30

FIELD MEASUREMENT SUMMARY

PROJECT NUMBER: R-2547 (Rogers Ln. Extension over US 64 Bypass)
MEASUREMENT DATE: October 19, October 26, & November 3, 2004

GIRDER DEFLECTIONS (data in inches, negative is deflection upwards)
POUR 3 MEASURED

	8/10 Span C Loading			4/10 Span C Loading			2/10 Span C Loading		
Point	**4/10 A**	**4/10 B**	**35/100 C**	**4/10 A**	**4/10 B**	**35/100 C**	**4/10 A**	**4/10 B**	**35/100 C**
G1	0.02	-0.23	0.82	0.15	-0.73	2.48	0.26	-1.03	3.53
G2	0.03	-0.21	0.82	0.16	-0.73	2.38	0.25	-1.04	3.45
G4	0.02	-0.21	0.82	0.16	-0.77	2.16	0.24	-1.12	3.35
G6	0.02	-0.22	0.95	0.17	-0.82	2.22	0.27	-1.18	3.63
G7	0.00	-0.22	1.05	0.17	-0.82	2.28	0.28	-1.19	3.86

	Middle Bent 2			Complete Loading		
Point	**4/10 A**	**4/10 B**	**35/100 C**	**4/10 A**	**4/10 B**	**35/100 C**
G1	0.36	-1.11	3.91	0.28	-0.75	3.56
G2	0.30	-1.14	3.81	0.22	-0.77	3.47
G4	0.28	-1.20	3.66	0.19	-0.83	3.35
G6	0.32	-1.23	3.86	0.23	-0.86	3.52
G7	0.34	-1.20	4.07	0.35	-0.82	3.73

TOTAL MEASURED

	Super-Imposed Total		
Point	**4/10 A**	**4/10 B**	**35/100 C**
G1	1.99	4.59	1.27
G2	1.73	4.38	1.13
G4	1.53	4.18	1.21
G6	1.77	3.99	1.41
G7	2.03	3.96	1.72

PREDICTIONS[4] (Single Girder-Line Model in SAP 2000)

	Pour 1			Pour 2		
Point	**4/10 A**	**4/10 B**	**35/100 C**	**4/10 A**	**4/10 B**	**35/100 C**
G1	2.36	-1.29	0.35	-1.04	5.95	-2.60
G2	2.52	-1.38	0.38	-1.09	6.35	-2.77
G3	2.52	-1.38	0.38	-1.09	6.35	-2.77
G4	2.52	-1.38	0.38	-1.09	6.35	-2.77
G5	2.36	-1.29	0.35	-1.04	5.95	-2.60

	Pour 3			Super-Imposed Total		
Point	**4/10 A**	**4/10 B**	**35/100 C**	**4/10 A**	**4/10 B**	**35/100 C**
G1	0.26	-1.06	3.57	1.59	3.60	1.33
G2	0.28	-1.11	3.80	1.70	3.85	1.40
G3	0.28	-1.11	3.80	1.70	3.85	1.40
G4	0.28	-1.11	3.80	1.70	3.85	1.40
G5	0.26	-1.06	3.57	1.59	3.60	1.33

[4] Using nominal slab thicknesses

FIELD MEASUREMENT SUMMARY

PROJECT NUMBER: R-2547 (Rogers Ln. Extension over US 64 Bypass)
MEASUREMENT DATE: October 19, October 26, & November 3, 2004

GIRDER DEFLECTIONS
CROSS SECTION VIEW

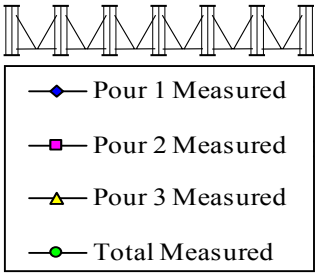

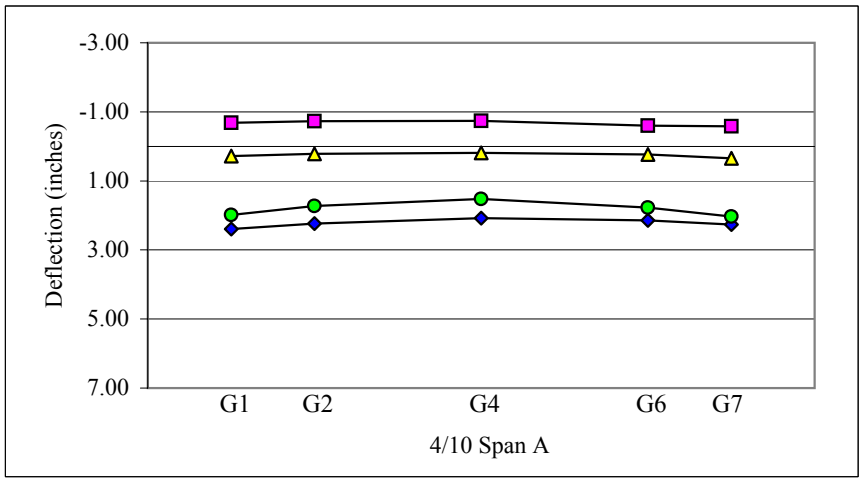

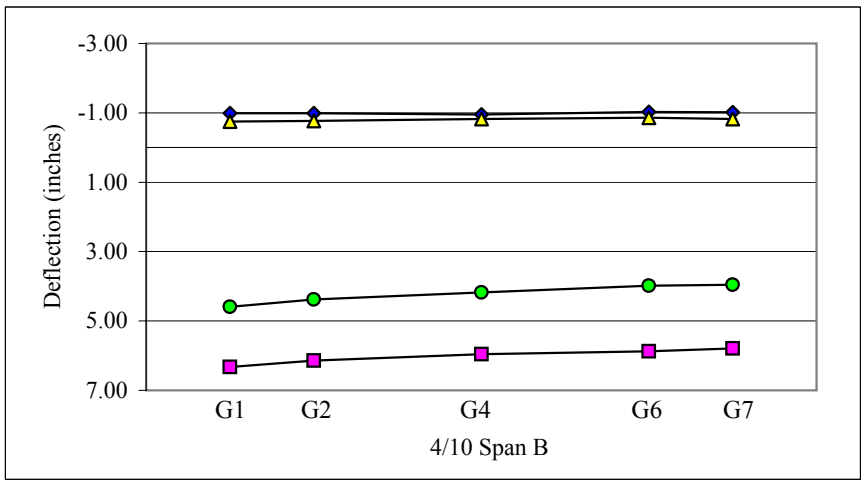

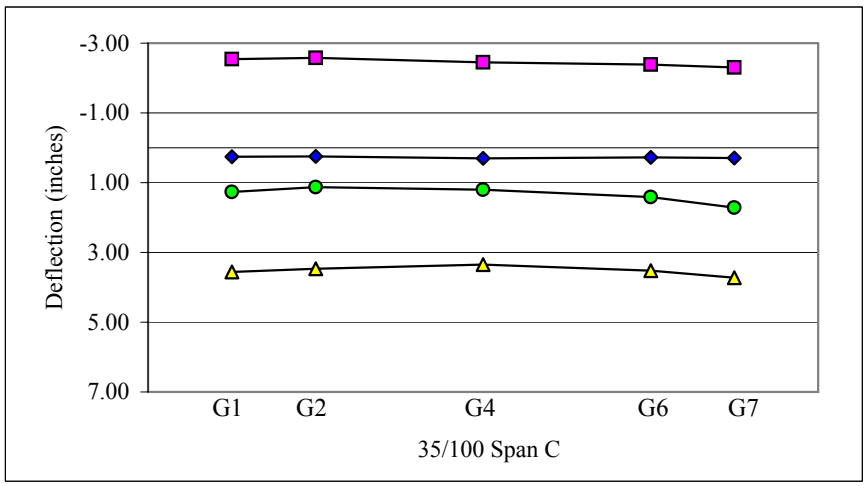

FIELD MEASUREMENT SUMMARY

PROJECT NUMBER: R-2547 (Rogers Ln. Extension over US 64 Bypass)
MEASUREMENT DATE: October 19, October 26, & November 3, 2004

GIRDER DEFLECTIONS
CROSS SECTION VIEW

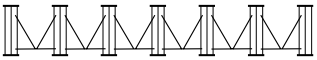

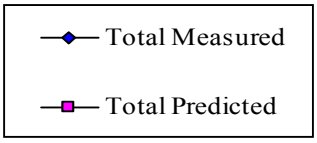

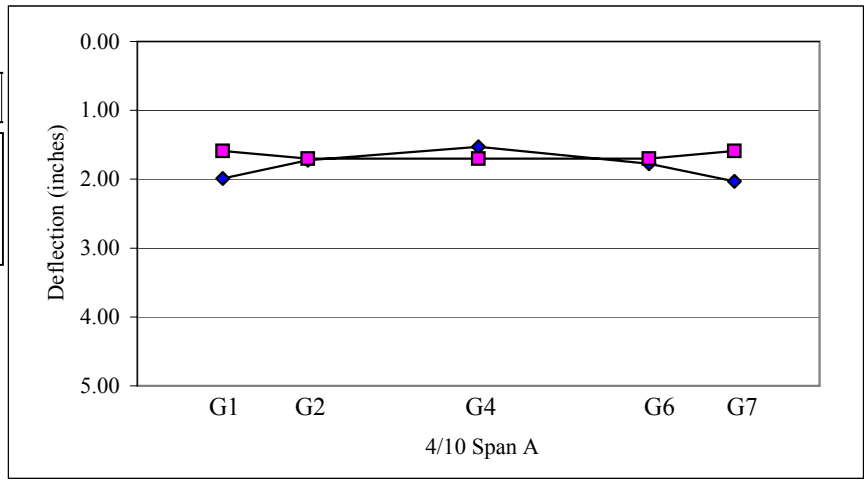

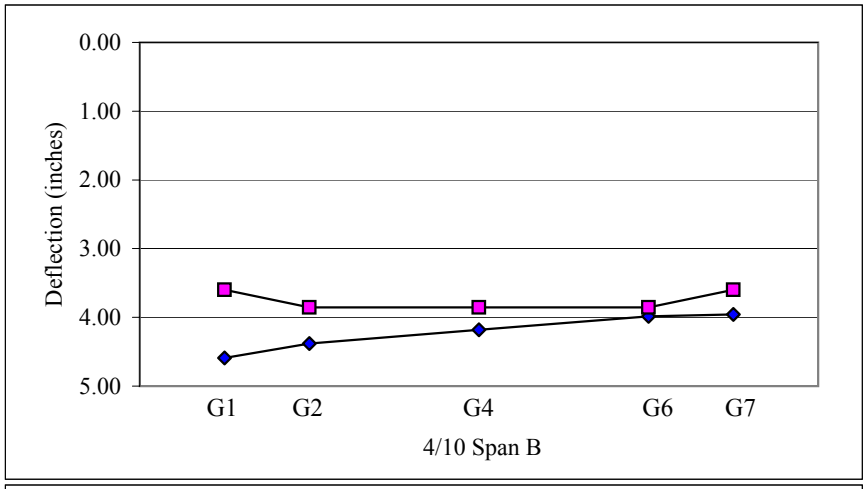

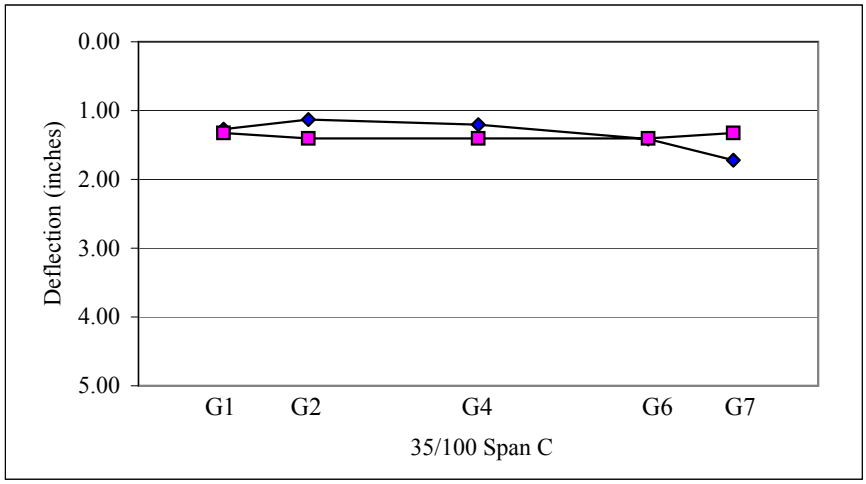

FIELD MEASUREMENT SUMMARY

PROJECT NUMBER: R-2547 (Rogers Ln. Extension over US 64 Bypass)
MEASUREMENT DATE: October 19, October 26, & November 3, 2004

GIRDER DEFLECTIONS
ELEVATION VIEW

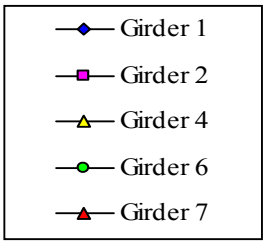

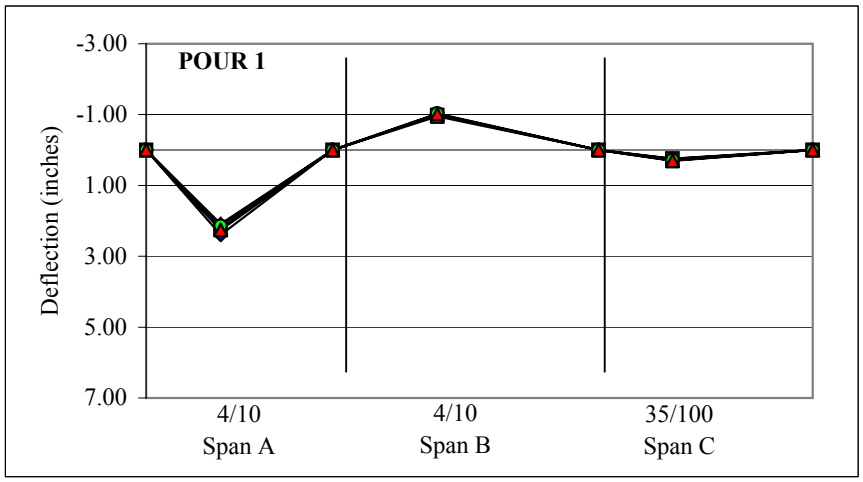

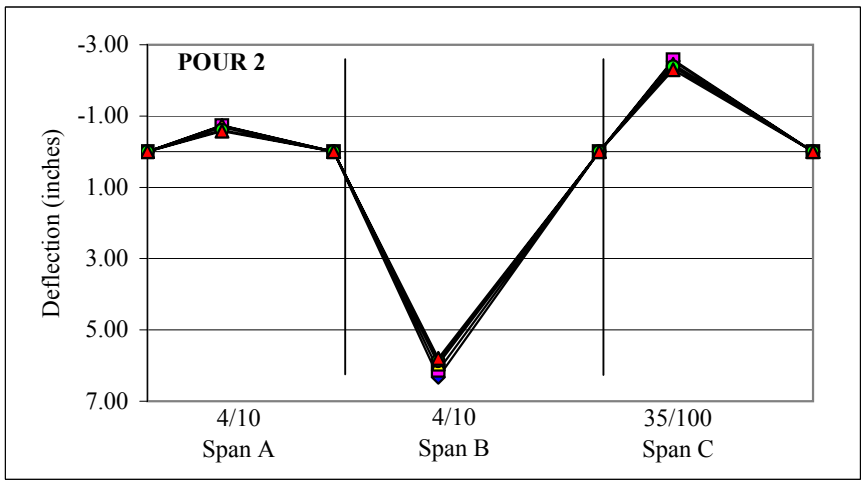

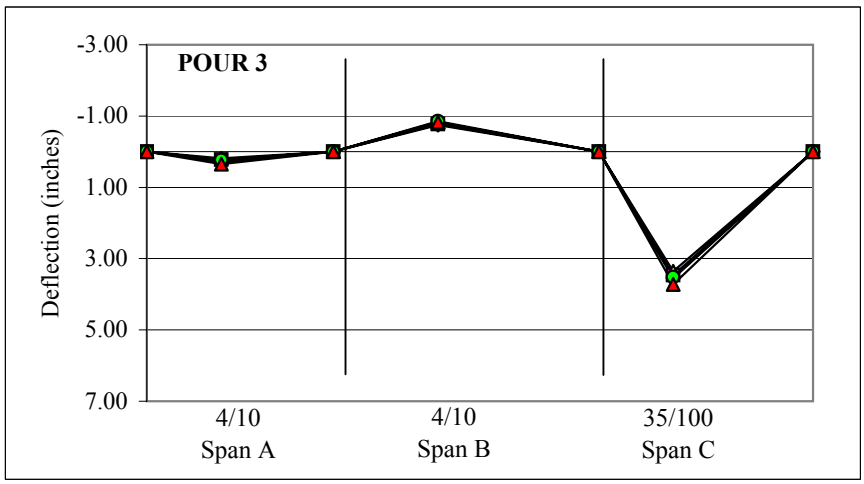

FIELD MEASUREMENT SUMMARY

PROJECT NUMBER: R-2547 (Rogers Ln. Extension over US 64 Bypass)
MEASUREMENT DATE: October 19, October 26, & November 3, 2004

GIRDER DEFLECTIONS
ELEVATION VIEW

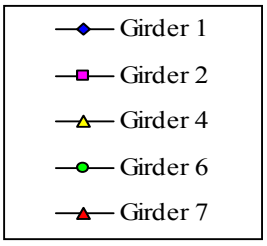

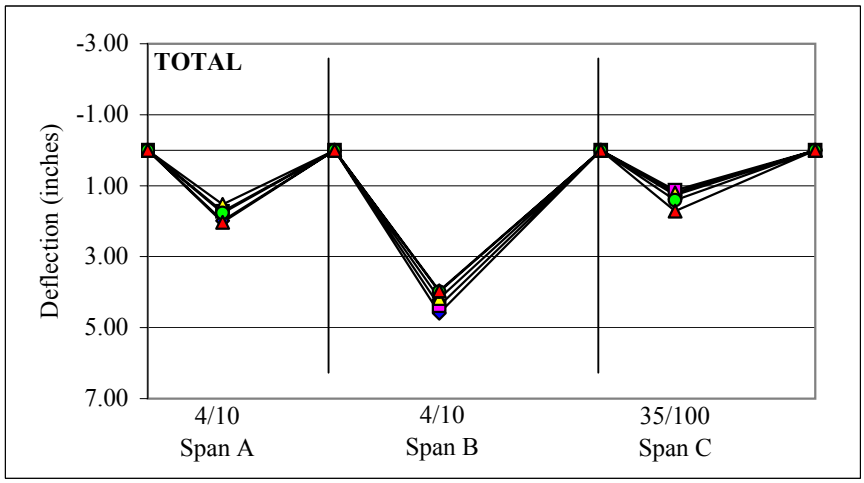

ANSYS FINITE ELEMENT MODELING SUMMARY

PROJECT NUMBER: R-2547 (Ramp (RPBDY1) Over US-64 Business)

MODEL PICTURE: (Steel Only, Oblique View)

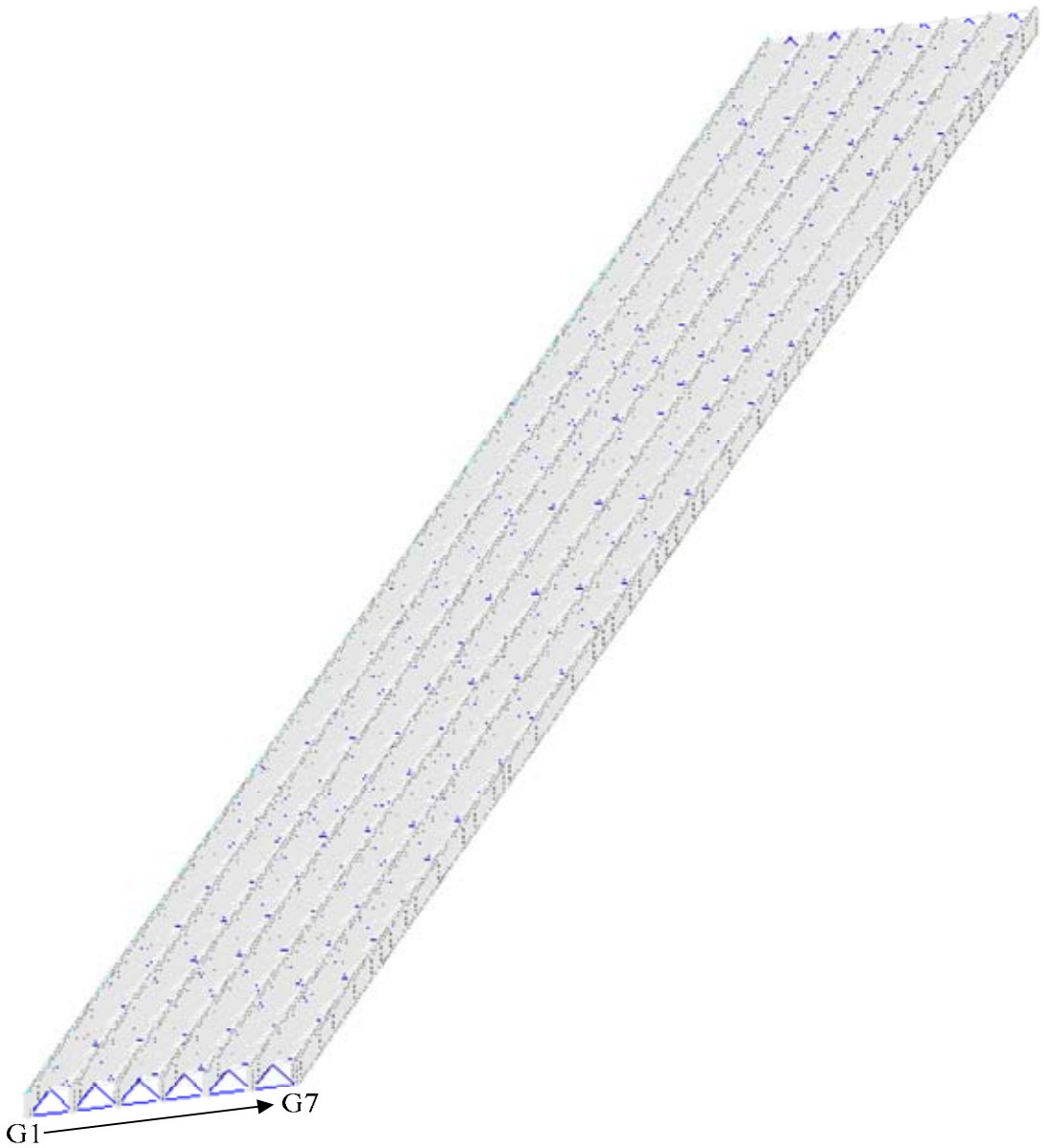

ANSYS FINITE ELEMENT MODELING SUMMARY

PROJECT NUMBER: R-2547 (Ramp (RPBDY1) Over US-64 Business)

MODEL DESCRIPTION

COMPONENT	**Element Type**
Girder:	SHELL93
Connector Plates:	SHELL93
Stiffener Plates:	SHELL93
Cross-frame Members:	LINK8 (diagonal)
	BEAM4 (horizontal)
Middle Diaphragm:	LINK8 (diagonal)
	BEAM4 (horizontal)
Stay-in-place Deck Forms:	LINK8
Concrete Slab:	SHELL63
Shear Studs:	MPC184

APPLIED LOADS

Girder	*Load	
	lb/ft	N/mm
G1	1109.37	16.19
G2	1183.37	17.27
G4	1183.37	17.27
G6	1183.37	17.27
G7	1109.37	16.19

*applied as a uniform pressure to area of top flange

	ANSYS Pour 1			ANSYS Pour 1 (SIP)			Pour 1 Measured		
Point	**4/10 A**	**4/10 B**	**35/100 C**	**4/10 A**	**4/10 B**	**35/100 C**	**4/10 A**	**4/10 B**	**35/100 C**
G1	2.34	-1.24	0.33	2.36	-1.25	0.33	2.39	-0.99	0.25
G2	2.32	-1.22	0.32	2.32	-1.22	0.32	2.23	-0.99	0.24
G4	2.31	-1.19	0.31	2.29	-1.19	0.31	2.08	-0.95	0.30
G6	2.30	-1.20	0.31	2.30	-1.19	0.31	2.14	-1.03	0.28
G7	2.32	-1.21	0.32	2.33	-1.20	0.31	2.26	-1.01	0.29
	ANSYS Pour 2			**ANSYS Pour 2 (SIP)**			**Pour 2 Measured**		
Point	**4/10 A**	**4/10 B**	**35/100 C**	**4/10 A**	**4/10 B**	**35/100 C**	**4/10 A**	**4/10 B**	**35/100 C**
G1	-1.01	6.02	-2.54	-1.01	6.05	-2.56	-0.69	6.33	-2.54
G2	-0.99	6.00	-2.49	-0.99	5.99	-2.50	-0.73	6.14	-2.58
G4	-0.98	5.99	-2.44	-0.97	5.95	-2.43	-0.74	5.96	-2.45
G6	-1.00	6.00	-2.45	-1.00	5.99	-2.43	-0.60	5.87	-2.38
G7	-1.03	6.03	-2.49	-1.03	6.05	-2.47	-0.58	5.80	-2.30
	ANSYS Pour 3			**ANSYS Pour 3 (SIP)**			**Pour 3 Measured**		
Point	**4/10 A**	**4/10 B**	**35/100 C**	**4/10 A**	**4/10 B**	**35/100 C**	**4/10 A**	**4/10 B**	**35/100 C**
G1	0.23	-1.00	3.60	0.22	-0.98	3.58	0.28	-0.75	3.56
G2	0.23	-0.99	3.58	0.22	-0.97	3.55	0.22	-0.77	3.47
G4	0.22	-0.99	3.56	0.22	-0.98	3.54	0.19	-0.83	3.35
G6	0.23	-1.01	3.60	0.23	-1.01	3.60	0.23	-0.86	3.52
G7	0.24	-1.02	3.64	0.24	-1.04	3.68	0.35	-0.82	3.73
	ANSYS Total			**ANSYS Total (SIP)**			**Total Measured**		
Point	**4/10 A**	**4/10 B**	**35/100 C**	**4/10 A**	**4/10 B**	**35/100 C**	**4/10 A**	**4/10 B**	**35/100 C**
G1	1.56	3.79	1.39	1.58	3.82	1.35	1.99	4.59	1.27
G2	1.55	3.79	1.41	1.55	3.80	1.38	1.73	4.38	1.13
G4	1.55	3.81	1.43	1.53	3.78	1.42	1.53	4.18	1.21
G6	1.53	3.79	1.46	1.52	3.79	1.48	1.77	3.99	1.41
G7	1.53	3.79	1.47	1.54	3.81	1.52	2.03	3.96	1.72

Note: When ANSYS numbers were compared with ANSYS (SIP) numbers, there was 1% difference, therefore, ANSYS with SIP will not be shown on graphs.

ANSYS FINITE ELEMENT MODELING SUMMARY

PROJECT NUMBER: R-2547 (Ramp (RPBDY1) Over US-64 Business)

GIRDER DEFLECTIONS
CROSS SECTION VIEW

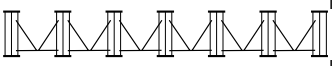

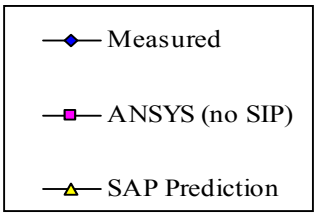

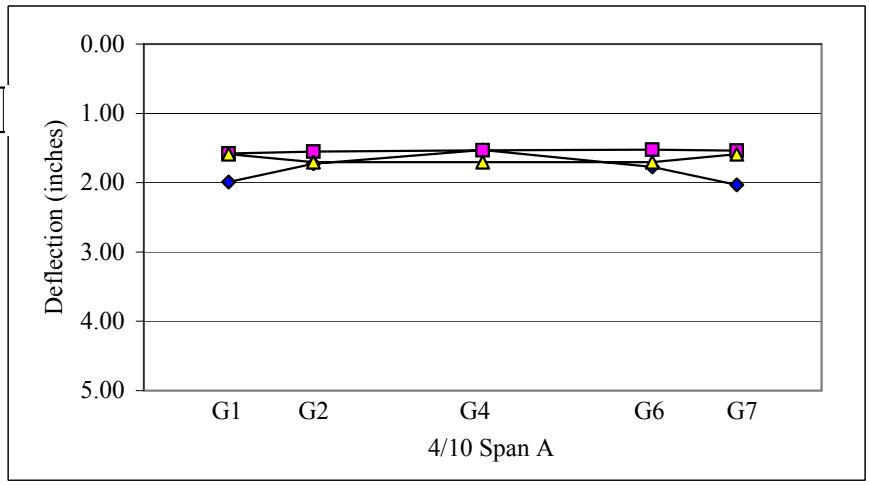

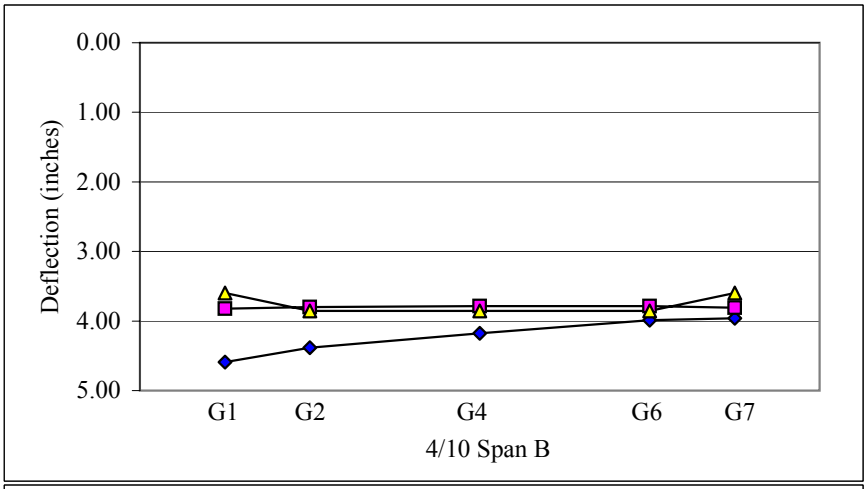

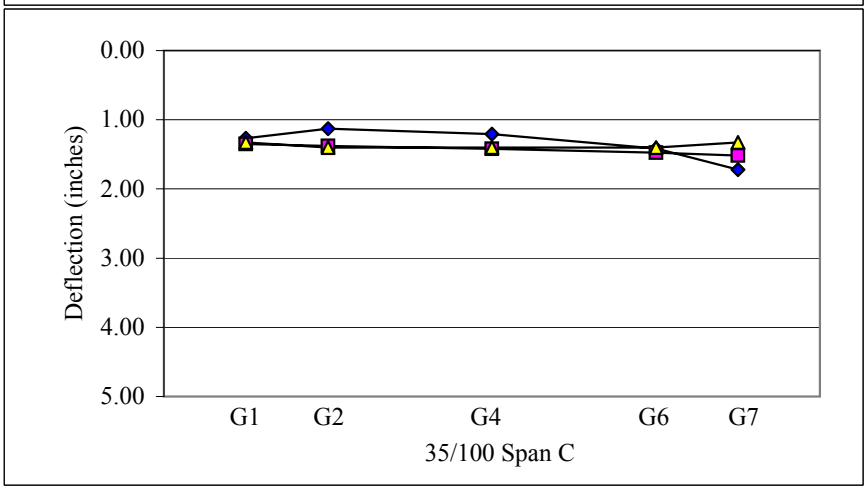

Appendix M

Sample Calculation of SIP Metal Deck Form Properties (ANSYS)

This appendix contains a step-by-step sample calculation of the SIP metal deck form properties that were used in the ANSYS bridge models. The geometry of the SIP metal deck form panels and the properties of the SIP X-braces used in the ANSYS models for each bridge were tabulated and included herein.

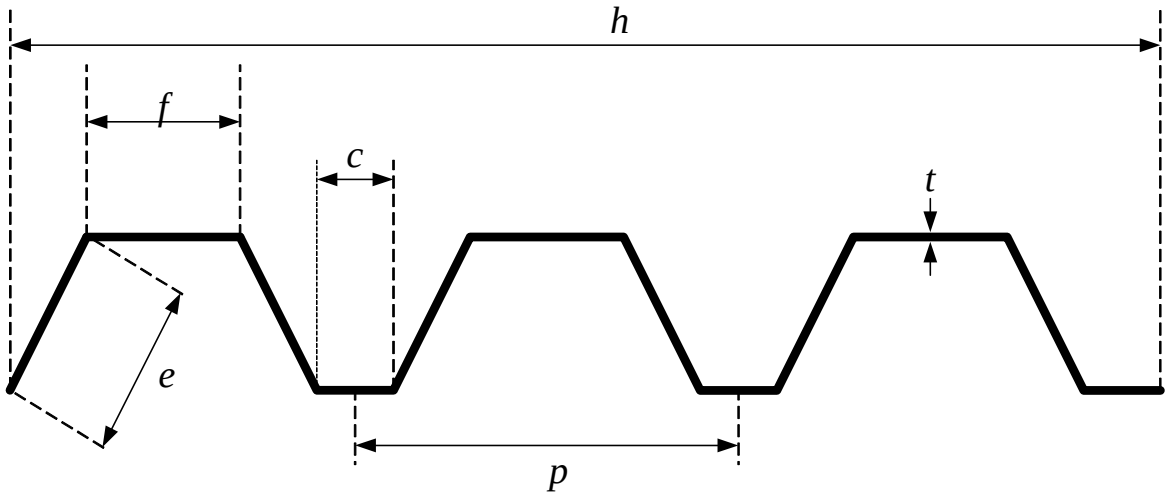

Figure M.1- Typical Stay-in-place Metal Deck Form Profile

Table M.1- Stay-in-place Metal Deck Form Data

SIP Data	Cover, *h* (inches)	Pitch, *p* (inches)	Depth, *d* (inches)	Thickness, *t* (gauge)
Eno	22.6	7.5	3.3	20
Bridge 8	24.0	8.0	3.0	15
Avondale	12.0	12.0	4.5	20
US-29	34.0	8.5	2.0	20
Camden (SB & NB)	24.0	24.0	3.0	20
Wilmington St	32.0	8.0	2.5	20
Bridge 14	24.0	8.0	3.0	20
Bridge 10	24.0	8.0	3.0	20
Bridge 1	24.0	8.0	3.0	20

Sample Calculation of Stay-in-place Metal Deck Form Properties for Camden Bridges:

Calculate flattened out panel width, *w* (see Figure M.1):

$$w = (6 \times e) + (3 \times f) + (3 \times c) = (6 \times 3.2) + (3 \times 4.0) + (3 \times 2.0) = 37.2 \text{ inches}$$

Calculate cross-sectional area, A_{panel}:

$$A_{panel} = w \times t = 37.2 \times 0.036 = 1.34 \text{ inches}^2$$

Calculate axial deflection, Δ_{panel}, of a slender rod of equal cross-sectional area:

$$\Delta_{panel} = \frac{PL}{A_{panel}E} = \frac{1 \times 44.1}{1.34 \times 29000} = 0.001 \text{ inches}$$

where: P = unit axial force
L = length of rod (equal to one half panel length)
E = elastic modulus of steel

Calculate screw flexibility, S_f:

$$S_f = \frac{1.3 \times 10^{-3}}{\sqrt{t}} = \frac{1.3 \times 10^{-3}}{\sqrt{0.036}} = 0.00685 \ \frac{\text{inches}}{\text{kip}} \text{ , SDI (1991)}$$

where: S_f = screw flexibility (in/kip)
t = thickness of panel material

Calculate stiffness of screw connection, k_{screw}:

$$k_{screw} = \frac{1}{n \times S_f} = \frac{1}{3 \times 0.00685} = 48.65 \ \frac{\text{kips}}{\text{inch}}$$

where: n = number of screws (assume 3 per panel end)
S_f = screw flexibility (in/kip)

Calculate cross-sectional area of a slender rod, A_{screw}, with axial stiffness equal to k_{screw}:

$$A_{screw} = \frac{k_{screw}L}{E} = \frac{48.65 \times 44.1}{29000} = 0.074 \text{ inches}^2$$

where: k_{screw} = stiffness of connecting screws
L = (equal to one half panel length)
E = elastic modulus of steel

Calculate axial deflection, Δ_{screw}, of a slender rod of equal cross-sectional area:

$$\Delta_{screw} = \frac{PL}{A_{screw}E} = \frac{1 \times 44.1}{0.074 \times 29000} = 0.021 \text{ inches}$$

where: P = unit axial force
L = length of rod (equal to one half panel length)
E = elastic modulus of steel

Calculate stiffness of support angle using analytical model and SAP2000 (see Figure M.2):

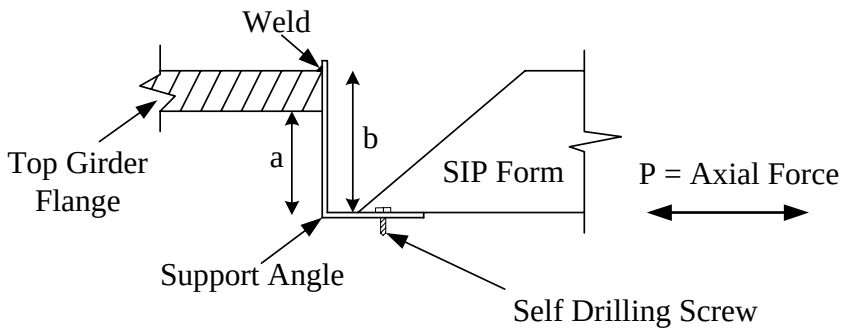

a) Connection Detail Assumed for Each Bridge

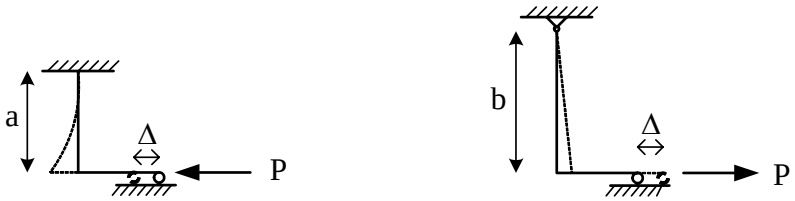

b) Analytical Models used in SAP2000

$$k_{angle} = \left[\left(\frac{P}{\Delta_{angle}} \right) / \text{unit length of panel width} \right] \times h = \left[\left(\frac{1}{0.47} \right) / 1 \right] \times 24 = 51.06 \ \frac{\text{kips}}{\text{inch}}$$

where: Δ_{angle} = displacement of angle from SAP2000
h = panel width

c) Stiffness Calculation from SAP2000 Results

Figure M.2- Support Angle Stiffness Analysis

Calculate cross-sectional area of a slender rod, A_{angle}, with axial stiffness equal to k_{angle}:

$$A_{angle} = \frac{k_{angle} L}{E} = \frac{51.06 \times 44.1}{29000} = 0.078 \text{ inches}^2$$

where: k_{angle} = largest stiffness of support angle
L = length of rod (equal to one half panel length)
E = elastic modulus of steel

Calculate axial deflection, Δ_{angle}, of a slender rod of equal cross-sectional area:

$$\Delta_{angle} = \frac{PL}{A_{angle}E} = \frac{1 \times 44.1}{0.078 \times 29000} = 0.020 \text{ inches}$$

where: P = unit axial force
L = length of rod (equal to one half panel length)
E = elastic modulus of steel

Calculate axial stiffness of entire system, k_{system}:

$$k_{system} = \frac{P}{\Delta_{system}} = \frac{P}{\Delta_{panel} + \Delta_{screw} + \Delta_{angle}} = \frac{1}{0.001 + 0.021 + 0.020} = 23.8 \ \frac{\text{kips}}{\text{inch}}$$

where: P = unit axial force

Calculate area of strut members, A_{strut}, with axial stiffness equal to k_{system}:

$$A_{strut} = \frac{k_{system}L}{E} = \frac{23.8 \times 44.1}{29000} = 0.036 \text{ inches}^2$$

where: k_{system} = axial system stiffness
L = length of rod (equal to one half panel length)
E = elastic modulus of steel

Calculate Δ of truss with shear stiffness equivalent to SIP form system (see Figure M.3):

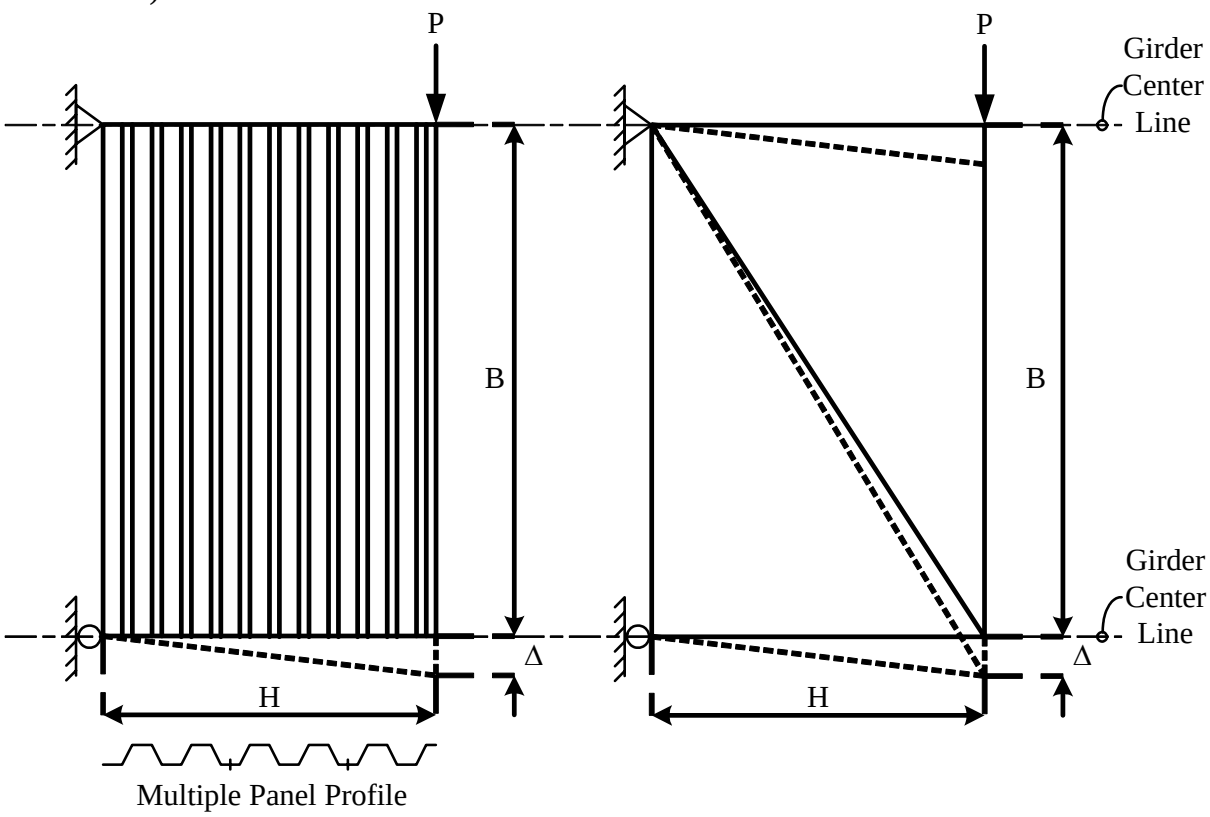

SIP Diaphragm System **Analogous Truss Model**

a) Truss Analogy, SDI (1991)

$$\Delta = \frac{P}{G'} \cdot \frac{h}{B} = \frac{1}{11} \cdot \frac{2.0}{7.35} = 0.025 \text{ inches}$$

where: P = unit axial force
h = panel width
B = panel length
G' = SIP system shear stiffness, Jetann et al. (2002)

b) Shear Deflection of Analogous Truss Model

Figure M.3- Shear Stiffness Analysis of SIP Forms

Calculate area of diagonals of X-frame truss system necessary to match Δ of analogous truss model using SAP2000 (see Figure G.4):

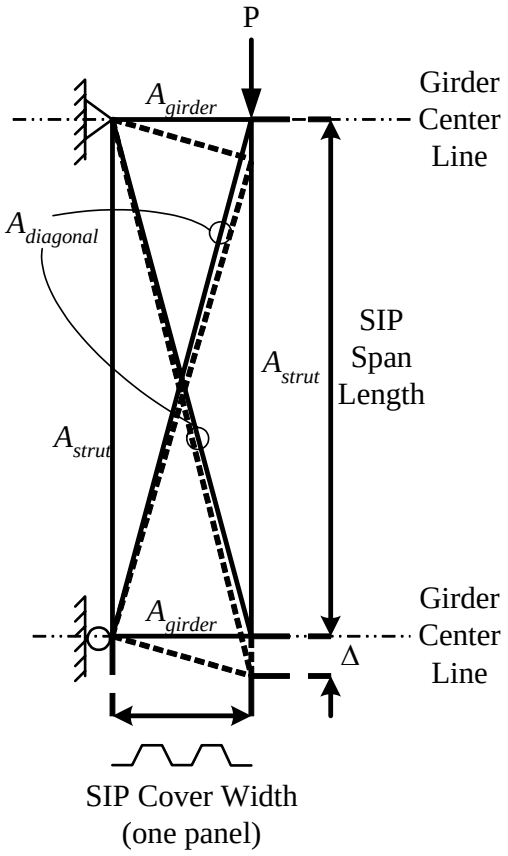

where: A_{girder} = girder cross-sectional area
A_{strut} = strut cross-sectional area
$A_{diagonal}$ = diagonal cross-sectional area
Δ = displacement equal to Δ of truss analogy

Figure M.4- X-frame Truss Model with Shear Stiffness Equivalent to Truss Analogy

Found by changing cross-sectional area (using SAP2000) until displacement equal to that of truss analogy. For this example:

A_{girder} = 78.0 inches^2
A_{strut} = 0.04 inches^2
$A_{diagonal}$ = 0.07 inches^2
Δ = 0.024 inches

The following table contains the SIP X-brace properties calculated for each bridge included in this study:

Table M.2- SIP X-Brace Data Calculated for Each Bridge

SIP X-Brace Data	A_{girder} (in^2)	A_{strut} (in^2)	$A_{diagonal}$ (in^2)
Eno	122.95	0.04	0.16
Bridge 8	95.50	0.04	0.04
Avondale	79.21	0.06	0.06
US-29	48.50	0.04	0.04
Camden (SB & NB)	121.00	0.04	0.16
Wilmington St	98.00	0.04	0.04
Bridge 14	110.50	0.04	0.04
Bridge 10	110.50	0.04	0.04
Bridge 1	120.00	0.04	0.04

Appendix N

Sample Calculation of SIP Metal Deck Form Properties (SAP)

This Appendix contains a sample calculation of the SIP metal deck form properties that were used in the SAP bridge models. The geometry and properties of the shell element used in SAP models for each bridge model were tabulated and are included herein.

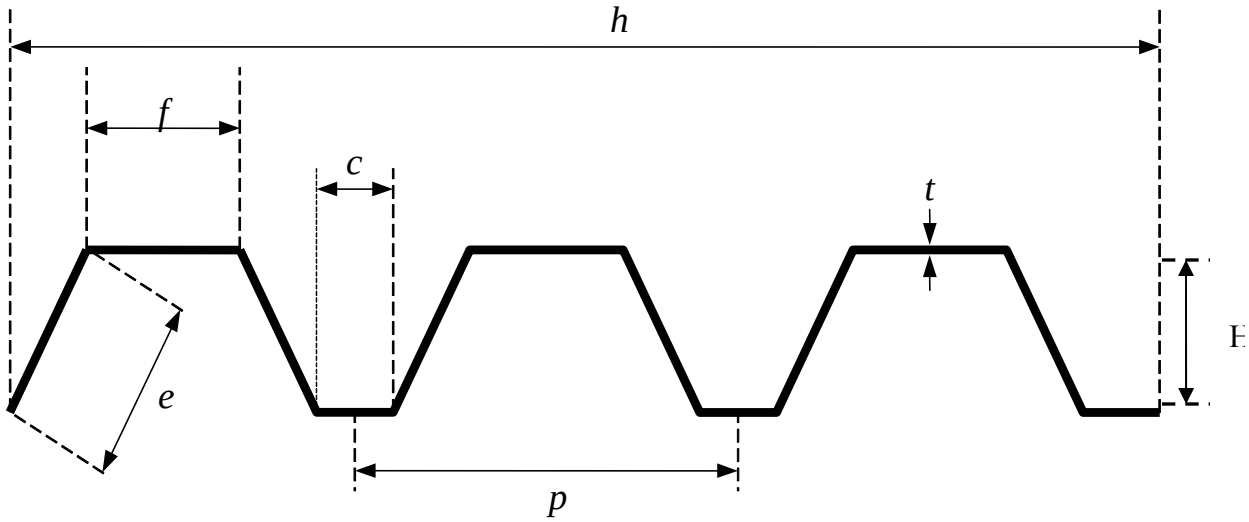

Figure N-1 Typical Stay-in-Place Metal Deck Form Profile

Table N-1 Stay-in-Place Metal Deck Form Data

Bridge	***H* (in.)**	***h* (in.)**	***p* (in.)**	***f* (in.)**	***c* (in.)**	***e* (in.)**	***t* (in.)**
US 29	2.5	32	8	5	2.5	2.51	0.036
Wilmington St.	2.5	32	8	5	2.5	2.51	0.036
Bridge 8	3	24	8	5.25	1.75	3.04	0.067
Eno	3	24	8	5.25	1.75	3.04	0.036
Bridge 10	3	24	8	5.25	1.75	3.04	0.036

Sample Calculation of Stay-in-place Metal Deck Form Properties for US 29:

Calculate flattened out panel width, *w*:

$$w = (8x\ e) + (4x\ f) + (4x\ c) = (8x2.51) + (4x5) + (4x2.5) = 50.08\ in.$$

Calculate total cross-area section of the panel, A_{Panel}.

$$A_{Panel} = w \times t = 50.08x.0.036 = 1.80\ in.^2$$

Calculate Shell Element thickness, *th*.

$$th = \frac{A_{Panel}}{w} = \frac{1.80}{32} = 0.056\ in.$$

Calculate Shell Element thickness of bending, *thb*.

$$I = \frac{1}{12} bt^3 : \frac{32}{12} x0.6302 = \frac{1}{12} x32xt^3$$

$$t = thb = 0.84\ in.$$

where: I = Moment of inertia of the SIP (CSI catalog)
b = Width of the SIP *(h)*
t = Thickness of Bending *(thb)*

Calculate the stiffness modifier, f_{11}.

$$f_{11} = \frac{Shell\ Element\ Thickness}{SIP\ Thickness} = \frac{0.056}{0.036} = 1.56\ in.$$

Using Trial & Error by changing the shear modulus of the panel until obtain the same deflection.

Calculate the shear stiffness of the Panel using Analytical model and SAP 2000

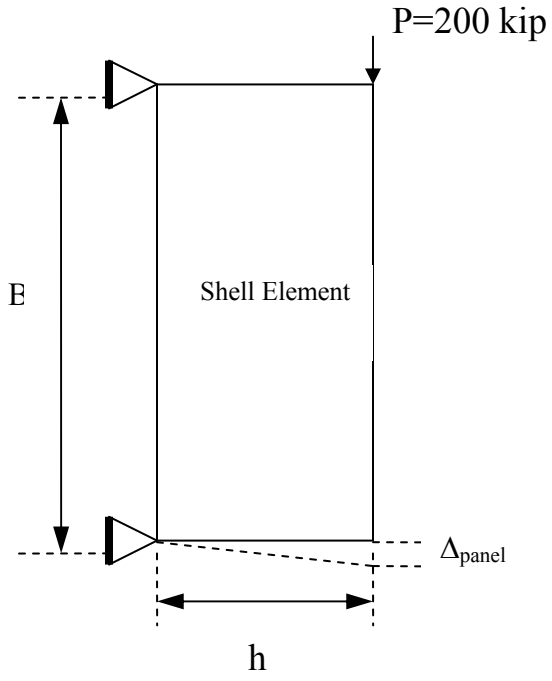

From Jetann (2002) G' = 11 *kip/in*.

$$\Delta_{panal} = \frac{Ph}{G'B} = \frac{200x32}{11x12x7.75} = 6.26\ ft$$

where: P = applied force (used 200 kip)
h = SIP width
B = Girder Spacing

Figure N-2 SAP, SIP Diaphragm Analytical Model, f_{12}

By assigning the thickness of the shell element equal to the real thickness of SIP form and using Trial & Error by changing the shear modulus of the panel until obtain the same deflection as analytical results.

By Trial & Error

Shear modulus = 26.445 *kip/ft*

Calculate the stiffness modifier, f_{12}

$$f_{12} = \frac{Shear\ modulus\ of\ Shell\ Element}{Shear\ Modulus\ of\ SIP} = \frac{26.445}{11153.846} \approx 0.00237$$

Calculate stiffness modifier f_{22} by using Trial & Error and SAP modeling.

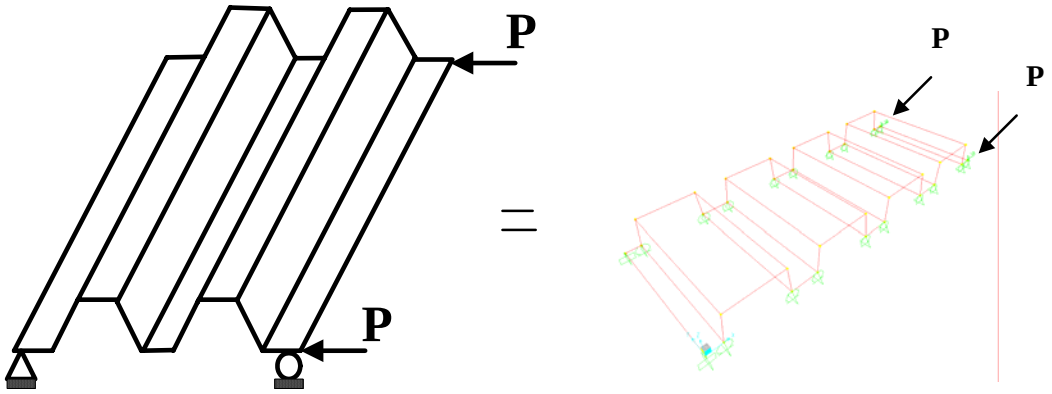

a) SAP, SIP Analytical Model

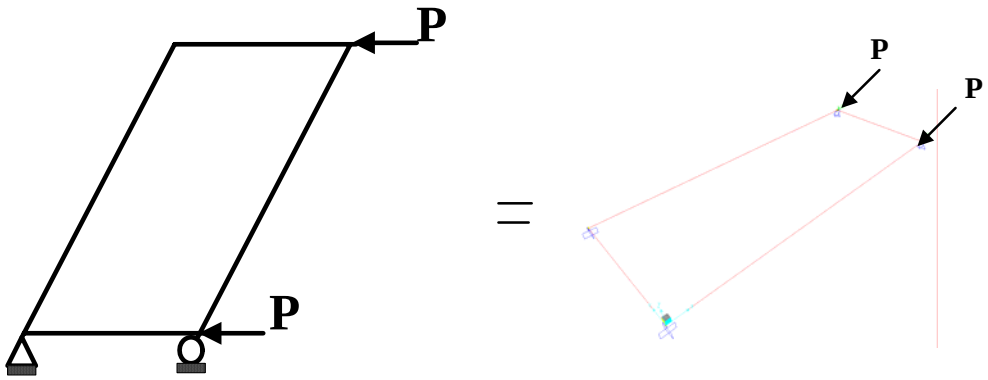

b) SAP, Shell Element Analysis

Figure N-3 SAP, f_{22} Analytical Models

Using Trial & Error to get the thickness of the simulate panel

Thickness of the panel = 2.5x10 $^{-6}$ *in.*

Calculate stiffness modifier, f_{22}

$$f_{22} = \frac{Thickness\ of\ Panel}{Thickness\ of\ SIP} = \frac{2.5x10^{-6}}{0.036} \approx 0.00007$$

Calculate stiffness modifier, m_{22}

$$Moment\ resistance\ of\ member \propto t^3$$
$$m_{22} = \frac{(Thickness\ in\ direction\ 22)^3}{(Thickness\ in\ direction\ 11)^3} = \frac{(0.036)^3}{(0.86)^3} \approx 0.00007$$

Calculate stiffness modifier, m_{12}

$$Moment\ resistance\ of\ member \propto t^3$$
$$m_{22} = \frac{(Thickness\ in\ direction\ 12)^3}{(Thickness\ in\ direction\ 11)^3} = \frac{(0.036)^3}{(0.86)^3} \approx 0.00007$$

The following tables contain the SIP properties and modifier calculated for each section followed CSI catalog:

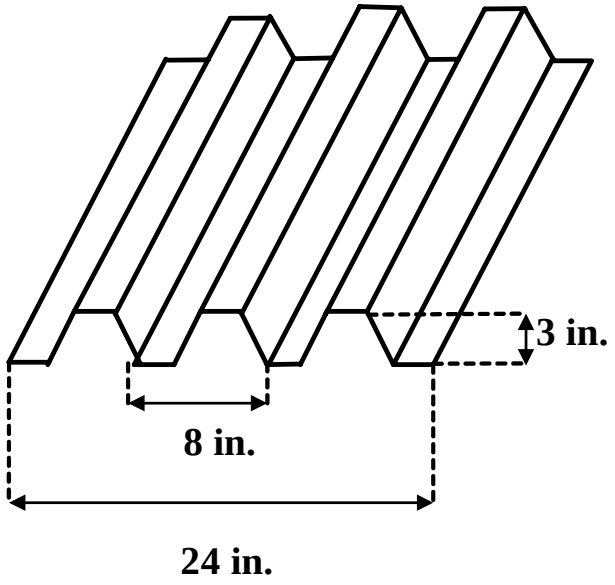

Figure N-4 SIP Form 24 in. Cover Width

Table N-2 SIP Form Properties used in SAP2000 Shell Element for SIP Form 24 in. Cover Width

Gage	Thickness (in.)	Cross Section Area (in.^2)	I (in.^4)	Thickness of Bending of simulated Pan (in.)	SIP stiffness modifier				
					f11	f22	m11	m22	m12
22	0.03	1.18	0.7704	0.917	1.635	0.00004	1	3.50E-05	3.50E-05
21	0.033	1.29	0.8601	0.951	1.635	0.00004	1	4.18E-05	4.18E-05
20	0.036	1.41	0.9511	0.983	1.635	0.00005	1	4.91E-05	4.91E-05
19	0.042	1.65	1.1368	1.044	1.635	0.00007	1	6.52E-05	6.52E-05
18	0.047	1.84	1.2946	1.090	1.635	0.00009	1	8.02E-05	8.02E-05
17	0.053	2.08	1.4872	1.141	1.635	0.00014	1	1.00E-04	1.00E-04
16	0.059	2.32	1.6593	1.184	1.635	0.00018	1	1.24E-04	1.24E-04
15	0.067	2.63	1.8843	1.235	1.635	0.00019	1	1.60E-04	1.60E-04
14	0.074	2.90	2.0811	1.277	1.635	0.00038	1	1.95E-04	1.26E-04

Table N-3 SIP Form Property, f_{12}, with Different Girder Spacing for SIP Form 24 in. Cover Width

Gage	Thickness (in.)	f 12 with different spacing (ft)						
		7	8	9	10	11	12	13
22	0.03	0.00270	0.00252	0.00243	0.00243	0.00250	0.00274	0.00274
21	0.033	0.00251	0.00231	0.00227	0.00227	0.00228	0.00250	0.00249
20	0.036	0.00224	0.00211	0.00202	0.00202	0.00228	0.00229	0.00226
19	0.042	0.00193	0.00179	0.00178	0.00178	0.00195	0.00197	0.00191
18	0.047	0.00175	0.00158	0.00158	0.00158	0.00173	0.00177	0.00174
17	0.053	0.00157	0.00142	0.00134	0.00134	0.00157	0.00156	0.00156
16	0.059	0.00142	0.00126	0.00126	0.00128	0.00141	0.00140	0.00141
15	0.067	0.00121	0.00114	0.00113	0.00113	0.00126	0.00123	0.00123
14	0.074	0.00108	0.00101	0.00101	0.00101	0.00116	0.00110	0.00112

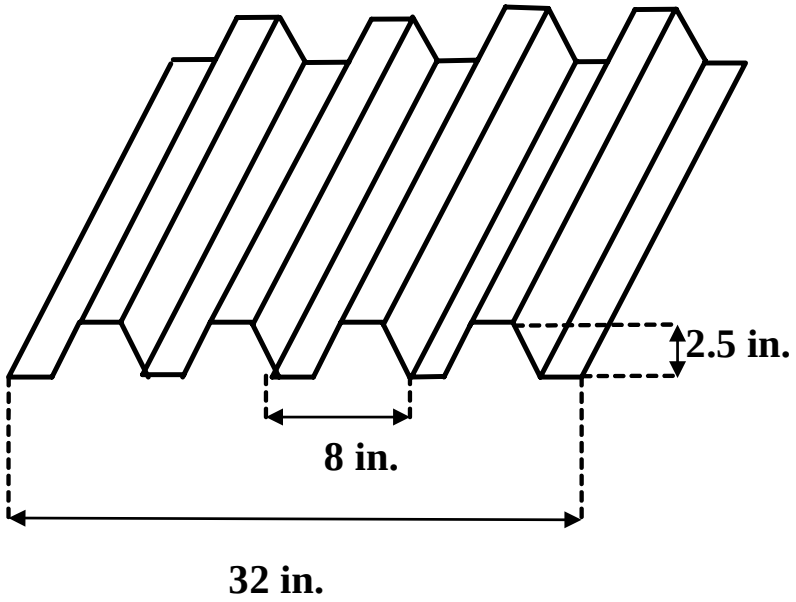

Figure N-5 SIP Form 32 in. Cover Width

Table N-4 SIP Form Properties used in SAP2000 Shell Element for SIP Form 32 in. Cover Width

Gage	Thickness (in.)	Cross Section Area (in.^2)	I (in.^4)	Thickness of Bending of simulated Pan (in.)	SIP stiffness modifier				
					f11	f22	m11	m22	m12
22	0.03	1.50	0.5251	0.807	1.565	0.00004	1	5.14E-05	5.14E-05
21	0.033	1.65	0.5777	0.833	1.565	0.00005	1	6.22E-05	6.21E-05
20	0.036	1.80	0.6302	0.857	1.565	0.00007	1	7.40E-05	7.40E-05

Table N-5 SIP Form Property, f_{12}, with Different Girder Spacing for SIP Form 32 in. Cover Width

Gage	Thickness (in.)	f 12 with different spacing (ft)						
		7	8	9	10	11	12	13
22	0.03	0.00272	0.00281	0.00281	0.00285	0.00283	0.00250	0.00274
21	0.033	0.00255	0.00256	0.00256	0.00248	0.00244	0.00249	0.00249
20	0.036	0.00237	0.00230	0.00230	0.00229	0.00229	0.00230	0.00229